Toxins and Signalling

Evelyne Benoit, Françoise Goudey-Perriere, Pascale Marchot, Denis Servent

Collection
Rencontres en Toxinologie

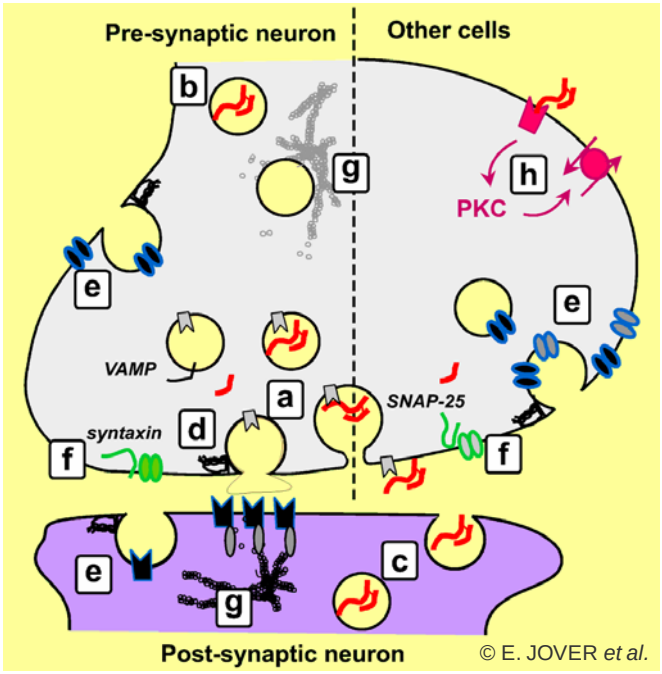

Toxines et Signalisation - *Toxins and Signalling*

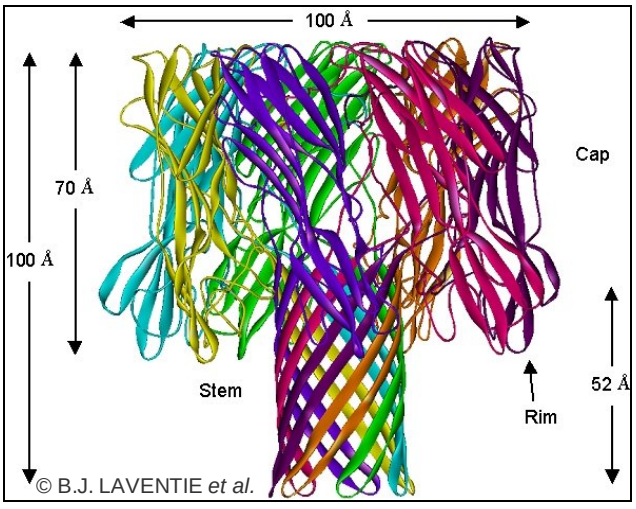

Comité d'édition – *Editorial committee :*
Evelyne BENOIT, Françoise GOUDEY-PERRIERE, Pascale MARCHOT, Denis SERVENT

Société Française pour l'Etude des Toxines
French Society of Toxinology

Illustrations de couverture – *Cover pictures* :

En haut – *Top* : Les effets intracellulaires multiples des toxines botuliques et de la toxine tétanique - *The multiple intracellular effects of the BoNTs and TeNT*. (*Copyright* Emmanuel JOVER, Fréderic DOUSSAU, Etienne LONCHAMP, Laetitia WIOLAND, Jean-Luc DUPONT, Jordi MOLGÓ, Michel POPOFF, Bernard POULAIN)

En bas - *Bottom* : Structure tridimensionnelle de l'alpha-toxine staphylocoque - *Tridimensional structure of* staphylococcal *alpha-toxin*. (*Copyright* Benoit-Joseph LAVENTIE, Daniel KELLER, Emmanuel JOVER, Gilles PREVOST)

Collection
Rencontres en Toxinologie

La collection « Rencontres en Toxinologie » est publiée à l'occasion des Colloques annuels « Rencontres en Toxinologie » organisés par la Société Française pour l'Etude des Toxines (SFET). Les ouvrages imprimés parus de 2001 à 2007 ont été édités par Elsevier (Paris, France) puis la Librairie Lavoisier (Cachan, France). Depuis 2008, ils sont édités par la SFET et diffusés sur le site http://www.sfet.asso.fr, en libre accès pour les auteurs et les lecteurs.

The series « Rencontres en Toxinologie » is published on the occasion of the annual Meetings on Toxinology organized by the French Society of Toxinology (SFET). The printed books of the series, from 2001 to 2007, were edited by Elsevier (Paris, France) and then the Librairie Lavoisier *(Cachan, France). Since 2008, they are edited by the SFET and are available on-line on the site http://www.sfet.asso.fr, with free access for authors and readers.*

Titres parus – *Previous titles*

Explorer, exploiter les toxines et maîtriser les organismes producteurs
Cassian Bon, Françoise Goudey-Perrière, Bernard Poulain, Simone Puiseux-Dao
Elsevier, Paris, 2001
ISBN : 2-84299-359-4

Toxines et recherches biomédicales
Françoise Goudey-Perrière, Cassian Bon, Simone Puiseux-Dao, Martin-Pierre Sauviat
Elsevier, Paris, 2002
ISBN : 2-84299-445-0

Toxinogenèse – Biosynthèse, ingénierie, polymorphisme et neutralisation des toxines
Françoise Goudey-Perrière, Cassian Bon, André Ménez, Simone Puiseux-Dao
Elsevier, Paris, 2003
ISBN : 2-84299-481-7

Envenimations, intoxinations
Françoise Goudey-Perrière, Evelyne Benoit, *Simone Puiseux-Dao*, *Cassian Bon*
Librairie Lavoisier, Cachan, 2004
ISBN : 2-7430-0749-4

Toxines et douleur
Cassian Bon, Françoise Goudey-Perrière, Max Goyffon, Martin-Pierre Sauviat
Librairie Lavoisier, Cachan, 2005
ISBN : 2-7430-0849-0

Toxines et cancer
Françoise Goudey-Perrière, Evelyne Benoit, Max Goyffon, Pascale Marchot
Librairie Lavoisier, Cachan, 2006
ISBN : 2-7430-0958-6

Toxines émergentes : nouveaux risques
Françoise Goudey-Perrière, Evelyne Benoit, Pascale Marchot, Michel R. Popoff
Librairie Lavoisier, Cachan, 2007
ISBN : 978-2-7430-1037-9

Toxines et fonctions cholinergiques neuronales et non neuronales
Evelyne Benoit, Françoise Goudey-Perrière, Pascale Marchot et Denis Servent
Publications de la SFET, Châtenay-Malabry, France, 2008
Epub on http://www.sfet.asso.fr - ISSN 1760-6004

Cet ouvrage est publié à l'occasion du colloque « 17èmes Rencontres en Toxinologie », organisé par la Société Française pour l'Etude des Toxines (SFET) les 2 et 3 décembre 2009 à Paris.

This book is published on the occasion of the 17th Meeting on Toxinology, organized by the French Society of Toxinology (SFET) on December 2nd and 3rd, 2009, in Paris.

Sommaire - *Content*

Toxines et Signalisation – Toxins and Signalling
Rencontres en Toxinologie – Meeting on Toxinology, 2009
Editions de la SFET – SFET Editions
Accès libre en ligne sur le site – Free access on line on the site : http://www.sfet.asso.fr

Signalling pathways activated by Clostridium perfringens *alpha-toxin*

Richard W. TITBALL[1]*, Andrew CARNEGIE[2], Ajit K. BASAK[2], Christopher GREEN[3], David S. MOSS[2], Claire E. NAYLOR[2]

[1] *School of Biosciences, University of Exeter, Devon, EX4 4QD UK ;* [2] *Department of Crystallography, Birkbeck College, Malet St., London, WC1E 7HY, UK ;* [3] *Defence Science and Technology Laboratory, Porton Down, Salisbury, Wilts, SP4 0JQ, UK*

Corresponding author ; Tel : +44 (0)1392 725157 ; Fax : +44 (0)1392 263434 ;
E-mail : R.W.Titball@exeter.ac.uk

Abstract

The α-toxin from Clostridium perfringens *is a phospholipase C which is active towards phospholipids in eukaryotic cell membranes. At high concentrations of the toxin cell lysis occurs but at sub-lytic concentrations there are subtle effects on cell metabolism because the cleavage of eukaryotic membrane phospholipids generates a number of secondary messengers within the cells. Two key messengers are diacylglycerol and inositol triphosphate. Diacylglycerol is able to activate the arachidonic acid pathway and protein kinase C. We have shown that α-toxin binds to the outer leaflet of cells and causes subsequent changes in intracellular calcium concentration. Our results suggest that initial changes in intracellular calcium concentrations were a consequence of calcium influx from the extracellular medium, with subsequent changes involving intracellular calcium stores.*

Voies de signalisation activées par la toxine alpha de Clostridium perfringens

La toxine alpha de Clostridium perfringens *possède une activité phospholipase C qui est active sur les phospholipides des membranes cellulaires eucaryotes. A forte concentration de toxine la lyse cellulaire se produit alors qu'à des concentrations sub-lytiques des effets subtils sur le métabolisme cellulaire apparaissent du fait de la libération de nombreux messagers secondaires à l'intérieur de la cellule suite au clivage des phospholipides de la membrane cellulaire. Les deux seconds messagers clés sont le diacylglycérol et l'inositol triphosphate, le diacylglycérol étant capable d'activer la voie de l'acide arachidonique et de la protéine kinase C. Nous avons montré que la toxine alpha se lie sur le feuillet externe de la cellule et provoque des changements de la concentration intracellulaire en calcium. Nos résultats suggèrent que les premières étapes de ce changement sont la conséquence d'un influx calcique à partir du milieu extracellulaire entrainant des modifications du stockage du calcium intracellulaire.*

Keywords : Clostridium perfringens*, α-toxin, phospholipase C, calcium signalling.*

Introduction

Clostridium perfringens is a Gram positive anaerobe which is found where decaying organic matter is present. The bacterium is found in virtually all soils and in the gut of almost all animal species and may be the most widely distributed pathogen known (Songer, 2002). The ability of the bacterium to cause disease is ascribed mainly to the production of a range of protein toxins. The differential production of the major toxins (α-, β-, γ- and ι-toxins) is used to assign strains into 1 of 5 biotypes (types A-E). These biotypes are associated with different diseases of humans and animals. Of the major toxins *C. perfringens* type A strains produce only the α-toxin. Type A strains are especially associated with gas gangrene, which usually arises as the result of the contamination of a traumatic injury site with bacteria. Over the past decade or so conclusive evidence has been presented that *C. perfringens* α-toxin is the major virulence determinant in gas gangrene (Awad *et al.*, 1995; Williamson and Titball 1993). It has also been suggested that α-toxin might play a role in non-gangrenous diseases of man and animals including necrotic enteritis in chickens (Heier *et al.*, 2001; Zekarias *et al.*, 2008) and a fatal enteritis in calves (Manteca *et al.*, 2001).

The α-toxin is a phospholipase C, and the preferred substrates are phosphatidylcholine and sphingomyelin (Krug and Kent 1984). Phospholipid hydrolysis yields a charged head group and a water-insoluble diacylglycerol group (or a ceramide group in the case of sphingomyelin). Unlike many bacterial phospholipases C, α-toxin is active towards phospholipids in eukaryotic cell membranes (Titball, 1998). It is believed that the ability of

α-toxin to interact with membrane phospholipids is a consequence of surface exposed hydrophobic amino acids and loops and the ability of the toxin to form calcium bridges with the phosphate groups of the phospholipids (Naylor *et al.*, 1998; Naylor *et al.*, 1999). When sufficient concentrations of α-toxin are incubated with eukaryotic cells, such as erythrocytes, fibroblasts and lymphocytes, obvious cytotoxicity occurs (Flores-Diaz *et al.*, 1998; Ochi *et al.*, 1996; Titball *et al.*, 1993). In the case of erythrocytes damage to the cell membrane can be quantified as haemolysis.

At sub-lytic concentrations of the toxin there are much more subtle effects on cell metabolism. These effects often involve the perturbation of cell signalling pathways and the modulation of these pathways may be of significance in the pathogenesis of disease. We review here the pathways which have been reported to be modulated in cells exposed to α-toxin, focussing especially on evidence that calcium ion fluxes occur.

Effect of α–toxin on signalling pathways in host cells

The cleavage of eukaryotic membrane phospholipids by α-toxin could potentially generate a number of secondary messengers within the cells. In addition, the effects of α-toxin on mammalian cells might be potentiated as a consequence of the activation of endogenous membrane phospholipases A_2, C and D (Gustafson and Tagesson, 1990; Ochi *et al.*, 1996; Sakurai *et al.*, 1993, 1994). In rabbit erythrocyte membranes treated with α-toxin it has been shown that endogenous phospholipase C is rapidly activated, followed later by the activation of endogenous phospholipase D. The mechanisms by which these membrane phospholipases are activated is not clear. It may involve activated protein kinase C (PKC), either directly or indirectly (Exton, 1990). Alternatively, α-toxin may mediate this effect via activation of guanine triphosphates (GTP) -binding proteins, which in turn activate mammalian phospholipases (Sakurai *et al.*, 1994).

Eukaryotic cells exposed to sub-lytic quantities of α-toxin have been shown to activate the arachidonic acid cascade (Fujii and Sakurai 1989; Gustafson and Tagesson 1990). The activation of the arachidonic acid cascade is dependent on the generation of diacylglcerol which is then converted by diacylglcerol lipase into arachidonic acid. The diacyglycerol might be generated directly as a consequence of the action of α-toxin on the cell membrane, or as a consequence of the activation of endogenous phospholipases. Diacyglycerol is then converted into prostaglandins, thromboxanes and/or leukotrienes in the arachidonic acid cascade (Samuelsson 1983). These compounds are able to regulate inflammatory processes. The production of thromboxanes is associated with platelet aggregation and significantly the aggregation of platelets occurs after the administration of α-toxin (Sugahara *et al.*, 1977). *In vivo* aggregates of platelets formed after the administration of α-toxin into mice occlude blood vessels and their formation is associated with a reduction in blood supply to tissues (Bryant *et al.*, 2000). This might enhance the anoxic state of tissues and allow the multiplication of *C. perfringens.* It is possible that platelet aggregation caused by α-toxin is due to the activation of the arachidonic acid cascade in these cells.

The diacylglycerol generated after the hydrolysis of phospholipids could also activate PKC which would then have short and long term effects on cellular metabolism (Bunting *et al.*, 1997; Nishizuka 1992; Ochi *et al.*, 2002). The activation of PKC in neutrophils exposed to α-toxin has been shown to be associated with the binding of cells to fibrinogen and fibronectin (Ochi *et al.*, 2002). This finding might explain the molecular basis of the observation that neutophils bind to endothelial cells lining blood vessels surrounding the site of gas gangrene infection. It is also clear that activated PKC plays a key role in the response of endothelial cells to α-toxin. Treated cells respond with the generation of the vasoactive lipids platelet-activating factor (PAF) and prostacyclin (Bunting *et al.*, 1997). The binding of neutrophils was also enhanced in α-toxin-treated cells, mediated by the upregulation of PAF receptor and P-selectin (Bunting *et al.*, 1997). Thus the binding of neutrophils to endothelial cells lining blood vessels might be dependent on PKC-mediated changes in both neutrophils and endothelial cells.

There is also good evidence that the secondary messenger inositol triphosphate is generated indirectly in cells exposed to α-toxin. Activated mammalian phospholipases C are able to hydrolyse phosphatidylinositol diphosphate (PIP_2), generating inositol triphosphate (IP_3) (Sakurai *et al.*, 1993). One of the key events triggered by IP_3 is the opening of calcium gates in the cell membrane (Fujii *et al.*, 1986). Elevated intracellular calcium levels would contribute to the activation of endogenous membrane phospholipases described above. It has previously been shown that muscle cells exposed to α-toxin become inexcitable (Boethius *et al.*, 1973) and the opening of calcium gates might explain the cardiotoxic effects of the α-toxin (Asmuth *et al.*, 1995).

Labelled α-toxin binds to the cell surface

Alpha-toxin with a sequence derived from the CER89L43 strain of *C. perfringens* was expressed in *E. coli*, purified as described previously (Titball *et al.*, 1991), and chemically labelled on its sole cysteine residue (169) using either Alexxa-Fluor 488 or Oregan Green maleimide (Molecular Probes). Cysteine 169 is both on the protein surface and distant from the active site and membrane-interaction surface, and was therefore not expected to affect the enzyme's fold or activity. Protein and label were mixed in a 1:20 molar ratio, in 0.1M Tris-HCl, pH 8.0, and stirred on ice for 2 hours. Unconjugated label was removed by size exclusion chromatography with Sephadex G-25 column. The procedure resulted in 70-80% of cysteine residues being modified, as assessed by absorbance. Unlabelled toxin was not removed as it would not affect the experiments. Retention of the enzymatic activity of the toxin (data not shown) was confirmed by measuring hydrolysis of *p*-nitrophenolphosphoryl choline (Stevens *et al.*, 1987) or egg yolk (Jepson *et al.*, 1999; Titball *et al.*, 1991), or by assessing cytotoxicity using neutral red cell viability assays (Borenfreund and Puerner, 1985).

A431 skin carcinoma or bovine pulmonary aortic lung endothelial (BPAE) cells were seeded at a density of 20,000 cells/ml in all experiments. The cell lines were shown by neutral red and 3-(4,5-dimethylthiazol-2-yl)-2,5-diphenyl tetrazolium bromide (MTT) cell viability (Denizot and Lang, 1986) assays to be susceptible to lysis by α-toxin in a dose-dependent manner (data not shown).

The cell lines were monitored by epifluorescence (Nikon Eclipse TE200 inverted microscope linked to an intensified Cairn CCD), or confocal microscopy (Olympus Fluoview FV200) and were continually perfused with HBBSS (HEPES-buffered balanced salt solution) medium to which labelled or unlabelled α-toxin was added as required at concentrations between 0.1 and 10 µg/mL. Subsequent image processing utilised the Axon Imaging Workbench or Olympus Fluoview software. The images show toxin binding strongly and immediately to the outer cell membranes, with no significant intracellular fluorescence observed. After a time period of between 20 min and several hours, dependent on toxin dose, intense fluorescence across what is apparently the entire volume of the cell is observed (*Figure 1*). This fluorescence can be attributed to loss of dead cells from the surface and subsequent binding of the toxin to debris. Further evidence that the toxin binds to the outer membrane but is not internalised can be observed by phase contrast light microscopy: images show that after a 5 hr exposure to 0.3 µg/mL α-toxin, the endothelial cell monolayer is highly disrupted and cells are rounded (not shown). If the toxin was removed and fresh medium is applied, 24 hr later the cells can clearly be seen to have recovered and their morphology returned to normal.

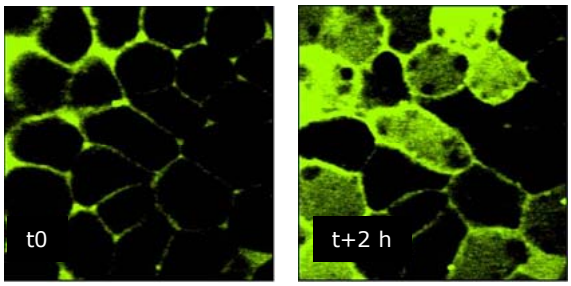

Fig 1. Confocal microscopy images of A431 skin carcinoma cells exposed to 10 µg/mL Alexa-488 labelled CER89L43 α-toxin. The left-hand image shows the cells shortly after toxin addition, and shows intense fluorescence on the outer cell membranes. The right-hand image shows the cells after 2 hours with some toxin having apparently entered the cells. Closer inspection reveals this actually corresponds to toxin binding to cell debris after a cell has died and detached from the coverslip surface.

Fig. 1. *Images en microscopie confocale de cellules A431 de carcinome de peau exposées à 10 µg/mL de toxine α CER89L43 marquée avec l'Alexa-488. Sur l'image de gauche, qui montre les cellules peu après l'addition de toxine, une fluorescence intense peut être observée au niveau de la membrane plasmique des cellules. L'image de droite montre, qu'après 2 heures, quelques molécules de toxine ont apparemment pénétré dans les cellules. Une observation plus attentive de cette image révèle qu'il s'agit en fait de molécules de toxine s'étant fixées aux débris cellulaires résultant de la mort dune cellule et de son absence d'adhésion au fond de la boîte de culture.*

These experiments established that at concentrations of between 0.1 and 1 µg/ml, the toxin bound strongly to the outer membrane of mammalian cell lines, but did not cause death for at least 6 hr, while between 1 and 10 µg/ml cell death occurred more rapidly. Therefore, a concentration of 1 µg/mL was selected to study intracellular calcium flux within cells caused by the presence of α-toxin bound to external cell membranes. Monolayers of A431 cells on 25 mm coverslips were incubated with 2.5 µM Fura-2/AM (Molecular Probes) for 30 min followed by a 10 min perfusion with PBS. Intracellular free calcium ion concentration variation in individual cells was then monitored by measuring the ratio of fluorescence at 340, 360 and 380 nm. Ratiometric measurements reduce the effects of uneven dye-loading, leakage and photobleaching and thus increase the sensitivity of the technique. Cells exposed to α-toxin showed alterations in the intracellular calcium ion concentration ($[Ca^{2+}]$), evidenced as changes in fluorescence (*Figure 1*). Following a 10 minute perfusion with PBS to establish a base line, A431 cells were perfused with varying concentrations of α-toxin in HBBSS. A variety of response times and behaviours were observed. These included a sudden and sustained increase in the 340/380 nm ratio (and therefore in intracellular calcium concentration, $[Ca^{2+}]_i$), but also $[Ca^{2+}]_i$ oscillations more typically associated with normal cell signalling in response to external stimuli. Both the time to the first peak in $[Ca^{2+}]$ entry and that to the highest $[Ca^{2+}]_i$ were dependent on α-toxin concentration, with the time to the first response being 34 min 41 sec (± 82 sec) and that to the peak response being 104 min 52 sec (± 187 sec) at 1 µg/mL toxin. Similar experiments performed in BPAE cells showed that this cell line was slightly more reactive with the first response after 27 min 7 sec (± 72 sec) and the peak response after 55 min 59 sec (± 453 sec) at the same α-toxin concentration.

In order to establish whether the source of the increase in $[Ca^{2+}]_i$ was from intracellular calcium stores or the extracellular medium, monolayers of Fura-2 incubated cells were perfused with α-toxin in a calcium-free buffer. No change in $[Ca^{2+}]_i$ was seen over the time course of the experiment, 1 hr 7 min. Calcium was then re-introduced into the external medium and there was an immediate increase in $[Ca^{2+}]_i$. This result suggested that α-toxin had bound to the outer cell membrane as previously shown, but that the initial source of the $[Ca^{2+}]_i$ increase following toxin exposure is due to influx of calcium from the extracellular medium, rather than release from intracellular calcium stores as previously postulated (Bryant *et al.*, 2003). However, if extracellular

calcium was withdrawn following initiation of an oscillatory $[Ca^{2+}]_i$ response, though on some occasions the response did stop, on others the response was unaffected or only slightly dampened (*Figure 2b*), suggesting some involvement of intracellular stores. We have also shown that the α-toxin binds Ca^{2+} (Naylor *et al.*, 1999) *via* its C-terminal domain, which is important for membrane interaction. This C-terminal domain is a C2-like domain that probably utilises Ca^{2+} to mediate membrane interactions (Naylor *et al.*, 1998). To confirm that the initial change in $[Ca^{2+}]$ was due to an influx from the extracellular medium we further observed Fura-2 fluorescence in the presence of manganese ion in the extracellular medium: this ion powerfully quenches Fura-2 fluorescence. In the presence of Mn^{2+}, the initial increase in 360/380 nm ratio on each occasion coincided with a significant drop in fluorescence intensity (at 360 nm excitation) indicating that the initial increase in $[Ca^{2+}]_i$ is due to influx from the extracellular medium.

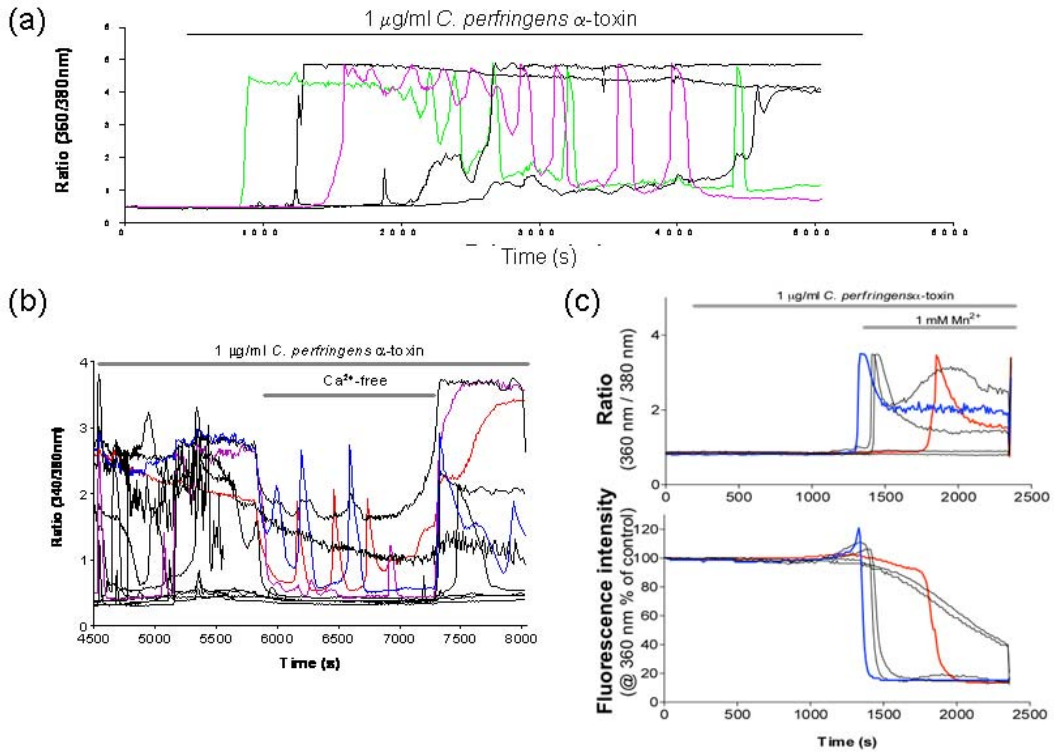

Fig. 2. Ratiometric measurement of free calcium concentration in individual A431 cells. Each curve represents the change in 340 or 360/380 nm fluorescence intensity ratio over time for a single cell that had been previously incubated with Fura-2/AM. The change in this ratio is an accurate indicator of the change in intracellular free calcium concentration. Bars represent the time period during which cells were perfused with the indicated substances. (**a**) After cells were perfused with α-toxin, a number of different responses were seen, including oscillations in calcium concentration, and a sharp and sustained rise in intracellular free calcium. (**b**) Cells initially perfused with α-toxin, and shown to respond were then perfused with calcium-free media. This reduces but does not eliminate the intensity of the signal. (**c**) Cells perfused with α-toxin in a calcium-free medium do not respond. Upon addition of calcium to the extracellular medium, an instantaneous response is observed. When calcium is replaced by manganese (upper graph), the response is accompanied by a drop in fluorescence intensity (lower graph) caused by quenching of Fura-2/AM fluorescence by manganese ions.

Fig. 2. *Mesures ratiométriques de la concentration de calcium libre dans des cellules A431 individuelles. Chaque courbe représente les variations du rapport des intensités de fluorescence entre 340 ou 360nm et 380 nm, en fonction du temps, pour une cellule donnée qui a été préalablement mise à incuber avec du Fura-2/AM. La variation de ce rapport est un indicateur adéquat du changement de la concentration intracellulaire de calcium libre. Les barres représentent les périodes durant lesquelles les cellules ont été perfusées avec les substances indiquées. (**a**) Après que les cellules aient été perfusées avec de la toxine α, un certain nombre de réponses a été observé, incluant des oscillations dans la concentration de calcium ainsi que des augmentations transitoires et soutenues du calcium libre intracellulaire. (**b**) Les cellules initialement perfusées avec de la toxine α et ayant montré une réponse ont ensuite été perfusées avec un milieu dépourvu de calcium, ce qui a pour conséquence de réduire mais pas d'éliminer l'intensité du signal. (**c**) Les cellules perfusées avec de la toxine α dans un milieu dépourvu de calcium ne répondent pas. Suite à l'addition de calcium au milieu extérieur, une réponse immédiate est observée. Quand le calcium est remplacé par du manganèse (en haut), la réponse est accompagnée d'une chute de l'intensité de fluorescence (en bas), provoquée par l'extinction de la fluorescence du Fura-2/AM par les ions manganèse.*

Finally, we observed variation in $[Ca^{2+}]$ resulting from toxin perfusion and initiation of an oscillatory response. After removal of toxin from the perfusion medium, as indicated above, cells, observed by phase-contrast light microscopy, were able to return to normal. In contrast, our ratiometric imaging results indicate that an oscillatory response continues for sometime after toxin withdrawal and that the resting calcium

concentration is higher than that prior to exposure (*Figure 2b*). It should be noted, however that the time course of this experiment (3.5 hr) is considerably shorter than that for the light microscopy (24 hr) and that an eventual return to resting [Ca^{2+}] is likely.

Conclusion

The membrane damaging toxins are often assumed to elicit their effects as a consequence of profound damage to cell membranes which results in cell lysis. However, it is increasingly apparent that subtle damage to the cell membrane can result in profound changes to cell metabolism which contribute to disease pathology. In this study we have monitored changes in calcium levels in cells exposed to *Clostridium perfringens* α-toxin. Our use of Fura-2/AM allowed the intracellular concentration of calcium to be monitored in real time following exposure to α-toxin. The treatment of cells with α-toxin resulted in changes in the level of intracellular calcium which were broadly proportional to the concentration of toxin applied. However, the intracellular calcium levels in cells exposed to sub-lethal doses of toxin typically showed an oscillatory response. We do not currently have a molecular explanation for this effect.

References

Asmuth DM, Olson RD, Hackett SP, Bryant AE, Tweten RK, Tso JY, Zollman T, Stevens DL (1995) Effects of *Clostridium perfringens* recombinant and crude phospholipase C and theta-toxin on rabbit hemodynamic parameters. *J Infect Dis* **172**: 1317-1323

Awad MM, Bryant AE, Stevens DL, Rood JI (1995) Virulence studies on chromosomal alpha-toxin and theta-toxin mutants constructed by allelic exchange provide genetic evidence for the essential role of alpha-toxin in *Clostridium perfringens*-mediated gas-gangrene. *Mo. Microbiol* **15**: 191-202

Boethius J, Rydqvist B, Mollby R, Wadstrom T (1973) Effect of a highly purified phospholipase C on some electrophysiological properties of the frog muscle fibre membrane. *Life Sci* **13**: 171-176

Borenfreund E, Puerner JA (1985) Toxicity determined in vitro by morphological alterations and neutral red absorption. *Toxicol Lett* **24**: 119-124

Bryant AE, Bayer CR, Hayes-Schroer SM, Stevens DL (2003) Activation of platelet gpIIbIIIa by phospholipase C from *Clostridium perfringens* involves store-operated calcium entry. *J Infect Dis* **187**: 408-417

Bryant AE, Chen RYZ, Nagata Y, Wang Y, Lee CH, Finegold S, Guth PH, Stevens DL (2000) Clostridial gas gangrene. II. Phospholipase C-induced activation of platelet gpIIbIIIa mediates vascular occlusion and myonecrosis in *Clostridium perfringens* gas gangrene. *J Infect Dis* **182**: 808-815

Bunting M, Lorant DE, Bryant AE, Zimmerman GA, McIntyre TM, Stevens DL, Prescott SM (1997) Alpha-toxin from *Clostridium perfringens* induces proinflammatory changes in endothelial cells. *J Clin Invest* **100**: 565-574

Denizot F, Lang R (1986) Rapid colorimetric assay for cell growth and survival. Modifications to the tetrazolium dye procedure giving improved sensitivity and reliability. *J Immunol Methods* **89**: 271-277

Exton JH (1990) Signalling through phosphatidylcholine breakdown. *J Biol Chem* **265**: 1-4

Flores-Diaz M, Alape-Giron A, Titball RW, Moos M, Guillouard I, Cole S, Howells AM, von Eichel-Streiber C, Florin I, Thelestam M (1998) UDP-glucose deficiency causes hypersensitivity to the cytotoxic effect of *Clostridium perfringens* phospholipase C. *J Biol Chem* **273**: 24433-24438

Fujii Y, Nomura S, Oshita Y, Sakurai J (1986) Excitatory effect of *Clostridium perfringens* alpha-toxin on the rat isolated aorta. *Br J Pharmacol* **88**: 531-539

Fujii Y, Sakurai J (1989) Contraction of the rat isolated aorta caused by *Clostridium perfringens* alpha toxin (phospholipase-C) - evidence for the involvement of arachidonic acid metabolism. *Br J Pharmacol* **97**: 119-124

Gustafson C, Tagesson C (1990) Phospholipase-C from *Clostridium perfringens* stimulates phospholipase-A2-mediated arachidonic acid release in cultured intestinal epithelial cells (Int-407). *Scand J Gastroenterol* **25**: 363-371

Heier BT, Lovland A, Soleim KB, Kaldhusdal M, Jarp J (2001) A field study of naturally occurring specific antibodies against *Clostridium perfringens* alpha toxin in Norwegian broiler flocks. *Avian Dis* **45**: 724-732

Jepson M, Howells A, Bullifent HL, Bolgiano B, Crane D, Miller J, Holley J, Jayasekera P, Titball RW (1999) Differences in the carboxy-terminal (putative phospholipid binding) domains of *Clostridium perfringens* and *Clostridium bifermentans* phospholipases C influence the hemolytic and lethal properties of these enzymes. *Infect Immun* **67**: 3297-3301

Krug EL, Kent C (1984) Phospholipase C from *Clostridium perfringens*: preparation and characterisation of homogenous enzyme. *Arch Biochem Biophys* **231**: 400-410

Manteca C, Daube G, Pirson V, Limbourg B, Kaeckenbeeck A, Mainil JG (2001) Bacterial intestinal flora associated with enterotoxaemia in Belgian Blue calves. *Vet Microbiol* **81**: 21-32

Naylor CE, Eaton JT, Howells A, Justin N, Moss DS, Titball RW, Basak AK (1998) Structure of the key toxin in gas gangrene. *Nat Struct Biol* **5**: 738-746

Naylor CE, Jepson M, Crane DT, Titball RW, Miller J, Basak AK, Bolgiano B (1999) Characterisation of the calcium-binding C-terminal domain of *Clostridium perfringens* alpha-toxin. *J Mol Biol* **294**: 757-770

Nishizuka Y (1992) Intracellular signalling by hydrolysis of phospholipids and activation of protein kinase C. *Science* **258**: 607-614

Ochi S, Hashimoto K, Nagahama M, Sakurai J (1996) Hemolysis and phospholipid metabolism elicited by *Clostridium perfringens* alpha-toxin through activation of GTP-binding protein in rabbit erythrocytes. *Jpn J Med Sci Biol* **49**: 266-267

Ochi S, Miyawaki T, Matsuda H, Oda M, Nagahama M, Sakurai J (2002) *Clostridium perfringens* alpha-toxin induces rabbit neutrophil adhesion. *Microbiology* **148**: 237-45

Sakurai J, Ochi S, Tanaka H (1993) Evidence for coupling of *Clostridium perfringens* alpha-toxin induced hemolysis to stimulated phosphatidic acid formation in rabbit erythrocytes. *Infect Immun* **61**: 3711-3718

Sakurai J, Ochi S, Tanaka H (1994) Regulation of *Clostridium perfringens* alpha-toxin activated phospholipase-C in rabbit erythrocyte membranes. *Infect Immun* **62**: 717-721

Samuelsson B (1983) Leukotrienes: mediators of immediate hypersensitivity reactions and inflammation. *Science* **220**: 568-575

Songer JG (2002) Gas gangrene and myonecrosis. In *Molecular Genetics, classification, pathology and ecology of the genus* Clostridium, Duchesnes C and Mainil J(eds) pp. 53-62. Presses de la Faculté de Médecine Vétérinaire de l'Université de Liège, Liège

Stevens DL, Mitten J, Henry C (1987) Effects of alpha-toxins and theta-toxins from *Clostridium perfringens* on human polymorphonuclear leukocytes. *J Infect Dis* **156**: 324-333

Sugahara T, Takahashi T, Yamaya S, Ohsaka A (1977) *In vitro* aggregation of platelets induced by alpha-toxin (phospholipase C) of *Clostridium perfringens*. *Jpn J Med Sci Biol* **29**: 255-263

Titball RW (1998) Bacterial phospholipases. *J Appl Microbiol* **84**: 127S-137S

Titball RW, Fearn AM, Williamson ED (1993) Biochemical and immunological properties of the C-terminal domain of the alpha-toxin of *Clostridium perfringens*. *FEMS Microbiol Lett* **110**: 45-50

Titball RW, Leslie DL, Harvey S, Kelly D (1991) Hemolytic and sphingomyelinase activities of *Clostridium perfringens* alpha-toxin are dependent on a domain homologous to that of an enzyme from the human arachidonic acid pathway. *Infect Immun* **59**: 1872-1874

Williamson ED, Titball RW (1993) A genetically engineered vaccine against the alpha-toxin of *Clostridium perfringens* protects mice against experimental gas-gangrene. *Vaccine* **11**: 1253-1258

Zekarias B, Mo H, Curtiss R 3rd (2008) Recombinant attenuated *Salmonella enterica* serovar typhimurium expressing the carboxy-terminal domain of alpha toxin from *Clostridium perfringens* induces protective responses against necrotic enteritis in chickens. *Clin Vaccine Immunol* **15**: 805-816

Toxines et Signalisation – Toxins and Signalling
Rencontres en Toxinologie – Meeting on Toxinology, 2009
Editions de la SFET – SFET Editions
Accès libre en ligne sur le site – Free access on line on the site : http://www.sfet.asso.fr

Lethal toxin from Clostridium sordellii *modifies, sequentially or independently, several cellular signalling pathways*

Blandine GENY*, Michel POPOFF

Institut Pasteur, Unité des Bactéries Anaérobies et Toxines, Département de Microbiologie, 25 rue du Docteur Roux, 75724 Paris cedex 15, France

** Corresponding author ; Tel : +33 (0)1 44 38 95 87 ; Fax : +33 (0)1 40 61 31 23 ;*
E-mail : blandine.geny@pasteur.fr

Abstract

The large clostridial lethal toxin (LT), from C. Sordellii*, possesses a glucosyltransferase activity that glucosylates and thus inactivates small GTPases including Rac, Ras, Rap and Ral. As a consequence of inactivation of these small GTPases, cells rounded up and actin is depolymerized. We have observed that several signalling pathways are sequentially inactivated downstream of small GTPase glucosylation, including alteration of phosphoinositide metabolism, disorganization of focal adhesions and adherens junctions that precedes actin depolymerization, decrease of phospholipase D activity and finally cell death by apoptosis starting at the mitochondrial level. Moreover, upon intoxication with LT from strain IP82 (LT-82) other cellular signalling pathways, the MAPK pathways, are modified as a consequence of the cytosolic entry of the N-terminal domain of LT-82. Activation of SAPK/JNK pathway facilitates glucosylation of LT-82 targets, however, independently of the toxin intrinsic catalytic activity. Here we summarize the main observations concerning the cellular signalling pathways modified by LT-82.*

La toxine létale de Clostridium sordellii *modifie, séquentiellement ou indépendamment, plusieurs voies de signalisation cellulaire*

La toxine létale (LT) de C. sordellii*, une grande toxine clostridiale, possède une activité glucosyltransférase qui glucosyle et, ainsi, inactive les petites GTPases, Rac, Ras, Rap et Ral. L'inactivation de ces petites protéines G conduit à un arrondissement des cellules et à la dépolymérisation de l'actine. En aval de la glucosylation des petites GTPases, plusieurs voies de signalisation sont inactivées séquentiellement. Elles incluent une altération du métabolisme des phosphoinositides, une désorganisation des points focaux d'adhésion et des jonctions adhérentes qui précèdent la dépolymérisation de l'actine ainsi qu'une diminution de l'activité de la phospholipase D et finalement la mort cellulaire par apoptose par voie intrinsèque. De plus, lors de l'intoxication des cellules par la LT purifiée à partir de la souche IP82 (LT-82) de* C. sordellii*, d'autres voies de signalisation sont modifiées lors de l'entrée du domaine catalytique de la toxine dans le cytosol, les voies MAPKs. L'activation de la voie SAPK/JNK facilite la glucosylation des cibles de la toxine LT-82 ; elle est cependant indépendante de l'activité enzymatique elle-même. Le présent travail résume l'ensemble des données connues sur les principales voies de signalisation modifiées par LT-82.*

Keywords : *Lethal toxin, actin, apoptose, SAPK/JNK.*

Introduction

Clostridium sordellii is an anaerobic, gram-positive, spore-forming rod. This bacterium is commonly found in the soil and in the intestines of animals and humans. Many strains are nonpathogenic, however, virulent strains produce toxins, amongst which the major pathogenic factor, lethal toxin (LT) also called edema-producing toxin (Arseculeratne *et al.*, 1969). These strains are responsible for lethal infections in several animal species, such as enteritis and enterotoxemia in sheep, lamb and cattle (Al-Mashat and Taylor, 1983 ; Popoff, 1984 ; Richards, 1982) and myonecrosis and gangrene (Pfeifer *et al.*, 2003 ; Rupnik *et al.*, 2005) often accompanied by a toxic shock syndrome in humans. Recently, several fatal toxic shocks due to *C. sordellii* LT were reported that occurred postpartum and after spontaneous or medical abortion with RU-486 (Bitty *et al.*, 1997 ; Cohen *et al.*, 2007 ; Fischer *et al.*, 2005 ; Rorbye *et al.*, 2000 ; Sinave *et al.*, 2002).

LT from *C. sordellii* has been shown to be closely related to the large clostridial toxin B from *C. difficile* (Bette *et al.*, 1991) as their amino acid sequences are 88 % identical and both toxins cross react immunologically (Martinez and Wilkins, 1992). Large clostridial toxins are single chain proteins with a MW of 250-300 kDa, which are active intracellularly and contain at least three functional domains (Just *et al.*, 2000 ; Thelen *et al.*, 1994). The C-terminal (C-ter) domain possesses multiple repeated sequences. It is

involved in the cell surface receptor recognition. The central part mediates the translocation into the cytosol of the N-terminal (N-ter) part across the endosomal membrane related to its hydrophobic segment. Recently, cleavage by autocatalysis of the N-ter part of the large clostridial toxin, ToxB, and its release into the cytosol have been well studied (Egerer *et al.*, 2007 ; Reineke *et al.*, 2007). The N-ter part contains the enzymatic site, a glucosyltransferase activity allowing glucosylation at threonin 35/37 of small G-proteins of the Ras superfamily by direct inhibition of effector binding (Popoff, 1987). Glucosylated small GTPases, *i.e.* inactivated by LT from strain 82 (LT-82), include Ras, Rap and Ral involved in signal transduction, and Rac implicated in actin cytoskeleton remodeling but also in a variety of cell functions such as cell cycle progression and gene transcription (Symons, 2000 ; Van Aelst and D'Souza-Schorey, 1997). The cellular effects of LT-82 have been studied using cell-lines of various origins and all cell-lines tested appeared sensitive to this toxin. After intoxication with LT-82 of adherent cells, cell rounding, assessing the depolymerization of actin cytoskeleton, was easily observed.

In the present report, we review the cellular signalling pathways modified by LT-82 downstream, upstream or concomitantly with the actin depolymerization, and we discuss their interconnection or independency.

Signaling pathways involved in cell death by apoptosis

LT-82 induces apoptosis by disruption of mitochondrial homeostasis and involves a cascade of events

After an overnight intoxication with 10^{-8} M LT-82, around 50 % of HL-60 cells exhibited nuclear fragmentation, a typical hallmark of apoptosis. Further confirmation was given by studying DNA fragmentation (not shown). As shown in *Figure 1*, after overnight intoxication with 10^{-8} M LT-82, the percentage of apoptotic cells was evaluated. Indeed, apoptotic cells exposed phosphatidylserine (PS) at their surface in the absence of cellular permeability to propidium iodide (*Figure 1A*). Mitochondria damages were assessed by measuring mitochondrial membrane potential ($\Delta\psi$m) that decreased upon LT-82 intoxication and caspase 3 activity that increased in apoptotic cells (*Figure 1B*). The pathway by which LT-82 induced apoptosis was further identified by studying the time-course of activation of caspase 8 first activated *via* the extrinsic pathway and caspase 9 *via* the intrinsic pathway. Clearly, caspase 9 was activated prior to caspase 8 indicating that LT-82 induced apoptosis *via* the intrinsic pathway (not shown ; Petit *et al.*, 2003).

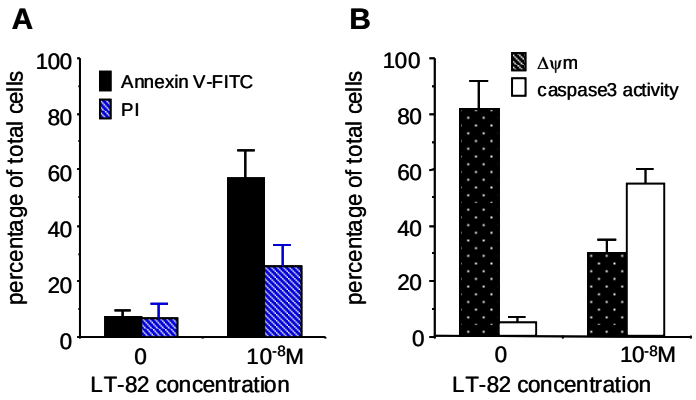

Fig. 1. LT-82 intoxication leads to apoptosis. (**A**) The importance of apoptosis was estimated by the percentage of cells exposing phosphatidylserine at their surface in the absence of plasma membrane permeability. HL-60 cells treated or not with a 16 h LT-82 exposure (10^{-8} M) were labeled with Annexin-V-FITC (filled bars) and PI (stripped bars) (Petit *et al.*, 2003). LT-82-treated cells labeled with Annexin-V represent the total dead cells (apoptotic and necrotic cells) amongst which cells labeled with PI were in secondary necrosis. Data, expressed in % ± SD of positive cells, are from duplicate measurements made in 3 independent experiments. (**B**) Apoptosis occurs by disruption of mitochondrial homeostasis. After a 16 h treatment of HL-60 cells with LT-82 (10^{-8} M), the percentage of cells with high mitochondrial membrane potential using DiOC6(3) ($\Delta\Psi$m high, spotted bars) and caspase 3-like activity using Phiphilux (empty bars) was measured by flow cytometry analysis (Petit *et al.*, 2003).

***Fig. 1**. **L'intoxication cellulaire par LT-82 conduit à une mort par apoptose.** (**A**) L'apoptose dans les cellules a été mesurée par le pourcentage des cellules ayant de la phosphatidylsérine exposée à la surface de leur membrane plasmique qui reste imperméable. Les cellules HL-60 sont intoxiquées ou non pendant 16 heures avec LT-82 (10^{-8} M) puis marquées avec de l'Annexine-V-FITC (colonnes pleines) et de l'iodure de propidium (PI, colonnes rayées) (Petit* et al.*, 2003). Les cellules traitées par LT-82 marquées par l'Annexine-V représentent le total des cellules mortes parmi lesquelles celles marquées avec PI ont subit une nécrose secondaire. Les données sont exprimées en % ± SD de cellules positivement marquées, et proviennent de 3 expériences différentes faites en duplicate. (**B**) L'apoptose débute au niveau mitochondrial. Après une intoxication de 16 heures avec LT-82 (10^{-8} M), le pourcentage des cellules ayant un haut potentiel de membrane mitochondriale ($\Delta\Psi$m haut) a été estimé par cytométrie de flux en utilisant du DiOC6(3) (colonnes en pointillés) et l'activité de la caspase 3 a été mesurée avec du Phiphilux (colonnes vides ; Petit* et al.*, 2003).*

Cell-death induced by LT-82 is also referred as the cytotoxic effect of this toxin. The early events leading to cell apoptosis upon LT-82 intoxication have been investigated. Indeed, Voth and Ballard have shown that this toxin was responsible for a rapid and strong decrease of phosphorylated Akt that required the enzymatic activity of the toxin. Downstream of Akt dephosphorylation, they observed a decrease of phosphoglycogen synthase kinase-3β (GSK-3β), the first characterized substrate of Akt (Voth and Ballard, 2007). These two

events occurred upstream of obvious signs of apoptosis such as caspase activation and were part of the cascade leading to apoptosis. Dreger *et al.* have also reported that LT induced a major decrease of phospho-Akt and showed that it led to an increase in RhoB exression, a protein with proapoptotic activity. In investigating which small GTPase family inactivated by large clostridial toxin (Ras or Rac) could be responsible for the cytotoxic effect of this toxin, they showed that only LT that inactivated Ras proteins, such as LT-82 or LT 6018, would induce apoptosis (Dreger *et al.*, 2009). This is in agreement with the role of Ras in the regulation of cell survival *via* the PI3K/Akt pathway (Cox and Der, 2002).

LT-82 inhibits phospholipase D activity and decreases the level of its cofactor, PI4,5P2

Phospholipase D is known to be regulated by many small GTPases under their GTP-bound form. Amongst the small GTPases that activate PLD, some are inactivated by LT-82: Rac implicated in the regulation of actin polymerization (Exton, 1997) and the oncogene p21Ras *via* RalA (Jiang *et al.*, 1995a ; Jiang *et al.*, 1995b). Thus, the effect of LT intoxication on PLD activity in HL-60 cells was investigated as detailed by Ben El Hadj *et al.* (Ben El Hadj *et al.*, 1999). These cells can be easily permeabilized by streptolysin O and thus are a good model to study PLD activity stimulated as well by small GTPases as by PKC. Although human cells possess two PLD isoforms, only PLD1 has been shown to be activated *via* small GTPases and PKCα1.

As shown in *Figure 2*, activity of PLD1 - stimulated either *via* small GTPases in their active form with guanosine 5'O-(3-thiotriphosphate) (GTPγS) in permeabilized cells or *via* PKCα1 in the presence of phorbol 12-myristate 13-acetate (PMA) in intact cells - was inhibited in a dose-dependent manner.

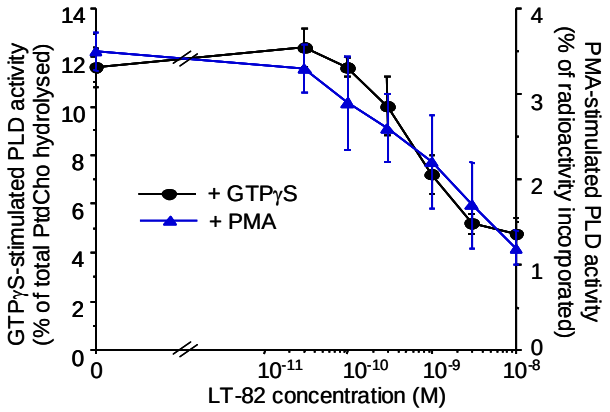

Fig. 2. Dose-dependent effect of LT-82 on GTPγS- or PMA-stimulated PLD activity. GTPγS-stimulated activity was measured in [^{3}H]choline-labeled cells intoxicated or not overnight with various concentrations of LT-82. PLD activity was determined in cells permeabilized with streptolysin O by measuring choline formation in the presence of 25 μM GTPγS as detailed elsewhere (Ben El Hadj *et al.*, 1999). PMA-stimulated PLD activity was measured in intact cells intoxicated overnight or not with various concentrations of LT-82. After intoxication, cells were labeled with [^{3}H]lyso-PAF for 30 min and after washing were re-suspended in a medium containing 1.5 % ethanol. After a pre-incubation of 10 min, PLD stimulation was started by adding PMA (10^{-7} M final). After 30 min, the reaction was stopped with chloroform/methanol, and samples were analyzed for phosphatidylethanol (Pet) content as detailed elsewhere (Ben El Hadj *et al.*, 1999). Data are expressed as the percentage of total incorporated radioactivity and represent means ± S.D.

Fig. 2. Effet dose-dépendant de LT-82 sur l'activité PLD stimulée soit par le GTPγS soit par le PMA. *L'activité stimulée par le GTPγS a été mesurée sur des cellules HL-60 intoxiquées ou non pendant une nuit par différentes doses de LT-82 et marquées avec de la choline tritiée. Après lavage, les cellules ont été perméabilisées avec de la streptolysine O puis stimulées avec 25 μM de GTPγS. La formation de choline libre représente l'activité PLD (Ben El Hadj* et al.*, 1999). L'activité PLD stimulée par le PMA a été mesurée dans des cellules intactes intoxiquées on non pendant la nuit avec différentes doses de LT-82. Après intoxication, les cellules ont été marquées pendant 30 min avec du lyso-PAF tritié puis lavées. Elles ont ensuite été re-suspendues dans un milieu contenant 1,5% d'éthanol. Après 10 min de pré-incubation la mesure a été initiée par l'addition de PMA (10^{-7} M final). Après 30 min, la réaction a été arrêtée avec un mélange chloroforme/méthanol et les échantillons ont été analysés pour leur contenu en phosphatidyléthanol (Pet) comme décrit précédemment (Ben El Hadj* et al.*, 1999). Les données sont exprimées en pourcentage de la radioactivité totale incorporée dans les cellules et représentent les moyennes ± S.D.*

PI4,5P2 (PIP2) which has been shown to be an essential cofactor for PLD activation (Liscovitch *et al.*, 1994) was markedly decreased upon an overnight LT-82 intoxication. Indeed, after overnight intoxication with 10^{-9} and 10^{-8} M LT-82, PIP2 level represented only 43±18 % and 27±7 %, respectively, of the PIP2 level observed in control cells. In contrast, its precursor PIP was decreased to a lesser extent. After intoxication with 10^{-9} and 10^{-8} M of LT-82, the amount of PIP corresponded to 82±27 % and 57±2 % of PIP measured in control cells. The effect of LT-82 on phosphoinositide metabolism and on different pathways modified by LT-82 will be discussed later.

Possible link between PLD activity and apoptosis

Although both apoptosis and inhibition of PLD activity occurred downstream of actin depolymerization, they did not appear to be its direct consequence. Indeed, actin depolymerization induced by an overnight treatment with 1μM cytochalasin D did not modify basal (0.51 ± 0.08 in control cells versus 0.50 ± 0.1 in cytochalasin D treated cells) and GTPγS-stimulated PLD activity (1.13 ± 0.8 in control cells versus 1.10 ± 0.4 in cytochalasin D treated cells). Moreover, another LT from *Clostridium sordellii,* strain 9048, and iota toxin

from *Clostridium perfringens,* both induced also actin depolymerization but not cell death by apoptosis (Ben El Hadj *et al.*, 1999).

Induction of apoptosis and decrease of PLD activity were both reported to be dependent of small GTPase inactivation by LT-82. Inactivation of RalA was proposed as the possible small GTPase responsible for the disturbance in these two pathways. As modifications in cell apoptosis and in PLD activity by LT-82 were both prevented by the overexpression of the anti-apoptotic mitochondrial protein, Bcl-2, it can be assumed that these effects are interrelated. As reported in *Figure 3*, time-course studies of these signalling pathways showed that LT-82 effect on PLD activity and apoptosis occurred simultaneously. Analysis of PLD1 has shown that an apoptotic motif, DEVD, is present near the N-terminal part of its sequence. A putative DEVD motif was also found in the middle of PLD1 sequence (*Figure 4A*). Therefore, proteolysis of this protein by a LT-82-activated caspase could be at the origin of PLD1 cleavage and thus induced its inactivation (*Figure 4B*).

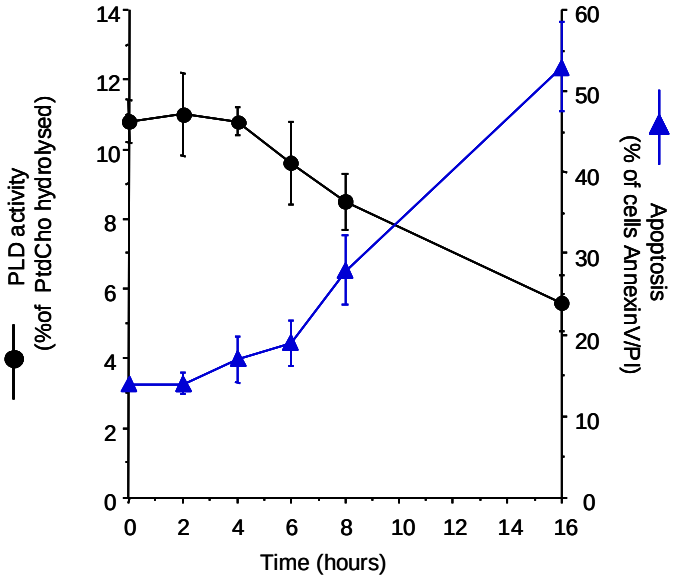

Fig. 3. Interrelationship between inhibition of PLD activity and apoptosis generated by LT-82. HL-60 cells were treated with LT-82 (10^{-8} M) and after various times, GTPγS-stimulated PLD activity was measured in SLO permeabilized cells as in *Figure 1* (circles). The percentage of apoptotic cells with PS exposure was determined as in *Figure 2A* (triangles).

Fig. 3. Interrelation entre l'inhibition de l'activité PLD et l'apoptose générée par LT-82*. Les cellules HL-60 ont été intoxiquées ou non avec LT-82 (10^{-8} M) pendant différents temps, l'activité PLD stimulée par le GTPγS a été mesurée dans les cellules perméabilisées par la streptolysine O comme dans la* Figure 1 *(cercles) et le pourcentage de cellules apoptotiques exposant la phosphatidylsérine sur la face externe de leur membrane plasmique a été déterminé comme dans la* Figure 2A *(triangles).*

Signaling pathways involved in cell morphology changes and actin depolymerization

LT-82 is well known to lead to cell rounding and actin depolymerization. This effect is sometimes reported as the cytopathic effect of this toxin. In two recent studies we have investigated the cascade of events leading to changes in cellular morphology. We have showed that in LT-treated cells, alterations of cell-cell interaction (adherens junctions) and cell substratum attachment (focal adhesions) occurred rapidly, concomitantly or upstream of actin depolymerization. These modifications can be assessed to LT-82 inactivation of Rac.

Sublocalization of adherens junction proteins and actin polymerization are modified simultaneously upon LT-82 intoxification

E-cadherin and catenins are the major proteins maintaining intercellular adherens junctions of epithelial and endothelial cells. As adherent cells loose their intercellular contacts and thus round up upon LT-82 intoxication, the toxin effect on polymerized actin and on E-cadherin and β-catenin was studied in epithelial cells (Boehm *et al.*, 2006). It was observed that apical cell membranes were not modified for at least 4 h upon intoxication with 10^{-8} M LT-82 (not shown). In contrast lateral and basal membranes were disorganized.

As shown in *Figure 5*, polymerized actin detected with fluorescent phalloidin was decreased (*Figure 5A*, left panel) and E-cadherin (and β-catenin, not shown) labeled with fluorescent specific antibodies exhibited a reduced, discontinuous and diffuse staining in lateral membranes (*Figure 5A*, right panel). Both alterations occurred with a similar time-course and were obvious in cells treated for 2 h with LT-82 at 10^{-8}M. Further investigations showed that whole E-cadherin-catenin complexes forming adherens junctions were redistributed from the plasma membrane into the cytosol (not shown). Studying how LT-82 kills animals (Geny *et al.*, 2007), we observed that the early major pathophysiology modification visualized by electron microscopy was a disappearance of well-organized adherens junctions of lung endothelial cells.

Immunofluorescent experiments showed that VE-cadherin was disorganized in lung vessel endothelium cells (*Figure 5B*).

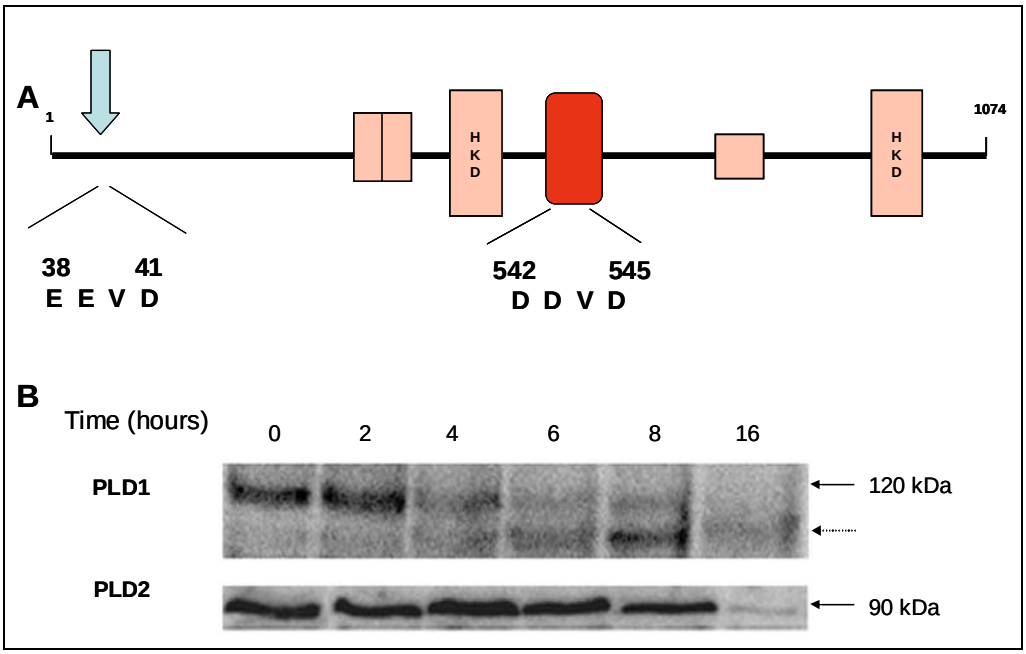

Fig. 4. Presence of a caspase 3 cleavage site in hPLD1 proteolysed during LT-induced apoptosis. Upon LT-82 intoxication, PLD1 cleavage is a consequence of caspase 3 activation. (**A**) Schematic representation of PLD1 isoform that contains a consensus motif for caspase 3 at its N-terminal part (arrow) and a putative motif in the middle part of the protein. (**B**) Western blot analysis of the two PLD isoforms upon LT-82 intoxication over time. PLD1 cleavage was observed after 4 h, and PLD2 was not modified for at least 8 h.

Fig. 4. Présence d'un site de clivage par la caspase 3 dans la PLD1 et lyse de la protéine lors de l'intoxication par LT-82. *(**A**) Représentation schématique de la PLD1 qui contient un motif consensus de clivage par la caspase 3 à son extrémité N-terminale (flèche) et un second site putatif dans la partie centrale de la protéine. (**B**) Analyse par western blot des 2 isoformes de PLD après différents temps d'intoxication par LT-82.*

Such modification of adherens junctions induced major vascular permeability at the origin of massive lung oedema, hemoconcentration and shock syndrome responsible for animal cell death (Geny *et al.*, 2007).

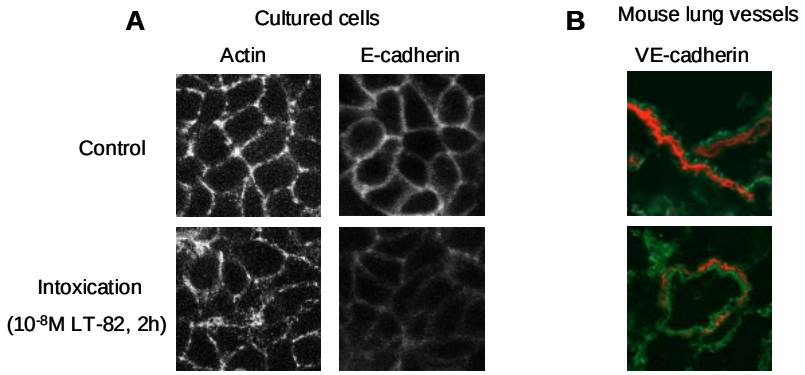

Fig. 5. LT-82 effect on actin and adherens junctions. LT modified actin polymerization and intracellular localization of E-cadherin, *in vitro* and *in vivo*. (**A**) Confluent MCCD cell monolayers grown on Transwell filters were incubated at 37°C with 10^{-8} M of LT82 for 2 h. After cell fixation with 4 % PFA, actin filaments were labeled with TRITC-phalloidin. (left panel) and E-cadherin, a protein from adherens junctions, was labeled using the relevant antibody (right panel). These structures were visualized by confocal microscopy. (**B**) After overnight intoxication of mice with LT-82, VE-cadherin decoration in lung vessels was analysis by immunohistology followed by confocal microscopy.

Fig. 5. Effet de LT-82* in vitro *et* in vivo *sur l'actine et les jonctions adhérentes. *LT modifie la polymérisation de l'actine et la localisation intracellulaire de l'E-cadherine, une protéine des jonctions adhérentes. (**A**) Des monocouches de cellules MCCD cultivées sur filtres Transwell ont été intoxiquées pendant 2 heures à 37°C avec 10^{-8} M de LT-82. Après fixation des cellules avec 4 % de PFA, les filaments d'actine ont été marqués avec de la phalloïdine-TRITC (photos de gauche) et l'E-cadherine a été marquée en utilisant des anticorps appropriés (photos de droite). Ces structures ont été visualisées par microscopie confocale (**B**) Après intoxication de souris pendant une nuit avec LT-82, la VE-cadherine des vaisseaux pulmonaires a été étudiée par immunohistologie et observée en microscopie confocale.*

Actin depolymerization and modifications of adherens junctions are likely to be interrelated. Indeed, disruption of actin filaments by iota toxin or cytochalasin D led to similar alteration of adherens junctions with cytosolic relocalization of E-cadherin-catenin complexes.

Small GTPase glucosylation resulting from LT-82 intoxication occurred rapidly, it was almost complete after a 30-60 min intoxication with a 10^{-8} M toxin concentration. Therefore we addressed the question of which early signalling pathways could lead to actin depolymerization observed after 2 h.

LT-82 disorganizes focal adhesions upstream of actin depolymerization

Adherent cells intoxicated with LT-82 round up and also become less adherent to the plastic dish. Therefore, we investigated alterations of focal adhesions and their possible causes induced by this toxin.

One of the earliest events observed so far in LT-treated HeLa cells was a decrease of phosphopaxillin starting after 30 min of intoxication in the absence of a change in the protein level (*Figure 6A*). Using specific antibodies to phosphopaxillin, a marked decrease of total cellular fluorescence was also observed in LT-82 intoxicated cells (*Figure 6B*). Paxillin is a multidomain adapter focal adhesion protein that functions as scaffold protein recruitment to focal adhesions and, thereby, facilitates protein networking and efficient signal transmission (Turner, 2000). Paxillin phosphorylation was recently reported to be regulated by Rac1 (Birukova *et al.*, 2008). Amongst the small GTPases inactivated by LT-82, Rac1 seems to be a good candidate as it is an essential protein in the regulation of the cytoskeleton and thus, of cell morphology. Indeed, in cells overexpressing constitutively active Rac1 (Rac^{V12}), no obvious decrease of phosphopaxillin upon LT-82 intoxication was observed (*Figure 6C*), indicating that paxillin dephosphorylation is a consequence of Rac1 inactivation.

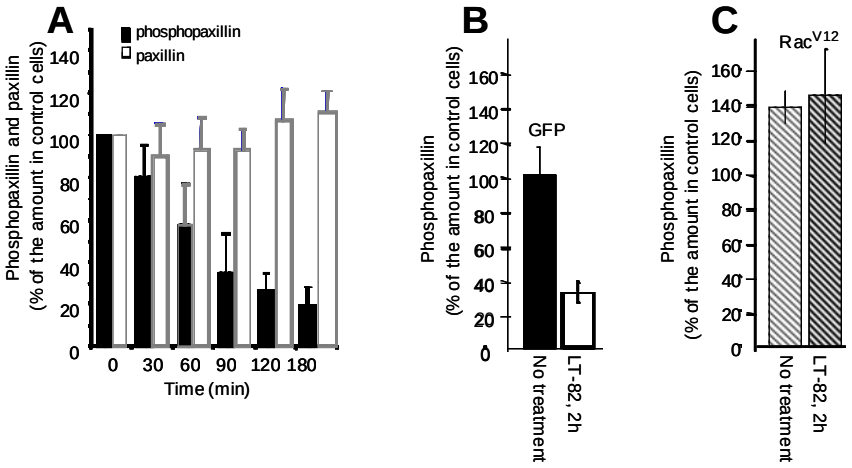

Fig. 6. LT-82 effect on phosphopaxillin, a protein regulating focal adhesion is a consequence of Rac1 inactivation. (**A**) HeLa cells were intoxicated with LT-82 for various times. After washing, cells were lysed with boiling Laemmli buffer and analyzed by western blot for their content in paxillin (empty bars) and phosphopaxillin (Y118 ; filled bars) with specific antibodies. (**B**, **C**) Cells were transfected either with the empty vector expressing eGFP (control cells) or with a vector expressing Rac^{V12} fused to c-myc. After 24 h expression, cells were intoxicated or not with LT-82 ($3x10^{-8}$ M). After washing, cells were lysed with Laemmli buffer. The level of phosphopaxillin was determined in cells expressing the empty vector (**B**) and in cells expressing $Rac1^{V12}$ (**C**). Results are the mean ± SD of 3 different experiments.

Fig. 6. L'effet de la LT-82 sur la phosphopaxilline, une protéine régulant les points focaux d'adhésion, est une conséquence de l'inactivation de Rac1. *(**A**) Les cellules Hela ont été intoxiquées pendant différents temps avec LT-82. Après lavage, les cellules ont été lysées avec du tampon Laemmli et analysées par western blot pour leur contenu en paxillin (colonnes vides) et en phosphopaxilline (Y118 ; colonnes pleines) en utilisant des anticorps spécifiques. (**B**, **C**) Les cellules ont été transfectées soit avec un vecteur vide exprimant l'eGFP soit avec un vecteur (cellules contrôles) soit avec un vecteur exprimant Rac^{V12} fusionné à c-myc. 24 heures après transfection, les cellules ont été intoxiquées ou non avec LT-82 ($3x10^{-8}$ M). Après lavage, les cellules ont été lysées avec du tampon Laemmli. Le contenu cellulaire en phosphopaxilline a été déterminé dans les cellules exprimant le vecteur vide (**B**) et dans les cellules exprimant $Rac1^{V12}$ (**C**) traitées ou non avec la toxine. Les résultats sont la moyenne ± SD de 3 différentes expériences.*

LT-82-induced changes in phosphoinositide metabolism are likely to play an important role in the toxin effects at various stages. Indeed, as indicated above, the decrease of PIP2, an essential cofactor for Phospholipase D, plays its part in the decrease of this enzyme activity. Moreover, PIP2 is an important regulator of the actin system dynamics and plays an important role in the interactions between the membrane and the cytoskeleton, which are critical for cell adhesion and morphology. Therefore, changes in membrane phosphoinositide content are likely related to Rac1 inactivation. Indeed, this small GTPase has been shown to interact with and activate a PI4P5-kinase, an enzyme responsible for PIP2 generation. Finally, the levels of phosphoinositides play also a role in lipid microdomain (raft) organization. Rafts are particularly important for scaffolding of focal adhesion protein complexes. A substantial decrease of PIP2 and PIP3 raft content is likely to modify the relationship between proteins forming adherens junction and/or focal adhesion complexes, and thus to destabilize these complexes. It is also noticeable that interaction between a protein

from focal adhesion, paxillin, and one from adherens junction, β-catenin, has been evidenced by co-immunoprecipitation experiments, linking these two structures (Birukova *et al.*, 2007).

LT-82 activates the three MAPK pathways prior to actin depolymerization and the SAPK/JNK pathway plays a role in enzymatic efficiency of this toxin specifically

In a recent work, we have reported that cell intoxication with LT-82 induced an activation of the three MAPKs with slightly similar time-course of activation (Geny and Popoff, 2009 ; see *Figure 7A*).

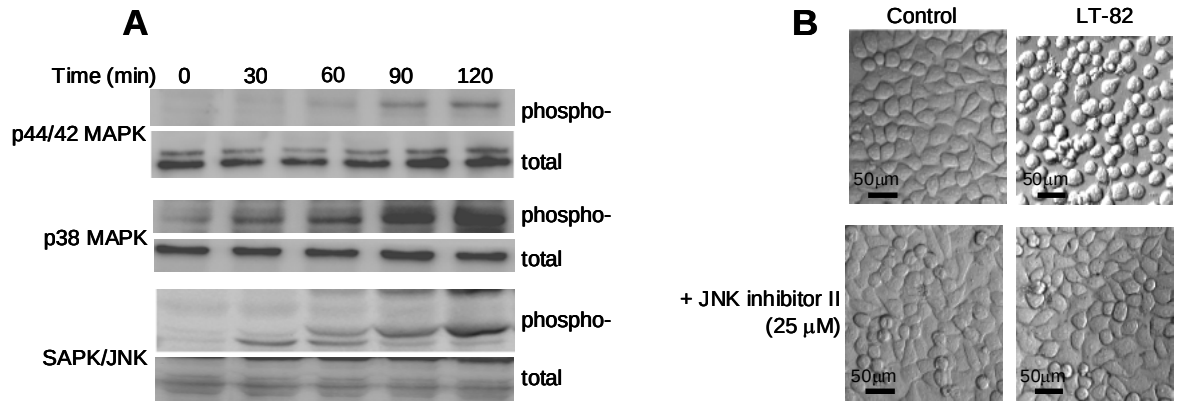

Fig. 7. A role for SAPK/JNK pathway in the glucosylation of small GTPases by LT-82. HeLa cells were intoxicated or not with LT-82 ($3x10^{-8}$ M) for various times. (**A**) After cell lysis with boiling Laemmli buffer, protein contents were analyzed by western blot using antibodies detecting total MAPK proteins and their active phosphorylated forms. (**B**) HeLa cells were either pretreated for 1 h with JNK inhibitor II (25 μM) or not. Then, as indicated, they were intoxicated for 2 h with LT-82 ($3x10^{-8}$ M) and photographed under phase microscopy.

Fig. 7. Un rôle pour la voie de la SAPK/JNK dans la glucosylation des petites protéines G, cibles de la LT-82*. Les cellules HeLa ont été intoxiquées ou non avec LT-82 ($3x10^{-8}$ M) pendant différents temps. (**A**) Après la lyse des cellules avec du tampon Laemmli bouillant, leur contenu a été analysé par western blot en utilisant des anticorps spécifiques des différentes MAPKs et de leurs formes actives phosphorylées. (**B**) Les cellules HeLa ont été pré-traitées ou non pendant 1 heure avec l'inhibiteur II de JNK (25 μM). Par la suite, les cellules ont été intoxiquées ou non pendant 2 heures avec LT-82 ($3x10^{-8}$ M) et photographiées au microscope en contraste de phase.*

However, only a permeable and specific JNK inhibitor, JNK inhibitor II, prevents toxin-dependent actin depolymerization and cell rounding (*Figure 7B*).

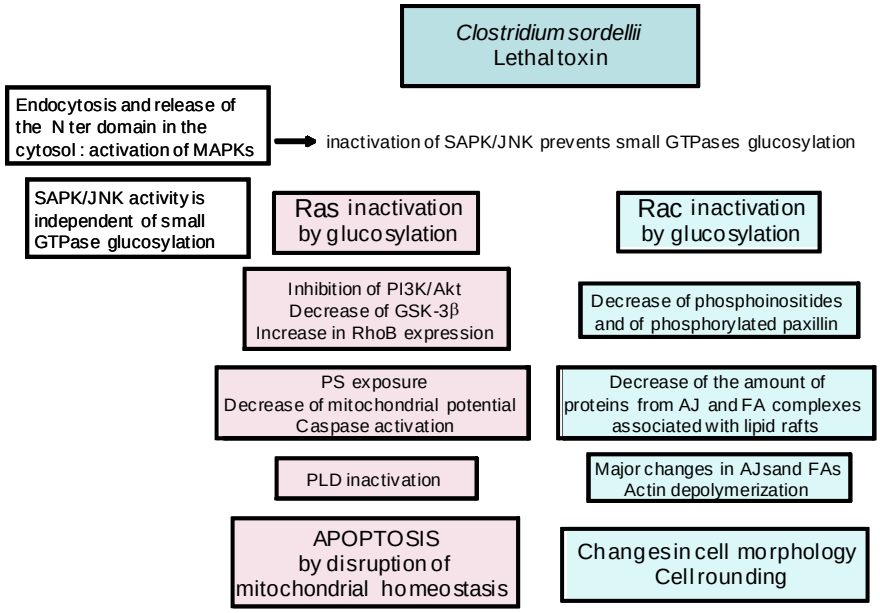

Fig. 8. Diagram of the signalling pathways modified by LT-82 : their cause and effects in cells.

Fig. 8. Diagramme des voies de signalisation modifiées par LT-82 *: leurs cause et effets dans les cellules.*

In this study, JNK activation was shown to be dependent on entry of the toxin N-terminal domain into the cytosol as bafilomycin A1, that prevents acidification of endocytic vesicles and subsequent cytosolic translocation of the toxin N-terminal domain, prevented JNK activation. Moreover, JNK inhibition was shown to delay small GTPase glucosylation generated by the N-terminal domain catalytic activity. Thus, activation of the SAPK/JNK pathway appears to facilitate the catalytic efficiency of LT-82 but not that of another large clostridial toxin such as ToxB from *C. difficile*. Interestingly, using a cell line mutant deficient in UDP-glucose, we observed that activation of JNK occurred even in the absence of small GTPase glucosylation and, thus, was independent of the toxin glucosyltransferase catalytic activity.

Conclusion

As summarized in *Figure 8*, most LT-82-induced cellular modifications involving the cytotoxic pathway leading to apoptosis and the cytopathic pathway leading to actin depolymerization and change in cell morphology were shown to require the enzyme activity and subsequent inactivation of small GTPases. Interestingly, through investigations from different laboratories, it appears that apoptosis and cell rounding are the consequence of the inactivation of the Ras GTPases and Rac GTPase respectively.

Moreover, LT-82 was also shown to activate the three MAPK pathways in relationship with the cytosolic release of the N-terminal part of the toxin from the endocytic vesicle. This effect appears to be independent from the toxin glucosyltransferase activity although activation of the SAPK/JNK pathway facilitates glucosylation of small GTPases by LT-82.

References

Al-Mashat RR, Taylor DJ (1983) Bacteria in enteric lesions of cattle. *Vet Rec* **112**: 5-10

Arseculeratne SN, Panabokké RG, Wijesundera S (1969) The toxins responsible for the lesions of *Clostridium sordellii* gas gangrene. *J Med Microbiol* **2**: 37-53

Ben El Hadj N, Popoff MR, Marvaud J-C, Payrastre B, Boquet P, Geny B (1999) GTPγS-stimulated PLD activity is inhibited by overnight treatment with lethal toxin from *Clostridium sordellii* in HL-60 cells. *J Biol Chem* **274**: 14021-14031

Bette P, Oksche A, Mauler F, von Eichel-Streiber C, Popoff MR, Habermann E (1991) A comparative biochemical, pharmacological and immunological study of *Clostridium novyi* alpha-toxin, *C. difficile* toxin B and *C. sordellii* lethal toxin. *Toxicon* **29**: 877-887

Birukova AA, Lekseeva E, Cokic I, Turner CE, Birukov KG (2008) Cross talk between paxillin and Rac is critical for mediation of barrier-protective effects by oxidized phospholipids. *Am J Physiol Lung Cell Mol Physiol* **295**: L593-L602

Birukova AA, Malyukova I, Poroyko V, Bikurov KG (2007) Paxillin-β-catenin interactions are involved in Rac.Cdc42-mediated endothelial barrier-protective to oxidized phospholipids. *Am J Physiol Lung Cell Mol Physiol* **193**: L199-L211

Bitty A, Manstrantonio P, Spigaglia P, Urru G, Spano AI, Moretti G, Cherchi GB (1997) A fatal postpartum *Clostridium sordellii* associated toxic shock syndrome. *J Clin Pathol* **50**: 259-260

Boehm C, Gibert M, Geny B, Popoff M, Rodriguez P (2006) Modification of epithelial cell barrier permeability and intercellular junctions by *Clostridium sordellii* lethal toxin. *Cell Microbiol* **8**: 1070-1085

Cohen AL, Bhatnagar J, Reagan S, Zane SB, D'Angeli MA, Fischer M, Killgore G, Kwan-Gett TS, Blossom DB, Shieh WJ, Guarner J, Jernigan J, Duchin JS, Zaki SR, McDonald LC (2007) Toxic shock associated with *Clostridium sordellii* and *Clostridium perfringens* after medical and spontaneous abortion. *Obstet Gynecol* **110**: 1027-1033

Cox AD, Der CJ (2002) Ras family signaling : therapeutic targeting. *Cancer Biol Ther* **1**: 599-606

Dreger SC, Schulz F, Huelsenbeck J, Gerhard R, Hofmann F, Just I, Genth H (2009) Killing rat basophilic leukemia cells by lethal toxin from *Clostridium sordellii* : critical role of phosphatidylinositide 3'-OH Kinase/Akt signaling. *Biochemistry* **48**: 1785-1792

Egerer M, Giesemann T, Jank T, Fullner Satchell KJ, Aktories K (2007) Auto-catalytic cleavage of *Clostridium difficile* toxins A and B depends on cystein protease activity. *J Biol Chem* **282**: 25314-25321

Exton JH (1997) Phospholipase D: Enzymology, mechanisms of regulation and function. *Physiol Reviews* **77**: 303-320

Fischer M, Bhatnagar J, Guarner J, Reagan S, Hacker JK, Van Meter SH, Poukens V, Whiteman DB, Iton A, Cheung M, Dassey DE, Shieh WJ, Zaki SR (2005) Fatal toxic shock syndrome associated with *Clostridium sordellii* after medical abortion. *New Engl J Med* **353**: 2352-2360

Geny B, Khun H, Fitting C, Zarantonelli L, Mazuet C, Cayet N, Szatanik M, Prevost M-C, Cavaillon J-M, Huerre M, Popoff M (2007) *Clostridium sordellii* lethal toxin kills mice by inducing a major increase in lung vascular permeability. *Am J Pathol* **170**: 1003-1017

Geny B, Popoff MR (2009) Activation of a c-Jun-NH2-terminal kinase pathway by the lethal toxin from *Clostridium sordellii*, TcsL-82, occurs independently of the toxin intrinsic enzymatic activity and facilitates small GTPase glucosylation. *Cell Microbiol* **11**: 1107-11013

Jiang H, Lu Z, Luo J-Q, Wolfman A, Foster DA (1995a) Ras mediates the activation of phospholipase D by v-Src. *J Biol Chem* **270**: 6006-6009

Jiang H, Luo J-Q, Urano T, Frankel P, Lu Z, Foster DA, Feig L (1995b) Involvement of Ral GTPase in v-Src-induced phospholipase D activation. *Nature* **378**: 409-412

Just I, Hofmann F, Aktories K (2000) Molecular mechanism of action of the large clostridial cytotoxins. In *Bacterial Protein Toxins*, Aktories K and Just I (eds) pp 307-331. Springer, Berlin

Liscovitch M, Chalifa V, Pertile P, Chen C-S, Cantley LC (1994) Novel function of phosphatidylinositol 4,5-bisphosphate as a cofactor for brain membrane phospholipase D. *J Biol Chem* **269**: 21403-21406

Martinez RD, Wilkins TD (1992) Comparison of *Clostridium sordellii* toxins HT and LT with toxins A and B of *C. difficile*. *J Med Microbiol* **36**: 30-32

Petit PX, Bréard J, Montalescot V, Ben El Hadj N, Levade T, Popoff M, Geny B (2003) Lethal toxin from *Clostridium sordellii* induces apoptotic cell death by disruption of the mitochondrial homeostasis in HL-60 cells. *Cell Microbiol* **5**: 761-771

Pfeifer G, Schirmer J, Leemhuis J, Busch C, Meyer DK, Aktories K, Barth H (2003) Cellular uptake of *Clostridium difficile* toxin B: translocation of the N-terminal catalytic domain into the cytosol of eukaryotic cells. *J Biol Chem* **278**: 44535-44541

Popoff MR (1984) Bacteriological examination in enterotoxaemia of sheep and lamb. *Vet Rec* **114**: 324

Popoff MR (1987) Purification and characterization of *Clostridium sordellii* lethal toxin and cross-reactivity with *Clostridium difficile* cytotoxin. *Infect Immun* **55**: 35-43

Reineke J, Tenzer S, Rupnik M, Koschinski A, Hasselmayer O, Schrattenholz A, Schild H, von Eichel-Streiber C (2007) Autocatalytic cleavage of *Clostridium difficile* toxin B. *Nature* **446**: 415-419

Richards SM (1982) *Clostridium sordellii* in lambs. *Vet Rec* **111**: 22

Rorbye C, Petersen IS, Nilas L (2000) Postpartum *Clostridium sordellii* infection associated with fatal toxic shock syndrome. *Acta Obstet Gynecol Scand* **79**: 1134-1135

Rupnik M, Pabst S, Rupnik M, von Eichel-Streiber C, Urlaub H, Söling H-D (2005) Characterization of the cleavage site and function of resulting cleavage fragment after limited proteolysis of *Clostridium difficile* toxin B (TcdB) by host cells. *Microbiology* **151**: 199-208

Sinave C, Le Templier G, Blouin D, Léveiller F, Deland E (2002) Toxic shock syndrome due to *Clostridium sordellii*: a dramatic postpartum and postabortion disease. *Clin Infect Dis* **35**: 1441-1443

Symons M (2000) Adhesion signaling: PAK meets Rac on solid ground. *Curr Biol* **10**: R535-R537

Thelen M, Wymann MP, Langen H (1994) Wortmannin binds specifically to 1-phosphatidylinositol 3-kinase while inhibiting guanine nucleotide-binding protein-coupled receptor signaling in neutrophil leukocytes. *Proc Natl Acad Sci USA* **91**: 4960-4964

Turner CE (2000) Paxillin and focal adhesion signalling. *Nature Cell Biol* **2**: E231-E236

Van Aelst L, D'Souza-Schorey C (1997) Rho GTPases and signaling networks. *Genes Dev* **11**: 2295-2322

Voth DE, Ballard JD (2007) Critical intermediate steps in *Clostridium sordellii* lethal toxin-induced apoptosis. *Biochem Biophys Res Commun* **363**: 959-964

Toxines et Signalisation – Toxins and Signalling
Rencontres en Toxinologie – Meeting on Toxinology, 2009
Editions de la SFET – SFET Editions
Accès libre en ligne sur le site – Free access on line on the site : http://www.sfet.asso.fr

De l'interaction avec les membranes des leucotoxines staphylococciques, à leur impact sur l'immunité innée

Benoit-Joseph LAVENTIE[1], Daniel KELLER[1], Emmanuel JOVER[2], Gilles PREVOST[1*]

[1] *EA-4438 Physiopathologie et Médecine Translationelle, Institut de Bactériologie de la faculté de médecine, 3 rue Koeberlé, 67 000 Strasbourg, France ;* [2] *INCI – UPR-CNRS 3212, Neurotransmission et sécrétion neuroendocrine, 5 rue Blaise Pascal, 67084 Strasbourg Cedex, France*

** Auteur correspondant ; Tél : +33 (0)3 68 85 37 57 ; Fax : +33 (0)3 68 85 38 08 ;*
Courriel : gilles.prevost@medecine.u-strasbg.fr

Résumé

Les leucotoxines de Staphylococcus aureus *sont une famille de toxines formant des pores, dont l'action activatrice et lytique est principalement dirigée contre les leucocytes. Cette courte revue se propose de prendre du recul par rapport aux connaissances accumulées et aux problématiques actuelles posées par ces toxines. Nous aborderons les relations structure/fonction des leucotoxines, et leurs interactions avec leurs cellules cibles, posant la question de l'existence de récepteurs. Des mécanismes d'activation des leucocytes à travers des voies de signalisation seront discutés. Le rôle des leucotoxines sur la modulation et l'altération du système immunitaire inné de l'hôte est à considérer au regard du cours de l'infection.*

From the interacting molecular surfaces of staphylococcal leucotoxins with membranes, to their different impact on innate immunity

Staphylococcal leukotoxins are a family of pore forming toxins, which mainly exert their activating and lytic activity against leukocytes. This short review intends to take a step back from the accumulated knowledges and current issues raised by these toxins. We discuss the structure-function relationships of leukotoxins, and their interactions with their target cells, raising the question of the existence of receptors. The mechanisms of leukocyte activation through signaling pathways will be discussed. The role of leukotoxins on the modulation and alteration of the host innate immune system is also to be considered regarding the course of infection.

Keywords : Staphylococcus aureus, *innate immunity, leucotoxins, PVL, receptor.*

Introduction

Staphylococcus aureus reste l'une des bactéries pathogènes les plus impliquées en clinique. Elle exerce sa virulence à travers la production d'un arsenal de facteurs, dont les leucotoxines qui activent et attaquent le système immunitaire de l'hôte. Les leucotoxines sont une famille de toxines formant des pores, composées en pathologie humaine de l'alpha-toxine et d'une série de toxines bipartites (association d'une protéine dite de classe S et d'une protéine de classe F) : les gamma-hémolysines (couples HlgA / HlgB et HlgC / HlgB), la leucocidine de Panton et Valentine ou « LPV » (LukS-PV / LukF-PV), et le couple LukE / LukD (*Tableau 1*).

Tableau 1. Liste des leucotoxines de *S. aureus* impliquées en pathologies humaines (M.M. = masse moléculaire).
Table 1. *List of staphylococcal leucotoxins involved in human diseases (M.M. = Molecular weight).*

Leucotoxine	Protéine	Classe	M.M. (Da)	EMBL	PDB
Toxine alpha (= alpha-hémolysine)	-	-	32.200	BA000033.2	7AHL
Gamma-hémolysine	HlgA	S	31.921	L01055	-
	HlgB	F	34.049	L01055	1LKF
	HlgC	S	32.565	L01055	-
Leucocidine de Panton et Valentine	LukS-PV	S	32.314	BAD89438	1T5R
	LukF-PV	F	34.445	BAD89439	1PVL
LukE / LukD	LukE	S	32.302	CP000255.1	-
	LukD	F	34.204	CP000730.1	-

L'alpha-toxine est produite par presque toutes les souches de *S. aureus*, et forme des homo-heptamères dans une série de cibles cellulaires comprenant des fibroblastes, des plaquettes, des érythrocytes et des lymphocytes T (Menestrina *et al.*, 2001). Elle est hémolytique (Prévost, 2005) et suggérée comme un facteur important de sévérité des sepsis (Grimminger *et al.*, 1997). Les gamma-hémolysines sont produites par 99% des souches de *S. aureus* (Prévost *et al.*, 1995) et sont décrites comme un facteur aggravant de la sévérité de l'infection. LukE-LukD est sécrétée par environ un tiers des souches, et est associée à des infections dermonécrotiques. Enfin, la leucocidine de Panton et Valentine est produite selon les pays par 1,6 - 12% des souches isolée en routine (Prévost *et al.*, 1995 ; Holmes *et al.*, 2005; Tristan *et al.*, 2007 ; Jahamy *et al.*, 2008). Elle est associée à des infections primaires nécrosantes de la peau, telles que les furoncles, l'anthrax, les panaris (Pia, 2006 ; Badiou *et al.*, 2008), et joue un rôle important dans les pneumopathies nécrosantes (Gillet *et al.*, 2002 ; Labandeira-Rey *et al.*, 2007 ; Diep *et al.*, 2008). Ces dernières surviennent principalement chez des patients jeunes et immunocompétents, et peuvent être aussi bien communautaires (Gonzalez *et al.*, 2005 ; Davis *et al.*, 2007) que contractées à l'hôpital (Webster *et al.*, 2007 ; Zilberberg, Shorr, 2009). La mortalité des pneumopathies nécrosantes peut approcher 75%, et le pronostic reste mauvais même en employant des traitement dédiés (Morgan, 2007).

Toutes les leucotoxines, comme leur nom le suggère, ciblent les leucocytes. Presque toutes les cellules immunitaires peuvent être ciblées : principalement les granulocytes (neutrophiles, basophiles, éosinophiles) et monocytes (macrophages, cellules dendritiques), mais aussi, pour certaines leucotoxines, les lymphocytes T (*Figure 1*). Bien qu'ayant des spectres d'action et des affinités variables, le même mode d'action est mis en œuvre : fixer les membranes des cellules cibles, s'oligomériser et former un pore dans les membranes des cellules cibles. Au site de l'infection, les leucotoxines provoquent une lyse des cellules de l'immunité et libèrent des chémokines, dont des facteurs pro inflammatoires.

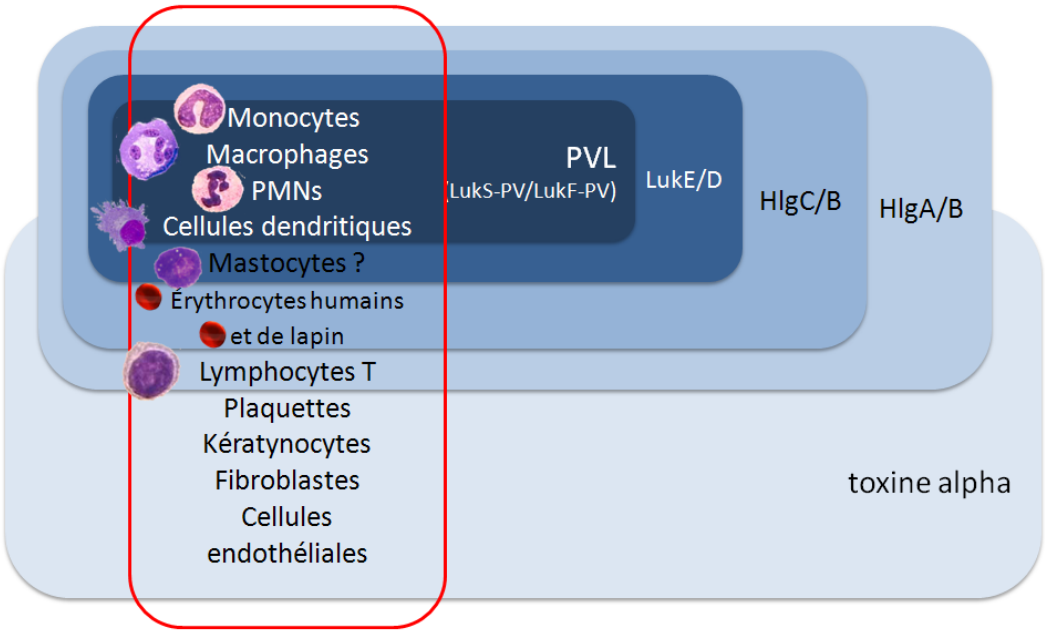

Fig. 1. Spectre d'action cellulaire des leucotoxines de *S. aureus*.

Fig. 1. *Cell spectrum of staphylococcal leucotoxins.*

Interaction avec les cellules cibles

Pour pouvoir exercer leur pouvoir toxique, et ce sur la bonne cible, la première étape cruciale de l'action des leucotoxines est la reconnaissance et la fixation aux membranes des cellules cibles.

Relations structure / fonction des leucotoxines

Les structures tridimensionnelles de la toxine alpha (Song *et al.*, 1996) et des composés de leucotoxines LukS-PV (Guillet *et al.*, 2004) (*Figure 2*), LukF-PV (Pédelacq *et al.*, 1999), et HlgB (Olson *et al.*, 1999) ont été résolues par cristallographie aux rayons X. Les protéines de classe F partagent 70% d'identité de séquence en acides aminés, les protéines de classe S entre 59 et 75%, alors qu'entre classes, l'identité n'est que de 26 à 30%. Les leucotoxines, qui dérivent probablement d'un ancêtre commun, ont toutes adopté une même configuration structurale en 3 domaines pour répondre aux contraintes imposées par leur double existence soluble (sécrétion, transport, accès aux cibles) et membranaire (formation de pore). Le domaine central est un beta-sandwich constituant plus de la moitié de la séquence de la protéine. Le « Stem » est un domaine déployable qui formera le pore transmembranaire. L'état soluble est facilité par son repliement rendant cryptique ses régions hydrophobes. Enfin le domaine « Rim » constitue la région probablement responsable de l'interaction des leucotoxines avec les membranes. Cette région possède une conformation assez souple, une organisation et une séquence variée selon les leucotoxines, probablement à

l'origine des spécificités cellulaires différentes pour chaque leucotoxine. L'organisation spatiale de ces domaines entre les monomères et sur les membranes lors de la formation du pore, a particulièrement été éclaircie par la résolution de la structure de l'heptamère de l'alpha-toxine (*Figure 2*).

Notre équipe à récemment étudié le domaine de fixation de LukS-PV. Une stratégie d'Ala-scanning a été choisie, en produisant des mutants recombinants de LukS-PV dans *Escherichia coli*. L'activité biologique et la capacité de fixation aux membranes des mutants ont été évaluées en cytométrie en flux. Une compétition avec un LukS-PV fluorescent a permis d'évaluer des constantes de dissociation apparentes ($k_{d\ app}$) des mutants, permettant de délimiter une région de quelques acides aminés entre T244 et Y250, plus le résidu Y184, essentiels à la fixation de LukS-PV aux neutrophiles. Ces acides aminés définissent une surface moléculaire dans la partie distale du « Rim ». Il est intéressant de noter que cette région partage une forte identité avec HlgC, qui partage la même cible membranaire que LukS-PV, mais correspond à un « gap » sur la séquence de HlgA. HlgA a un spectre cellulaire plus éloigné et large que celui de LukS-PV et HlgC.

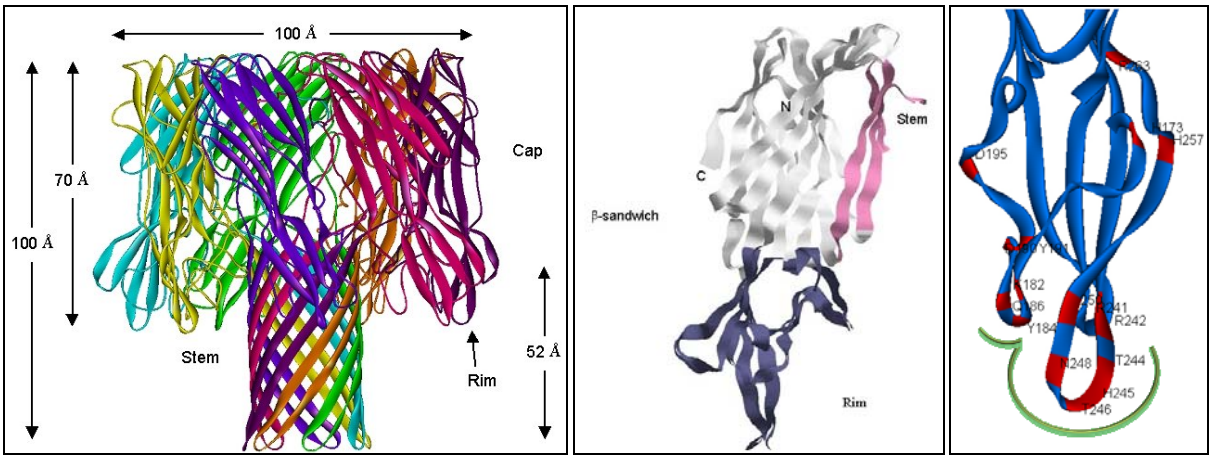

Fig. 2. Structure tridimensionnelle de l'heptamère de l'alpha-toxine (à gauche, PDB : 7AHL), de LukS-PV (au milieu, PDB : 1T5R), et un détail du « Rim » de LukS-PV (à droite) où est représenté en rouge des positions ciblées par mutagénèse dirigée et en vert la surface moléculaire d'interaction responsable de la fixation de cette protéine.

Fig. 2. *Tridimensional structure of alpha-toxin (left), LukS-PV (center), and LukS-PV "Rim" domain detail (right) with its interacting molecular surface.*

Cibles membranaires des leucotoxines

Un rôle proéminant de la protéine de classe S (LukS-PV, HlgA, HlgC, LukE) semble acquis, dans la mesure où cette protéine assure la spécificité de reconnaissance de la cible, et parfois même conditionne la fixation secondaire de la protéine de classe F (*e.g.* : HlgB ne fixe les membranes qu'après ajout préalable d'un composé de classe S). Un récepteur représente une solution d'arrimage pour une toxine. Dans le cas des leucotoxines, cette interaction est probablement transitoire, et plus ou moins nécessaire selon les leucotoxines. Pour l'alpha-toxine, quelques acides aminés pourraient directement être ancrés dans l'environnement lipidique (Vecsey-Semjen *et al.*, 1996 ; Valeva *et al.*, 1997). Le couple HlgA / HlgB, plutôt sensible à une composition lipidique, peut se fixer sur une bicouche lipidique artificielle et y former des pores (Ferreras *et al.*, 1998). Il en est autrement dans le cas de la LPV et du couple HlgC / HlgB. LukS-PV, le composé de classe S de la LPV, est décrit comme ayant le k_d le plus faible des leucotoxines (k_d = 0,07 nM), représentant une très forte affinité pour les membranes de ses cellules cibles, une fixation saturable (Gauduchon *et al.*, 2001), et le spectre cellulaire le plus étroit (neutrophiles, monocytes, macrophages). Ceci suggère l'existence d'un récepteur, qui reste à identifier. HlgC est décrit comme entrant en compétition avec LukS-PV à la surface des membranes, et partagerait le même site de fixation que LukS-PV (Gauduchon *et al.*, 2001), qui se situerait dans les radeaux lipidiques riches en glycosphingolipides et cholestérol (Nishiyama *et al.*, 2006), par ailleurs bien connus comme siège des interactions de protéines synthétisées par des pathogènes (Montecucco, 1986 ; Brown, 1998). Des travaux suggèrent un rôle de la protéine MD-2 dans l'activité de HlgC, mais sans démontrer son rôle direct sur l'étape de fixation (Nishiyama *et al.*, 2006). Globalement, les capacités de fixation et spectres cellulaires des leucotoxines sont relativement bien connues ; en revanche l'existence de récepteurs ou de ligands reste très peu documentée.

Activités des leucotoxines et conséquences sur les cellules cibles

La fixation des composés de classe S et F sur les membranes, qui peut être simultanée (Meyer *et al.*, 2009) ou séquentielle (Finck-Barbançon *et al.*, 1993), est suivie d'une étape d'oligomerisation des monomères. L'alpha-toxine forme un heptamètre comme le montre la *Figure 1*. Les leucotoxines bipartites forment des hétéro-oligomères de stœchiométrie toujours débattue S_3F_3 ou S_4F_4, avec une alternance des 2 composés (Sugawara *et al.*, 1999 ; Miles *et al.*, 2002 ; Joubert *et al.*, 2006 ; Viero *et al.*, 2006). Une fois l'oligomère formé, les domaines « Stem » se reconfigurent pour former le pore transmembranaire. L'ouverture du pore, spécifiquement perméable aux cations monovalents, entraine la fuite de potassium et l'entrée de sodium et d'eau, déséquilibrant l'homéostasie ionique et osmotique de la cellule. L'ajout d'éthidium dans le milieu permet par conséquent de suivre la formation des pores en cytométrie en flux. Une dose suffisante de toxine

(ordre de la nM) va conduire à la lyse de la cellule. Ce mécanisme a longtemps été considéré comme le mécanisme d'action principal des leucotoxines.

Mais il semble qu'un autre mécanisme a jusque là été sous estimé : en effet, indépendamment de la formation du pore, l'oligomère ou « prépore » provoque très rapidement une augmentation de la concentration en calcium intracellulaire, dépendante de la présence de calcium extracellulaire (Staali *et al.*, 1998). Le pic d'entrée de calcium et les études des changements morphologiques des cellules montrent leur activation, même à des concentrations sublytiques de toxines. Ceci a pour effet la sécrétion des granules chez les neutrophiles, la libération d'IL8 (König *et al.*, 1995), IL6 et IL12 (Prévost *et al.*, 2001), leucotriène B4 (Hensler *et al.*, 1994), NO (Colin et Monteil, 2003), et d'histamine (König *et al.*, 1995). Des concentrations sublytiques de leucotoxines auraient une activité sur les mitochondries et déclencheraient l'apoptose des cellules (Genestier *et al.*, 2005).

La bibliographie est quasi inexistante sur les mécanismes conduisant à l'entrée de calcium dans les cellules cibles. Il est décrit une modulation de l'entrée de calcium par la PKC, restaurée par son inhibiteur : la staurosporine. La nature du canal calcique reste inconnue malgré les nombreux essais de pharmacologie calcique, et suggèrent une voie d'activation complexe. Jover et collaborateurs ont récemment décrit l'activité de HlgC / HlgB sur des neurones, et ont proposé une voie de signalisation conduisant à cette entrée de calcium (Jover, en préparation). Notre équipe teste actuellement cette voie sur des neutrophiles, avec des résultats préliminaires encourageants. Le dynasore, un inhibiteur de l'endocytose dépendante de la dynamine, réduit fortement le flux calcique provoqué par HlgC / HlgB sur des neutrophiles. Il est intéressant de noter qu'il est sans effet sur les flux calciques entraînés par le couple HlgA / HlgB et la LPV. Le Thio-NADP, un inhibiteur du NAADP qui permet le fonctionnement des canaux calciques TPC dans les membranes des vésicules d'endocytose, réduit également fortement le flux calcique. Ces résultats, bien qu'à compléter, viennent appuyer l'utilisation de la voie décrite par Jover et ses collaborateurs.

L'existence de tels mécanismes montre bien que les leucotoxines sont bien plus que de simples toxines formant des pores entrainant une lyse cellulaire. Elles sont capables, indépendamment de leur activité de formation de pores, d'activer les cellules cibles par le jeu de voie de signalisation qui restent à décrire.

Impact sur l'immunité innée

En tant que pathogène, *S. aureus* a évolué de manière à exploiter l'abondance de nutriments fournis par l'hôte. En contrepartie, *S. aureus* doit pour survivre faire face au système immunitaire qui a co-évolué avec les bactéries. Les bactéries peuvent utiliser pour cela des mécanismes d'échappement (bactérie intracellulaire, zones cryptiques, …), de dévoiement du système immunitaire, … Dans ce contexte, les leucotoxines sont un moyen d'agir directement contre les cellules du système immunitaire (*Figure 3*).

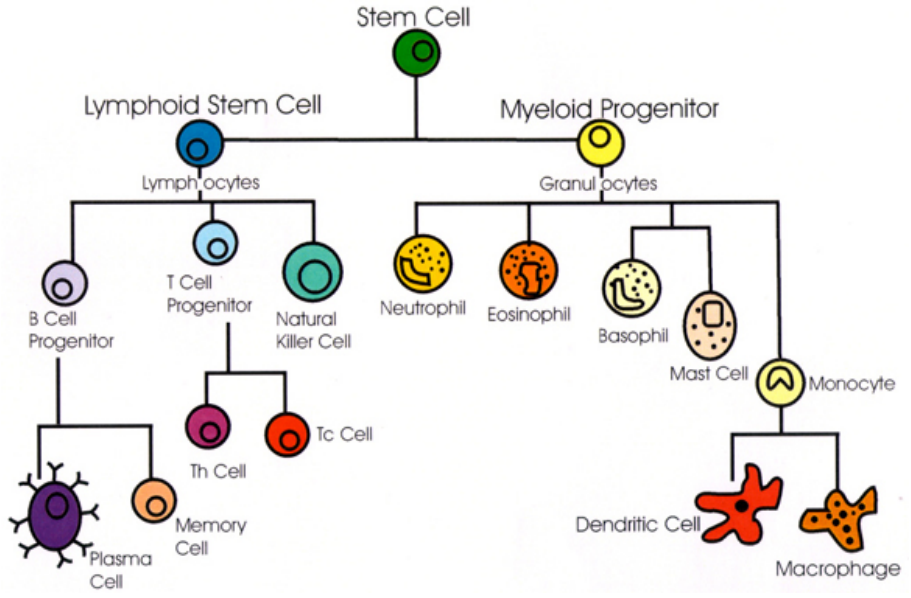

Fig. 3. Cellules du système immunitaire adaptatif (lignée lymphoide, à gauche) et inné (lignée myéloide, à droite) (Todar, 2008).

Fig. 3. *Cells of the immune system (Todar, 2008).*

La présence de la bactérie en elle-même va initier une réponse innée inflammatoire, *via* la reconnaissance de structures bactériennes spécifiques : les PAMPs (pour *Pathogen-Associated Molecular Patterns*). Cette reconnaissance se fait par l'intermédiaire de récepteurs au niveau des macrophages et des cellules dendritiques: les PRRs (pour *Pattern Recognition Receptors*) tels que les TLRs (pour *Toll-Like Receptors*) et les protéines de la famille des Nod-like receptors (NLRs). L'infection est marquée par une infiltration leucocytaire, principalement de neutrophiles (Wagner *et al.*, 2006). Bien que l'infiltration soit un processus très étudié (Melnicoff *et al.*, 1989 ; Savill, 1997 ; Kaplanski *et al.*, 2003), le devenir des

neutrophiles ayant migré est moins bien connu. Des études histomorphologiques, des infections induites expérimentalement, des expériences *in vitro* ont permis de déduire que la phagocytose des bactéries, ou même la stimulation de récepteurs impliqués dans la phagocytose, initie la mort cellulaire programmée des neutrophiles (Watson *et al.*, 1996 ; Kobayashi *et al.*, 2003 ; Zhang *et al.*, 2003). Subséquemment, les macrophages infiltrés « nettoient » le site en phagocytant les neutrophiles apoptotiques, et ce phénomène est un pré-requis pour la résolution de l'inflammation associée à l'infection.

Les leucotoxines peuvent faire pencher la balance en faveur de *S. aureus*. Au site de l'infection, ces toxines activent et détruisent les cellules immunitaires résidentes (macrophages, cellules dendritiques) et provoquent la libération de chémokines pro-inflammatoires telles que l'interleukine-8 et le leucotriène B4, qui sont de puissants chémoattractants des neutrophiles. Les leucotoxines accroissent l'inflammation et le recrutement de leucocytes circulants au site d'infection (neutrophiles principalement, quelques lymphocytes T, de rares lymphocytes B et monocytes) (Wagner *et al.*, 2006). La LPV en particulier est décrite comme étant sécrétée en quantité toxique dans des abcès de la peau (Badiou *et al.*, 2008) et associée à une augmentation dans un premier temps de la numération leucocytaire au site d'infections cutanées superficielles La LPV pourrait ainsi grandement contribuer à la sévérité de l'infection et moduler l'efficacité de la réponse immunitaire locale (Mertz *et al.*, 2007).

Tout au long du cours de l'infection, les leucotoxines lysent les cellules présentatrices d'antigènes (neutrophiles, macrophages, cellules dendritiques). Dans les cas les plus sévères, comme les pneumopathies nécrosantes, en quelques jours les patients souffrent de leucopénie. L'échec des neutrophiles à entrer dans un processus contrôlé d'apoptose crée une situation pathologique (Savill, 1993 ; Watson *et al.*, 1996 ; Kobayashi *et al.*, 2003 ; Zhang *et al.*, 2003). Le relargage non contrôlé de molécules cytotoxiques (*e.g.* : monoxide d'azote (Grimminger *et al.*, 1997) et protéolytiques (protéases des granules de sécrétion) par les granulocytes lysés peut détruire les tissus environnants. Le relargage de médiateurs pro-inflammatoires produits par les neutrophiles ayant échappé à l'apoptose pourrait soutenir une réaction inflammatoire et participer à sa progression vers la chronicité, aussi bien qu'au développement d'un sepsis, une défaillance multiviscérale (SDMV) et une destruction des tissus environnants (Savill, 1993 ; Haslett, 1999 ; Harter *et al.*, 2003).

Mais l'impact sur le système immunitaire pourrait être plus subtil. Récemment, notre équipe a étudié l'impact d'autres facteurs de virulence de *S. aureus* (Zhang *et al.*, 2009) sur la maturation de précurseurs de peptides antimicrobiens, tels que les chromogranines. Un rôle des leucotoxines est à l'étude. Ce dévoiement entrainerait le système immunitaire inné vers une réponse antifongique inadaptée contre la bactérie *S. aureus*.

Conclusion

Les leucotoxines constituent une famille de facteurs de virulence de *S. aureus* connus depuis plus de 50 ans, et surtout étudiés depuis 30 ans avec l'essor de la biologie moléculaire et cellulaire. Ainsi, leur mode d'action et leurs cibles cellulaires ont pu être décrits en grande partie. Néanmoins, l'étude de récepteurs membranaires reste difficile et n'a donné que peu de résultats pour les leucotoxines. Aujourd'hui, de nouvelles cibles cellulaires et l'importance de leur effet activateur des leucocytes doivent être reconsidérés. La compréhension de leurs interactions et de leurs effets sur le système immunitaire, inné en particulier, bien au-delà de la simple formation de pore, est la clef de l'étiologie des pathologies staphylococciques et en même temps une opportunité de créer des moyens d'agir dans l'intérêt du patient. Il s'agit notamment d'élaborer des drogues dirigées directement contre les leucotoxines, ce qui s'inscrit naturellement dans la recherche de nouveaux médicaments alors même que l'industrie pharmaceutique est à la recherche de nouvelles classes d'antibiotiques et que les souches de *S. aureus* de plus en plus résistantes (SARM, GISA) se répandent.

Remerciements. *Le travail de B-J.L. et de l'EA-4438 a été soutenu par une bourse du ministère de l'enseignement supérieur de la recherche.*

Références bibliographiques

Badiou C, Dumitrescu O, Croze M*, et al.* (2008) Panton-Valentine leukocidin is expressed at toxic levels in human skin abscesses. *Clin Microbiol Infect* **14**: 1180-1183

Colin DA, Monteil H (2003) Control of the oxidative burst of human neutrophils by staphylococcal leukotoxins. *Infect Immun* **71**, 3724-3729

Davis SL, Perri MB, Donabedian SM*, et al.* (2007) Epidemiology and outcomes of community-associated methicillin-resistant *Staphylococcus aureus* infection. *J Clin Microbiol* **45**: 1705-1711

Diep BA, Palazzolo-Ballance AM, Tattevin P*, et al.* (2008) Contribution of Panton-Valentine leukocidin in community-associated methicillin-resistant *Staphylococcus aureus* pathogenesis. *PLoS ONE* **3**: e3198

Ferreras M, Hoper F, Dalla Serra M*, et al.* (1998) The interaction of *Staphylococcus aureus* bi-component gamma-hemolysins and leucocidins with cells and lipid membranes. *Biochim Biophys Acta* **1414**: 108-126

Finck-Barbançon V, Duportail G, Meunier O, Colin DA (1993) Pore Formation by a 2-Component Leukocidin from *Staphylococcus aureus* within the Membrane of Human Polymorphonuclear Leukocytes. *Biochim Biophys Acta* **1182**v 275-282

Gauduchon V, Werner S, Prévost G, Monteil H, Colin DA (2001) Flow cytometric determination of Panton-Valentine leucocidin S component binding. *Infect Immun* **69**: 2390-2395

Genestier AL, Michallet MC, Prévost G*, et al.* (2005) *Staphylococcus aureus* Panton-Valentine leukocidin directly targets mitochondria and induces Bax-independent apoptosis of human neutrophils. *J Clin Invest* **115**: 3117-3127

Gillet Y, Issartel B, Vanhems P*, et al.* (2002) Association between *Staphylococcus aureus* strains carrying gene for Panton-Valentine leukocidin and highly lethal necrotising pneumonia in young immunocompetent patients. *Lancet* **359**: 753-759

Gonzalez BE, Hulten KG, Dishop MK, *et al.* (2005) Pulmonary manifestations in children with invasive community-acquired *Staphylococcus aureus* infection. *Clin Infect Dis* **41**: 583-590

Grimminger F, Rose F, Sibelius U, *et al.* (1997) Human endothelial cell activation and mediator release in response to the bacterial exotoxins Escherichia coli hemolysin and staphylococcal alpha-toxin. *J Immunol* **159**: 1909-1916

Guillet V, Roblin P, Werner S, *et al.* (2004) Crystal structure of leucotoxin S component: new insight into the Staphylococcal beta-barrel pore-forming toxins. *J Biol Chem* **279**: 41028-41037

Harter L, Mica L, Stocker R, Trentz O, Keel M (2003) Mcl-1 correlates with reduced apoptosis in neutrophils from patients with sepsis. *J Am Coll Surg* **197**: 964-973

Haslett C (1999) Granulocyte apoptosis and its role in the resolution and control of lung inflammation. *Am J Respir Crit Care Med* **160**: S5-11

Hensler T, König B, Prévost G, *et al.* (1994) Leukotriene B4 generation and DNA fragmentation induced by leukocidin from *Staphylococcus aureus*: protective role of granulocyte-macrophage colony-stimulating factor (GM-CSF) and G-CSF for human neutrophils. *Infect Immun* **62**: 2529-2535

Holmes A, Ganner M, McGuane S, *et al.* (2005) *Staphylococcus aureus* isolates carrying Panton-Valentine leucocidin genes in England and Wales: frequency, characterization, and association with clinical disease. *J Clin Microbiol* **43**: 2384-2390

Jahamy H, Ganga R, Al Raiy B, *et al.* (2008) *Staphylococcus aureus* skin/soft-tissue infections: the impact of SCCmec type and Panton-Valentine leukocidin. *Scand J Infect Dis* **40**: 601-606

Joubert O, Viero G, Keller D, *et al.* (2006) Engineered covalent leucotoxin heterodimers form functional pores: insights into S-F interactions. *Biochem J* **396**: 381-389

Kaplanski G, Marin V, Montero-Julian F, Mantovani A, Farnarier C (2003) IL-6: a regulator of the transition from neutrophil to monocyte recruitment during inflammation. *Trends Immunol* **24**: 25-29

Kobayashi SD, Voyich JM, Somerville GA, *et al.* (2003) An apoptosis-differentiation program in human polymorphonuclear leukocytes facilitates resolution of inflammation. *J Leukoc Biol* **73**: 315-322

König B, Prévost G, Piémont Y, König W (1995) Effects of *Staphylococcus aureus* leukocidins on inflammatory mediator release from human granulocytes. *J Infect Dis* **171**: 607-613

Labandeira-Rey M, Couzon F, Boisset S, *et al.* (2007) *Staphylococcus aureus* Panton-Valentine leukocidin causes necrotizing pneumonia. *Science* **315**: 1130-1133

Melnicoff MJ, Horan PK, Morahan PS (1989) Kinetics of changes in peritoneal cell populations following acute inflammation. *Cell Immunol* **118**: 178-191

Menestrina G, Dalla Serra M, Prévost G (2001) Mode of action of beta-barrel pore-forming toxins of the staphylococcal alpha-hemolysin family. *Toxicon* **39**: 1661-1672

Mertz PM, Cardenas TC, Snyder RV, *et al.* (2007) Staphylococcus aureus virulence factors associated with infected skin lesions: influence on the local immune response. *Arch Dermatol* **143**: 1259-1263

Meyer F, Girardot R, Piémont Y, Prévost G, Colin DA (2009) Analysis of the specificity of Panton-Valentine leucocidin and gamma-hemolysin F component binding. *Infect Immun* **77**: 266-273

Miles G, Movileanu L, Bayley H (2002) Subunit composition of a bicomponent toxin: staphylococcal leukocidin forms an octameric transmembrane pore. *Protein Sci* **11**: 894-902

Morgan MS (2007) Diagnosis and treatment of Panton-Valentine leukocidin (PVL)-associated staphylococcal pneumonia. *Int J Antimicrob Agents* **30**: 289-296

Nishiyama A, Kaneko J, Harata M, Kamio Y (2006) Assembly of staphylococcal leukocidin into a pore-forming oligomer on detergent-resistant membrane microdomains, lipid rafts, in human polymorphonuclear leukocytes. *Biosci Biotechnol Biochem* **70**: 1300-1307

Olson R, Nariya H, Yokota K, Kamio Y, Gouaux E (1999) Crystal structure of staphylococcal LukF delineates conformational changes accompanying formation of a transmembrane channel. *Nat Struct Biol* **6**: 134-140

Pédelacq JD, Maveyraud L, Prévost G, *et al.* (1999) The structure of a *Staphylococcus aureus* leucocidin component (LukF-PV) reveals the fold of the water-soluble species of a family of transmembrane pore-forming toxins. *Structure* **7**: 277-287

Pia SP, Kristina G. Hulten, Blanca E. Gonzalez, Edward O. Mason, Jr., and Sheldon L. Kaplan. (2006) Infective Pyomyositis and Myositis in Children in the Era of Community-Acquired, Methicillin-Resistant *Staphylococcus aureus* Infection. *Clin Infect Dis* **43**: 953-960

Prévost G (2005) Toxins in *Staphylococcus aureus* pathogenesis. In *Microbial Toxins: Molecular and Cellular Biology*. T. Proft, ed. Horizon Bioscience Press, Norfolk (UK), 243-284

Prévost G, Couppie P, Prevost P, *et al.* (1995) Epidemiological data on *Staphylococcus aureus* strains producing synergohymenotropic toxins. *J Med Microbiol* **42**: 237-245

Prévost G, Mourey L, Colin DA, Menestrina G (2001) Staphylococcal pore-forming toxins. *Curr Top Microbiol Immunol* **257**: 53-83.

Savill J (1993) The fate of the neutrophil in vasculitis. *Clin Exp Immunol* **93 Suppl 1**: 2-5

Savill J (1997) Apoptosis in resolution of inflammation. *J Leukoc Biol* **61**: 375-380

Song L, Hobaugh MR, Shustak C, *et al.* (1996) Structure of staphylococcal alpha-hemolysin, a heptameric transmembrane pore. *Science* **274**: 1859-1866

Staali L, Monteil H, Colin DA (1998) The staphylococcal pore-forming leukotoxins open Ca2+ channels in the membrane of human polymorphonuclear neutrophils. *J Membr Biol* **162**: 209-216

Sugawara N, Tomita T, Sato T, Kamio Y (1999) Assembly of *Staphylococcus aureus* leukocidin into a pore-forming ring-shaped oligomer on human polymorphonuclear leukocytes and rabbit erythrocytes. *Biosci Biotechnol Biochem* **63**: 884-891

Todar K (2008) Immune Defense against Microbial Pathogens: Innate Immunity. *Online Textbook of Bacteriology* *www.textbookofbacteriology.net*.

Tristan A, Bes M, Meugnier H, *et al.* (2007) Global distribution of Panton-Valentine leukocidin--positive methicillin-resistant *Staphylococcus aureus*. *Emerg Infect Dis* **13**: 594-600

Valeva A, Palmer M, Bhakdi S (1997) Staphylococcal alpha-toxin: formation of the heptameric pore is partially cooperative and proceeds through multiple intermediate stages. *Biochemistry* **36**: 13298-13304

Vecsey-Semjen B, Mollby R, van der Goot FG (1996) Partial C-terminal unfolding is required for channel formation by staphylococcal alpha-toxin. *J Biol Chem* **271**: 8655-8660

Viero G, Cunaccia R, Prévost G*, et al.* (2006) Homologous versus heterologous interactions in the bicomponent staphylococcal gamma-haemolysin pore. *Biochem J* **394**: 217-225

Wagner C, Iking-Konert C, Hug F*, et al.* (2006) Cellular inflammatory response to persistent localized Staphylococcus aureus infection: phenotypical and functional characterization of polymorphonuclear neutrophils (PMN). *Clin Exp Immunol* **143**: 70-77

Watson RW, Redmond HP, Wang JH, Condron C, Bouchier-Hayes D (1996) Neutrophils undergo apoptosis following ingestion of Escherichia coli. *J Immunol* **156**: 3986-3992

Webster D, Chui L, Tyrrell GJ, Marrie TJ (2007) Health care-associated *Staphylococcus aureus* pneumonia. *Can J Infect Dis Med Microbiol* **18**: 181-188

Zhang B, Hirahashi J, Cullere X, Mayadas TN (2003) Elucidation of molecular events leading to neutrophil apoptosis following phagocytosis: cross-talk between caspase 8, reactive oxygen species, and MAPK/ERK activation. *J Biol Chem* **278**: 28443-28454

Zhang D, Shooshtarizadeh P, Laventie BJ*, et al.* (2009) Two chromogranin a-derived peptides induce calcium entry in human neutrophils by calmodulin-regulated calcium independent phospholipase A2. *PLoS ONE* **4**: e4501

Zilberberg MD, Shorr AF (2009) Epidemiology of healthcare-associated pneumonia (HCAP). *Semin Respir Crit Care Med* **30**: 10-15

Toxines et Signalisation – Toxins and Signalling
Rencontres en Toxinologie – Meeting on Toxinology, 2009
Editions de la SFET – SFET Editions
Accès libre en ligne sur le site – Free access on line on the site : http://www.sfet.asso.fr

Intracellular actions of botulinum and tetanus neurotoxins : SNARE cleavage but not only !

Emmanuel JOVER[1], Fréderic DOUSSAU[1], Etienne LONCHAMP[1], Laetitia WIOLAND[1], Jean-Luc DUPONT[1], Jordi MOLGÓ[2], Michel POPOFF[3], Bernard POULAIN[1*]

[1] *Université de Strasbourg et CNRS UPR-3212, Institut des Neurosciences Cellulaires et Intégratives, 5 rue Blaise Pascal, 67084 Strasbourg ;* [2] *CNRS, Institut de Neurobiologie Alfred Fessard - FRC2118, Laboratoire de Neurobiologie Cellulaire et Moléculaire - UPR9040, 91198 Gif-sur-Yvette ;* [3] *Unité des Bactéries anaérobies et Toxines, Institut Pasteur, 75724 Paris, France*

** Corresponding author ; Tel : +33 (0)3.88.45.66.77 ; Fax : +33 (0)3.88.60.16.64 ;*
E-mail : poulain@inci-cnrs.unistra.fr

Abstract

The SNARE protein complex that helps vesicles to fuse and deliver neurotransmitters into the synaptic cleft are now clearly identified as specific targets for the clostridial toxins TeNT and BoNTs. The proteolytic activity of these toxins is so precise that, from the eminent position of the most potent poisonous toxins, their status is moving to that of powerful tools for basic cell biology research and for medical therapeutic purposes. However, as basic work continues to grow, other actions due to their intracellular transfer are coming to light. This review intends to focus the attention on settled and recent data concerning behindhand actions of TeNT and BoNTs. The first part presents a reminder of the covered way from distant diseases to the identification of closely related structures and activity. Then, we review recent data on the effect of clostridial toxins on the transport to the membrane of neurotransmitter receptors. Moreover, examples showing that ionic conductances can be disrupted by the interactions between cleaved SNARE proteins and channels are reviewed. Finally, observations that suggest a disturbance of the actin network due to TeNT or BoNTs are also mentioned. Overall, some of these effects could shed light on the cellular mechanism of unexplained clinical advantages observed with the increasing use of BoNTs.

Effets intracellulaires des toxines botuliques et tétanique : le clivage des SNARES, mais pas uniquement !

Les protéines SNARE, qui facilitent la fusion des vésicules et la libération des neuromédiateurs dans la fente synaptique, sont bien identifiées comme la cible spécifique des toxines clostridiales TeNT et BoNTs. L'activité protéolytique de ces toxines est tellement particulière qu'elles sont passées du statut des toxines les plus puissantes à celui d'outils éminents pour la recherche fondamentale en biologie cellulaire et à celui de médicament. Néanmoins, de nouvelles données sur des effets intracellulaires de ces toxines continuent d'émerger. Cette revue tente d'attirer l'attention sur des données établies et récentes à propos des effets de BoNTs et TeNT restés au second plan. Une première partie rappelle le chemin parcouru depuis la description déjà ancienne des pathologies provoquées par les toxines et l'identification de leurs analogies de structure et d'activité. Il est ensuite fait état des données récentes sur l'effet des toxines sur le transport à la membrane de récepteurs de neuromédiateurs. Des exemples sont aussi apportés qui illustrent le fait que des conductances ioniques peuvent être perturbées du fait des interactions entre des SNAREs clivées et des canaux ioniques. Enfin, on rappelle des observations montrant que les TeNT et BoNTs peuvent aussi perturber le réseau des neurofilaments d'actine. En définitive, certains de ces effets peuvent clarifier les mécanismes moléculaires à la base de plusieurs observations cliniques positives obtenues grâce à l'utilisation médicale croissante des BoNTs.

Keywords : *Botulinum neurotoxins, Tetanus toxin, unconventional intracellular activity.*

Introduction

Most bacterial proteins with demonstrable "toxic" activity interact with various cell types. More than one third of all bacterial toxins are pore-formers which recognize ubiquitous membrane components as receptors, such as cholesterol, gangliosides, and proteins. Others have developed various internalization processes, therefore specifically modifying an intracellular target. This comprises several bacterial protein toxins produced by members of the *Clostridium* genus. Among them, two unique classes of neurotoxins, the

botulinum (BoNTs) and tetanus toxin (TeNT), have evolved as specific inhibitors of the neuroexocytosis machinery, the former appearing specific for cholinergic transmission in the peripheral nervous system ; the latter proposed to be specific of GABA- and glycinergic transmission in the central nervous system. The specificity of these toxic proteins has enabled them to become useful tools in therapeutics and basic sciences. Indeed they were helpful to elucidate and characterize crucial processes for eukaryotic cells, which include neurotransmitter release, physiological signaling pathways, and constitutive cellular mechanisms. However, it is very intriguing that toxins produced by environmental bacteria as the *Clostridia* possess such specific and highly sophisticated tools directed against certain types of chemical synaptic transmission. Since the "screening" leading to assignation of these bacterial protein toxins as neurotoxins was based on the initial observations of potent neurological disorders, a bias has been introduced in the way we think their actions. We here investigate the limits of their selectivity and specificity and review evidences supporting the notion that these neurotoxins have a broader spectrum of action than usually believed, not only in terms of cellular targets but also, more importantly, in their intracellular mechanisms.

Distinct diseases led to identification of toxins, initially thought very different

The botulinum toxins and tetanus toxin have been identified upon unraveling the etiology of two diseases, botulism and tetanus, which are characterized by severe neurological components. Botulism is characterized by dysautonomia and flaccid paralysis of peripheral origin, while tetanus comprises dysautonomia and spastic paralysis, both of central origin (for comprehensive reviews, see Bleck, 1989 ; Tacket and Rogawski, 1989 ; Niemann *et al.*, 1991 ; Popoff and Poulain 2005 ; Popoff *et al.*, 2009).

Botulism has been recognized at the beginning of the 19th century and described as a particular form of food-born poisoning due to ingestion of 'sausage poison'. The term *botulism* has been coined from the Latin word *botulus* = 'sausage' (for an historical perspective, see Schantz and Johnson, 1992 ; Erbguth and Naumann, 1999 ; Erbguth, 2008). The microorganism producing botulinum toxin has been identified at the end of the XIXth century as an anaerobic sporulating bacillus, initially named *bacillus botulinus* (van Ermengem, 1897), then renamed *Clostridium botulinum*. The strains of *Clostridia* producing botulinum toxin also synthesize other proteins -as botulinolysin-, however they have not been established participating in the etiology of botulism. Pure botulinum toxin type A was obtained in 1946 (Lamanna *et al.*, 1946), but fractionation studies allowed establishing it as a multi-protein complex comprising a neuroactive moiety - termed botulinum neurotoxin (BoNT), which is closely related to tetanus toxin (see below) - and several associated non-toxic proteins (ANTPs, with or without hemagglutinin activity ; DasGupta *et al.*, 1966). The associated non-toxic proteins play a role in the passage of the intestinal barrier, and may display some cytotoxicity (Matsumura *et al.*, 2008 ; Jin *et al.*, 2009) ; however, they do not participate in the neurological aspects of botulism. Existence of several distinct botulinum toxin serotypes (A through G) and the corresponding BoNT toxinotypes have been revealed all along the XXth century. Extensive sequencing of the genes from *C. botulinum* and other *Clostridia* producing botulinum toxin revealed the existence of more than 40 sub-types of botulinum neurotoxin (Smith *et al.*, 2005b, 2007 ; Arndt *et al.*, 2006). A major progress in understanding the prominent symptoms of botulism has been the discovery that the botulinum toxins block acetylcholine (ACh) release at the neuromuscular junction (Burgen *et al.*, 1949), reviewed by Molgó *et al.* (1990). This effect is at the origin of the use of botulinum toxins as well as neurotoxins in human therapy.

Tetanus is derived from the Greek word τετανοσ that means rigidity or tension. Hippocratos (~ 470-360 BC, in Kos island) was first to describe a disease in which the main physical manifestation was a general spasm. It is only at the end of the XIXth century that Carle and Rattone (1884) proposed the neurological origin of the manifestations of the disease. Later, Kitasato (1889) isolated *Clostridium tetani* from necrotic wounds in Man (for historical considerations, see Prevot, 1967 ;Hatheway, 1990 ; Niemann *et al.*, 1991 ; Popoff and Poulain, 2005). Tetanus neurotoxin (TeNT), also called tetanospasmin, is produced by *C. tetani* and is responsible for all the neurological disorders of tetanus caused by this bacterium. Only one toxinotype of TeNT is known, and those bacteria producing TeNT display homogeneous bacteriological characteristics that uniformly form *C. tetani*. At variance of the botulinum toxins, TeNT is produced without other proteins aimed to form a complex. However, *C. tetani* produces also tetanolysin O (a cholesterol-dependent pore-forming toxin) together with several additional virulence factors. They may participate in the *C. tetani* invasion into host tissues (Brüggemann *et al.*, 2003), but not in the neurological disorders.

Botulinum and tetanus neurotoxins are closely related and share similar molecular and cellular mechanisms

Determination of the amino acid sequences and the corresponding genes of the tetanus and different botulinum neurotoxin serotypes started with TeNT (Eisel *et al.*, 1986 ; Fairweather and Lyness, 1986), followed by BoNT/A (Binz *et al.*, 1990 ; Thompson *et al.*, 1990) and the other BoNT toxinotypes (Arndt *et al.*, 2006). A very close homology between TeNT and the BoNTs was revealed. Both toxin types share a common tri-dimensional structure (Lacy *et al.*, 1998 ; Hanson and Stevens, 2000 ; Swaminathan and Eswaramoorthy, 2000 ; Breidenbach and Brunger, 2005 ; Kumaran *et al.*, 2008, 2009 ; see also reviews by Chaddock and Marks, 2006 ; Singh, 2006) and a cellular/molecular mode of action that ultimately leads to inhibiting vesicular neurotransmitter release. According to the heuristic model initially proposed by Simpson (1981), the cellular mode of action of the clostridial neurotoxins can be depicted according to a multi-step model. The toxin's heavy chain mediates binding to specific receptors comprising a ganglioside moiety and a protein.

Binding implicates a subdomain of the neurotoxin localized into its C-terminus fourth. The BoNTs are well known binding to gangliosides (Kitamura *et al.*, 1980) and to a protein. The protein receptor for most of the BoNTs has been identified: BoNT/A, /C, /E, /F exploit the three isoforms of the vesicle protein SV2 as specific receptors, while BoNT/B and /G bind to synaptotagmin I or II (Nishiki *et al.*, 1994 ; Rummel *et al.*, 2004, 2009 ; Dong *et al.*, 2006, 2007, 2008 ; Mahrhold *et al.*, 2006 ; for a recent review, see Binz and Rummel, 2009). The identity of TeNT receptor still remains elusive. Van Heyningen (1961) reported early that TeNT binds to gangliosides in the nervous tissue, and several recent studies show that TeNT can bind simultaneously to two gangliosides (Chen *et al.*, 2009). However, as pinpointed early by Montecucco *et al.* (1988), the ubiquitous distribution of the gangliosides cannot explain the high neuroselectivity of TeNT. Critchley *et al.* (1986) were first to suggest that TeNT binds both to ganglioside and protein receptors. Consistent with the localisation of TeNT binding in lipid raft, the GPI-anchored membrane protein Thy-1 has been proposed to act as a TeNT receptor (Herreros *et al.*, 2001 ; Munro *et al.*, 2001), but this idea is now abandoned. Thus, unravelling the protein receptor of TeNT remains elusive and needed. Overall, whatever the considered Clostridial neurotoxin, the identified protein receptors are not neurospecific and are expressed on several cell types including crypt epithelial cells in the intestine (Couesnon *et al.*, 2008). The distribution of the gangliosides is distinct from that of the protein receptors. Thus, co-presence of the *ad hoc* ganglioside(s) and protein receptors identifies a set of target cells against which TeNT and the BoNTs display a higher affinity than for other cell types (Chai *et al.*, 2006 ; Jin *et al.*, 2006 ; Rummel *et al.*, 2007 ; Binz and Rummel, 2009 ; reviewed by Binz and Rummel, 2009), these comprise numerous neurons but not all (see *Tables 1-3*).

Table 1. The BoNT block release of many different small neurotransmitter molecules.

Tableau 1. *Le blocage induit par les BoNTs de la libération de nombreuses et différentes petites molécules de neurotransmetteurs.*

Neurotransmitter	Model system	References
ACh	Skeletal neuromuscular junction	Burgen *et al*., 1949
	Torpedo electric organ	Dunant *et al*., 1987
	Aplysia CNS	Poulain et al, 1988
Glutamate	Brain synaptosomes	Sanchez-Prieto *et al*., 1987
	Hind paw / Mass spectrometry	Cui *et al.*, 2004
	Cultured rat cerebellar neurons/radioactive evaluation	Foran *et al*., 2003
	Cultured rat cerebellar neurons/enzymatic ev aluation	Khairallah *et al*., 2008
Aspartate	Brain synaptosomes	McMahon *et al*., 1992
GABA	Brain synaptosomes	Ashton and Dolly, 1988 ; McMahon *et al*., 1992
Glycine	Spinal cord neurons (culture)	Neale *et al*., 1999
DA, A, NA	Brain synaptosomes	Ashton and Dolly, 1988 ; Maisey *et al*., 1988
5-HT	Brain synaptosomes	Najib *et al*., 1999
ATP (co-release with ACh)	*Torpedo* synaptosomes	Marsal *et al*., 1989
	Rat bladder urothelium	Khera *et al.*, 2004 ; Smith *et al*., 2005a
	Guinea pig stellate neurons	Tompkins and Parsons, 2006
NAD	Canine mesenteric artery	Smyth *et al.*, 2006b
	Human urinary bladder detrusor muscle	Breen *et al*., 2006

Table 1 summarizes some of small neurotransmitter molecules which release or co-release is blocked by the BoNTs. *Table 2* summarized a large body of literature indicating, even though indirectly, the inhibition of peptide secretion.

Table 2. BoNT/A can inhibit release of CGRP and Substance P.

Tableau 2. *La BoNT/A peut inhiber la libération de CGRP et de la Substance P.*

Transmitter	Toxin (A type) effect	Concentration / amount	Model system (References)
Substance P (SP)	Inhibition of KCl evoked SP release	100 nM	Cultured DRG neurons (Purkiss *et al.*, 1997 ; Welch *et al*., 2000)
CGRP	Inhibition of release	BoNT/A	Cultured DRG neurons (Welch *et al*., 2000)
		Retagged BoNT/A	Cultured DRG neurons (Duggan *et al.*, 2002)
		1.6 to 3.1 units BTXA/well (3-24 hrs)	CGRP secretion evoked by KCl, or capsaicin, or bradykinin + histamine + 5HT + PGE2, pH5,5 in cultured rat trigeminal nerve cells; (Durham *et al.*, 2004)
		6 hrs, 50 µM !	Isolated rat bladder (Rapp *et al.*, 2006)
	Upregulated synthesis, retention ; increased immunoreactivity	Intra-muscle injection	Ventral horn of spinal cord and neuromuscular junction (mouse, rat) (Hassan *et al.*, 1994 ; Meunier *et al*., 1996 ; Sala *et al*., 1995 ; Tarabal *et al*., 1996)

Table 3 lists several examples of non-neuronal cell types, targeted by the toxins, and whose release process is depressed by BoNTs. Note that in the case of the chromaffin cells, high extracellular concentration of toxin is required, but incubation with gangliosides increases by 2 order of magnitude their susceptibility to the neurotoxins (Marxen *et al.*, 1989).

Table 3. At high concentrations, BoNTs can target non-neuronal cells.

Tableau 3. *A de fortes concentrations, les BoNTs peuvent cibler les cellules non neuronales.*

Cell type	References
Chromaffin cells	Penner *et al.*, 1986 ; Ahnert-Hilger *et al.*, 1989a ; Ahnert-Hilger *et al.*, 1989b
Glial cells : astrocytes or Schwann cells	Abdipranoto *et al.*, 2003 ; Araque *et al.*, 2000 ; Verderio *et al.*, 1999
Exocrine pancreas (100 nM)	Rosado *et al.*, 2005b
Platelets	Redondo *et al.*, 2004

We also provide in *Table 4* examples of release of neuroactive substances that are not affected by BoNTs. These include neurotransmitters that in other neuron/cell types are blocked by the BoNTs. This highlights the notion that distribution of receptors determines susceptibility to the toxins. However, as discussed below, this may also relate to the absence of appropriate intracellular targets.

Table 4. Examples of neurotransmitter release resistant to BoNTs.

Tableau 4. *Exemples de libération de neurotransmetteur résistante aux BoNTs.*

Transmitter	Published data	References / Comments
VIP, CGRP	No change in immunoreactivity 3 months after BTX-A. Periglandular innervations in sweat gland	Swartling *et al.*, 2004
Neuropeptide Y	Vasoconstrictor neurons afferent to vena cava and uterine artery from guinea pig	Morris *et al.*, 2002
SP	Capsaicin evoked release from cultured DRG	Welch *et al.*, 2000
NO	Non vesicular	Jones *et al.*, 2004 ; Morris *et al.*, 2001
ACh	Fraction of 5-HT evoked ACh release at bronchiolar smooth muscle	Moffatt *et al.*l, 2004 Hypothesis: ACh release by epithelial cells
GABA	Cultured inhibitory hippocampal interneurons	Verderio *et al.*, 2004 BoNT-resistant SNAP-25 related isoform ?

The binding of BoNT or TeNT is followed by the endocytotic internalisation of the neurotoxin/receptor complex (*step a* in *Figure 1*). When the neurotoxin is sorted into endocytotic vesicle that acidifies, the heavy chain N-terminus half inserts into the vesicle membrane to make a pore through which the unfolded light chain of the neurotoxin can translocate into the cytosol (Boquet and Duflot, 1982 ; Koriazova and Montal, 2003 ; Fischer and Montal, 2007). When the neurotoxin (TeNT as well as BoNT) is sorted in neutral vesicles, it undergoes retroaxonal ascent (*step b* in *Figure 1*), followed by its release in the central nervous system (*step c* in *Figure 1*) and secondary recapture, *i.e.* transcytosis (Bohnert and Schiavo, 2005 ; Deinhardt *et al.*, 2006 ; Verderio *et al.*, 2007 ; Antonucci *et al.*, 2008 ; review by Caleo and Schiavo, 2009). Note, however, that transcytosis of TeNT is by far more intense than that of BoNTs, and that within BoNTs, susceptibility varies with the toxinotype (Antonucci *et al.*, 2008).

BoNTs and TeNT sequences have revealed the presence of a consensus amino-acid motif characteristic of the catalytic site of zinc-metalloproteases leading to demonstration that TeNT and BoNT/A are indeed metalloproteases (Schiavo *et al.*, 1992b, 1992c ; but see also below). Their targets are the SNARE proteins (for example, see Blasi *et al.*, 1993a, 1993b ; Schiavo *et al.*, 1992a, 1992b), which have been assigned as the key actors governing synaptic vesicle fusion and thus neurotransmitter release (Sollner *et al.*, 1993 ; Jahn and Scheller, 2006). To summarise, VAMP-synaptobrevin is the target of TeNT, and the BoNT/B, /D, /F and /G. SNAP-25 is that of BoNT/A, /C and /E, and syntaxin is targeted by BoNT/C. Since SNAP-25, VAMP-synaptobrevin and syntaxin play a major role in regulated fusion of synaptic vesicles with the plasma membrane at the release sites, their cleavage induces blockade of neurotransmitter exocytosis (*step d* in *Figure 1*). Since the BoNT and TeNT receptors and their intracellular targets are present at all nerve terminals, neither BoNTs nor TeNT are specific for a given type of molecule or cell type (see *Tables 1-2*). Note that in most of the examples listed in these tables, susceptibility to the toxins (when applied extracellularly) is determined by presence of the *ad hoc* membrane receptors and appropriate SNAREs. Several examples of neurotransmission resistant to the BoNTs have been reported (see *Table 3*). In the case of the release of nitric oxide (NO), resistance to BoNT (Morris *et al.*, 2001 ; Jones *et al.*, 2004) is due to the fact that NO release is mediated by diffusion through the membrane, independently of vesicular exocytosis. More interesting is the resistance of GABA release to BoNT observed in certain brain structures, although SNARE-mediated, quantal GABA release seems to implicate neither SNAP-25 nor a related isoform (Verderio *et al.*, 2004).

With the refinement of the understanding of the role played by the SNAREs in exocytosis, the question has arisen of how their cleavage may result in neurotransmitter exocytosis blockade. Moreover, cleaving the SNAREs does not prevent synaptic vesicle tethering to the release site. Two scenarios have emerged (reviewed by Poulain *et al.*, 2008) : *(i)* Proteolytic attack of VAMP by TeNT or the BoNT/B, /D, /F, /G, Syntaxin by BoNT C, or SNAP-25 by BoNT/E does allow formation of either a SNARE complex disconnected of the synaptic vesicle or the plasma membrane, or unstable, thus compromising the priming of the synaptic vesicles at the active zone ; *(ii)* Cleaving SNAP-25 by BoNT/A or /C deeply alters the coupling between detecting Ca^{2+} and synaptic vesicle triggering (for example, see Sakaba *et al.*, 2005). Since the synaptic vesicles docked with unproductive complexes cannot fuse or undock, they stay at the fusion sites (with slightly increased numbers) irreversibly plugging the fusion sites that would normally accommodate intact

vesicles. This progressively reduces the number of release sites to which exocytosis can occur as recently demonstrated for TeNT at identified *Aplysia* cholinergic synapses (Humeau and Luthi, 2007).

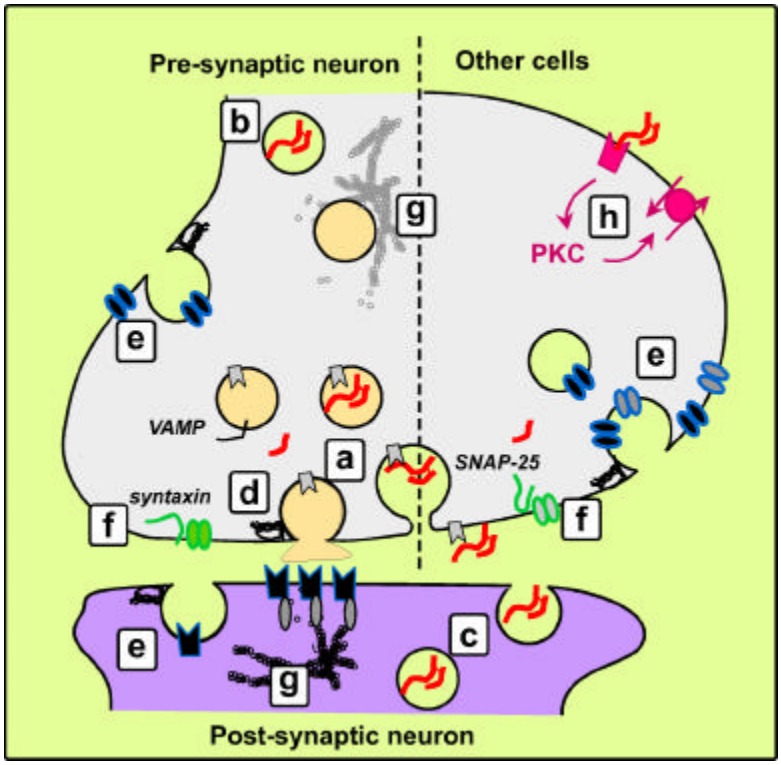

Fig. 1. The multiple intracellular effects of the BoNTs and TeNT. Upon vesicle fusing with plasma membrane, neurotoxin receptors are exposed at the surface of the neuron nerve ending or other target cell neurons (**a**). Then neurotoxin (red) is entrapped inside endocytotic vesicle. Its traffic into acidic vesicles (light orange) allows L chain translocation into the cytosol. When sorted into neutral vesicles, the neurotoxin can undergo retrograde transport (**b**), eventually followed by release (**c**). Inside the cytosol, the neurotoxin L chain cleaves one among the SNARE proteins (VAMP, SNAP-25 or Syntaxin). Following SNARE cleavage, synaptic vesicles containing neurotransmitter (**d**) as well as other cargo implicated in incorporation of integral proteins to plasma membrane, as ionic channels, ionotropic or metabotropic receptors, aquaporins (**e**) can no longer fuse with plasma membrane. Since Syntaxin and SNAP-25 are directly regulating a variety of voltage dependent ionic channels, their cleavage alters the functioning of the latter (**f**). Modification of actin-based cytoskeleton (either following non-proteolytic activation of TGAse type II by TeNT, or other mechanism) may impact traffic of both synaptic vesicle and receptors (**g**). Moreover, binding of TeNT can activate a PKC signaling pathway, resulting in changes in the activity of certain transporters (**h**).

Fig. 1. Les multiples effets intracellulaires des toxines BoNTs et TeNT. *Suite à la fusion des vésicules à la membrane plasmique, le récepteur protéique des neurotoxines se trouve exposé à la surface de la terminaison axonale ou du neurone cible (**a**). La neurotoxine (en rouge) peut se trouver ainsi piégée à l'intérieur de la vésicule d'endocytose. Son passage dans une vésicule qui devient acide (orange clair) facilite la translocation de la chaine L vers le cytosol. Lorsque la toxine est maintenue dans une vésicule restant à pH neutre, elle peut faire l'objet d'un transport rétrograde (**b**), qui pourra éventuellement être suivi de fusion vésiculaire et de libération (**c**). La chaine L de la neurotoxine transférée au cytosol peut cliver l'une des protéines SNARE (VAMP, SNAP-25 ou Syntaxine). En conséquence du clivage des SNARE, les vésicules synaptiques chargées de neuromédiateur (**d**), comme toute vésicule cargo impliquée dans l'incorporation à la membrane de protéines telles que des canaux ioniques, récepteurs métabotropiques ou aquaporines (**e**), sont empêchées de fusionner. Par ailleurs, la Syntaxine et la SNAP-25 peuvent réguler directement l'activité de canaux ioniques dépendant du potentiel, le clivage de ces SNARE pouvant altérer le fonctionnement normal des canaux (**f**). Des modifications du cytosquelette actinique (entrainées par une action non protéolytique de TeNT sur la TGase de type II, ou par un autre mécanisme) peuvent avoir des conséquence sur le trafic des vésicules synaptiques ou des récepteurs (**g**). Enfin, la fixation à la membrane de la sous-unité H de TeNT peut activer la voie de signalisation de la PKC, avec la possibilité d'aboutir à des variations dans l'activité de certains transporteurs de neuromédiateurs (**h**).*

By cleaving the SNARE, the TeNT and BoNTs can alter cell mechanisms other than neurotransmitter release

Exocytosis is a general mechanism that is exploited not only to secrete molecular products, but also to incorporate both lipids and integral membrane proteins to the plasmalemma (*step e* in *Figure 1*). It has arise that some of the SNARE proteins susceptible of proteolysis by TeNT or the BoNTs are implicated in the trafficking of many different membrane proteins resulting in the alteration of mechanisms unrelated to neurotransmitter release. *Table 5* provides several examples of membrane receptors and channels affected by clostridial toxins on their trafficking or their recycling.

These initially unexpected actions of the BoNTs and TeNT may explain some of the new potential applications of these toxins in therapy. Notably, BoNT/A can decrease neurogenic inflammation (Cui *et al.*, 2004) and reduce pain (Favre-Guilmard *et al.*, 2009). During neurogenic inflammation, release of CGRP and SP induces dilatation of small arteries and small veins and BoNT can inhibit CGRP release (see refs in *Table 2*). Of interest, protein kinase C induced membrane incorporation of TRPV1 channels in DRG neurons is prevented by BoNT (Morenilla-Palao *et al.*, 2004) which suggest an explanation to the anti-nociceptive properties of BoNT. Indeed, in response to activation of TRPV1 receptors, non-myelinated axons can release CGRP (Bernardini *et al.*, 2004 ; Fischer and Reeh, 2007). Moreover, in trigeminal ganglionic neurons only a recombinant chimera of BoNT/A and BoNT/E is able to overcome the elevation of CGRP release induced by the activation of the capsaicin receptor TRPV1 channel (Meng *et al.*, 2009).

Table 5. Examples on the sensitivity of receptors or channels trafficking to TeNT or BoNTs.

Tableau 5. *Exemples de sensibilité du trafic des récepteurs ou canaux à la TeNT ou aux BoNTs.*

Receptor	BoNT effect	Remarks	Model system (References)
Glu R (AMPA-R)	Decrease in LTP amplitude Decrease in AMPA-R insertion	BoNT/B LC intra-pipette	LTP in CA1 (Lledo *et al.*, 1998) ; Cerebellar NO-induced PF-LTP (Kakegawa and Yuzaki, 2005) ; L-type channel driven insertion of AMPA-R in mouse CA1 (Baxter and Wyllie, 2006)
NMDA-R (NR1)	Decrease insertion	BoNT/A intra-pipette	mGluR1 driven insertion of NR1 in Xenopus oocyte membrane (Lan *et al.*, 2001)
Gephyrin (Glycine-Receptors)	Decrease in immunoreactivity	Inhibition of inhibitory potentials on motor neurons, but reduction of synaptic covering due to silencing.	2 month injection in cat abducens motoneurons (Moreno-Lopez *et al.*, 1998)
α7-nAChR	Reduced activity driven trafficking	BoNT/C1 or /D	Somatic spines in cultured chick ciliary ganglion (Liu *et al.*, 2005)
H^+-ATPase	Reduced trafficking	BoNT/A or/E (25-50 nM) extracellular, 45 min.	SNAP-23 dependent trafficking of H^+-ATPase in cultured inner medullary collecting duct cells of the rat (Banerjee *et al.*, 2001)
Transferrin-R synaptic vesicle	Reduced recycling	TeNT	(Knight, 2002 ; Salem *et al.*, 1998)
Aquaporin 2	Inhibition of the membrane insertion of water channels		Rabbit renal cortical collecting tubule (Quigley *et al.*, 2005)
TRPV1 channels	Membrane incorporation in DRG neurons		(Morenilla-Palao *et al.*, 2004)
Membrane resealing	Block of membrane resealing in sea urchin eggs and embryos		(Bi *et al.*, 1995 ; Steinhardt *et al.*, 1994)
Orai1	Reduction of the store operated Ca^{2+} entry (SOCE)		(Woodard *et al.*, 2008)

Overall, the above mentioned examples are consistent with the current notion that the SNAREs control fusion of cargo vesicles with plasma membrane. Likewise, several step of the synaptic vesicle cycle are altered by the toxin action. For example, VAMP cleavage abolishes the interaction of VAMP with the adaptor protein AP3 and affect synaptic vesicle recycling *via* early endosomes (Salem *et al.*, 1998).

The SNARE cleavage products have also the potential to interfere with fusion processes (Cornille *et al.*, 1995 ; Tucker *et al.*, 2004). Truncated SNAP-25 can behave as a dominant negative mutant upon the exocytotic process suggesting that after BoNT/A, the block of release is due to both functional elimination of SNAP-25 and the accumulation of the cleavage product which competitively inhibits exocytosis (Gutierrez *et al.*, 1997 ; Keller and Neale, 2001 ; Apland *et al.*, 2003). Consistent with synaptophysin-1 controlling specifically the targeting of VAMP2 but not VAMP1 to synaptic vesicles, is the observation that the cytosolic cleavage product of VAMP2 but not VAMP1, released upon TeNT or BoNT/B activity, blocks neurotransmitter release (Cornille *et al.*, 1995). This result suggests an alteration of the exocytosis due to a disturbance of the synaptophysin-1/VAMP2 interaction.

Action of toxins on calcium dynamics

The SNAREs are able to interact, directly or indirectly, with other proteins present in the plasma membrane ; their cleavage would indirectly affect the functioning of their partners. For example, syntaxin promotes inactivation of N- or P/Q-, R-, L-types Ca^{2+} channels, and this inactivation is removed when proteins of the fusion complex (SNAP-25, VAMP, synaptotagmin ...) bind to syntaxin and/or Ca^{2+}-channels (Wiser *et al.*, 1999 ; Degtiar *et al.*, 2000 ; Stanley *et al.*, 2003 ; Cohen and Atlas, 2004). In this line, SNAP-25 has been reported to control calcium responsiveness to depolarization (Verderio *et al.*, 2004 ; *step f* in *Figure 1*). Syntaxin cleavage may indirectly alter Ca^{2+}-channel functioning : slow Ca^{2+} influx has been found

potentiated after BoNT/C (Bergsman and Tsien, 2000), while in *Torpedo* preparations, Ca^{2+} entry was reported to be significantly decreased by BoNT/C (Aleu *et al.*, 2002). Moreover, BoNT/C abolishes the regulation of Ca^{2+}-channel by heterotrimeric G-proteins (Stanley and Mirotznik, 1997). SNAP-25 modulates L-Type channels (Ji *et al.*, 2002), and entry of Ca^{2+} mediated by store operated-channels in pancreatic acini secreting amylase, or human platelets. In these cells, Ca^{2+} influx is strongly depressed after SNAP-25 cleavage by BoNT, possibly contributing to the blockade of Ca^{2+}-dependent exocytosis by BoNT/A (Rosado *et al.*, 2005b). Note however, these non-neuronal effects have been detected using very high concentration of toxin (~100 nM). Overall, these observations suggests that in certain preparations, the blockade of secretion resulting from SNAP-25 cleavage can relate to inhibition of the exocytotic machinery and changes in Ca^{2+} influx at the nerve terminals.

A significant reduction of the store operated Ca^{2+} entry (SOCE) due to BoNT/A has been observed in different cells. The SOCE normally follows a depletion of intracellular Ca^{2+} stores ant this Ca^{2+} influx is carried out by store-operated Ca^{2+} channels (SOCC) (Putney, 1986 ; Smyth *et al.*, 2006a ; Lewis, 2007). Working with *Xenopus* oocytes, Yao *et al.* (1999) demonstrated that the activation of a store-operated Ca^{2+} current required SNAP-25 since the current was found to be inhibited by BoNT/A in a dose-dependent manner with an apparent Ki of 8 nM. Similarly, the store-operated Ca^{2+} current was almost completely abolished by expression of C-terminal truncated SNAP-25 mutants (Yao *et al.*, 1999). The BoNT/A light chain and TeNT significantly reduced SOCE when directly microinjected in human embryonic kidney (HEK) cells (Alderton *et al.*, 2000). SOCE was also significantly reduced by BoNT/A or BoNT/E in murine pancreatic acinar cells and in human platelets (Redondo *et al.*, 2004 ; Rosado *et al.*, 2005b). The molecular identity of the channel carrying the Ca^{2+} current in SOCE is in the process of clarification, then, it remains difficult to assert a role to SNAP-25 in the regulation of the conductance or in the process of protein secretion. A direct interaction of SNAP-25 with TRPC1 channel has been postulated (Rosado *et al.*, 2005a) and, more recently, the inhibition of exocytotic-like insertion of Orai1 into the plasma membrane in human HeLa and HEK 293T cells was shown to be partially affected by BoNTA (Woodard *et al.*, 2008).

Likewise, physical and functional interactions between syntaxin 1A and brain voltage gated K^+ -channels Kv1.1 type have been found (Fili *et al.*, 2001). The activity of Kv2.1 channel, the prevalent delayed rectifier channel in endocrine and neuroendocrine cells, is also strongly modulated by syntaxin and SNAP-25 (Michaelevski *et al.*, 2003 ; Tsuk *et al.*, 2004). This suggests that SNARE proteins can regulate membrane excitability *via* K^+ channels, thus tuning exocytosis. This raises the question of whether exocytosis may be altered by BoNTs *via* changes in activation of Kv2.1 currents.

Non-proteolytic molecular actions of BoNTs and TeNT

Yet a direct cause-effect relationship exists between the cleavage of the SNAREs and the blockade of neuroexocytosis by TeNT or the BoNTs (Humeau *et al.*, 2000 ; Rossetto *et al.*, 2006 ; Poulain *et al.*, 2008), a controversial possibility is that the BoNTs and TeNT may interfere with exocytosis and other cell functions *via* molecular actions unrelated to their proteolytic activity. Indeed, when mutated in the catalytic site at positions crucial for either Zn^{2+} binding (His^{233} and His^{237}) or cleavage of the Gln-Phe bond in VAMP-2 (Glu^{234}), TeNT-light chain cannot cleave VAMP-2 *in vitro* (Li *et al.*, 1994 ; Yamasaki *et al.*, 1994). However, several of the point-mutated TeNT L chain constructs are able to produce inhibition of neurotransmitter release (His^{233}->Ala^{233}, Leu^{233} or Val^{233} ; Glu^{234}->Ala^{234} ; His^{237}->Ala^{237} ; Asp^{237}, Gly^{237} or Val^{237}) albeit with reduced potency as compared to wild-type TeNT-light chain (Niemann *et al.*, 1994 ; Ashton *et al.*, 1995). Such a non-proteolytic mechanism may explain why endopeptidase blockers, which abolish VAMP-2 cleavage *in vitro,* counteract only partially the inhibitory action of TeNT on neurotransmitter release (de Paiva *et al.*, 1993 ; Ashton *et al.*, 1995). Moreover, the observation that antagonism of the intracellular action of BoNT/A can be relieved fast by the mean of injecting monoclonal antibodies directed against the BoNT/A L chain (Cenci di Bello *et al.*, 1994) is difficult to conciliate with the proteloytic activity of the neurotoxin, protein cleavage being in essence irreversible.

The observation that TeNT binds with high affinity to, and strongly activates, the GTP-binding protein transglutaminase type II (TGase II) *in vitro,* suggests that TGase II may participate in the intracellular action of TeNT (Facchiano and Luini, 1992 ; Facchiano *et al.*, 1993a, 1993b). However, the precise contribution of TGase II to the blockade of neurotransmission by TeNT has never been clarified and conflicting data exist in the literature (Coffield *et al.*, 1994 ; Ashton *et al.*, 1995 ; Gobbi *et al.*, 1996).

TGase II belongs to a large family of bifunctional and Ca^{2+}-dependent cross-linking enzymes (Fesus and Piacentini, 2002 ; Lorand and Graham, 2003) abundant in neurons and nerve endings (Facchiano and Luini, 1992 ; Maggio *et al.*, 2001) which has been implicated in secretory mechanisms (Pastuszko *et al.*, 1986 ; Driscoll *et al.*, 1997 ; Walther *et al.*, 2003). The identification of the vesicular protein synapsin-I as one of the two main substrates crosslinked by TGase II needs to be considered for explaining part of the non-proteolytic TeNT-induced decrease in neurotransmitter release. Indeed, synapsin-I regulates synaptic vesicle trafficking *via* interactions with the actin cytoskeleton (*step g* in *Figure 1*) and participates in post-docking steps of exocytosis (Humeau *et al.*, 2001 ; Baldelli *et al.*, 2007). Possibly, TeNT stimulation of TGase II leads to reduced synaptic vesicle availability for release. This view is supported by several observations: *(i)* the depolarization-stimulated phosphorylation and redistribution of SynI is altered after the action of TeNT (Presek *et al.*, 1992) ; *(ii)* the blocking action of TeNT is diminished after disassembly of microfilaments (Ashton and Dolly, 1997) and *(iii)* the amplitude of post-tetanic potentiation, a plasticity paradigm which involves synapsin I in *Aplysia* synapses, is highly reduced after TeNT treatment (Humeau *et al.*, 2001, 2007). As TeNT can access VAMP-2 only during a defined “physiological window” (Humeau *et al.*, 2000 ;

Poulain *et al.*, 2008), TGase-II activation may modulate this access *via* the modification of proteins involved in regulation of the synaptic vesicle cycle (*i.e.* synapsin I) or its other substrate(s).

The importance of the proteolytic and non-proteolytic mechanisms of TeNT may be variable from one model systems to other, and may depend on differential expression of endogenous TGase-II. Contrasting with the observations made using brain synaptosomes or *Aplysia* preparations (Niemann *et al.*, 1994 ; Ashton *et al.*, 1995), non-proteolytic TeNT mutants were found ineffective at the mouse hemidiaphragm (Li *et al.*, 1994) or neurohypophysial nerve endings (Dayanithi *et al.*, 1994) and participation of TGase-II activation in the blockade of secretion by TeNT has been ruled out at the mouse neuromuscular junction and in NG108 cells (Coffield *et al.*, 1994).

In vitro, BoNT/E light chain has been reported cleaving actin and all the 11 cleavages sites identified involved Arg or Lys residues in *P*'1 position exactly as in SNAP-25 (DasGupta and Tepp, 1993). Thus another unexpected intracellular effect of TeNT is the modification of actin cytoskeleton (*step g* in *Figure 1*). This is supported by several observations : TeNT inhibits the rearrangements of subcortical microfilaments that accompany secretion in chromaffin cells (Marxen and Bigalke, 1991). Actin cytoskeleton network is altered when TeNT light chain is expressed in Sertoli cells in mice (Eisel *et al.*, 1993). Consistent with the well documented implication of small GTPases Rho in the dynamics and organization of actin-based cytoskeleton (Hall, 1998), BoNT/A has been reported to target RhoB to the proteasome, causing both blockade of exocytosis and actin cystoskeleton disorganization (Ishida *et al.*, 2004). This may relate to a crosstalk between actin cytoskeleton remodeling, SNARE- and Rho-GTPase-dependent mechanisms of exocytosis, as recently illustrated for Cdc42 and VAMP-2 during insulin secretion (Nevins and Thurmond, 2005).

TeNT shows unconventional cellular actions time before its classical proteolytic effects became evident. Aguliera and Yavin first reported the *in vivo* activation and translocation of protein kinase C in rat brain (Aguilera *et al.*, 1990 ; Aguilera and Yavin, 1990). Concomitantly, an increase of phosphoinositide hydrolysis was observed (Gil *et al.*, 1998). The intracellular pathway activates phospholipase C-1 and other kinases (Gil *et al.*, 2000). Among the different targets these enzymes can attain, the best characterized is the 5-HT transporter which is phosphorylated and has its activity modulated at low toxin concentration (10^{-12} M) in less than 30 minutes (Inserte *et al.*, 1999 ; Najib *et al.*, 2000 ; Pelliccioni *et al.*, 2001) (*step h* in *Figure 1*). These effects are carried out by the half C-terminal part of the heavy subunit, the portion that carries the binding domain of the toxin to the receptor (Gil *et al.*, 2003 ; Chaïb-Oukadour *et al.*, 2004). It is of interest to note that this portion of the heavy chain is able to protect from death neuronal cells, *in vitro* as well as *in vivo* (Chaïb-Oukadour *et al.*, 2004 ; Chaïb-Oukadour *et al.*, 2009 ; Mendieta *et al.*, 2009).

Conclusion

As the use of botulinum toxins for medical purposes continues to expand, novel observations will emerge that fit poorly with the conventional view of the specific inhibition of acetylcholine release at the neuromuscular junction. This underlies the need for giving more thoughts to the published unconventional effects of clostridial TenT and BoNTs. Some of the results reviewed here already complement the rationale behind empiric clinical observations. It will be of a general interest for basic sciences as well as clinical knowledge to continue depend our understanding of these unconventional effects of clostridial toxins.

Acknowledgements. *E.L. and L.W are recipients of a doctoral grant from the Mission pour la Recherche et l'Innovation Scientifique - Délégation Générale à l'Armement (M.R.I.S/D.G.A-Gilles Vergnaud.*

References

Abdipranoto A, Liu GJ, Werry EL, Bennett MR (2003) Mechanisms of secretion of ATP from cortical astrocytes triggered by uridine triphosphate. *Neuroreport* **14**(17): 2177-2181

Aguilera J, Lopez LA, Yavin E (1990) Tetanus toxin-induced protein kinase C activation and elevated serotonin levels in the perinatal rat brain. *FEBS Lett* **263**(1): 61-65

Aguilera J, Yavin E (1990) *In vivo* translocation and down-regulation of protein kinase C following intraventricular administration of tetanus toxin. *J Neurochem* **54**(1): 339-342

Ahnert-Hilger G, Bader MF, Bhakdi S, Gratzl M (1989a) Introduction of macromolecules into bovine adrenal medullary chromaffin cells and rat pheochromocytoma cells (PC12) by permeabilization with streptolysin O: inhibitory effect of tetanus toxin on catecholamine secretion. *J Neurochem* **52**(6): 1751-1758

Ahnert-Hilger G, Weller U, Dauzenroth ME, Habermann E, Gratzl M (1989b) The tetanus toxin light chain inhibits exocytosis. *FEBS Lett* **242**(2): 245-248

Alderton JM, Ahmed SA, Smith LA, Steinhardt RA (2000) Evidence for a vesicle-mediated maintenance of store-operated calcium channels in a human embryonic kidney cell line. *Cell Calcium* **28**(3): 161-169

Aleu J, Blasi J, Solsona C, J. M (2002) Calcium-dependent acetylcholine release from *Xenopus* oocytes: simultaneous ionic currents and acetylcholine release recordings. *Eur J Neurochem* **8**: 1442-1448

Antonucci F, Di Garbo A, Novelli E, Manno I, Sartucci F, Bozzi Y, Caleo M (2008) Botulinum neurotoxin E (BoNT/E) reduces CA1 neuron loss and granule cell dispersion, with no effects on chronic seizures, in a mouse model of temporal lobe epilepsy. *Exp Neurol* **210**(2): 388-401

Apland JP, Adler M, Oyler GA (2003) Inhibition of neurotransmitter release by peptides that mimic the N-terminal domain of SNAP-25. *J Prot Chem* **22**(2): 147-153

Araque A, Li N, Doyle RT, Haydon PG (2000) SNARE protein-dependent glutamate release from astrocytes. *J Neurosci* **20**(2): 666-673

Arndt JW, Jacobson MJ, Abola EE, Forsyth CM, Tepp WH, Marks JD, Johnson EA, Stevens RC (2006) A structural perspective of the sequence variability within botulinum neurotoxin subtypes A1-A4. *J Mol Biol* **362**(4): 733-742

Ashton AC, Dolly JO (1988) Characterization of the inhibitory action of botulinum neurotoxin type A on the release of several transmitters from rat cerebrocortical synaptosomes. *J Neurochem* **50**(6): 1808-1816

Ashton AC, Dolly JO (1997) Microtubules and microfilaments participate in the inhibition of synaptosomal noradrenaline release by tetanus toxin. *J Neurochem* **68**(2): 649-658

Ashton AC, Li Y, Doussau F, Weller U, Dougan G, Poulain B, Dolly JO (1995) Tetanus toxin inhibits neuroexocytosis even when its Zn-dependent protease activity is removed. *J Biol Chem* **270**(52): 31386-31390

Baldelli P, Fassio A, Valtorta F, Benfenati F (2007) Lack of synapsin I reduces the readily releasable pool of synaptic vesicles at central inhibitory synapses. *J Neurosci* **27**(49): 13520-13531

Banerjee A, Li G, Alexander EA, Schwartz JH (2001) Role of SNAP-23 in trafficking of H^+-ATPase in cultured inner medullary collecting duct cells. *Am J Physiol Cell Physiol* **280**(4): C775-781

Baxter AW, Wyllie DJA (2006) Phosphatidylinositol 3 Kinase activation and AMPA receptor subunit trafficking underlie the potentiation of miniature EPSC amplitudes triggered by the activation of L-Type calcium channels. *J Neurosci* **26**(20): 5456-5469

Bergsman JB, Tsien RW (2000) Syntaxin modulation of calcium channels in cortical synaptosomes as revealed by botulinum toxin C1. *J Neurosci* **20**: 4368-4378

Bernardini N, Neuhuber W, Reeh PW, Sauer SK (2004) Morphological evidence for functional capsaicin receptor expression and calcitonin gene-related peptide exocytosis in isolated peripheral nerve axons of the mouse. *Neuroscience* **126**(3): 585-590

Bi G, Alderton J, Steinhardt R (1995) Calcium-regulated exocytosis is required for cell membrane resealing. *J Cell Biol* **131**(6): 1747-1758

Binz T, Kurazono H, Wille M, Frevert J, Wernars K, Niemann H (1990) The complete sequence of botulinum neurotoxin type A and comparison with other clostridial neurotoxins. *J Biol Chem* **265**(16): 9153-9158

Binz T, Rummel A (2009) Cell entry strategy of clostridial neurotoxins. *J Neurochem* **109**(6): 1584-1595

Blasi J, Chapman ER, Link E, Binz T, Yamasaki S, De Camilli P, Sudhof TC, Niemann H, Jahn R (1993a) Botulinum neurotoxin A selectively cleaves the synaptic protein SNAP-25. *Nature* **365**(6442): 160-163

Blasi J, Chapman ER, Yamasaki S, Binz T, Niemann H, Jahn R (1993b) Botulinum neurotoxin C1 blocks neurotransmitter release by means of cleaving HPC-1/syntaxin. *EMBO J* **12**(12): 4821-4828

Bleck TP (1989) Clinical aspects of Tetanus. In *Botulinum Neurotoxin and Tetanus Toxin*, Simpson LL (ed) pp 379-398. Academic Press, Inc: San Diego, California 92101

Bohnert S, Schiavo G (2005) Tetanus toxin is transported in a novel neuronal compartment characterized by a specialized pH regulation. *J Biol Chem* **280**(51): 42336-42344

Boquet P, Duflot E (1982) Tetanus toxin fragment forms channels in lipid vesicles at low pH. *Proc Natl Acad Sci U S A* **79**(24): 7614-7618

Breen LT, Smyth LM, Yamboliev IA, Mutafova-Yambolieva VN (2006) beta-NAD is a novel nucleotide released on stimulation of nerve terminals in human urinary bladder detrusor muscle. *Am J Physiol Renal Physiol* **290**(2): F486-495

Breidenbach MA, Brunger AT (2005) 2.3 A crystal structure of tetanus neurotoxin light chain. *Biochemistry* **44**(20): 7450-7457

Brüggemann H, Baumer S, Fricke WF, Wiezer A, Liesegang H, Decker I, Herzberg C, Martinez-Arias R, Merkl R, Henne A, Gottschalk G (2003) The genome sequence of *Clostridium tetani*, the causative agent of tetanus disease. *Proc Natl Acad Sci U S A* **100**(3): 1316-1321

Burgen AS, Dickens F, Zatman LJ (1949) The action of botulinum toxin on the neuro-muscular junction. *J Physiol* **109**(1-2): 10-24

Caleo M, Schiavo G (2009) Central effects of tetanus and botulinum neurotoxins. *Toxicon* **54**(5): 593-599

Carle A, Rattone G (1884) Studio esperimentale sull'eziologia del tetano. *Giorn Accad Mede Torino* **32** 174-179.

Cenci di Bello I, Poulain B, Shone CC, Tauc L, Dolly JO (1994) Antagonism of the intracellular action of botulinum neurotoxin type A with monoclonal antibodies that map to light-chain epitopes. *Eur J Biochem* **219**(1-2): 161-169

Chaddock J, Marks P (2006) Clostridial neurotoxins: structure-function led design of new therapeutics. *Cell Mol Life Sci* **63**(5): 540-551

Chai Q, Arndt JW, Dong M, Tepp WH, Johnson EA, Chapman ER, Stevens RC (2006) Structural basis of cell surface receptor recognition by botulinum neurotoxin B. *Nature* **444**(7122): 1096-1100

Chaïb-Oukadour I, Gil C, Aguilera J (2004) The C-terminal domain of the heavy chain of tetanus toxin rescues cerebellar granule neurones from apoptotic death: involvement of phosphatidylinositol 3-kinase and mitogen-activated protein kinase pathways. *J Neurochem* **90**(5): 1227-1236

Chaïb-Oukadour I, Gil C, Rodríguez-Alvarez J, Ortega A, Aguilera J (2009) Tetanus toxin HC fragment reduces neuronal MPP+ toxicity. *Mol Cell Neurosci* **41**(3): 297-303

Chen C, Fu Z, Kim JJ, Barbieri JT, Baldwin MR (2009) Gangliosides as high affinity receptors for tetanus neurotoxin. *J Biol Chem* **284**(39): 26569-26577

Coffield JA, Considine RV, Jeyapaul J, Maksymowych AB, Zhang RD, Simpson LL (1994) The role of transglutaminase in the mechanism of action of tetanus toxin. *J Biol Chem* **269**(39): 24454-24458

Cohen R, Atlas D (2004) R-type voltage-gated Ca(2+) channel interacts with synaptic proteins and recruits synaptotagmin to the plasma membrane of *Xenopus* oocytes. *Neurosci* **128**: 831-841

Cornille F, Deloye F, Fournie-Zaluski MC, Roques BP, Poulain B (1995) Inhibition of neurotransmitter release by synthetic proline-rich peptides shows that the N-terminal domain of vesicle-associated membrane protein/synaptobrevin is critical for neuro-exocytosis. *J Biol Chem* **270**(28): 16826-16832

Couesnon A, Pereira Y, Popoff MR (2008) Receptor-mediated transcytosis of botulinum neurotoxin A through intestinal cell monolayers. *Cell Microbiol* **10**(2): 375-387

Critchley DR, Habig WH, Fishman PH (1986) Reevaluation of the role of gangliosides as receptors for tetanus toxin. *J Neurochem* **47**(1): 213-222

Cui M, Khanijou S, Rubino J, Aoki KR (2004) Subcutaneous administration of botulinum toxin A reduces formalin-induced pain. *Pain* **107**(1-2): 125-133

DasGupta BR, Boroff DA, Rothstein E (1966) Chromatographic fractionation of the crystalline toxin of *Clostridium botulinum* type A. *Biochem Biophys Res Commun* **22**(6): 750-756

DasGupta BR, Tepp W (1993) Protease activity of botulinum neurotoxin type E and its light chain: cleavage of actin. *Biochem Biophys Res Commun* **190**(2): 470-474

Dayanithi G, Stecher B, Hohne-Zell B, Yamasaki S, Binz T, Weller U, Niemann H, Gratzl M (1994) Exploring the functional domain and the target of the tetanus toxin light chain in neurohypophysial terminals. *Neuroscience* **58**(2): 423-431

de Paiva A, Poulain B, Lawrence GW, Shone CC, Tauc L, Dolly JO (1993) A role for the interchain disulfide or its participating thiols in the internalization of botulinum neurotoxin A revealed by a toxin derivative that binds to ecto-acceptors and inhibits transmitter release intracellularly. *J Biol Chem* **268**(28): 20838-20844

Degtiar VE, Scheller RH, Tsien RW (2000) Syntaxin modulation of slow inactivation of N-type calcium channels. *J Neurochem* **20**: 4355-4367

Deinhardt K, Berninghausen O, Willison HJ, Hopkins CR, Schiavo G (2006) Tetanus toxin is internalized by a sequential clathrin-dependent mechanism initiated within lipid microdomains and independent of epsin1. *J Cell Biol* **174**(3): 459-471

Dong M, Liu H, Tepp WH, Johnson EA, Janz R, Chapman ER (2008) Glycosylated SV2A and SV2B mediate the entry of botulinum neurotoxin E into neurons. *Mol Biol Cell* **19**(12): 5226-5237

Dong M, Tepp WH, Liu H, Johnson EA, Chapman ER (2007) Mechanism of botulinum neurotoxin B and G entry into hippocampal neurons. *J Cell Biol* **179**(7): 1511-1522

Dong M, Yeh F, Tepp WH, Dean C, Johnson EA, Janz R, Chapman ER (2006) SV2 is the protein receptor for botulinum neurotoxin A. *Science* **312**(5773): 592-596

Driscoll HK, Adkins CD, Chertow TE, Cordle MB, Matthews KA, Chertow BS (1997) Vitamin A stimulation of insulin secretion: effects on transglutaminase mRNA and activity using rat islets and insulin-secreting cells. *Pancreas* **15**(1): 69-77

Duggan MJ, Quinn CP, Chaddock JA, Purkiss JR, Alexander FC, Doward S, Fooks SJ, Friis LM, Hall YH, Kirby ER, Leeds N, Moulsdale HJ, Dickenson A, Green GM, Rahman W, Suzuki R, Shone CC, Foster KA (2002) Inhibition of release of neurotransmitters from rat dorsal root ganglia by a novel conjugate of a *Clostridium botulinum* toxin A endopeptidase fragment and Erythrina cristagalli lectin. *J Biol Chem* **277**(38): 34846-34852

Dunant Y, Esquerda JE, Loctin F, Marsal J, Muller D (1987) Botulinum toxin inhibits quantal acetylcholine release and energy metabolism in the *Torpedo* electric organ. *J Physiol* **385**: 677-692

Durham PL, Cady R, Cady R (2004) Regulation of Calcitonin Gene-Related Peptide secretion from trigeminal nerve cells by botulinum toxin type A: implications for migraine therapy. *Headache: The Journal of Head and Face Pain* **44**(1): 35-43

Eisel U, Jarausch W, Goretzki K, Henschen A, Engels J, Weller U, Hudel M, Habermann E, Niemann H (1986) Tetanus toxin: primary structure, expression in *E. coli*, and homology with botulinum toxins. *EMBO J* **5**(10): 2495-2502

Eisel U, Reynolds K, Riddick M, Zimmer A, Niemann H, Zimmer A (1993) Tetanus toxin light chain expression in Sertoli cells of transgenic mice causes alterations of the actin cytoskeleton and disrupts spermatogenesis. *EMBO J* **12**: 3365-3372

Erbguth FJ (2008) From poison to remedy: the chequered history of botulinum toxin. *J Neural Transm* **115**(4): 559-565

Erbguth FJ, Naumann M (1999) Historical aspects of botulinum toxin: Justinus Kerner (1786-1862) and the "sausage poison". *Neurology* **53**(8): 1850-1853

Facchiano F, Benfenati F, Valtorta F, Luini A (1993a) Covalent modification of synapsin I by a tetanus toxin-activated transglutaminase. *J Biol Chem* **268**(7): 4588-4591

Facchiano F, Luini A (1992) Tetanus toxin potently stimulates tissue transglutaminase. A possible mechanism of neurotoxicity. *J Biol Chem* **267**(19): 13267-13271

Facchiano F, Valtorta F, Benfenati F, Luini A (1993b) The transglutaminase hypothesis for the action of tetanus toxin. *Trends Biochem Sci* **18**(9): 327-329

Fairweather NF, Lyness VA (1986) The complete nucleotide sequence of tetanus toxin. *Nucleic Acids Res* **14**(19): 7809-7812

Favre-Guilmard C, Auguet M, Chabrier P-E (2009) Different antinociceptive effects of botulinum toxin type A in inflammatory and peripheral polyneuropathic rat models. *Eur J Pharmacol* **617**(1-3): 48-53

Fesus L, Piacentini M (2002) Transglutaminase 2: an enigmatic enzyme with diverse functions. *Trends Biochem Sci* **27**(10): 534-539

Fili O, Michaelevsk iI, Bledi Y, Chikvashvili D, Singer-Lahat D, Boshwitz H, Linial M, Lotan I (2001) Direct interaction of a brain voltage-gated K^+ channel with syntaxin 1A: functional impact on channel gating. *J Neurochem* **21**: 1964-1974

Fischer A, Montal M (2007) Crucial role of the disulfide bridge between botulinum neurotoxin light and heavy chains in protease translocation across membranes. *J Biol Chem* **282**(40): 29604-29611

Fischer MJM, Reeh PW (2007) Sensitization to heat through G-protein-coupled receptor pathways in the isolated sciatic mouse nerve. *Eur J Neurosci* **25**(12): 3570-3575

Foran PG, Mohammed N, Lisk GO, Nagwaney S, Lawrence GW, Johnson E, Smith L, Aoki KR, Dolly JO (2003) Evaluation of the therapeutic usefulness of botulinum neurotoxin B, C1, E, and F compared with the long lasting type A. Basis for distinct durations of inhibition of exocytosis in central neurons. *J Biol Chem* **278**(2): 1363-1371

Gil C, Chaïb-Oukadour I, Pelliccioni P, Aguilera J (2000) Activation of signal transduction pathways involving trkA, PLC[gamma]-1, PKC isoforms and ERK-1/2 by tetanus toxin. *FEBS Lett* **481**(2): 177-182

Gil C, Najib A, Aguilera J (2003) Serotonin transport is modulated differently by tetanus toxin and growth factors. *Neurochem Int* **42**(7): 535-542

Gil C, Ruiz-Meana M, Álava M, Yavin E (1998) Tetanus toxin enhances protein kinase C activity translocation and increases polyphosphoinositide hydrolysis in rat cerebral cortex preparations. *J Neurochem* **70**(4): 1636-1643

Gobbi M, Frittoli E, Mennini T (1996) Role of transglutaminase in [3H]5-HT release from synaptosomes and in the inhibitory effect of tetanus toxin. *Neurochem Int* **29**(2): 129-134

Gutierrez LM, Viniegra S, Rueda J, Ferrer-Montiel AV, Canaves JM, Montal M (1997) A peptide that mimics the C-terminal sequence of SNAP-25 inhibits secretory vesicle docking in chromaffin cells. *J Biol Chem* **272**(5): 2634-2639

Hall A (1998) Rho GTPases and the actin cytoskeleton. *Science* **279**(5350): 509-514

Hanson MA, Stevens RC (2000) Cocrystal structure of synaptobrevin-II bound to botulinum neurotoxin type B at 2.0 A resolution. *Nat Struct Mol Biol* **7**(8): 687-692

Hassan SM, Jennekens FG, Wieneke G, Veldman H (1994) Calcitonin gene-related peptide-like immunoreactivity, in botulinum toxin-paralysed rat muscles. *Neuromuscul Disord* **4**(5-6): 489-496

Hatheway CL (1990) Toxigenic clostridia. *Clin Microbiol Rev* **3**(1): 66-98

Herreros J, Ng T, Schiavo G (2001) Lipid rafts act as specialized domains for tetanus toxin binding and internalization into neurons. *Mol Biol Cell* **12**(10): 2947-2960

Humeau Y, Doussau F, Grant NJ, Poulain B (2000) How botulinum and tetanus neurotoxins block neurotransmitter release. *Biochimie* **82**(5): 427-446

Humeau Y, Doussau F, Popoff MR, Benfenati F, Poulain B (2007) Fast changes in the functional status of release sites during short-term plasticity: involvement of a frequency-dependent bypass of Rac at *Aplysia* synapses. *J Physiol* **583**(Pt 3): 983-1004

Humeau Y, Doussau F, Vitiello F, Greengard P, Benfenati F, Poulain B (2001) Synapsin controls both reserve and releasable synaptic vesicle pools during neuronal activity and short-term plasticity in *Aplysia*. *J Neurosci* **21**(12): 4195-4206

Humeau Y, Luthi A (2007) Dendritic calcium spikes induce bi-directional synaptic plasticity in the lateral amygdala. *Neuropharmacology* **52**(1): 234-243

Inserte J, Najib A, Pelliccioni P, Gil C, Aguilera J (1999) Inhibition by tetanus toxin of sodium-dependent, high-affinity [^{3}H]5-hydroxytryptamine uptake in rat synaptosomes. *Biochem Pharmacol* **57**(1): 111-120

Ishida H, Zhang X, Erickson K, Ray P (2004) Botulinum toxin type A targets RhoB to inhibit lysophosphatidic acid-stimulated actin reorganization and acetylcholine release in nerve growth factor-treated PC12 cells. *J Pharmacol Exp Ther* **310**(3): 881-889

Jahn R, Scheller RH (2006) SNAREs-engines for membrane fusion. *Nat Rev Mol Cell Biol* **7**(9): 631-643

Ji J, Tsuk S, Salapatek AMF, Huang X, Chikvashvili D, Pasyk EA, Kang Y, Sheu L, Tsushima R, Diamant N, Trimble WS, Lotan I, Gaisano HY (2002) The 25-kDa synaptosome-associated protein (SNAP-25) binds and inhibits delayed rectifier potassium channels in secretory cells. *J Biol Chem* **277**(23): 20195-20204

Jin R, Rummel A, Binz T, Brunger AT (2006) Botulinum neurotoxin B recognizes its protein receptor with high affinity and specificity. *Nature* **444**(7122): 1092-1095

Jin Y, Takegahara Y, Sugawara Y, Matsumura T, Fujinaga Y (2009) Disruption of the epithelial barrier by botulinum haemagglutinin (HA) proteins - differences in cell tropism and the mechanism of action between HA proteins of types A or B, and HA proteins of type C. *Microbiology* **155**(Pt 1): 35-45

Jones OM, Brading AF, Mortensen NJ (2004) Mechanism of action of botulinum toxin on the internal anal sphincter. *Br J Surg* **91**(2): 224-228

Kakegawa W, Yuzaki M (2005) A mechanism underlying AMPA receptor trafficking during cerebellar long-term potentiation. *Proc Natl Acad Sci U S A* **102**(49): 17846-17851

Keller JE, Neale EA (2001) The role of the synaptic protein snap-25 in the potency of botulinum neurotoxin type A. *J Biol Chem* **276**(16): 13476-13482

Khairallah G, Andreoletti JB, Jover E, Simon E (2008) Measurement of botulinum toxin activity: towards a new cellular culture assay ? *Ann Chir Plast Esthet* **53**(5): 424-429

Khera M, Somogyi GT, Kiss S, Boone TB, Smith CP (2004) Botulinum toxin A inhibits ATP release from bladder urothelium after chronic spinal cord injury. *Neurochem Int* **45**(7): 987-993

Kitamura M, Iwamori M, Nagai Y (1980) Interaction between *Clostridium botulinum* neurotoxin and gangliosides. *Biochim Biophys Acta* **628**(3): 328-335

Kitasato S (1889) Die Widerstandsfähigkeit der Cholerabacterien gegen das Eintrocknen und gegen Hitze. *Zeitschrift für Hygiene Infektionskrankh* **5**: 134-140

Knight DE (2002) Calcium-dependent transferrin receptor recycling in bovine chromaffin cells. *Traffic* **3**(4): 298-307

Koriazova LK, Montal M (2003) Translocation of botulinum neurotoxin light chain protease through the heavy chain channel. *Nat Struct Biol* **10**(1): 13-18

Kumaran D, Eswaramoorthy S, Furey W, Navaza J, Sax M, Swaminathan S (2009) Domain organization in *Clostridium botulinum* neurotoxin type E is unique: Its implication in faster translocation. *J Mol Biol* **386**(1): 233-245

Kumaran D, Rawat R, Ahmed SA, Swaminathan S (2008) Substrate binding mode and its implication on drug design for botulinum neurotoxin A. *PLoS Pathog* **4**(9): e1000165

Lacy DB, Tepp W, Cohen AC, DasGupta BR, Stevens RC (1998) Crystal structure of botulinum neurotoxin type A and implications for toxicity. *Nat Struct Biol* **5**(10): 898-902

Lamanna C, McElroy OE, Eklund HW (1946) The purification and crystallization of *Clostridium botulinum* type A toxin. *Science* **103**(2681): 613-614

Lan JY, Skeberdis VA, Jover T, Zheng X, Bennett MV, Zukin RS (2001) Activation of metabotropic glutamate receptor 1 accelerates NMDA receptor trafficking. *J Neurosci* **21**(16): 6058-6068

Lewis RS (2007) The molecular choreography of a store-operated calcium channel. *Nature* **446**(7133): 284-287

Li Y, Foran P, Fairweather NF, de Paiva A, Weller U, Dougan G, Dolly JO (1994) A single mutation in the recombinant light chain of tetanus toxin abolishes its proteolytic activity and removes the toxicity seen after reconstitution with native heavy chain. *Biochemistry* **33**(22): 7014-7020

Liu Z, Tearle AW, Nai Q, Berg DK (2005) Rapid activity-driven SNARE-dependent trafficking of nicotinic receptors on somatic spines. *J Neurosci* **25**(5): 1159-1168

Lledo PM, Zhang X, Sudhof TC, Malenka RC, Nicoll RA (1998) Postsynaptic membrane fusion and long-term potentiation. *Science* **279**(5349): 399-403

Lorand L, Graham RM (2003) Transglutaminases: crosslinking enzymes with pleiotropic functions. *Nat Rev Mol Cell Biol* **4**(2): 140-156

Maggio N, Sellitti S, Capano CP, Papa M (2001) Tissue-transglutaminase in rat and human brain: light and electron immunocytochemical analysis and *in situ* hybridization study. *Brain Res Bull* **56**(3-4): 173-182

Mahrhold S, Rummel A, Bigalke H, Davletov B, Binz T (2006) The synaptic vesicle protein 2C mediates the uptake of botulinum neurotoxin A into phrenic nerves. *FEBS Lett* **580**(8): 2011-2014

Maisey EA, Wadsworth JD, Poulain B, Shone CC, Melling J, Gibbs P, Tauc L, Dolly JO (1988) Involvement of the constituent chains of botulinum neurotoxins A and B in the blockade of neurotransmitter release. *Eur J Biochem* **177**(3): 683-691

Marsal J, Egea G, Solsona C, Rabasseda X (1989) Botulinum toxin type A blocks the morphological changes induced by chemical stimulation on the presynaptic membrane of *Torpedo* synaptosomes. *Proc Natl Acad Sci U S A* **86**(1): 372-376

Marxen P, Bigalke H (1991) Tetanus and botulinum A toxins inhibit stimulated F-actin rearrangement in chromaffin cells. *Neuroreport* **2**(1): 33-36

Marxen P, Fuhrmann U, Bigalke H (1989) Gangliosides mediate inhibitory effects of tetanus and botulinum A neurotoxins on exocytosis in chromaffin cells. *Toxicon* **27**(8): 849-859

Matsumura T, Jin Y, Kabumoto Y, Takegahara Y, Oguma K, Lencer WI, Fujinaga Y (2008) The HA proteins of botulinum toxin disrupt intestinal epithelial intercellular junctions to increase toxin absorption. *Cell Microbiol* **10**(2): 355-364

McMahon HT, Foran P, Dolly JO, Verhage M, Wiegant VM, Nicholls DG (1992) Tetanus toxin and botulinum toxins type A and B inhibit glutamate, gamma-aminobutyric acid, aspartate, and met-enkephalin release from synaptosomes. Clues to the locus of action. *J Biol Chem* **267**(30): 21338-21343

Mendieta L, Venegas B, Moreno N, Patricio A, Martínez I, Aguilera J, Limón ID (2009) The carboxyl-terminal domain of the heavy chain of tetanus toxin prevents dopaminergic degeneration and improves motor behavior in rats with striatal MPP+-lesions. *Neurosci Res* **65**(1): 98-106

Meng J, Ovsepian SV, Wang J, Pickering M, Sasse A, Aoki KR, Lawrence GW, Dolly JO (2009) Activation of TRPV1 mediates calcitonin gene-related peptide release, which excites trigeminal sensory neurons and is attenuated by a retargeted botulinum toxin with anti-nociceptive potential. *J Neurosci* **29**(15): 4981-4992

Meunier FA, Colasante C, Faille L, Gastard M, Molgó J (1996) Upregulation of calcitonin gene-related peptide at mouse motor nerve terminals poisoned with botulinum type-A toxin. *Pflugers Arch* **431**(6 Suppl 2): R297-298

Michaelevski I, Chikvashvili D, Tsuk S, Singer-Lahat D, Kang Y, Linial M, Gaisano HY, Fili O, Lotan I (2003) Direct interaction of target SNAREs with the Kv2.1 channel. Modal regulation of channel activation and inactivation gating. *J Biol Chem* **278**(36): 34320-34330

Moffatt JD, Cocks TM, Page CP (2004) Role of the epithelium and acetylcholine in mediating the contraction to 5-hydroxytryptamine in the mouse isolated trachea. *Br J Pharmacol* **141**(7): 1159-1166

Molgó J, Comella JX, Angaut-Petit D, Pecot-Dechavassine M, Tabti N, Faille L, Mallart A, Thesleff S (1990) Presynaptic actions of botulinal neurotoxins at vertebrate neuromuscular junctions. *J Physiol (Paris)* **84**(2): 152-166

Montecucco C, Schiavo G, Gao Z, Bauerlein E, Boquet P, DasGupta BR (1988) Interaction of botulinum and tetanus toxins with the lipid bilayer surface. *Biochem J* **251**(2): 379-383

Morenilla-Palao C, Planells-Cases R, Garcia-Sanz N, Ferrer-Montiel A (2004) Regulated exocytosis contributes to protein kinase C potentiation of vanilloid receptor activity. *J Biol Chem* **279**(24): 25665-25672

Moreno-Lopez B, de la Cruz RR, Pastor AM, Delgado-Garcia JM, Alvarez FJ (1998) Effects of botulinum neurotoxin type A on the expression of gephyrin in cat abducens motoneurons. *J Comp Neurol* **400**(1): 1-17

Morris JL, Jobling P, Gibbins IL (2001) Differential inhibition by botulinum neurotoxin A of cotransmitters released from autonomic vasodilator neurons. *Am J Physiol Heart Circ Physiol* **281**(5): H2124-2132

Morris JL, Jobling P, Gibbins IL (2002) Botulinum neurotoxin A attenuates release of norepinephrine but not NPY from vasoconstrictor neurons. *Am J Physiol Heart Circ Physiol* **283**(6): H2627-2635

Munro P, Kojima H, Dupont JL, Bossu JL, Poulain B, Boquet P (2001) High sensitivity of mouse neuronal cells to tetanus toxin requires a GPI-anchored protein. *Biochem Biophys Res Commun* **289**(2): 623-629

Najib A, Pelliccioni P, Gil C, Aguilera J (1999) *Clostridium* neurotoxins influence serotonin uptake and release differently in rat brain synaptosomes. *J Neurochem* **72**(5): 1991-1998

Najib A, Pelliccioni P, Gil C, Aguilera J (2000) Serotonin transporter phosphorylation modulated by tetanus toxin. *FEBS Lett* **486**(2): 136-142

Neale EA, Bowers LM, Jia M, Bateman KE, Williamson LC (1999) Botulinum neurotoxin A blocks synaptic vesicle exocytosis but not endocytosis at the nerve terminal. *J Cell Biol* **147**(6): 1249-1260

Nevins AK, Thurmond DC (2005) A direct interaction between Cdc42 and vesicle-associated membrane protein 2 regulates SNARE-dependent insulin exocytosis. *J Biol Chem* **280**(3): 1944-1952

Niemann H, Binz T, Grebenstein O, Kurazono H, Thierer J, Mochida S, Poulain B, Tauc L (1991) Clostridial neurotoxins: from toxins to therapeutic tools? *Behring Inst Mitt* **89**: 153-162

Niemann H, Blasi J, Jahn R (1994) Clostridial neurotoxins: new tools for dissecting exocytosis. *Trends Cell Biol* **4**(5): 179-185

Nishiki T, Kamata Y, Nemoto Y, Omori A, Ito T, Takahashi M, Kozaki S (1994) Identification of protein receptor for *Clostridium botulinum* type B neurotoxin in rat brain synaptosomes. *J Biol Chem* **269**(14): 10498-10503

Pastuszko A, Wilson DF, Erecinska M (1986) A role for transglutaminase in neurotransmitter release by rat brain synaptosomes. *J Neurochem* **46**(2): 499-508

Pelliccioni P, Gil C, Najib A, Sarri E, Picatoste F, Aguilera J (2001) Tetanus toxin modulates serotonin transport in rat-brain neuronal cultures. *J Mol Neurosci* **17**(3): 303-310

Penner R, Neher E, Dreyer F (1986) Intracellularly injected tetanus toxin inhibits exocytosis in bovine adrenal chromaffin cells. *Nature* **324**(6092): 76-78

Popoff M, Carlier J-P, Poulain B. (2009) Botulisme. In *Maladies infectieuses*, pp 8-038-H-050. EMC (Elsevier Masson SAS): Paris

Popoff MR, Poulain B (2005) Tétanos: physiopathologie, épidémiologoe, formes cliniques, traitements et vaccination. *Antibiotiques* **7**: 23-41

Poulain B, Popoff M, Molgó J (2008) How do the botulinum neurotoxins block neurotransmitter release: from botulism to the molecular mechanism of action. *The Botulinum J* **1**(1): 14-87

Poulain B, Tauc L, Maisey EA, Wadsworth JD, Mohan PM, Dolly JO (1988) Neurotransmitter release is blocked intracellularly by botulinum neurotoxin, and this requires uptake of both toxin polypeptides by a process mediated by the larger chain. *Proc Natl Acad Sci U S A* **85**(11): 4090-4094

Presek P, Jessen S, Dreyer F, Jarvie PE, Findik D, Dunkley PR (1992) Tetanus toxin inhibits depolarization-stimulated protein phosphorylation in rat cortical synaptosomes: effect on synapsin I phosphorylation and translocation. *J Neurochem* **59**(4): 1336-1343

Prevot AR (1967) A century of Pasteur Institute discoveries in anaerobic animal pathology. *Bull Off Int Epizoot* **67**(11): 1622-1634

Purkiss JR, Welch MJ, Doward S, Foster KA (1997) Capsaicin stimulates release of substance P from dorsal root ganglion neurons *via* two distinct mechanisms. *Biochem Soc Trans* **25**(3): 542S

Putney JW (1986) A model for receptor-regulated calcium entry. *Cell Calcium* **7**: 1-12

Quigley R, Chu PY, Huang CL (2005) Botulinum toxins inhibit the antidiuretic hormone (ADH)-stimulated increase in rabbit cortical collecting-tubule water permeability. *J Membrane Biol* **204**(3): 109-116

Rapp DE, Turk KW, Bales GT, Cook SP (2006) Botulinum toxin type a inhibits calcitonin gene-related peptide release from isolated rat bladder. *J Urol* **175**(3 Pt 1): 1138-1142

Redondo PC, Harper AGS, Salido GM, Pariente JA, Sage SO, Rosado JA (2004) A role for SNAP-25 but not VAMPs in store-mediated Ca^{2+} entry in human platelets. *J Physiol* **558**(1): 99-109

Rosado JA, Redondo PC, Sage SO, Pariente JA, Salido GM (2005a) Store-operated Ca^{2+} entry: Vesicle fusion or reversible trafficking and de novo conformational coupling ? *J Cell Physiol* **205**(2): 262-269

Rosado JA, Redondo PC, Salido GM, Sage SO, Pariente JA (2005b) Cleavage of SNAP-25 and VAMP-2 impairs store-operated Ca^{2+} entry in mouse pancreatic acinar cells. *Am J Physiol Cell Physiol* **288**(1): C214-221

Rossetto O, Morbiato L, Caccin P, Rigoni M, Montecucco C (2006) Presynaptic enzymatic neurotoxins. *J Neurochem* **97**(6): 1534-1545

Rummel A, Eichner T, Weil T, Karnath T, Gutcaits A, Mahrhold S, Sandhoff K, Proia RL, Acharya KR, Bigalke H, Binz T (2007) Identification of the protein receptor binding site of botulinum neurotoxins B and G proves the double-receptor concept. *Proc Natl Acad Sci U S A* **104**(1): 359-364

Rummel A, Häfner K, Mahrhold S, Darashchonak N, Holt M, Jahn R, Beermann S, Karnath T, Bigalke H, Binz T (2009) Botulinum neurotoxins C, E and F bind gangliosides *via* a conserved binding site prior to stimulation-dependent uptake with botulinum neurotoxin F utilising the three isoforms of SV2 as second receptor. *J Neurochem* **110**(6): 1942-1954

Rummel A, Karnath T, Henke T, Bigalke H, Binz T (2004) Synaptotagmins I and II act as nerve cell receptors for botulinum neurotoxin G. *J Biol Chem* **279**(29): 30865-30870

Sakaba T, Stein A, Jahn R, Neher E (2005) Distinct kinetic changes in neurotransmitter release after SNARE protein cleavage. *Science* **309**(5733): 491-494

Sala C, Andreose JS, Fumagalli G, Lomo T (1995) Calcitonin gene-related peptide: possible role in formation and maintenance of neuromuscular junctions. *J Neurosci* **15**(1 Pt 2): 520-528

Salem N, Faundez V, Horng JT, Kelly RB (1998) A v-SNARE participates in synaptic vesicle formation mediated by the AP3 adaptor complex. *Nat Neurosci* **1**(7): 551-556

Sanchez-Prieto J, Sihra TS, Evans D, Ashton A, Dolly JO, Nichols DG (1987) Botulinum toxin A blocks glutamate exocytosis from guinea-pig cerebral cortical synaptosomes. *Eur J Biochem* **165**(3): 675-681

Schantz EJ, Johnson EA (1992) Properties and use of botulinum toxin and other microbial neurotoxins in medicine. *Microbiol Rev* **56**(1): 80-99

Schiavo G, Benfenati F, Poulain B, Rossetto O, Polverino de Laureto P, DasGupta BR, Montecucco C (1992a) Tetanus and botulinum-B neurotoxins block neurotransmitter release by proteolytic cleavage of synaptobrevin. *Nature* **359**(6398): 832-835

Schiavo G, Poulain B, Rossetto O, Benfenati F, Tauc L, Montecucco C (1992b) Tetanus toxin is a zinc protein and its inhibition of neurotransmitter release and protease activity depend on zinc. *EMBO J* **11**(10): 3577-3583

Schiavo G, Rossetto O, Santucci A, DasGupta BR, Montecucco C (1992c) Botulinum neurotoxins are zinc proteins. *J Biol Chem* **267**(33): 23479-23483

Simpson LL (1981) The origin, structure, and pharmacological activity of botulinum toxin. *Pharmacol Rev* **33**(3): 155-188

Singh BR (2006) Botulinum neurotoxin structure, engineering, and novel cellular trafficking and targeting. *Neurotox Res* **9**(2-3): 73-92

Smith CP, Vemulakonda VM, Kiss S, Boone TB, Somogyi GT (2005a) Enhanced ATP release from rat bladder urothelium during chronic bladder inflammation: effect of botulinum toxin A. *Neurochem Int* **47**(4): 291-297

Smith TJ, Hill KK, Foley BT, Detter JC, Munk AC, Bruce DC, Doggett NA, Smith LA, Marks JD, Xie G, Brettin TS (2007) Analysis of the neurotoxin complex genes in *Clostridium botulinum* A1-A4 and B1 strains: BoNT/A3, /Ba4 and /B1 clusters are located within plasmids. *PLoS One* **2**(12): e1271

Smith TJ, Lou J, Geren IN, Forsyth CM, Tsai R, Laporte SL, Tepp WH, Bradshaw M, Johnson EA, Smith LA, Marks JD (2005b) Sequence variation within botulinum neurotoxin serotypes impacts antibody binding and neutralization. *Infect Immun* **73**(9): 5450-5457

Smyth JT, DeHaven WI, Jones BF, Mercer JC, Trebak M, Vazquez G, Putney JJW (2006a) Emerging perspectives in store-operated Ca^{2+} entry: Roles of Orai, Stim and TRP. *Biochim Biophys Acta - Mol Cell Res* **1763**(11): 1147-1160

Smyth LM, Breen LT, Mutafova-Yambolieva VN (2006b) Nicotinamide adenine dinucleotide is released from sympathetic nerve terminals *via* a botulinum neurotoxin A-mediated mechanism in canine mesenteric artery. *Am J Physiol Heart Circ Physiol* **290**(5): H1818-1825

Sollner T, Bennett MK, Whiteheart SW, Scheller RH, Rothman JE (1993) A protein assembly-disassembly pathway in vitro that may correspond to sequential steps of synaptic vesicle docking, activation, and fusion. *Cell* **75**(3): 409-418

Stanley EF, Mirotznik RR (1997) Cleavage of syntaxin prevents G-protein regulation of presynaptic calcium channels. *Nature* **385**(6614): 340-343

Stanley EF, Reese TS, Wang GZ (2003) Molecular scaffold reorganization at the transmitter release site with vesicle exocytosis or botulinum toxin C1. *Eur J Neurosci* **18**(8): 2403-2407

Steinhardt RA, Bi G, Alderton JM (1994) Cell membrane resealing by a vesicular mechanism similar to neurotransmitter release. *Science* **263**(5145): 390-393

Swaminathan S, Eswaramoorthy S (2000) Structural analysis of the catalytic and binding sites of *Clostridium botulinum* neurotoxin B. *Nat Struct Mol Biol* **7**(8): 693-699

Swartling C, Naver H, Pihl-Lundin I, Hagforsen E, Vahlquist A (2004) Sweat gland morphology and periglandular innervation in essential palmar hyperhidrosis before and after treatment with intradermal botulinum toxin. *J Am Acad Dermatol* **51**(5): 739-745

Tacket AC, Rogawski MA (1989) Botulism. In *Botulinum neurotoxin and Tetanus toxin*, Simpson LL (ed) pp 351-357. Academic Press Inc: San Diego

Tarabal O, Caldero J, Ribera J, Sorribas A, Lopez R, Molgó J, Esquerda JE (1996) Regulation of motoneuronal calcitonin gene-related peptide (CGRP) during axonal growth and neuromuscular synaptic plasticity induced by botulinum toxin in rats. *Eur J Neurosci* **8**(4): 829-836

Thompson DE, Brehm JK, Oultram JD, Swinfield TJ, Shone CC, Atkinson T, Melling J, Minton NP (1990) The complete amino acid sequence of the *Clostridium botulinum* type A neurotoxin, deduced by nucleotide sequence analysis of the encoding gene. *Eur J Biochem* **189**(1): 73-81

Tompkins JD, Parsons RL (2006) Exocytotic release of ATP and activation of P2X receptors in dissociated guinea pig stellate neurons. *Am J Physiol Cell Physiol* **291**(5): C1062-1071

Tsuk S, Michaelevski I, Bentley GN, Joho RH, Chikvashvili D, Lotan I (2004) Kv2.1 channel activation and inactivation is influenced by physical interactions of both syntaxin 1A and the t-SNARE complex with the C-terminus of the channel. *Mol Pharmacol* **67**(2): 480-488

Tucker WC, Weber T, Chapman ER (2004) Reconstitution of Ca2+-Regulated Membrane Fusion by Synaptotagmin and SNAREs. *Science* **304**(5669): 435-438

van Ermengem EP (1897) Über einen neuen anaeroben Bacillus und seine Beziehung zum Botulismus. *Z Hyg Infektionskrankh* **26**: 1-56 [English version: Van Ermengem EP (1979) A new anaerobic bacillus and its relation to botulism. *Rev Infect Dis* **1971**: 1701-1719]

Van Heyningen WE (1961) The relation between the fixation and inactivation of tetanus toxin by ganglioside. *Br J Exp Pathol* **42**: 397-398

Verderio C, Coco S, Rossetto O, Montecucco C, Matteoli M (1999) Internalization and proteolytic action of botulinum toxins in CNS neurons and astrocytes. *J Neurochem* **73**(1): 372-379

Verderio C, Grumelli C, Raiteri L, Coco S, Paluzzi S, Caccin P, Rossetto O, Bonanno G, Montecucco C, Matteoli M (2007) Traffic of botulinum toxins A and E in excitatory and inhibitory neurons. *Traffic* **8**(2): 142-153

Verderio C, Pozzi D, Pravettoni E, Inverardi F, Schenk U, Coco S, Proux-Gillardeaux V, Galli T, Rossetto O, Frassoni C, Matteoli M (2004) SNAP-25 modulation of calcium dynamics underlies differences in GABAergic and glutamatergic responsiveness to depolarization. *Neuron* **41**(4): 599-610

Walther DJ, Peter JU, Winter S, Holtje M, Paulmann N, Grohmann M, Vowinckel J, Alamo-Bethencourt V, Wilhelm CS, Ahnert-Hilger G, Bader M (2003) Serotonylation of small GTPases is a signal transduction pathway that triggers platele*t al.*pha-granule release. *Cell* **115**(7): 851-862

Welch MJ, Purkiss JR, Foster KA (2000) Sensitivity of embryonic rat dorsal root ganglia neurons to *Clostridium botulinum* neurotoxins. *Toxicon* **38**(2): 245-258

Wiser O, Trus M, Hernandez A, Renstrom E, Barg S, Rorsman P, Atlas D (1999) The voltage sensitive Lc-type Ca^{2+} channel is functionally coupled to the exocytotic machinery. *Proc Natl Acad Sci U S A* **96**(1): 248-253

Woodard GE, Salido GM, Rosado JA (2008) Enhanced exocytotic-like insertion of Orai1 into the plasma membrane upon intracellular Ca^{2+} store depletion. *Am J Physiol Cell Physiol* **294**(6): C1323-1331

Yamasaki S, Baumeister A, Binz T, Blasi J, Link E, Cornille F, Roques B, Fykse EM, Sudhof TC, Jahn R, *et al.* (1994) Cleavage of members of the synaptobrevin/VAMP family by types D and F botulinal neurotoxins and tetanus toxin. *J Biol Chem* **269**(17): 12764-12772

Yao Y, Ferrer-Montiel AV, Montal M, Tsien RY (1999) Activation of store-operated Ca^{2+} current in *Xenopus* oocytes requires SNAP-25 but not a diffusible messenger. *Cell* **98**(4): 475-485

Toxines et Signalisation – Toxins and Signalling
Rencontres en Toxinologie – Meeting on Toxinology, 2009
Editions de la SFET – SFET Editions
Accès libre en ligne sur le site – Free access on line on the site : http://www.sfet.asso.fr

Activation of heterotrimeric G proteins by Pasteurella multocida *toxin*

Joachim H.C. ORTH, Klaus AKTORIES*

Institut für Experimentelle und Klinische Pharmakologie und Toxikologie, Albert-Ludwigs Universität Freiburg, Albertstraße 25, 79104 Freiburg, Germany.

** Corresponding author ; Tel : +49 (0)761-2035301 ; Fax : +49 (0)761-2035311 ;*
E-mail: Klaus.Aktories@pharmakol.uni-freiburg.de

Abstract

Pasteurella multocida *toxin (PMT) is a 146 kDa protein toxin, which is a major virulence factor of the facultative pathogen bacteria. PMT acts as a deamidase to activate heterotrimeric G proteins. The toxin causes deamidation of an essential glutamine residue of Gα subunits resulting in glutamic acid. This exchange blocks the intrinsic GTPases activity and causes persistent activation of the G protein.*

Activation des protéines G hétérotrimériques par la toxine de Pasteurella multocida

La toxine de Pasteurella multocida *(PMT) est une protéine de 146 kDa, qui constitue le facteur de virulence majeur des bactéries pathogènes facultatives. PMT agit avec une activité déamidase pour activer une protéine G hétérotrimérique. La toxine cause une déamidation d'un résidu glutamine essentiel de la sous-unité Gα ainsi transformé en acide glutamique. Cette modification bloque l'activité GTPasique intrinsèque de la protéine G et induit ainsi son activation permanente.*

Keywords : *Bacterial protein toxin, deamidation, Gα, Gβγ, GTPase.*

Introduction

Pasteurella multocida is a gram-negative coccobacillus colonizing the gastrointestinal tract and nasopharynx of wild and domesticated animals including cats and dogs. The bacteria are facultative pathogens, which cause bite wound infections, pneumonia, endocarditis and septicemia in men. In pigs, *Pasteurella multocida* induces atrophic rhinitis, which is characterized by a loss of nasal turbinate bone (Kamp and Kimman, 1988). Major virulence factor of the pathogen is the 146 kDa protein toxin *Pasteurella multocida* toxin (PMT). This toxin is the causative agent of atrophic rhinitis and was shown to be responsible for the osteolytic activity of bacteria (Chanter, 1990;Kamp *et al.*, 1988;Lax and Chanter, 1990;Lax and Grigoriadis, 2001). Recently the molecular mechanism of the toxin has been elucidated (Orth *et al.*, 2009).

The structure of PMT

PMT consists of 1285 amino acid residues and is structured according to an AB toxin. Whereas the biologically active domain is located in the C-terminal part of the protein (Busch *et al.*, 2001;Pullinger *et al.*, 2001), the N-terminal part is involved in receptor binding and translocation into the cytosol of target cells. The latter part of the toxin exhibits significant sequence similarity with the N-terminal part of the cytotoxic necrotizing factor of *E. coli* that is also involved in binding and translocation.

Recently, the crystal structure of the C-terminal fragment of PMT, covering amino acids 569 to 1285, was solved (Kitadokoro *et al.*, 2007), showing 3 domains. Whereas the C1 domain (residues 569-719) should contribute to intracellular localization of the toxin, the function of the C2 domain (residues 720-1104) remains enigmatic. Most exciting is the C-terminal C3 domain (residues 1105-1285), which resembles a papain-like fold. This domain harbors a catalytic triad characteristic of thiol proteases, harboring the essential amino acids cysteine-1165 (Busch *et al.*, 2001;Ward *et al.*, 1998), histidine-1205 (Orth *et al.*, 2003) and aspartic acid-1220 (*Figure 1*).

PMT activates various cellular signal pathways

PMT is an extremely potent mitogen and stimulates DNA synthesis and proliferation of several cell lines (Dudet *et al.*, 1996;Higgins *et al.*, 1992;Mullan and Lax, 1996;Rozengurt *et al.*, 1990). The mitogenic action of PMT depends on the stimulation of the MAP-kinase ERK (extracellular signal regulated kinase) (Seo *et al.*, 2000). PMT was shown to stimulate phospholipase Cβ1 (PLC-β1). This causes calcium mobilization, accumulation of diacylglycerol and activation of protein kinase C (Staddon *et al.*, 1991). The toxin activates

PLC-β1 by an action on the heterotrimeric G_q protein (Wilson *et al.*, 1997). Heterotrimeric G proteins are grouped in at least 4 families: the G_s-, $G_{i/o}$-, $G_{q/11}$- and $G_{12/13}$- families. It was shown by gene deletion of the α-subunits of G_q and G_{11} that PMT acts on PLC-β *via* $G\alpha_q$ but not *via* $G\alpha_{11}$ (Zywietz *et al.*, 2001). This is remarkable, because $G\alpha_q$ and $G\alpha_{11}$ share 89% of their amino acid residues. The helical domain of $G\alpha_q$ was identified to be essential for activation of PLCβ by PMT (Orth *et al.*, 2004).

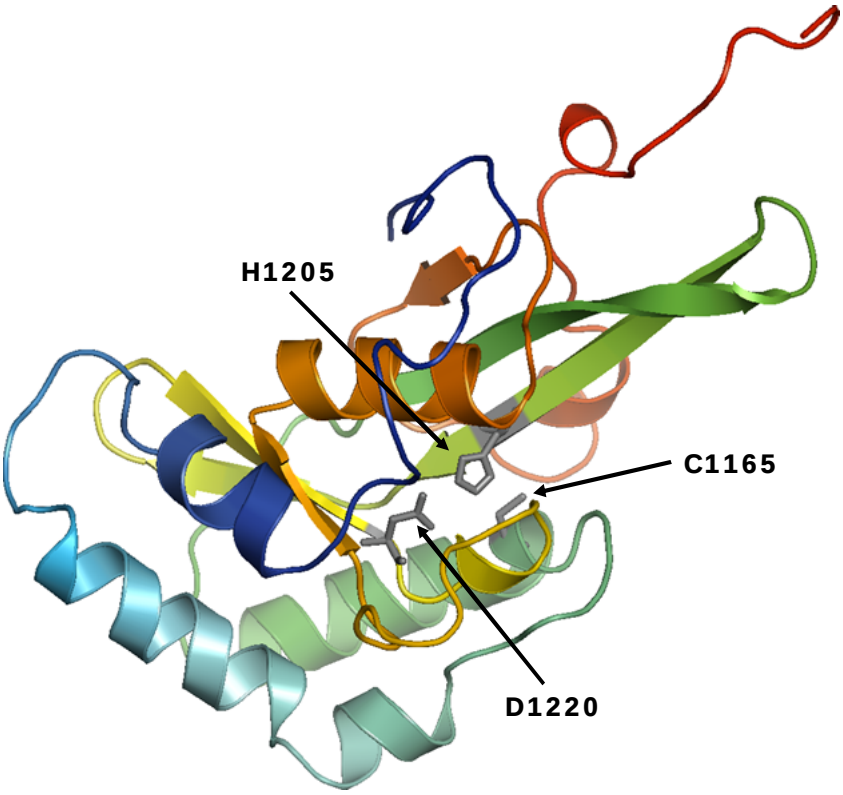

Fig. 1. Structure of the very C-terminal C3 domain harboring the biological activity of PMT. The catalytic triad cysteine-1165, histidine-1205 and aspartic acid-1220 is highlighted in the folds. Image was generated using PyMOL and PDB data file 2EBF.

Fig. 1. *Structure du domaine C-terminal C3 porteur de l'activité biologique de la PMT. La triade catalytique Cys1165, His1205 et Asp1220 est indiquée sur la structure. L'image est générée à l'aide de PyMOL et la référence PDB est 2EBF.*

In addition, PMT activates the small GTPase RhoA, thereby inducing formation of stress fibers, focal adhesions and tyrosine phosphorylation of focal adhesion kinase and paxillin (Dudet *et al.*, 1996;Lacerda *et al.*, 1996). The activation of Rho, ERK and Jun kinase depends not only on G_q (Zywietz *et al.*, 2001). In addition to $G\alpha_q$, PMT activates $G\alpha_{13}$ of the $G_{12/13}$ family, which activates the small GTPase RhoA and causes formation of stress fibers (Orth *et al.*, 2005). More recently, it was observed that PMT is also a potent activator of $G\alpha_i$. PMT inhibits beta-adrenoceptor- or forskolin-induced activation of adenylyl cyclase in cell membrane preparations and in intact cells (Orth *et al.*, 2008). Moreover, G_i activation by PMT results in release of βγ-subunits and activation of PI3-kinase γ (Preuss *et al.*, 2009) (*Figure 2*).

Regulation of heterotrimeric G proteins

Heterotrimeric G proteins consist of the GTP-binding Gα-, the Gβ- and the Gγ-subunits. The G proteins are regulated by a GTPase cycle and are inactive in the heterotrimeric complex with GDP-bound at the α-subunit. Activation starts with the release of GDP. This process is greatly facilitated by interaction with GPCRs, which function as GEF proteins (guanine nucleotide exchange factors). Subsequent binding of GTP causes conformational changes, which promote separation of the α-subunit from the βγ-subunit. Both, the α-subunit and the βγ-subunit activate effector proteins (*e.g.*, enzymes or channels) (Cabrera-Vera *et al.*, 2003). The activated state is terminated by hydrolysis of bound GTP catalyzed by the intrinsic GTPase activity of the α-subunit following re-association to form the inactive heterotrimeric complex. GTP-hydrolysis can be accelerated by GTPase-activating proteins called RGS proteins (regulators of G protein signaling), which speed up inactivation of the G proteins.

The molecular mechanism of PMT

Until recently the molecular mechanism of PMT was enigmatic. Four scientific steps were of major importance to elucidate the mode of action of PMT. First, it was observed that activation of $G\alpha_q$ by PMT is independent of G protein-coupled membrane receptors (GPCR). This was shown by using $G\alpha_q$ subunits, which were C-

terminally deleted in 5 amino acid residues (Orth *et al.*, 2007). Without the C-terminus, the interaction of the G protein with the GPCR is blocked. Second, it was shown that the activation of G_q by PMT is persistent and does not depend on the permanent presence of the toxin (Orth *et al.*, 2007). Third, the finding that G_i is a substrate of the toxin was of special importance for analysis of the molecular mechanism of PMT, because G_i proteins are readily accessible for analyses and recombinant expression. Moreover, G_i is a substrate for ADP-ribosylation by pertussis toxin but activation of G_i by PMT turns the G protein into a pertussis toxin-insensitive state (Orth *et al.*, 2008).

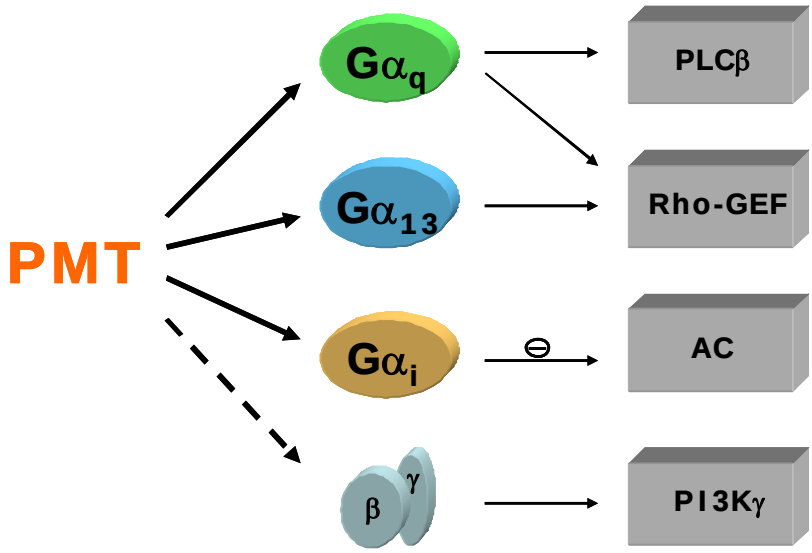

Fig. 2. Overview on PMT-activated G proteins and subsequent signal transduction pathways. PMT activates $G\alpha_q$ to induce stimulation of phospholipase Cβ (PLCβ) and activation of RhoA *via* Rho guanine nucleotide exchange factors (Rho-GEF). Activation of $G\alpha_{12/13}$ leads also to Rho-GEF-dependent RhoA activation. Toxin-induced activation of $G\alpha_i$ inhibits adenylyl cyclase (AC) activity. By activation of the α-subunits, Gβγ-subunits are released, which stimulate *e.g.* phosphoinositide-3-kinase γ (PI3Kγ) activity.

Fig. 2. *Revue des protéines G activées par la PMT et des cascades de signalisation impliquées. PMT active $G\alpha_q$ et induit la stimulation de la phospholipase Cβ (PLCβ) et l'activation de RhoA* via *le facteur d'échange de nucléotide guanine de Rho (Rho-GEF). L'activation de $G\alpha_{12/13}$ conduit aussi à l'activation de RhoA dépendant de Rho-GEF. L'activation de $G\alpha_i$ par la toxine inhibe l'activité de l'adénylate cyclase (AC). En activant la sous-unité α, les sous-unités Gβγ sont relarguées, stimulant ainsi l'activité phosphoinositide-3-kinase γ (PI3Kγ).*

Therefore, ADP-ribosylation by pertussis toxin can be used to monitor PMT effects. However, although having recombinant G_i protein and PMT in hand, initial studies did not show any G protein activation by incubation of purified proteins *in vitro*. The crucial step was the coexpression of $G\alpha_i$ and PMT in *E. coli*. Subsequent *in vitro*-ADP-ribosylation of $G\alpha_i$ by pertussis toxin (to monitor the activation state of the G protein) indicated that wild-type PMT activated $G\alpha_i$, whereas an inactive PMT mutant was without effect. To analyze the reason for the activation of the G-protein, the inherent GTPase activity of the G protein was studied showing that PMT causes inhibition of the hydrolysis of bound GTP. Moreover, RGS proteins were not able to activate the GTPase activity. With the purified PMT-activated $G\alpha_i$ proteins it was possible to perform mass spectrometric analyses. These studies revealed that PMT-treated $G\alpha_i$ has glutamic acid instead of glutamine in position 205 (Orth *et al.*, 2009). These data indicated that PMT causes deamidation of a specific glutamine residue and acts like a deamidase (*Figure 3*).

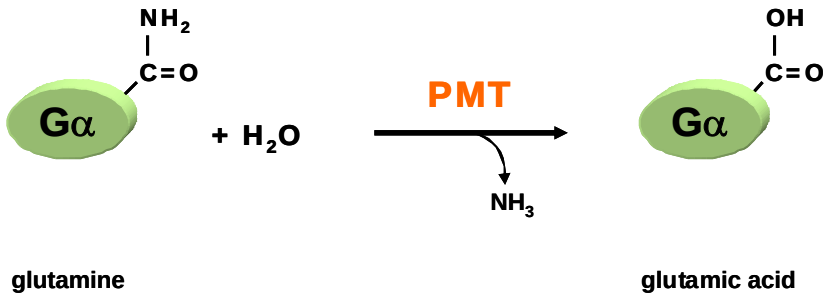

Fig. 3. Scheme of deamidation of PMT. The toxin deamidates a specific glutamine residue essential for GTPase activity of the α-subunit. As compared to transglutaminases PMT utilizes a water molecule as cosubstrate instead of an amine. During the reaction the NH_2-group of the glutamine is released as ammonia and a carboxyl group is formed resulting in a glutamic acid residue.

Fig. 3. *Schéma de l'activité déamidase de la PMT. La toxine déamide le résidu glutamine essentiel à l'activité GTPase de la sous-unité α. Comparé à une activité transglutaminase, la PMT utilise une molécule d'eau comme co-substrat plutôt qu'une amine. Au cours de la réaction, le groupement amine de la glutamine est substitué par le groupement carboxyl de l'acide glutamique.*

The data obtained with recombinant $G\alpha_i$ protein were corroborated with native G_i protein from PMT-pretreated intact cells. Moreover, it was also shown that PMT causes deamidation of glutamine 209 of G_q. This residue of G_q is equivalent to glutamine-205 of $G\alpha_i$. By contrast $G\alpha_{11}$ is not deamidated by PMT, a finding which is in full agreement with the reported insensitivity of $G\alpha_{11}$ towards the toxin (Orth *et al.*, 2009).

Functional consequences of PMT-induced deamidation

Glutamine-205 of $G\alpha_i$ is known to be essential for GTPase activity. This amino acid is not only conserved in heterotrimeric G proteins but also in the superfamily of GTPases including small GTPases like Ras and Rho. The residue has been frequently exchanged for leucine to construct constitutively active G-proteins (De Vivo *et al.*, 1992;Majumdar *et al.*, 2006). Glutamine-205 of $G\alpha_i$ is reportedly a key catalytic residue of the endogenous GTPase activity of $G\alpha_i$ (Coleman *et al.*, 1994;Sprang, 1997;Tesmer *et al.*, 1997). It stabilizes the pentavalent transition state of GTP hydrolyses and is essential for orientation of the incoming water nucleophile. Therefore, the deamidation of this glutamine residue to glutamic acid prevents GTP hydrolysis and turns the $G\alpha$ subunit into a persistently active state. Glutamine-209 of $G\alpha_q$, which is activated by PMT, has the same function in GTP hydrolysis and in regulation of the activity state as glutamine-205 in $G\alpha_i$.

PMT as a member of a family of deamidating toxins

Deamidation of target proteins by bacterial protein toxins is not a unique mechanism of PMT. The cytotoxic necrotizing factors CNF, which are produced by *E. coli* and *Yersinia* strains cause deamidation of Rho proteins at glutamine-61(63), which is functionally equivalent to glutamine-205 of $G\alpha_i$. (Flatau *et al.*, 1997;Schmidt *et al.*, 1997). In addition dermonecrotic toxin (DNT) from *Bordetella pertussis* and *B. bronchiseptica* belongs to the family of deamidating toxins. DNT deamidates Rho proteins at glutamine-61(63) like CNF. Moreover, DNT can act as a transglutaminase on Rho proteins (Horiguchi *et al.*, 1997;Masuda *et al.*, 2000). Notably, PMT has sequence similarity with CNF and DNT in the N-terminal binding and translocation domains. By contrast, PMT has no obvious structural similarity with CNFs or DNT at the C-terminal catalytic domain (Buetow *et al.*, 2001;Kitadokoro *et al.*, 2007). Both PMT and CNF1 share the catalytic residues cysteine and histidine. A third catalytic residue is aspartate in PMT and valine in CNF1 (*Figure 4A*). Accordingly, the 3D-structure of the catalytic domain of PMT is different from that of CNF1. The active site of DNT is similar to PMT and CNF in respect to the catalytic cysteine and histidine. The supposed third catalytic active amino acid residue is not known in the case of DNT. Together with the lack of a crystal structure of DNT, it is not possible to answer the question, whether the catalytic site of PMT is structurally related to the active site of the deamidating and transglutaminating toxin DNT.

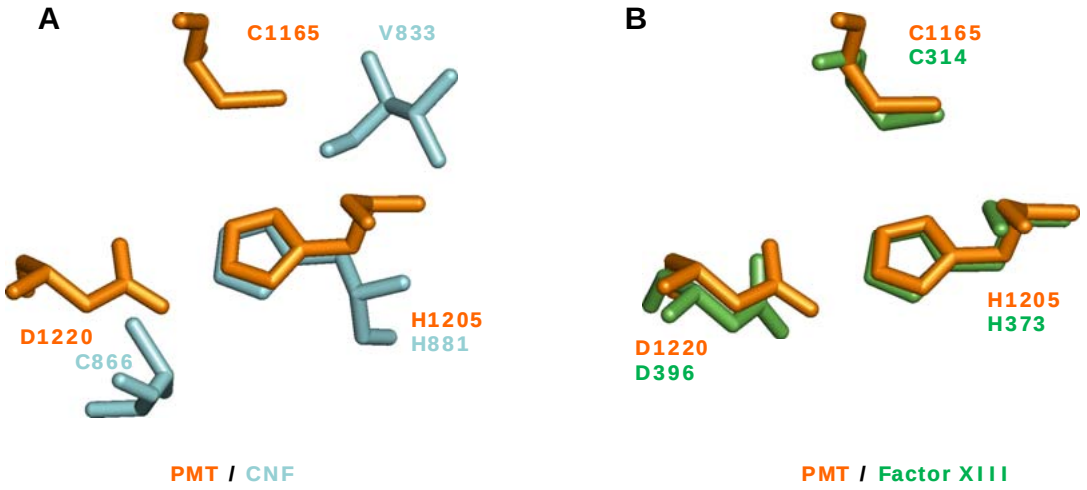

Fig. 4. Differences in catalytic triads of deamidating toxins. (**A**) The catalytic triads of PMT (cysteine-1165, histidine-1205 and aspartic acid-1220) and CNF1 (valine-833, cysteine-866 and histidine-881) are compared after superimposing the catalytic histidines. (**B**) The catalytic triads of PMT (cysteine-1165, histidine-1205 and aspartic acid-1220) and the transglutaminase human factor XIII (cysteine-314, histidine-373 and aspartic acid-396) are compared after superimposing the catalytic histidines. Image was generated using PyMOL and PDB data file 2EBF (PMT), 1HQO (CNF1) and 1GGT (factor XIII).

Fig. 4. *Différences entre les triades catalytiques des toxines à activité déamidase. Les triades catalytiques de la PMT (cystéine-1165, histidine-1205 et acide aspartique-1220) et du CNF1 (valine-833, cystéine-866 et histidine-881) (**A**) ou du facteur XIII* (cystéine-314, histidine-373 et acide aspartique-396) (***B***) *sont comparées après superposition des histidines. L'image est générée par PyMOL et les coordonnées PDB sont 2EBF (PMT), 1HQO (CNF1) et 1GGT (facteur XIII).*

The catalytic triad of PMT is similar to the catalytic triad of the thiol protease papain. This was the reason to suggest that PMT may act as a protease (Kitadokoro *et al.*, 2007). Comparing the structure of thiol proteases with transglutaminases (e.g. human factor XIII) shows high homology. The typ of chemical reaction is comparable: Transglutaminases replace the NH_2-group of an amide with another NH_2-group of an amine. Thiol proteases catalyze the reverse reaction. Deamidases in turn are acting like transglutaminases

using a H_2O instead of an amine. Structural comparison of the active centers of deamidases and thiol proteases with transglutaminases shows similar orientation of the active site. Transglutaminases (e.g. human factor XIII), which possess a similar catalytic triad as PMT proteases, replace the NH_2-group of the amide of glutamine by another amine residue and (Buetow *et al.*, 2001;Chao *et al.*, 2006;Kashiwagi *et al.*, 2002;Noguchi *et al.*, 2001;Pedersen *et al.*, 1994). Although the catalytic triad of PMT perfectly matches the catalytic site of a transglutaminase (*Figure 4B*), until to date no transglutaminating activity could be detected for PMT.

Conclusion

PMT acts as a deamidase to activate heterotrimeric G proteins. The toxin causes deamidation of an essential glutamine residue of Gα subunits resulting in glutamic acid. This exchange blocks the intrinsic GTPases activity and causes persistent activation of the G protein. The mitogenic effect of PMT has been repeatedly discussed as a possible source of cancerogenic activity. Interestingly, it was reported recently that frequent somatic mutations in the gene *Gnaq*, encoding $G\alpha_q$, are found in melanoma of the uvea (46%) and in blue naevi (83%). This mutations results in change of glutamine-209 in a manner similar to the constitutive activation as found for PMT (Van Raamsdonk *et al.*, 2008). It remains to be elucidated whether PMT-induced activation of G proteins by deamidation plays a role in cancer development.

Acknowledgements. *Studies from the laboratory of the authors reported in this review were supported by the Sonderforschungsbereich 746 (project P17).*

References

Buetow L, Flatau G, Chiu K, Boquet P, Ghosh P (2001) Structure of the Rho-activating domain of *Escherichia coli* cytotoxic necrotizing factor 1. *Nature Struct Biol,* **8**: 584-588

Busch C, Orth J, Djouder N, Aktories K (2001) Biological activity of a C-terminal fragment of *Pasteurella multocida* toxin. *Infect Immun,* **69**: 3628-3634

Cabrera-Vera TM, Vanhauwe J, Thomas TO, Medkova M, Preininger A, Mazzoni MR, Hamm HE (2003) Insights into G protein structure, function, and regulation. *Endocr Rev,* **24**: 765-781

Chanter N (1990) Molecular aspects of the virulence of *Pasteurella multocida*. *Can J Vet Res,* **54 Suppl**: S45-S47

Chao X, Muff TJ, Park SY, Zhang S, Pollard AM, Ordal GW, Bilwes AM, Crane BR (2006) A receptor-modifying deamidase in complex with a signaling phosphatase reveals reciprocal regulation. *Cell,* **124**: 561-571

Coleman DE, Berghuis AM, Lee E, Linder ME, Gilman AG, Sprang SR (1994) Structures of active conformations of Gi alpha 1 and the mechanism of GTP hydrolysis. *Science,* **265**: 1405-1412

De Vivo M, Chen J, Codina J, Iyengar R (1992) Enhanced phospholipase C stimulation and transformation in NIH-3T3 cells expressing Q209LGq-alpha-subunits. *J Biol Chem,* **267**: 18263-18266

Dudet LI, Chailler P, Dubreuil D, Martineau-Doize B (1996) *Pasteurella multocida* toxin stimulates mitogenesis and cytoskeleton reorganization in swiss 3T3 fibroblasts. *J Cell Physiol,* **168**: 173-182

Flatau G, Lemichez E, Gauthier M, Chardin P, Paris S, Fiorentini C, Boquet P (1997) Toxin-induced activation of the G protein p21 Rho by deamidation of glutamine. *Nature,* **387**: 729-733

Higgins TE, Murphy AC, Staddon JM, Lax AJ, Rozengurt E (1992) *Pasteurella multocida* toxin is a potent inducer of anchorage-independent cell growth. *Proc Natl Acad Sci U S A,* **89**: 4240-4244

Horiguchi Y, Inoue N, Masuda M, Kashimoto T, Katahira J, Sugimoto N, Matsuda M (1997) *Bordetella bronchiseptica* dermonecrotizing toxin induces reorganization of actin stress fibers through deamidation of Gln-63 of the GTP-binding protein Rho. *Proc Natl Acad Sci USA* **94**: 11623-11626

Kamp EM, Kimman TG (1988) Induction of nasal turbinate atrophy in germ-free pigs, using *Pasteurella multocida* as well as bacterium-free crude and purified dermonecrotic toxin of *P multocida*. *Am J Vet Res,* **49**: 1844-1849

Kashiwagi T, Yokoyama K, Ishikawa K, Ono K, Ejima D, Matsui H, Suzuki E (2002) Crystal structure of microbial transglutaminase from *Streptoverticillium mobaraense*. *J Biol Chem,* **277**: 44252-44260

Kitadokoro K, Kamitani S, Miyazawa M, Hanajima-Ozawa M, Fukui A, Miyake M, Horiguchi Y (2007) Crystal structures reveal a thiol protease-like catalytic triad in the C-terminal region of *Pasteurella multocida* toxin. *Proc Natl Acad Sci U S A,* **104**: 5139-5144

Lacerda HM, Lax AJ, Rozengurt E (1996) *Pasteurella multocida* toxin, a potent intracellularly acting mitogen, induces $p125^{FAK}$ and paxillin tyrosine phosphorylation, actin stress fiber formation, and focal contact assembly in Swiss 3T3 cells. *J Biol Chem,* **271**: 439-445

Lax AJ, Chanter N (1990) Cloning of the toxin gene from *Pasteurella multocida* and its role in atrophic rhinitis. *J Gen Microbiol,* **136**: 81-87

Lax AJ, Grigoriadis AE (2001) *Pasteurella multocida* toxin: the mitogenic toxin that stimulates signalling cascades to regulate growth and differentiation. *Int J Med Microbiol,* **291**: 261-268

Majumdar S, Ramachandran S, Cerione RA (2006) New insights into the role of conserved, essential residues in the GTP binding/GTP hydrolytic cycle of large G proteins. *J Biol Chem,* **281**: 9219-9226

Masuda M, Betancourt L, Matsuzawa T, Kashimoto T, Takao T, Shimonishi Y, Horiguchi Y (2000) Activation of Rho through a cross-link with polyamines catalyzed by *Bordetella* dermonecrotizing toxin. *EMBO J* **19**: 521-530

Mullan PB, Lax AJ (1996) *Pasteurella multocida* toxin is a mitogen for bone cells in primary culture. *Infect Immun,* **64**: 959-965

Noguchi K, Ishikawa K, Yokoyama K, Ohtsuka T, Nio N, Suzuki E (2001) Crystal structure of red sea bream transglutaminase. *J Biol Chem,* **276**: 12055-12059

Orth JH, Blöcker D, Aktories K (2003) His1205 and His 1223 are essential for the activity of the mitogenic *Pasteurella multocida* toxin. *Biochemistry,* **42**: 4971-4977

Orth JH, Fester I, Preuss I, Agnoletto L, Wilson BA, Aktories K (2008) Activation of Galphai and subsequent uncoupling of receptor-Galphai signaling by *Pasteurella multocida* toxin. *J Biol Chem,* **283**: 23288-23294

Orth JH, Lang S, Aktories K (2004) Action of *Pasteurella multocida* toxin depends on the helical domain of Galphaq. *J Biol Chem,* **279**: 34150-34155

Orth JH, Lang S, Preuss I, Milligan G, Aktories K (2007) Action of *Pasteurella multocida* toxin on Galpha(q) is persistent and independent of interaction with G-protein-coupled receptors. *Cell Signal,* **19**: 2174-2182

Orth JH, Lang S, Taniguchi M, Aktories K (2005) *Pasteurella multocida* toxin-induced activation of RhoA is mediated *via* two families of G{alpha} proteins, G{alpha}q and G{alpha}12/13. *J Biol Chem,* **280**: 36701-36707

Orth JH, Preuss I, Fester I, Schlosser A, Wilson BA, Aktories K (2009) *Pasteurella multocida* toxin activation of heterotrimeric G proteins by deamidation. *Proc Natl Acad Sci U S A,* **106**: 7179-7184

Pedersen LC, Yee VC, Bishop PD, Trong IL, Teller DC, Stenkamp RE (1994) Transglutaminase factor XIII uses proteinase-like catalytic triad to crosslink macromolecules. *Protein Sci,* **3**: 1131-1135

Preuss I, Kurig B, Nurnberg B, Orth JH, Aktories K (2009) *Pasteurella multocida* toxin activates Gbetagamma dimers of heterotrimeric G proteins. *Cell Signal,* **21**: 551-558

Pullinger GD, Sowdhamini R, Lax AJ (2001) Localization of functional domains of the mitogenic toxin of *Pasteurella multocida*. *Infect Immun,* **69**: 7839-7850

Rozengurt E, Higgins T, Chanter N, Lax AJ, Staddon JM (1990) *Pasteurella multocida* toxin: potent mitogen for cultured fibroblasts. *Proc Natl Acad Sci USA,* **87**: 123-127

Schmidt G, Sehr P, Wilm M, Selzer J, Mann M, Aktories K (1997) Gln63 of Rho is deamidated by *Escherichia coli* cytotoxic necrotizing factor 1. *Nature,* **387**: 725-729

Seo B, Choy EW, Maudsley WE, Miller WE, Wilson BA, Luttrell LM (2000) *Pasteurella multocida* toxin stimulates mitogen-activated protein kinase *via* $G_{q/11}$-dependent transactivation of the epidermal growth factor receptor. *J Biol Chem,* **275**: 2239-2245

Sprang SR (1997) G protein mechanisms: insights from structural analysis. *Annu Rev Biochem,* **66**: 639-678

Staddon JM, Barker CJ, Murphy AC, Chanter N, Lax AJ, Michell RH, Rozengurt E (1991) *Pasteurella multocida* toxin, a potent mitogen, increases inositol 1,4,5-triphosphate and mobilizes Ca^{2+} in swiss 3T3 cells. *J Biol Chem,* **266**: 4840-4847

Tesmer JJ, Berman DM, Gilman AG, Sprang SR (1997) Structure of RGS4 bound to AlF4--activated G(i alpha1): stabilization of the transition state for GTP hydrolysis. *Cell,* **89**: 251-261

Van Raamsdonk CD, Bezrookove V, Green G, Bauer J, Gaugler L, O'Brien JM, Simpson EM, Barsh GS, Bastian BC (2008) Frequent somatic mutations of GNAQ in uveal melanoma and blue naevi. *Nature,* **457**: 599-602

Ward PN, Miles AJ, Sumner IG, Thomas LH, Lax AJ (1998) Activity of the mitogenic *Pasteurella multocida* toxin requires an essential C-terminal residue. *Infect Immun,* **66**: 5636-5642

Wilson BA, Zhu X, Ho M, Lu L (1997) *Pasteurella multocida* toxin activates the inositol triphosphate signaling pathway in *Xenopus* oocytes *via* G_{qa}-coupled phospholipase C-b1. *J Biol Chem,* **272**: 1268-1275

Zywietz A, Gohla A, Schmelz M, Schultz G, Offermanns S (2001) Pleiotropic effects of *Pasteurella multocida* toxin are mediated by Gq-dependent and -independent mechanisms. Involvement of Gq but not G11. *J Biol Chem,* **276**: 3840-3845

Toxines et Signalisation – Toxins and Signalling
Rencontres en Toxinologie – Meeting on Toxinology, 2009
Editions de la SFET – SFET Editions
Accès libre en ligne sur le site – Free access on line on the site : http://www.sfet.asso.fr

Recent advances in marine phycotoxin mechanisms of action

Amparo ALFONSO[1*], Carmen VALE[1], Natalia VILARIÑO[1], Juan RUBIOLO[2], M. Carmen LOUZAO[1], Mercedes R. VIEYTES[2], Luis M. BOTANA[1]

[1] *USC, Departamentos de Farmacología, Facultad de Veterinaria, Campus Universitario, 27002 Lugo, Spain ;*
[2] *USC, Departamentos de Fisiología, Facultad de Veterinaria, Campus Universitario, 27002 Lugo, Spain*

** Corresponding author ; Tel : 34982252242 ; E-mail : amparo.alfonso@usc.es*

Abstract

Marine toxins are important tools for research due to the variety of their mechanisms of action. Several intracellular signals are involved in these toxin actions. Yessotoxins (YTXs) effect is related to cyclic nucleotides and calcium signals. Azaspiracids (AZAs) modulate cytosolic calcium levels, intracellular pH and cAMP, and anion channels are also involved in their effects. Intracellular calcium levels are not modified, while cAMP levels are slightly increased in the presence of pectenotoxins (PTXs). Na^+-K^+-ATPase has been pointed as the cellular target of palytoxins. Depending on the cellular model used, excitable or non-excitable cells, palytoxin induces an important cytosolic calcium increase modulated either by extracellular calcium and/or sodium. The knowledge of the early signals modulated by marine toxins is very important to later understand the final toxin effects.

Avancées récentes dans les mécanismes d'action des phycotoxines marines

Les toxines marines sont des outils importants pour la recherche à cause de la variété de leurs mécanismes d'action. Plusieurs signaux intracellulaires sont impliqués dans les actions de ces toxines. L'effet des yessotoxines (YTXs) est relié aux signaux des nucléotides cycliques et du calcium. Les azaspiracides (AZAs) modulent les taux de calcium cytosolique, le pH intracellulaire, et l'AMPc, et les canaux anioniques sont aussi impliqués dans leurs effets. Les taux de calcium intracellulaire ne sont pas modifiés alors que les taux d'AMPc sont légèrement augmentés en présence de pecténotoxines (PTXs). L'ATPase Na^+-K^+ a été montrée comme étant la cible cellulaire de la palytoxine. Selon le modèle cellulaire utilisé, cellules excitables ou non excitables, la palytoxine induit une augmentation importante du calcium cytosolique, modulée par le calcium externe et/ou par le sodium. La connaissance des signaux précoces modulés par les toxines marines est très importante pour comprendre, par la suite, les effets finaux des toxines.

Keywords : *Marine phycotoxins, cAMP, cytosolic calcium, intracellular pH.*

Introduction

Cytosolic calcium, cyclic nucleotides and intracellular pH are early steps in the activation pathways of cellular signaling. These signals are the molecular target, or are involved in the initial effect, of some marine phycotoxins that, through complex cross-talks, induce other long-term effects.

Calcium and cyclic nucleotides are second messengers extensively studied and documented in eukaryotic cells. The modulation of cellular pH is associated, in a complex way, to cellular function. Several studies show that the cellular response to a variety of factors, including cytosolic calcium increase, is associated to cytosolic alkalinization, and also a cellular acidification is related to cell death. Therefore, these cellular signals are useful tools to study the mechanism of action of marine toxins.

Yessotoxins

Yessotoxins (YTXs) are polyether compounds produced by the planktonic algae *Proteceratium reticulatum* and *Lingulodinium polyedrum*, and originally isolated from *Patinopecten yessoensis* (Satake, 1997). These toxins present a high acute toxicity after intraperitoneal (i.p.) injection to mice. However, much less toxicity has been reported after oral administration (Munday, 2008b), and no reports about human intoxications caused by YTXs have been published. In the last ten years, many studies have been done to describe YTXs mechanism of action.

Cytosolic calcium levels and calcium channels are early steps in cellular activation. YTX induces a small

increase (40 nM) in cytosolic calcium levels in human lymphocytes. This increase is due to the activation of calcium influx through nifedipine and SKF-96365 sensitive channels. By contrast, in the same cellular model YTX inhibits the influx of calcium either activated by thapsigargin, a tumor-promoting sesquiterpene lactone that inhibits calcium-ATPase from intracellular pools and activates store-operated calcium influx, or by pre-incubation in a calcium-free medium (De la Rosa, 2001a). However, the effect of YTX in cytosolic calcium levels is different depending on the cellular model; the toxin activates calcium release from intracellular pools and influx from extracellular media in some tumor cell lines.

Maitotoxin is a potent, water-soluble, marine phycotoxin associated with ciguatera food poisoning, that induces a high and massive calcium influx in several cellular models. In human lymphocytes, the influx of calcium evoked by maitotoxin was increased in the presence of YTX. This summative result is due to the activation of different channels since each toxin effect is blocked by different drugs (De la Rosa, 2001b).

The chemical structure of YTX, more than 10 contiguous ether rings (Satake, 1996), resembles those of brevetoxins and ciguatoxins. The action of these toxins is mediated through voltage-gated sodium channels. However, YTX did not induce any direct effect on sodium channels; besides, the toxin did not induce any competitive displacement of brevetoxins from site 5 of sodium channels (Inoue, 2003). Therefore, these results point out that the effect of YTX on cytosolic calcium levels is a direct consequence of calcium channels activation and it is not linked to sodium channels as it happens with brevetoxins and ciguatoxins. In summary, calcium influx seems to be an important and necessary event in YTX mechanism of action.

The cyclic nucleotides adenosine 3'-5'cyclic monophosphate (cAMP) and guanine 3'-5'cyclic monophosphate (cGMP) are second messengers related to early activation pathways of cellular signaling. Cells regulate the levels of these second messengers by a balance between adenylyl cyclases (synthesis) and phosphodiesterases (PDEs) (hydrolysis). YTX induces a dose-dependent decrease of cAMP and cGMP levels after 10 minutes incubation (*Figure 1*). These effects are calcium-dependent and can be modified by specific PDEs inhibitors (Alfonso, 2008).

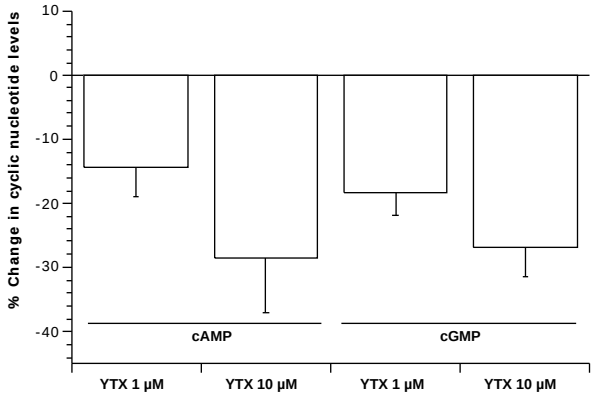

Fig. 1. Changes in cyclic nucleotide levels in the presence of YTX in human lymphocytes.

Fig. 1. *Modifications des niveaux de nucléotides cycliques dans les lymphocytes humains en présence d'YTX.*

PDEs are a group of isozymes that includes several families with different substrate specificity, affinity, sensitivity to inhibitors and tissue localization. YTX induces a dose-dependent increase in PDEs activity (*Figure 2*). In parallel, the toxin decreases cAMP levels and increases the rate of hydrolysis of this second messenger. All these effects can be mimicked by PDEs activators and are modulated by enzyme inhibitors (Alfonso, 2003).

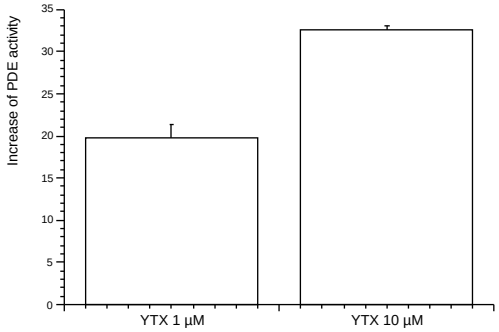

Fig. 2. PDE (from bovine brain) activity in the presence of YTX.

Fig. 2. *Activité de la PDE (du cerveau de bœuf) en présence d'YTX.*

All these results point out PDEs as a cellular target for YTX and calcium as an important key factor for toxin effect. The interaction between these enzymes and YTX was demonstrated by immobilizing PDEs in a biosensor surface. When different concentrations of toxin were added over immobilized PDEs, typical association curves indicative of interaction were observed (*Figure 3*). In these conditions, the value of the kinetic equilibrium dissociation constant (K_D) for YTX-PDEs association is $3.74x10^{-6}$ M (Pazos, 2004). The K_D value increases when YTX molecule is modified, indicating a structure-activity relationship. Under the same conditions, the K_D for hydroxy-YTX-PDEs interaction is $7.36x10^{-6}$ M, and that for carboxy-YTX-PDEs interaction is $23x10^{-6}$ M (Pazos, 2005). These results point out a structure-selectivity of YTX-PDEs association, and agree with the toxic effect decrease observed with some YTX analogs (Tubaro, 2003). The PDEs-YTX interaction was later confirmed by measuring changes in fluorescence polarization of an enzyme-dye conjugate in the presence of YTX (Alfonso, 2005). By using different enzyme families in a sensor surface and by measuring changes in fluorescence polarization, it was concluded that YTX binds to cyclic nucleotide PDE 1, PDE 3 and PDE4, and shows high affinity for exonuclease PDE I (Alfonso, 2005 ; Pazos, 2006).

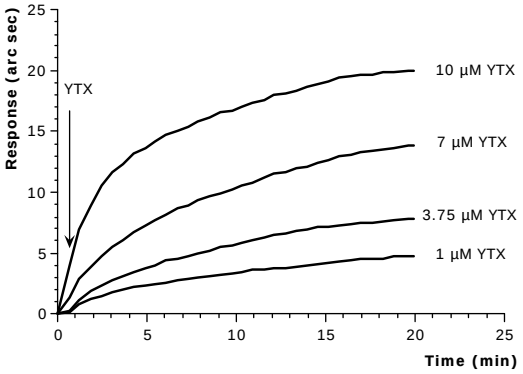

Fig. 3. Typical association PDEs-YTX curves obtained after addition of different concentrations of YTX over immobilized PDEs in a resonant mirror biosensor surface.

Fig. 3. *Association typique PDEs-YTX obtenue après l'addition de différentes concentrations d'YTX sur des PDEs immobilisées à la surface biosensitive d'un miroir à résonnance.*

Other cellular signals were checked to study YTX mechanism of action. On one hand, YTX increases interleukin-2 production in human lymphocytes after 24 hours incubation (Alfonso, 2003). This increase is functionality related to the decrease of cAMP levels since it has been described that cellular function is inhibited by agents that increase the levels of this second messenger in human lymphocytes. In addition, after i.p. YTX injection, the thymus and the immune system are affected, and some inflammatory response is also reported (Franchini, 2004). On the other hand, YTX affects mast cells response (unpublished data). PDEs modulation is often used to regulate the activity of a number of inflammatory cell types, and several drugs used in the asthma therapy interfere within this pathway. Therefore, all these results on immune cells are very interesting and, again, point out PDEs as the YTX target. YTXs often coexist with diarrheic shellfish poisoning (DSP) toxins but their effects are different. DSP toxins are specific and potent inhibitors of Ser/Thr protein phosphatases PP1 and PP2A. These enzymes play a critical role in phosphorylation/dephosphorylation processes within eukaryotic cells. YTX also inhibits protein phosphatases, but the effect is four orders of magnitude lower than the one induced by DSP toxins (Ogino, 1997). Therefore, it has been concluded that YTX mechanism of action was not mediated by the inhibition of these enzymes.

In summary, PDEs are pointed out as an intracellular target for YTX, and the cytosolic calcium levels have an important role in YTX cellular response.

Azaspiracids

Azaspiracids (AZAs) are a family of polyether marine neurotoxins found in shellfish associated to human intoxications. The symptoms related to such poisonings are vomiting, stomach cramps and severe diarrhea, very similar to those of DSP. After i.p. injection of AZA-contaminated shellfish extracts into mice or rats, neurological symptoms with progressive paralysis, fatigue, breathing difficulties and death were reported. In addition to pathological effects, some histological alterations in the pancreas, spleen, liver and thymus have been described. To date, 32 different AZA analogues have been identified, AZA-1 to -32 (Twiner, 2008). The structure of AZA-1 was originally proposed by Satake, Yasumoto and co-workers (Satake, 1998). However, a total synthesis by the Nicolaou group (Nicolaou, 2003a, 2003b) proved the structure to be misassigned. AZAs structures are distinct from other marine toxins and are characterized by a trioxadispiroacetal system fused onto a tetrahydrofuran ring (ABCD domain), an azaspiro-ring system fused onto a 2,9-dioxabicyclo [3.3.1] nonane system (FGHI domain), and a terminal carboxylic acid moiety (James, 2008). The predominant natural analogues are AZA-1, known as azaspiracid, AZA-2, 8-methylazaspiracid, and AZA-3, 22-demethylazaspiracid. Since AZA-1 is the most abundant in nature, most research was centered on its intracellular target. However,

neither its mechanism of action nor its pharmacokinetic behavior have been elucidated, principally because of the lack of standards and reference tissues, even recent advances in purification methodology and toxin stability have been done (Alfonso, 2008a, 2008b).

Several *in vitro* approaches have been undertaken to know the biological target of these toxins. On one hand, *in vitro* experiments reveal that AZAs toxicity is related to the alteration of the actin cytoskeleton arrangement, which is accompanied by changes in cell shape and loss of cell adherence to the substrate. AZA effects on the actin cytoskeleton are irreversible. They take place after long incubation periods and are not related to early activation pathways (Vilariño, 2007, 2008a, 2008c). On the other hand, AZAs treatment increases the phosphorylation state of Jun-N-terminal kinase (JNK) and causes nuclear accumulation of phosphorylated JNK. This pathway is associated to the cytotoxic effect of AZAs (Vale, 2007, 2008c). These results could provide the basis to identify the mechanism of action of this group of toxins. However, it is still important to connect these later activated signaling pathways to early transduction pathways modulated by these toxins.

AZA-1 increases cytosolic calcium and cAMP levels and does not affect intracellular pH. The increase in cytosolic calcium is dependent on both the release of calcium from intracellular pools and the influx from extracellular media (Roman, 2002). AZA-2 and AZA-3 increase cytosolic calcium levels. AZA-2 has the same effect than AZA-1, while AZA-3 does not empty intracellular stores but increases cytosolic calcium levels. AZA-2 did not modify intracellular pH, but AZA-3 slightly alkalinizes the cytosol (0.16 pH units). These toxins increase cAMP levels and the modulation of this pathway inhibits AZA-2- and AZA-3-evoked calcium increase and AZA-3-induced pH rise (Román, 2004). Surprisingly, AZA-4 did not modify cytosolic calcium in resting cells. However, the toxin dose-dependently inhibited the increase in cytosolic calcium levels induced by thapsigargin, even if no effect on calcium release from internal stores was observed. These effects are not related to cAMP pathway. AZA-4 also inhibits maitotoxin-stimulated calcium influx. AZA-4 increases cAMP levels and inhibits intracellular alkalinization independently of the calcium presence (Alfonso, 2005). AZA-5 does not modulate cytosolic calcium or intracellular pH (Alfonso, 2006).

Clearly, each AZA analogue has different effects on the same intracellular targets, depending on their structure (Botana, 2007). The importance of calcium, anionic fluxes and intracellular pH changes in AZAs cytotoxicity is still unknown. However, it seems that some of these primary targets are involved in the mechanism of action of this group of natural toxins.

Pectenotoxins

Pectenotoxins (PTXs) are a group of cyclic polyether macrolide compounds, macrolactones, isolated from the scallop *Patinopectem yessoensis* and produced by dinoflagellates from the genus *Dinophysis*. This group of toxins was first included in the DSP toxins group. However, since the chemical structures and effects of both groups are different, PTXs are classified by themselves.

To date, fifteen PTX analogs have been identified. The toxicity of each analog is related to the structure, and the hydrolysis of the lactone bond rends less toxic compounds (Vilariño, 2008b).

The mechanism of action of PTXs has not been completely elucidated, even though the actin cytoskeleton seems to be involved in the effect of these toxins (Leira, 2002). The rearrangement of the actin cytoskeleton with a reduction of stress fibers and total polymerized actin has been found with different PTX analogs in various cell types (Ares, 2005, 2007 ; Espiña, 2008). PTX-6 does not modify cytosolic calcium levels in human lymphocytes. However, the toxin modifies either calcium influx or release from intracellular pools when it is added in the presence of thapsigargin. When the store-operated calcium influx is activated, PTX-6 inhibits calcium influx (the toxin inhibits calcium entry when the ionic channel is open). Nevertheless, when PTX-6 is added before pools depletion, a significant increase in calcium release from intracellular stores and a consequent higher influx from extracellular media take place. Under these conditions, PTX-6 did not modify cAMP levels in human lymphocytes. However, when the toxin is added in a calcium-free medium, cAMP levels were significantly increased (Leira, 2002).

In summary, actin cytoskeleton is clearly affected by PTXs. The precise mechanism that induces this effect and the relationships with the signal transduction pathways implicated in cell survival, in normal somatic and tumoral cells, are currently been studied. This is important since PTXs show selective cytotoxicity against some tumor cell lines. In addition, these toxins induce apoptosis of p53-deficient cells, which could convert these toxins in very useful therapeutic tools.

Palytoxin

Palytoxin, produced by dinoflagellates from the genus *Ostreopsis* and isolated from marine soft coral of the genus *Palythoa,* is one of the most potent non-protein animal toxins, highly toxic to mammalian cells. This toxin is a large, non-peptide molecule with a chain of more than 100 carbons and a complex variety of organic side groups. Palytoxin was identified on the basis of its striking lethality when injected into mice ; this lethality is mainly due to rapid disruption of cardiac function together with severe vasoconstriction. However, many studies have revealed that PTX affects most cell types by depolarizing the plasma membrane as a secondary consequence of inducing a small-conductance, non-selective cation channel activity. The Na^+-K^+-ATPase has been proposed as the cellular target for palytoxin: by binding to the pump, it converts it into an open channel that stimulates sodium influx and potassium efflux (Vale-Gonzalez, 2007 ; Vale, 2008b). Ostreocin and ovatotoxin are toxins from the same group as palytoxin, with similar effects and toxicities (Vale, 2008a).

Palytoxin induces important calcium increase in excitable cells, secondary to the membrane depolarization. The exact mechanism by which this effect is generated is not clear and seems to vary among the different cell types (Shimahara, 1990 ; Vale, 2006 ; Louzao, 2007). This effect is abolished in the absence of external calcium, and reduced in the absence of sodium or in the presence of inhibitors of calcium and sodium channels. The calcium increase induced by palytoxin was strongly reduced after inhibition of the Na^+/Ca^{2+} exchanger (Vale, 2006) and totally abolished in the presence of ouabain (Vale-Gonzalez, 2007 ; Cagide, 2009). In addition, palytoxin induces an irreversible intracellular acidification of cerebellar neurons. This acidification was due to the influx of extracellular calcium since it was suppressed by the use of a calcium-free medium. This effect was completely prevented by several inhibitors of the plasma membrane calcium ATPase including orthovanadate, lanthanum, high extracellular pH, and caloxin 2A1. The palytoxin-evoked increase in cytosolic calcium levels should activate calcium extrusion through the membrane calcium ATPase which, in turn, decreases intracellular pH by countertransport of H^+ ions. This effect of palytoxin on neuronal pH could be a potential factor contributing to the high cytotoxicity of this toxin in excitable cells (Vale-González, 2007a). This effect on intracellular pH does not occur in non-excitable cells.

Other pharmacological targets have been evaluated in the presence of palytoxin. In this sense, a direct effect on calcium channels at high toxin concentrations, an effect as an agonist for a family of low-conductance channels and/or a calcium increase not related to the depolarizating effect were shown in some cell models (Vale, 2008a). In addition, palytoxin shows high toxicity to several cellular models (Munday, 2008a). Depending on the cell type used, cytotoxicity is related to different pathways and inhibited by different systems (Vale-González, 2007b ; Espiña, 2009). This is currently being evaluated since the results obtained strongly suggest more than one site of action for palytoxin and singular effects depending on the cells studied.

Conclusion

Marine toxins are important tools for research because of their variety of mechanisms of action. The knowledge of the early signals modulated by these toxins is very important to later understand the final toxin effects. YTXs, AZAs, PTXs and palytoxin are toxins with different effects and mechanisms of action. However, all of them share effects on early cellular signal pathways connected with the final toxic effect.

References

Alfonso A, Alfonso C (2008) Yessotoxin: Pharmacology and mechanism of action. Biological Detection. In *Seafood and Freshwater Toxins*. Second Edition, Botana LM (ed) pp 315-327. CRC Press, Taylor and Francis Group: London

Alfonso A, de la Rosa LA, Vieytes MR, Yasumoto T, Botana LM (2003) Yessotoxin a novel phycotoxin, activates phosphodiesterase activity. Effect of yessotoxin on cAMP levels in human lymphocytes. *Biochem Pharmacol* **65**: 193-208

Alfonso A, Román Y, Vieytes MR, Ofuji K, Satake M, Yasumoto T, Botana LM (2005) Azaspiracid-4 inhibits Ca^{2+} entry by stored operated channels in human T lymphocytes. *Biochem Pharmacol* **69**: 1627-1636

Alfonso A, Vieytes MR, Ofuji K, Satake M, Nicolaou KC, Frederick MO, Botana LM (2006) Azaspiracids modulate intracellular pH levels in human lymphocytes. *Biochem Biophys Res Commun* **346**: 1091-1099

Alfonso C, Alfonso A, Otero P, Rodríguez P, Vieyte MR, Elliot C, Higgins C, Botana LM (2008a) Purification of five azaspiracids from mussel samples contaminated with DSP toxins and azaspiracids. *J Chromatogr B Analyt Technol Biomed Life Sci* **865**: 133-140

Alfonso C, Alfonso A, Vieytes MR, Yasumoto T, Botana LM (2005) Quantification of yessotoxin using the fluorescence polarization technique, and study of the adequate extraction procedure. *Anal Biochem* **344**: 266-74

Alfonso C, Rehmann N, Hess P, Alfonso A, Wandscheer CB, Abuín M, Vale C, Otero P, Vieytes MR, Botana LM (2008b) Evaluation of various pH and temperature conditions on the stability of azaspiracids and their importance in preparative isolation and toxicological studies. *Anal Chem* **80**: 9672-9680

Ares IR, Louzao MC, Espiña B, Vieytes MR, Miles CO, Yasumoto T, Botana LM (2007) Lactone ring of pectenotoxins: a key factor for their activity on cytoskeletal dynamics. *Cell Physiol Biochem* **19**: 283-292

Ares IR, Louzao MC, Vieytes MR, Yasumoto T, Botana LM (2005) Actin cytoskeleton of rabbit intestinal cells is a target for potent marine phycotoxins. *J Exp Biol* **208**: 4345-4354

Botana LM, Vale C, Vilariño N (2007) Mechanisms of action of palytoxin and azaspiracids. In *Toxins émergentes: nouveaux risques*, Goudey-Perrière F, Benoit E, Marchot P and Popoff MR (eds) pp 149-156. Lavoisier : Paris

Cagide E, Louzao MC, Espiña B, Vieytes MR, Jaen D, Maman L, Yasumoto T, Botana LM (2009) Production of functionally active palytoxin-like compounds by Mediterranean *Ostreopsis cf. siamensis*. *Cell Physiol Biochem* **23**: 431-440

De la Rosa LA, Alfonso A, Vilariño N, Vieytes MR, Botana LM (2001a) Modulation of cytosolic calcium levels of human lymphocytes by yessotoxin, a novel marine phycotoxin. *Biochem Pharmacol* **61**: 827-833

De la Rosa LA, Alfonso A, Vilariño N, Vieytes MR, Yasumoto T, Botana LM (2001b) Maitotoxin-induced calcium entry in human lymphocytes - Modulation by yessotoxin, Ca^{2+} channel blockers and kinases. *Cell Signal* **13**: 711-716

Espiña B, Cagide E, Louzao MC, Fernandez MM, Vieytes MR, Katikou P, Villar A, Jaen D, Maman L, Botana LM (2009) Specific and dynamic detection of palytoxins by *in vitro* microplate assay with human neuroblastoma cells. *Biosci Rep* **29**: 13-23

Espiña B, Louzao MC, Ares I, Cagide E, Vieytes MR, Vega FV, Rubiolo JA, Miles CO, Suzuki T, Yasumoto T, Botana LM (2008) Cytoskeletal toxicity of pectenotoxins in hepatic cells. *Br J Pharmacol* **155**: 934-944

Franchini A, Marchesini E, Poletti R, Ottaviani E (2004) Lethal and sub-lethal yessotoxin dose-induced morpho-functional alterations in intraperitoneal injected Swiss CD1 mice. *Toxicon* **44**: 83-90

Inoue M, Hirama M, Satake M, Sugiyama K, Yasumoto T (2003) Inhibition of brevetoxins binding to the voltage-gated sodium channel by gambierol and gambieric acid-A. *Toxicon* **41**: 469-474

James KJ, O´Driscoll D, García Fernández J, Furey A (2008) Azaspiracids: Chemistry, bioconversion, and determination. In *Seafood and Freshwater Toxins*. Second Edition, Botana LM (ed) pp 763-773. CRC Press, Taylor and Francis Group: London

Leira F, Cabado AG, Vieytes MR, Roman Y, Alfonso A, Botana LM, Yasumoto T, Malaguti C, Rossini GP (2002) Characterization of F-actin depolymerization as a major toxic event induced by pectenotoxin-6 in neuroblastoma cells. *Biochem Pharmacol* **63**: 1979-1988

Louzao MC, Ares IR, Vieytes MR, Valverde I, Vieites JM, Yasumoto T, Botana LM (2007) The cytoskeleton, a structure that is susceptible to the toxic mechanism activated by palytoxins in human excitable cells. *FEBS J* **274**: 1991-2004

Munday R (2008a) Occurrence and toxicology of palytoxins. In *Seafood and Freshwater Toxins*. Second Edition, Botana LM (ed) pp 693-713. CRC Press, Taylor and Francis Group: London

Munday R., Aune T, Rossini GP (2008b) Toxicology of the yessotoxins. In *Seafood and Freshwater Toxins*. Second Edition, Botana LM (ed) pp 371-380. CRC Press, Taylor and Francis Group: London

Nicolaou KC, Chen DY, Li Y, Qian W, Ling T, Vyskocil S, Koftis TV, Govindasamy M, Uesaka N (2003a) Total synthesis of the proposed azaspiracid-1 structure, Part 2: Coupling of the C1-C20, C21-C27, and C28-C40 fragments and completion of the synthesis. *Angew Chem Int Ed Engl* **42**: 3649-3653

Nicolaou KC, Li Y, Uesaka N, Koftis TV, Vyskocil S, Ling T, Govindasamy M, Qian W, Bernal F, Chen DY, Tachibana H (2003b) Total synthesis of the proposed azaspiracid-1 structure, Part 1: Construction of the enantiomerically pure C1-C20, C21-C27, and C28-C40 fragments. *Angew Chem Int Ed Engl* **42**: 3643-3648

Ogino H, Kumagai M, Yasumoto T (1997) Toxicological evaluation of yessotoxin. *Natural Toxins* **5**: 255-259

Pazos M, Alfonso A, Vieytes M, Yasumoto T, Botana L (2004) Resonant mirror biosensor detection method based on yessotoxin-phosphodiesterase interactions. *Analytical Biochemestry* **335**: 112-118

Pazos M, Alfonso A, Vieytes M, Yasumoto T, Botana L (2005) Kinetic analysis of the interaction between yessotoxin and analogs and immobilized phosphodiesterases using a resonant mirror optical biosensor. *Chem Res Toxicol* **18**: 1155-60

Pazos M, Alfonso A, Vieytes M, Yasumoto T, Botana L (2006) Study of the interaction between different phosphodiesterases and yessotoxin using a resonant mirror biosensor. *Chem Res Toxicol* **19**: 794-800

Roman Y, Alfonso A, Louzao MC, de la Rosa LA, Leira F, Vieites JM, Vieytes MR, Ofuji K, Satake M, Yasumoto T, Botana LM (2002) Azaspiracid-1, a potent, nonapoptotic new phycotoxin with several cell targets. *Cell Signal* **14**: 703-716

Román Y, Alfonso A, Vieytes MR, Ofuji K, Satake M, Yasumoto T, Botana LM (2004) Effects of azaspiracids 2 and 3 on intracellular cAMP, [Ca^{2+}], and pH. *Chem Res Toxicol* **17**: 1338-1349

Satake M, MacKenzie L, Yasumoto T (1997) Identification of *Protoceratium reticulatum* as the biogenetic origin of yessotoxin. *Nat Toxins* **5**: 164-167

Satake M, Ofuji K, Naoki H, James KJ, Furey A, McMahon T, Silke J, Yasumoto T (1998) Azaspiracid, a new marine toxin having unique spiro ring assemblies, isolated from Irish mussels, *Mytilus edulis*. *J Am Chem Soc* **120**: 9967-9968

Satake M, Terasawa K, Kadowaki Y, Yasumoto T (1996) Relative configuration of yessotoxin and isolation of two new analogs from toxic scallops. *Tetrahedron Lett* **37**: 5955-5958

Shimahara T, Molgo J (1990) Palytoxin enhances quantal acetylcholine release from motor nerve terminals and increases cytoplasmic calcium levels in a neuronal hybrid cell line. *Life Sci Adv Pharmacol* **9**: 785-792

Tubaro A, Sosa S, Carbonatto M, Altinier G, Vita F, Melato M, Satake M, Yasumoto T (2003) Oral and intraperitoneal acute toxicity studies of yessotoxin and homoyessotoxins in mice. *Toxicon* **41**: 783-792

Twiner MJ, Rehmann N, Hess P, Doucette GJ (2008) Azaspiracid shellfish poisoning: a review on the chemistry, ecology, and toxicology with an emphasis on human health impacts. *Mar Drugs* **6**: 39-72

Vale C (2008a) Palytoxins: Pharmacology and biological detection methods. In *Seafood and Freshwater Toxins*. Second Edition, Botana LM (ed) pp 675-691. CRC Press, Taylor and Francis Group: London

Vale C, Alfonso A, Suñol C, Vieytes MR, Botana LM (2006) Modulation of calcium entry and glutamate release in cultured cerebellar granule cells by palytoxin. *J Neurosci Res* **83**: 1393-1406

Vale C, Alfonso A, Vieytes MR, Romarís XM, Arévalo F, Botana AM, Botana LM (2008b) *In vitro* and *in vivo* evaluation of paralytic shellfish poisoning toxin potency and the influence of the pH of extraction. *Anal Chem* **80**: 1770-1776

Vale C, Gómez-Limia B, Nicolaou KC, Frederick MO, Vieytes MR, Botana L (2007) The c-Jun-N-terminal kinase is involved in the neurotoxic effect of azaspiracid-1. *Cell Physiol Biochem* **20**: 957-966

Vale C, Wandscheer C, Nicolaou KC, Frederick MO, Alfonso C, Vieytes MR, Botana LM (2008c) Cytotoxic effect of azaspiracid-2 and azaspiracid-2-methyl ester in cultured neurons: involvement of the c-Jun N-terminal kinase. *J Neurosci Res* **86**: 2952-2962

Vale-González C, Gómez-Limia B, Vieytes MR, Botana LM (2007a) Effects of the marine phycotoxin palytoxin on neuronal pH in primary cultures of cerebellar granule cells. *J Neurosci Res* **85**: 90-98

Vale-González C, Gómez-Limia B, Vieytes MR, Botana LM (2007b) Mitogen-activated protein kinases regulate palytoxin-induced calcium influx and cytotoxicity in cultured neurons. *Br J Pharmacol* **152**: 256-266

Vale-Gonzalez C, Pazos MJ, Alfonso A, Vieytes MR, Botana LM (2007) Study of the neuronal effects of ouabain and palytoxin and their binding to Na,K-ATPases using an optical biosensor. *Toxicon* **50**: 541-552

Vilariño N (2008a) Marine toxins and the cytoskeleton: azaspiracids. *FEBS J* **275**: 6075-6081

Vilariño N, Espiña B (2008b) Pharmacology of pectenotoxins. In *Seafood and Freshwater Toxins*. Second Edition, Botana LM (ed) pp 361-369. CRC Press, Taylor and Francis Group: London

Vilariño N, Nicolaou KC, Frederick MO, Cagide E, Alfonso C, Alonso E, Vieytes MR, Botana LM (2008c) Azaspiracid substituent at C1 is relevant to *in vitro* toxicity. *Chem Res Toxicol* **21**: 1823-1831

Vilariño N, Nicolaou KC, Frederick MO, Vieytes MR, Botana LM (2007) Irreversible cytoskeletal disarrangement is independent of caspase activation during in vitro azaspiracid toxicity in human neuroblastoma cells. *Biochem Pharmacol* **74**: 327-335

Toxines et Signalisation – Toxins and Signalling
Rencontres en Toxinologie – Meeting on Toxinology, 2009
Editions de la SFET – SFET Editions
Accès libre en ligne sur le site – Free access on line on the site : http://www.sfet.asso.fr

Proteomic analyses for the characterization of toxicity pathways and their interactions in human cells : learning from marine biotoxins

Gian Luca SALA[1], Giuseppe RONZITTI[2], Mirella BELLOCCI[1], Makoto SASAKI[3], Haruhiko FUWA[3], Takeshi YASUMOTO[4], Albertino BIGIANI[1], Gian Paolo ROSSINI[1*]

[1] *Dipartimento di Scienze Biomediche, Università di Modena e Reggio Emilia, Via Campi 287, 41100 Modena, Italy ;* [2] *Present address: Neuroscience and Brain Technologies Department, Italian Institute of Technology, Via Morego 30, 16163 Genova, Italy ;* [3] *Graduate School of Life Sciences, Tohoku University, Sendai 981-8555, Japan ;* [4] *Okinawa Science and Technology Promotion Center, Okinawa, 904-2234, Japan*

**Corresponding author ; Tel : +39.059.205.5388 ; Fax : +39.059.205.5410 ; E-mail : rossini@unimore.it*

Abstract

The analysis of molecular families by "omic" approaches is increasingly used in investigations onto signaling pathways. We have exploited proteomic analyses to probe the molecular responses of living systems exposed to marine biotoxins, and found that these components cause changes in the levels of expression of many proteins in MCF-7 cells. By an integration of different means of protein detection and analysis, we observed changes in molecular components that reveal the involvement of complex sets of covalent modifications of hsp 27 in the signaling pathways responsible for the death response of MCF-7 cells exposed to okadaic acid. The integration of results obtained by complementary analytical techniques and means of analyte detection facilitates a better exploitation of proteomic approaches.

La caractérisation de voies de signalisation reliées à la toxicité et leurs interactions dans les cellules humaines par l'analyse protéomique : apprendre par les biotoxines marines

L'analyse par les méthodes « omiques » de familles de molécules est de plus en plus utilisée pour les études des voies de signalisation. Nous avons utilisé l'analyse protéomique pour étudier les réponses moléculaires des systèmes biologiques qui ont été exposés aux biotoxines marines, et nous avons trouvé que ces substances changent les concentrations de plusieurs protéines dans les cellules MCF-7. L'intégration des différentes méthodes d'analyse nous a permis de détecter des changements moléculaires qui suggèrent l'existence d'un ensemble complexe de modifications covalentes des protéines hsp 27 dans les voies de signalisation qui causent la mort des cellules MCF-7 exposées à l'acide okadaïque. L'intégration des résultats obtenus par des techniques analytiques et de détection complémentaires soutient une meilleure exploitation des méthodes protéomiques.

Keywords : *Heat shock protein, protein phosphorylation, proteome, shellfish contamination, signaling pathways.*

Introduction

The characterization of the molecular mechanism of action of toxins is a key achievement for the understanding of adverse effects and their dynamics in living systems.

The identification of the molecular targets of toxins is only one, albeit important, step towards the clarification of their mechanisms of action, whose full characterization stems from a description of the mechanistic links existing in the chain of events that brings about individual responses in living systems. In this perspective, the mechanisms of actions of toxins can be viewed as signaling pathways (Rossini, 2005), and the capacity of toxins to alter, either directly or indirectly, the regulatory mechanisms of proper cellular functioning, is the basis for the contention that toxicity pathways essentially represent normal mechanisms of cellular functioning that, whenever sufficiently perturbed by a noxious stimulus, lead to adverse effects in sensitive systems (Andersen *et al*., 2005 ; National Research Council, 2007).

The level of complexity inherent into the characterization of toxicity pathways is a challenging obstacle to the development of studies on the molecular mechanisms of action of toxins in living systems, but recent technological achievements have allowed investigations at a system level. The "omic" approaches, in fact,

that provide accounts of full molecular families in living systems, are paving the way for the description of large sets of molecules and their changes over time in perturbed systems (Benninghoff, 2007).

We have exploited the potential of proteomic approaches to probe the molecular responses of living systems exposed to marine biotoxins. The model systems we have used in our studies have included both naturally contaminated samples and cultured cells. In the first case, we have investigated onto the changes that may occur in the proteome of digestive glands as a consequence of shellfish contamination with a marine biotoxin (Ronzitti *et al*., 2008). The exposure of cultured cells to toxins under controlled *in vitro* conditions, in turn, is being exploited to characterize toxicity pathways of marine biotoxins and their interactions (Sala *et al*., 2009).

The wealth of data provided by those studies has shown the potential of "omic" approaches for the characterization and understanding of toxicity pathways and their networks.

In this contribution, we wish to outline the general features of our studies on the mechanisms of action of biotoxins by proteomic analyses using cultured cells, and highlight some critical issues that we have encountered in the course of those investigations, to support a wider exploitation of "omics" in the characterization of toxicity pathways.

Materials and methods

The methodology used in our studies has been previously reported (Sala *et al*., 2009). In summary, the MCF-7 human breast cancer cell line has been used in our studies, and the characterization of the protein profiles of these cells under different experimental conditions has been pursued by established procedures. Protein extracts were prepared by cell lyses with buffers containing detergents, and the proteins contained in the extracts were separated by two dimensional gel electrophoresis. The protein profiles were next obtained by protein staining, image capture and its analysis using standardized procedures and software. The proteins of interest were found by matching of images of virtual gels, and based on significant quantitative differences of protein spots, as set by the software. Proteins in relevant spots were subjected to tryptic digestion, the characterization of peptides was then obtained by mass spectrometry, and their MASCOT analysis led to identification of individual proteins.

Results

Our original study on the effects of okadaic acid (OA) and gambierol (Gb) showed that these two toxins modify the protein profile in MCF-7 cells. The phosphorylation state of the hsp 27 protein, in particular, was affected by OA, but not Gb (Sala *et al*., 2009), in keeping with the different mechanisms of action of the two toxins (Bialojan and Takai, 1988 ; Ghiaroni *et al*., 2005).

That conclusion was based on the different intensity of protein spots detectable in the stained gels, as shown in *Figure 1*, where components A and B were clearly detectable in the extracts from OA-treated cells but were either absent (A) or barely detectable (B) in the extracts prepared from control and Gb-treated cells. The mass spectra of peptides obtained from spots A and B indicated that the most abundant isoform of hsp 27 present in those spots included the phosphorylated protein in Ser_{82}, whereas the most abundant protein of spot B consisted of an hsp 27 isoform containing phosphorylated residues Ser_{82} and Ser_{83}. Smaller changes, in turn, were detected in the relative intensities of other hsp 27 isoforms present in the extracts (Sala *et al*., 2009).

In order to obtain a better characterization of experimental findings and confirm the results obtained by densitometric scanning of stained gels, immunoblotting analyses of proteins can be employed. This procedure was used for analysis of hsp 27 in our cell extracts, and, in keeping with the MS results outlined above, we employed antibodies (Ab) recognizing either total hsp 27 (including both non-phosphorylated and phosphorylated protein isoforms) or the hsp 27 phosphorylated in Ser_{82} (*Figure 2*).

The immunoblotting procedure was employed after separation by two dimensional electrophoresis of proteins, because one-dimensional SDS-PAGE may not resolve components having similar molecular masses but different isoelectric points, as is the case for hsp 27 isoforms differing in their phosphorylation state. The results we obtained are reported in *Figure 2*, and show that three major spots are detectable with the ab recognizing total hsp 27 in extracts prepared from control cells. Two spots were detected when the same sample was immunoblotted with the ab specific for hsp 27 isoforms phosphorylated in Ser_{82}, and the alignment of spots using an internal protein standard revealed that they consist of components A and B in *Figure 1*. Only component B was detected with the Ab recognizing total hsp 27, suggesting that very low concentrations of component A were present in samples from control cells, that could be detected only by immunoblotting analysis, and represented a "tail" on the left of component B visualized by the Ab recognizing total hsp 27 (*Figure 2*, upper panel, left). Similar findings were obtained with extracts from Gb-treated cells (*Figure 2*). The extracts prepared from OA-treated cells, in turn, contained six hsp 27 isoforms detectable with the Ab recognizing total hsp 27. Four of those isoforms were also detected with the Ab specific for hsp 27 phosphorylated in Ser_{82}, including prominent spots of components A and B, confirming the results obtained with stained gels (*Figure 1*), and indicating that two other hsp 27 isoforms phosphorylated in Ser_{82} exist in MCF-7 OA-treated cells, but their low levels would not allow detection in stained gels (*Figure 1*).

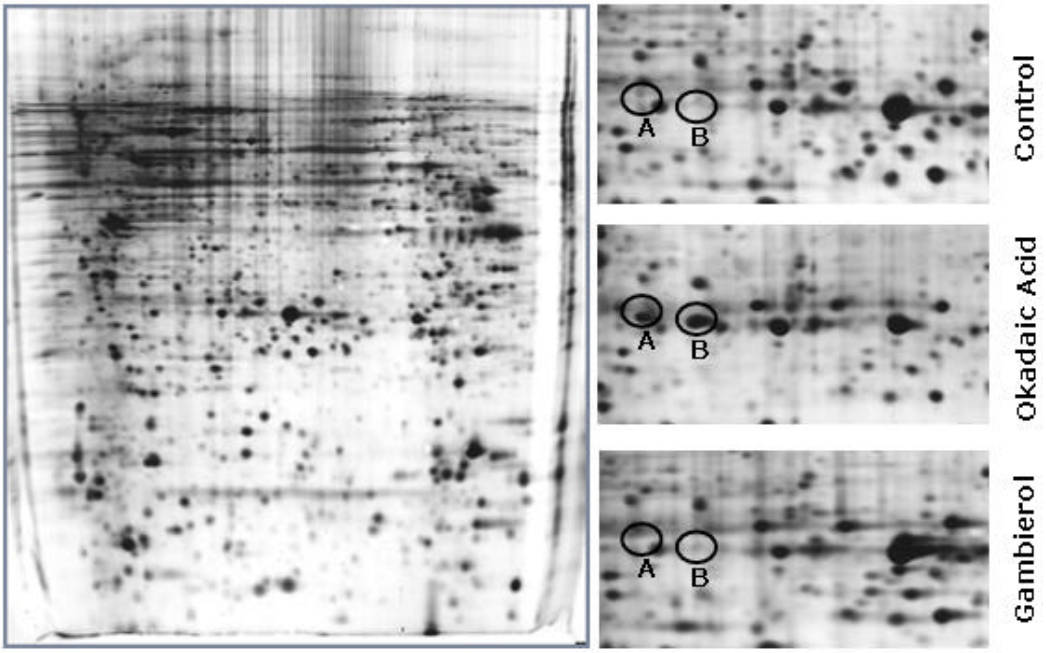

Fig. 1. Effect of okadaic acid and gambierol on the proteome of MCF-7 cells. Cells were treated for 24 h with either ethanol as control, 50 nM okadaic acid, or 50 nM gambierol as indicated, before being used for the preparation of the cell extracts, that were subjected to two dimensional electrophoresis. The gel obtained in a typical experiment after silver staining is shown on the left, and the portions of the gels containing the relevant hsp 27 isoforms in the three different experimental conditions are on the right.

Fig. 1. *Effet de l'acide okadaïque et du gambiérol sur le protéome des cellules MCF-7. Les cellules ont été exposées 24 h à l'acide okadaïque 50 nM, au gambiérol 50 nM ou à l'éthanol comme contrôle, comme indiqué, avant d'être utilisées pour la préparation des extraits cellulaires qui ont été fractionnés par électrophorèse bidimensionelle. Un gel typique (coloration argentique) est montré sur la gauche, et les portions des gels qui contiennent les isoformes des protéines hsp 2 obtenues dans les trois conditions différentes, sont montrées sur la droite.*

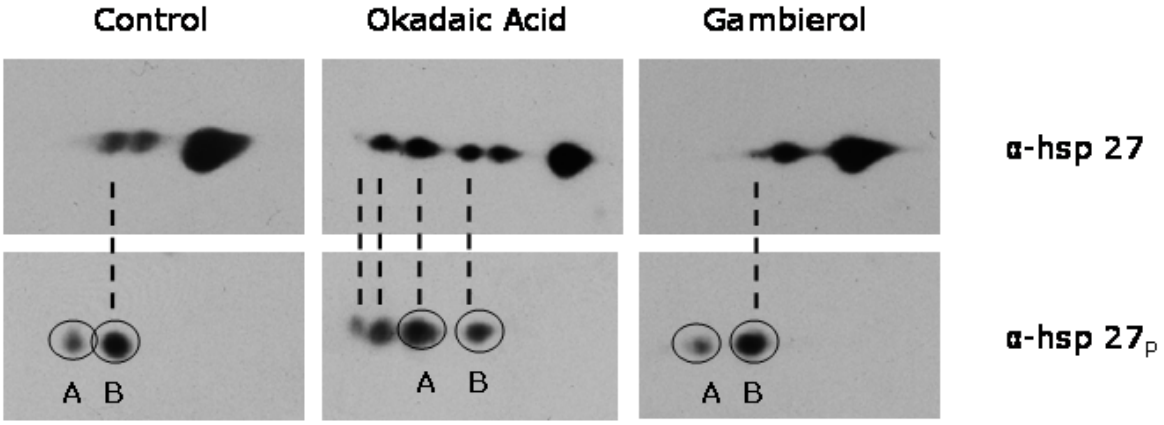

Fig. 2. Effect of okadaic acid and gambierol on the hsp 27 proteins in MCF-7 cells. Cells were treated for 24 h with either vehicle, 50 nM okadaic acid, or 50 nM gambierol, as indicated, before being used for the preparation of the cell extracts, that were subjected to two dimensional electrophoresis. At the end of the electrophoresis, proteins were transferred onto a nitrocellulose membrane and were subjected to immunoblotting, using antibodies recognizing either total hsp 27 or the hsp 27 phosphorylated in Ser_{82}, as indicated. The antibodies were obtained from Cell Signaling Technology, and the immunoblotting procedure was as already reported (Malaguti and Rossini, 2002), adjusting the antibody concentrations and the incubation conditions, following the information sheet of individual products.

Fig. 2. *Effet de l'acide okadaïque et du gambiérol sur les protéines hsp 27 des cellules MCF-7. Les cellules ont été exposées 24 h à l'acide okadaïque (50 nM), au gambierol (50 nM) ou à l'éthanol, comme indiqué, avant d'être utilisées pour la préparation des extraits cellulaires, qui ont été fractionnées par électrophorèse bidimensionnelle. Après l'électrophorèse, les protéines ont été transférées sur une membrane de nitrocellulose et analysées par immunoblotting, avec des anticorps dirigés contre la hsp 27 totale (hsp 27), ou la hsp 27 phosphorylée sur la* Ser_{82} *(hsp* 27_P*). Les anticorps ont été obtenus par Cell Signaling Technology, et la procédure d'analyse par immunoblotting (Malaguti et Rossini, 2002) a été réalisée en accord avec les indications contenues dans la brochure des anticorps.*

Discussion

The proteomic analysis of extracts from MCF-7 cells had revealed that the cellular pool of hsp 27 is affected both by OA and Gb, that cause qualitative and quantitative changes of these particular protein isoforms and fragments (Sala *et al*., 2009). In this system, OA seems to favour the stabilization of the phosphorylated forms of the hsp 27 protein and to induce cell death, whereas Gb does not significantly alter the phosphorylated pool of the protein and is not causing significant cell death under our experimental conditions (Malaguti and Rossini, 2002 ; Sala *et al*., 2009).

The general model of hsp 27 functioning in cell stress responses with regard to the death /survival opposition is primarily based on the equilibrium between phosphorylated and non-phosphorylated pools of this protein and their supramolecular arrangements (Lanneau *et al*., 2008).

The data we obtained by probing the effects of OA and Gb on the hsp 27 system, using antibodies recognizing different hsp 27 isoforms, confirm our original observations, and provide additional data showing that complex sets of phosphorylated hsp 27 isoforms exist in MCF-7 cells. Several considerations can be discussed, but we will confine our attention onto major issues raised by the data we have reported in this study.

In the first instance, a direct inspection of results reported in *Figure 2*, reveals that at least four hsp 27 isoforms phosphorylated in Ser_{82} can be detected by immunoblotting in extracts prepared from cells exposed to OA. This finding has impacts on both the mechanistic and the methodological aspects of an investigation aimed at characterizing the molecular events involved in a cell's response to an external signal by the use of proteomic tools.

On the methodological side, four hsp 27 isoforms phosphorylated in Ser_{82} have been detected by immunoblotting, whereas only two of them can be detected by gel staining (Sala *et al*., 2009). These findings imply that the analytical potential of proteomic analyses is best exploited when complementary means of detection are applied to methodologies of protein separation.

In mechanistic terms, in turn, the detection of low levels of two isoforms of hsp 27 phosphorylated in Ser_{82} in control cells indicate that the functional roles of the hsp 27 system should depend on defined sets of phosphorylated amino-acids, rather than a simple opposition between phosphorylated and non-phosphorylated states of the protein in the cells. Hence, the cell fate would most likely be controlled by the relative levels of individual hsp 27 isoforms in this experimental model.

Several interpretations are available to account for the four hsp 27 isoforms phosphorylated in Ser_{82} that we detected, but further data are needed to provide robust experimental support to possible proposals. Within these limitations, the detection of four components that have been separated in the course of iso-electrofocusing would imply that they differ with regard to the number of phosphate groups covalently bound to amino-acid residues in the hsp 27 protein, one of which being Ser_{82}.

Our original data showed that several aspects of molecular responses triggered by OA and Gb are maintained also when MCF-7 cells are challenged with a mixture of these toxins (Sala *et al*., 2009). The immunoblotting analyses we have used in this study are a drive for further investigations, to get more data on the details of molecular mechanisms involved in the combined response and the role played by the hsp 27 system.

Conclusions

The potential of proteomic analyses in the characterization of molecular responses of biological systems to internal and external signals is being uncovered. The use of proteomic tools in the study of signaling pathways of marine biotoxins are providing increased amounts of data allowing a detailed characterization of their molecular modes of action, and the integration of results obtained by complementary analytical techniques and means of analyte detection appears of particular value for a full exploitation of experimental data.

Acknowledgements. *Our investigations are supported by the Italian MUR, MS and by Fondazione Cassa di Risparmio di Modena.*

References

Andersen ME, Dennison JE, Thomas RS, Conolly RB (2005) New directions in incidence-dose modeling. *Trends Biotechnol* **23**: 122-127

Benninghoff AD (2007) Toxicoproteomics – The next step in the evolution of environmental biomarkers ? *Toxicol Sci* **95**: 1-4

Bialojan C, Takai A (1988) Inhibitory effect of a marine sponge toxin, okadaic acid, on protein phosphatases. *Biochem J* **256**: 283-290

Ghiaroni V, Sasaki M, Fuwa H, Rossini GP, Scalera G, Yasumoto T, Pietra P, Bigiani A (2005) Inhibition of voltage-gated potassium currents by gambierol in mouse taste cells. *Toxicol Sci* **85**: 657-665

Lanneau D, Brunet M, Frisan E, Solary E, Fontenay M, Garrido C (2008) Heat shock proteins: essential proteins for apoptosis regulation. *J Cell Mol Med* **12**: 743-761

Malaguti C, Rossini GP (2002) Recovery of cellular E-cadherin precedes replenishment of estrogen receptor and estrogen-dependent proliferation of breast cancer cells rescued from a death stimulus. *J Cell Physiol* **192**: 171-181

National Research Council of the National Academies (2007) *Toxicity testing in the 21st century*. The National Academies Press: Washington

Ronzitti G, Milandri A, Scortichini G, Poletti R, Rossini GP (2008) Protein markers of algal toxin contamination in shellfish. *Toxicon* **52**: 705-713

Rossini GP (2005) Functional assays in marine biotoxin detection. *Toxicology* **208**: 451-462

Sala GL, Ronzitti G, Sasaki M, Fuwa H, Yasumoto T, Bigiani A, Rossini GP (2009) Proteomic analysis reveals multiple patterns of response in cells exposed to a toxin mixture. *Chem Res Toxicol* **22**: 1077-1085

Toxines et Signalisation – Toxins and Signalling
Rencontres en Toxinologie – Meeting on Toxinology, 2009
Editions de la SFET – SFET Editions
Accès libre en ligne sur le site – Free access on line on the site : http://www.sfet.asso.fr

Use of maurocalcine analogues as biotechnological tools for the penetration of cell-impermeable compounds

Cathy POILLOT[1,2], Michel DE WAARD[1,2*]

[1] *Inserm U836, Grenoble Neuroscience Institute, Site Santé Tronche, Chemin Fortuné Ferrini, BP 170, 38042 Grenoble cedex 09 ;* [2] *Université Joseph Fourier, Grenoble, France*

** Corresponding author ; Tel : +33 (0) 456520563 ; Fax : +33 (0) 456520637 ;*
E-mail : michel.dewaard@ujf-grenoble.fr

Abstract

Maurocalcine is unique in the sense that its natural molecular target, the ryanodine receptor, is localized inside cells. While studying how this toxin could reach its target, it was found that it represents a new member of a family of cell penetrating peptides. Indeed, maurocalcine is a highly basic peptide and most of the positively charged amino-acids are located on one face of the molecule according to a distribution that resembles that seen in Tat and penetratin. Since the initial discovery that maurocalcine can serve as a vector for the intracellular delivery of fluorescent streptavidin, accumulating data highlight the incredible biotechnological value of this toxin. Several new analogues have been designed that segregate the pharmacological and cell penetrating properties of the peptide. Maurocalcine was shown to be efficient for the cell delivery of nanoparticles opening a wealth of possible high tech applications. Also, maurocalcine has been covalently coupled to doxorubicine, an anti-tumour agent, to reverse chemo-resistance of cancer cells. It appears that this toxin is only at the start of his career as biotechnological tool, but also that it may still prove useful for deciphering fine mechanistic details of the functioning of the ryanodine receptor.

Utilisation d'analogues de la maurocalcine comme outils biotechnologiques de la pénétration cellulaire de composés non perméables

La maurocalcine est une toxine unique en ce sens que sa cible moléculaire naturelle, le récepteur à la ryanodine, est localisée à l'intérieur des cellules. En étudiant comment cette toxine pouvait atteindre sa cible, nous avons montré qu'elle représente un nouveau membre d'une famille de peptides de pénétration cellulaire. En effet, la maurocalcine est un peptide hautement basique et la plupart des acides aminés chargés positivement sont localisés sur une face de la molécule en accord avec la distribution observée sur des molécules telles que Tat et pénétratine. Depuis la découverte que la maurocalcine peut servir de vecteur à la délivrance intracellulaire de streptavidine fluorescente, les données se sont accumulées pour illustrer l'incroyable valeur biotechnologique de cette toxine. Plusieurs nouveaux analogues ont été produits qui séparent les propriétés pharmacologiques et de pénétration cellulaire du peptide. La maurocalcine s'est avérée efficace pour la délivrance cellulaire de nanoparticules ouvrant ainsi une myriade d'applications high tech. Enfin, la maurocalcine a été couplée à la doxorubicine, un agent anti-tumoral, pour rendre chimio-sensibles des cellules cancéreuses devenues chimio-résistantes. Il semble donc que la maurocalcine débute sa carrière comme outil biotechnologique, mais aussi que cette toxine s'avèrera utile pour déchiffrer finement les détails mécanistiques du fonctionnement du récepteur à la ryanodine.

Keywords : *Acetylcholine, pathogenicity, embryotoxicity, pain,* Cerastes cerastes.

Introduction

Maurocalcine initially triggered the interest of our research group based on the finding that it has strong sequence homology with imperatoxin A, an activator of the ryanodine receptor (el-Hayek *et al.*, 1995). The first characterization of maurocalcine dates back to 2000, date at which it was first chemically synthesized by peptide chemistry by the group of Dr. Jean-Marc Sabatier in Marseille, France. The toxin however originates from the group led by Pr. Mohamed El Ayeb at the Institut Pasteur of Tunis (Tunisia) where it was purified from the venom of the scorpion *Scorpio maurus palmatus*. Maurocalcine is a 33-mer basic peptide cross-linked by three disulfide bridges with the following pairing: Cys^{3}-Cys^{17}, Cys^{10}-Cys^{21}, and Cys^{16}-Cys^{32}. The solution structure of the peptide was determined by ^{1}H-NMR (Mosbah *et al.*, 2000). Its three dimensional structure consists of a double-stranded antiparallel beta-sheet comprising residues 20-23 and 30-33, and a third

extended strand from residues 9 to 11 that is perpendicular to the beta-sheet. Interestingly, this was the first description of a scorpion toxin folding according to an Inhibitor Cystine Knot fold (ICK), a motif previously described for various protease inhibitors. *In vivo*, maurocalcine was lethal to mice only upon intracerebroventricular inoculation (LD_{50} of 20 µg/mouse).

Maurocalcine is a member of a growing family of toxins

Maurocalcine is the second discovered member of an increasing family of new calcin toxins active on ryanodine receptors. The first member of this family, imperatoxin A, was isolated in 1995 from the venom of scorpion *Pandinus imperator* (el-Hayek *et al.*, 1995). Since that time, five more analogous peptides were subsequently discovered, first maurocalcine in 2000 from the scorpion *Scorpio maurus palmatus* (Mosbah *et al.*, 2000), followed by both opicalcine 1 and 2 from the scorpion *Opistophthalmus carinatus* in 2003 (Zhu *et al.*, 2003), hemicalcin from the scorpion *Hemiscorpius* lepturus in 2007 (Shahbazzadeh *et al.*, 2007), and finally hadrucalcin in 2009 from the scorpion *Hadrurus gertschi* (Schwartz *et al.*, 2009). The homology between these peptides ranges from 76 to 91%. All these peptides share common features that include a length of 33 to 35 amino acids, three disulfide bridges paired according to the motif Cys^1-Cys^4, Cys^2-Cys^5 and Cys^3-Cys^6 (see *Figure 1*). Hadrucalcin is a quite interesting new member in the sense that it is significantly divergent from the five other members. With this member, the number of variable amino acids rises from 7 to 12 and demonstration is made that the toxin can accommodate 13 positively charged amino acids instead of 12 and that the sequence can be extended at its N-terminus (the sequence length goes from a constant value of 33 for all other members to 35 with this analogue). This finding suggests that the calcin family will probably be soon incremented with new members from other scorpion sources. Also, it provides interesting new clues on how to design novel calcin toxins that would conserve activity on RyR and penetrate into cells.

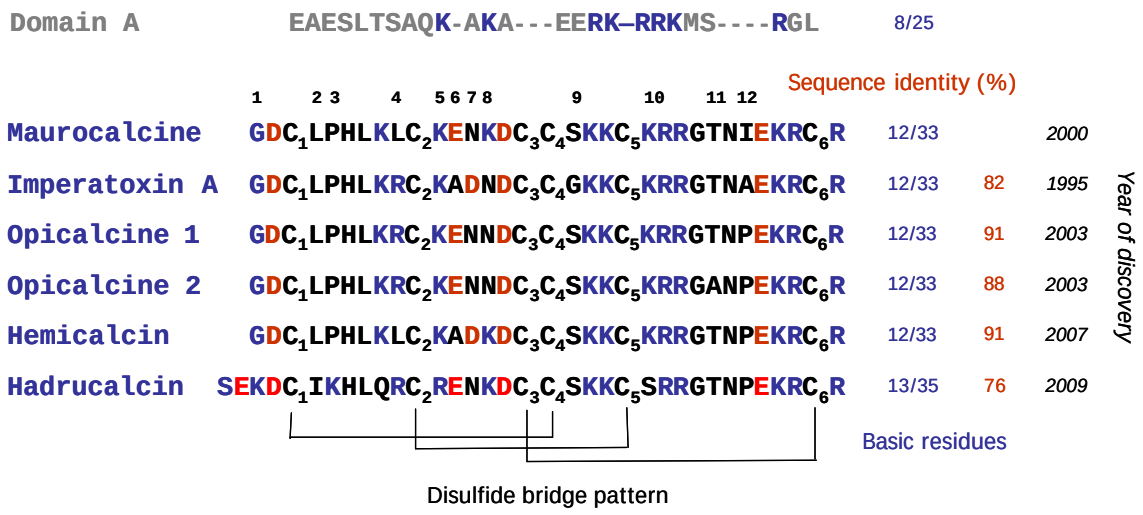

Fig. 1. Maurocalcine-like scorpion toxins. Sequence alignment of maurocalcine with five analogous toxins, imperatoxin A, opicalcine 1, opicalcine 2, hemicalcin and hadrucalcin. Maurocalcine, imperatoxin A, hemicalcin and hadrucalcin have all shown to be active on the ryanodine receptor. Opicalcine 1 and 2 have not been tested for pharmacological activity. Toxins have between 12 and 13 positively charged amino acid residues (the N-terminal residue, six or seven lysine residues, and four to six arginine residues as indicated in blue). Negatively charged amino acids are represented in red as well as sequence identities with maurocalcine. Highlighted residues (twelve possible positions) indicate variable amino acids among toxins. The year of discovery of each toxin is also provided in italics. Sequence alignment with domain A of the L-type calcium channel is also illustrated.

Fig. 1. *Toxines de scorpion du type maurocalcine. Alignement de séquence de la maurocalcine avec 5 toxines analogues, l'imperatoxine A, l'opicalcine 1, l'opicalcine 2, l'hemicalcine et l'hadrucalcine. Maurocalcine, imperatoxine A, hemicalcine et hadrucalcine sont tous connus pour être actif sur le récepteur à la ryanodine. Les opicalcines 1 et 2 n'ont pas été testé pour leurs activités pharmacologiques. Les toxines possèdent entre 12 et 13 acides aminés chargés positivement (le résidu N-terminal, 6 ou 7 résidus lysine, 4 à 6 résidus arginine, indiqués en bleu). Les acides aminés chargés négativement sont en rouge ainsi que les identités de séquence avec la maurocalcine. Les résidus surlignés (12 positions possibles) indiquent les acides aminés variables entre toxines. L'année de découverte de chaque toxine est aussi indiquée en italique. L'alignement de séquence avec le domaine A du canal calcique de type L est aussi montré.*

Calcin toxins are active on the ryanodine receptor

Ryanodine receptors are calcium channels that allow calcium cations to exit the lumen of endoplasmic reticulum. They contribute therefore to calcium signalling events in the cell cytoplasm. These channels are present therefore within the membrane of the endoplasmic reticulum and are constituted of an ion pore and a large cytoplasmic bulk. None of the sequence of the channel is integrated in the plasma membrane or present at the extracellular surface. For this reason, the ryanodine receptor is an unusual target for a toxin. Three genes encode for ryanodine receptor type I, II and III. The type I ryanodine receptor is mainly expressed in skeletal muscles, the type II is mostly cardiac and cerebral, whereas the type III is predominantly neuronal. Most calcin toxins have been tested on type I ryanodine receptor, essentially because this type is easier to

purify from the skeletal muscle, a rich source of that type of channel. Calcin toxins induce similar effects on the ryanodine receptor that can be summarized as follows. (i) Application of a calcin toxin to purified sarcoplasmic reticulum induces Ca^{2+} release, suggesting that one effect of the toxin is channel activation. (ii) Calcin toxins converts low affinity [^{3}H]-ryanodine binding sites to high affinity ones (el-Hayek *et al.*, 1995 ; Esteve *et al.*, 2003). High affinity [^{3}H]-ryanodine binding has been interpreted to a change of channel conformation compatible with the open state conformation of the channel. Using this assay, it was estimated that calcin toxins should bind to ryanodine receptors with an affinity in the 10 to 50 nM range (Zamudio *et al.*, 1997 ; Esteve *et al.*, 2003 ; Schwartz *et al.*, 2009). (iii) Calcin toxins have complex effects on channel activity recorded from ryanodine receptors incorporated into lipid bilayers. The first effect observed is generally an increase in open-state probability, followed by the appearance of a long-lasting subconductance state, which is rarely reversible. Higher concentration of toxins induce complete channel block meaning that calcin toxins are considered as activators at low concentrations and blockers at high concentrations. This complex set of effects is probably due to the fact that ryanodine receptor are organized as homo-tetramers, implying that toxins can occupy one to at least four potential sites on the channel. Multi-site occupancy likely triggers different channel behaviours (Chen *et al.*, 2003). The interaction of calcin toxin with the ryanodine receptor is direct since a biotinylated derivative of maurocalcine bound to streptavidin-coated beads pulls down purified skeletal muscle RyR (Altafaj *et al.*, 2005). Also, it was shown that maurocalcine directly binds onto a cytoplasmic domain of the ryanodine receptor. This domain is of functional importance for increased [^{3}H]-ryanodine binding in the presence of maurocalcine. The cytoplasmic nature of the calcin toxin binding site on the ryanodine receptor is confirmed by the observation that maurocalcine alters the activity of channels reconstituted into lipid bilayers only when applied to the cytoplasmic face of the channel (Fajloun *et al.*, 2000). Altogether, these data demonstrate that calcin toxins are pharmacological modulators of the ryanodine receptors by directly binding onto a site located in the cytoplasm.

Existence of a curious sequence homology between calcin toxins and a voltage-dependent calcium channel domain

One amazing property of calcin toxins is their limited sequence homology with a voltage-dependent calcium channels. Skeletal muscle L-type channel come as a complex of four subunits: the pore-forming and voltage-sensing subunit $Ca_v1.1$, associated to three auxiliary subunits β, $\alpha_2\delta$ and γ. This channel type is peculiar in the sense that it transmits changes in membrane potential directly to the ryanodine receptor. This process termed excitation-contraction coupling ensures that action potentials trigger enough calcium elevation in the cytoplasm to produce muscle contraction. Since most of the calcium originates from the sarcoplasmic reticulum through opening of the ryanodine receptor, the voltage-dependent calcium channel transmits the necessary information to the ryanodine receptor directly by changes in conformation. This entire chain of events is still poorly understood at the mechanistic level, but several channel determinants have been identified that serve as lead in the understanding of the process. One such determinant is called domain A, a small 20 amino acid sequence of $Ca_v1.1$ that is located in the cytoplasmic II-III loop of the channel. Sequence homology of domain A with calcin toxins is restricted to a basic patch of amino acids, but it was found that both domain A and calcin toxins share structural homology (Green *et al.*, 2003), they similarly induce an increase in [^{3}H]-ryanodine binding, activate channel activity (Gurrola *et al.*, 1999), and finally they bind onto identical sites (Lee *et al.*, 2004 ; Altafaj *et al.*, 2005). The finding that calcin toxins bind to the ryanodine receptor with higher affinity than domain A (20 nM versus 1 µM) indicates that these toxins may be used as interesting molecular tools to dissect the functional role of domain A in excitation-contraction coupling. This goal has been partially reached by the demonstration that maurocalcine induces a default in the closure of the ryanodine-sensitive calcium channel following activation by membrane depolarisation (Szappanos *et al.*, 2005). These data seem to imply that maurocalcine is able to substitute to domain A while the ryanodine receptor is activated by membrane depolarization. During repolarisation, ryanodine receptor closure is slowed presumably because of the greater affinity of maurocalcine for the binding site it shares in common with domain A. Obviously, calcin toxins still have to reveal many intimate mechanistic details on the process of excitation-contraction coupling.

Firsts evidences that maurocalcine penetrates into cells

The location of the pharmacological target of calcin toxins (intracellular) and the position of maurocalcine binding site on the ryanodine receptor with regard to the channel topology (cytoplasm) are strong evidences that calcin toxins need to cross the plasma membrane before reaching their target. For a long period, criticisms had been formulated with regard to the pharmacological target of imperatoxin A, the first discovered calcin toxin. It was estimated that peptides could not cross the plasma membrane, and therefore doubts were expressed about the pharmacological reality of the ryanodine receptor as target for calcin toxins. To sort this question out, two sorts of experiments were performed. On one hand, it was observed that extracellular application of 100 nM maurocalcine to myotubes produces a rapid rise (within a few seconds) of intracellular calcium (Esteve *et al.*, 2003). Similarly, it was shown that hadrucalcin elicits discharges of internal calcium stores within seconds in ventricular myocytes (Schwartz *et al.*, 2009). On the other hand, we evidenced that a biotinylated derivative of maurocalcine had the ability to trigger cell entry of fluorescent streptavidine (Esteve *et al.*, 2005). The cell entry of this vector / cargo couple was unique in the history of toxinology, and the first demonstration that (i) maurocalcine enters into cells, and (ii) can be used for the cell entry of cargoes that would otherwise not enter the cell. These data illustrate the succession of molecular events undergone by calcin toxins until calcium release from the lumen of the endoplasmic reticulum: (i) very rapid plasma membrane crossing, (ii) elevation of the cytoplasm concentration of the toxin to a level close or above 10 nM to reach the K_D value for RyR, (iii) binding onto the RyR site, (iv) opening of RyR channels, and (v) calcium release from internal stores.

Separating the pharmacological properties from the cell penetration properties

The discovery that maurocalcine may serve as a vector for the cell penetration of various cargoes turns out of great interest. Contrary to many cell penetrating peptides whose sequences have been derived from larger proteins, maurocalcine is a functional entity on its own. More importantly, a functional readout of the effects of maurocalcine can easily be measured (calcium release or alteration in excitation-contraction coupling). Since these effects all require the presence of the toxin in the cytoplasm, these functional readouts ensure that cell entry of maurocalcine coincides with cytoplasmic localization. This issue is essential since the fate of cell penetrating peptides is diverse. Two modes of cell entry exist: direct translocation through the plasma membrane through a mechanism(s) still unexplained, but that results in accumulation in the cytoplasm, or endocytosis, generally macropinocytosis, with significant accumulation in endosomes and little escapes from there into the cytoplasm. In that sense, maurocalcine presents an incredible advantage over other cell penetrating peptides in that complicated cell assays don't need to be developed alongside with chemical modification of the cell penetrating peptide.

This being stated, it is also obvious that the cell penetrating peptide virtue of maurocalcine is an advantage provided that pharmacological effects of the peptide are not obscuring the beneficial technological effects. This implies that structural analogues of maurocalcine ought to be designed that conserve cell penetration properties but are significantly impaired with regard to the pharmacological activation of the ryanodine receptor. This aim has been reached by different methods. A first approach consisted by site directed mutagenesis of maurocalcine (Mabrouk *et al.*, 2007). This approached taught us that it was possible to drastically reduce the pharmacological activity of maurocalcine while largely preserving the cell penetration of fluorescent streptavidin. For instance ; the R24A-maurocalcine mutant totally lost its effect on the ryanodine receptor (both stimulation of [^{3}H]-ryanodine binding and activation of channel activity (Lukacs *et al.*, 2008)), while keeping more than half the cell penetration properties of the peptide. The advantage of this approach was that it precisely maps the amino acid residues involved in the pharmacological action or in the cell penetrating one. Conclusions were that pharmacology has more stringent structural requirements than cell penetration. This was good news because it suggested that alternative strategies could be envisioned. Finally, this approach also yielded a novel analogue E12A-maurocalcine that possesses better cell penetration properties than the wild-type sequence. A second approach was based on two observations: i) other cell penetrating peptides are disulfide-less, and ii) disulfide bridges contribute to the fold of toxins and thus presumably to pharmacological activity. We therefore assumed that removing the disulfide bridges of maurocalcine would alter its 3D structure and consequently its functional effects, but possibly without inhibiting cell penetration. This is indeed what we observed by synthesizing an analogue in which all internal cysteine residues were substituted by Abu derivatives. The peptide was unfolded as assessed by circular dichroism and lost the ability to regulate ryanodine receptor activity (Ram *et al.*, 2008b). The added advantage of this approach was the possibility to add a cysteine residue at the N-terminus of the sequence to chemically couple cargoes through thiol chemistry. Unfolded MCa was slightly less efficient for cell penetration than its folded counterpart suggesting that folding is an advantage in maurocalcine over other cell penetrating peptides such as Tat or penetratin. Nevertheless, in a comparative study, we found that this unfolded analogue is as potent as other cell penetrating peptides demonstrating that it represents a good vector for biotechnical applications (unpublished observations). From there, we start to investigate shorter maurocalcine sequences to determine the minimal structural requirement for cell penetration. Preliminary results indicate that the basic region of maurocalcine is responsible for its cell penetration, in agreement with the data obtained by single amino acid substitution (Ram *et al.*, 2008b). The third approach that is currently in development in our laboratory is the production of a D-maurocalcine, synthesized with D-amino acids instead of L-amino acids. The synthesis is a challenge because this new analogue should fold according to the motif observed in L-maurocalcine. Our preliminary results indicate that we are successful in the production of this analogue that is a mirror structure of L-maurocalcine. Peptides produced this way lose target recognition and binding, and preserve cell penetration, again because the structural requirements for pharmacology and cell penetration are significantly different. D-maurocalcine is indeed unable to activate the ryanodine receptor, yet still penetrates into cells.

How does maurocalcine enter cells ?

There is no trivial answer to that question. Let's simply emphasize that the mechanism of cell entry of cell penetrating peptides is crucial for the application that is programmed. By definition, a "real" cell penetrating peptide is one that accumulates in the cytoplasm and not into endosomes! Yet, most manuscripts dealing about cell penetrating peptides relate to peptide accumulation into endosomes. To be honest, the fate of the peptide into cells does not simply rely on the nature of the cell penetrating peptide itself, but also frequently to the nature of the cargo being transported or the type of cell under consideration. It is interesting to observe that maurocalcine can adopt both types of cell entry: translocation for cytoplasmic accumulation or endocytosis for endosome localization. When streptavidine is the cargo, we observed mainly punctuate distribution coinciding with endosomes (Boisseau *et al.*, 2006). Now, we also observed a predominant cytoplasmic localization with other cargoes such as fluorescent peptides, doxorubicine or quantum dots (Ram et al., 2008b ; Aroui et al., 2009). It is difficult to decide in advance what type of cell distribution to expect with a given cargo and no general rule seem to emerge. It is possible that cargo size may be a factor as membrane translocation may accommodate only small cargoes. But it would be reductionist to limit this differential distribution to this sole factor. One way to better understand by which mechanism maurocalcine enters into cells is to determine the nature of the molecular partner that takes maurocalcine in charge at the surface of the cell and to analyze how it may contribute to the cell penetration. We found two types of interacting molecules: glycoaminoglycans (Ram *et al.*, 2008a) and several negatively charged lipids (Boisseau *et al.*, 2006). Maurocalcine interacts with

heparin, heparin sulphate, and chondroitin sulphate. Incubating maurocalcine with soluble GAGs can inhibit up to 80 % of the cell uptake of maurocalcine for two reasons: (i) soluble GAGs screen the positive charges of maurocalcine required for cell entry, and (ii) they compete for the interaction of maurocalcine with cell surface bounds GAGs. Interactions with GAGs are however not totally required for cell entry of maurocalcine since penetration is partially preserved in GAG-deficient CHO cells. In these same cells, the mode of penetration is not modified suggesting that membrane receptors of maurocalcine are not associated with a particular type of cell penetration. We assume that GAGs contribute to cell penetration of maurocalcine at the quantitative level by favoring local accumulation of the peptide at the cell membrane. It is possible that it acts as a reservoir of peptide for delivery to membrane lipids. In that sense, it is interesting that the affinity of maurocalcine for GAGs (1-2 µM) is lower than for lipids. For instance, maurocalcine interacts with GD3 (disialoganglioside NeuAca2-8NeuAca2-3Galß1-4Glcß1-Cer) at an affinity in the 100 nM range (Boisseau *et al.*, 2006). This is an affinity that is more in agreement with the concentration-dependence of cell penetration of maurocalcine, suggesting that lipids may well represent the final/true penetrating partners of maurocalcine. It makes sense for the translocation process through the plasma membrane. However, considerably more work is required at the biophysical level to determine how the complex of maurocalcine / lipids evolves during the translocation process. Also, because of the multiplicity of intervening partners, it would be highly desirable to identify what lipid, if there a specific one, is responsible for the cell entry of maurocalcine. Knowledge of this information would be of tremendous help in the design of more efficient analogues of maurocalcine for cell penetration.

Examples of biotechnological applications

Doxorubicine-maurocalcine : a chimera molecule to treat chemo resistance of tumor cells

Although it is of conceptual interest to develop novel analogues of cell penetrating peptides and to understand their mode of cell entry, the main interest of these peptides resides in the applications that can be envisioned. We therefore sought to develop a novel therapeutic application using our pharmacologically inert, but still efficient cell penetrating Abu-derivative maurocalcine analogue. Doxorubicine is an anti-tumor agent but that also induces chemo-resistance in cancer cells. One mechanism of chemo-resistance is the over-expression of multidrug resistance protein in cells that expels efficiently doxorubicine that is normally capable to enter freely into cells. We therefore investigated whether coupling doxorubicine to maurocalcine could oppose cell resistance presumably by inhibiting this expulsion process. To that purpose, we used two cancer cell lines, MCF7 and MDA-MB-231, described as having a different sensitivity/resistance for doxorubicine and tested doxorubicine itself and various cell penetrating peptides coupled to doxorubicine, such as Tat and penetratin besides the Abu-derivative maurocalcine analogue. All peptides were synthesized with a cysteine residue at the N-terminus to couple them to doxorubicine via SMCC (succinimidyl-4-(*N*-maléimidomethyl)cyclohexane-1-carboxylate, according to the method of Liang and Yang (Liang and Yang, 2005). Two parameters were investigated at short and long-term in culture: cell penetration and cell survival (Aroui *et al.*, 2009). Because doxorubicine has intrinsic fluorescent properties, the subcellular localization of the complexes could be followed by confocal microscopy and FACS analyses allowed the quantification of the entry of the complexes. We demonstrated that doxorubicine, coupled to cell penetrating peptides, is mainly localized in the cytoplasm of the cells, while it is predominantly concentrated in the nucleus when it is uncoupled. FACS analyses demonstrate that evident cell penetration of doxorubicine is detected at 0.5 µM and saturates at 10 µM for both the free form and cell penetrating coupled forms. We observed a clear accumulation of doxorubicine in MDA-MB-231 cells only when it is coupled to cell penetrating peptides, suggesting that the coupling process blocks doxorubicine expulsion in this chemo-resistant cell line. Accordingly, we observed that the conjugation of doxorubicine to cell penetrating peptides greatly enhances MDA-MB-231 cell death, even at very low concentrations, while it reduces cell death of MCF7 cells (see *Figure 2*). The reduced doxorubicine distribution in the nucleus is correlated with reduced toxicity in MCF7 cells, while the enhanced cell accumulation of the drug in MDA-MB-231 cells is associated with enhanced cell death. It has been shown that the toxic action of doxorubicine depends of its DNA intercalating properties and of the modifications in activity and expression levels of its target topoisomerase II. The toxicity induced by cell penetrating peptide coupled doxorubicine, while the drug is mostly present in the cytoplasm, appears to occur through different mechanisms, namely the induction of apoptosis. What our data have shown is that the Abu-derivative maurocalcine analogue is at least as efficient as other cell penetrating peptides for the cell penetration and retention of doxorubicine. The drug remains highly toxic in spite of chemical conjugation to cell penetrating peptides and of altered subcellular distribution. This approach suggests that cell penetrating peptides may constitute a significant progress when it comes to re-sensitize cancer cells to doxorubicine. We hope to complement these analyses by *in vivo* studies demonstrating the usefulness of maurocalcine for cancer therapy.

Coupling maurocalcine to nanoparticles : new diagnostic and therapeutic applications in perspective

Semiconductor quantum dots are new classes of fluorescent probes with a large surface to volume ratio. This property can be exploited to graft new functional entities at their surface, such as peptides, proteins, nucleic acids, antibodies and drugs. They possess excellent photo stability, far exceeding that of conventional organic fluorophores, and high emission quantum yield, which leads to increased fluorescence detection sensitivity. Quantum dots consist of a core of semi-conducting material, typically cadmium-telluride (CdTe) or cadmium-selenium (CdSe) for emission in the visible to the near infrared domain, for which tissue auto-fluorescence and absorption are reduced.

This core is generally covered by a shell composed of zinc sulfide (ZnS), in order to improve the chemical stability and emission quantum yield of the quantum dot (Lim *et al.*, 2003 ; Michalet *et al.*, 2005). These

nanocrystals are surface-modified for their stabilization in aqueous media and biological functionalization. In particular, coating of nanoparticles by a polyethylene glycol polymer (PEGylation) improves colloidal stability (Lee *et al.*, 2008) and blood circulation time (Ballou *et al.*, 2004).

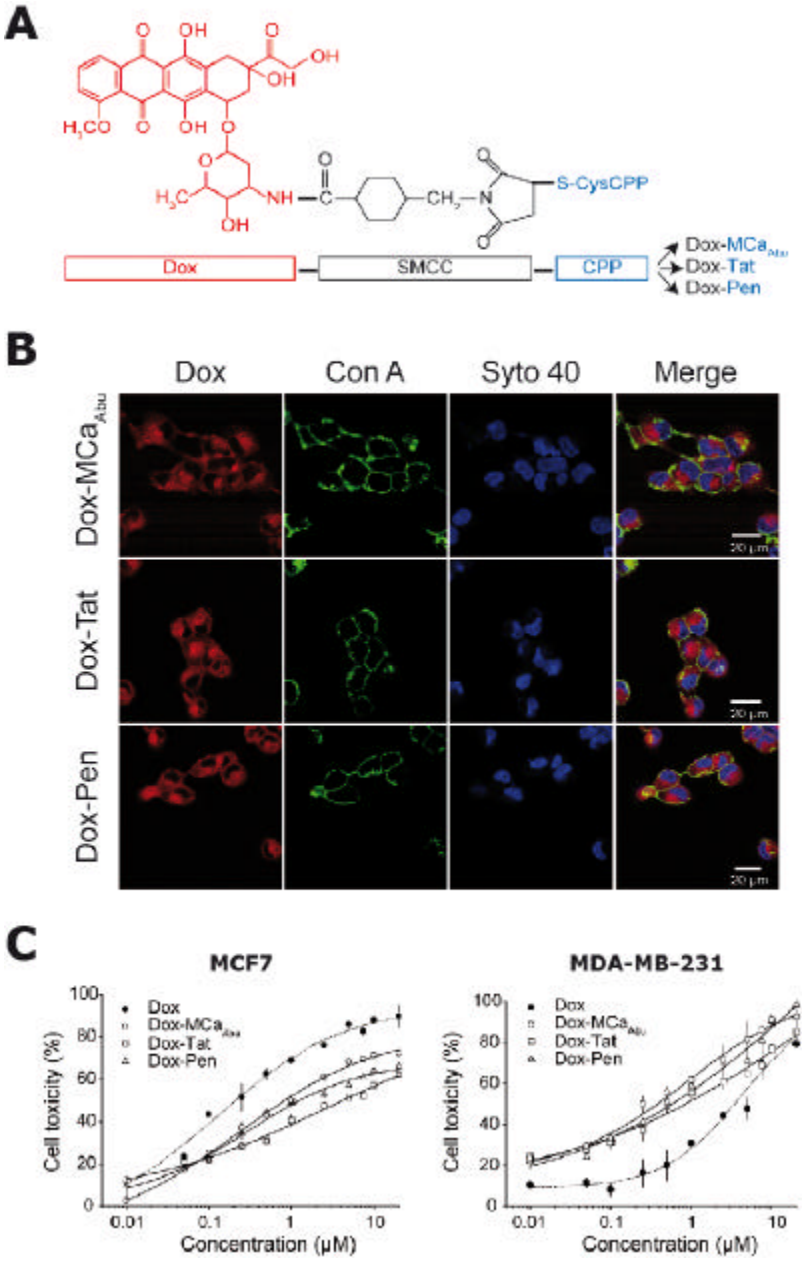

Fig. 2. (**A**) Structure of doxorubicine-cell penetrating peptide (CPP) complexes. (**B**) Cell distribution of doxorubicine conjugates in MDA-MB-231 cells showing the predominant presence in the cytoplasm. (**C**) Cell death induction by 24 hrs exposure to doxorubicine or doxorubicine-conjugates in MCF7 or MDA-MB-231 cells.

Fig. 2. *(**A**) Structures des complexes doxorubicine / peptide de pénétration cellulaire. (**B**) Distribution cellulaire des conjugués de doxorubicine dans les cellules MDA-MB-231 démontrant leurs présences prédominantes dans le cytoplasme. (**C**) Induction de la mort cellulaire après une exposition de 24 heures à la doxorubicine ou les conjugués de doxorubicine dans les cellules MCF7 ou MDA-MB-231.*

The emission spectra of quantum dots is size-tunable which enables their simultaneous excitation and tracking with the same excitation source (Biju *et al.*, 2008). Their properties are so useful that they have been used in several biological applications. In particular, quantum dots have proven useful for immunostaining of membrane proteins (Sukhanova *et al.*, 2004) and staining of organelles like mitochondria or nuclei (Hoshino *et al.*, 2004) in fixed cells, and for tracking single molecules in living cells by videomicroscopy (Dahan *et al.*, 2003 ; Lidke *et al.*, 2004 ; Mansson *et al.*, 2004). *In vivo* imaging applications have also been reported (Akerman *et al.*, 2002 ; Dubertret *et al.*, 2002 ; Gao *et al.*, 2004 ; Michalet *et al.*, 2005 ; Choi *et al.*, 2007).

Peptides have been used to improve quantum dot solubility in aqueous solution and for targeting cell surface proteins of interest *(Pinaud et al.*, 2004). Nevertheless, the use of quantum dots for intracellular applications *in vitro* or *in vivo* has been hampered by their inability to cross the plasma membrane. Several experimental strategies have been developed to physically deliver quantum dots, including direct microinjection, but this limits the number of cells that can be studied, or electroporation (Chen, 2004 ; Derfus, 2004 ; Voura *et al.*, 2004). Cell delivery of quantum dots using lipofectamine results in the formation of aggregates (Voura *et al.*, 2004). None of these delivery systems seem promising for *in vivo* applications because of their limited cell penetration efficiencies. Recently, the cell penetrating peptides, polyarginine (Silver and Ou, 2005) or TAT (Santra *et al.*, 2005), have been used for the delivery of quantum dots into living cells *in vitro* or across the blood brain barrier *in vivo*. This delivery approach appears very promising because many applications rely on the efficient cell delivery of cargoes such as peptides, proteins, siRNA, peptide nucleic acids, cDNA or drugs (Wadia and Dowdy, 2002).

Using biotinylated maurocalcine, we were the first group to report that streptavidine-coated quantum dots can be physically delivered within cells (see *Figure 3*).

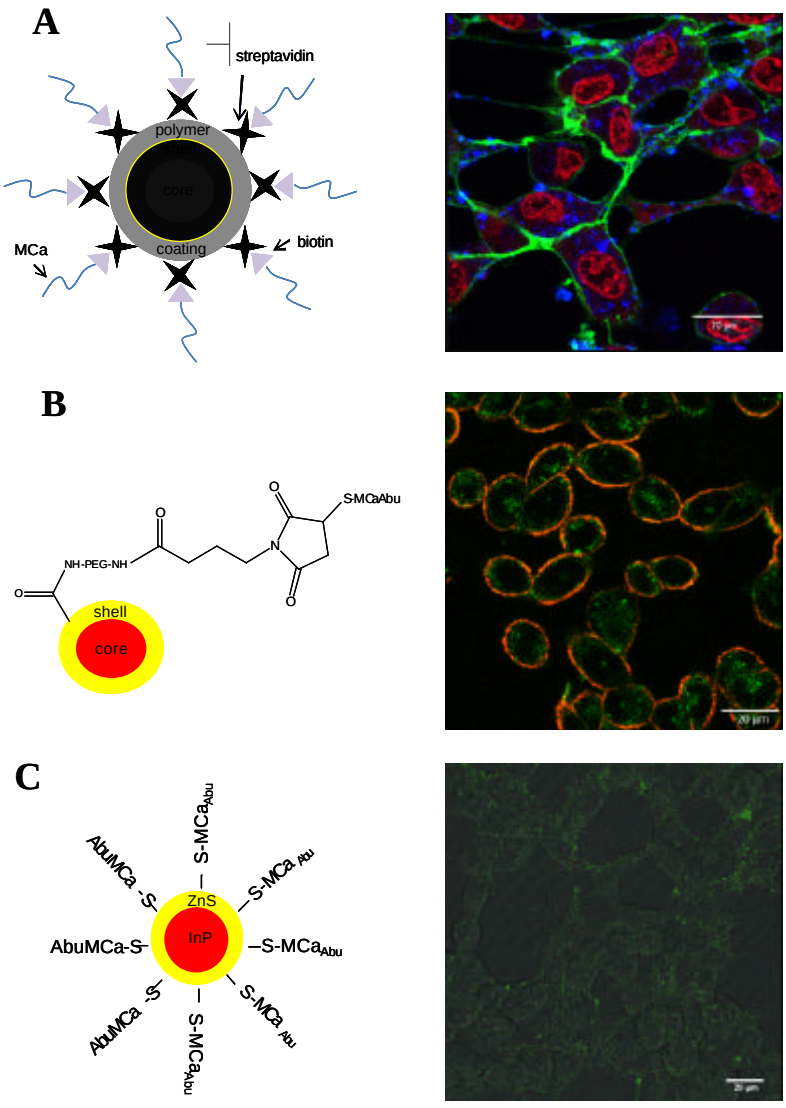

Fig. 3. Maurocalcine is an efficient vector for the entry of nanoparticles into CHO cells. (**A**) Cell delivery of streptavidine-coated CdSe/ZnS quantum dots by biotinylated folded maurocalcine. Punctate distribution is indicative of endosomal localization. (**B**) Cell delivery of CdSe/ZnS quantum dots directly coupled to Abu-derivative unfolded maurocalcine. Localization is predominantly cytoplasmic. (**C**) Cell delivery of InP/ZnS nanoparticles directly coupled to Abu-derivative unfolded maurocalcine.

Fig. 3. *Maurocalcine est un vecteur efficace pour la pénétration cellulaire de nanoparticules dans les cellules CHO. (**A**) Délivrance cellulaire de quantum dots CdSe/ZnS recouverts de streptavidine par une maurocalcine foldée biotinylée. La distribution ponctiforme est indicative d'une localisation endosomale. (**B**) Délivrance cellulaire de quantum dots CdSe/ZnS directement couplé à un analogue non foldé de la maurocalcine. La localisation est essentiellement cytoplasmique. (**C**) Délivrance cellulaire de nanoparticules InP/ZnS directement couplé à un analogue non foldé de la maurocalcine.*

One peculiar property of these quantum dots is that the maurocalcine / streptavidine linkage automatically is always associated with endosomal localization. Using a different chemical linkage, that makes abstraction of streptavidin, and using the Abu-derivative maurocalcine as cell penetrating peptide, we found a very different subcellular distribution of the quantum dots. Most of the nanoparticles were found in the cytoplasm suggesting that membrane translocation of peptide / quantum dots complexes is possible. More recently, through a targeted collaboration with Drs. Peter Reiss and Isabelle Texier of the CEA Grenoble, we successfully produced nanoparticules of InP/ZnS, functionalized with penicillamin, which have beeen coupled to our abu-derivative maurocalcine analogue. The data demonstrate the efficient cell penetration of this new generation of nanoparticles that present three decisive advantages for *in vivo* applications: i) preliminary data indicate that, owing to their relatively small size, these nanoparticles can be eliminated *in vivo* by urine secretion (unpublished data), ii) none of the materials used present the known cell toxicity of free cadmium, and iii) these nanoparticules emit at near infrared wavelengths indicating their good suitability for imaging across tissues.

In one specific applications, the ability of maurocalcine to deliver quantum dots to cells were used for imaging of atherosclerosis (Jayagopal *et al.*, 2009). In this application, the authors used biotinylated maurocalcine to deliver streptavidine coated CdSe/ZnS quantum dots *in vitro* to isolated monocytes and T-lymphocytes. Quantum dot labeled cells were then injected into ApoE-/- mice, a model of atherosclerosis. It was shown that cells incorporated aortic lesions and that quantum dots were present in atherosclerotic plaques 2 days after injection. This fluorescence could be monitored for up to four weeks demonstrating the remarkable stability of these quantum dots *in vivo*. During that study, it was confirmed that maurocalcine / quantum dots complexes present no toxicity for the cells, similarly to what was observed for streptavidine alone (Boisseau *et al.*, 2006).

Nanotechnology is destined to a fabulous future and many of the applications will require intracellular delivery of active compounds. Maurocalcine is one of the promising cell delivery peptide vector that holds great promises for these applications. Although it is more complex to synthesize than other cell penetrating peptides, it has some competitive advantages such as a cell penetration at lower concentration, absence of cell toxicity, greater resistance to protease degradation.

Acknowledgements. *We acknowledge financial support from CEA (Program TIMOMA2), ANR PNANO (Program SYNERGY), and from Inserm.*

References

Akerman ME, Chan WC, Laakkonen P, Bhatia SN, Ruoslahti E (2002) Nanocrystal targeting *in vivo*. *Proc Natl Acad Sci USA* **99**: 12617-12621

Altafaj X, Cheng W, Esteve E, Urbani J, Grunwald D, Sabatier JM, Coronado R, De Waard M, Ronjat M (2005) Maurocalcine and domain A of the II-III loop of the dihydropyridine receptor Cav 1.1 subunit share common binding sites on the skeletal ryanodine receptor. *J Biol Chem* **280**: 4013-4016

Arou S, Ram N, Appaix F, Ronjat M, Kenani A, Pirollet F, De Waard M (2009) Maurocalcine as a Non Toxic Drug Carrier Overcomes Doxorubicin Resistance in the Cancer Cell Line MDA-MB 231. *Pharm Res* **26**: 836-845

Ballou B, Lagerholm BC, Ernst LA, Bruchez MP, Waggoner AS (2004) Noninvasive imaging of quantum dots in mice. *Bioconjug Chem* **15**: 79-86

Biju V, Itoh T, Anas A, Sujith A, Ishikawa M (2008) Semiconductor quantum dots and metal nanoparticles: syntheses, optical properties, and biological applications. *Anal Bioanal Chem* **391**: 2469-2495

Boisseau S, Mabrouk K, Ram N, Garmy N, Collin V, Tadmouri A, Mikati M, Sabatier JM, Ronjat M, Fantini J*, et al.* (2006) Cell penetration properties of maurocalcine, a natural venom peptide active on the intracellular ryanodine receptor. *Biochim Biophys Acta* **1758**: 308-319

Chen F, Gerion D (2004) Fluorescent CdSe/ZnS nanocrystal-peptide conjugates for long-term, nontoxic imaging and nuclear targeting in living cells. *Nano Lett* **4**: 1827-1832

Chen L, Esteve E, Sabatier JM, Ronjat M, De Waard M, Allen PD, Pessah IN (2003) Maurocalcine and peptide A stabilize distinct subconductance states of ryanodine receptor type 1, revealing a proportional gating mechanism. *J Biol Chem* **278**: 16095-16106

Choi HS, Liu W, Misra P, Tanaka E, Zimmer JP, Itty Ipe B, Bawendi MG, Frangioni JV (2007) Renal clearance of quantum dots. *Nat Biotechnol* **25**: 1165-1170

Dahan M, Levi S, Luccardini C, Rostaing P, Riveau B, Triller A (2003) Diffusion dynamics of glycine receptors revealed by single-quantum dot tracking. *Science* **302**: 442-445

Derfus AM, Chen WCW, Bhatia SN (2004) Intracellular delivery of quantum dots for live cell labeling and organelle tracking. *Adv Mater* **16**: 961-966

Dubertret B, Skourides P, Norris DJ, Noireaux V, Brivanlou AH, Libchaber A (2002) In vivo imaging of quantum dots encapsulated in phospholipid micelles. *Science* **298**: 1759-1762

el-Hayek R, Lokuta AJ, Arevalo C, Valdivia HH (1995) Peptide probe of ryanodine receptor function. Imperatoxin A, a peptide from the venom of the scorpion Pandinus imperator, selectively activates skeletal-type ryanodine receptor isoforms. *J Biol Chem* **270**: 28696-28704

Esteve E, Mabrouk K, Dupuis A, Smida-Rezgui S, Altafaj X, Grunwald D, Platel JC, Andreotti N, Marty I, Sabatier J*M, et al.* (2005) Transduction of the scorpion toxin maurocalcine into cells. Evidence that the toxin crosses the plasma membrane. *J Biol Chem* **280**: 12833-12839

Esteve E, Smida-Rezgui S, Sarkozi S, Szegedi C, Regaya I, Chen L, Altafaj X, Rochat H, Allen P, Pessah IN*, et al.* (2003) Critical amino acid residues determine the binding affinity and the Ca^{2+} release efficacy of maurocalcine in skeletal muscle cells. *J Biol Chem* **278**: 37822-37831

Fajloun Z, Kharrat R, Chen L, Lecomte C, Di Luccio E, Bichet D, El Ayeb M, Rochat H, Allen PD, Pessah IN*, et al.* (2000)

Chemical synthesis and characterization of maurocalcine, a scorpion toxin that activates Ca(2+) release channel/ryanodine receptors. *FEBS Lett* **469**: 179-185

Gao X, Cui Y, Levenson RM, Chung LW, Nie S (2004) In vivo cancer targeting and imaging with semiconductor quantum dots. *Nat Biotechnol* **22**: 969-976

Green D, Pace S, Curtis SM, Sakowska M, Lamb GD, Dulhunty AF, Casarotto MG (2003) The three-dimensional structural surface of two beta-sheet scorpion toxins mimics that of an alpha-helical dihydropyridine receptor segment. *Biochem J* **370**: 517-527

Gurrola GB, Arevalo C, Sreekumar R, Lokuta AJ, Walker JW, Valdivia HH (1999) Activation of ryanodine receptors by imperatoxin A and a peptide segment of the II-III loop of the dihydropyridine receptor. *J Biol Chem* **274**: 7879-7886

Hoshino A, Fujioka K, Oku T, Nakamura S, Suga M, Yamaguchi Y, Suzuki K, Yasuhara M, Yamamoto K (2004) Quantum dots targeted to the assigned organelle in living cells. *Microbiol Immunol* **48**: 985-994

Jayagopal A, Su YR, Blakemore JL, Linton MF, Fazio S, Haselton FR (2009) Quantum dot mediated imaging of atherosclerosis. *Nanotechnology* **20**: 165102

Lee CW, Lee EH, Takeuchi K, Takahashi H, Shimada I, Sato K, Shin SY, Kim do H, Kim JI (2004) Molecular basis of the high-affinity activation of type 1 ryanodine receptors by imperatoxin A. *Biochem J* **377**: 385-394

Lee J, Kim J, Park E, Jo S, Song R (2008) PEG-ylated cationic CdSe/ZnS QDs as an efficient intracellular labeling agent. *Phys Chem Chem Phys* **10**: 1739-1742

Liang JF, Yang VC (2005) Synthesis of doxorubicin-peptide conjugate with multidrug resistant tumor cell killing activity. *Bioorganic & medicinal chemistry letters* **15**: 5071-5075

Lidke DS, Nagy P, Heintzmann R, Arndt-Jovin DJ, Post JN, Grecco HE, Jares-Erijman EA, Jovin TM (2004) Quantum dot ligands provide new insights into erbB/HER receptor-mediated signal transduction. *Nat Biotechnol* **22**: 198-203

Lim YT, Kim S, Nakayama A, Stott NE, Bawendi MG, Frangioni JV (2003) Selection of quantum dot wavelengths for biomedical assays and imaging. *Mol Imaging* **2**: 50-64

Lukacs B, Sztretye M, Almassy J, Sarkozi S, Dienes B, Mabrouk K, Simut C, Szabo L, Szentesi P, De Waard M*, et al.* (2008) Charged surface area of maurocalcine determines its interaction with the skeletal ryanodine receptor. *Biophys J* **95**: 3497-3509

Mabrouk K, Ram N, Boisseau S, Strappazzon F, Rehaim A, Sadoul R, Darbon H, Ronjat M, De Waard M (2007) Critical amino acid residues of maurocalcine involved in pharmacology, lipid interaction and cell penetration. *Biochim Biophys Acta* **1768**: 2528-2540

Mansson, A., Sundberg, M., Balaz, M., Bunk, R., Nicholls, I.A., Omling, P., Tagerud, S., and Montelius, L. (2004). In vitro sliding of actin filaments labelled with single quantum dots. B*iochem Biophys Res Commun* **314**: 529-534

Michalet X, Pinaud FF, Bentolila LA, Tsay JM, Doose S, Li JJ, Sundaresan G, Wu AM, Gambhir SS, Weiss S (2005) Quantum dots for live cells, in vivo imaging, and diagnostics. *Science* **307**: 538-544

Mosbah A, Kharrat R, Fajloun Z, Renisio JG, Blanc E, Sabatier JM, El Ayeb M, Darbon H (2000) A new fold in the scorpion toxin family, associated with an activity on a ryanodine-sensitive calcium channel. *Proteins* **40**: 436-442

Pinaud F, King D, Moore HP, Weiss S (2004) Bioactivation and cell targeting of semiconductor CdSe/ZnS nanocrystals with phytochelatin-related peptides. *J Am Chem Soc* **126**: 6115-6123

Ram N, Aroui S, Jaumain E, Bichraoui H, Mabrouk K, Ronjat M, Lortat-Jacob H, De Waard M (2008a) Direct Peptide Interaction with Surface Glycosaminoglycans Contributes to the Cell Penetration of Maurocalcine. *J Biol Chem* **283**: 24274-24284

Ram N, Weiss N, Texier-Nogues I, Aroui S, Andreotti N, Pirollet F, Ronjat M, Sabatier JM, Darbon H, Jacquemond V*, et al.* (2008b) Design of a disulfide-less, pharmacologically-inert and chemically-competent analog of maurocalcine for the efficient transport of impermeant compounds into cells. *J Biol Chem*. **283**: 27048-27056

Santra S, Yang H, Stanley JT, Holloway PH, Moudgil BM, Walter G, Mericle RA (2005) Rapid and effective labeling of brain tissue using TAT-conjugated CdS:Mn/ZnS quantum dots. *Chem Commun (Camb),* **25**: 3144-3146

Schwartz EF, Capes EM, Diego-Garcia E, Zamudio FZ, Fuentes O, Possani LD, Valdivia HH (2009) Characterization of hadrucalcin, a peptide from Hadrurus gertschi scorpion venom with pharmacological activity on ryanodine receptors. *Br J Pharmacol* **157**: 392-403

Shahbazzadeh D, Srairi-Abid N, Feng W, Ram N, Borchani L, Ronjat M, Akbari A, Pessah IN, De Waard M, El Ayeb M (2007) Hemicalcin, a new toxin from the Iranian scorpion *Hemiscorpius lepturus* which is active on ryanodine-sensitive Ca2+ channels. *Biochem J* **404**: 89-96

Silver J, Ou W (2005) Photoactivation of quantum dot fluorescence following endocytosis. *Nano Lett* **5**: 1445-1449

Sukhanova A, Devy J, Venteo L, Kaplan H, Artemyev M, Oleinikov V, Klinov D, Pluot M, Cohen JH, Nabiev I (2004) Biocompatible fluorescent nanocrystals for immunolabeling of membrane proteins and cells. *Anal Biochem* **324**: 60-67

Szappanos H, Smida-Rezgui S, Cseri J, Simut C, Sabatier JM, De Waard M, Kovacs L, Csernoch L, Ronjat M (2005) Differential effects of maurocalcine on Ca^{2+} release events and depolarization-induced Ca2+ release in rat skeletal muscle. *J Physiol* **565**: 843-853

Voura EB, Jaiswal JK, Mattoussi H, Simon SM (2004) Tracking metastatic tumor cell extravasation with quantum dot nanocrystals and fluorescence emission-scanning microscopy. *Nat Med* **10**: 993-998

Wadia JS, Dowdy SF (2002) Protein transduction technology. *Curr Opin Biotechnol* **13**: 52-56

Zamudio FZ, Gurrola GB, Arevalo C, Sreekumar R, Walker JW, Valdivia HH, Possani LD (1997) Primary structure and synthesis of Imperatoxin A (IpTx(a)), a peptide activator of Ca^{2+} release channels/ryanodine receptors. *FEBS Lett* **405**: 385-389

Zhu S, Darbon H, Dyason K, Verdonck F, Tytgat J (2003) Evolutionary origin of inhibitor cystine knot peptides. *Faseb J* **17**: 1765-1767

Toxines et Signalisation – Toxins and Signalling
Rencontres en Toxinologie – Meeting on Toxinology, 2009
Editions de la SFET – SFET Editions
Accès libre en ligne sur le site – Free access on line on the site : http://www.sfet.asso.fr

Les Amoebophrya*, parasitoïdes de dinoflagellés toxiques*

Aurélie CHAMBOUVET, Laure GUILLOU*

Station Biologique de Roscoff, UMR 7144, Centre national de recherche scientifique (CNRS), Université Pierre et Marie Curie (Paris VI), place G. Tessier, 29680 Roscoff, France

** Auteur correspondant ; Tél : 33 2 98 29 23 79 ; Fax : 33 2 98 29 23 24 ; Courriel : lguillou@sb-roscoff.fr*

Résumé

Les Syndiniales (Alveolata) forment un groupe constitué de protistes dinoflagellés parasites marins ubiquistes, infectant de nombreuses espèces planctoniques, depuis le phytoplancton jusqu'à des larves de poissons. En particulier, le genre Amoebophrya *(Syndiniales, Alveolata) est capable d'infecter certaines micro-algues toxiques responsables d'efflorescences (appelées aussi marées rouges). La virulence de ces parasitoïdes est extrême, car ils empêchent la reproduction de leur hôte et le tuent obligatoirement pour accomplir leur cycle de vie. Au bout de 2 à 4 jours, chaque cellule hôte infectée aboutit à la libération de plusieurs centaines de nouvelles cellules infectives dans l'eau. De plus, ce parasite paraît hautement spécifique d'une espèce donnée, le même clade génétique revenant infecter la même espèce hôte d'une année sur l'autre. Toutes ces caractéristiques lui confèrent les capacités de réguler et d'empêcher la prolifération de micro-algues toxiques. Ainsi, l'existence même d'efflorescences algales toxiques a été récemment réinterprétée comme une absence de ces contrôles parasitaires, permettant à la micro-algue de devenir localement invasive. Ce découplage entre microalgues et pathogènes naturels pourrait être favorisé par le déplacement de nombreuses souches, accéléré aujourd'hui par le réchauffement climatique et par le transport maritime.*

The Amoebophrya*, parasitoid of toxic dinoflagellates*

Syndiniales (Alveolata) are a group of ubiquitous marine parasitic dinoflagellates infecting a wide range of planktonic species, from phytoplankton to fish larvae. Amoebophrya *genus (Syndiniales, Alveolata) are able to infect toxic micro-algae which are responsible of toxic algal blooms (also called red tides). The extreme virulence of these parasitoids avoids the host duplication. After 2-4 days, each infected cell allows the release of hundreds of free-living new infective parasites, and obligatory include the host death. Furthermore, this parasite appears to be species specific, the same genotype infecting the same host species, year after year. All these features allow this parasite to control and prevent noxious algal proliferations. Hence, the toxic algal blooms may occur in absence (or inefficiency) of their natural parasites leading to these micro-algae to become locally invasive. Such disruptive connection between micro-alga and their natural pathogen could be favoured by the transfer of non-endemic species into novel environments, increasing today because of the global warming and multiple shipping transportations.*

Keywords : Amoebophrya*, biological control, Dinoflagellates, harmful algal blooms, parasitoid.*

Introduction

Depuis 20 ans, le nombre d'espèces de micro-algues toxiques recensées sur les côtes françaises ne cesse d'augmenter (données du REPHY - réseau national de surveillance du phytoplancton, IFREMER). L'arrivée massive de ces nouvelles espèces toxiques, souvent invasives, a plusieurs explications. Avec le réchauffement climatique, les populations se déplacent sensiblement, et peuvent coloniser de nouvelles aires géographiques. L'eutrophisation de nos côtes (produit par l'agriculture intensive ou le développement de zones touristiques) apporte les conditions idéales au développement phytoplanctonique. Enfin, l'utilisation du transport maritime permet le déplacement de souches sur de très grandes distances géographiques, *via* les ballasts des cargos. Une fois installées, ces micro-algues peuvent devenir de véritables fléaux. Le développement de micro-algues toxiques entraine chaque année la fermeture de nombreux bassins de production aquacole (moules, huîtres, coquilles Saint-Jacques).

Les toxines produites par ces micro-algues s'accumulent dans les tissus de ces bivalves filtreurs jusqu'à des concentrations parfois mortelles pour l'Homme. Il n'existe aucun antidote. De plus, ces toxines ne s'éliminent pas à la cuisson. L'interdiction des ventes ainsi que la fermeture des zones contaminées restent les seules mesures préventives actuelles. La plupart de ces espèces phytoplanctoniques toxiques appartiennent au groupe des dinoflagellés. Ces micro-algues contaminent généralement les écosystèmes à long terme, car la plupart sont capables de produire des kystes de résistance qui se déposent dans les sédiments en attendant des conditions plus favorables.

Si les facteurs favorisant le transport ou le développement de ces micro-algues sont relativement bien connus, en revanche les causes de mortalité, et en particulier le rôle de bio-contrôles naturels, comme celui de certains parasites, reste très mal connu. Ainsi depuis quelques années, il a été observé que certaines micro-algues invasives, capables de produire localement des efflorescences toxiques durant plusieurs années consécutives, finissaient par voir leur population diminuer avec le temps. Nous reportons ici le rôle d'un groupe particulier de Dinoflagellés endoparasites, les *Amoebophrya*, dans le contrôle de nombreuses espèces du plancton marin.

Des eucaryotes parasites du plancton marin

Des parasites révélés par des études de diversité génétique

Le début des années 2000 a été marqué par une véritable révolution dans notre connaissance de la richesse spécifique du plancton marin. En effet, l'utilisation de la biologie moléculaire a offert une alternative à l'isolement et a permis de mieux décrire les communautés naturelles, en particulier les plus petites fractions de taille. Ces études consistent à extraire l'ADN génomique d'un échantillon environnemental, puis à étudier la diversité génétique d'un gène cible, en général celui codant la petite sous-unité de l'ARN ribosomal (ou ADNr 18S). Ainsi, le séquençage à haut débit d'une grande variété d'environnements a permis l'accumulation dans les bases de données d'un nombre important de séquences de protistes inconnus.

De nouveaux groupes d'eucaryotes ont ainsi pu être découverts, en particulier de très nombreuses séquences environnementales appartenant au phylum des Alvéolés. Les nouveaux Alvéolés marins (MALV), décrits grâce à ces techniques, se répartissent en quatre groupes principaux (Lopez-Garcia*, et al.*, 2001 ; Moon-van der Staay *et al.*, 2001 ; Guillou *et al.*, 2008). Les séquences appartenant aux groupes I et II sont les plus nombreuses et ont été détectées dans tous les écosystèmes marins étudiés : depuis la surface des océans (Díez*, et al.*, 2001 ; Moon-van der Staay *et al.*, 2001) jusqu'à 3.000 mètres de profondeur (Edgcomb *et al.*, 2002 ; Lopez-Garcia *et al.*, 2003), ainsi qu'au niveau des sources hydrothermales de profondeur (Lopez-Garcia *et al.*, 2001). Ces séquences représentent en moyenne près de 20 à 50% des séquences environnementales récupérées au sein des librairies génétiques eucaryotes (Lopez-Garcia *et al.*, 2001 ; Moon-van der Staay *et al.*, 2001) Ces groupes apparaissent d'une importance écologique considérable au vu de leur abondance relative dans toutes les banques de clones, même s'il est probable que des biais de PCR existent et que ces résultats sont loin d'être quantitatifs.

Nous savons aujourd'hui que toutes ces séquences appartiennent aux Syndiniales, une classe de protistes exclusivement composée à ce jour de parasites dont certains sont décrits et connus depuis plus d'un siècle! Prises dans leur ensemble, les espèces décrites au sein des Syndiniales sont capables d'infecter tous les compartiments du réseau trophique marin (Guillou *et al.*, 2008), depuis certaines micro-algues (les dinoflagellés), des consommateurs primaires de ces micro-algues (Ciliés, Copépodes, Radiolaires), jusqu'à des consommateurs secondaires ou des détritivores type larves de poissons, crabes ou langoustines. L'impact écologique de ces parasites n'est pas sans conséquence. Ainsi le parasite *Hematodinium* induisant le syndrome de « Bitter crab disease » a fait de très nombreux dégâts dans les pêcheries de ces crustacés, comme en France entre 1984 et 1988 où la récolte de l'étrille (*Necora puber*) a diminué de 96% (Wilhelm *et al.*, 1996).

Généralement, l'infection se révèle très rapidement fatale pour l'hôte, et aboutit dans tous les cas à la production et à la libération dans l'eau de cellules nageuses de très petite taille (environ 2 µm dans le cas de *Amoebophrya ceratii)*, appelées dinospores, qui représentent le stade infectieux. Les séquences environnementales retrouvées dans le micro et nano-plancton (de 0,2 µm à 20 µm) marin proviennent très certainement de cette phase libre (Guillou *et al.*, 2008).

Cycle de vie du parasite *Amoebophrya ceratii*

Amoebophrya ceratii est capable d'infecter de nombreuses espèces de dinoflagellés (si ce n'est toutes) (Cachon, 1964). Comme dans le cas de nombreuses autres Syndiniales, l'infection est initiée par l'entrée dans l'hôte d'une ou plusieurs dinospores (*Figure 1a*). Après plusieurs cycles de réplication actifs du matériel génétique, ces dinospores produisent une structure multi-nucléée appelée trophonte (stade endocellulaire). Ce trophonte, en forme de nid d'abeille (« beehive stage » en anglais) est caractéristique du genre *Amoebophrya* sp. (*Figures 1b et c*). La pression du trophonte à la dernière étape de maturation est telle que la cellule hôte se déforme et double de taille (*Figure 1c*). A maturité, le parasite va alors subir une métamorphose surprenante. Par une ultime évagination, il sort de son hôte sous la forme d'un long filament de cellules, le vermiforme (*Figures 2e et f*). Cette structure temporaire est parfaitement libre et mobile. Chaque cellule constitutive de ce vermiforme finira par s'individualiser en quelques heures pour redonner une nouvelle dinospore. Ce type de parasite est appelé parasitoïde. Bien qu'habituellement utilisé dans le cas de parasites d'insectes, le terme parasitoïde signifie que le parasite tue son hôte pour accomplir son cycle de vie (Combes, 2001).

Spécificité et impact écologique d'*Amoebophrya ceratii*

Spécificité d'infection d'*Amoebophrya ceratii*

La spécificité est probablement la caractéristique principale d'un parasite, mais elle reste très souvent difficile à définir avec certitude. Par exemple, il est très difficile, voire impossible, de distinguer différentes souches du parasite *Amoebophrya* infectant différentes espèces hôtes sur des critères morphologiques, ce qui a fait penser pendant longtemps que ce parasite était capable d'infecter un très grand nombre d'espèces, sans grande spécificité. Cependant, cette homogénéité morphologique masque une très grande variabilité génétique (Cachon,

1964 ; Nishitani *et al.*, 1985). Finalement, la validité même de l'espèce *A. ceratii* est remise en cause, étant plutôt considérée aujourd'hui comme un « complexe d'espèces » (Coats *et al.*, 1996 ; Janson *et al.*, 2000).

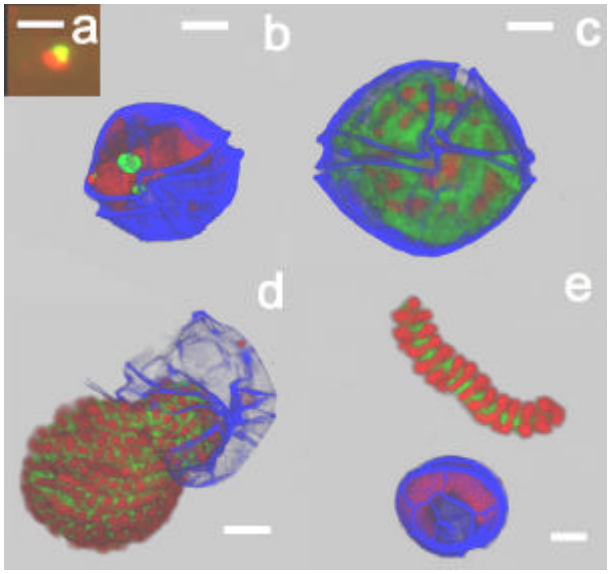

Fig. 1. Cycle de vie d'*Amoebophrya ceratii* infectant la micro-algue toxique *Alexandrium minutum* (dinoflagellé). Observations à partir d'échantillons naturels (Estuaire de la Penzé, Finistère). Fluorescence verte : sonde oligonucléotidique spécifique des parasites Syndiniales du groupe II, fluorescence rouge : marquage des noyaux à l'iodure de propidium, fluorescence bleue : thèque de l'hôte marquée au calcofluor. (**a**) Une dinospore, stade libre. (**b**) Stade précoce d'infection, début de formation du stade trophonte. (**c**) Trophonte mature (également appelé "beehive stage"). (**d**) Après maturation du parasite, la cellule hôte est complètement vidée de toute substance. (**e**) Stade vermiforme. La barre d'échelle représente 3 µm (**a**) ou 10 µm (**b** - **e**) (Chambouvet *et al.*, 2008).

Fig. 1. *Life cycle of* Amoebophrya ceratii *(Syndiniales, Alveolata) infecting the toxic micro-algae* Alexandrium minutum *(Dinoflagellate, Alveolata) from natural samples (Penzé estuary, Finistère France). Green fluorescence: Group II (Syndiniales, Alveolate) specific oligonucleotidique probe, red fluorescence: nuclear genomic DNA stained by propidium iodide, blue fluorescence: cellulosic host theca labelled by calcofluore. (**a**) Free living stage of parasite, the dinospore. (**b**) Early stage of* A. minutum *infection, early trophont stage formation. (**c**) Mature trophont stage ("beehive stage"). (**d**) Very late stage of trophont maturation of parasite, the parasite disrupts the wall host cell and leaves behind him the empty host theca (**e**) Vermiform stage. The scale bars represents 3 µm (**a**) or 10 µm (**b** - **e**) (Chambouvet et al., 2008).*

Les tests de spécificité en culture ont produit des résultats contradictoires. Coats et collaborateurs ont montré qu'une souche d'*A. ceratii* infectant initialement le dinoflagellé *Akashiwo sanguinea* n'était pas capable d'infecter d'autres dinoflagellés comme *Ceratium furca, Gyrodinium uncatenum* ou encore *Scrippsiella trochoidea* (Coats *et al.,* 1996). Par contre, Kim a montré en 2006 qu'une souche ayant pour hôte primaire *Gonyaulax polygramma*, était également capable d'infecter au moins 5 autres espèces de dinoflagellés appartenant à 5 genres différents (Kim, 2006). Il est aujourd'hui accepté que les barrières de spécificité d'un parasite dépendent largement des conditions environnementales, et sont souvent plus perméables en laboratoire que dans le milieu naturel plus complexe (Poulin *et al.*, 2007). La spécificité d'un parasite devrait donc s'évaluer *in situ*.

L'élaboration de sondes ADN spécifiques de différents clades génétiques d'*Amoebophrya* a permis de visualiser par fluorescence (technique du FISH-TSA) ce parasite directement dans des échantillons naturels, et d'en étudier la spécificité. Dans l'estuaire de la Penzé (Finistère Nord), cette technique a permis de démontrer que toutes les espèces de dinoflagellés présentes sont infectées, ce qui confirme l'importance écologique de ce groupe de parasites. Cependant, chaque espèce hôte est infectée par un parasite très différent génétiquement. Au cours de temps, la spécificité de ces attaques parasitaires induit une succession rapide des espèces de dinoflagellés, l'espèce dominante changeant d'une semaine sur l'autre (Chambouvet *et al.*, 2008). Sur trois années consécutives, il a été observé que le même parasite revenait infecter la même espèce hôte, année après année.

Cependant, si l'on compare l'histoire évolutive de ces parasites avec celle de leurs hôtes, on s'aperçoit rapidement de l'absence totale de co-évolution. En effet, deux clades complètement différents peuvent infecter deux espèces du même genre. Par exemple, des souches appartenant aux clades 2 et 4 sont respectivement capables d'infecter les espèces toxiques *Alexandrium tamarense* et *Alexandrium affine*. A l'inverse, des souches de parasites appartenant à un même clade peuvent infecter deux genres différents. Ainsi, des parasites infectant le genre *Scrippsiella* appartiennent également au clade 2. Cette absence de co-évolution entre les parasites et leurs hôtes est typique d'une histoire évolutive complexe, incluant de fréquents changements d'hôtes (Guillou *et al.*, 2008).

En conclusion, la spécificité des parasites appartenant aux Amoebophryidae se révèle être souche dépendante, engendrant dans l'écosystème une forte pression de sélection spécifique sur les dinoflagellés cibles. Ces parasites jouent donc un rôle majeur dans la dynamique des populations, et peut-être sont-ils capables à terme de s'adapter localement à une nouvelle espèce hôte.

Impact de la toxicité de l'hôte sur le parasite

Certaines espèces de dinoflagellés produisent de puissantes toxines. Actuellement deux hypothèses expliqueraient l'utilité de ces toxines. Résultantes du métabolisme secondaire, elles pourraient être excrétées et jouer un rôle dans le signal allélopathique (Legrand *et al.*, 2003). Egalement, ces toxines pourraient être un moyen de défense efficace contre les prédateurs naturels, tels que dinoflagellés hétérotrophes (John *et al.*, 2002), Ciliés (Hansen *et al.*, 1992), Copépodes (Carlsson *et al.*, 1995) et autres groupes zooplanctoniques (Pogorelov *et al.*, 1996). Cependant, ces toxines semblent parfaitement inefficaces dans la protection contre le parasite *Amoebophrya* sp. Des expériences *in vitro* ont même démontré par l'utilisation de différentes souches du dinoflagellé *Karlodinium veneficum* plus ou moins toxiques que l'infection était positivement corrélée à la toxicité (Bai *et al.*, 2007). Ainsi, ce parasite semblerait insensible aux karlotoxines (KmTx1 et KmTx2), produites par *K. veneficum*. Pourtant, ces dernières ont la capacité de perméabiliser les membranes cellulaires des cellules cibles aux ions et aux petites molécules conduisant par lyse osmotique à la mort cellulaire (Deeds *et al.*, 2003). De plus, il semblerait que ces toxines ne soient pas directement dégradées par le parasite (Bai *et al.*, 2007).

L'effet des karlotoxines pourrait bien dépendre de la composition en stérol de la membrane. De façon intéressante, les compositions en stérol des membranes du parasite et de son hôte sont très proches, composées de gymnodinostérol et de brévestérol qui interagissent peu avec les karlotoxines comparés au cholestérol ou autres diméthylstérols (Deeds *et al.*, 2006 ; Leblond *et al.*, 2006). Afin de se protéger des toxines, ces parasites pourraient adopter les mêmes stratégies que leur hôte. Ces résultats ont été retrouvés dans deux autres couples hôte/parasite, *Amoebophrya*/*Akashiwo sanguinea* et *Amoebophrya*/*Gymnodinium instriatum* (Place *et al.*, 2009). Néanmoins, cette règle ne semble pas universelle et ne s'applique pas au couplage *Amoebophrya*/*Alexandrium tamarense*, chaque partenaire possédant une composition membranaire en stérol différente. Un spectre d'hôte plus large pour cette souche de parasite est invoqué pour expliquer cette différence (Place *et al.*, 2009).

Impact écologique d'*Amoebophrya ceratii* sur les populations hôtes

Le temps de génération du parasite, sa progéniture (nombre de dinospores produites par cellule infectée) et la prévalence (% d'hôtes infectés) sont d'importants paramètres pour estimer la mortalité induite par le parasitisme. En culture, ce type de parasite est hautement virulent : une fois infectée, la cellule hôte est incapable de se reproduire et aucune ne survit à l'infection. Le temps de génération est compris entre 2 et 4 jours (Coats *et al.*, 2002 ; Park *et al.*, 2002) et aboutit à la libération de plusieurs centaines de dinospores. Ainsi, une prévalence de 1% est théoriquement suffisante pour infecter l'ensemble de la population hôte après deux-trois générations de parasites, c'est-à-dire une dizaine de jours. Dans le milieu naturel, les prévalences observées sont généralement inférieures à 10% (Fritz *et al.*, 1992 ; Coats *et al.*, 1994) mais de fortes prévalences (> 50%) ont été occasionnellement corrélées au déclin rapide des populations hôtes (Fritz *et al.*, 1992 ; Coats *et al.*, 1996).

L'estimation de la prévalence à partir d'échantillons naturels se heurte à des difficultés d'ordre méthodologique. D'une part, la méthode classiquement utilisée (coloration nucléaire) ne permet d'observer que les stades d'infection matures. En effet, les premiers stades d'infection sont très difficiles à détecter ce qui conduit à la sous-estimation des prévalences. D'autre part, la dynamique hôte/parasite est très rapide, et seul un échantillonnage journalier de la même masse d'eau peut permettre une bonne estimation de ce paramètre.

Enfin, la colonne d'eau est un milieu complexe où de nombreuses interactions existent. En effet, des facteurs abiotiques (*e.g.* facteurs environnementaux) et biotiques (*e.g.* broutage) peuvent influencer aussi bien la dynamique des hôtes que celle des parasites. En particulier, le broutage est un facteur probablement très important car les micro-prédateurs (Ciliés) sont des organismes capables de consommer aussi bien l'hôte (Calbet *et al.*, 2003), la partie libre du parasite, que les hôtes infectés (Johansson *et al.*, 2002). Ainsi, en culture, la présence de Ciliés de petite taille tels que *Strombilidium* sp. broutant des dinospores diminue de 70 à 80% le nombre de cellules hôtes *Akashiwo sanguinea* infectées (Johansson *et al.*, 2002).

Le découplage hôte-parasite à l'origine des efflorescences algales toxiques ?

Pour synthétiser ces interactions complexes, il faut faire appel à la modélisation. Pour cela, un modèle hôte-microparasite de type Anderson-May a été intégré à un modèle classique du réseau trophique microbien (nano- et microphytoplancton, nano- et microzooplancton). Les données disponibles dans la littérature concernant ces interactions en milieu estuarien, ainsi que la physiologie de la micro-algue toxique *Alexandrium minutum,* ont ensuite servi à paramétrer ce modèle. Les simulations utilisant ce modèle sont sans appel ; le broutage seul semble incapable de prévenir l'apparition d'une efflorescence toxique par *Alexandrium minutum*. Par contre, l'ajout du parasite *Amoebophrya*, même à de très faibles concentrations, induit la régulation rapide du développement de la microalgue toxique et le parfait contrôle de sa population en quelques jours seulement (Montagnes *et al.*, 2008).

Et ce scénario mime à s'y méprendre certaines observations récurrentes, en particulier celles effectuées en baie de Penzé. L'espèce toxique *Alexandrium minutum* fut détectée pour la première fois sur les côtes finistériennes en 1988. A partir de cette période, cette micro-algue a proliféré annuellement pendant près de 10

ans, dépassant des dizaines de million de cellules par litre conduisant à de nombreuses fermetures des zones de productions aquacoles. Aujourd'hui, bien qu'elle soit présente chaque année, les densités de cette micro-algue n'ont plus jamais dépassé des centaines de milliers cellules par litre avec la disparition des événements toxiques depuis bientôt 6 ans, et ce malgré des conditions environnementales propices à son développement. En 2004, grâce à des techniques de biologie moléculaire, nous avons montré que ce phénomène est corrélé à la présence des parasitoïdes de type *Amoebophrya* sp. Depuis, nous savons que cette microalgue est parasitée avec des prévalences de l'ordre de 10 à 20% impliquant un rôle important des parasites dans la régulation de la microalgue toxique. Autrement dit, les efflorescences de dinoflagellés (ou marées rouges) pourraient tout simplement traduire l'incapacité de certains pathogènes du type parasites à infecter localement une espèce, qui deviendrait alors invasive si les conditions le permettent.

Cette hypothèse est à rapprocher de celle plus générale qui consiste à expliquer la capacité d'une espèce à devenir localement invasive par l'absence d'ennemis adaptés ou « « the Enemy Release Hypothesis » (Keane *et al.*, 2002). Le cas certainement le plus médiatisé en milieu marin est celui de la macro-algue *Caulerpa taxifolia* introduite accidentellement sur les côtes méditerranéennes françaises en 1984 (Meinesz *et al.*, 1995). Depuis, en absence de tout prédateur, elle est devenue invasive, avec des conséquences désastreuses pour l'environnement (Meinesz *et al.*, 1995).

Conclusion

En conclusion, depuis sa première apparition en 1988 suivie de sa régulation en 1998, 10 ans ont donc été nécessaires à la mise en place d'un contrôle naturel de la micro-algue toxique *Alexandrium minutum* dans l'estuaire de la Penzé. Cet exemple n'est pas isolé. Ce phénomène a été observé dans le port d'Alexandrie (Egypte) où *A. minutum,* après 30 ans d'efflorescences toxiques régulières*,* paraît aujourd'hui régulé à de faibles concentrations cellulaires. Il reste à comprendre encore dans bien des cas l'origine et l'identité de ces régulations (Ismael, 2003).

En 1968, Taylor proposa l'utilisation de bio-contrôle comme *Amoebophrya* pour lutter contre les efflorescences algales toxiques (Taylor, 1968). En effet, l'utilisation d'*Amoebophrya* dans cette lutte biologique pourrait finalement s'envisager au vu de la spécificité apparente de ces parasites. Cependant, même si les efflorescences toxiques sont en pleine augmentation, l'histoire nous rappelle qu'il est souvent dangereux d'introduire une espèce pour en contrôler une autre. En effet, l'utilisation de bio-contrôles a souvent abouti à une cascade d'événements ayant parfois des conséquences encore plus désastreuses que le problème initial. Il n'en demeure pas moins que les mécanismes de cette régulation et de la spécificité de ces parasites sont autant de voies à explorer, pouvant aboutir à une meilleure compréhension de ce phénomène naturel.

Remerciements. *Nous tenons à remercier Françoise Goudey-Perrière pour nous avoir offert la possibilité de présenter notre modèle de recherche. Ce travail de recherche a été supporté financièrement par le projet ANR « Aquaparadox » ainsi que le Groupement d'Intérêt Scientifique Génomique Marine.*

Références bibliographiques

Bai X, Adolf JE, Bachvarof T, Place AR, Coats DW (2007) The interplay between host toxins and parasitism by *Amoebophrya*. *Harmful algae* **6**: 670-678

Cachon J (1964) Contribution à l'étude des péridiniens parasites. Cytologie, cycles évolutifs. *Ann Sci Nat, Zool, Paris,* VI ser 12, **6**: 1-15

Calbet A, Vaque D, Felipe J, Vila M, Sala MM, Alcaraz M, Estrada M (2003) Relative grazing impact of microzooplankton and mesozooplankton on a bloom of the toxic dinoflagellate *Alexandrium minutum*. *MEPS* **259**: 303-309

Carlsson P, Graneli E, Finenko G, Maestrini SY (1995) Copepod grazing on phytoplankton community containing the toxic dinoflagellate *Dinophysis acuminata. J Plank Res* **17**: 1925-1938

Chambouvet A, Morin P, Marie D, Guillou L (2008) Control of toxic marine dinoflagellate blooms by serial parasitic killers. *Science* **322**: 1254-1257

Coats D, Park M (2002) Parasitism of photosynthetic dinoflagellates by three strains of *Amoebophrya* (Dinophyta): Parasite survival, infectivity, generation time, and host specificity. *J Phycol* **38**: 520-528

Coats DW, Adam EJ, Gallegos CL, Hedrick S (1996) Parasitism of photosynthetic dinoflagellates in a shallow subestuary of Chesapeake Bay, USA. *Aquat Micro Ecol* **11**: 1-9

Coats DW, Bockstahler KR (1994) Occurrence of the Parasitic Dinoflagellate *Amoebophrya ceratii* in Chesapeake Bay Populations of *Gymnodinium sanguineum*. *J Eukaryot Microbiol* **41**: 586-593

Combes C (2001) Interactions durables, écologie et évolution du parasitisme. In *Collection Ecologie*, n°26, Masson (ed). Dunod: Paris, France

Deeds JR, Kao JPY, Hoesch RE, Place AR (2003) Toxic mode of action of KmTx 2, a fish-killing toxin from *Karlodinium micrum* (Dinophyceae). In *Proceedings of the second Symposium on Harmful Marine Algae in the U.S. (December 9-13, 2003),* Symposium Agenda, Abstract and Participants, p 19. Woods Hole, Massachusetts

Deeds JR, Place AR (2006) Sterol specific membrane interactions with the toxins from *Karlodinium micrum* (Dinophyceae) - a strategy for self-protection. *Harmful Algae 2004, Afr J Mar Sci* **28**: 421-427

Díez B, Pedrós-Alió C, Massana R (2001) Study of genetic diversity of eukaryotic picoplankton in different oceanic regions by small-subunit rRNA gene cloning and sequencing. *Appl Environ Microbiol* **67**: 2932-2941

Edgcomb VP, Kysela DT, Teske A, Gomez AD, Sogin ML (2002) Benthic eukaryotic diversity in the Guaymas Basin hydrothermal vent environment. *PNAS* **99**: 7658-7662

Fritz L, Nass M (1992) Development of the endoparasitic dinoflagellate *Amoebophrya ceratii* within host dinoflagellate species. *J Phycol* **28**: 312-320

Guillou L, Viprey M, Chambouvet A, Welsh RM, Kirkham AR, Massana R, Scanlan DJ, Worden AZ (2008) Widespread occurrence and genetic diversity of marine parasitoids belonging to Syndiniales (Alveolata). *Environ Microbiol* **10**: 3349-3365

Hansen PJ, Cembella AD, Moestrup O (1992) The marine dinoflagellate *Alexandrium ostenfeldii*: paralytic shellfish toxin concentration, composition, and toxicity to a tintinnid ciliate. *J Phycol* **28**: 597-603

Ismael AA (2003) Succession of heterotrophic and mixotrophic dinoflagellates as well as autotrophic microplankton in the harbour of Alexandria, Egypt. *J Plank Res* **25**: 193-202

Janson S, Gisselson P, Salomon P, Graneli E (2000) Evidence for multiple species within the endoparasitic dinoflagellate *Amoebophrya ceratii* as based on 18S rRNA gene-sequence analysis. *Parasitol Res* **86**: 929-933

Johansson M, Coats D (2002) Ciliate grazing on the parasite *Amoebophrya* sp. decreases infection of red-tide dinoflagellate *Akashiwo sanguinea*. *Aquat Microb Ecol* **28**: 69-78

John U, Tillmann U, Medlin L (2002) A comparative approach to study inhibition of grazing and lipid composition of a toxic and non toxic clone of *Chrysochromulina polylepis*. *Harmful algae* **1**: 45-47

Keane RM, Crawley MJ (2002) Exotic plant invasions and the enemy release hypothesis. *Trends Ecol Evol.* **17**: 164-170

Kim S (2006) Patterns in host range for two strains of *Amoebophrya* (Dinophyta) infecting thecate dinoflagellates: *Amoebophrya* spp. ex *Alexandrium affine* and ex *Gonyaulax polygramma*. *J Phycol* **42**: 1170-1173

Leblond J, Sengco M, Sikman J, Dahmen J, Anderson D (2006) Sterols of the Syndinian Dinoflagellate *Amoebophrya* sp., a Parasite of the Dinoflagellate *Alexandrium tamarense* (Dinophyceae). *J Eukaryot Microbiol* **53**: 211-216

Legrand C, Regenfors K, Fistarol GO, Graneli E (2003) Allelopathy in phytoplankton-biochemical and evolutionary aspects. *Phycologia* **42**: 406-419

Lopez-Garcia P, Philippe H, Gail F, Moreira D (2003) Autochthonous eukaryotic diversity in hydrothermal sediment and experimental microcolonizers at the Mid-Atlantic Ridge. *PNAS* **100**: 697-702

Lopez-Garcia P, Rodriguez-Valera F, Pedros-Alios C, Moreira D (2001) Unexpected diversity of small eukaryotes in deep-sea Antartic plankton. *Nature* **409**: 603-607

Meinesz A, De Vaugelas J, Hesse B, Mari X (1995) Spread of the introduced tropical green alga *Caulerpa taxifolia* in northern Mediterranean waters. *J Appl Phycol* **5**: 141-147

Montagnes DJS, Chambouvet A, Guillou L, Fenton A (2008) Responsibility of microzooplankton and parasite pressure for the demise of toxic dinoflagellate blooms. *Aquat Microb Ecol* **53**: 211-225

Moon-van der Staay SY, De Wachter R, Vaulot D (2001) Oceanic 18S rDNA sequences from picoplankton reveal unsuspected eukaryotic diversity. *Nature* **409**: 607-610

Nishitani L, Erickson G, Chew K (1985) Role of the parasitic dinoflagellate *Amoebophrya ceratii* in control of *Gonyaulax catenella* populations. In *Toxic dinoflagellates*, Anderson DM, White A and Baden DG (eds) pp 225-232. Elsevier: New York, USA

Park MG, Cooney SK, Yih W, Coats DW (2002) Effects of two strains of the parasitic dinoflagellate *Amoebophrya* on growth, photosynthesis, light absorption, and quantum yield of bloom-forming dinoflagellates. *MEPS* **227**: 281-292

Place AR, Bai X, Kim S, Sengco MR, Coats DW (2009) Dinoflagellate host-parasite sterol profiles dictate karlotoxin sensitivity. *J Phycol* **45**: 375-385

Pogorelov VI, Van Emmerik REA, Wagenaar RC, Pennington BF, Ozonoff S, Teegarden GJ, Cembella AD (1996) Grazing of toxic dinoflagellates, *Alexandrium* spp. by adult copepods of coastal Maine: implications for the fate of paralytic shellfish toxins in the marine food webs. *J Exp Mar Biol Ecol* **32**: 145-176

Poulin R, Keeney DB (2007) Host specificity under molecular and experimental scrutiny. *Trends Parasitol* **24**:24-28

Taylor FJR (1968) Parasitism of Toxin-Producing Dinoflagellate *Gonyaulax catenella* by Endoparasitic Dinoflagellate *Amoebophrya ceratii*. *J Fish Res Board Can* **25**: 2241-2245

Wilhelm G, Mialhe E (1996) Dinoflagellate infection associated with the decline of *Necora puber* crab populations in France. *Dis Aquat Org* **26**: 213-219

Toxines et Signalisation – Toxins and Signalling
Rencontres en Toxinologie – Meeting on Toxinology, 2009
Editions de la SFET – SFET Editions
Accès libre en ligne sur le site – Free access on line on the site : http://www.sfet.asso.fr

Gymnodimines : a family of phycotoxins contaminating shellfish

Riadh MARROUCHI[1,2], Evelyne BENOIT[2], Riadh KHARRAT[1], Jordi MOLGO[2*]

[1] *Laboratoire des Toxines Alimentaires, Institut Pasteur de Tunis, 13 Place Pasteur, B.P. 74, 1002 Tunis-Belvédère, Tunisie ;* [2] *CNRS, Institut de Neurobiologie Alfred Fessard, FRC2118, Laboratoire de Neurobiologie Cellulaire et Moléculaire, UPR9040, 91198 Gif-sur-Yvette cedex, France*

** Corresponding author ; Tel : +33 (0)1 69 82 36 42 ; Fax : +33 (0)1 69 82 41 41 ;*
E-mail : molgo@nbcm.cnrs-gif.fr

Abstract

Gymnodimines (GYMs) are phycotoxins belonging to the group of spiro-imines. They are the most recently discovered marine biotoxins in first New Zealand and then Tunisian coasts. The agent, responsible for the production of these toxins, is the dinoflagellate Karenia selliformis*, with a subhemispheric to conic epitheca, a big hypotheca and a central position of the nucleus. Following intraperitoneal injections of shellfish samples contaminated with GYM-A, mice present an acute neurotoxicity (flattening then paralysis of hind legs, respiratory difficulties) leading to the rapid death of animals. This toxin is also highly toxic when administered by intracerebroventricular injection. Nevertheless, it is less toxic when administrated by force-feeding, and even less toxic when ingested with food. At the cellular level, it contributes to decrease the number of neurons and to sensitize these cells to the apoptotic effects of okadaic acid. At the molecular level, it targets nicotinic acetylcholine receptors with high affinity and low specificity. Despite these effects, currently no regulatory control has been established for GYMs since, until now, the toxicity of GYMs to human remains to be determined.*

Les gymnodimines : une famille de phycotoxines contaminant les coquillages

Les gymnodimines (GYMs) sont des phycotoxines qui appartiennent au groupe des spiro-imines. Ce sont les biotoxines marines les plus récemment détectées qui soient, d'abord sur les côtes de Nouvelle Zélande puis sur les côtes tunisiennes. L'agent responsable de la production de ces toxines est le dinoflagellé Karenia selliformis *qui se distingue par une épithèque subhémisphérique puis conique, une grande hypothèque et un noyau en position centrale. Suite à des injections intrapéritonéales d'échantillons de coquillages contaminés par la GYM-A, les souris présentent une neurotoxicité aiguë (aplatissement puis paralysie des pattes postérieures, difficultés respiratoires) qui provoque la mort rapide des animaux. Cette toxine est également fortement toxique lorsqu'elle est injectée par voie intracérébro-ventriculaire. Cependant, elle est moins toxique lorsqu'elle est administrée par gavage et encore moins toxique lorsqu'elle est ingérée avec de la nourriture. Au niveau cellulaire, elle contribue à la réduction du nombre de neurones et sensibilise ces cellules aux effets apoptotiques de l'acide okadaique. Au niveau moléculaire, elle bloque, avec une haute affinité et une faible spécificité, les récepteurs nicotiniques de l'acétylcholine. En dépit de ces effets, le problème de santé publique posé par les GYMs demeure controversé. Jusqu'à présent, aucun seuil réglementaire n'a été établi dû au fait que la toxicité des GYMs vis-à-vis de l'homme reste encore à déterminer.*

Keywords : *Gymnodimines,* Karenia selliformis*, nicotinic acetylcholine receptors, regulatory control.*

Introduction

During the two past decades, the frequency, intensity and geographic distribution of harmful algal blooms have increased along with the number of toxic compounds found through the marine food chain (FAO, 2004). The marine biotoxins, produced by some species of micro-algae, are secondary metabolites with unknown explicit role in the metabolism of organisms that produce them although showing very specific activities in mammals. They are probably used by their producers as a way to compete for space, fight predation and/or as a defense against the overgrowth of other organisms (Botana *et al.*, 1996).

Recently, in 1994, novel seafood toxins have been discovered during routine toxin monitoring of bivalve mollusks from Foveaux Strait, in the South Island of New Zealand (Mackenzie *et al.*, 1994). This family of toxins, named gymnodimines (GYMs), is composed of three congeners (GYM-A, GYM-B and GYM-C ; *Figure 1*)

that were later detected in harvested clams from Tunisia (Biré *et al.*, 2002) and unequivocally in shellfish from European and North American coasts.

Until now, there is little information regarding the toxicological properties of GYMs, and no regulatory control has been established for these toxins.

Karenia selliformis, the producer of GYMs

Karenia selliformis is a well-known producer of GYMs in New Zealand (Mackenzie *et al.*, 2002 ; Miles *et al.*, 2003). This species has also been identified in Kuwait (Gilbert *et al.*, 2001 ; Heil *et al.*, 2001), and was recently discovered in Australia when GYMs were detected in phytoplankton samples (Takahashi *et al.*, 2007). Since 1990, *Karenia selliformis* appears every summer in the Boughrara Lagoon of Gabes Golf in Tunisia (Dammak *et al.*, 2009).

The size range of *Karenia selliformis* is 25-35 µm long, 17.5-27.5 µm wide and 5-10 µm thickness, as measured in cells from seawater samples, and 25-37.5 µm long, 20-30 µm wide, and 5-13 µm thickness, as measured in cultured cells. The characteristic detail of this dinoflagellate is located in the epitheca which appears subhemispheric to conic. When observed using a scanning electronic microscope, an apical groove extending vertically, to at least one third of both ventral and dorsal epitheca, is noted, as for other species of the genus *Karenia*. The hypotheca is generally bigger than the epitheca, with a convex dorsal side and an antapical indentation. The cingulum is wide and displaces at least one width. The hypothecal excavation of *Karenia selliformis* is more pronounced than that of *Karenia mikomotoi*. Finally, another structurally distinct feature of *Karenia selliformis* is the central position of the nucleus and the peripheral organization of 10-27 yellow-green chloroplasts (Dammak *et al.*, 2009).

The *Karenia* species identified in Tunisia presents some morphological and physiological differences when compared to European and Japanese strains (Hansen *et al.*, 2000), mainly because of its dorso-ventrally compressed and rounded shape appearance (Dammak *et al.*, 2009).

Mackenzie and collaborators (2002) found that about 30% of total GYMs were free in the medium during most of the growth phase of *Karenia selliformis*. This strongly suggests a possible ectocrine function for these compounds.

Structure elucidation and physicochemical characteristics of GYMs

The first chemical structure of GYMs to be solved was that of GYM-A. It was initially elucidated by nuclear magnetic resonance (NMR) spectroscopy (Seki *et al.*, 1995) and later confirmed by X-ray crystallographic analysis of its p-bromobenzamide derivative, which revealed its absolute stereochemistry (Stewart *et al.*, 1997). Then, two new analogs of GYM-A, GYM-B and GYM-C, were isolated from cell culture extracts of the dinoflagellate *Karenia selliformis* (Miles *et al.*, 2000, 2003). Although various synthesis approaches for GYMs have been developed, as recently reviewed (O'Connor and Brimble, 2007), total synthesis has not been reported to date.

GYM-A and analogs exhibit unusual structural features, including a spirocyclic imine ring system and a trisubstituted tetrahydrofuran embedded within a 16-membered macrocycle (*Figure 1*). The presence of the spirocyclic imine places these marine toxins in the same family as spirolides (Hu *et al.*, 1995 ; Cembella *et al.*, 1999), pinnatoxins (Uemura *et al.*, 1995 ; Chou *et al.*, 1996a), pteriatoxins (Takada *et al.*, 2001) and prorocentrolides (Chou *et al.*, 1996b). GYM-B is similar in structure to GYM-A, but contains an exocyclic methylene at C-17 and an allylic hydroxyl group at C-18 (Miles *et al.*, 2000), while GYM-C is an oxidized analog of GYM-A that was found to be isomeric with GYM-B at C-18 position (Miles *et al.*, 2003).

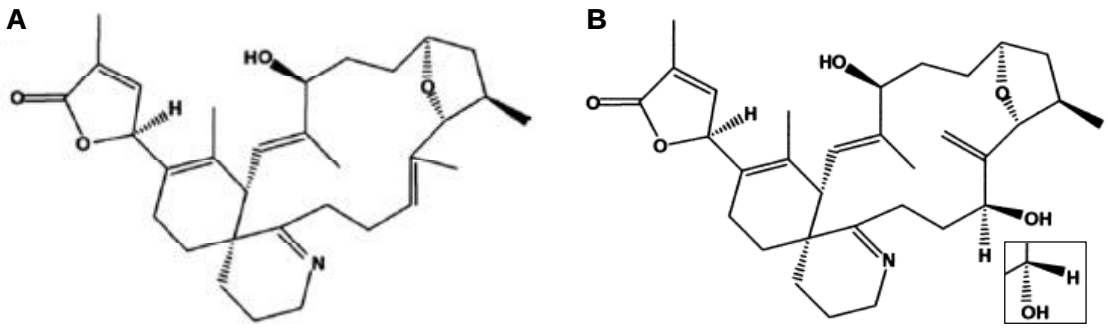

Fig. 1. Chemical structures of (**A**) GYM-A and (**B**) GYM-B and GYM-C (inset). From Kharrat *et al.* (2008).

Fig. 1. *Structures chimiques de (**A**) la GYM-A et (**B**) les GYM-B et GYM-C (encart). D'après Kharrat* et al. *(2008).*

GYMs decomposed in aqueous solutions, following first-order kinetics with half-lives at 37°C of 1020 h at pH 5.2, 33.2 h at pH 7.6 and 8.1 h at pH 9.6. No significant decomposition was detected at pH 1.8 and 2.8, or in methanol solutions at 37°C or 280°C over 2 weeks (Munday *et al.*, 2004).

Toxicity of GYMs

When injected to mice at lethal doses, GYMs are responsible for immediate hyperactivity followed, soon after, by reduction in exploratory movements. Afterwards, hind legs became paralyzed and extended. Subsequently, animals became completely immobile and unresponsive to stimuli. Severe dyspnea occurred followed by rapid death within 3 min after injection (Munday *et al.*, 2004 ; Kharrat *et al.*, 2008 ; Marrouchi *et al.*, 2009). The necropsy of mice revealed no organ lesion and no significant change in their body weight compared to uninjected animals (Munday *et al.*, 2004).

The dose of GYM-A producing death to 50% of mice (LD_{50}) was in the range of 80-96 µg/kg, when injected by intraperitoneal route (Munday *et al.*, 2004 ; Kharrat *et al.*, 2008). The toxin was also highly toxic when injected by intracerebroventricular route, with a LD_{50} of 3 µg/kg. However, it was less toxic when administered subcutaneously, with a LD_{50} of 100 µg/kg, and even more less toxic when administered by force-feeding (gavage) or ingested with food, with a LD_{50} of 755 mg/kg. GYM-B also produced toxic effects to mice but was about 10 fold less toxic than GYM-A since its LD_{50} was 800 µg/kg after intraperitoneal injection (Munday *et al.*, 2004 ; Kharrat *et al.*, 2008).

In addition to its toxicity to murins, GYM-A also showed potent ichthyotoxicity against a small freshwater fish *Tanichthys albonubes* at 0.1 ppm at pH 8 (Seki *et al.*, 1995).

At the cellular level, GYM-A was reported to contribute to decrease the number of neurons and to sensitize these cells to the apoptotic effects of the okadaic acid, also produced by *Karenia selliformis* (Dragunow *et al.*, 2005).

Mechanism of action of GYMs

The mechanism of action of GYM-A has been recently determined. In isolated mouse phrenic hemidiaphragm preparations, the toxin was shown to produce a concentration- and time-dependent block of twitch responses evoked by electric phrenic-nerve stimulation, without affecting the directly elicited muscle contraction (Kharrat *et al.*, 2008). This strongly suggests that GYM-A blocked muscle-type nicotinic acetylcholine (ACh) receptors (nAChRs). This was confirmed by the blockade of miniature endplate potentials and the recordings of subthreshold endplate potentials from GYM-A-paralyzed neuromuscular preparations isolated from frog and mouse. In addition, patch-clamp recordings from *Xenopus* skeletal myocytes revealed that the nicotinic currents evoked by constant iontophoretical ACh pulses were inhibited by GYM-A in a reversible manner. The toxin also blocked, in a voltage-independent manner, homomeric human α7 nAChRs expressed in *Xenopus* oocytes. Finally, competition-binding assays confirmed that GYM-A is a powerful ligand interacting with muscle-type nAChRs, heteropentameric $\alpha3\beta2$, $\alpha4\beta2$, and chimeric α7-5HT3 neuronal nAChRs (Kharrat *et al.*, 2008). In conclusion, GYM-A broadly targets muscle- and neuronal-types of nAChRs with a high affinity.

GYMs and human health risk

With respect to toxicity and until now, only data on the acute oral toxicity are available for the majority of the marine toxins, both in experimental animals and humans. However, repeated exposure to lower sublethal dose levels may be a common feature. In addition, administration of toxins by force-feeding can give an artifactual high estimate of their risk to human health (Mantle, 2002). Therefore, it was considered likely that administration of GYM-A by gavage may have given an artificially high estimate of the oral toxicity of the toxin, due to the semi-solid nature of mouse stomach contents. In this case, rapid uptake from this absorptive tissue has to be expected, and the delivery of the toxin into the duodenum would be assumed to be associated with rapid and severe toxic effects (Munday *et al.*, 2004).

At present, the toxicity of GYMs to humans remains unknown (Vilariño *et al.*, 2009) since no human intoxication has been unequivocally linked to GYMs poisoning (Richard *et al.*, 2000), as it is the case for the cyclic-imine toxin group (Marrouchi *et al.*, 2009). Currently, no regulatory control has been established for these toxins (Fux *et al.*, 2007).

Methods of GYMs detection

Officially, the mouse bioassay, adapted from that of Yasumoto and collaborators (1978), is the only method used for the detection of GYMs. Because of the low sensitivity and selectivity of this assay, many alternative chemical methods have been developed to monitor these toxins during the last years. Marrouchi and collaborators (2009) recently developed a new method to detect and quantify GYM-A from contaminated clams by High Performance Liquid Chromatography (HPLC)-UV. This method is of particular efficiency since recovery rates exceeded 96%, and limits of detection (LOD) and quantification (LOQ) were 5 ng/mL and 8 ng/g digestive glands, respectively.

A fast, non radioactive, quantitative method for the detection of cyclic-imines in shellfish was also recently developed, based on the high affinity binding of GYMs and spirolides to nAChRs. This method, which also does not require the use of laboratory animals, was designed as an inhibition assay according which, the binding of fluorescent α-bungarotoxin to *Torpedo* nAChRs was detected by fluorescence polarization and was inhibited by GYMs (Vilariño *et al.*, 2009).

Depuration of GYMs

Since GYMs are known to have a slow depuration rate in oysters (Stirling, 2001), there is high probability that the toxins remain in the ecosystems for a prolonged period.

The kinetics of GYM-A discharge was recently studied from starved clams in controlled medium : the depuration tanks used seawater of daily monitored salinity, dissolved oxygen and temperature (15 ± 2 °C) that was disinfected through a large sand filter and with UV. Toxicity of samples and changes in the amount of sequestered GYM-A in the shellfish digestive glands were evaluated using the mouse bioassay and HPLC method, respectively. During one month, depuration rate was found to be 85% of the total amount of sequestered GYM-A. It is worth noting that the kinetics of discharge was not the same during all the experimental periods since a fast exponential reduction of the total toxicity was noted in the first period (12 days) followed by a moderated one (>10% of the total amount) in the later period (Marrouchi *et al.*, 2009).

Conclusion

As a conclusion, the consumption of a variety of shellfish and fish causes an increasing number of human intoxications around the world, and safety of these products becomes until now the first challenge to preserve human health. One of the most serious problems to regulate the family of GYMs is the lack of information regarding the toxicological proprieties and especially the effects of repeated exposure to this emerging family of biotoxins.

Acknowledgements. *This study was performed in the frame of a Franco-Tunisian cooperation program funded by the French and Tunisian governments (PHC project 08G0903 to R.K. and J.M.).*

References

Biré R, Krys S, Fremy JM, Dragacci S, Stirling D, Kharrat R (2002) First evidence on occurrence of gymnodimine in clams from Tunisia. *J Nat Toxins* **11**: 269-275

Botana LM, Rodriguez-Vieytes M, Alfonso A, Louzao MC (1996) Phycotoxins: paralytic shellfish poisoning and diarrhetic shellfish poisoning. In *Handbook of food analysis*. Nollet LML (ed) Volume 2, Residues and other food component analysis, pp 1147-1169. Marcel Dekker: New York

Cembella AD, Lewis NI Quilliam MA (1999) Spirolide composition of micro-extracted pooled cells isolated from natural plankton assemblages and from cultures of the dinoflagellate *Alexandrium ostenfeldii. J Nat Toxins* **7**: 197-206

Chou T, Haino T, Kuramoto M Uemura D (1996a) Isolation and structure of pinnatoxin D: new shellfish poison from the Okinawan bivalve *Pinna muricata*. *Tetrahedron Lett* **37**: 4027-4030

Chou TT, de Freitas ASW, Curtis JM, Oshima Y, Walter JA, Wright JLC (1996b) Isolation and structure of prorocentrolide B a fast-acting toxin from *Prorocentrum maculosum*. *J Nat Prod* **59**: 1010-1014

Dammak-Zouari H, Hamza A, Bouain A (2009) Gymnodiniales in the Gulf of Gabes (Tunisia). *Cah Biol Mar* **50**: 153-170

Dragunowa M, Trzoss M , Brimble M. A, Camerona R, Beuzenberg V, Holland P, Mountfort D (2005) Investigations into the cellular actions of the shellfish toxin gymnodimine and analogues. *Environ Toxicol Pharmacol* **20**: 305–312

FAO (2004) Marine biotoxins. FAO food and nutrition, paper 80

Fux E, McMillan D, Biré R, Hess P (2007) Development of an ultra-performance liquid chromatography–mass spectrometry method for the detection of lipophilic marine toxins. *J Chromatogr A* **1157**: 273-280

Gilbert PM, Landesberg JH, Evans JJ, Al-Sarawi MAM, Faraj M, Al-Jarallah MA, Haywood A, Ibrahem S, Kleius P, Powell C, Shoemaker C (2001) A fish kill of massive proportion in Kuwait Bay, Arabian Gulf, 2001: the roles of bacterial disease, harmful algae, and eutrophication. *Harmful Algae* **1**: 215-231

Hansen G, Moestrup Ø, Roberts K (2000) Light and electron microscopical observations on the type species of *Gymnodinium*, *G. fuscum* (Dinophyceae). *Phycologia* **39**:365-376

Heil CA, Gilbert PM, Al-Sarawi MA, Faraj M, Behbehani M, Husain M (2001) First record of a fish-killing *Gymnodinium sp*. bloom in Kuwait Bay, Arabian Sea: chronology and potential causes. *Mar Ecol Prog Ser* **214**: 15-23

Hu T, Curtis JM, Oshima Y, Quilliam MA, Walter JA, Watson-Wright WM, Wright JLC (1995) Spirolides B and D, two novel macrocycles isolated from the digestive glands of shellfish. *J Chem Soc Chem Commun* **20**: 2159-2161

Kharrat R, Servent D, Girard E, Ouanounou G, Amar M, Marrouchi R, Benoit E, Molgó J (2008) The marine phycotoxin gymnodimine targets muscular and neuronal nicotinic acetylcholine receptor subtypes with high affinity. *J Neurochem* **21**: 952-963

Mackenzie L (1994) More blooming problems: toxic algae and shellfish biotoxins in the South Island (January–May 1994). *Seafood NZ* **2**: 47–52

Mackenzie L, Holland P, McNabb P, Beuzenberg V, Selwood A, Suzuki T (2002) Complex toxin profiles in phytoplankton and Green shell mussels (*Perna canaliculus*), revealed by LC-MS/MS analysis. *Toxicon* **40**: 1321-1330

Mantle PG (2002) Risk assessment and the importance of ochratoxins. *Int Biodeterior Biodegrad* **50**: 143–146

Marrouchi R, Dziri F, Hamza A, Benoit E, Molgó J, Kharrat R (2009) Quantitative determination of gymnodimine-A by high performance liquid chromatography in contaminated clams from Tunisia coastline. *Mar Biotech* (in press)

Miles CO, Wilkins AL, Stirling DJ, Mackenzie AL (2000) New analogue of gymnodimine from a *Gymnodinium* species. *J Agric Food Chem* **48**: 1373-1376

Miles CO, Wilkins AL, Stirling DJ, Mackenzie AL (2003) Gymnodimine C, an isomer of gymnodimine B, from *Karenia selliformis*. *J Agric Food Chem* **51**: 4838-4840

Munday R, Towers NR, Mackenzie L, Beuzenberg V, Holland PT, Miles CO (2004) Acute toxicity of gymnodimine to mice. *Toxicon* **44**: 173-178

O'Connor PD, Brimble MA (2007) Synthesis of macrocyclic shellfish toxins containing spiroimine moieties. *Nat Prod Rep* **24**: 869-885

Richard D, Arsenault E, Cembella AD, Quilliam M (2000) Investigations into the toxicology and pharmacology of spirolides, a novel group of shellfish toxins. In *Harmful Algal Blooms*. Hallegraeff GM, Blackburn SI, Bolch CJ and Lewis RJ (eds) pp 383-386. Intergovernmental Oceanographic Commission of Unesco 2001: Paris, France

Seki T, Satake M, Mackenzie L, Kaspar HF, Yasumoto T (1995) Gymnodimine, a new marine toxin of unprecedented structure isolated from New Zealand oysters and the dinoflagellate *Gymnodinium sp*. *Tetrahedron Lett* **36**: 7093-7096

Stewart M, Blunt JW, Munro MHG, Robinson WT, Hannah DJ (1997) The absolute stereochemistry of the New Zealand shellfish toxin gymnodimine. *Tetrahedron Lett* **38**: 4889-4890

Stirling DJ (2001) Survey of historical New Zealand shellfish samples for accumulation of gymnodimine. *NZ J Mar Freshwater Res* **35**: 851-857

Takada N, Umemura N, Suenaga K, Uemura D (2001) Structural determination of the pteriatoxins A, B, and C, extremely potent toxins from the bivalve *Pteria penguin*. *Tetrahedron Lett* **42**: 3495-3497

Takahashi E, Yu Q, Eaglesham G, Connell DW, McBroom J, Costanzo S, Shaw GR (2007) Occurrence and seasonal variations of algal toxins in water, phytoplankton and shellfish from North Stradbroke Island, Queensland, Australia. *Mar Environ Res* **64**: 429-442

Uemura D, Chou T, Hainao T, Nagatsu A, Fukuzawa S, Zheng SZ, Chen HS (1995) Pinnatoxin A: a toxic amphoteric macrocycle from the Okinawan bivalve *Pinna muricata*. *J Am Chem Soc* **117**: 1155-1156

Vilariño N, Fonfría ES, Molgó J, Aráoz R, Botana LM (2009) Detection of gymnodimine-A and 13-desmethyl C spirolide phycotoxins by fluorescence polarization. *Anal Chem* **81**: 2708-2714

Yasumoto T, Oshima Y, Yamaguchi M (1978) Occurrence of a new type shellfish poisoning in the Tohoku district. *Bull Jap Soc Sc Fish* **44**: 1249-1255

Toxines et Signalisation – Toxins and Signalling
Rencontres en Toxinologie – Meeting on Toxinology, 2009
Editions de la SFET – SFET Editions
Accès libre en ligne sur le site – Free access on line on the site : http://www.sfet.asso.fr

Effets thérapeutiques, antidotiques, antiparasitaires et toxiques des inhibiteurs de l'acétylcholinestérase : importance des phytotoxines et de leurs dérivés

Nicole PAGES[1,2*], Françoise GOUDEY-PERRIERE[2], Patrick BRETON[3]

[1] *Toxicologie, Faculté de Pharmacie, 67400 Illkirch ;* [2] *Biologie animale, Faculté de Pharmacie, 92296 Châtenay-Malabry ;* [3] *Centre d'Etudes du Bouchet, 91710 Vert le Petit, France*

** Auteur correspondant ; Fax : 33 (0)1 60 19 01 31 ; Courriel : nicole.pages4@hotmail.fr*

Résumé

Les inhibiteurs de l'acétylcholinestérase (AChEI), surtout des phytotoxines et leurs dérivés, sont utilisés pour inhiber la dégradation de l'acétylcholine (ACh). Les inhibiteurs périphériques réversibles sont utilisés dans le traitement du glaucome, de la myasthénie commune et des blocs neuromusculaires résiduels. Les inhibiteurs centraux réversibles permettent de diminuer les symptômes de diverses démences attribuées à une baisse du fonctionnement cholinergique, comme la maladie d'Alzheimer (AD), la démence vasculaire et autres affections psychiatriques et donc d'améliorer la vie quotidienne des malades. Ils représentent la première ligne de défense dans les formes légères et modérées d'AD. Leurs effets secondaires principaux sont d'ordre cholinergique, essentiellement digestifs à dose thérapeutique, mais deviennent plus dangereux à dose toxique. Certains AChEI sont employés comme antidotes dans les intoxications produites par l'atropine, par différents psychotropes et médicaments utilisés en anesthésie et en réanimation ou encore, en prévention d'intoxication par les organophosphates. A l'inverse, les AChEI chimiques irréversibles sont utilisés soit comme pesticides, soit exceptionnellement comme armes chimiques.

Therapeutic, antidotic, antiparasite and toxic effects of acetylcholinesterase inhibitors : importance of phytotoxins and derivates

Acetylcholinesterase inhibitors (AChEI), mainly phytotoxins and derivates, are used to inhibit the degradation of the neurotransmitter acetylcholine (ACh). Peripheral reversible inhibitors are used in the treatment of glaucoma, myasthenia, and residual neuromuscular blockade. Central reversible inhibitors allow an improvement of daily living and behavioural symptoms in various dementia attributed to a decrease in cholinergic function such as Alzheimer disease (AD), vascular dementia and other psychiatric affections. They represent the first line therapy in mild and moderate AD. Their major adverse effects are cholinergic disorders, mostly digestive at therapeutic doses and more severe at toxic doses. Some of AChEI can be employed as antidotes in the intoxications induced by atropine, as well as by various psychotrops and drugs used in anaesthesia or intensive care or organophosphates. In contrast, chemical irreversible AChEI are used either as pesticides or considered as potential weapons.

Keywords : *Alzheimer disease, central anticholinergic syndrome (CAS), cholinesterase inhibitors, galanthamine, physostigmine and derivates, phytotoxins.*

Introduction

Certaines pathologies telles que le glaucome, la myasthénie commune, les blocages neuromusculaires résultant d'une curarisation prolongée, ou les démences séniles au premier rang desquelles vient la maladie d'Alzheimer (AD, pour *Alzheimer Disease*), sont asociées à une baisse des concentrations d'acétylcholine (ACh). En inhibant sa dégradation physiologique par l'acétylcholinestérase (AChE), les inhibiteurs de l'AChE (AChEI) restaurent, au moins en partie, la transmission cholinergique. Beaucoup de molécules naturelles (Akhondzadeh et Abassi, 2006 ; dos Santos Neto *et al*., 2006 ; Houghton *et al*., 2006 ; Adams *et al*., 2007 ; Mukherjee *et al*., 2007), ainsi que des molécules d'hémisynthèse et de synthèse, inhibent l'AChE de façon réversible. Cependant, très peu sont aujourd'hui utilisées en thérapeutique, car la plupart sont trop toxiques. Il existe aussi des AChEI qui agissent de manière irréversible, plutôt utilisés comme pesticides (et potentiellement comme armes de destruction massive).

Transmission cholinergique et cholinestérases

L'ACh est un des neurotransmetteurs majeurs impliqués dans le fonctionnement du système nerveux

périphérique ou SNP (synapses ganglionnaires du système nerveux autonome, jonction neuromusculaire, muscle lisse, cœur) et dans celui du système nerveux central ou SNC (Dutar et Lamour, 1992). Après libération, elle se lie à un récepteur membranaire (nicotinique ou muscarinique). Les récepteurs nicotiniques sont impliqués au niveau périphérique dans la contraction des muscles squelettiques et dans le système nerveux sympathique et parasympathique et, au niveau central, dans les processus de mémorisation et autres fonctions cognitives telles que langage, pensée, raisonnement, jugement, facultés d'adaptation… (Houghton *et al*., 2006). Les récepteurs muscariniques sont responsables, au niveau périphérique, d'effets parasympathiques : baisse de la fréquence cardiaque et de la pression artérielle, hypersalivation, stimulation des sécrétions digestives, augmentation du péristaltisme intestinal, relâchement des sphincters, contraction des bronches et des muscles de la pupille, dépolarisation membranaire des cellules de la chaîne ganglionnaire et des fibres musculaires (Dutar et Lamour, 1992). Au niveau central, ils inhibent les conductances potassiques et calciques, ce qui provoque une dépolarisation de longue durée (Dutar et Lamour, 1992 ; [1]). Deux estérases sont responsables de la dégradation physiologique de l'ACh : l'acétylcholinestérase (AChE) et la butyrylcholinestérase (BuChE) (Wright *et al*., 1993).

L'AChE (EC 3.1.1.7) a pour fonction la dégradation spécifique et très rapide de l'ACh qu'elle coupe en choline et acétate, terminant ainsi la transmission des influx nerveux. Cette enzyme a une structure bien conservée à travers les espèces. Sa structure et son fonctionnement ont été déterminés chez le poisson *Torpedo californica* (qui sert de référence) ainsi que chez les Mammifères et l'Homme (Houghton *et al*., 2005 ; Silman et Sussman, 2005). Elle possède notamment un site anionique périphérique, sur lequel se fixe l'ACh et qui est la cible de nouveaux AChEI, et un site actif au fond d'une gorge. Le site actif contient une sérine (associée à la triade catalytique) et deux sous domaines, un noyau aromatique qui positionne la choline et une poche acyl qui limite la taille des ligands susceptibles d'entrer dans le site (Silman et Sussman, 2005 ; Houghton *et al*., 2006).

La BuChE (EC 3.1.1.8) a une structure analogue à celle de l'AChE. Elle se distingue par l'organisation du site périphérique en surface, les résidus aromatiques le long de la gorge qui facilitent le mouvement de l'ACh et la taille de la poche acyl. Il en résulte que la BuCh peut entrer dans le site actif de la BuChE mais pas dans celui de l'AChE. La BuChE est abondante dans de nombreux tissus (Li *et al*., 2000 ; Houghton *et al*., 2006).

L'AChE et la BuChE agissent différemment chez l'individu sain et chez le patient atteint d'AD. Chez le sujet sain, 80% de l'activité enzymatique est assurée par l'AChE, qui est 10^{13} fois plus rapide que la BuChE. Cependant, la BuChE est capable de compenser l'AChE lorsque la fonction de celle-ci est perturbée. L'AChE agit très sélectivement sur l'ACh alors que la BuChE agit sur différents substrats. Ces deux enzymes sont actives sous deux formes : une forme G4, formée de 4 sous-unités et une forme monomérique G1 qui ne joue qu'un rôle mineur chez le sujet sain. Chez le patient atteint d'AD, l'activité de l'AChE peut être réduite de 65% alors que celle de la BuChE (notamment la forme G1) augmente, ce qui se traduit par une modification du rapport BuChE/AChE qui passe de 0,5 chez le sujet sain à 15 chez le malade. Il est à noter que la BuChE accélère l'agrégation du peptide A-béta en fibrilles amyloïdes, caractéristiques de l'AD (Perry *et al*., 1978 ; Guillozet *et al*., 1997 ; Silman et Sussman, 2005). Les deux enzymes s'accumulent ensuite dans les plaques séniles et les neurofibrilles (Wright *et al*., 1993 ; Mesulam et Geula, 1994).

En plus de son rôle enzymatique, l'AChE intervient comme protéine d'adhésion, protéine de la matrice osseuse et dans la croissance des neurites (axone ou dendrites) (Silman et Sussman, 2005).

Inhibiteurs de l'acétylcholinestérase (AChEI)

En inhibant momentanément la dégradation physiologique de l'ACh, les AChEI permettent de renforcer la transmission synaptique cholinergique, là où elle est épargnée (Jeffrey et Cummings, 2000). Les différentes classes d'AChEI diffèrent par le type de liaison (réversible ou irréversible, en fonction de la durée de la liaison à l'AChE) et le mode d'inhibition de l'ACh (compétitif ou non-compétitif).

On distingue ainsi des AChEI qui sont ou ont été utilisés en thérapeutique pour obtenir un effet central ou périphérique.

AChEI réversibles

- Les premiers, sélectifs (donépézil, galantamine) ou non de l'AChE (tacrine), entraînent une inhibition réversible, rapide, dépendante de la concentration. L'effet thérapeutique n'est obtenu qu'en présence permanente de l'inhibiteur.
- Les seconds ont une durée d'action plus prolongée, car ils forment un complexe carbamylé stable (physostigmine, néostigmine, rivastigmine). Ainsi, l'enzyme est libérée lentement et l'effet persiste longtemps (au moins 10 h) bien que l'inhibiteur ait disparu. Toutefois, les effets centraux s'accompagnent d'effets indésirables périphériques rendant ces thérapies difficiles à manipuler. La rivastigmine est employée dans le traitement de l'AD, la physostigmine, la néostigmine ayant plutôt des indications antidotiques.

AChEI irréversibles

Ces AChEI d'origine chimique [dérivés organophosphorés (OP), carbamates, métrifonate] sont responsables

[1] *http://www.cea.fr/le_cea/actualites/observation_medicaments_anti_alzheimer*

d'une inhibition irréversible par liaison covalente avec l'enzyme : la disparition de l'effet nécessite une néosynthèse de l'enzyme. Ce type d'AChEI est utilisé comme insecticide en agriculture, en hygiène générale (élimination des vecteurs de maladies humaines) ou domestique. Certains d'entre eux, plus toxiques encore, peuvent aussi être utilisés comme gaz de combat (soman, sarin, tabun, VX).

Utilisations thérapeutiques des AChEI réversibles

Historiquement, la physostigmine (ou ésérine) a été le premier AChEI d'origine naturelle, utilisé en thérapeutique. Elle est extraite de la fève de Calabar, graine de *Physostigma venenosum* (Fabacée), qui se développe à l'état sauvage en Afrique, dans la région du Niger. C'est un AChEI efficace (IC_{50} de 0,25 µM sur érythrocytes de bœuf). La fonction carbamate est indispensable à son activité. Elle forme un ester stable avec l'AChE, qui ne récupère sa forme active que lentement. Après absorption, elle est distribuée dans tout l'organisme et sa structure d'amine tertiaire lui permet de franchir la barrière hémato-encéphalique (BHE), mais en petite quantité car elle est assez polaire. Elle agit donc à la fois sur le SNC et le SNP. Elle été utilisée dans le traitement de l'iléus paralytique, l'atonie intestinale, le glaucome, la myasthénie, la décurarisation post-anesthésique[2]. Elle a été testée dans le traitement de la maladie d'Alzheimer (AD) par voie orale (Davies *et al*., 1983) ou par voie intra-veineuse (Christie *et al*., 1981 ; Davies *et al*., 1982 ; Mohs *et al*., 1985 ; Harrell *et al*., 1990 ; Cummings *et al*., 1993), et, plus récemment, par des formulations orales à libération prolongée ou par des patchs transdermiques permettant d'assurer une concentration plasmatique relativement stable (Coelho Filho et Birks, 2001). Il semblerait qu'elle améliore de façon passagère la mémoire des patients, sous réserve qu'elle atteigne le cerveau (le marqueur en étant une augmentation du cortisol plasmatique) (Mohs *et al*., 1985) et qu'il persiste suffisamment de neurones cholinergiques fonctionnels (AD modérée). Elle a, en revanche, deux inconvénients majeurs : sa courte demi-vie plasmatique (30 min) (Whelpton et Hurst, 1985) et ses nombreux effets indésirables (en particulier nausées, vomissements et diarrhées pour ne citer que les plus fréquents). De ce fait, la physostigmine est un médicament assez difficile à manier et sans bénéfice par rapport aux AChEI actuellement commercialisés. Son usage est donc remis en question et considéré comme obsolète dans le traitement de l'AD (Coelho Filho et Birks, 2001-2008). En revanche, elle est encore utile comme antidote dans les intoxications cholinergiques. Par ailleurs, elle a servi de modèle à la synthèse d'autres carbamates encore utilisés (néostigmine, pyridostigmine, rivastigmine, physostigmine) ou non (éptastigmine). Les principales applications thérapeutiques périphériques et centrales sont rapportées ci-après.

Au niveau périphérique

Au niveau périphérique, les AChEI réversibles ont des indications ophtalmiques et musculaires.

- Le **glaucome** est dû à une accumulation de fluide dans l'œil, lié à un défaut de drainage. L'ACh permet de dilater les vaisseaux responsables du drainage. La physostigmine a d'abord été utilisée en collyre mais on lui préfère maintenant un cholinomimétique direct (pilocarpine) (Houghton *et al*., 2006).
- La **myasthénie commune** est une maladie neuromusculaire de la musculature striée squelettique. Elle résulte d'une atteinte de la transmission neuro-musculaire, entraînant une faiblesse musculaire fluctuante et une fatigabilité excessive. C'est l'une des maladies auto-immunes les plus connues : les anticorps circulants entraînent la réduction du nombre des récepteurs de l'ACh à la jonction neuromusculaire post-synaptique et s'opposent donc à l'effet stimulant de l'ACh. La myasthénie est traitée par immunosuppression et par des AChEI. La physostigmine n'ayant pas donné les résultats escomptés, trois analogues synthétiques très hydrosolubles ont été synthétisés : la néostigmine (Prostigmine®), l'edrophonium (Tensilon®) et la pyridostigmine (Mestinon®). Ces AChEI ne concernent que le SNP, car ils ne traversent pas la BHE (Houghton *et al*., 2006).
- Traitement de la **curarisation résiduelle post-opératoire** (CRPO) avec blocage neuromusculaire. L'incidence de la CRPO est liée à la grande variabilité de la durée d'action des curares non dépolarisants. La physostigmine a été utilisée dès les années 1942 comme antidote du curare utilisé en anesthésie. Aujourd'hui, la néostigmine lui est préférée à la dose de 40 µg/kg, même dans les cas sévères, car une des caractéristiques de l'action des AChEI est qu'à partir d'une certaine concentration, l'effet atteint une valeur de plateau. Augmenter les doses n'améliorerait pas la vitesse de récupération et pourrait provoquer des effets secondaires graves (Jones *et al*., 1988 ; Baurin *et al*., 1996 ; Beaussier et Boughaba, 2005).

Au niveau central

Au niveau central, les AChEI réversibles ont un rôle dans les démences. Les concentrations cérébrales d'ACh diminuent spontanément lors du vieillissement, par suite d'une dégénérescence des neurones cholinergiques du cortex et de l'hippocampe, ce qui se traduit par une réduction de la fonction cholinergique. Cette baisse peut être considérable dans certaines démences séniles [AD, démence vasculaire, Chorée de Huntington, BPSD (pour *Behavioural and Psychological Symptoms of Dementia*)] (Perry *et al*., 1978 ; Palmer, 1996 ; Giacobini, 2000). Il a donc été proposé de stimuler le système cholinergique afin d'améliorer la mémoire et le fonctionnement cérébral de ces patients. Trois types de substances cholinomimétiques ont été testés dans ce but :

- **Les précurseurs de l'acétylcholine** (choline et lécithine) dont l'efficacité est modérée ou nulle en

[2] *http://www.pharmacorama.com/Rubriques/Output/Acetylcholinea4_3.php*

raison de la faible quantité du transporteur à haute affinité de la choline et de son induction lente (Thal *et al*., 1981 ; Amenta *et al*., 2001 ; Hartmann *et al*., 2008).

- **Les agonistes cholinergiques** (arécoline, oxotrémorine) qui, chez l'animal, provoquent une amélioration des capacités mnésiques en agissant directement sur le récepteur postsynaptique mais présentent de nombreux effets secondaires liés à leurs effets périphériques.

- **Les AChEI** qui, en augmentant les concentrations d'ACh dans la fente synaptique, permettent d'améliorer les performances cognitives, les activités de la vie quotidienne et le comportement des malades souffrant d'AD (Jeffrey et Cummings, 2000 ; Pirot, 2000 ; [1]). La thérapie compensatrice par les AChEI pourrait avoir un intérêt dans d'autres pathologies neurologiques associées à un déficit cholinergique et à des troubles neuropsychiatriques et comportementaux : démence avec corps de Lewy (donépézil), démences des parkinsoniens, troubles bipolaires de l'humeur et chez certains patients schizophrènes (Hutchinson et Fazini, 1996 ; White et Cummings, 1996 ; Jan et McKeith, 1998 ; Shea *et al*., 1998 ; Aarsland *et al*., 1999 ; Burt *et al*., 1999 ; Pirot, 2000).

Trois médicaments, dits de deuxième génération, sont actuellement commercialisés : donépézil (Exelon®), galantamine (Reminyl®) et rivastigmine (Aricept®) (Clegg *et al*., 2001 ; Doody *et al*., 2001). Le premier est un produit de synthèse, le second un produit d'origine naturelle et le troisième un dérivé hémi-synthétique de la physostigmine. Les deux premiers, rapidement réversibles sont considérés comme spécifiques de l'AChE (Bryson et Benfield, 1997), le troisième est un inhibiteur lentement réversible de l'AChE et de la BuChE (Weinstock, 1999 ; Onor *et al*., 2007). Tous les trois ont les mêmes effets secondaires, cholinergiques dépendants (nausées, vomissements, céphalées, diarrhées). Leur capacité à améliorer la mémoire et les fonctions centrales pourraient être liées à d'autres propriétés que la seule inhibition de l'AChE cérébrale (Narahashi *et al*., 2004 ; Wilkinson *et al*., 2004 ; Moriguchi *et al*., 2005). Les principales propriétés pharmacologiques de ces AChEI sont colligées dans le *Tableau 1*. Puis un paragraphe est consacré à chaque molécule.

Tableau 1. Comparaison des propriétés pharmacologiques des inhibiteurs de cholinestérases actuellement commercialisés (2e génération)(Pirot, 2000 ; Allain *et al*., 2001).

Table 1. *Pharmacological properties of cholinesterase inhibitors currently marketed.*

DCI	*Donépézil*	*Galantamine*	*Rivastigmine*
Nom déposé en France	Exelon®	Reminyl®	Aricept®
Sélectivité	AChE>>BuChE	AChE>>>BuCHE	AChE>BuChE
Classe chimique	Pipéridine	Alcaloïde phénanthérénique	Carbamate
Mécanisme de l'inhibition ➢ Réversibilité ➢ Type d'inhibition	réversible mixte compétitif /non compétitif	réversible compétitif	pseudo-irréversible non compétitif
Durée de l'inhibition enzymatique	courte	courte	intermédiaire
Posologie quotidienne (mg)	5-10	12-24	6-12
Nombre d'administrations quotidiennes	1	3	2 ou 3
1/2 vie plasmatique (h)	70 - 80	5 - 7	0,6 – 2
Biodisponibilité (%)	100	85	40
Tmax (h)	3 - 5	0,5 - 1	0,5 - 2
Liaison aux protéines (%)	96	0	40
Ajustement posologique progressif	Oui	Oui	Oui
% de patients arrêtant le traitement à cause des effets indésirables	5-13	6-21	25
Métabolisme hépatique Interaction au niveau des cytochromes P450	oui CYP2D6 et 3A4	oui CYP2D6	non
Surveillance des enzymes hépatiques	non	non	Non

Donépézil (Exelon®)

C'est un AChEI de synthèse qui, outre ses propriétés d'AChEI réversible et spécifique, est capable, à concentration thérapeutique (0,01–1 µM), de potentialiser l'activité du système NMDA, ce qui pourrait contribuer à son effet thérapeutique (Moriguchi *et al*., 2005). Ceci peut sembler contradictoire avec l'effet pharmacologique antagoniste de la mémantine sur ce même récepteur. En fait dans l'AD, il y une régulation négative du système NMDA mais au cours de la maladie, des radicaux libres s'accumulent et, à partir d'un certain seuil, provoquent une réponse brutale du récepteur NMDA, que bloque la mémantine. Moriguchi *et al*. (2005) supposent que le donépézil pourrait éviter ce type de décharge brutale en permettant au récepteur de fonctionner de façon plus régulière.

La biodisponibilité par voie orale du donépézil est totale. Il franchit très bien la BHE. Sa longue demi-vie (70 h) permet de l'administrer une seule fois par jour. La dose initiale est de 5 mg/j et peut être portée à 10 mg/j après une période d'adaptation de 4 semaines. Son efficacité clinique (amélioration des fonctions cognitives, de la qualité de vie et du comportement) a été démontrée à l'issue de traitements de 12, 24 et 52 semaines chez des malades souffrant de formes légères ou modérées et parfois sévères d'AD (Birks et Harvey, 2003 ; Dooley et Lamb, 2000). Il a aussi fait la preuve de son efficacité dans les démences vasculaires (Malouf et Birks, 2004).

Galantamine (Réminyl®)

C'est un alcaloïde naturel, isolé initialement du bulbe du Perce-neige (*Galanthus nivalis* L.) et d'autres Amaryllidaceae (Heinrich et Lee Teoh, 2004). Cet alcaloïde phénanthrénique est aujourd'hui produit par synthèse (Marco et Do Carmo Carreiras, 2006). Son métabolisme conduit à 4 composés, dont l'un est un AChEI plus puissant que la galantamine elle-même.

De nombreux dérivés soit naturels, issus des Amaryllidaceae*,* soit semi synthétiques, ont également été testés afin d'optimiser l'activité thérapeutique et de réduire les effets secondaires (Houghton *et al*., 2005 ; Marco et Do Carmo Carreiras, 2006). La galantamine a d'abord été utilisée en Bulgarie pour traiter les contractions musculaires des poliomyélitiques. Mais son utilisation s'est vite élargie au traitement de l'AD.

Elle inhibe spécifiquement l'AChE. Son activité est puissante (IC_{50} de 1,27 µM, *in vitro*) (Lopez *et al*., 2002). Elle franchit la BHE (Harvey, 1995 ; cf. Pagès *et al*., 2009a). Après administration orale, la molécule est rapidement absorbée (T_{max} de 52 min). Sa demi-vie plasmatique varie de 5 à 7 heures. La posologie initiale (8 mg/kg) est augmentée par paliers de 4 semaines jusqu'à la dose thérapeutique de 16 mg/kg (dose maximum : 24 mg/kg). Ses effets secondaires se limitent aux effets indésirables classiques qui sont généralement modérés et peuvent disparaître en réduisant la posologie (Mayeux et Sano, 1999 ; Shadlen et Larson, 1999 ; Scott et Goa, 2000 ; Akhondzadeh et Noroozian, 2002 ; Bullock, 2002). Les données cumulées de quatre essais randomisés chez des patients avec des formes légères ou modérées d'AD indiquent que les patients ayant reçu 24 mg/j pendant 6 mois présentaient une amélioration des symptômes cognitifs, fonctionnels et comportementaux par rapport à ceux ayant reçu un placebo (Raskind *et al*., 2000 ; Lopez *et al*., 2002 ; Winblad *et al.*, 2008). La galantamine semble même capable d'améliorer les fonctions cognitives des malades présentant des formes graves d'Alzheimer ou d'Alzheimer accompagné d'une pathologie vasculaire cérébrale ou encore de démence vasculaire (Feldman *et al*., 2009 ; Burns *et al.*, 2009). En revanche, elle n'améliore pas l'attention, la mémoire ou les performances visuo-spatiales de patients parkinsoniens non déments (Grace *et al*., 2009).

En plus de ses capacités d'AChEI, la galantamine est capable de potentialiser l'activité des récepteurs cholinergiques nicotiniques et celle des récepteurs glutamatergiques NMDA (Moriguchi *et al*., 2005). Elle induit une modulation allostérique des récepteurs nicotiniques (Scott et Goa, 2000 ; Sramek *et al*., 2000 ; Coyle et Kershaw , 2001 ; Maelicke *et al*., 2001 ; Samochocki *et al*., 2003). Elle augmenterait ainsi l'action intrinsèque de l'ACh et donc la transmission cholinergique (Pontecorvo et Parys, 1998 ; Razay et Willcock, 2008). Toutefois des travaux récents remettent en cause ce mécanisme d'action. En effet, Reid et Sabbagh (2008) ont montré chez le Rat que les 3 AChEI commercialisés avaient tous le même effet après 15 jours de traitement (augmentation du nombre de récepteurs alpha-7 et non alpha-7 (ou alpha-4béta-2) dans le cortex et augmentation des non alpha-7 dans l'hippocampe). En parallèle, ils ont montré, *in vitro*, qu'en présence des 3 AChEI, la liaison d'agonistes radiomarqués spécifiques des récepteurs nicotiniques alpha-7 et non alpha-7 n'était pas modifiée. Leur conclusion est que l'augmentation du nombre des récepteurs nicotiniques serait seulement due à l'augmentation des concentrations synaptiques d'ACh. Par ailleurs, une étude réalisée *ex vivo*, chez des patients atteints d'AD modérée et traités pendant 12 semaines par galantamine n'a montré aucune modification régionale ou globale du nombre et de l'affinité des récepteurs nicotiniques non alpha-7 avant et après traitement (Ellis *et al*., 2009). En revanche, dans un modèle de maladie de Huntington chez le Rat, la galantamine réduit la neurodégénérescence striatale. Elle atténue les déficits neurologiques et réduit, en diminuant l'apoptose, la taille des lésions striatales. Ces effets disparaissent lors de la co-administration de la galantamine et d'un antagoniste d'un récepteur nicotinique (Park *et al*., 2008). D'autres études sont donc encore nécessaires pour préciser ce point.

Par ailleurs, la galantamine potentialise les courants évoqués par l'activation des récepteurs NMDA dans des neurones corticaux de Rat. Cette action serait exercée par l'intermédiaire de la protéine kinase (PKC). La modulation des récepteurs NMDA pourrait donc intervenir dans l'amélioration des fonctions cognitives (Moriguchi *et al*., 2004).

Rivastigmine (Aricept®)

Deux carbamates de synthèse dérivés de la physostigmine, plus liposolubles et donc capables de franchir la BHE, ont été synthétisés pour traiter avec succès l'AD : rivastigmine et éptastigmine. L'éptastigmine a été abandonnée en raison de sa toxicité (granulocytopénie) (Imbimbo *et al*., 1998, 1999). En revanche, la rivastigmine est l'un des trois AChEI actuellement sur le marché (Houghton *et al*., 2005). Elle a une sélectivité centrale (Gottwald et Rozanski, 1999) et inhibe à la fois l'AChE et la BuChE, en particulier sous leur forme G1 (Ballard, 2002). Elle protègerait ainsi le patient de l'agrégation du peptide A-béta dans les plaques (Inestrosa *et al.*, 1996). Elle se lie au site estérasique de l'enzyme plus longuement que l'acétate de l'ACh. Ainsi, l'AChE est inactivée longtemps après la disparition du composé parent de la circulation. L'AChE clive la rivastigmine et libère un produit de clivage phénolique, pharmacologiquement inactif, éliminé par le rein.

Par voie orale, elle est bien absorbée. Comme tout AChEI, la posologie initiale, est de 3 mg/jour et doit être augmentée progressivement, par paliers de deux à quatre semaines (phase de dosage) jusqu'à la dose orale maximum recommandée de 12 mg/jour (Corey-Bloom *et al*., 1998). Sa biocinétique est linéaire jusqu'à 3 mg et non linéaire au-delà. Le pic plasmatique est vite atteint (1h), la concentration maximum dans le liquide céphalo-rachidien étant atteinte plus tard (1,4–3,8 h). 40% de la molécule se lie aux protéines plasmatiques (Jann *et al*., 2002). Son métabolisme est assuré par l'AChE (*vide supra*), et non par les isoenzymes hépatiques du cytochrome P450, ce qui limite les risques d'interactions avec d'autres médicaments (Jann, 2000). Ceci a un

intérêt majeur, car ce type de patients est très souvent polymédiqué. Administrée par patch transdermique, la rivastigmine atteint une concentration plasmatique plus faible et présente moins de fluctuations que par voie orale (ce qui limite les effets secondaires) (Cummings *et al*., 2007). Le patch, dosé à 9,5 mg/24 h, est équivalent à 12 mg/jour apportés par voie orale (Cummings *et al*., 2007 ; [3]).

La rivastigmine a démontré son efficacité sur les plans cognitif (pensée et mémoire), fonctionnel (activités quotidiennes) et comportemental des patients atteints d'AD (Corey-Bloom *et al*., 1998 ; Rösler *et al*., 1998, 1999 ; Finkel, 2004) en particulier chez ceux présentant des carences nutritionnelles, une maladie précoce, un développement agressif de la maladie, ou ceux qui ont des idées délirantes ou des hallucinations (Finkel, 2004). La rivastigmine est également efficace dans les démences dues à la maladie de Parkinson (Emre *et al*., 2004). Son efficacité est comparable à celle du donépézil et de la tacrine. Des doses inférieures à un seuil de 6 mg/jour pourraient être inefficaces [3].

Sa sécurité est bonne en dehors des effets indésirables classiques, cholinergique-dépendants (nausées, vomissements, céphalées, diarrhées), avec des signes plus marqués pour la voie transdermique (Inglis, 2002). En cas de surdosage, d'autres effets peuvent apparaitre (hypersécrétions, incontinence, crampes, fasciculations et tout autre symptôme de décharge du parasympathique).

Intérêt des trois AChEI de 2e génération

Les premiers essais cliniques semblaient indiquer de meilleurs résultats avec le donépézil qu'avec la galantamine (Jones *et al*., 2002) et des effets similaires pour le donépézil et la rivastigmine (Wilkinson *et al*., 2002). Mais des études plus récentes ont montré que l'efficacité clinique des trois AChEI de deuxième génération était la même (Clegg *et al*., 2001 ; Wilkinson *et al*., 2004 ; Hansen *et al*., 2006, 2008). Ces essais indiquent aussi que le donépézil est généralement mieux supporté que la galantamine (Jones *et al*., 2002) ou la rivastigmine (Wilkinson *et al*., 2002; Lanctôt *et al*., 2003).

Des recherches en cours indiquent que l'effet combiné d'un AChEI efficace dans le traitement de l'AD et de la mémantine chez des patients aux stades modéré à avancé de l'AD pourrait améliorer les résultats cliniques, parfois plus que la somme des effets de chaque médicament pris individuellement. Toutefois, des essais sur un plus grand nombre de sujets sont encore nécessaires pour confirmer ces premiers résultats prometteurs [4]. Des travaux récents suggèrent que leur administration par voie nasale qui présente plusieurs avantages (large surface d'absorption, obtention rapide des concentrations sanguines efficaces, absence de premier passage hépatique, distribution rapide au cerveau, administration non invasive permettant une bonne compliance au traitement) est une option d'avenir (Costantino *et al*., 2008).

Rôle des AChEI réversibles dans l'arsenal thérapeutique de l'AD

La lutte contre la maladie d'Alzheimer est considérée comme une priorité nationale et mondiale : en 2006, sa prévalence mondiale était estimée à plus de 25 millions de personnes. Cette maladie neurodégénérative est complexe. Elle est caractérisée par une détérioration de la mémoire et des fonctions cognitives associées à une perte massive de neurones et un dépôt de plaques séniles (Whitehouse *et al*., 1981, 1982 ; Xiao *et al*., 2002). L'accumulation du peptide amyloïde serait responsable de la neurodégénéresence (Hardy, 1997 ; Selkoe, 2000) en induisant l'apoptose des neurones (Cotman, 1998), en favorisant une hyperphosphorylation de la protéine tau (Luo *et al*., 1995), en modifiant l'homéostasie calcique (Mattson *et al*., 1992), et en augmentant la production de radicaux libres oxygénés (Behl *et al*., 1994 ; Hensley *et al*., 1994 ; Mattson et Goodman, 1995 ; Bus *et al*., 1999 ; Huang *et al*., 1999).

Les recherches actuelles ciblent les mécanismes étiologiques responsables de la dégénérescence neuronale : de nombreux agents empêchant l'agrégation des peptides d'amyloïde béta, ou favorisant son élimination (par la glycoprotéine P (P-gp) au niveau de la BHE dont l'expression est modifiée dans l'AD) sont en cours d'évaluation, mais d'autres pistes sont ouvertes (thérapies ciblant la protéine tau, neuroprotection, neurorestauration) (Piau *et al*., 2009). Cependant, les AChEI ont été les premiers à apporter une lueur d'espoir dans le traitement symptomatique de l'AD, avec la mise sur le marché, en 1997, de la tacrine (Cognex®) (Kaufer *et al*., 1996, 1998), qui n'est plus commercialisée depuis 2007 du fait de sa courte demi vie et surtout de sa sévère toxicité hépatique. Mais les trois AChEI de deuxième génération déjà cités sont mieux tolérés et constituent la première ligne de défense de l'AD dans ses formes légères à modérément sévères (*Tableau I*). Dans les cas plus sévères, un antagoniste du récepteur NMDA, la mémantine peut être utilisée, seule ou en association avec l'un des AChEI précédents (Parsons *et al.,* 1999 ; Danysz et Parsons, 2003). Cependant des doutes subsistent sur l'efficacité de ces médicaments qui, au mieux, retardent les manifestations de l'AD sans agir sur sa cause (Birks, 2006).

Utilisations antidotiques des AChEI réversibles

La physostigmine, capable de franchir la BHE, est encore utilisée comme antidote dans des empoisonnements provoqués par différents médicaments neurotropes et pour traiter la somnolence et la dépression respiratoire postopératoires. C'est aussi un antidote puissant dans les empoisonnements par les organophosphates (Rygnestad, 1992). Ses effets secondaires les plus fréquents sont d'ordre digestif (nausées, vomissements). Beaucoup de médecins hésitent néanmoins à l'utiliser, en particulier chez les enfants, car des asystolies ont été

[3] *http://en.wikipedia.org /wiki/Rivastigmine*
[4] *http://www.alzheimer.ca/french/treatment/treatments-exelon.htm*

décrites dans le traitement d'intoxications par les antidépresseurs tricycliques (ADT). Des travaux récents ont montré aussi l'apparition de convulsions (Frascogna, 2007).

Toutefois, dans les intoxications anticholinergiques pures, avec des symptômes sévères, la physostigmine permet de contrôler l'agitation et de stopper le délire : elle semble plus efficace et moins dangereuse que les benzodiazépines dans ce cas (Oakley, 2001 ; Burns *et al*., 2002 ; Frascogna, 2007). La physostigmine devra donc être utilisée avec précaution chez les patients présentant des symptômes cholinergiques d'origine inconnue, ou chez ceux présentant des problèmes cardiaques (Frascogna, 2007).

Antidote des intoxications atropiniques pures (ingestion de plantes, champignons ou surdosage médicamenteux)

L'intoxication atropinique est due au fait que l'atropine se fixe aux récepteurs muscariniques de l'acétylcholine dans le SNC et le SNP et agit donc comme un antagoniste cholinergique. En cas d'intoxication par l'atropine et ses dérivés (homatropine, scopolamine, hyoscyamine) apportés par l'ingestion de plantes (*Datura stramonium, Hyoscyamus niger*, *Atropa belladonna, Solanum pseudocapsicum, Solanum tuberosum)*, de champignons (*Amanita muscaria* ou amanite tue-mouches), ou de médicaments (cigarettes anti-asthmatiques qui ne sont plus commercialisées), un syndrome anticholinergique central (CAS) peut survenir (confusion, agitation, dépression respiratoire, hallucinations allant jusqu'au délire, convulsions et coma), accompagné d'effets périphériques (mydriase, sécheresse et rougeur de la peau et des muqueuses, rétention urinaire et atonie intestinale, arythmie cardiaque) [5]. La physostigmine est utile à la fois pour diagnostiquer les intoxications atropiniques difficiles à identifier (diagnostic différentiel d'une encéphalite) et pour traiter l'intoxication.

La physostigmine (Anticholium®) (dose initiale, chez l'adulte, de 2 mg dilué dans 10 mL de sérum physiologique en injection intra-veineuse (IV) lente (1 mg/min, à répéter toutes les 30 min à 2 h aussi souvent que nécessaire) agit à la fois sur les symptômes anticholinergiques centraux et périphériques. Normalement, dans les 10 minutes suivant l'administration de la première dose, les symptômes disparaissent. Il n'y pas de décès si l'intoxication est traitée à temps (Daunderer, 1980). La néostigmine (Prostigmine®) (0,03 mg/kg) qui pourtant ne franchit pas la BHE, a été utilisée avec succès pour traiter un enfant présentant un CAS sévère après ingestion de *Solanum pseudocapsicum* (Parisi et Francia, 2000).

Antidote de médicaments provoquant un syndrome cholinergique

De nombreux médicaments inhibent la transmission cholinergique en bloquant les récepteurs muscariniques : antihistaminiques (chlophéniramine, diphenhydramine, prométhazine) ; antidépresseurs tricycliques (amitryptiline, desimipramine, doxépine, imipramine) ; antipsychotiques (thioridazine, chlorpromazine, butyrophénones) (Jastak, 1985). La physostigmine, en augmentant la quantité d'ACh disponible permet de réverser ces intoxications. Toutefois, son utilisation dans le traitement des intoxications par les ADT doit être entourée d'un maximum de précautions en raison de la survenue possible mais exceptionnelle d'asystolie et de convulsions (Schneir, 2004-2009).

Antidote lors d'usage excessif de psychotropes

De nombreuses substances utilisées en anesthésie et en soins intensifs peuvent provoquer un blocage de la neurotransmission centrale cholinergique et provoquer un CAS : c'est le cas des opiacés, des benzodiazépines, des antipsychotiques, de la kétamine, du gamma-hydroxybutyrate (GHB), de l'étomidate, du propofol, du NO, des anesthésiques halogénés. L'incidence du CAS qui varie de 1 à 40% en post-anesthésie, peut être réduite en administrant de la physostigmine au cours de l'anesthésie (Drummond *et al*., 1979 ; Burns *et al*., 2001). En soins intensifs, le CAS peut survenir chez des patients sous ventilation mécanique assistée (surtout lors de sédation prolongée induite par de fortes doses). La physostigmine peut éviter chez de tels malades le CAS lors de l'arrêt de la respiration assistée. Enfin, le CAS peut s'observer lors du sevrage des toxicomanies par opiacés, alcool, hallucinogènes et NO (Schneck et Rupreht, 1989). La physostigmine ne doit pas être utilisée après anesthésie à la kétamine (Drummond *et al*., 1979) ou au GHB (Zvosec *et al*., 2007) ; elle est également proscrite chez les sujets présentant des signes de Parkinson. La dose doit être réduite à 0,5 mg par voie intra veineuse chez les patients âgés de plus de 65 ans (Wiklund, 1986).

Antidotes des neurotoxiques organophosphorés (cf. page suivante)

Utilisations antiparasitaires des AChEI irréversibles ou lentement réversibles

Différents AChEI chimiques irréversibles ou lentement réversibles (organophosphorés et carbamates) sont utilisés pour détruire les Arthropodes. Ils ont des applications en agriculture (amélioration des rendements), en hygiène publique (lutte contre les vecteurs de maladies parasitaires et virales comme les moustiques et les simulies), et dans la lutte contre des nuisibles domestiques (cafards) ou humains (poux : Para Plus® et Prioderm® à base de malathion). Les plus utilisés comme produits phytosanitaires sont les organophosphorés. Il en existe une quarantaine, dont les DL_{50} varient de quelques mg à quelques g par kg, la majorité étant "toxiques" ou "très toxiques". Leur effet persiste de quelques jours à quelques mois. En revanche, ils sont peu rémanents dans l'environnement. Les carbamates sont moins employés actuellement : ils entrent dans la formulation de produits ménagers (insecticides de plantes d'appartement), de jardinage et surtout de produits phytosanitaires (insecticides vétérinaires). Leur toxicité aiguë est moins sévère que celle des

[5] *http://www.poisoncentre.be/article.php?id_article=23# anticholinergique*

organophosphorés. Leur synthèse a été suggérée par la présence, dans la structure de la physostigmine, d'un groupe carbamate indispensable à son activité (Houghton *et al*., 2006).

Utilisation toxique des AChEI irréversibles comme arme chimique

A l'heure actuelle, les neurotoxiques organophosphorés (NOP) sont considérés comme des menaces potentielles lors d'opérations militaires ou d'actes de terrorisme (Lallement et Dorandeu, 2002). Il en existe deux groupes : les agents « G » [tabun (GA), sarin (GB), soman (GD) et cyclosarin (GF)] et les agents « V » (VX). Ils n'ont pas servi durant la 2e guerre mondiale, mais ont été utilisés durant le conflit Iran-Irak associés à l'ypérite, et en 1995 dans l'attentat du métro de Tokyo (sarin). Ils sont liquides à température ambiante. Les agents G sont très volatils alors que les agents V, plus huileux, persistent et peuvent contaminer plus durablement les milieux.

Les NOP sont des inhibiteurs irréversibles des AChE périphériques et centrales. Ils se lient au site actif de l'enzyme et la stabilité de la liaison dépend de la structure du composé : quelques heures pour les groupes méthyl et éthyl, indéfiniment pour les groupes alkyle de taille supérieure. Cette liaison se renforce au cours du temps par la formation de liaisons hydrogènes supplémentaires entre le NOP et l'AChE. Ce processus porte le nom d' «*ageing* ». Le temps de 1/2 vie de l'*ageing* en minutes est fonction du NOP (5, 150, 420 et plus pour GD, GB, GA et VX respectivement). Il est donc fondamental d'administrer des oximes, réactivateurs des cholinestérases, le plus vite possible après l'intoxication, car lorsque l'*ageing* s'est produit, l'enzyme ne peut plus être réactivée (Weinbroum, 2005).

L'exposition se fait par voie cutanée et surtout, respiratoire. Le tableau clinique résulte de l'hyperstimulation des récepteurs muscariniques et nicotiniques périphériques et centraux. Il impose une prise en charge rapide pour empêcher l'apparition de symptômes cholinergiques sévères (hypersécrétion des glandes sécrétoires, paralysie musculaires sévère, brady-asystolie, insuffisance respiratoire, convulsions, coma et mort). Les principales stratégies font appel à l'atropine qui inhibe les symptômes muscariniques et aux oximes (chlorhydate de pralidoxime) qui, en réactivant l'enzyme phosphorylée, réverse les signes nicotiniques (Weinbroum, 2005). Un traitement symptomatique complémentaire (anticonvulsivants, sédatifs, ventilation mécanique) permet une amélioration des intoxiqués (Weinbroum, 2005).

La pyridostigmine, carbamate inhibiteur réversible de l'AChE est efficace, à titre préventif, seule ou en association avec d'autres principes actifs, chez l'animal de laboratoire et les populations à risque (Gordon *et al*., 1978 ; Sharabi *et al*., 1991 ; Von Bredow *et al*., 1991 ; Lallement *et al*., 1999 ; Bagjar, 2004 ; Smythies et Golomb, 2004 ; Kim *et al.* , 2005 ; Weinbroum, 2005 ; Wetherell *et al*., 2006, 2007). Lorsque l'enzyme est inhibée par la pyridostigmine, elle résiste à l'inhibition par les NOP (Bajgar, 2004). La pyridostigmine est active par voie IV (préférée à l'hôpital), intramusculaire et orale (conseillées sur les champs de bataille). Pour la voie IV, la dose est de 1-2 mg pour un adulte (0,02 mg/kg chez l'enfant avec un maximum de 0,5 mg) à administrer lentement (5-10 min). Ainsi sont stoppés les signes nicotiniques déjà évoqués. L'effet est rapide, la ½ vie est courte (16 min) mais la durée d'action est 5 fois supérieure (1h30 environ). Des patchs transdermiques associant physostigmine et procyclidine ont été testés (Kim *et al.*, 2005). La physostigmine est également efficace dans l'intoxication par un agent incapacitant anticholinergique, BZ (3 quinuclidinyl benzylate ou QNB ou EAA-2277). Cependant, comme la durée d'action de BZ est longue, plusieurs injections de physostigmine sont nécessaires (Roy, 2004).

Cependant, la pyridostigmine ne pénètre pas dans le cerveau et n'apporte aucune protection contre les crises d'épilepsie et la neuropathologie induites par les NOP (Lallement et Dorandeu, 2002). Des travaux récents chez l'animal de laboratoire montrent que des AChEI à activité centrale sont efficaces tels que le donépézil, utilisé dans le traitement de l'AD (Janowski *et al*., 2005), ou l'huperzine, une phytotoxine en cours de développement, qui associe les propriétés d'AChEI réversible, peu toxique et capable de franchir la BHE (Lallement et Dorandeu, 2002 ; cf. Pagès *et al*., 2009b).

En conclusion, cette revue permet de montrer que tous les AChEI dotés de propriétés thérapeutiques et d'une toxicité modérée sont, à l'exception du donépézil, des phytotoxines ou des dérivés d'hémisynthèse de la physostigmine.

Références bibliographiques

Adams M, Gmünder F, Hamburger M (2007) Plants traditionally used in age related brain disorders--a survey of ethnobotanical literature. *J Ethnopharmacol* **113**: 363-381

Akhondzadeh S, Abassi SH (2006) Herbal medicine in the treatment of Alzheimer's disease. *Am J Alzheimers Dis Other Demen* **21**: 113-118

Akhondzadeh S, Noroozian M (2002) Alzheimer's disease: pathophysiology and pharmacotherapy. *Drugs* **5**:1062-1069

Allain H, Tribut O, Reymann JM, Polard E, Lecavorzin P, Bentue-Ferrer D (2001) Perspectives médicamenteuses dans la maladie d'Alzheimer. www.med.univ-rennes1.fr/etud/pharmaco

Amenta F, Parnetti L, Gallai V, Wallin A (2001) Treatment of cognitive dysfunction associated with Alzheimer's disease with cholinergic precursors. Ineffective treatments or inappropriate approaches? *Mech Ageing Dev* **122**: 2025-2040

Bagjar J (2004) Organophosphates/nerve agent poisoning: mechanism of action, diagnosis, prophylaxis, and treatment. *Adv Clin Chem* **38**: 151-216

Ballard CG (2002) Advances in the treatment of Alzheimer's disease: benefits of dual cholinesterase inhibition. *Eur Neurol* **47**:64-70

Baurin M, Hoton F, Dhollander A, Cantraine F (1996) Is recovery of neuromuscular transmission complete after the use of physostigmine to antagonize block produced by rocuronium, vecuronium, atracurium and pancuronium? *Brit J Anaesth* **77**: 496-499

Behl C, Davis JB, Lesley R, Schubert D (1994) Hydrogen peroxide mediates amyloid β-protein toxicity. *Cell* **77**: 817-827

Birks J (2006) Cholinesterase inhibitors for Alzheimer's disease. *Cochrane Database Syst Rev* **1**: CD005593

Birks JS, Harvey R (2003) Donepezil for dementia due to Alzheimer's disease. *Cochrane Database Syst Rev* **3**: CD001190

Bryson HM, Benfield P (1997) Donepezil. *Drugs Aging* **10**: 234-239

Bullock R (2002) New drugs for Alzheimer's disease and other dementias. *Br J Psychiatry* **80**: 135-139

Burns MJ, Linden CH, Graudins A, Brown RM, Fletcher KE (2002) A comparison of physostigmine and benzodiazepines for the treatment of anticholinergic poisoning. *Ann Emerg Med* **35**: 374-381

Burns A, Bernabei R, Bullock R, Cruz Jentoft AJ, Frölich L, Hock C, Raivio M, Triau E, Vandewoude M, Wimo A, Came E, Van Baelen B, Hammond GL, van Oene JC, Schwalen S (2009) Safety and efficacy of galantamine (Reminyl) in severe Alzheimer's disease (the SERAD study): a randomised, placebo-controlled, double-blind trial. *Lancet Neurol* **8**: 22-23

Burt T, Sachs G, Demopulos C (1999) Donepezil in treatment resistant bipolar disorder. *Biol Psychiatry* **45**: 959-964

Christie JE, Shering A, Ferguson J, Glen AI (1981) Physostigmine and arecoline: effects of intravenous infusions in Alzheimer presenile dementia. *Br J Psychiatry* **138**:46-50

Clegg A, Bryant J, Nicholson T, McIntyre L, De Broe S, Gerard K, Waugh N (2001) Clinical and cost-effectiveness of donepezil, rivastigmine and galantamine for Alzheimer's disease: a rapid and systematic review. *Health Technol Assess* **5**: 1-137

Coelho Filho JM, Birks J (2001) Physostigmine for dementia due to Alzheimer disease. *Cochrane Database Syst Rev* **2**: CD001499, last assessed June 02,2008

Corey-Bloom J, Anand R, Veach J (1998) A randomized trial evaluating the efficacy and safety of ENA 713 (rivastigmine tartrate), a new acetylcholinesterase inhibitor, in patients with mild to moderately severe Alzheimer's disease. *Int J Geriatr Psychopharmacol* **1**: 55–65

Costantino HR, Leonard AK, Brandt G, Jonhson PH, Quay SC (2008) Intranasal administration of acetylcholinesterase inhibitors. *BMC Neurosci* **9** (supp3): S6. Published online 2008 December 10. doi: 10.1186/1471-2202-9-S3-S6

Cotman CW (1998) Apoptosis decision cascades and neuronal degeneration in Alzheimer's disease. *Neurobiol Aging* **19**: S29-S32

Coyle J, Kershaw P (2001) Galantamine, a cholinesterase inhibitor that allosterically modulates nicotinic receptors: effects on the course of Alzheimer's disease. *Biol Psychiatry* **49**: 289-299

Cummings JL, Gorman DG, Shapira J (1993) Physostigmine ameliorates the delusions of Alzheimer's disease. *Biol Psychiatry* **33**: 536-541

Cummings J, Lefevre G, Small G, Appel-Dingemanse S. (2007) Pharmacokinetic rationale for the rivastigmine patch. *Neurology* **69** (Suppl 1): S10–13

Danysz W, Parsons CG (2003) The NMDA receptor antagonist memantine as a symptomatological and neuroprotective treatment for Alzheimer's disease: preclinical evidence. *Int J Geriatr Psychiatry* **18**: S23–S32

Daunderer M (1980) Physostigmine salicylate as an antidote. *Int J Clin Pharmacol Ther Toxicol*. **18**: 523-535

Davis KL, Mohs RC, Davis BM, Horvath TB, Greenwald BS, Rosen WG, Levy MI, Johns CA (1983) Oral physostigmine in Alzheimer's disease. *Psychopharmacol Bull.* **19**: 451-453

Davis KL, Mohs RC (1982) Enhancement of memory processes in Alzheimer's disease with multiple-dose intravenous physostigmine. *Am J Psychiatry* **139**: 1421-1424

Dos Santos-Neto LL, de Vilhena Toledo MA, Medeiros-Souza P, de Souza GA (2006) The use of herbal medicine in Alzheimer's disease-a systematic review. *Evid Based Complement Alternat Med.* 3 : 441-445

Doody RS, Stevens JC, Beck C, Dubinsky RM, Kaye JA, Gwyther L, Mohs RC, Thal LJ, Whitehouse PJ**,** DeKosky ST, Cummings JL (2001) Practice parameter: management of dementia (an evidence-based review). *Report of the quality standards subcommittee of the American Academy of Neurology. Neurology* **56**: 1154–1166

Dooley M, Lamb HM (2000) Donepezil: a review of its use in Alzheimer's disease. *Drugs Aging* **16**: 199-226

Drummond JC, Brebner J, Galloon S, Young PS (1979) A randomized evaluation of the reversal of ketamine by physostigmine. *Can Anaesth Soc J.* **26**: 289-295

Dutar P., Lamour Y (1992) Acétylcholine in Neuropeptides et neuromédiateurs. Epelbaum J (ed). Laboratoires Sandoz

Ellis JR, Nathan PJ, Villemagne VL, Mulligan RS, Saunder T, Young K, Smith CL, Welch J, Woodward M, Wesnes KA, Savage G, Rowe CC (2009) Galantamine-induced improvements in cognitive function are not related to alterations in alpha(4)beta (2) nicotinic receptors in early Alzheimer's disease as measured *in vivo* by 2-[18F]fluoro-A-85380 PET. *Psychopharmacology (Berl)* **202**: 79-91

Emre M, Aarsland D, Albanese A, Byrne EJ, Deuschl G, De Deyn PP, Durif F, Kulisevsky J, van Laar T, Lees A, Poewe W, Robillard A, Rosa MM, Wolters E, Quarg P, Tekin S, Lane R (2004) Rivastigmine for dementia associated with Parkinson's disease. *N Engl J Med.* **351**: 2509–2518

Feldman HH**,** Pirttila T**,** Dartigues JF**,** Everitt B**,** Van Baelen B**,** Brashear HR**,** Berlin JA**,** Battisti WP**,** Kavanagh S (2004) Analyses of mortality risk in patients with dementia treated with galantamine. *Acta Neurol Scand* **119**: 22-31

Finkel SI (2004) Effects of rivastigmine on behavioral and psychological symptoms of dementia in Alzheimer's disease. *Clin Ther* **26**: 980–990

Frascogna N (2007) Physostigmine: is there a role for this antidote in pediatric poisonings? *Curr Opin Pediatr* **19**: 201-205

Giacobini E (2000) Cholinesterase inhibitor therapy stabilizes symptoms of Alzheimer's disease. *Alzheimer Dis Assoc Disord* **14** (Suppl 1): S3–S10.

Gordon JJ, Leadbeater L, Maidment MP (1978) The protection of animals against organophosphate poisoning by pre-treatment with a carbamate. *Toxicol Appl Pharmacol* **43**: 207-216

Gottwald MD, Rozanski RI (1999) Rivastigmine, a brain-region selective acetylcholinesterase inhibitor for treating Alzheimer's disease: review and current status. *Expert Opin Investig Drugs* **8**:1673-1682

Grace J, Amick MM, Friedman JH (2009) A double-blind comparison of galantamine hydrobromide ER and placebo in Parkinson disease. *J Neurol Neurosurg Psychiatry* **80**: 18-23

Guillozet A, Smiley JF, Mash DC, Mesulam MM (1997) Butyrycholinesterase in the life cycle of amyloid plaques. *Ann Neurol* **42**: 909–918

Hansen RA, Gartlehner G, Kaufer DJ, Lohr KN, Carey T (2006) Drug class Review on Alzheimer's drugs. OHSU Final Report, Juin 2006

Hansen RA, Gartlehner G, Webb AP, Morgan LC, Moore CG, Jonas DE (2008) Efficacy and safety of donepezil, galantamine, and rivastigmine for the treatment of Alzheimer's disease: a systematic review and meta-analysis. *Clin Interv Aging* **3**: 211-225

Hardy J (1997) Amyloid, the presenilins and Alzheimer's disease. *Trends Neurosci* **20**: 154-159

Harrell LE, Calloway R, Morere D, Falgout J (1990) The effect of long-term physostigmine administration in Alzheimer's disease. *Neurology* **40**: 1350-1354

Hartmann J, Kiewert C, Duysen EG, Lockridge O, Klein J (2008) Choline availability and acetylcholine synthesis in the hippocampus of acetylcholinesterase-deficient mice. *Neurochem Int* **52**: 972-978

Harvey AL (1995) The pharmacology of galanthamine and its analogues. *Pharmacol Ther* **68**: 113-128

Heinrich M, Lee Teoh H (2004) Galanthamine from snowdrop--the development of a modern drug against Alzheimer's disease from local Caucasian knowledge. *J. Ethnopharmacol* **92**: 147-162

Hensley K, Carney JM, Mattson MP, Aksenova M, Harris M, Wu JF, Floyd RA, Butterfield DA (1994) A model for b-amyloid aggregation and neurotoxicity based on free radical generation by the peptide: relevance to Alzheimer disease. *Proc Natl Acad Sci USA* **91**: 3270-3274

Houghton PJ, Ren Y, Howes MJ (2005) Acetylcholinesterase inhibitors from plants and fungi. *Nat Prod Rep* **23**: 181-199

Huang X, Atwood CS, Hartshorn MA, Multhaup G, Goldstein LE, Scarpa RC, Cuajungco MP, Gray DN, Lim J, Moir RD, Tanzi RE, Bush AI (1999) The Aβ peptide of Alzheimer's disease directly produces hydrogen peroxide through metal ion reduction. *Biochemistry* **38**: 7609-7616

Hutchinson M, Fazini E (1996) Cholinesterase inhibition in Parkinson's disease. *J Neurol Neurosurg Psychiatry* **61**: 324-325

Imbimbo BP, Lucca U, Lucchelli F, Alberoni M, Thal LJ (Eptastigmine Study Group) (1998) A 25-week placebo controlled study of eptastigmine in patients with Alzheimer's disease. *Alzheimer Sis Assoc Disord* **12**: 313-322

Imbimbo BP, Martelli P, Troetel WM, Lucchelli F, Lucca U, Thal LJ (Eptastigmine Study Group) (1999) Efficacy and safety of eptastigmine for the treatment of patients with Alzheimer's disease. *Neurology* **52**: 700-708

Inestrosa NC, Alvarez A, Pérez CA, Moreno RD, Vicente M, Linker C, Casanueva OI, Soto C, Garrido J (1996) Acetylcholinesterase accelerates assembly of amyloid-beta-peptides into Alzheimer's fibrils: possible role of the peripheral site of the enzyme. *Neuron* **16** : 881-891

Inglis F (2002) The tolerability and safety of cholinesterase inhibitors in the treatment of dementia. *Int J Clin Pract* **127**: 45-63

Jan G, McKeith IG (1998) Special workshop in dementia with Lewy bodies (abstract). *Neurobiol Aging* **19**: 45

Jann MW (2000) Rivastigmine, a new-generation cholinesterase inhibitor for the treatment of Alzheimer's disease. *Pharmacotherapy* **20**: 1-12

Jann MW, Shirley KL, Small GW (2002) Clinical pharmacokinetics and pharmacodynamics of cholinesterase inhibitors. *Clin Pharmacokinet* **41**: 719-739

Janowski D, Davis J, Overstreet DH (2005) Anticholinesterase (DFP) toxicity antagonism by chronic donezepil: a potential nerve agent treatment. *Parmacol Biochem Behav* **81**: 917-922

Jastak JT (1985) Physostigmine: an antidote for excessive central nervous system depression or paradoxical rage reactions resulting from intravenous diazepam. *Anesth Prog* **32**: 87-92

Jeffrey L, Cummings MD (2000) Cholinesterase Inhibitors: a New Class of Psychotropic Compounds. *Am J Psychiatry* **157**: 4-15

Jones J, Parker J, Hunter J (1988) Antagonism of blockade produced by atracurium or vecuronium with low doses of neostigmine. *Br J Anaesth* **61**: 560-564

Jones RW, Passmore P, Wetterberg P, Soininen H, Bullock R, Murthy A (2002) First head-to-head study comparing the tolerability and efficacy of donepezil and galantamine in Alzheimer's disease. *7th International Geneva/Springfield Symposium on Advances in Alzheimer Therapy (AAT)*; 3-6 avril 2002, Genève, Suisse

Kaufer D, Cummings JL, Christine D (1998) Differential neuropsychiatric symptom responses to tacrine in Alzheimer's disease : relationship to dementia severity. *J. Neuropsychiatry Clin Neurosci* **10**: 55-63

Kaufer DI, Cummings JL, Christine D (1996) Effect of tacrine on behovioral symptoms in Alzheimer's disease : an open label study. *J Geriatr Psychiatry Neurol* **9**: 1-6

Kim WS, Cho Y, Kim JC, Huang ZZ, Park SH, Choi EK, Shin S, Nam SY, Kang JK, Hwang SY, Kim YB (2005) Protection by a transdermal patch containing physostigmine and procyclidine of soman poisoning in dogs. *Eur J Pharmacol* **525**: 135-142

Lallement G, Dorandeu F (2002) Une nouvelle perspective pour le prétraitement de l'intoxication organophosphorée : l'huperzine A : données expérimentales. *Médecine et armées* **30**: 219-224

Lallement G, Baubichon D, Clarençon D, Galonnier M, Peoc'h M, Carpentier P (1999) Review of the value of gacyclidine (GK-11) as adjuvant medication to conventional treatments of organophosphate poisoning: primate experiments mimicking various scenarios of military or terrorist attack by soman. *Neurotoxicology* **20**: 675-684

Lanctôt KL, Herrmann N, Yau KK, Khan LR, Liu BA, LouLou MM, Einarson TR (2003) Efficacy and safety of cholinesterase inhibitors in Alzheimer's disease: a meta-analysis. *CMAJ* **169**: 557-564

Li B, Stribley JA, Ticu A, Xie W, Schopfer LM, Hammond P, Brimijoin S, Hinrichs SH, Lockridge O (2000) Abundant tissue butyrylcholinesterase and its possible function in the acetylcholinesterase knockout mouse. *J Neurochem* **75**: 1320-1331

López S, Bastida J, Viladomat F, Codina C (2002) Acetylcholinesterase inhibitory activity of some Amaryllidaceae alkaloids and *Narcissus* extracts. *Life Sci* **71**: 2521-2529

Luo YQ, Hirashima N, Li YH, Alkon DL, Sunderland T, Etcheberrigaray R, Wolozin B (1995) Physiological levels of beta-amyloid increase tyrosine phosphorylation and cytosolic calcium. *Brain Res* **681**: 65-74

Maelicke A, Samochocki M, Jostock R, Fehrenbacher A, Ludwig J, Albuquerque EX, Zerlin M (2001) Allosteric sensitization of nicotinic receptors by galantamine, a new treatment strategy for Alzheimer's disease. *Biol Psychiatry* **49**: 279-288

Malouf R, Birks J (2004) Donepezil for vascular cognitive impairment. *Cochrane Database Syst Rev* **1**: CD004395

Mattson MP, Goodman Y (1995) Different amyloidogenic peptides share a similar mechanism of neurotoxicity involving reactive oxygen species and calcium. *Brain Res* **676**: 219-224

Marco L, Do Carmo Carreiras M (2006) Galanthamine, a natural product for the treatment of Alzheimer's disease. *Recent Pat CNS Drug Discov* **1**: 105-111

Mattson MP, Cheng B, Davis D, Bryant K, Lieberburg I, Rydel RE (1992) b-Amyloid peptides destabilize calcium homeostasis and render human cortical neurons vulnerable to excitotoxicity. *J Neurosci* **12**: 376-389

Mayeux R, Sano M (1999) Treatment of Alzheimer's disease. *N Engl J Med* **341**: 1670-1679

Mesulam M, Geula C (1994) Butyrylcholinesterase reactivity differentiates the amyloid plaques of aging from those of dementia. *Ann Neurol* **36**: 722–727

Mohs RC, Davis BM, Johns CA, Mathé AA, Greenwald BS, Horvath TB, Davis KL (1985) Oral physostigmine treatment of patients with Alzheimer's disease. *Am J Psychiatry* **142**: 28-33

Moriguchi S, Marszalec W, Zhao X, Yeh JZ, Narahashi T (2004) Mechanism of action of galantamine on *N*-methyl-D-aspartate receptors in rat cortical neurons. *J Pharmacol Exp Ther* **310**: 933-942

Moriguchi S, Zhao X, Marszalec W, Yeh JZ, Narahashi T (2005) Modulation of N-Methyl-D-aspartate Receptors by Donepezil in Rat Cortical Neurons**.** *J Pharm Exp Therap* **5**:125-135

Mukherjee PK., Kumar V, Mal M, Houghton PJ (2007) Acetylcholinesterase inhibitors from plants. *Phytomedicine* **14**: 289-300

Narahashi T, Moriguchi S, Zhao X, Marszalec W, Yeh JZ (2004) Mechanisms of action of cognitive enhancers on neuroreceptors. *Biol Pharma Bull* **27**: 1701-1706

Oakley P (2001) Physostigmin versus diazepines for anticholinergic poisoning. *Ann Emerg Med* **37**: 239-241

Onor ML, Trevisiol M, Aguglia E (2007) Rivastigmine in the treatment of Alzheimer's disease : an update. *Clin Interv Aging* **2**: 17-32

Pagès N, Breton P, Goudey-Perrière F (2009a) Characterization of new phytotoxins targeting cholinesterases : a potential therapeutic use in Alzheimer disease? In *Toxins and Signalling*, Benoit E, Goudey-Perrière F, Marchot P and Servent D (eds) pp 109-121. SFET Publications, Châtenay-Malabry, France, Epub on http://www.sfet.asso.fr (ISSN 1760-6004)

Pagès N, Goudey-Perrière F, Breton P (2009b) L'huperzine A, un inhibiteur de l'acétychlinestérase prometteur. In *Toxins and Signalling*, Benoit E, Goudey-Perrière F, Marchot P and Servent D (eds) pp 97-108. SFET Publications, Châtenay-Malabry, France, Epub on http://www.sfet.asso.fr (ISSN 1760-6004)

Palmer AM (1996) Neurochemical studies of Alzheimer's disease. *Neurodegeneration* **5**: 381-391

Parisi P, Francia A (2000) A female with central anticholinergic syndroem resposive to neostigmine. *Pediatr Neurol* **23**: 185-187

Park JE, Lee ST, Im WS, Chu K, Kim M (2008) Galantamine reduces striatal degeneration in 3-nitropropionic acid model of Huntington's disease. *Neurosci Lett* **448**: 143-147

Parsons CG, Danysz W, Quack G (1999) Memantine is a clinically well tolerated N-methyl-D-aspartate (NMDA) receptor antagonist - a review of preclinical data. *Neuropharmacology* **38**: 735–767

Perry EK, Perry RH, Blessed G, Tomlinson BE (1978) Changes in brain cholinesterases in senile dementia of Alzheimer type. *Neuropathol Appl Neurobiol* **4**: 273–277

Piau A, Hein C., Nourhashémi F., Vellas B (2009) Nouvelles thérapeutiques dans la maladie d'Alzheimer : vers un traitement visant à ralentir la progression de la maladie. *Cah. Année Gérontol* **1**: 15-25

Pirot S (2000) Intérêt des inhibiteurs de l'acétylcholinestérase dans la maladie d'Alzheimer. *Neuropsychiatrie : Tendances et Débats* **9**: 33-36

Pontecorvo MJ, Parys W (1998) Clinical development of galantamine: evaluation of a compound with possible acetylcholinesterase inhibiting and nicotinic modulating activity (abstract). *Neurobiol Aging* **19** (suppl 7): 57

Raina P, Santaguida P, Ismaila A, Patterson C, Cowan D, Levine M, Booker L, Oremus M (2008) Effectiveness of cholinesterase inhibitors and memantine for treating dementia: evidence review for a clinical practice guideline. *Ann Intern Med* **148**:379-397

Raskind MA, Peskind ER, Wessel T, Yuan W (2000) Galantamine in AD: A 6-month randomized, placebo-controlled trial with a 6-month extension. *The Galantamine USA-1 Study Group. Neurology* **54**: 2261-2268

Razay G, Wilcock GK (2008) Galantamine in Alzheimer's disease. *Expert Rev Neurother* **8**: 9-17

Reid RT, Sabbagh MN (2008) Effects of cholinesterase inhibitors on rat nicotinic receptor levels *in vivo* and *in vitro*. *J Neural Transm* **115**: 1437-1444

Rösler M, Anand R, Cicin-Sain A, Gauthier S, Agid Y, Dal-Bianco P, Stähelin HB, Hartman R, Gharabawi M (1999) Efficacy and safety of rivastigmine in patients with Alzheimer's disease: international randomised controlled trial. *Br Med J* **318**: 633–640

Rosler M, Retz W, Retz-Junginger P, Dennler HJ (1998) Effects of two-year treatment with the cholinesterase inhibitor rivastigmine on behavioural symptoms in Alzheimer's disease. *Behav Neurol* **11**: 211–216

Roy MJ (2004) Physician's guide to terrorist attack. Humana press

Rygnestad T (1992) Development of physostigmine from a poisonous plant to an antidote. One of the most important drug in the development of modern medicine? *Tidsskr. Nor. Laegeforen* **112**: 1300-1303

Samochocki M, Hoffle A, Fehrenbacher A, Jostock R, Ludwig J, Christner C, Radina M, Zerlin M, Ullmer C, Pereira EF, Lübbert H, Albuquerque EX, Maelicke A (2003) Galantamine is an allosterically potentiating ligand of neuronal nicotinic but not muscarinic acetylcholine receptors. *J Pharmacol Exp Ther* **305**: 1024–1036

Schneck HJ, Rupreht J (1989) Central anticholinergic syndrome (CAS) in anesthesia and intensive care. *Acta Anaesthesiol Belg* **40**: 219-228

Schneir A (2004) Physostigmine. *California Poison Control System* **3**: Update 2009

Scott LJ, Goa KL (2000) Galantamine: a review of its use in Alzheimer's disease. *Drugs* **60**:1095-1122

Selkoe DJ (2000) Toward a comprehensive theory for Alzheimer's disease. Hypothesis: Alzheimer's disease is caused by the cerebral accumulation and cytotoxicity of amyloid beta-protein. *Ann N Y Acad Sci* **924**: 17-25

Shadlen MF, Larson EB (1999) What's new in Alzheimer's disease treatment? Reasons for optimism about future pharmacologic options. *Postgrad Med* **105**: 109-118

Sharabi Y, Danon YL, Berkenstadt H, Almog S, Mimouni-Bloch A, Zisman A, Dani S, Atsmon J (1991) Survey of symptoms following intake of pyridostigmine during the Persian Gulf war. *Isr Med Sci* **27**: 656-658

Shea C, MacKnight C, Rockwood K (1998) Aspects of dementia : donepezil for treatment of dementia with Lewy bodies : a case series of nine patients. *Int Psychogeriatr* **10**: 229-238

Silman I, Sussman JL (2005) Acetylcholinesterase: 'classical' and 'non-classical' functions and pharmacology. *Curr Opin Pharmacol* **5**: 293-302

Smythies J, Golomb B (2004) Nerve gas antidotes. *JR Soc Med* **97**: 32

Sramek JJ, Frackiewicz EJ, Cutler NR (2000) Review of the acetylcholinesterase inhibitor galanthamine. *Expert Opin Investig Drugs* **9**: 2393-2402

Thal LJ, Rosen W, Sharpless NS, Crystal H (1981) Choline chloride fails to improve cognition of Alzheimer's disease. *Neurobiol Aging* **2**: 205-208

Von Bredow JD, Adams NL, Groff WA, Vick JA (1991) Effectiveness of oral pyridoxime and cholinolytic-oxime therapy against soman intoxication in non human primates. *Fundam Appl Toxicol* **17**: 761-770

Weinbroum AA (2005) Pathophysiological and clinical aspects of combat anticholinesterase poisoning. *Br Med Bull* **72**: 119-133

Weinstock M (1999) Selectivity of cholinesterase inhibition. *CNS Drugs* **12**: 307–323

Wetherell J, Price M, Mumford H (2006) A novel approach for medical countermeasures to nerve agent poisoning in the guinea pig. *Neurotoxicol* **27**: 485-491

Wetherell J, Price M, Mumford H, Armstrong S, Scott L (2007) Development of next generation medical countermeasures to nerve agent poisoning. *Toxicol* **233**: 120-127

Wilkinson DG, Passmore AP, Bullock R, Hopker SW, Smith R, Potocnik FC, Maud CM, Engelbrecht I, Hock C, Ieni JR, Bahra RS (2002) A multinational, randomised, 12-week, comparative study of donepezil and rivastigmine in patients with mild to moderate Alzheimer's disease. *Int J Clin Pract* **56**: 441-446

Wilkinson DG, Francis PT, Schwam E, Payne-Parrish J (2004) Cholinesterase inhibitors used in the treatment of Alzheimer's disease: the relationship between pharmacological effects and clinical efficacy. *Drugs Aging* **21**: 453-478

Winblad B, Gauthier S, Scinto L, Feldman H, Wilcock GK, Truyen L, Mayorga AJ, Wang D, Brashear HR, Nye JS (2008) GAL-INT-11/18 Study Group. Safety and efficacy of galantamine in subjects with mild cognitive impairment. *Neurology* **70**: 2024-2035

Whelpton R, Hurst P (1985) Bioavailability of oral physostigmine. *N Engl J Med* **313**: 1293-1294

Wiklund L (1986) Reversal sedation and respiratory depression after anaesthesia by the combined use of physostigmine and naloxone in neurosurgical patients. *Acta Anaesthesiol Scand* **30**: 374-377

White K, Cummings JL (1996) Schizophrenia and Alzheimer's disease: clinical and pathophysiologic analogies. *Compar Psychiatry* **37**: 188-195

Whitehouse PJ, Price DL, Clark AW, Coyle JT, Delong MR (1981) Alzheimer's disease : evidence for selective loss of cholinergic neurons in the nucleus basalis. *Ann Neurol* **10**: 122-126

Whitehouse PJ, Price DL, Struble RG, Clark AW, Coyle JT (1982) Alzheimer's disease and senile dementia : loss of neurons in the basal forebrain. *Science* **215**: 1237-1239

Wright CI, Geula C, Mesulam MM (1993) Neurological cholinesterases in the normal brain and in Alzheimer's disease: relationship to plaques, tangles, and patterns of selective vulnerability. *Ann Neurol* **34**: 373-384

Xiao XQ, Zhang HY, Tang XC (2002) Huperzine A attenuates amyloid beta-peptide fragment 25-35-induced apoptosis in rat cortical neurons via inhibiting reactive oxygen species formation and caspase-3 activation. *J Neurosci Res* **67**: 30-36

Zvosec DL, Smith SW, Litonjua R, Westfal RE (2007) Physostigmine for gamma-hydroxybutyrate coma : inefficacy, adverse events and review. *Clin Toxicol (Phila)* **45**: 261-265

Autres sites à consulter :

http://www.alzheimer.ca/french/research/resprog-awards08-descriptions/AubertIsabelle.htm

http://ispb.univ-lyon1.fr/ms/volume2/28-medicaments_alzheimer2.pdf

http://www.vulgaris-medical.com/encyclopedie/alzheimer-traitement-medicamenteux-de-la-maladie-d-9366.html

http://www.em-consulte.com/article/89983

http://michel.cavey-lemoine.net/spip.php?article81

Toxines et Signalisation – Toxins and Signalling
Rencontres en Toxinologie – Meeting on Toxinology, 2009
Editions de la SFET – SFET Editions
Accès libre en ligne sur le site – Free access on line on the site : http://www.sfet.asso.fr

L'huperzine A, un inhibiteur prometteur de l'acétylcholinestérase

Nicole PAGES[1,2*], Françoise GOUDEY-PERRIERE[2], Patrick BRETON[3]

[1] *Toxicologie, Faculté de Pharmacie, 67400 Illkirch ;* [2] *Biologie animale, Faculté de Pharmacie, 92296 Châtenay-Malabry ;* [3] *Centre d'Etudes du Bouchet, 91710, Vert le Petit, France*

** Auteur correspondant ; Fax : (0)1 60 19 01 31 ; Courriel : nicole.pages4@hotmail.fr*

Résumé

L'huperzine A (HUP) est un inhibiteur spécifique de l'acétylcholinestérase, réversible et capable de traverser la barrière hémato-encéphalique. Elle a d'autres fonctions neuroprotectrices qui ont un intérêt clinique évident parmi lesquelles on retiendra la régulation du métabolisme du précuseur de la protéine b-amyloïde (APP), la protection contre la neurotoxicité induite par le peptide A-béta (stress oxydatif, apoptose, dysfonctionnement mitochondrial), un effet anti-inflammatoire et antagoniste des récepteurs NMDA. L'HUP est actuellement autorisée en Chine pour le traitement de la maladie d'Alzheimer et des essais cliniques sont encore menés en Chine et aux USA. L'HUP est aussi utilisée aux USA comme stimulant cérébral. Les essais cliniques de phase IV en Chine ont montré que l'HUP est une drogue efficace et non toxique qui améliore la fonction cognitive de personnes âgées souffrant de pertes de mémoire liées à l'âge et celle de patients atteints de la maladie d'Alzheimer et de démence vasculaire, avec des effets secondaires mineurs de type cholinergique. L'HUP a aussi un intérêt dans la prévention des intoxications par les organophosphorés.

Huperzine A, a promising anticholinesterase inhibitor

Huperzine A (HUP) is a specific, reversible AChE inhibitor that crosses the blood-brain barrier. It also possesses other protective functions which might yield additional clinical beneficial effects : they include regulation of b-amyloid precursor protein (APP) metabolism, protection against A-beta- mediated neurotoxicity including oxidative stress, apoptosis and mitochondrial dysfunction, together with anti-inflammatory activity and NMDA receptor antagonist effects. HUP is presently approved for human use in China or is in course of clinical trials in China and USA for the treatment of Alzheimer's disease. HUP is also used as supplementary drug in the USA for correction of memory impairment. The phase IV clinical trials in China have demonstrated that HUP is an effective and safe drug that improves cognitive function in elderly people with benign senescent forgetfulness, and patients with Alzheimer's disease and vascular dementia, with minimal peripheral cholinergic side effects. HUP can also be used as a protective agent against organophosphate poisoning.

Keywords : *Acetylcholinesterase inhibitor (AChEI), Alzheimer disease, huperzine, neuroprotection, plant, organophosphate intoxication.*

Introduction

L'Huperzine A (ou HUP, HupA, Sélagine) est extraite d'une plante chinoise, *Huperzia serrata* (anciennement appelée *Lycopodium serratum*) qui appartient à la famille des Huperziaceae. Elle est également présente, en moins grande quantité, dans *Lycopodium selago.* Les extraits de ces plantes sont utilisés en médecine traditionnelle chinoise comme antipyrétiques et anti-inflammatoires (Pilotaz et Masson, 1999) et dans le traitement des contusions, de divers troubles sanguins et de certaines schizophrénies (Zangara, 2003 ; Ward et Caprio, 2006) mais ces applications ne reposent sur aucun travail scientifique sérieux (Zangara, 2003). En revanche, l'efficacité clinique de l'HUP dans la maladie d'Alzheimer (AD), les troubles mnésiques liés à l'âge et la démence vasculaire a d'abord été démontrée en Chine, où elle a un statut de médicament dans ces indications depuis 1994. D'autres travaux plus récents ont confirmé l'efficacité de l'HUP dans le traitement de l'AD à des stades modérés ou moyens et dans celui des troubles mnésiques liés à l'âge (Schachter *et al*., 2009). L'HUP pourrait également être utilisée comme antidote d'une intoxication par les neurotoxiques organophosphorés.

Son procédé d'extraction (1986) n'ayant pas été breveté, l'HUP a, aux USA, le statut de supplément alimentaire (et non de médicament) avec l'indication «stimulant de la mémoire». On peut se la procurer sur internet ou dans des magasins de diététique. Les produits commercialisés ont des noms évoquant le neurotropisme de la molécule : Brain Elevate, Huperzine Rx-Brain (Nature's Plus) ; Huperzine A ; Memorall (PharmAssure) (Hao *et al*., 2009). Mais tous les produits ne se valent pas : certains sont des extraits préparés à partir de la plante et donc hautement enrichis en HUP, d'autres des produits synthétiques beaucoup moins

actifs[1]. Pourtant, parce que l'HUP possède des effets pharmacologiques puissants, elle ne devrait être utilisée que sous contrôle médical.

De fait, l'HUP est un inhibiteur hautement spécifique et réversible de l'acétylcholinestérase (AChE). Elle augmente donc la concentration synaptique d'acétylcholine (ACh) dans la synapse et améliore ainsi la neurotransmission. Elle est efficace à très faible dose, de l'ordre du µg[2]. Comparée aux inhibiteurs de l'acétylcholinestérase (AChEI) actuellement sur le marché, l'HUP traverse mieux la barrière hémato-encéphalique (BHE), présente une meilleure biodisponibilité et inhibe pendant plus longtemps l'AChE (Wang *et al*., 2006). Son index thérapeutique est supérieur à celui du donépézil (Bai *et al*., 2000). Enfin, elle semble assez peu toxique : c'est sans doute l'une des molécules les plus prometteuses comme AChEI dans les différentes indications thérapeutiques qui ont été rappelées par Pagès *et al.* (2009).

Propriétés physico-chimiques

L'huperzine [CAS number : 102518-79-6] est un alcaloïde sesquiterpénique. C'est une molécule très stable, soluble dans l'eau et le chloroforme. Sa formule moléculaire est $C_{15}H_{18}N_2O$ (*Figure 1*). Sa masse molaire est de 242,32 ; son point d'ébullition de 217-219°C en conditions standard (à 25°C, 100 kPa) (Geib *et al*., 1991).

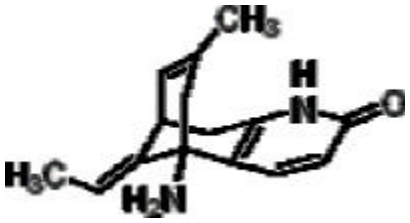

Fig. 1. Structure de l'huperzine.
Fig. 1. *Huperzine structure.*

Phytobiologie

A ce jour, la présence d'HUP n'est connue que chez les Huperziacées, notamment dans les genres *Huperzia* et *Phlegmariurus.* Les espèces du genre *Huperzia* sont distribuées dans les zones tropicales, subtropicales et tempérées chinoises. En revanche, celles appartenant au genre *Phlegmariurus* se trouvent surtout en zones tropicales et subtropicales. L'utilisation traditionnelle des *Phlegmariurus* spp. est très voisine de celle des *Huperzia* spp. (Ma et Gang, 2004). Des extraits d'alcaloïdes préparés à partir de *Huperzia saururus* (Amérique du Sud) possèdent aussi une activité AChEI (Ortega *et al*., 2004a, 2004b, 2006 ; Vallejo *et al*., 2007). Ces plantes ne sont pas abondantes, poussent très lentement (la maturité est atteinte en 15 - 20 ans) et ne se rencontrent que dans des habitats particuliers. Par conséquent, l'augmentation de la demande exerce une pression énorme sur ces plantes qui risquent de disparaître. La culture d'*Huperzia* est pour l'instant un échec et sa propagation par cultures *in vitro* très difficile. En revanche, la production par cultures *in vitro* de *Phlegmariurus squarrosus,* une espèce plus riche en HUP qu'*Huperzia serrata,* a déjà été réalisée (Ma *et al*., 2006) et pourrait répondre à la demande croissante de préparations titrées en HUP tout en préservant les ressources naturelles (Ma et Gang, 2004 ; Ma *et al*., 2007).

Huperzia serrata a été la plus anciennement étudiée : elle contient des terpénoïdes qui semblent impliqués dans une partie des utilisations traditionnelles de la plante ainsi que différents alcaloïdes (0,2%) dont la lycodoline, la lycoclavine, la serratinine et les huperzines (Liu *et al*., 1986a, 1986b ; Ma, 1997 ; Ma *et al*., 2006) Ces alcaloïdes sont tétracycliques, l'un des cycles pouvant être ouvert. Les huperzines présentent à la fois un azote intracyclique et un résidu aminé.

Ces huperzines existent sous différentes formes : l'huperzine A (HUP) présente à raison d'environ 0,011% (exprimé en poids sec de plante entière, *H. serrata*) (Liu *et al*., 2005) et l'huperzine B qui est un AChEI 10 fois moins puissant. L'HUP naturelle est une molécule chirale aussi appelée L-huperzine A ou (-)-huperzine A. Depuis que son activité AChEI est connue (Liu *et al*., 1986a, 1986b), beaucoup d'efforts ont été faits pour produire des analogues ou des dérivés plus actifs et moins toxiques. La première synthèse totale a été réalisée par Qian et Ji (1989). Puis de nombreux analogues ont été synthétisés par Kozikowski et Xia, (1989), Högenauer *et al*. (2001), Lucey *et al*. (2007), certains de ces procédés se prêtant à une synthèse à l'échelle industrielle. L'HUP de synthèse est un mélange racémique appelé (±)-huperzine A qui contient à la fois une forme active (lévogyre) et une forme inactive (dextrogyre). De ce fait, l'HUP naturelle est environ 3 fois plus efficace que le racémique *in vitro* (Hao *et al*., 2009).

Des dérivés de l'HUP ont été développés pour des applications pharmaceutiques[1]. L'HUP peut être administrée chez l'Homme par voie orale ou transcutanée (patch) mais la voie nasale (gel) pourrait aussi avoir un intérêt (cf. paragraphe pharmacocinétique). Par voie orale, la libération est presque totale et conduit à un pic de concentration élevé responsable de fluctuations de la concentration sanguine au cours du temps. La mise au point d'une nouvelle forme galénique utilisant des microsphères de [poly(d,l-lactide-*co*-glycolide) ou PLG-H] couplées à l'HUP permet une libération régulière du principe actif et l'obtention d'une réponse pharmacologique

[1] *http://www.passeportsante.net/fr/ Solutions/PlantesSupplements/Fiche.aspx?doc=huperzine_ps*

prolongée chez le Rat, après injection sous-cutanée (Gao *et al*., 2007 ; Liu *et al*., 2005). Un dérivé semi-synthétique de l'HUP, ZT-1 (une base de Schiff obtenue par condensation d'HUP et de 5-Cl-*O*-vanilline), dont la préparation est facile et peu onéreuse, possède une activité AChEI semblable à celle de l'HUP, mais il est plus sélectif pour l'AChE, agit encore moins sur la butyrylcholinestérase (BuCHE), et se révèle moins toxique chez la Souris. Les autres caractéristiques sont celles de l'HUP (franchissement de la BHE, grande biodisponibilité orale et longue durée d'action (Tang, 1996 ; Tang et Han, 1999 ; Ma et Gang, 2004 ; Tamchès *et al*., 2006 ; Wang *et al*., 2006 ; Zangara *et al*., 2006).

Pharmacocinétique

Chez l'animal

Les études de pharmacocinétique sont peu nombreuses (Zangara, 2003). Chez la **Souris**, après injection intra-veineuse (IV) de 183 µg/kg d'HUP radiomarquée, la radioactivité se retrouve au bout d'1 h dans tout le cerveau, en particulier dans le cortex frontopariétal, le striatum, l'hippocampe et le *nucleus accumbens*. Elle est également présente dans le foie et les reins 15 min après l'injection. Elle est totalement éliminée après 12h (Tang *et al*., 1989). Une autre expérience chez la Souris montre que la majorité de l'huperzine est excrétée en moins de 24h dans les urines sous forme native ou métabolisée, le reste (2,4%) passant dans les fèces. Chez la Souris gravide, une petite quantité passe chez le fœtus (Wang *et al*., 1988).

Chez le **Rat**, l'administration d'une dose de 177 µg/kg apportée soit par voie intranasale, soit par voie IV, conduit à une ASC (pour *Aire Sous la Courbe*) plasmatique très proche (94% pour la voie intranasale *vs* IV) mais la voie intranasale donne des ASC plus élevées dans le liquide céphalorachidien et dans différentes aires cérébrales, tout particulièrement le cortex et l'hippocampe (130, 150 et 130% respectivement *vs* IV). Lorsque la dose de 177 µg/kg par voie intranasale est comparée aux effets d'une dose 2 à 3 fois plus élevée apportée par des comprimés du commerce (500 µg/kg), l' ASC plasmatique est proche (94 *vs* 98% *per os*) mais les ASC du liquide céphalorachidien, du cortex et de l'hippocampe sont beaucoup plus élevées (260, 270 et 220% respectivement *vs per os*). L'administration intranasale de l'HUP est donc une voie non invasive et très efficace pour atteindre des concentrations cérébrales plus élevées que celles obtenues par les voies orale et IV, en particulier dans le cortex et l'hippocampe qui sont très atteints au cours de l'AD (Tao *et al*., 2006 ; Yue *et al*., 2007 ; Zhao *et al*., 2007).

Quelques études réalisées chez le **Chien** ont comparé la voie orale à la voie IV (Chu *et al*., 2006 ; Ye *et al*., 2008). Après administration orale, l'HUP est rapidement et presque totalement absorbée (94,4% *vs* IV) et largement distribuée dans les tissus (Chu *et al*., 2006). Par voie transdermique, l'application d'un seul patch à la dose de 4 mg/20cm^2 augmente progressivement la concentration sérique pendant 12 à 24 h (T_{max} de 24 h *vs* 3 h *per os*) jusqu'à un plateau qui se prolonge pendant 84 h. La valeur du C_{max} est plus faible que par voie orale (3,4 vs 9,8 mg/L *per os*), ce qui évite des fluctuations brutales de l'huperzinémie. L'application de 2 patchs par semaine permet de stabiliser cette concentration à une valeur comprise entre 2,4 et 4,3 mg/L. Le patch permet donc une libération contrôlée, maintient une concentration sérique assez constante pendant 3,5 jours et limite le traitement à deux applications par semaine (Ye *et al*., 2005).

Chez l'Homme

Un essai réalisé sur des **volontaires sains** montre que l'HUP, par voie orale, est rapidement absorbée (T_{max} 80 min et $t_{1/2}$ 288 min), ce qui imposerait 2 ou 3 administrations quotidiennes. Le temps d'élimination est lent. Aucun effet secondaire n'a été noté aux doses testées (comprises entre 0,18 et 0,54 mg) (Qian *et al*., 1995).

Toxicité

Les études chez l'animal et les essais de tolérance cliniques ont montré que l'HUP n'a que des effets périphériques cholinergiques modérés et pas d'effet indésirables inattendus comme la redoutable hépatotoxicité de la Tacrine qui a entraîné son retrait du marché (Wang et Tang, 1998a, 1998b ; Bai *et al*., 2000 ; Zangara, 2003 ; Wang *et al*., 2006).

Chez l'animal

Les études toxicologiques réalisées dans différentes espèces animales ont montré que l'HUP était peu toxique (Zangara, 2003). Chez la Souris, les DL_{50} sont de 4,6 mg *per os*, 3 mg par voie sous-cutanée, 1,8 mg par voie intrapéritonéale (IP), et 0,63 mg par voie IV. L'administration quotidienne d'HUP, pendant 180 jours, à des chiens (0,6 mg/kg par voie intra-musculaire, IM) ou à des rats (1,5 mg/kg, par voie orale) n'a provoqué aucune modification histologique du foie, des reins, du cœur, des poumons ou du cerveau. Aucune mutagénicité n'est apparue chez le Rat (Zenghong et Melying, 1990). Aucun effet reprotoxique n'a été observé chez la Souris ou le Lapin bien que l'HUP traverse la barrière foeto-placentaire chez la Souris (Wang *et al*., 1988).

Chez l'Homme

L'HUP n'a pas d'effets délétères connus, chez l'Homme sain (Qian *et al*., 1995 ; Lallement *et al*., 2002 ; Zangara, 2003). Elle ne provoque notamment pas l'hépatotoxicité de la Tacrine (Xu *et al*., 1995 ; 1999 ; Zhang et Wang, 1990 ; Zhang *et al*., 1991).

Pharmacologie

Chez l'animal et l'Homme, l'HUP permet d'améliorer la mémoire et est neuroprotectrice (Zangara, 2003 ; [2]).

[2] *http://www.clinicaltrials.gov/show/NCT00083590*

Chez l'animal

Profil neuroprotecteur *:* Des effets positifs de l'HUP sur la mémoire et la cognition ont été observés après administration d'HUP chez des rongeurs nouveaux-nés (Wang *et al*., 2003) ainsi que sur des rongeurs et des singes en bonne santé, adultes ou âgés. Il a aussi été montré, dans différents modèles animaux, que l'HUP (à des doses de l'ordre de 0,1 mg/kg par voie IP ou IM) est capable de réverser ou d'atténuer les déficits cognitifs induits par injection de produits neurotoxiques, traitements physiques ou actes chirurgicaux (Tang *et al*., 1986 ; Vincent *et al*., 1987 ; Zhu et Tang, 1987, 1988 ; Liu *et al*., 1988 ; Xiong et Tang, 1995 ; Cheng et Tang, 1998 ; Liu *et al*., 1998 ; Wang et Tang, 1998b ; Xiong et al., 1998 ; Ye *et al*., 1999, 2000 ; Ou *et al*., 2001 ; Zangara, 2003 ; Wang et Tang, 2005).

L'HUP provoque une augmentation de la concentration d'ACh dans le cerveau (Tang *et al*., 1989 ; Zhu et Giacobini, 1995). Des expériences de dialyse cérébrale chez le Rat ont montré que l'HUP était respectivement 8 et 2 fois plus puissante que le donépézil et la rivastigmine et que son effet durait plus longtemps (Liang et Tang, 2004).

Profil anticonvulsivant *:* L'HUP est active, 1 heure après injection, dans différents tests d'épilepsie (pentylènetétrazole test ; 6-Hz modèle) mais pas dans le *maximum electroshock seizure* test (MES), chez la Souris (White *et al*., 2005). Aux doses de 1, 2 et 4 mg/kg, la protection maximum a été de 62,5% des animaux testés mais, à partir de 2 mg/kg, le test du rotarod est perturbé, indiquant une atteinte du comportement. Des doses inférieures, non toxiques dans le test du rotarod sont efficaces dans le 6-Hz modèle, ce qui donnerait un avantage à l'HUP sur les antiépileptiques couramment utilisés (Schachter *et al*., 2006).

Profil antinociceptif *:* L'HUP possède aussi un effet antinociceptif puissant chez la Souris, dès la dose de 1 mg/kg IP, mis en évidence dans un modèle de douleur provoquée par injection de formol (Murphee *et al*., 2006).

Chez l'Homme

Des essais cliniques de phase IV, réalisés en Chine (et rédigés le plus souvent en chinois !) (Yan *et al*., 2007) ont montré que l'HUP (60 µg à 400 µg d'HUP par jour, généralement en une ou deux prises) est efficace dans le traitement de maladies neurodégénératives comme l'AD (Xu *et al*., 1995, 1999 ; Yang *et al*., 2003) ou la démence vasculaire (Wei *et al*., 2001 ; Yin *et al*., 2001 ; Zhong et Liang, 2004). Elle permet aussi d'améliorer la mémoire et d'autres déficits cognitifs causés par des maladies telles que la schizophrénie (Fang *et al*., 2002 ; Ma *et al*., 2003 ; Yang, 2003), les traumatismes crâniens et les carences en iode (Qu *et al*., 1995) ou encore par le vieillissement (Wang et Tang, 2005). Ces essais cliniques ont aussi montré qu'elle avait des effets secondaires mineurs de type cholinergique. Il semble donc de toute évidence que l'HUP ait un effet bénéfique sur les fonctions cognitives, le statut global clinique, les troubles comportementaux et les performances fonctionnelles, sans effets secondaires majeurs chez les patients souffrant d'AD. Cependant, selon Li *et al*., (2008), une seule de ces études répond aux normes de recherche clinique en termes de protocole et de taille de l'échantillon étudié. Ces auteurs soulignent la nécessité de réaliser des essais multicentriques randomisés sur de larges échantillons de population, dans des conditions de recherche rigoureuses pour confirmer les effets de l'HUP dans l'AD. L'utilisation croissante de l'HUP par des patients souffrant ou non d'AD aux USA a conduit les américains à initier une étude de ce type. Dans les études de phase I (deux fois quatre semaines), avec augmentation progressive des doses, l'HUP a fait la preuve de son innocuité et de sa bonne tolérance chez des individus sains, âgés de 65-79 ans. Même à la dose de 800 µg par jour, les effets secondaires rapportés étaient très modérés. Une étude multicentrique de phase II a alors été entreprise. Elle a porté sur 150 participants, dispersés dans 28 sites différents. C'est une étude en double aveugle, placebo-contrôle, qui est maintenant terminée. Les participants ont été répartis de manière aléatoire en trois groupes recevant soit un placebo, soit 200 ou 400 µg d'HUP deux fois par jour. Cette étude a évalué non seulement la fonction cognitive mais aussi les modifications de l'attitude générale, des activités quotidiennes et du statut neuropsychiatrique de chaque patient. Elle a déterminé aussi le lien existant entre l'activité AChE dans le sang et les fonctions cognitives chez les individus traités. A l'issue des 24 semaines de traitement, Neuro-Hitech proposera aux personnes souhaitant participer à un complément d'étude ouverte de poursuivre le traitement à base d'HUP[2]. Lors de l'ICAD (International Conference on Alzheimer's Disease) de 2008, des résultats encourageants ont été présentés (Sabbagh, 2009). Les données préliminaires montrent en effet que l'HUP peut améliorer la cognition ; ainsi, après 8 à 12 semaines, des améliorations sur l'échelle MMSE (*Mini Mental Status Examination*) de 1 à 5 points ont pu être mesurées (Desilets *et al*., 2009). L'efficacité des comprimés et des capsules d'HUP, de même concentration en molécule active, semble identique (Zangara, 2003).

Mécanisme d'action

L'AD est une pathologie d'origine multifactorielle. Les concentrations cérébrales en ACh sont réduites et s'accompagnent d'altérations pathologiques du tissu cérébral. Comme dans la plupart des maladies neuro-dégénératives, il se produit un stress oxydatif (Wang *et al*., 2006). D'autres altérations participent aussi au développement de l'AD : altération du séquençage de l'APP (*Amyloid Precursor Protein)*, dysfonctionnement mitochondrial, augmentation de l'apoptose, perturbation de la neurotransmission glutamatergique et inflammation (Xiao *et al*., 2000 ; Grundman *et al*., 2002 ; Wang *et al*., 2003 ; Tang *et al*., 2005a ; Wang et Tang, 2005 ; Wang *et al*., 2006).

Or, l'HUP agit sur les démences par l'intermédiaire de mécanismes multiples (Wang et Tang, 2005) favorisant la neurotransmission (effet sur l'ACh et les catécholamines) et la neuroprotection : protection contre

la formation et les effets du peptide béta-amyloïde (stress oxydatif, dépôt de la plaque amyloïde, apoptose), inhibition du récepteur NMDA et de l'inflammation (Wang et Tang, 2005 ; Schachter *et al*., 2006 ; Li *et al*., 2008).

HUP et neurotransmission

Acétylcholine *:* Il existe une corrélation entre la baisse de l'activité cholinergique corticale et la détérioration des tests dans l'AD (Perry *et al*., 1978) qui a conduit à l'«hypothèse cholinergique », selon laquelle toute substance capable d'augmenter les concentrations d'ACh devrait réduire les troubles neurodégénératifs de l'AD. Et de fait, les AChEI ont été les premiers à ralentir l'évolution de cette maladie (Wang *et al*., 2006). Durant les années 80, les scientifiques chinois ont montré que l'HUP était un puissant AChEI (Wang *et al*., 1986, 1998a ; Ashani *et al*., 1992 ; Saxena *et al*., 1994) et possédait d'autres propriétés qui contribuent à son efficacité dans le traitement de l'AD (Gao *et al*., 2007 ; Little *et al*., 2008).

L'HUP est un inhibiteur réversible et hautement spécifique de l'AChE, capable de traverser la BHE, et ayant donc à la fois des effets périphériques et centraux (Cheng *et al*., 1996). Sa spécificité tient au fait qu'elle s'intègre dans le site actif de l'AChE et s'y attache par de multiples liaisons chimiques (Ashani *et al*., 1992 ; Raves *et al*., 1997). Ainsi, l'enzyme ne peut plus jouer son rôle. Ce mécanisme a été démontré par de nombreuses études sophistiquées incluant la modélisation par ordinateur de la forme de la molécule d'HUP (Pang et Kozikowski, 1994). Les autres AChEI fonctionnent de la même façon, mais le complexe HupA–AChE a une plus longue durée de vie (Ma et Gang, 2004). De nombreuses autres études comparant les AChEI commercialisés et l'HUP *in vivo* et *in vitro*, ont montré que l'HUP était au moins égale ou supérieure aux autres AChEI dans le traitement de l'AD (Wang *et al*., 1986 ; Wang et Tang, 1998 ; Liang et Tang, 2004 ; Ma et Gang, 2004 ; Wang *et al*., 2006). *In vitro*, l'HUP inhibe différemment l'AChE et la BuChE (Wang et Tang, 1998) (*Tableau 1*). Les activités inhibitrices de l'AChE sont par, ordre décroissant : donépézil > HUP > tacrine > physostigmine > galantamine > rivastigmine alors que l'HUP est l'inhibiteur le moins puissant de la BuChE sérique. Par ailleurs, les constantes d'inhibition de l'AChE corticale sont toutes exprimées en nanomoles, ce qui signifie que ces inhibiteurs ont une forte affinité pour l'AChE. Cependant, les doses de donépézil et de tacrine utilisées par voie orale sont très supérieures à celles d'HUP, ce qui peut provenir de leur faible biodisponibilité et/ou de leur rapide dégradation. De plus, des études*, in vivo* chez le Rat, ont montré que l'HUP était respectivement 8 et 2 fois plus puissante (en termes molaires) que le donépézil et la rivastigmine pour augmenter les concentrations d'ACh corticale. Par ailleurs, l'effet dure plus longtemps. Enfin, l'inhibition de la BuChE par la tacrine est significativement supérieure à celle des autres AChEI. Or la tacrine est l'AChEI le plus toxique, ce qui suggère que l'inhibition de la BuChE pourrait contribuer à cette toxicité. Par conséquent, il semble qu'un rapport élevé des IC_{50} BuChE/AChE soit très favorable pour les médicaments qui ciblent le système cholinergique, et dans cette hypothèse, l'HUP occupe une place de choix ! (*Tableau 1*) (Ma *et al*., 2007).

Tableau 1. Effets de l'HUP et des autres AChEI sur les activités AChE corticale et BuChE sérique du Rat (Ma *et al*., 2007).

Table 1. *Effects of HUPA and other AChEI on AChE activity in rat cortex and BuChE activity in rat serum.*

ChEI	IC_{50} (µM)		Rapport de IC_{50} BuChEI / AChEI	Ki (nM)
	AchE cortex	BuChE sérum		
HUP	0,082	74,43	907,7	24,9
Tacrine	0,093	0,074	0,8	105
Donépézil	0,010	5,01	501	12,5
Physostigmine	0,251	1,26	5	–
Rivastigmine	181,39	31.07	0,17	–
Galantamine	1,995	12.59	6,3	210

Monoamines cérébrales : Chez le Rat, l'HUP augmente les concentrations cérébrales en noradrénaline et dopamine mais pas celles de sérotonine (Liang et Tang, 2004 ; Desilets *et al.,* 2009).

Récepteurs : L'HUP n'agit ni sur le nombre ni sur l'affinité des récepteurs nicotiniques ou muscariniques à l'ACh (Fayuk et Yakel, 2004), ni sur le nombre de récepteurs NMDA au glutamate. Il a un faible effet inhibiteur sur le récepteur alpha-1 adrénergique et sur le récepteur aux benzodiazépines (Gordon *et al*., 2001).

HUP et neuroprotection

Les effets neuroprotecteurs de l'HUP sont liés à sa capacité à interférer avec le métabolisme de l'APP, à atténuer le stress oxydatif, à réguler l'expression des protéines impliquées dans l'apoptose (Bcl-2, Bax, P53 et caspase-3), à protéger les mitochondries et à réguler la sécrétion du NGF *(Nerve Growth Factor*) et de ses voies de signalisation (pour une revue détaillée, voir Zangara, 2003 ; Wang et Tang, 2005 ; Zhang et Tang, 2006).

Effet sur le clivage du précurseur de la protéine amyloïde (APP) : L'APP, glycoprotéine transmembranaire, peut être coupée par un processus physiologique non amyloïdogène qui fait intervenir les alpha et gamma sécrétases libèrant un fragment APPs (s pour soluble) ou APP_{695}, et qui évite la formation du peptide A-beta (Esch *et al*., 1990 ; Busciglio *et al*., 1993).

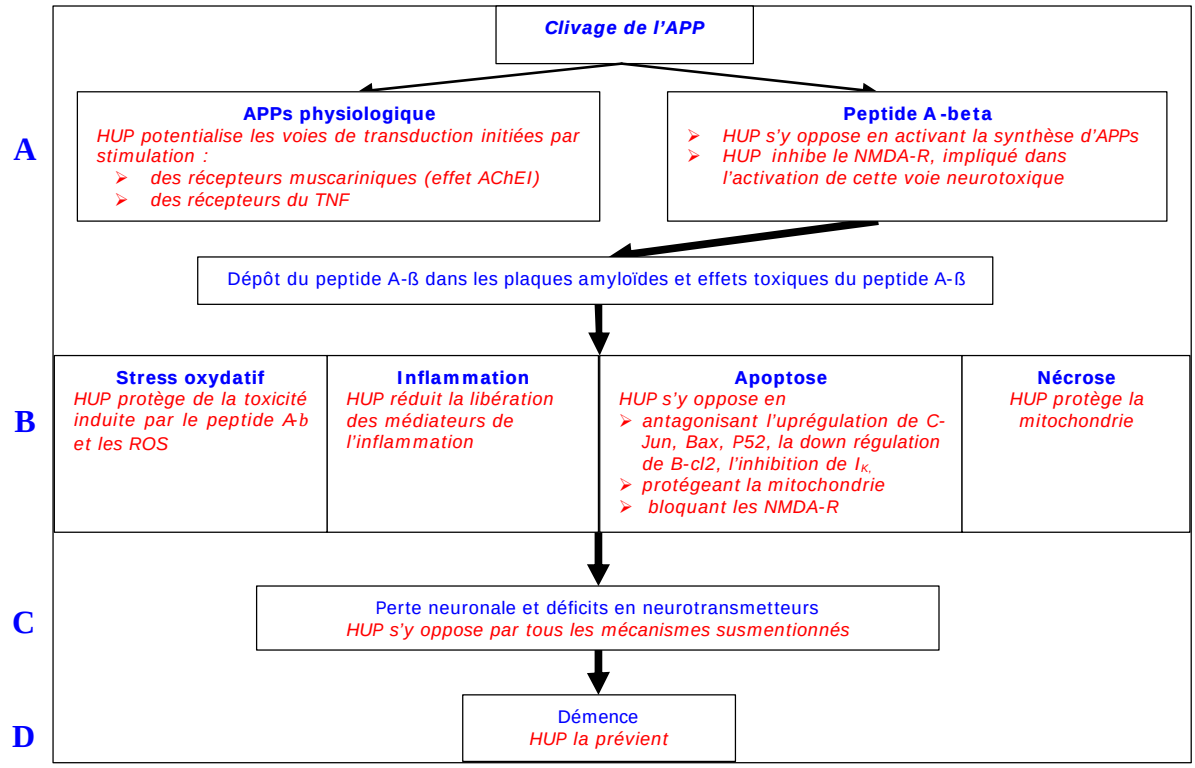

Fig. 2. Multiples effets de l'HUP sur les altérations présentes dans l'AD.

Fig. 2. *Multiple effects of HUP on AD alterations.*

L'APPs a de multiples fonctions neurotrophiques et neuroprotectrices. Ce processus physiologique peut être potentialisé par deux voies de transduction, qui convergent vers une étape commune de phosphorylation de la tyrosine d'une protéine responsable de l'activation de l'alpha-sécrétase (Peng *et al*., 2007 ; Zhang et Tang, 2008) :

- la cascade dépendant de la protéine kinase C (PKC), initiée par les récepteurs muscariniques M1 et M3, couplés à la phosphorylase C (Nitsch *et al*., 1992). L'HUP, comme tout AChEI, en augmentant la concentration d'ACh, stimule les récepteurs muscariniques et s'oppose au clivage anormal de l'APP ; elle diminue ainsi les différentes causes d'altérations neurodégénératives (Buxbaum *et al*., 1993 ; Mori *et al*., 1995 ; Giacobini *et al*., 1996) ;

- la cascade dépendant de Ras/MAPK (*Mitogen-Activated Protein Kinase*, encore appelée Erk), initiée par le NGF et son récepteur de haute affinité TrkA (*Tyrosine Kinase Receptor type 1*). L'HUP exerce une régulation positive (up-regulation) du NGF et de ses récepteurs, notamment dans le noyau basal de Meynert d'où partent les neurones à ACh dans tout le cerveau (Tang *et al*., 2005a, 2005b ; Zhang et Tang, 2006, 2008).

Mais, l'APP peut aussi être clivé par une autre voie impliquant les beta et gamma sécrétases, produisant des peptides bêta-amyloïdes neurotoxiques de 39 à 43 aminoacides (ou peptides beta-A4 ou A-beta), rendus insolubles par leur conformation en feuillets ß (*Figure 2*). Il est probable que le métabolisme aberrant de l'APP soit le mécanisme pathogène central des démences (*étape A*). Ce peptide A-beta est, en effet, responsable de multiples changements neurodégénératifs (dépôt des plaques amyloïdes caractéristiques de l'AD, stress oxydatif, hyperphosphorylation de la protéine tau, mort neuronale par apoptose et nécrose, réponses inflammatoires) (*étapes B*). Tous ces changements conduisent à la perte de synapses et à une altération de la neurotransmission (*étape C*) responsables de la démence (*étape finale D*).

Il a été montré, dans des cultures de neurones corticaux, que l'activation du récepteur NMDA inhibe l'alpha-sécrétase et promeut donc la voie alternative conduisant à la synthèse de peptide béta-amyloïde (Lesné *et al*., 2005).

Effet antiradicalaire : Le stress oxydatif est impliqué dans la cascade d'événements conduisant à la démence de l'AD et d'autres troubles neurodégénératifs. Il pourrait intervenir, en particulier, lors de la formation des plaques séniles, quand le peptide A-béta produit en excès s'agrège.

- ***In vitro***, l'HUP protège des cultures primaires de neurones corticaux des effets toxiques de l'H_2O_2 et du peptide A-beta ; elle diminue la lipopéroxydation (LPO) et augmente l'activité des enzymes antioxydantes. Son action neuroprotectrice passe donc, au moins en partie, par une moindre formation de ROS (*Radical Oxygen Species* ou radicaux libres oxygénés) (Xiao *et al*., 2000).

- ***In vivo,* chez le Rat** : l'administration préventive d'HUP par voie IV pendant 12 jours évite l'apparition des déficits cognitifs classiquement induits par injection du peptide A-beta (Wang *et al*., 2001). De même, l'administration d'HUP à des rats âgés montre une diminution de la LPO dans l'hippocampe, le cortex et le sérum.
- ***In vivo,* chez l'Homme :** l'administration d'HUP diminue les ROS dans le plasma et les globules rouges des patients souffrant d'AD (Xu *et al*., 1999).

Ces résultats indiquent que l'HUP protège de la neurotoxicité induite par le peptide A-beta par l'intermédiaire des ROS (Wang et Tang, 2005). Les mêmes résultats ont été obtenus avec l'huperzine B qui est un AChEI beaucoup moins puissant : cela signifie que l'action antiradicalaire est indépendante de l'effet inhibiteur de l'AChE (Wang et Tang, 2005).

Amélioration de la fonction mitochondriale : La mitochondrie joue un rôle majeur dans le fonctionnement physiologique cellulaire. Son dysfonctionnement est l'une des lésions intracellulaires majeures associées à la pathogénie de l'AD. Dans la mitochondrie, l'accumulation d'A-beta et l'interaction directe d'A-beta avec l'ABAD (pour *Ab-binding alcool deshydrogenase*) perturbent le fonctionnement de la mitochondrie. De fait, l'accumulation d'A-beta provoque une surproduction de ROS et perturbe à la fois le fonctionnement de la chaîne respiratoire et celui du cycle des acides tricarboxyliques. L'A-beta cause ainsi une déplétion en ATP et la perte du potentiel membranaire qui conduit à l'apoptose. L'HUP diminue les concentrations de ROS et rétablit le fonctionnement de la chaîne respiratoire et du cycle des acides tricarboxyliques (Zheng *et al*., 2008). Une augmentation prolongée de la perméabilité de la mitochondrie conduit à la mort de la cellule par nécrose (Wang et Tang, 2005).

Effet antiapoptotique : L'apoptose des cellules nerveuses est de règle dans les maladies neuro-dégénératives. Elle se traduit par une fragmentation du noyau, une convolution des membranes cytoplasmiques et nucléaires et une condensation du cytoplasme entraînant la formation de corps apoptotiques (Wang et Tang, 2005). Le mécanisme de l'apoptose est gouverné par deux voies principales d'activation : une voie dite extrinsèque, impliquant des récepteurs appartenant à la superfamille des récepteurs au TNF et une voie dite intrinsèque, mettant particulièrement en jeu la mitochondrie. Ce dernier résulte d'un déséquilibre des protéines anti-apoptotiques (Bcl-2) et pro-apoptotiques (C-Jun, P53 et Bax). Bcl-2 supprime l'apoptose en inhibant la libération de cytochrome c hors de la mitochondrie. Au contraire, Bax provoque la libération du cytochrome c et de l'AIF (*Apoptosis Inducing Factor*). Le cytochrome c est responsable de l'activation de la cascade des caspases (Graham et Chen, 2001) qui active des protéases et des DNAses responsables de la mort cellulaire par apoptose.

Différentes études ont montré que l'HUP protège, *in vitro*, les cellules de l'apoptose induite par le peptide A-beta ou d'autres stress (privation de sérum, staurosporine) : diminution de l'activité de la caspase 3, de la libération de cytochrome c, de la fragmentation de l'ADN, de la régulation négative de Bcl-2, de la régulation positive de Bax et de la formation des corps apototiques (Xiao *et al*., 2000 ; Zhou et Tang, 2002 ; Zhang et Tang, 2003). Par ailleurs, l'HUP inhibe réversiblement *in vitro*, dans les neurones d'hippocampe de rat, un courant retardé sortant d'ions K^+ dénommé I_K (Yu *et al*., 1998) dont la régulation positive induite notamment par le peptide A-beta, participe à différentes formes d'apoptose neuronale. *In vivo*, l'administration de 0,1 à 0,2 mg/kg d'HUP par voie IP à des rats, diminue le nombre de cellules apoptotiques et réverse la régulation négative de Bcl-2 et la régulation positive de Bax et P52 lors de l'injection intra-cérébroventriculaire (3 fois 800 µmoles) de peptide A-beta (Wang et Tang, 2005). Cet effet anti-apoptotique pourrait être dû, en partie, à l'inhibition de la production des ROS (Xiao *et al*., 2002).

Par conséquent, les effets anti-apoptotiques de l'HUP sont liés à l'inhibition de la production de ROS, à une action antagoniste sur les protéines impliquées dans l'apoptose et à l'inhibition du courant retardé I_K.

Effets antiglutamatergiques : Une stimulation excessive des récepteurs au glutamate, en particulier du récepteur NMDA, est impliquée dans la plupart des désordres neurodégénératifs (Lipton et Rosenberg, 1994 ; Hynd *et al*., 2004). Il en résulte une entrée excessive d'ions Ca^{2+} dans la cellule, responsable de la mort cellulaire par nécrose ou apoptose. L'HUP inhibe de façon dose-dépendante la toxicité induite par le NMDA dans des cultures de neurones (Wang *et al*., 1999), en se fixant au niveau du site de liaison des polyamines du récepteur NMDA (NMAD-R) (Gordon *et al*., 2001). Elle agirait comme un antagoniste non-compétitif des NMDA-R. Cette action n'est pas stéréospécifique puisque les mêmes résultats sont obtenus avec l'HUP naturelle et synthétique. L'HUP serait le plus puissant de tous les AChEI testés à protéger les neurones matures et à antagoniser les NMDA-R (Zhang et Hu, 2001).

Effet anti-inflammatoire : Les mécanismes inflammatoires ont été fortement liés à la pathogénie de l'AD et de la démence vasculaire (VD). La production chronique de cytokines de l'inflammation comme l'IL-2beta, le TNF-alpha ou l'IL-6 au voisinage des plaques amyloïdes pourrait être cytotoxique et stimuler la production du peptide A-beta. L'effet anti-inflammatoire de l'HUP a été démontré *in vitro* dans différents modèles d'ischémie cérébrale ; elle induit une diminution de la production des cytokines, inhibe l'activation du NF-κB (pour *Nuclear Factor Kappa B*), atténue la surexpression de la NO synthase inductible (iNOS), de la cyclooxygénase 2 (COX-2), du NO et promeut la survie des cellules (Zhang *et al*., 2008).

Utilisations cliniques de l'huperzine

Maladie d'Alzheimer : La plupart des essais cliniques, y compris des essais de phase IV, ont été effectués en

Chine, et l'on estime à 100.000 le nombre de malades qui ont été ainsi traités (Chiu et Zhang, 2000). Ces essais ont montré que l'HUP améliore considérablement la fonction cognitive, le comportement, les activités quotidiennes et l'humeur des patients souffrant d'AD (Xu *et al*., 1995, 1999 ; Zhang *et al*., 2002a). Comparée aux autres AChEI actuellement sur le marché, l'HUP traverse mieux la BHE, a une meilleure biodisponibilité et une durée action d'AChEI plus longue (Wang *et al*., 2006). Elle serait aussi un peu mieux tolérée (Zhang *et al*., 2002b ; Bialer *et al*., 2009). Son efficacité est améliorée lorsque l'HUP est utilisée en combinaison avec de la nicergoline, un œstrogène, ou du nilestriol (pour les femmes souffrant d'AD) (Zhou *et al*., 2004 ; Ma *et al*., 2007) ou avec un entrainement quotidien pendant 8 semaines chez des patients présentant une forme légère ou modérée d'AD (Wang *et al*., 2002). ZT-1 est généralement bien toléré, et les effets gastro-intestinaux habituels des AChEI sont considérablement réduits. Le principe actif est libéré de façon progressive et semble approprié pour le traitement de l'AD (Cervenka et Jahodar, 2006 ; Tamchès *et al*., 2006 ; Zangara *et al*., 2006).

Démence vasculaire (VD) : Il n'existe pas actuellement de traitement médical ou chirurgical de la VD qui résulte de l'accumulation de multiples petits accidents ischémiques cérébraux. Cette pathologie est la deuxième cause de démence en Europe et aux USA. Dans les pays développés d'Asie, l'incidence de VD excède celle d'AD (Wang et Tang, 2005). L'HUP administrée par voie intramusculaire chez 55 patients souffrant de VD, à la dose de 0,05 mg deux fois par jour pendant 4 semaines, a amélioré la mémoire de la plupart d'entre eux (Zhang *et al*., 1991 ; Skolnick, 1997 ; [3]). D'autres études ont également rapporté des effets bénéfiques dans cette indication (Ma *et al*., 1998 ; Li et Min, 2001 ; Wang *et al*., 2002 ; Pi *et al*., 2004). Cependant une méta-analyse récente est beaucoup plus réservée, indiquant que l'huperzine n'a pas d'intérêt dans le traitement de VD (Hao *et al*., 2009).

Pertes de mémoire liées à l'âge : L'HUP est évaluée dans cette indication aux USA [4]. Par ailleurs, l'administration IM quotidienne de 0,03 mg d'HUP pendant deux semaines chez 100 personnes âgées souffrant de troubles légers ou modérés de la mémoire liés à l'âge a amélioré la mémoire de la plupart d'entre eux. Certains se sont plaints de légers vertiges qui n'ont pas nécessité l'arrêt du traitement (Zhang *et al*., 1991 ; Skolnick, 1997 ; Mazurek, 2000 ; Chang *et al*., 2002 ; Zhang *et al*., 2002b ; Wang *et al*., 2006). Les résultats obtenus doivent néanmoins être pris avec réserve en raison du petit nombre d'individus considérés et du protocole de cet essai (Sun *et al*., 1999).

Schizophrénie : L'HUP a un effet très favorable sur les désordres mnésiques des patients schizophrènes (Fang *et al*., 2002 ; Ma *et al*., 2003 ; Yang 2003).

Amélioration des performances scolaires : Un essai à double insu avec placebo a été mené auprès de 68 adolescents en bonne santé qui se plaignaient de troubles de la mémoire : la prise quotidienne de 2 capsules de 50 microgrammes d'HUP, en deux fois, a amélioré la mémoire et l'apprentissage des participants dès le premier mois (Sun *et al*., 1999).

Epilepsie : Une étude pilote utilisant différentes doses d'HUP est en cours pour évaluer la tolérabilité et l'efficacité de l'HUP chez des patients présentant une épilepsie réfractaire aux autres traitements (Schachter *et al.,* 2009).

Myasthénie commune : Les résultats d'études cliniques chez l'Homme montrent que l'HUP A améliore les symptômes de la myasthénie. En augmentant la quantité d'ACh disponible, elle permet aux récepteurs non bloqués par les anticorps de fonctionner plus efficacement. La détérioration de la fonction musculaire peut être retardée ou stoppée [5].

Antidote des neurotoxiques organophosphorés : Lors d'une intoxication par des AChEI irréversibles tels que les neurotoxiques organophosphorés (NOP) qui peuvent être utilisés sur un champ de bataille ou dans le cadre d'une action terroriste, la mort peut survenir au cours de convulsions incontrôlables (état de mal) ou par arrêt respiratoire dû à une hypercontraction des muscles respiratoires. Cette intoxication peut être prévenue par administration d'HUP (Grunwald *et al.,* 1994 ; Lallement, 1997, 2002 ; Ricordel et Meunier, 2000 ; Zangara, 2003 ; Wang *et al*., 2006).

Différentes études ont, en effet, montré chez l'animal, que des doses faibles mais répétées d'HUP administrées avant exposition aux organophosphorés (comme le soman) évitaient les convulsions et protégeaient le tissu nerveux. En revanche, aucune donnée n'est actuellement disponible chez l'Homme [5].

L'efficacité de l'HUP serait due, au niveau périphérique, à sa sélectivité pour l'AChE érythrocytaire qui sauvegarderait la capacité scavenger de la BChE plasmatique. Son activité neuroprotectrice centrale provient du fait qu'elle franchit la BHE, et réduit la neurotransmission excitatrice glutamatergique (Lallement *et al*., 2002).

Conclusion

L'HUP est un alcaloïde naturel doté de propriétés anticholinestérasiques spécifiques, centrales et périphériques. Elle possède, en outre des propriétés neuroprotectrices multiples qui en font un candidat tout désigné pour le traitement de la maladie d'Alzheimer et de nombreuses autres pathologies neurodégénératives. Elle a de

[3] *http://www.healthy.net/scr/column.asp? Id= 281*
[4] *http://www.clinicaltrials.gov/ show/NCT00083590*
[5] *http://www.drugdigest. org/wps/PA_1_DHFHCNL218J630276FL8L614D2/pages/common/ddPrintPage.jsp*

multiples intérêts pharmacocinétiques et ne présente qu'une très faible toxicité. Elle devrait, si les essais cliniques standardisés en cours sont concluants, être rapidement utilisée en clinique.

Références bibliographiques

Ashani Y, Peggins JO III, Doctor BP (1992) Mechanism of inhibition of cholinesterases by huperzine A. *Biochem Biophys Res Commun* **184**: 719–726

Bai DL, Tang XC, He XC (2000) Huperzine A, a potential therapeutic agent for treatment of Alzheimer's disease. *Curr Med Chem* **7**: 355-374

Bialer M., Johannessen SI, Levy RH, *et al.* (2009) Progress report on new antiepileptic drugs: A summary of the Ninth Eilat Conference (EILAT IX). *Epilepsy Res* **83**: 1-43

Busciglio J, Gabuzda DH, Matsudaira P, *et al.* (1993) Generation of beta-amyloid in the secretory pathway in neuronal and nonneuronal cells. *Proc Natl Acad Sci USA* **90**: 2092-2096

Buxbaum JD, Koo EH, Greengard P (1993) Protein phosphorylation inhibits production of Alzheimer amyloid beta/A4 peptide. *Proc Natl Acad Sci USA* **90**: 9195-9198

Cervenka F, Jahodar L (2006) [Plant metabolites as nootropics and cognitives]. *Ceska Slov Farm* **55**: 219-229

Chang SY, Chen SM, Cao QL, *et al.* (2002) A clinical study of the effect of huperzine A to improve the ability of verbal recall, retention and repetition in middle-aged and elderly patients with dysmnesia. *Herald of Medicine* **21**: 263–265

Cheng DH, Ren H, Tang XC (1996) Huperzine A, a novel promising acetylcholinesterase inhibitor. *Neuroreport* **8**: 97-101

Cheng DH, Tang XC (1998) Comparative studies of huperzine A, E2020, and tacrine on behavior and cholinesterase activities. *Pharmacol Biochem Behav* **60**: 377-386

Chiu HF, Zhang M (2000) Dementia research in China. *Int J Geriatric Psychiatry* **15**: 947–953

Chu D, Liu W, Li Y, *et al.* (2006) Pharmacokinetics of huperzine A in dogs following single intravenous and oral administrations. *Planta Med* **72**: 552-555

Desilets AR, Gickas JJ, Dunican K (2009) Rôle de l'Huperzine-A dans le Traitement de la Maladie d'Alzheimer. *Ann Pharmacother* **43**: 514-518

Esch FS, Keim PS, Beattie EC, *et al.* (1990) Cleavage of amyloid beta peptide during constitutive processing of its precursor. *Science* **248**: 1122-1124

Fang CX, Guo CR, Wu B (2002) Effect of huperzine on memory of schizophrenia patients. *Sandong Arch Psychiatry* **15**: 39-40

Fayuk D, Yakel JL (2004) Regulation of nicotinic acetylcholine receptor channel function by acetylcholinesterase inhibitors in rat hippocampal CA1 interneurons. *Mol Pharmacol* **66**: 658-666

Gao P, Hui Xu, Ding HXP, *et al.* (2007) Controlled release of huperzine A from biodegradable microspheres: *In vitro* and *in vivo* studies. *Int J Pharm* **330**: 1-5

Geib SJ, Tückmantel W, Kozikowski AP (1991) Huperzine A-a potent acetylcholinesterase inhibitor of use in the treatment of Alzheimer's disease. *Acta Crystallogr* **47**: 824-827

Giacobini E, Mori F, Lai CC (1996) The effects of cholinesterase inhibitors on the secretion of APPs from rat brain cortex. *Ann NY Acad Sci* **777**: 393-398

Gordon RK, Nigam SV, Weitz JA, *et al.* (2001) The NMDA receptor ion channel: A site for binding of huperzine A. *J Appl Toxicol* **21**(suppl 1): S47-S51

Graham SH, Chen J (2001) Programmed cell death in cerebral ischemia. *J Cereb Blood Flow Metab* **21**: 99-109

Grundman M, Grundman M, Delaney P (2002) Antioxidant strategies for Alzheimer's disease. *Proc Nutr Soc* **61**: 191-202

Grunwald J, Raveh L, Doctor BP, *et al.* (1994) Huperzine A as a pretreatment candidate drug against nerve agent toxicity. *Life Sci* **54**: 991-997

Hao Z, Liu M, Liu Z, *et al.* (2009) Huperzine A for vascular dementia. *Cochrane Database Syst Rev* **2**: Art. No CD007365

Högenauer K, Baumann K, Enz A, *et al.* (2001) Synthesis and acetylcholinesterase inhibition of 5-desamino huperzine A derivatives. *Bioorg Med Chem Lett* **11**: 2627-2630

Hynd MR, Scott HL, Dodd PR (2004) Glutamate-mediated excitotoxicity and neurodegeneration in Alzheimer's disease. *Neurochem Int* **45**: 583-595

Kozikowski KR, Xia Y (1989) practical synthesis of the Chinese "nootropic" agent huperzine A: a possible lead in the treatment of Alzheimer's disease. *J Am Chem Soc* **111**: 4116-4117

Lallement G, Baille V, Baubichon D, *et al.* (2002) Review of the value of huperzine as pretreatment of organophosphate poisoning. *Neurotoxicology* **23** : 1-5

Lallement G, Veyret J, Masqueliez C, *et al.* (1997) Efficacy of huperzine in preventing soman-induced seizures, neuropathological changes and lethality. *Fundam Clin Pharmacol* **11**: 387-394

Lesné S, Ali C, Gabriel C, *et al.* (2005) NMDA receptor activation inhibits a-secretase and promotes neuronal amyloid production. *J Neurosci* **25**: 9367-9377

Li HN, Min QY (2001) Huperzine A improved the cognition of vascular dementia: a report of 30 patients in therapeutics. *Xian Dai Kang Fu* **5**: 59-63

Li J, Wu HM, Zhou RL, *et al.* (2008) Huperzine A for Alzheimer's disease. *Cochrane Database of Systematic Reviews* **2**: Art. No.: CD005592

Liang YQ, Tang XC (2004) Comparative effects of huperzine A, donezepil and rivastigmine on cortical acetylcholine level and cholinesterase activity in rats. *Neurosci Lett* **361**: 56-59

Lipton SA, Rosenberg PA (1994) Excitatory amino acids as a final common pathway for neurologic disorders. *N Engl J Med* **330**: 613-622

Little JT, Walsh S, Aisen PS (2008) An update on huperzine A as a treatment for Alzheimer's disease. *Exp Opin Invest Drugs* **17**: 209-215

Liu J, Zhang HY, Tang XC, *et al.* (1998) Effects of synthetic (-)-huperzine A on cholinesterase activities and mouse water maze performance. *Acta Pharmacol Sin* **19**: 413-416

Liu JS, Yu CM, Zhou YZ, *et al.* (1986a) Study on the chemistry of huperzine-A and huperzine-B. *Acta Chim Sin*. **44**: 1035–1040

Liu JS, Zhu YL, Yu CM, *et al.* (1986b) The structures of huperzine A and B, two new alkaloids exhibiting marked anticholinesterase activity, *Can J Chem* **64**: 837–839

Liu WH, Shou J, Tang XC (1988) Improving effect of huperzine A on discrimination performance in aged rats and adult rats with experimental cognitive impairment. *Acta Pharmacol Sin* **9**: 11-15

Liu WH, Song JL, Liu K, *et al.* (2005) Preparation and *in vitro* and *in vivo* release studies of Huperzine A loaded microspheres for the treatment of Alzheimer's disease. *J Control Release* **107**: 417-427

Lucey C, Kelly SA, Mann J (2007) A concise and convergent (formal) total synthesis of huperzine A. *Org Biomol Chem* **5**: 301-306

Ma JD, Zheng H, Wang YJ (2003) Effets of huperzine on the memory disorders of schizophrenia patients during rehabilitation period. *Health Psychol J* **11**: 340-341

Ma XQ (1997) Chemical studies on natural resources of *huperzia* and its related genera in China. *Chinese Academy of Sciences [D]*, Shanghai

Ma XQ, Gang DR (2004) The *Lycopodium* alkaloids. *Nat Prod Reports* **21**: 752–772

Ma XQ, Tan CH, Zhu D, *et al.* (2006) Survey of potential huperzine A natural resources in China: the Huperziaceae. *J Ethnopharmacol* **104**: 54–67

Ma XQ, Tan CH, Zhu D, *et al.* (2007) Huperzine A from *Huperzia* species—An ethnopharmacolgical review. *J Ethnopharmacol* **113**: 15-34

Ma YX, Zhu Y, Gu YD, *et al.* (1998) Double-blind trial of huperzine-A on cognitive deterioration in 314 cases of benign senescent forgetfulness, vascular dementia and Alzheimer's disease. *Ann NY Acad Sci* **854**: 506-507

Mazurek AA (2000) Treatment of Alzheimer's disease. New Engl J Med **342**: 821-822

Mori F, Lai CC, Fusi F, *et al.* (1995) Cholinestesrase inhibitors increase secretion of APPs in rat brain cortex. *NeuroReport* **6**: 633-636

Murphree L, Schachter S, White HS, *et al.* (2006) Antinociceptive activity of Huperzine A, an alkaloid extract of Chinese club moss (*Huperzia serrata*). *Epilepsia* **47** (Suppl): AES abstract

Nitsch RM, Slack BE, Wurtman RJ, *et al.* (1992) Release of Alzheimer amyloid precursor derivative stimulated by activation of muscarinic acetylcholine receptors. *Science* **258**: 304-307

Ortega MG, Agnese AM, Cabrera JL (2004a) Sauroine-a novel Lycopodium alkaloid from *Huperzia saururus*, *Tetrahedron Lett* **45**: 7003–7005

Ortega MG, Agnese AM, Cabrera JL (2004b) Anticholinesterase activity in an alkaloid extract of *Huperzia saururus*. *Phytomedicine* **11**: 539–543

Ortega MG, Vallejo MG, Cabrera JL, *et al.* (2006) *Huperzia saururus*, activity on synaptic transmission in the hippocampus. *J Ethnopharmacol* **104**: 374–378

Ou LY, Tang XC, Cai JX (2001). Effect of huperzine A on working memory in reserpine- or yohimbine-treated monkeys. *Eur J Pharmacol* **433**: 151-156

Pagès N, Goudey-Perrière F, Breton P (2009) Effets thérapeutiques, antidotiques, antiparasitaires et toxiques des inhibiteurs de l'acétylcholinestérase : importance des phytotoxines et de leurs dérivés. In *Toxins and Signalling,* Benoit E, Goudey-Perrière F, Marchot P, Servent D (eds) pp 85-96. SFET Publications, Châtenay-Malabry, France, Epub on http://www.sfet.asso.fr (ISSN 1760-6004)

Pang YP, Kozikowski AP (1994) Prediction of the binding sites of huperzine A in acetylcholinesterase by docking studies. *J Comput Aided Mol Des* **8**: 669–681

Peng Y, Lee DY, Jiang L, *et al.* (2007) Huperzine A regulates amyloid precursor protein processing via protein kinase C and mitogen-activated protein kinase pathways in neuroblastoma SK-N-SH cells over-expressing wild type human amyloid precursor protein 695. *Neuroscience* **150**: 386-395

Perry EK, Tomlinson BE, Blessed G, *et al.* (1978) Correlation of cholinergic abnormalities with senile plaques and mental test scores in senile dementia. *Br Med J* **2**: 1457-1459

Pi X, Liu Y, Jiang ZY, *et al.* (2004) Clinical observations on treatment of light and moderate vascular dementia with meclofenoxate plus huperzine A. *Shangai Med Pharmaceut J* **255**: 409-411

Pilotaz F, Masson P (1999) Huperzine A: an acetylcholinesterase inhibitor with high pharmacological potential. *Ann Pharm Fr* **57**: 363-373

Qian BC, Wang M, Zhou ZF, *et al.* (1995) Pharmacokinetics of tablet huperzine in six volunteers. *Acta Pharmacol Sin* **16**: 396-398

Qian L, Ji R (1989) A total synthesis of (±) Huperzine A. *Tetrahedron Lett* **30**: 2089-2090

Qu CY, Wang HM, Yu W *et al.* (1995) A pilot report on huperzine A in treating amentia in iodine-lacking area. *Shanxi Med J* **24**: 47-48

Raves ML, Harel M, Pang YP, *et al.* (1997) Structure of acetylcholinesterase complexed with the nootropic alkaloid, (-)-huperzine A. *Nat Struct Biol* **4**: 57–63

Ricordel I, Meunier J (2000) Armes chimiques : antidotes. Aperçu sur les moyens actuels, perspectives. *Ann Pharm Fr* **58**: 5-12

Sabbagh MN (2009) Drug development for Alzheimer's disease: where are we now and where are we headed? *Am J Geriatr Pharmacother* **7**: 167-185

Schachter S, White HS, Murphree L, *et al.* (2006) Anticonvulsant activity of Huperzine A, an alkaloid extract of Chinese club moss (*Huperzia serrata*), in the 6-Hz model of psychomotor seizures. http://www.aesnet.org/go/publications/aes-abstracts/abstractsearch/? Abstract 4.087

Schachter S, White HS, Stables J (2009) Huperzine A. Progress report on new antiepileptic drugs: A summary of the Ninth Eilat Conference (EILAT IX). *Epilepsy Res* **83**: in press

Skolnick AA (1997) Old Chinese herbal medicine used for fever yields possible new Alzheimer Disease therapy. *J Amer Med Assoc* **277**: 776

Sun QQ, Xu SS, Pan JL, *et al.* (1999) Huperzine-A capsules enhance memory and learning performance in 34 pairs of matched adolescent students. *Chung Kuo Yao Li Hsueh Pao* **20**: 601-603

Tamchès E., Orgogozo J.M., Wilkinson D., *et al.* (2006) ZT-1 for the Symptomatic Treatment of Mild to Moderate Alzheimer's Disease: Preliminary Results of a Multicentre, Randomised, Double-blind Placebo and Active Controlled Phase II Study. *The Alzheimer's Association,* Published by Elsevier B.V., doi:10.1016/j.jalz.2006.05.2107

Tang LL, Wang R, Tang XC (2005a) Huperzine A protects SHSY5Y neuroblastoma cells against oxidative stress damage via nerve growth factor production. *Eur J Pharmacol* **519**: 9-15

Tang LL, Wang R, Tang XC (2005b) Effects of huperzine A on secretion of nerve growth factor in cultured rat cortical astrocytes and neurite outgrowth in rat PC12 cells. *Acta Pharmacol Sin* **26**: 673-678

Tang XC (1996). Huperzine A shuangyiping: a promising drug for Alzheimer's disease. *Zhongguo Yao Li Xue Bao* **17**: 481–484

Tang XC, De Sarno P, Sugaya K, *et al.* (1989) Effect of huperzine A, a new cholinesterase inhibitor, on the central cholinergic system of the rat. *J Neurosci Res* **24**: 276-285

Tang XC, Han YF (1999) Pharmacological profile of huperzine A, a novel acetylcholinesterase inhibitor from Chinese herb. *CNS Drug Reviews* **5**: 281–300

Tang XC, Han YF, Chen XP, *et al.* (1986) Effects of huperzine A on learning and retrieval process of discrimination performance in rats. *Acta Pharmacol Sin* **7**: 507-511

Tao T, Zhao Y, Yue P, *et al*. (2006) [Preparation of huperzine A nasal in situ gel and evaluation of its brain targeting following intranasal administration]. *Yao Xue Xue Bao* **41**: 1104-1110

Vallejo MG, Ortega MG, Cabrera JL, *et al.* (2007) *Huperzia saururus* increases memory retention in rats. *J Ethnopharmacol* **111**: 685–687

Vincent XP, Rumennik L, Cumin R, *et al.* (1987) The effects of huperzine A, an acetylcholinesterase inhibitor, on the enhancement of memory in mice, rats and monkeys. *Neurosci Abstr* **13**: 844

Wang H, Tang XC (1998a) Anticholinesterase effects of huperzine A, E2020, and tacrine in rats. *Acta Pharmacol Sin* **19**: 27-30

Wang T, Tang XC (1998b) Reversal of scopolamine-induced deficits in radial maze performance by (-)-huperzine A: comparison with E2020 and tacrine. *Eur J Pharmacol* **349**: 137-142

Wang R, Tang XC (2005) Neuroprotective effects of huperzine A. A natural cholinesterase inhibitor for the treatment of Alzheimer's disease. *Neurosignals* **14**: 71-82

Wang LS, Zhou J, Shao XM, *et al.* (2003) Huperzine A attenuates cognitive deficits and brain injury after hypoxia-ischemic brain damage in neonatal rats. *Zhonghua Er Ke Za Zhi* **41**: 42-45

Wang R, Yan H, Tang XC (2006) Progress in studies of huperzine A, a natural cholinesterase inhibitor from Chinese herbal medicine. *Acta Pharmacol Sin* **27**: 1-26

Wang R, Zhang HY, Tang XC. (2001) Huperzine A attenuates cognitive dysfunction and neuronal degeneration caused by beta-amyloid protein-(1-40) in rat. *Eur J Pharmacol* **421**: 149-156

Wang RQ, Meng HY, Liu W (2002) Therapeutic effects of huperzine A complementing with 3R mental stimulation program in senile dementia patients. *Chin J Clin Rehabilitation* **6**: 2560–2561

Wang XD, Zhang JM, Yang HH, *et al.* (1999) Modulation of NMDA receptor by huperzine A in rat cerebral cortex. *Acta Pharmacol Sin* **20**: 31-35

Wang YE, Feng J, Lu WH, *et al.* (1988) [Pharmacokinetics of huperzine A in rats and mice]. *Zhongguo Yao Li Xue Bao* **9**: 193-196

Wang YE, Yue DX, Tang XC (1986) Anticholinesterase activity of huperzine A. *Acta Pharmacol Sin* **7**: 110-113

Ward J, Caprio V (2006) A radical mediated approach to the core structure of Huperzine A. *Tetrahedron Lett* **47**: 553–556

Wei YF, He JY, Song FG (2001) Observation on clinical effect of huperzine A on 50 vascular dementia patients. *Shandong Med J* **41**: 25-26

White HS, Schachter S, Lee D, *et al.* (2005) Anticonvulsant activity of Huperzine A, an alkaloid extract of Chinese club moss (*Huperzia serrata*), *Epilepsia* **46** (Suppl. 8): 220

Xiao XQ, Wang R, Tang XC (2000) Huperzine A and tacrine attenuate beta-amyloid peptide-induced oxidative injury. *J Neurosci Res* **61**: 564-569

Xiao XQ, Zhang HY, Tang XC (2002) Huperzine A attenuates amyloid beta-peptide fragment 25-35-induced apoptosis in rat cortical neurons via inhibiting reactive oxygen species formation and caspase-3 activation. *J Neurosci Res* **67**: 30-36

Xiong ZQ, Cheng DH, Tang XC (1998) Effects of huperzine A on nucleus basalis magnocellularis lesion-induced spatial working memory deficit. *Zhongguo Yao Li Xue Bao* **19**: 128-132

Xiong ZQ, Tang XC (1995) Effect of huperzine A, a novel acetylchilinesterase inhibitor, on radial maze performance in rats. *Pharmacol Biochem Behav* **51**: 415-419

Xu SS, Cai ZY, Qu ZW (1999) Huperzine A in capsules and tablets for treating patients with Alzheimer's disease. *Acta Pharmacol Sin* **20**: 486-490

Xu SS, Gao ZX, Weng Z (1995) Efficacy of tablet huperzine-A on memory, cognition, and behavior in Alzheimer's disease. *Zhongguo Yao Li Xue Bao* **16:** 391-395

Yan H, Li L, Tang XC (2007) Treating senile dementia with traditional medicine. *Clin Inter Aging* **2**: 201-208

Yang CY, Lv ZP, Zheng CG (2003) Efficacy and reliability of huperzine A in mild and moderate Alzheimer's disease. *Chin J Clin Rehabil* **7**: 4258-4259

Yang JZ (2003) Effect of huperzine A on the memory deficits of schizophrenia patients during rehabilitation period. *Chin J Clin Rehab*. **5**: 74-75

Ye JC, Zeng S, Zheng GL (2008) Pharmacokinetics of Huperzine A after transdermal and oral administration in beagle dogs. *Int J Pharm* **356**: 187-192

Ye J, Zeng S, Zhang W, *et al*. (2005) Ion-pair reverse-phase high performance liquid chromatography method for determination of Huperzine-A in beagle dog serum. *J Chromatogr B Analyt Technol Biomed Life Sci* **817**: 187-191

Ye JW, Cai JX, Wang LM (1999) Improving effects of huperzine A on spatial working memory in aged monkeys and young adult monkeys with experimental cognitive impairment. *J Pharmacol Exp Ther* **288**: 814-819

Ye JW, Shang YZ, Wang ZM (2000) Huperzine ameliorates the impaired memory of aged rats in the Morris water maze performance. *Acta Pharmacol Sin* **21**: 65-69

Yin FM, Du YY, Wang LE (2001) Analyze of intervention effect of huperzine A on vascular dementia. *Mod Rehabil* **5**: 74-75

Yu SP, Farhangrazi ZS, Ying HS (1998) Enhancement of outward potassium current may participate in beta-amyloid peptide-induced cortical neuronal death. *Neurobiol Dis* **5**: 81-88

Yue P, Tao T, Zhao Y, *et al.* (2007) Huperzine A in rat plasma and CSF following intranasal administration. *Int J Pharm* **337**: 127-132

Zangara A (2003) The psychopharmacology of huperzine A: an alkaloid with cognitive enhancing and neuroprotective properties of interest in the treatment of Alzheimer's disease. *Pharmacol Biochem Behav* **75**: 675-686

Zangara A, Edgar C, Wesnes K (2006) Reversal of Scopolamine-related Deficits in Cognitive Functions by ZT-1, a Huperzine-A Derivative, *9th International Geneva Springfield Symposium on Advanced Alzheimer Therapy,* poster accessible sur http://www.debiopharm.com/publications/debio-9902-zt-1/reversal-of-scopolamine-related-deficits-in-cognitive-functions-by-zt-1-a-huperzine-a-derivative.html

Zenghong T, Melying W (1990) Mutagenicity and comutagenicity of three nootropics: huperzine A, aniracetam and piracetam. *New drugs Clin Remed* **9**: 65-68

Zhang CL, Wang GZ (1990) Effects of huperzine A tablet on memory. *New Drugs Clin Remed*. **9**: 339-341

Zhang HY, Tang XC (2003) Huperzine A attenuates the neurotoxic effect of staurosporine in primary rat cortical neurons. *Neurosci Lett* **340**: 91-94

Zhang HY, Tang XC (2006) Neuroprotective effects of huperzine A: new therapeutic targets for neurodegenerative disease. *Trends Pharmacol Sci* **27**: 619-625

Zhang HY, Tang XC (2008) Non-cholinergiic effects of huperzine A: beyond inhibition of acetylcholinesterase. *Cell Mol Neurobiol* **28**: 173-183

Zhang HY, Zheng CY, Yan H (2008) Potential therapeutic targets of huperzine A for Alzheimer's disease and vascular dementia. *Chemico-Biological Interactions* **175**, 396-402

Zhang JH, Fan JZ, Deng AW (2002a) A clinical study of huperzine A on mild and moderate traumatic brain injury in memory and cognitive impairment. *Chin J Rehabil Med* **17**: 162–164

Zhang JM, Hu GY (2001) Huperzine A, a nootropic alkaloid, inhibits N-methyl-*D*-aspartate-induced current in rat dissociated hippocampal neurons. *Neuroscience* **105**: 663-669

Zhang RW, Tang XC, Han YY (1991) [Drug evaluation of huperzine A in the treatment of senile memory disorders]. *Acta Pharmacol Sin* **12**: 250-252

Zhang Z, Wang X, Chen Q (2002b) [Clinical efficacy and safety of huperzine Alpha in treatment of mild to moderate Alzheimer disease, a placebo-controlled, double-blind, randomized trial]. *Zhonghua Yi Xue Za Zhi* **82**: 941-944

Zhao Y, Yue P, Tao T, *et al.* (2007) Drug brain distribution following intranasal administration of Huperzine A *in situ* gel in rats. *Acta Pharmacol Sin* **28**: 273-278

Zheng CY, Zhang HY, Tang XC (2008) Huperzine A attenuates mitochondrial dysfunction after middle cerebral artery occlusion in rats. *J Neurosci Res* **86**: 2432-2440

Zhong ZG, Liang KZ (2004) Clinical observation of effect of huperzine A on 29 vascular dementia patients. *J Hainan Med Coll* **10**: 251-252

Zhou BR, Xu ZQ, Kuang YF (2004) Effectiveness of polydrug therapy for senile dementia. *Chin J Clin Rehab* **8**: 1214-1215

Zhou J, Tang XC (2002) Huperzine A attenuates apoptosis and mitochondria-dependent caspase-3 in rat cortical neurons. *FEBS Lett* **526**: 21-25

Zhu XD, Giacobini E (1995) Second generation cholinesterase inhibitors : effect of (L)-huperzine-A on cortical biogenic amines. *J Neurosci Res* **41**: 828-835

Zhu XD, Tang XC (1987) Facilitatory effects of huperzine A and B on learning and memory spatial discrimination in mice. *Acta Pharmacol Sin* **22**: 812-817

Zhu XD, Tang XC (1988) Improvement of impaired memory in mice by huperzine A and huperzine B. *Acta Pharmacol Sin* **9**: 492-497

Autres sites à consulter :

http://www.alzheimersreadingroom.com

http://www.drugdigest.org/wps/PA_1_DHFHCNL218J630276FL8L614D2/pages/common/ddPrintPage.jsp

http://www.healthy.net/scr/column.asp?Id=281

Toxines et Signalisation – Toxins and Signalling
Rencontres en Toxinologie – Meeting on Toxinology, 2009
Editions de la SFET – SFET Editions
Accès libre en ligne sur le site – Free access on line on the site : http://www.sfet.asso.fr

Characterization of new phytotoxins targeting cholinesterases : a potential therapeutic use in Alzheimer's disease ?

Nicole PAGES[1,2*], Patrick BRETON[3] , Françoise GOUDEY-PERRIERE[1]

[1] *Laboratoire de Biologie animale appliquée, Faculté de Pharmacie, 3 rue Jean-Baptiste Clément, 92296 Châtenay-Malabry ;* [2] *Laboratoire de Toxicologie, Faculté de Pharmacie, Université de Strasbourg, 67400 Illkirch ;* [3] *Centre d'études du Bouchet, 91710 Vert le Petit, France.*

** Auteur correspondant ; Fax : 33 (01) 60 19 01 31 ; Courriel : nicole.pages4@hotmail.fr*

Abstract

In traditional medicines, many plant extracts have been used to treat neurodegenerative disorders, including Alzheimer's disease (AD). With the growing importance of the disease in recent years, modern researchers have focused their in vitro *screening studies on inhibition of cholinesterases by either full extracts of plants or their components (toxins) because acetylcholinesterase inhibitors (AChEI) have been the first promising clinical approach for the treatment of AD. Plants are an exceptional source of bioactive compounds. Many plant families have demonstrated AChEI activity but animal and clinical results into protective and preventive effects of herbal drugs are rather scarce. This review describes the main naturally-occurring compounds obtained from plants which have been shown to inhibit cholinesterases, thereby displaying a potential medicinal interest. The rare studies dealing with their therapeutic efficiency and toxicity* in vivo *are also reported.*

Caractérisation de nouvelles phytotoxines ciblant les cholinestérases : une utilisation thérapeutique potentielle dans le traitement de la maladie d'Alzheimer ?

Dans la plupart des médecines traditionnelles, les extraits de plantes occupent une place de choix dans le traitement des troubles neurodégénératifs tels que la maladie d'Alzheimer (AD). Avec l'accroissement du nombre de patients atteints par cette maladie, les chercheurs modernes se sont focalisés sur la recherche in vitro *d'inhibiteurs de l'acétylcholinestérase (AChEI) extraits de ces plantes [extraits totaux ou leurs composants (toxines)] parce que les AChEI ont apporté la première lueur d'espoir sur le plan clinique. Les plantes contiennent une grande diversité de molécules pouvant se prêter au développement de nouveaux produits thérapeutiques. Beaucoup de familles ont une activité AChEI mais les recherches chez l'animal et chez l'Homme sont assez rares. Cette revue décrit une partie des composés produits par les plantes et doués de propriétés inhibitrices de l'AChE, qui présentent donc un intérêt médical potentiel. Les rares études consacrées à leur efficacité thérapeutique et leur toxicité* in vivo *sont aussi rapportées.*

Keywords : *Cholinesterase inhibitors, plant, toxins.*

Introduction

Plants are a potential source of bioactive compounds and offer a promising strategy for the treatment of neurological disorders such as Alzheimer's disease (AD). So far, AChE inhibitors (AChEI) are the most effective approach to treat the cognitive symptoms of AD and other neurodegenerative disorders (cf. Pagès *et al*., 2009a). The AChEI of first generation (physostigmine and tacrine) were banned for the treatment of AD because of their short-half-lives and/or unfavourable side-effects. Donepezil, rivastigmine and galanthamine are the only drugs currently approved in that indication but still induce undesired side effects. The most common adverse effects, related to cholinergic stimulation in the brain and peripheral tissues, include mainly gastrointestinal effects, and, less often, cardiorespiratory, extrapyramidal, genito-urinary, and musculoskeletal symptoms, as well as sleep disturbances (Thompson *et al*., 2004 ; Chattipakorn *et al*., 2007). Huperzine is now approved in China for the treatment of AD and seems well tolerated. New cholinesterase inhibitors with good safety and therapeutic profile are still needed (Birks, 2006 ; Khan *et al*., 2006 ; Nino *et al*., 2006). Plants belonging to different families (*Table 1*) have been reported to have AChEI potential (Barbosa-Filho *et al*., 2006 ; Adams *et al*., 2007 ; Mukherjee *et al*., 2007). So far, many alkaloids and various terpenoids, glycosides and coumarins have been involved in this effect (Mukherjee *et al*., 2007). Generally, plants that are used in traditional medicine are screened as full extract and their active principles are investigated thereafter. However,

for most plants and compounds that have demonstrated AChEI activity relevant to AD therapy, clinical data are very limited. Clinical efficacy and potential toxicity in large trials requires further assessment, before recommendations concerning their routine clinical use for AD and other neurodegenerative disorders can be identified (Mukherjee *et al*., 2007). Based on their traditional use in folk medicine as complex herbal formulas and their documented AChEI activity, the following plants and isolated compounds have been described according to the different plant families in alphabetical order.

Table 1. Main natural substances with strong AChEI activity detected by Ellman's reaction.

Tableau 1. *Principales substances naturelles présentant une forte activité d'AChEI (réaction d'Ellman).*

Plant	Molecules	IC50 (µM)	References
Alkaloids			
Galanthus spp. (Amaryllidaceae)	Galanthamine	1.07	Houghton *et al*., 2006
Lycoris radiata (Amaryllidaceae)	Lycoramine, Sanguinine 11-hydroxygalanthamine Assoanine Galanthamine	0.7 0.1 1.61 3.87	Lopez *et al*., 2002
Nerine bowdenii (Amaryllidaceae)	Ungeremine	0.35	Rhee *et al*., 2004
various Iberian *Narcissus* species (Amaryllidaceae)	Sanguinine 11- hydroxygalanthamine 1-O-acetyllycorine	0.10 1.61 0.96	Houghton *et al*., 2006
Tabernaemontana australis (Apocynaceae)	Coronaridine, Voacangine, Voacangine hydroxyindolenine, Rupicoline	id. galanthamine	Andrade *et al*., 2005 Pratchayakul *et al*., 2008
Tabernaemontana divaricata (Apocynaceae) roots	19,20-dihydrotabernamine 19,20-dihydroervahanine A	0.227 0.071	Ingkaninan *et al*., 2006
Sarcococca hookeriana (Buxaceae)	Sarcovagenine-C Hookerianamide-F Sarcovagine-D Many alcaloids	1.6 1.5 2.2 AChE :5.21- 22.7 BuChE 2.18-38.37	Orhan and Sener, 2003
Buxus papillosa and *B. hyrcana* (Buxaceae)	Buxamine C Other alcaloids	7.5 AChE : 83-468 BuChE : 1.1-350	Choudhary *et al*., 2006
Physostigma venenosum (Fabaceae)	Physostigmine = eserine	0.25	Houghton *et al*., 2006
Caragana chamlague (Fabaceae)	α-viniferin	2.0	Sung *et al*., 2002
Huperzia serrata (Huperziaceae) Other species	Huperzine A Huperzine B	0.023 2.0	Wang *et al*., 2006 Ma and Gang, 2004
Lycopodium (Lycopodiaceae) *Lycopodium clavatum*	Sieboldine α-onocerin	2.0 5.2	Ma and Gang, 2004 Sener and Orhan, 2005
Chelidonium majus (Papaveraceae)	8- hydroxydihydrochelerythrine, 8-hydroxydihydro-sanguinarine Berberine	AChE : 0.61 BuChE : 34.6 AChE :1.37 BuChE : 12.8 AChE :1.85 BuChE 78.9	Cho *et al*., 2006
Corydalis (Papaveraceae)	Palmatine Sanguinarine Berberine Chelidonine	5.8 0.23 0.23	Kim *et al.,* 2004 Houghton *et al*., 2006 Houghton *et al*., 2006 Houghton *et al*., 2006
Fumaria (Papaveraceae)	Ophiocarpine α-allocryptopine Berberine Ophiocarpine-N-oxide Protopine	1.1 1.3 1.6 1.79 1.8	Sener, 2002
Prosopis juliflora (Papilionaceae)	Juliflorine	AChE : 0.42 BuChE : 0.12	Houghton *et al*., 2006
Chimarrhis turbinata (Rubiaceae)	Turbinatine Desoxycordifoline	0,1 1.0	Houghton *et al*., 2006
Euodia rutaecarpa (Rutaceae)	Dehydroevodiamine	37.8	Houghton *et al*., 2006
Solanum (Solanaceae)	α-Solanine α-Chaconine	AChE : 33.8 BuChE : 0.17 AChE : 33.4 BuChE : 0.066	Nigg *et al*., 1996
Terpenoids			
Angelica acutiloba (Apiaceae) furanocoumarins	Xanthotoxin Isopimpinellin	0.58 0.32	Houghton *et al*., 2006
Salvia miltiorrhiza (Lamiaceae)	Dihydrotanshinone Cryptotanshinone	1 7.0	Houghton *et al*., 2006
Salvia fruticosa, *Salvia officinalis* var. *purpurea*, *Salvia officinalis,* *Salvia lavandulifolia*	Huiles essentielles Activité BuChE en mg/mL	BuChE : 0.05 BuChE : 0.4 BuChE : 0.03 BuChE : 0.07	Adams *et al*., 2007

Several methods for screening of AChE inhibitory activity *in vitro* from natural resources has been used based on Ellman's reactions. Moreover, spectrophotometric determination using thin-layer chromatography method has been reported to be useful. HPLC method for detection of AChE inhibition on immobilized AChE column and HPLC with on-line coupled UV–MS–biochemical detection for AChE inhibitory activity have also been reported (Mukherjee *et al*., 2007). The IC_{50} values may vary from one paper to another according to the method used to evaluate the AChEI effect and to the origin of the enzyme (Lopez *et al*., 2002 ; Mukherjee *et al*., 2007). In order to simplify the presentation, we will indicate the absolute IC_{50} values without their interval of confidence.

Some plants inhibit AChE and butyryl-ChE (BuChE), an enzyme not associated with cholinergic neurotransmission. Therefore, adverse effects associated with BuChE inhibition may occur. However, BuChE has recently been implicated in the aetiology and progression of AD (Guillozet *et al*., 1997). BuChE inhibition may therefore develop as a therapeutic target in AD (Howes *et al*., 2003).

Acanthaceae

Avicennia officinalis, a mangrove plant, which is used as folk medicine in Indian tropical countries, inhibited 50% AChE and BuChE activities *in vitro* at concentrations less than 2 mg/mL, like the standard drug Donepezil. It contains many alkaloids that might be correlated to its ChEI activities (Suganthy *et al*., 2009).

Aizoaceae

Sesuvium portulacastrum is also a mangrove plant used as folk medicine in Indian tropical countries. It has AChEI activity and a rich alkaloid content (Suganthy *et al*., 2009).

Amaranthaceae

New piperidine alkaloids, **haloxylines A** and **B** have been isolated from the chloroform soluble fraction of *Haloxylon salicornicum* and displayed antifungal and ChEI potentials (Ferheen *et al*., 2005).

Amaryllidaceae

Amaryllidaceae (genus *Leucojum*, genus *Narcissus*) were extensively studied during the last 10 years. They were used in different folk medicines for neurological conditions for a long time, perhaps Antiquity. More than 500 alkaloids have been identified in that family ; among them, 140 were tested for their AChEI properties (Zhong, 2003). It appeared that only the alkaloids belonging to the galanthamine (IC_{50} 1.07 µM) and lycorine groups exhibited AChEI activity *in vitro* (Lopez *et al*., 2002 ; Elgorashi *et al*., 2004 ; Houghton *et al*., 2006). Lycorine and galanthamine type alkaloids are phylogenetically constrained and a phylogeny of *Narcissus* can be used to predict the presence of active alkaloids in uninvestigated species (Rønsted *et al*., 2008). **Galanthamine** (CAS number 357-70-0, MW = 287.35) was initially obtained from the bulbs and flowers of Caucasian snowdrop (*Galanthus woronowii*). Later, galanthamine has been found in other Amaryllidaceae (*Lycoris radiata,* genus *Leucojum* and genus *Narcissus*). Its HBr salt was licensed as Reminyl® in the US and some European countries. It binds at the base of the active site gorge of *Torpedo californica* AChE (TcAChE), interacting with both the choline-binding site (Trp-84) and the acyl-binding pocket (Phe-288, Phe-290) (Batolucci *et al*., 2001). The hydroxyl group of the inhibitor makes a strong hydrogen bond with Glu-199 (Greenblatt *et al*., 2004). Galanthamine, a long-acting alkaloid, selective, reversible and competitive AChEI, is now approved for the treatment of AD in most developed countries (cf. Pagès *et al*., 2009a). It easily crosses the blood-brain barrier (BBB). It decreases AChE activity of the cerebral cortex, medulla oblongata, and thalamus [1]. It also stimulates nicotinic receptors, which may enhance cholinergic function and memory, which may be interesting in AD treatment. It has been reviewed previously (cf. Pagès *et al*., 2009a). **Lycoramine** (CAS number: 21133-52-8) is less active than galanthamine (Lopez *et al*., 2002). It is also present in both *Lycorus radiata* and in the *Narcissus* genus. The methiodide and hydrochloride of lycoramine derivatives were used for their AChEI peripheral effects : both salts are of equal potency on muscles but are more active than neostigmine or physostigmine (Irwin *et al*., 1961). Like galanthamine, lycoramine analogs also exert modulation of nicotinic receptors. This effect is useful in improving attentional functions, relieving pain, treating nicotine and similar addictions, treating anxiety and depression, treating and retarding the progression of Alzheimer's and Parkinson's diseases (patent WO/2001/043697).

Lycoris radiata, a chinese plant used in folk medicine, contains many alkaloids. Both galanthamine (IC_{50} 1.07) and lycoramine are AChEI. The most active alkaloids of galanthamine structural type were **sanguinine** (IC_{50} 0.1 µM) which was 10-fold more active than galanthamine, and **11-hydroxygalanthamine** (IC_{50} 1.61 µM) which showed an AChEI similar to that of galanthamine (Lopez *et al*., 2002) whereas epinorgalanthamine (IC_{50} 9.6 µM) was less potent. AChEI alkaloids of the lycorine type were assoanine (IC_{50} 3.87 µM), oxoassoanine (IC_{50} 47.21 µM) and pseudolycorine (IC_{50} 152.3 µM).

Amaryllidaceae AChEI potential was also evaluated in plant extracts. Among 26 Iberian *Narcissus* species, 2 *Pseudonarcissus* bulb extracts, *Narcissus confusus* (IC_{50} 0.05 mg dry weight of plant material per mL) and *Narcissus perez-chiscanoi* (IC_{50} 0.08 µg/mL) had strong AChEI activity. All the extracts of other *Narcissus* species with the highest AChEI activity contained galanthamine except *N. assosanus*, a lycorine type-bearing species (Lopez *et al*., 2002). In the Turkish flora, *Galanthus ikariae* and *N. tazetta* subsp. *tazetta* extracts afforded 8 Amaryllidaceae-type alkaloids responsible for AChEI activity (Orhan and Sener, 2003).

[1] *http://www.herbs-tech.com/product/lycoramine.asp*

Finally, the methanol extract of *Nerine bowdenii* showed a strong AChEI activity. The active compound was **ungeremine** (IC_{50} 0.35 µM), with stronger activity than galanthamine (IC_{50} 2.2 µM) (Rhee *et al*., 2004).

Apiaceae

Angelica archangelica has been used in traditional Chinese medicine for cerebral diseases. The crude alcohol extract of *A. archangelica* displaced nicotine binding to nicotine receptors in a concentration dependent manner and inhibited AChE *in vitro*. It is also reported to enhance blood flow (Howes *et al*., 2003). AChE inhibitory activity-guided fractionation of *A. gigas* root extract led to isolation of 12 coumarins, of which **decursinol** was the most potent *in vitro* (Kang *et al*., 2001). Three dihydrofuranocoumarins exhibited significant neuroprotective activities against glutamate-induced toxicity *in vitro.* All together, these activities could be of interest for AD treatment (Kang and Kim, 2007).

Centella asiatica leaf is an ancient Indian remedy used to strengthen nervous system and memory. Its essential oil contains monoterpenes and sesquiterpenes (bornyl acetate, α- and β-pinene, and γ-terpinene), which are known to inhibit AChE. In mice, an extract of *C. asiatica* leaf was sedative, antidepressant and showed cholinomimetic activity which was blocked by atropine. It also improved learning and memory processes in rats and modulated monoamine systems in the central nervous system (CNS) *in vivo*. Finally, the triterpene asiatic acid and its derivatives have been shown to protect cortical neurons from glutamate induced toxicity (Howes *et al*., 2003).

Apocynaceae

Tabernaemontana is a large genus including approximately 100 species which are widely distributed in tropical parts of the world. *Tabernaemontana* is one of the genera that is used in Chinese, Ayurvedic (Indian) and Thai traditional medicines for the treatment of fever, pain and dysentery (van Beek *et al*., 1984). In Thai herbal medicine, these remedies are believed to improve memory (Ingkaninan *et al*., 2003). In addition, native people in America, Africa and Continental Asia have used this plant as a central nervous system stimulant (Taesotikul *et al*., 1998 ; Chattipakorn *et al*., 2007). One of the most interesting species is *Tabernaemontana divaricata* (L.) R. Br. Ex Roem. & Schult. (synonym : *Ervatamia coronaria, Ervatamia microphylla, Ervatamia divaricata, T. coronaria*) (Pratchayasakul *et al*., 2008). Observational or behaviour screenings in rats of methanol extract from *T. divaricata* and *T pandacaqui* indicated that both have depressive effects on the CNS (Taesotikul *et al*., 1989).

***Tabernaemontana divaricata* methanolic extract (TDE) :** The higher AChEI activity was found in stem and root extracts while leaf and flower extracts gave lower activity. *In vitro* studies have shown that methanolic extracts from roots of *Tabernaemontana divaricata* inhibited more than 90% of AChE activity (Ingkaninan *et al*., 2003, 2006). These results were confirmed by Chattipakorn *et al*. (2007), who showed that TDE inhibited AChE activity (IC_{50} 2.56 µg/mL) more than BuChE activity (IC_{50} 76.95 µg/mL). The AChEI effect of TDE was ten times less potent than that of galanthamine used as reference (IC_{50} for AChE and BuChE : 0.22 ± 0.04 and 23.96 ± 9.03 µg/mL respectively). Exceptionnally, TDE gave rise to *in vivo* studies which showed in Wistar rats that, 2 hrs after intra-peritoneal (i.p.) injection, an enhanced neuronal activity (evaluated from Fos expression) was recorded in the cerebral cortex, a brain region critical for learning and memory, together with a 20% AChEI effect (at the same time point BuChE activity was undetectable, which is consistent with *in vitro* results). Consequently, the capacity of the drug to pass the BBB is low since the effects previously reported could be measured only 2 hrs after i.p. administration. The same type of response was observed 2 hrs after i.p administration of 10 mg/kg of galanthamine [AChE inhibition (28 ± 6%) ; BuChE inhibition (0.6 ± 4%)] (Chattipakorn *et al*., 2007). Noteworthy, the percentage inhibition of AChE activity in the **cerebral cortex** compared to that in controls was rather constant (17.4, 22.7 and 16.6%) whatever the dose used (250, 500 and 1000 mg/kg TDE respectively). This absence of dose-dependent AChEI effect of TDE may depend on AChE level in the brain. If the 250 mg/kg of TDE inhibits all of the AChE activity in the brain, increasing the dose of TDE should not further inhibit AChE activity. As a whole, those results suggested that TDE may not be a potent AChEI as other commercially available AChEI since their percentage inhibition in rats were evaluated 30-46%, 0.5-2 hrs after a single administration of 2.5 mg/kg of donepezil, 10 mg/kg of tacrine and 2.5 mg/kg of rivastigmine (Kosasa *et al*., 1999). TDE significantly inhibited circulating AChE 10, 30 and 60 min after administration whereas this effect disappeared after 2 hrs, a schedule which is similar to that of galanthamine. This indicates that TDE may be a short-acting and reversible agent in inhibiting AChE activity similar to galanthamine (Chattipakorn *et al*., 2007, 2008).

Recently *T. divaricata* root extract was shown to exert a neuroprotective effect on amyloid β-peptide 25-35 induced cognitive deficit in mice (Nikbakt and Sheibani, 2008). Other alkaloids of the plant could intervene in its neuroprotective effect such as ibogamine that block NMDA receptors.

***Tabernaemontana divaricata* alkaloids :** At least 66 alkaloids were extracted from *T. divaricata* (Rastogi *et al*., 1980), but only some of them showed AChEI activity. The possible cholinergic candidate alkaloids in *T. divaricata* are coronaridine, voacangine, isovoacristine, 19, 20 dihydrotabernamine, and 19, 20 dihydroervahanine A (Pratchayasakul *et al*., 2008). **19,20-dihydrotabernamine** ($C_{40}H_{50}N_4O_4$; MW 618.86) and **19,20-dihydroervahanine A** ($C_{42}H_{52}N_4O_3$; MW 676.89) were isolated from the roots. They inhibited AChE in a dose-dependent, specific, reversible and competitive manner. In addition, the compounds showed 2 fold greater inhibitory activity on AChE (IC_{50} 227 nM) than galanthamine (IC_{50} 594 nM) (Ingkaninan *et al*., 2006). **Coronaridine** ($C_{21}H_{26}N_2O_2$; MW 338.4) is an alkaloid found in the leaves, stems, barks and roots. It has also recently been shown to have a significant AChEI activity, at the same concentration as physostigmine and galanthamine *in vitro* (Pratchayakul *et al*., 2008). In addition, coronaridine has both analgesic and anti-

inflammatory activities in rats (Taesotikul *et al*., 2003) that may contribute to their potential efficiency in AD (see Pagès *et al*., 2009b). However it displayed dose-related hypotensive and bradycardial responses after IV injection in rats that might limit its therapeutic use in AD (Rastogi *et al*., 1980 ; Taesotikul *et al*., 1989). **Voacangine** is an alkaloid found in the leaves, stems, bark and roots of *T. divaricata*. It potentiated the hypnotic effects of barbiturates, had an analgesic as well as a local anesthetic activity in a mouse model (Oyukama *et al*., 1992). It dysplayed negative chronotropic and inotropic activities (Pratchayasakul *et al*., 2008). Its AChEI effect, demonstrated *in vitro* (Andrade *et al*., 2005), might explain its negative chronotropic effect *in vivo*. **Isovoacristine** induced both anti-cholinergic and antihistaminic activities on the isolated guinea pig ileum (Dagnino *et al*., 1998). Its AChEI effect is probably involved in its muscle relaxing effect and its negative chronotropic effect in both frog and rabbit (Dagnino *et al*., 1998).

***Tabernaemontana australis* chloroform extracts** *: Tabernaemontana australis* (Müell. Arg) Miers (sin *Peschiera australis*) flourishes in Brazil, Argentina, Uruguay and Paraguay. Among ten indole alkaloids isolated from the chloroform extract of stalk, only **coronaridine**, **voacangine, voacangine hydroxyindolenine** and **rupicoline** showed AChEI activity (Andrade *et al*., 2005), but no values to compare activities were reported (Houhgton *et al*., 2006).

Tabernaemontana laeta and ***T. hystrix*** extracts : Alkaloids obtained from root bark of *T. laeta* and *T. hystrix* showed AChE and BuChE inhibitory activities. The alkaloids **heyneanine** and **Nb-methylvoachalotine** selectively inhibited BuChE, **19-epi-isovoacristine** selectively inhibited AChE, whereas **olivacine, affinisine, ibogamine, affinine, conodurine** and **hystrixnine** inhibited both enzymes (Vieira *et al*., 2008).

Finally, the genus *Tabernaemontana* is especially rich in complex mixtures of monoterpenic indole alkaloids and several Brazilian native species have been chemically investigated being good candidates to furnish cholinesterase inhibitory compounds (Vieira *et al*., 2008).

Haplophyton crooksii L. Benson contains many AChEI indole alkaloids (10-methoxy-*N1*-methylpericyclivine, 16-decarbomethoxyvinervinine, crooksiine, yohimbine, ®-yohimbine, crooksidine, decarbomethoxytetrahydro-secodine, akuammicine, tubotaiwine, lanceomigine, lanceomigine *N*-oxide, haplophytine, cimicine, cimicidine and akuammidine. *In vitro*, the most active of the *H. crooksii* alkaloids is about 38 times less active than physostigmine (IC_{95} 4.8 × 10^{-6} M) (Mroue *et al*., 1996).

Asteraceae

From selected Pakistani medicinal plants, crude extracts of *Carthamus oxyacantha, Conyza bonariensis* and *Tanacetum artemisoides* were found to exhibit a low dose-dependent AChEI effect (maximum inhibition 34, 0 and 41%) and a marked BuChE inhibition (maximum 80, 68 and 79.5%) at a concentration of 1 mg/mL (Gilani *et al*., 2005). The results suggest that these extracts have marked inhibitory effects against BuChE with weaker action on AChE opening the possibility of finding other leading natural ChEI compounds (Khan *et al*., 2006).

Berberidaceae

Various species of Berberidaceae are reputed for helping age related cognitive and memory deficit. *Berberis* species, a Chinese herb contains **berberine** [also found in various *Corydalis species (*Papaveraceae*)* and *Coptis chinensis* (Ranunculaceae)] and also provides **berbamine, palmatine, isotetrandrine** and **jatrorrhizine**. **Berberine** has been more studied in the other families. **Palmatine** have strong AChEI activity. **Isotetrandrine** also found in *Stephania* species (Menispermaceae) antagonizes ileal contraction induced by histamine or acetylcholine. **Jatrorrhizine** reduces spontaneous activity of mice and prolongs the animals sleep elicited by pentobarbital ; it induces sleep in mice given subthreshold doses of pentobarbital (Dharmananda, 1996).

Boraginaceae

Isolated flavanones isolated from *Onosma hispida* have AChEI activity (Ahmad *et al*., 2003).

Buddlejaceae

From selected Pakistani medicinal plants, crude extracts of *Buddleja crispa* was found to exhibit dose dependent inhibitory effects against both AChE and BuChE (Gilani *et al*., 2005). At a concentration of 1 mg/mL, the maximum inhibitory effect against AChE was 28% and 60 % against BuChE (with IC_{50} values ranging from 0.2 to 0.4 mg/mL) (Khan *et al*., 2006).

Burseraceae

The genus *Boswelia* includes 23 species of small trees widely spread throughout the world, mainly in Arabia, on eastern cost of Africa and in India, the oleogum resins of which are used in folk medicine. The resins give by hydrodistillation, essential oils (EO) rich in monoterpenoids, which are generally weaker AChEI as compared to physostigmine (Howes *et al*., 2003). *B. socatrana* from Soqotra Island is different in that it contains mainly the diterpene verticiol (52.4%) and the sesquiterpene caryophellene (39.1%). EO AChEI activity was 59.3% at concentration of 200 µg/mL, whereas, at the same concentration, two other EO from endemic plants (*B. elongata* and *B. ameero*) were less efficient (29.6 and 41.6%). In addition, the EO had interesting antioxidant properties that could account for AD treatment (Ali *et al*., 2008).

Buxaceae

Sarcococca species are rich in steroidal alkaloids. There are four species of *Sarcococca* (*S. coriacea, S. hookeriana, S. saligna, S. wallichii*) reported from different ecological zones of Nepal (Kalauni *et al*., 2002). *S.*

saligna leaves contain 27 steroidal alkaloids of pregnene-type. The alkaloids inhibited *in vitro* both AChE (IC_{50} between 5.21- 22.7 µM) and BuChE (2.18-38.37 µM) in a dose-dependent manner (Orhan and Sener, 2003). *S. coriacea* (Hook) contains 2 steroidal alkaloids, **epoxynepapakistamine-A** and **epoxysarcovagenine-D** and two known compounds **funtumafrine C** and **N-methylfuntumine.** The compounds (except funtumarine C) inhibit in a concentration dependent fashion the activities of both AChE and BuChE (Kalauni *et al*., 2002).

Buxus hyrcana Pojark leaf extracts contain 8 alkaloids which are AChEI and BuChEI. The IC_{50} values were in the range of 83-468 µM against AChE and 1.1-350 µM against BuChE. The presence of dimethylamino moieties at C(3) and C(20) would be the most important factor influencing the activity of these compounds against the ChE enzymes (Choudhary *et al*., 2006).

Three new triterpenoid alkaloids, **buxakashmiramine**, **buxakarachiamine** and **buxahejramine** were isolated from the leaves of *Buxus papillosa* together with known bases, **cycloprotobuxine-C, cyclovirobuxeine-A, cyclomicrophylline-A** and **semperviraminol** which exhibited ChEI activity (Atta-ur-Rahman *et al*., 2001).

Combretaceae

Rangoon creeper (*Quisqualis indica*) is a tropical flowering vine up to 12 feet long. In Thai traditional medicine, seeds are used as anthelminthic. Its leaves could cure abscess and its flowers were used as food and antidiarrhea. Methanolic extract of *Q. indica* flower exhibited an AChE non competitive inhibition (Wetwitayaklung *et al*., 2007) with an IC_{50} of 0.77 µg/mL, a lower AChEI activity than physostigmine (IC_{50} 1.65 10^{-3} µg/mL). The kinetic constants obtained from Lineweaver-Burk plots suggested that the extract had low affinity for AChE. Methanolic flower extract contained many active compounds that could potentially inhibit AChE and act by a synergistic effect.

Convolvulaceae

At least seven plants known as Shankhapushpi are used in Indian system of medicine for improving memory function, including *Evolvulus alsinoides* and *E. nummularius*. Both inhibited AChE in a dose dependent manner together with radical scavenging and antioxidant effects (Nag and De, 2008).

Euphorbiaceae

Securinega suffruticosa contains many alkaloids, mainly **securinine** and its derivatives. Securinine is a CNS stimulant that antagonizes the inhibitory action of meprobamate. It inhibits cholinesterase activity, but it is weaker than galanthamine (Dharmananda, 1996). At a dose of 40 mg/kg, it significantly improved the cognitive deficits and reduced the glial inflammatory responses induced by peptide A-beta (*i.e.* neurodegeneration), in rats (Lin and Jun-Tian, 2004).

Fabaceae

Physostigma venenosum contains **physostigmine**, the first discovered alkaloid which has been a model for some semi-synthetic drugs with AChEI activity such as rivastigmine (Exelon®), neostigmine and pyridostigmine with clinical applications (see Pagès *et al*., 2009a). It inhibited AChE (G1 and G4 forms) and BuChE with similar potency. It has improved cognitive function in several *in vivo* studies (Howes *et al*., 2003). It has also shown cognitive benefits in both normal and AD patients. However, its short action duration and severe cholinergic side effects have limited its therapeutic use in AD.

A total methanolic extract of the underground parts of *Caragana chamlague* showed significant AChEI activity. Two active stilbene oligomers were isolated and inhibited AChE activity in a dose dependent manner : α-viniferin (IC_{50} 2 µM) and kobophenol A (IC_{50} 115.8 µM). The AChEI activity of α-viniferin was specific, reversible and non competitive (Sung *et al*., 2002).

Gentianaceae

The methanol extract of *Gentiana campestris* leaves exhibited significant AChEI activity. A bioactivity-guided fractionation approach revealed four AChEI xanthones, **bellidin, bellidifolin, bellidin 8-*O*-ß-glucopyranoside** and **bellidifolin 8-*O*-ß-glucopyranoside. Bellidifolin** had the same activity as galanthamine *in vitro* (Urbain *et al*., 2004).

At least seven plants known as Shankhapushpi are used in Indian system of medicine for improving memory function, including *Canscora decussata* and *C. diffusa* (Gargi and Bratati, 2008). Both inhibited AChE in a dose-dependent manner together with radical scavenging and antioxidant effects. *C. decussata* has the highest AChEI and the best antioxidant effects (Nag and De, 2008).

Huperziaceae

Huperzine A (HUP) has been traditionally used in China to alleviate memory loss, promote circulation and for fever and inflammation. It is now approved for AD treatment in China and is used in the USA as brain booster. It is a specific, reversible AChE inhibitor (IC_{50} 0.023 µM) with additional antioxidant and neuroprotective properties that cross the BBB, has an excellent bioavailability, inhibits AChE for a long time, without major side effects (Wang *et al*., 2006 ; Pagès *et al*., 2009b). It improved memory in cognitively impaired aged and adult rats. In a multi-center, double blind trial, it significantly improved memory and behaviour in AD patients (Howes *et al*., 2003). This alkaloid is present in *Huperzia serrata* and in other species of *Huperzia* and the

related genus *Lycopodium* (Lycopodiaceae) together with huperzine B and sieboldine (IC_{50} 2.0 µM) (Ma and Gang, 2004 ; Houghton *et al*., 2006).

Huperzia saururus (Lam.) Trevis is used widely in Argentine traditional medicine as an aphrodisiac and for memory improvement. An aqueous extract from the aerial parts showed a marked inhibition of AChE (IC_{50} 0.58 µg/mL).

Lamiaceae

Research into old European literature reveals that sage (*Salvia* species) had memory-improving properties that may be considered today to be relevant to the treatment of AD (Perry *et al*., 1998 ; Houghton, 2004). Cholinergic activity has been identified in both a 96% ethanolic extract and a steam-distilled essential oil (EO) of *S. officinalis* and *S. lavandulifolia*. AChE inhibition was apparent in EO from *S. officinalis* (52%) and *S. lavandulifolia* (63%) at 0.1 µl/mL and in alcoholic extracts of fresh (47%) and dried (68%) *S. officinalis* at 2 mg/mL (Perry *et al*., 1996). The IC_{50} values determined *in vitro*, for human AChE in different brain areas (cerebral cortex, striatum and cerebellum) were respectively 0.07, 0.15 and 0.18 µg/mL (Perry *et al*., 1996). EO was a more effective inhibitor of striatal AChE (50%) than BuChE (7%) at 0.1 µg/mL. Several cyclic monoterpenes were identified as the most active AChEI compounds, *in vitro* (Perry *et al*., 2000). This effect was likely due to the monoterpene **1,8-cineole** (IC_{50} 0.67 mM), with some contribution from other constituents perhaps by acting synergistically (Howes *et al*., 2003). 1,8 cineole is considerably less active than the alkaloid physostigmine (by a factor of at least 10^3). In a recent study, an 80% ethanolic extract from sage leaf exhibited dose-dependent ChEI activity which was more selective of BuChE (IC_{50} 0.054 mg/mL) than of AChE (IC_{50} 0.365 mg/mL) (Kennedy *et al*., 2006). In addition, several antioxidant compounds have been identified in both methanol and ethanol extracts and in the EO of *S. officinalis.* Anti-inflammatory effects were also reported in alcohol extracts and EO of *S. officinalis* and *S. lavandulifolia* (Howes *et al*., 2003). Finally, the extracts of both *Salvia* species were able to displace [^{3}H]-(N)-nicotine and [^{3}H]-(N)-scopolamine from nicotinic receptors and muscarinic receptors, respectively in homogenates of human cerebral cortical cell membranes (IC_{50} < 1 mg/mL) (Wake *et al*., 2000).

In vivo, oral administration of *S. lavandulifolia* once daily for 5 days to rats decreased striatal AChE activity (with doses of 20 µL) whereas a higher dose (50 µL) decreased it in both the striatum and the hippocampus as compared to controls. No changes appeared in cortex (Perry *et al*., 2002). This indicates that some components of *S. lavandulifolia* oil cross the BBB and inhibit AChE in select brain area. A study in healthy volunteers reported a number of significant effects on cognition and mood at doses of 50 µL (Howes *et al*., 2003). Clinical studies showed that AD patients (65-80 years of age) treated with a sage leaf extract experienced significant benefits in cognitive function after 16 weeks of treatment (Akhondzadeh *et al*., 2003) and in reducing anxiety (Kennedy *et al*., 2006). The side effects were generally of cholinergic type and were similar to those reported with commercially AChEI (Wake *et al*., 2000).

A new lupene triterpenetriol was isolated from the acetone extract of the aerial parts of *S. sclareoides* and characterised as **(1ß,3ß)-lup-20(29)-ene-1,3,30-triol**. In addition, **nepetidin**, **nepeticin**, **lupendiol**, **(1ß,11a)-dihydroxy-lup-20(29)-en-3-one**, **ursolic acid**, **sumaresinolic acid** and **hederagenin**, were identified in this *Salvia* species. All the acetone, ethanol, butanol and water extracts of the plant inhibited AChE activity at 10 µg/mL, whereas the standard drug rivastigmine has no AChEI activity at the same concentration. Only, the acetone extract at 1 mg/mL was able to inhibit completely BuChE activity when the butanol and ethanol extracts, at this concentration, produced a potent inhibition of BuChE (Rauter *et al*., 2007).

The dried root of *S. miltiorhiza,* a chinese herb, has been used for the treatment of cerebrovascular disease and CNS deterioration in old age for over one thousand years. Four AChE inhibitory compounds, **dihydrotanshinone, cryptotanshinone, tanshinone I** and **tanshinone IIA** were identified. The inhibitory activities of dihydrotanshinone (IC_{50} 1.0 µM) and cryptotanshinone (IC_{50} 7.0 µM) were dose-dependent. The log P values (logarithm of its partition coefficient between n-octanol and water $\log(c_{octanol}/c_{water})$ of dihydrotanshinone, cryptotanshinone, tanshinone I and tanshinone IIA were 2.4, 3.4, 4.8 and 5.8, respectively, which indicate that these compounds have potential to penetrate the BBB. This is the first example of diterpenoids as inhibitors of AChE (Ren *et al*., 2004).

Melissa officinalis (lemon balm) is also reputed to improve memory in traditional European medicine. AChE inhibition was important in two EO from *M. officinalis* (76 and 100% at 0.1 µL/mL according to the source), giving an IC_{50} value of 0.017 µg/mL (Perry *et al*., 1996). *M. officinalis* was able to displace radiolabeled agonists from nicotinic receptors and muscarinic receptors in homogenates of human cerebral cortical cell membranes (IC_{50} < 1 mg/mL) (Wake *et al*., 2000). A randomised, placebo-controlled, double-blind, balanced-crossover study investigated the acute effects on cognition and mood of a standardised extract of *M. officinalis* in twenty healthy, young participants who received single doses of 300, 600 and 900 mg of *M. officinalis* (Pharmaton) or a matching placebo at 7-day intervals. Cognitive performance was progressively improved following 600 mg of *Melissa* whereas the alertness was significantly reduced at all time points following the highest dose (Kennedy *et al*., 2002). Finally, *M. officinalis* treatment for four months improved cognitive function and reduces agitation in 42 patients with mild to moderate AD. No significant difference in the frequency of side effects appeared between treated patients and the placebo group. However the frequency of agitation was higher in the placebo group (Akhondzadeh *et al*., 2003).

The **ursolic acid** of *Origanum majorana* L. inhibited AChE activity in a dose-dependent and competitive /non-competitive type. The K_i value (representing the affinity of the enzyme and inhibitor) of *O. majorana* L. **ursolic acid** was 6 pM (tacrine 0.4 nM) and the IC_{50} value was 7.5 nM (tacrine 1 nM). Ursolic acid appears as a potent AChEI (Chung *et al*., 2001).

The genus *Otostegia* comprises *ca.* 33 species, mainly occurring in the Mediterranean region. The species of genus *Otostegia* are widely used by the traditional practitioners against various diseases, and their constituents have shown to possess anti-ulcer, antispasmodic, antidepressant, anxiolytic and sedative activities (Farooq *et al*., 2007). In Pakistan, only two species have been found, namely *O. aucheri* BOISS and *O. limbata* (BTH) BOISS. (Syn. *Ballota limbata* BTH). *O. limbata* is widely distributed in the North-West Frontier Province and lower hills of West Punjab in Pakistan. New tricyclic *cis*-clerodane type diterpenoids **limbatolide A**, **limbatolide B** and **limbatolide C** have been isolated from the roots of *O. limbata*. They displayed inhibitory potential in a concentration-dependent manner against AChE and BChE (Ahmad *et al*., 2005).

Liliaceae

Two new cevanine steroidal alkaloids, impericine and forticine along with known alkaloids were isolated from the bulbs of *Fritillaria imperialis*. These steroidal bases showed AChEI and BuChEI activities (Atta-ur-Rahman, 2002).

Lycopodiaceae

Lycopodium is a large group of 500 species that are commonly known as club mosses (Ma and Gang, 2004). Seven *Lycopodium* alkaloids have been identified : **sauroxine, 6-hydroxylycopodine, N-acetyllycodine, lycopodine, lycodine, N-methyllycodine** and **clavolonine,** some of which being probably responsible for AChEI activity [2].

From the screening of some turkish plant extracts in the genus *Lycopodium* (Orhan et Sener, 2003), a new triterpenoid AChEI was identified from *Lycopodium clavatum* : **a-onocerin.** It showed a better AChEI activity than donepezil at 1 and 3 mg/mL concentrations (IC_{50} 5.2 µM) (Sener and Orhan, 2005), but could not reach the inhibition rates of galanthamine (Orhan *et al*., 2003a, 2003b). In addition, the petroleum ether extract of *Lycopodium complanatum* L. ssp. *chamaecyparissus* (A. Br.) exhibited a remarkable activity against both AChE and BChE at 1 mg/mL (76.5 and 69.6%, respectively) (Orhan *et al*., 2009). Finally, *Lycopodium sieboldii* contains a tetracyclic alkaloid, Sieboldine A which exhibited a potent inhibitory activity against AChE and a modest cytotoxicity (Hirasawa *et al*., 2003).

Magnoliaceae

The bark of the root and stem of *Magnolia officinalis* has been used in Chinese traditional medicine to treat anxiety and nervous disturbances (Howes *et al*., 2003). Its isolated phenolic compounds, honokiol and magnolol, have been demonstrated to increase choline acetyltransferase activity, inhibit AChE, promote potassium-induced ACh release and exhibit neurotrophic function *in vitro* studies. *In vivo*, 10^{-4}-10^{-6} M of honokiol or magnolol perfused into rat hippocampus *via* a dialysis probe, markedly increased extracellular ACh release to 165 and 237% of the basal level, respectively (Hou *et al*., 2000).

Menispermaceae

The methanolic extracts from *Stephania suberosa* roots used as Thai traditional rejuvenating and neurotonic remedies had a high AChEI activity at the concentration of 0.1 mg/mL (Ingkaninan *et al*., 2003, 2006).

Olacaceae

Ptychopetalum olacoides (PO) roots used in traditional Amazonian medicine for treating various CNS diseases, including AD, possess AChEI. Its ethanol extract significantly inhibited AChE activity *in vitro* in a dose- and time-dependent manner in rat frontal cortex, hippocampus and striatum (Siqueira *et al*., 2003).

Papaveraceae

In the course of screening plants used in Danish folk medicine to treat memory dysfunction, significant AChEI activity in dose-dependent manner was observed for aqueous and methanolic extracts of *Corydalis cava*, *C. intermedia*, *C. solida* ssp. *laxa* and *C. solida* ssp. *slivenensis* (Adersen *et al*., 2006). *C. cava* is a rich source of benzylisoquinoline alkaloids and various modified molecules including **corydaline, bulbocapnine** and **corydine** (Rueffer *et al*., 1994). Corydaline inhibited AChE in a dose-dependent manner (IC_{50} 15 µM), bulbocapnine inhibited AChE (40 µM) as well as BuChE (IC_{50} 83 µM). Corydine inhibited BuChE (IC_{50} 52 µM) (Adersen *et al*., 2007). Four isoquinoline alkaloids were isolated from the methanolic extract of the aerial parts of *C. speciosa*, a Korean species : **corynoxidine, protopine, palmatine** and **berberine.** These compounds inhibited AChE with IC_{50} values of 89, 16.1, 5.8 and 3.3 µM respectively (Kim *et al.,* 2004). **Berberine** was also present in the methanol extract of Korean *Corydalis* tubers, and appeared as a reversible and specific AChEI having 90% inhibitory effect at the concentration of 2.5 µM (Hwang *et al*., 1996 ; Young *et al*., 1996). **Protopine** was also isolated from the methanolic extract of *C. ternata* tuber. It inhibited AChE activity in a specific, reversible, competitive dose-dependent manner. The concentration required for 50% inhibition was 50 µM. *In vivo*, pre-treatment of mice with protopine significantly alleviated scopolamine-induced memory impairment, in a similar way as velnacrine, a tacrine derivative (Kim *et al*., 1999).

From the genus *Fumaria* were isolated isoquinoline alkaloids and among them, **ophiocarpine** (IC_{50} 1.1 µM) which had the most potent inhibitory activity followed by a - **allocryptopine** (IC_{50} 1.3 µM), **berberine** (IC_{50} 1.6 µM), **ophiocarpine-N-oxide** (IC_{50} 1.79 µM) and **protopine** (IC_{50} 1.8 µM) (all have tetrahydro-protoberberine and protoberberine skeletons) (Sener, 2002).

[2] *http://www.find-health-articles.com/rec_pub_15500266-anticholinesterase-activity-alkaloid-extract-huperzia-saururus.htm*

Chelidonium majus has been traditionally used as an herbal medicine for treatment of gastric ulcer, gastric cancer, oral infection, liver disease and general pains in Asian and European countries. Ethanol extract of the aerial portion of *C. majus* inhibited AChE activity by 98%, at a concentration of 200 µg/mL, with no significant inhibition of BuChE (Cho *et al*., 2006). Three active compounds were isolated : **8-hydroxydihydro-chelerythrine**, **8-hydroxydihydro-sanguinarine** and **berberine** with AChEI IC_{50} (µM) values of 0.61, 1.37 and 1.85 compared with IC_{50} for BuChE of 34.6, 12.8, 78.9 respectively (Cho *et al*., 2006).

Macleaya cordata contains several alkaloids including **sanguinarine, chelerythine, protopine and allocryptopine**. Sanguinarine is an AChEI (Dharmananda, 1996).

Ranunculaceae

Coptis chinensis has been used in traditional chinese medicine for several conditions. A methanol extract of *C. chinensis* presents an AChEI activity. It contains mainly **berberine** alkaloids (cf. Berberidaceae and Papaveraceae) but also **palmatine** ($C_{21}H_{22}NO_4$, MW 387.8) and **columbamine**. **Berberine** is a benzylisoquinoline (CAS number : 633-6-9 ; $C_{20}H_{18}NO_4$; MW 371.81) with strong AChE inhibition activity (IC_{50} 0.23 µM) suggesting that quaternary nitrogen is necessary for strong activity in alkaloids possessing a benzylisoquinoline skeleton. **Palmatine** has also an AChEI activity (Howes *et al*., 2003). Four isoquinoline alkaloids isolated from *C. chinensis* have radical scavenging properties. At a 1 mM concentration, **berberrubine** (85%) showed the strongest activity, **coptisine** (79%), **berberine** (23%), and **palmatine** (22%). These effects were attributed to their ferrous ion chelating activities (Jang *et al*., 2009).

C. chinensis administered orally for 1 week improved a scopolamine induced learning and memory deficit in rats (Hsieh *et al*., 2000). The protective effects on neurodegeneration induced by aluminium overload of the total base from rhizoma *C. chinensis* and of berberine were investigated in rats. Both the total base extract and berberine significantly improved the learning and memory ability impairment and hippocampal neuronal death. They also had antioxidant, AChEI activities and MAO-B inhibiting effects. The total extract (110 mg/kg) had more powerful neuroprotective effect than berberine (Zhang *et al*., 2009). The numerous effects observed both *in vivo* and *in vitro* may be of interest in AD treatment.

Rhizophoraceae

Rhizophora lamarckii, a mangrove plant, which is used as Indian folk medicine in tropical countries, showed 50% inhibitory activity to both AChE and BChE at concentrations less than 2 mg/mL, which was comparable to the standard drug Donepezil. The presence of alkaloids in high concentration might be correlated to its ChEI activity (Suganthy *et al*., 2009).

Rosaceae

From a screening for AChEI from 180 medicinal plants, Jung and Park (2007) found that the ethyl acetate extract of the whole plants of *Agrimonia pilosa* showed significant AChE inhibition. It is a perennial plant native to Northern Asia and Eastern Europe. The genus included some fifteen species in the temperate zones of the North hemisphere. *Agrimonia pilosa* plant has long been used for medicinal purposes, in the treatment of abdominal pain, sore throat, headaches, bloody and mucoid dysentery and heat stroke. Isolation of four flavonoids with AChEI activity was performed (Jung and Park, 2007) : **tiliroside** (IC_{50} = 23.5 µM), **3-methoxy quercetin** (IC_{50} 37.9 µM), **quercitrin** (IC_{50} 66.9 µM) and **quercetin** (IC_{50} 19.8 µM) which are less effective than tacrine (IC_{50} 0.1 µM) and berberine (IC_{50} 0.7 µM).

Rubiaceae

By studying Brazilian rainforest *Chimarrhis turbinata*, Cardoso *et al*. (2004) isolated two new glucoalkaloids, **3,4-dehydro-strictosidine** and **3,4-dehydro-strictosidinic acid**, along with seven known glucoalkaloids, **cordifoline** (with a strong free-radical scavenging and antioxidant activities), **strictosidinic acid**, **strictosidine**, **5a-carboxystrictosidine**, **turbinatine**, **desoxycordifoline** and **harman-3-carboxylic acid**. Both turbinatine and desoxycordifoline were shown to be moderate AChEI at a concentration of 0.1 and 1.0 µM, respectively. In an *in vitro* rat brain assay, turbinatine showed lower activity (IC_{50} 1.86 µM), compared to the standard compound, galanthamine (IC_{50} 0.92 µM).

Rutaceae

The unripe fruit of *Evodia rutaecarpa* Bentham (syn. *Tetradium ruticarpum*) has been used frequently as a traditional medicine against inflammatory diseases in Korea, China and Japan. *E. rutaecarpa* showed a strong inhibitory effect on AChEI *in vitro* and an anti-amnesic effect *in vivo.* The active component is **dehydroevodiamine hydrochloride** (DHED). DHED inhibited AChE activity (IC50 37.8 µM) in a dose-dependent and non-competitive manner. A single administration of DHED to rats (6.25 mg/kg) significantly reversed the scopolamine-induced memory impairment in a passive avoidance test. The anti-amnesic effect of DHED was more potent than that of tacrine. This potent anti-amnesic effect of DHED was thought to be due to the combined effects of AChEI and the known cerebral blood flow enhancement (Park *et al*., 1996).

Schisandraceae

Schisandra chinensis is used in folk medicine in Japan, Korea, China and Russia. It is a wild arborescent creeper plant from the North-East of China. Pharmacological studies on animals have shown that *Schizandra* presents phyto-adaptogen properties by increasing physical working capacity and affording a stress-protective effect against a broad spectrum of harmful factors (Panossian and Wikman, 2008). In healthy subjects, *S. chinensis*

increases endurance and accuracy of movement, mental performance and working capacity. Numerous clinical trials have demonstrated the efficiency of *Schizandra* in asthenia, neuralgic and psychiatric (neurosis, psychogenic depression, astheno-depressive states, schizophrenia and alcoholism) disorders (Panossian and Wikman, 2008). A hexane-soluble extract of the fruits of *S. chinensis*, exhibited AChE inhibitory activity. Among the fourteen lignans isolated (all of them bear a dibenzocyclootene structure), the compounds having both aromatic methylenedioxy and hydroxyl groups on their cyclooctadiene ring, such as **Gomisin G** (IC_{50} 6.55 µM), **Gomisin C (**IC_{50} 6.71µM), **Gomisin D (**IC_{50}7.84 µM), schisandrol B (IC_{50} 12.57 µM) and **Gomisin A** (IC_{50} 13.28 µM) showed significant dose-dependent AChEI which were less important than the tacrine control (IC_{50} = 0.18) (Hung *et al*., 2007). These toxins cross the BBB. The determination of Michaelis-Menten constant (Km) and maximum velocity (Vmax) suggested that gomisin may bind at both the active site and an additional site of the AChE. It was shown that gomisin A may improve spatial long-term and short-term memories by enhancing the cholinergic nervous system (Hung *et al*., 2007).

Solanaceae

In general, in the Solanaceae family there has been reported many species with strong AChE inhibitory properties. *Withania somnifera* (known as Indian Ginseng), are used in Indian medicine to attenuate cerebral functional deficits, including amnesia, in geriatric patients. *W. somnifera* roots are one of the most highly regarded herbs in Indian medicine. Steroid lactones (whithanolides A-Y, glycowithanolides, dehydrowithanolide-R, whithasomniferin-A, whithasomidienone, whithasomniferols A-C, whithaferin, whitanone) have been isolated from the root and leaf. Phytosterols (sitoindosines VII-X and β-sitosterol) and many alkaloids were also isolated (Adams *et al*., 2007). *W. somnifera* roots contains three withanolides that inhibited in a concentration-dependent fashion AChE (IC_{50} 20.5-49.2 µM) and BuChE (IC_{50} 29.0-85.2 µM). Molecular docking study revealed that all the ligands are completely buried inside the aromatic gorge of AChE and lie parallel to the surface of the gorge (Choudhary *et al*., 2004). Whithanoside IV or VI produced dendritic outgrowth, whereas withanolide A produced axonal outgrowth in normal cortical neurons of isolated rat cells. Neuritic regeneration or synaptic reconstruction was induced by withanoside IV and VI in amyloid-β peptide-induced damaged cortical neurons (Adams *et al*., 2007). *In vivo*, the extract reversed ibotenic acid induced cognitive deficit and reversed the reduction in cholinergic markers, such as ACh (Schliebs *et al.*, 1997). An extract containing various steroids (Sitoindosides VII-X and withaferin-A), injected i.p. at dose of 40 mg/kg of body weight for 7 days to mice, led to differential effects on AChE activity in basal forebrain nuclei : slightly enhanced AChE activity in the lateral septum and *globus pallidus*, and reduced AChE activity in the vertical diagonal band. These changes were accompanied by enhanced M1-muscarinic receptor binding (in lateral and medial septum, and in frontal cortices), whereas the M2-muscarinic receptor binding sites were increased in cortical regions (Schliebs *et al*., 1997). The steroidal derivatives (sitoindosides IX and X) from *W. somnifera* root increased learning and memory in both young and old rats. The root extract also reversed scopolamine induced memory deficit in mice. In addition, it has also antioxidant and anti-inflammatory activities (Howes *et al*., 2003 ; Adams *et al*., 2007).

Solanum nigrum known as Morelle noire in french, is an annual plant with toxic fruits, commensal of crops and widely distributed. The plant contains the **solanine** glyco-alkaloid. Solanine is found throuhout the plant, the highest concentrations being in the unripened fruit. The molecule is soluble in water and destroyed at a temperature of about 243°C ; boiling is ineffective in decreasing the concentrations of the glycoalkaloids. It is also present in plants of the family Solanaceae such as potato, eggplanty and tomato. The level of glycoalkaloids in potato tubers may increase substantially as a result of improper handling and storage. Using the plant extracts, a crude alkaloid preparation is normally obtained with ammonia at pH >10 at 70°C. It contains two major alkaloids : α-**chaconine** ($C_{45}H_{73}NO_{14}$, MW 852.07) and α-**solanine** (CAS number : 20562-02-1; $C_{45}H_{73}NO_{15}$, MW 868.07). The proportion of each alcaloid varies widely in different potato varieties. Solanine and chaconine have the same chemical structure and are both glycosylate derivatives of the aglycone solanidine. They differ only in their sugar moieties. Solanine was used in folk medicine as sedative and anticonvulsant and was formely used in the treatment of bronchitis, epilepsy and asthma. It has also been used as an agricultural insecticide. α-**solanine** (IC_{50} 14 µM) and α-**chaconine** (IC_{50} 17 µM) have a moderate anticholinesterase action (McGehee *et al*., 2000). On an AChE of another origin, the respective IC_{50} values were 33.8 and 33.4 µM and their inhibition percentages were 26.8 and 26.3% (Bushway *et al*., 1987). In contrast both solanine and chaconine substantially inhibited BuChE activity (IC_{50} 0.17 and 0.066 µM respectively). At concentration of 2.88 µM, both glycoalkaloids reversibly inhibited human plasma BuChE by 70 and 50% respectively (Nigg *et al*., 1996). However, solanine markedly decreases spontaneaous activity in mice and prolongs the sleeping time induced by pentobarbital (Dharmananda, 1996). These adverse effects together with its toxic effects may limit its clinical use. Indeed, when ingested Solanine can induce severe signs of intoxication strongly resembling those produced by inhibition of AChE (McGehee *et al*., 2000). Symptoms which generally occur 8 to 12 hrs after ingestion, include gastrointestinal disturbances and neurological disorders. Doses of 2 to 5 mg/kg induce toxic symptoms in humans and doses of 3 to 6 mg/kg are fatal (OMS, 1992 ; Zeiger, 1998). Signs of intoxication included nausea, vomiting, stomach cramps, headaches, decrease of blood pressure, fever and dizziness. In the most severe cases, these signs are followed by neurological disturbances like vertigo, tremor, hallucination and possibly increased heart, pulse, and respiratory rates, sedation and coma.

An AChEI activity is also displayed by the methanol extracts of two species of the Colombian flora belonging to the Solanaceae family : *Solanum leucocarpum* (IC_{50} 204.59 mg/L) and *Witheringia coccoloboides* (IC_{50} 220.68 mg/L) (Niño *et al*., 2006). Their AChEI activity could be due to the presence of steroidal glycoalkaloids which are characteristic to the Solanaceae family (Roddick, 1989). The importance of the aglycone moiety structure (also found in solanine and chaconine), evidenced the fact that heterocycle nitrogen of steroidal alkaloids plays an important feature on AChE inhibition. Isolation and characterization of the phyto-compounds responsible for this biological activity remain to be done (Niño *et al*., 2006).

Conclusion

It appears that a variety of plants show various activities that may be relevant to the treatment of neurodegenerative disorders such as AD. However, all the plants with AChEI effects could not be reported in the present paper (for more informations, see Gupta and Gupta, 1997 ; Lee *et al*., 1997 ; Howes *et al*., 2003 ; Ingkaninan *et al*., 2003 ; Orhan and Sener, 2003 ; Orhan *et al*., 2004 ; Barbosa Filho *et al.,* 2006 ; Houghton *et al.,* 2006 ; Adams *et al*., 2007 ; Mukherjee *et al*., 2007 ; Vinutha *et al*., 2007). Presently, screening researches are focused on plants used in folk medicine for memory improvement. Analyses using *in vitro* experiments mainly demonstrated the ChE inhibitory activity (more or less specific for one type of enzyme) of their extracts allowing a bioactivity-guided fractionation approach of their constituents with AChEI activity. However, their ability to pass the BBB and to enhance cholinergic activity in the CNS is generally still to be investigated. Examining the great diversity of sources and isolated molecules, the research appears promising. Possibly, many molecules could be useful therapeutic agents for several neurodegenerative diseases but further detailed studies of alkaloids and other compounds *in vivo* are needed to investigate this possibility. Mainly, behavioural studies, therapeutic indices, pharmacokinetics and complete toxicological evaluation are necessary to determine their therapeutic potential. Finally, the numerous plants that may improve memory dysfunctions through other mechanisms of action than cholinergic enhancement, such as antioxidant, anti-inflammatory, anti-glutamatergic, anti-apoptotic or anti peptide A–beta were discarded from the present work but must also be kept in mind for AD treatment.

References

Adams M, Gmünder F, Hamburger M (2007) Plants traditionally used in age related brain disorders-a survey of ethnobotanical literature. *Ethnopharmacol* **113**: 363-381

Adsersen A, Gauguin B, Gudiksen L, Jäger AK (2006) Screening of plants used in Danish folk medicine to treat memory dysfunction for acetylcholinesterase inhibitory activity. *J Ethnopharmacol* **104**: 418-422

Adsersen A, Kjolbye A, Dall O, Jäger AK (2007) Acetylcholinesterase and butyrylcholinesterase inhibitory compounds from *Corydalis cava*. *J Ethnopharmacol* **113:** 179-182

Ahmad I, Anis I, Malik A, Nawaz SA, Choudhary MI (2003) Cholinesterase Inhibitory Constituents from *Onosma hispida. Chem Pharm Bull* **51**: 412-414

Ahmad VU, Khan A, Farooq U, Kousar F, Khan SS, Ahmad Nawaz S, Athar Abbasi M, Choudhary MI (2005) Three New Cholinesterase-Inhibiting *cis*-Clerodane Diterpenoids from *Otostegia limba.Chem Pharm Bull* **53**: 378-381

Akhondzadeh S, Noroozian M, Mohammadi M, Ohadinia S, Jamshidi AH, Khani M (2003) *Salvia officinalis* extract in the treatment of patients with mild to moderate Alzheimer's disease: a double blind randomized and placebo-controlled trial. *J Clin Pharm Ther* **28**: 53-59

Ali NA, Wurster M, Arnold N, Teitchert A, Schmidt J, Lindequist U, Wessjohann L (2008) Chemical composition and biological activities of essential oils from oleogum resins of three endemic soqotraen *Boswellia* species. *Rec Nat Prod* **2**: 6-12

Andrade MT, Lima JA, Pinto AC, Rezende CM, Carvalho MP, Epifanio RA (2005) Indole alkaloids from *Tabernaemontana australis* (Muell. Arg) Miers that inhibit acetylcholinesterase enzyme. *Bioorg Med Chem* **13**: 4092-4095

Atta-ur-Rahman, Akhtar MN, Choudhary MI, Tsuda Y, Sener B, Khalid A, Parvez M (2002) New steroidal alkaloids from *Fritillaria imperialis* and their cholinesterase inhibiting activities. *Chem Pharm Bull* **50**: 1013-1016

Atta-ur-Rahman, Parveen S, Khalid A, Farooq A, Choudhary MI (2001) Acetyl and butyrylcholinesterase-inhibiting triterpenoid alkaloids from *Buxus papillosa. Phytochemistry* **58**: 963-968

Barbosa-Filho JM, Paula Medeiros KC, Diniz FM, Batista LM, Athayde-Filho PF, Silva MS, da-Cunha EVL, Silva Almeida JRG, Quintans J (2006) Natural products inhibitor of the enzyme acetylcholineesterase. *Rev Bras Farmacogn* **16**: 258-285

Batolucci C, Perola E, Pilger C, Fels G, Lamba D (2001) Three-dimensional structure of a complex of galanthamine (Nivalin) with acetylcholinesterase from *Torpedo californica* : implications for the design of new anti-Alzheimer drugs. *Proteins* **42**: 182-191

Birks J (2006) Cholinesterase inhibitors for Alzheimer's disease. *Cochrane database syst. Rev*. **1** DOI: 10.1002/14651858. CD005593

Bushway RS, Savage SA, Ferguson BS (1987) Inhibition of acetylcholinesterase by solanaceous glycoalkaloids and alkaloids. *Am Potato J* **64**: 409-414

Cardoso CL, Castro-Gamboa I, Helena Siqueira Silva D, Furlan M, Epifanio R, Cunha Pinto A, Moraes de Rezende C, Alencar Lima J, da Silva Bolzani V (2004) Indole Glucoalkaloids from *Chimarrhis turbinata* and Their Evaluation as Antioxidant Agents and Acetylcholinesterase Inhibitors. *Phytomedicine J Nat Prod* **67**:1882–1885

Chattipakorn S, Pongpanparadorn A, Pratchayasakul W, Pongchaidacha A, Ingkaninan K, Chattipakorn N (2007) *Tabernaemontana divaricata* extract inhibits neuronal acetylcholinesterase activity in rats. *J Ethnopharmacol* **110**: 61-68

Chattipakorn S, Pongpanparadorn A, Pratchayasakul W, Pongchaidacha A, Ingkaninan K, Chattipakorn N (2008) *Tabernaemontana divaricata* extract inhibits neuronal acetylcholinesterase activity in rats. *Food Chem Toxicol* **46**: 2922-2927

Cho KM, Yoo ID, Kim WG (2006) 8-hydroxydihydrochelerythrine and 8-hydroxydihydrosanguinarine with a potent acetylcholinesterase inhibitory activity from *Chelidonium majus. Biol Pharm Bull* **29**: 2317-2320

Choudhary MI, Shahnaz S, Parveen S, Khalid A, Mesaik MA, Ayatollahi SA, Atta-ur-Rahman (2006) New cholinesterase inhibiting triterpenoid alkaloids from *Buxus hyrcana*. *Chem Biodivers* **3**: 1039-1052

Choudhary MI, Yousuf S, Nawas SA, Ahmed S, Atta-ur-Rahman (2004) Cholinesterase inhibiting withanolides from *Withania somnifera*. *Chem Pharm Bull* **52**: 1358-1361

Chung YK, Heo HJ, Kim EK, Kim HK, Huh TL, Lim Y, Kim SK, Shin DH (2001) Inhibitory effect of ursolic acid purified from *Origanum majorana L* on the acetylcholinesterase. *Mol Cells* **11**: 137-43

Dagnino D, Schripsema J, Verpoorte R (1998) Comparison of terpenoid indole alkaloid production and degradation in two cell lines of *Tabernaemontana divaricata. Plant Cell Rep* **13**: 95-98

Dharmananda S (1996) Alzheimer's disease: treatment with Chinese herbs. http://www.itmonline.org/arts/alzheimers.htm

Elgorashi EE, Stafford GI, van Staden J (2004) Acetylcholinesterase enzyme inhibitory effects of Amaryllidaceae alkaloids. *Planta Med* **70**: 260-262

Farooq U, Khan A, Ahmad VU, Khan SS, Kousar F, Arshad S (2007) Two New Rare-Class Tetracyclic Diterpenoids from *Otostegia limbata*. *Chem Pharm Bull* **55**: 471-473

Ferheen S, Ahmed E, Afza N, Malik A, Shah MR, Nawaz SA, Choudhary MI (2005) Haloxylines A and B, antifungal and cholinesterase inhibiting piperidine alkaloids from *Haloxylon salicornicum*. *Chem Pharm Bull* (Tokyo) **53**: 570-572

Gargi N, Bratati D (2008) Antioxidant and acetylcholinesterase inhibitory properties of the indian medicinal plant Shankhapushpi Used for Enhancing Memory Function. *J Compl Integ Med* **5**: 26

Gilani AH, Bukhari IA, Khan RA, Khan A, Ullah F, Ahmad VU (2005) Cholinomimetic and calcium channel blocking activities of *Carthamus oxyacantha*. *Phytother Res* **19**: 679-683

Greenblatt HM, Guillou C, Guenard D, Argaman A, Botti S, Badet B, Thai C, Silman I, Sussman JL (2004) The complex of a bivalent derivative of galanthamine with *Torpedo* acetylcholinesterase displays drastic deformation of the active-site gorge: implications for structure-based drug design. *J Am Chem Soc* **126**: 15405-15411

Guillozet AL, Smiley JF, Mash DC, Mesulam MM (1997) Butyrylcholinesterase in the life cycle of amyloid plaques. *Ann Neurol* **42**: 909-918

Gupta A, Gupta R (1997) A survey of plants for presence of cholinesterase activity. *Phytochemistry* **46**: 827-831

Hirasawa Y, Morita H, Shiro M, Kobayashi J (2003) Sieboldine A, a novel tetracyclic alkaloid from *Lycopodium sieboldii*, inhibiting acetylcholinesterase. *Org Lett* **5**: 3991-3993

Hou YC, Chao PD, Chen SY (2000) Honokiol and magnolol increased hippocampal acetylcholine release in freely-moving rats. *Am J Chin Med* **28**: 379-384

Houghton PJ (2004) Activity and constituents of sage relevant to the potential treatment of symptoms of Alzheimer disease. *HerbalGram* **61**: 38-53

Houghton PJ, Ren Y, Howes MJ (2006) Acetylcholinesterase inhibitors from plants and fungi. *Nat Prod Rep* **23**: 181-199

Howes MJR, Perry NSL, Houghton PJ (2003) Plants with traditional uses and activities, relevant to the management of Alzheimer's disease and other cognitive disorders. *Phytother Res* **17**: 1-18

Hsieh MT, Peng WH, Wu CR, Wang WH (2000) The ameliorating effects of the cognitive-enhancing Chinese herbs on scopolamine-induced amnesia in rats. *Phytother Res* **14**: 375-377

Hung TM, Na M, Min BS, Ngoc TM, Lee I, Zhang X, Bae K (2007) Acetylcholinesterase inhibitory effect of ligand isolated from *Shizandra chinensis*. *Arch Pharm Res* **30**: 685-690

Hwang SY, Chang YP, Byun SJ, Jeon MH, Kim YC (1996) An acetylcholinesterase inhibitor isolated from *Corydalis* tuber and its mode of action. *Korean J Pharmacogn* **27**: 91-95

Ingkaninan K, Changwijit K, Suwanboriux K (2006) Vobasinyl-iboga bisindole alkaloids, potent acetylcholinesterase inhibitors from *Tabernaemontana divaricata* root. *J Pharm Pharmacol* **58**: 847-852

Ingkaninan K, Temkitthawon P, Chuenchom K, Yuyaem T, Thongnoi W (2003) Screening for acetylcholinesterase inhibitory activity in plants used in Thai traditional rejuvenating and neurotonic remedies. *J Ethnopharmacol* **89**: 261-264

Irwin RL, Smith HJ, Hein MM (1961) The activity of certain lycoramine derivatives on muscle. *J Pharm Exper Ther* **134**: 53-59

Jang MH, Kim HY, Kang KS, Yokozawa T, Park JH (2009) Hydroxyl radical scavenging activities of isoquinoline alkaloids isolated from *Coptis chinensis*. *Arch Pharm Res* **32**: 341-345

Jung M, Park M (2007) Acetylcholinesterase inhibition by flavonoids from *Agrimonia pilosa*. *Molecules* **12**: 2130-2139

Kalauni SK, Choudhary MI, Khalid A, Manandhar MD, Shaheen F, Atta-ur-Rahman, Gewali MB (2002) New cholinesterase inhibiting steroidal alkaloids from the leaves of *Sarcococca coriacea* of Nepalese origin. *Chem Pharm Bull* (Tokyo) **50**: 1423-1426.

Kang SY, Lee KY, Sung SH, Park MJ, Kim YC (2001) Coumarins isolated from *Angelica gigas* inhibit acetylcholinesterase: structure-activity relationships. *J Nat Prod* **64**: 683-685

Kang SY, Kim YC (2007) Neuroprotective coumarins from the root of *Angelica gigas*: structure-activity relationships. *Arch Pharm Res* **30**: 1368-1373

Kennedy DO, Pace S, Haskell C, Okello EJ, Milne A, Scholey AB (2006) Effects of cholinesterase inhibiting sage (*Salvia officinalis*) on mood, anxiety and performance on a psychological stressor battery. *Neuropsychopharm* **31**: 845-852

Kennedy DO, Scholey AB, Tildesley NT, Perry EK, Wesnes KA (2002) Modulation of mood and cognitive performance following acute administration of *Melissa officinalis* (lemon balm). *Pharmacol Biochem Behav* **72**: 953-964

Khan RA, Buukhani IA, Nawaz SA, Choudhary MI (2006) Acetylcholinesterase and butyrylcholinesterase inhibitory potential of some Pakistani medicinal plants. *J Bas Appl Sci* **2**: 1-7

Kim DK, Lee KT, Baek NI, Kim S.H., Park HW, Lim JP, Shin TY, Eom DO, Yang JH, Eun JS (2004) Acetylcholinesterase inhibitors from aerial parts of *Corydalis speciosa*. *Arch Pharm Res* **27**: 1127-1131

Kim SR, Hwang SY, Jang YP, Park MJ, Markelonis GJ, Oh TH, Kim YC (1999) Protopine from *Corydalis ternata* has anticholinesterase and antiamnesic activities. *Planta Med* **65**: 218-221

Kosasa T, Kuriya Y, Yamanishi Y (1999) Effect of donepezil hydrochloride (E2020) on extracellular acetylcholine concentration in the cerebral cortex of rats. *Jpn J Pharmacol* **81**: 216-222

Lee BH, Choi BW, Ryu GS, Kang KJ, Hwang DY, Hong ND (1997) Screening of the acetylcholinesterase inhibitors from medicinal plants. *Korean J Pharmacogn* **28**: 167-173

Lin X, Jun-Tian Z (2004) Neuroprotection by D-securinine against neurotoxicity induced by beta-amyloid (25-35). *Neurol Res* **26**: 792-796

Lopez S, Bastida J, Viladomat F, Codina C (2002) Acetylcholinesterase inhibitory activity of some Amaryllidaceae alkaloids and *Narcissus* extracts. *Life Sciences* **71**: 2521-2529

Ma X, Gang DR (2004) The lycopodium alkaloids. *Nat Prod Rep* **21**: 752-772

McGehee DS, Krasowski MD, Fung DL, Wilson B, Gronert GA, Moss J (2000) Cholinesterase inhibition by potato glycoalkaloids slows mivacurium metabolism. *Anesth* **93**: 510-519

Mroue MA, Euler K L, Ghuman M A, Alam M (1996) Indole Alkaloids of *Haplophyton crooksii*. *J Nat Prod* **59**: 890-893

Mukherjee PK, Venkatesan MM, Houghton PJ (2007) Acetylcholinesterase inhibitors from plants. *Phytomed Inter J Phytother Phytopharmacol* **14**: 621-627

Nag G, De B (2008) Antioxidant and acetylcholinesterase inhibitory properties of the indian medicinal plant "shankhapushpi" used for enhancing memory function. *J Compl Integ Med* **5**: 26

Nigg HN, Romas LE, Graham EM, Sterling J, Brown S, Cornell JA (1996) Inhibition of human plasma and serum butyrylcholinesterase (E. C. 3.1.1.8) by α-chaconine and α-solanine. *Fund Appl Toxicol* **33**: 272-281

Nikbakt F, Sheibani V (2008) The neuroprotective effect of *T. divaricata* root extract on amyloid β-peptide 25-35 induced cognitive deficit in mice. 3rd FAONS symposium 2008

Nino J, Hernandez JA, Correa YM, Mosquera OM (2006) *In vitro* inhibition of acetylcholinesterase by crude plant extracts from Colombian flora. *Mem Inst Oswaldo Cruz* **101**: 783-785

OMS rapport technique 828 (1992) Evaluation de certains additifs alimentaires et de certains produits toxiques naturels

Orhan I, Ozcelik B, Aslan S, Kartal M, Karaoglu T, Sener B, Terzioglu S, Choudhary MI (2009) *In vitro* biological activity screening of *Lycopodium complanatum* L. ssp. *chamaecyparissus* (A. Br.) Doll. *Nat Prod Res* **23**: 514-526

Orhan I, Sener B (2003) Acetylcholinesterase inhibitors from natural resources. *FABAD J Pharm Sci* **28**: 51-58

Orhan I, Sener B, Choudhary MI, Khalid A (2004) Acetylcholinesterase and butyrylcholinesterase inhibitory activity of some Turkish medicinal plants. *J Ethnopharmacol* **91**: 57-60

Orhan I, Terzioglu S, Fiener B (2003a) α-Onocerin: acetylcholinesterase inhibitor from *Lycopodium clavatum* , *Planta Med* **69**: 1-3

Orhan I, Terzioglu S, Sener B (2003b) α-Onocerin: an acetylcholinesterase inhibitor from *Lycopodium clavatum. Planta Med* **69**: 265-267

Oyukama E, Gao LH, Yamazaki M (1992) Analgesic components from bornean medicinal plants, *Tabernaemontana pauciflora* Blume and *Tabernaemontana pandacaqui* Poir. *Chem Pharm Bull (Tokyo)* **40**: 2075-2079

Pagès N, Goudey-Perrière F, Breton P (2009a) Effets thérapeutiques, antidotiques, antiparasitaires et toxiques des inhibiteurs de l'acétylcholinestérase : importance des phytotoxines et de leurs dérivés. *In* Toxins and Signalling, Benoit E, Goudey-Perrière F, Marchot P, Servent D (eds) pp 85-96. SFET Publications, Châtenay-Malabry, France, Epub on http://www.sfet.asso.fr (ISSN 1760-6004)

Pagès N, Goudey-Perrière F, Breton P (2009b) L'huperzine A, un inhibiteur de l'acétychlinestérase prometteur. In *Toxins and Signalling*, Benoit E, Goudey-Perrière F, Marchot P, Servent D (eds) pp 97-108. SFET Publications, Châtenay-Malabry, France, Epub on http://www.sfet.asso.fr (ISSN 1760-6004)

Panossian A, Wikman G (2008) Pharmacology of *Schisandra chinensis* Bail: an overview of Russian research and uses in medicine. *J Ethnopharmacol* **118**: 183-212

Park CH, Kim SH, Choi W, Lee YJ, Kim JS, Kang SS, Suh YH (1996) Novel anticholinesterase and antiamnesic activities of dehydroevodiamine, a constituent of *Evodia rutaecarpa*. *Planta Med* **62**: 405-409

Patent WO/2001/043697. Analogs of galanthamine and lycoramine as modulators of nicotinic receptors

Perry EK, Pickering AT, Wang WW, Houghton PJ, Perry NSL (1998) Medical plants and Alzheimer's disease: integrating ethnobotanical and contemporary scientific evidence. *J Alt Complementary Med* **4**: 419-428

Perry N, Court G, Bidet N, Court J, Perry E (1996) European herbs with cholinergic activities: potential in dementia therapy. *Int J Geriatr Psych* **11**: 1063-1069

Perry NSL, Houghton PJ, Jenner P, Keith A, Perry EK (2002) *Salvia lavandulaefolia* essential oil inhibits cholinesterase *in vivo*. *Phytomedicine* **9**: 48-51

Perry NS, Houghton PJ, Theobald A, Jenner P, Perry EK (2000) *In-vitro* inhibition of human erythrocyte acetylcholinesterase by *Salvia lavandulaefolia* essential oil and constituent terpenes. *J Pharm Pharmacol* **52**: 895-902. Erratum in: *J Pharm Pharmacol* 2000 **52**: 203

Pratchayasakul W, Pongchaidecha A, Chattipakorn N, Chattipakorn S (2008) Ethnobotany and ethnopharmacology of *Tabernaemontana divaricata*. *Indian J Med Res* **127**: 317-335

Rastogi K, Kapil RS, Popli SP (1980) New alkaloids from *Tabernaemontana divaricata*. *Phytochem* **19**: 1209-1212

Rauter A, Branco I, Lopes Rg, Justino J, Silva F, Noronha JP, Cabrita EJ, Brouard I, Bermejo J (2007) A new lupene triterpenetriol and anticholinesterase activity of *Salvia sclareoides*. *Fitoterapia* **78**: 474-481

Ren Y, Houghton PJ, Hider RC, Howes MR (2004). Novel Diterpenoid Acetylcholinesterase Inhibitors from *Salvia miltiorhiza. Planta Med* **70**: 201-204

Rhee IK, Appels N, Hofte B, Karabatak B, Erkelens C, Stark LM, Flippin LA, Verpoorte R (2004) Isolation of the acetylcholinesterase inhibitor ungeremine from *Nerine bowdenii* by preparative HPLC coupled on-line to a flow assay system. *Biol Pharm Bull* **27**:1804-1809

Roddick JG (1989) The acetylcholinesterase inhibitory activity of steroidal glycoalkaloids and their aglycones. *Phytochemistry* **28***:* 2631-2634

Rønsted N, Savolainen V, Mølgaard P, Jâger AK (2008) Phylogenetic selection of *Narcissus* species for drug discovery. *Biochem System Ecol* **36**: 417-422

Rueffer M, Bauer W, Zenk MH (1994) The formation of corydaline and related alkaloids in *Corydalis cava in vivo* and *in vitro*. *Can J Chem* **72**: 170-175

Schliebs R, Liebmann A, Bhattacharya SK, Kumar A, Ghosal S, Bigl V (1997) Systemic administration of defined extracts from *Withania somnifera* (Indian Ginseng) and Shilajit differentially affects cholinergic but not glutamatergic and GABAergic markers in rat brain. *Neurochem Int* **30**: 181-190

Sener R (2002) Molecular diversity in the alkaloids of Turkish *Fumaria* L. species. *Acta Pharm Turc* **44**: 205-212

Sener B, Orhan I (2005) Discovery of drug candidates from some Turkish plants and conservation of biodiversity. *Pure Appl Chem* **77**: 53-64

Siqueira IR, Fochesatto C, da Silva AL, Nunes DS, Battastini AM, Netto CA, Elisabetsky E (2003) *Ptychopetalum olacoides*, a traditional Amazonian "nerve tonic", possesses anticholinesterase activity. *Pharmacol Biochem Behav* **75**: 645-650

Suganthy N, Pandian SH, Pandima Devi K (2009) Cholinesterase inhibitory effects of *Rhizophora lamarckii, Avicennia officinalis, Sesuvium portulacastrum and Suaeda monica:* Mangroves inhabiting an Indian coastal area (Vellar Estuary). *J Enzyme Inhib Med Chem* **24**: 702-707

Sung SH, Kang SY, Lee KY, Park MJ, Kim JH, Park JH, Kim YC, Kim J, Kim YC (2002) (+)-α-Viniferin, a stilbene trimer from *Caragana chamlague*, inhibits acetylcholinesterase. *Biol Pharm Bull* ***25***: 125-127

Taesotikul T, Panthong A, Kanjanapothi D, Verpoorte R, Scheffer JJ (1989) Hippocratic screening of ethanolic extracts from two *Tabernaemontana species. J Ethnopharmacol* **27**: 99-102

Taesotikul T, Panthong A, Kanjanapothi D, Verpoorte R, Scheffer JJ (1998) Neuropharmacological activities of the crude alkaloidal fraction from stems of *Tabernaemontana pandacaqui* Poir. *J Ethnopharmacol* **62**: 229-234

Taesotikul T, Panthong A, Kanjanapothi D, Verpoorte R, Scheffer JJ (2003) Anti-inflammatory, antipyretic and antinociceptive activities of *Tabernaemontana pandacaqui* Poir. *J Ethnopharmacol* **84**: 31-35

Thompson S, Lanctot KL, Herrmann N (2004) The benefits and risks associated with cholinesterase inhibitor therapy in Alzheimer's disease, *Expert Opinion on Drug Safety* **3**: 425-440

Urbain A, Marston A, Ferreira Queiroz E, Ndjoko K, Hostettmann K (2004) Xanthones from *Gentiana campestris* as New Acetylcholinesterase Inhibitors. *Planta Med* **70**: 1011-1014

Van Beek TA, Verpoorte R, Svendsen AB, Leeuwenberg AJ, Bisset NG (1984) *Tabernaemontana* L. (Apocynaceae): a review of its taxonomy, phytochemistry, ethnobotany and pharmacology. *J Ethnopharmacol* **10**: 1-156

Vieira IJ, Medeiros WL, Monnerat CS, Souza JJ, Mathias L, Braz-Filho R, Pinto AC, Sousa PM, Rezende CM, Epifanio Rde A (2008) Two fast screening methods (GC-MS and TLC-ChEI assay) for rapid evaluation of potential anticholinesterasic indole alkaloids in complex mixtures. *An Acad Bras Cienc* **80**: 419-426

Vinutha B, Prashanth D, Salma K, Sreeja SL, Pratiti D, Padmaja R, Radhika S, Amit A, Venkateshwarlu K, Deepak M (2007) Screening of selected Indian medicinal plants for acetylcholinesterase inhibitory activity. *J Ethnopharmacol* **109**: 359-363

Wake G, Court J, Pickering A, Lewis R, Wilkins R, Perry E (2000) CNS acetylcholine receptor activity in European medicinal plants traditionally used to improve failing memory. *J Ethnopharmacol* **69**: 105-114

Wang R, Yan H, Tang XC (2006) Progress in studies of huperzine A, a natural cholinesterase inhibitor from Chinese herbal medicine. *Acta Pharmacol Sin* **27**: 1-26

Wetwitayaklung P, Limmatvapirat C, Phaechamud T, Keokitichai S (2007) Kinetics of acetylcholinesterase inhibition of *Quisqualis indica* Linn. Flower extract. *Silpakorn Sci Tech J* **2**: 20-28

Young HS, Pyo CY, Jung BS, Hee JM, Choong KY (1996) An acetylcholinesterase inhibitor isolated from *Corydalis* tuber and its mode of action. *Saengyak Hakhoechi* **27**: 91-95

Zeiger E (1998) Alpha-chaconine and alpha-solanine, review of toxicological literature. *Testing Status of Agents at NTP (National Toxicology Program)*

Zhang J, Yang JQ, He BC, Zhou QX, Yu HR, Tang Y, Liu BZ (2009) Berberine and total base from rhizoma *Coptis chinensis* attenuate brain injury in an aluminum-induced rat model of neurodegenerative disease. *Saudi Med J* **30**: 760-766

Zhong J (2003) Amaryllidaceae and *Sceletium* alkaloids. *Nat Prod Rep* **20**: 606–614

Toxines et Signalisation – Toxins and Signalling
Rencontres en Toxinologie – Meeting on Toxinology, 2009
Editions de la SFET – SFET Editions
Accès libre en ligne sur le site – Free access on line on the site : http ://www.sfet.asso.fr

A non-invasive method to appraise time-dependent effects of toxins on the mouse neuromuscular excitability in vivo*, and its clinical applications*

Delphine BOERIO-GUEGUEN[1,2*], Jean-Pascal LEFAUCHEUR[2,3], Alain CREANGE[2,4], Evelyne BENOIT[1]

[1] *CNRS, Institut de Neurobiologie Alfred Fessard - FRC2118, Laboratoire de Neurobiologie Cellulaire et Moléculaire - UPR9040, 91198 Gif sur Yvette cedex ;* [2] *EA 4391 Excitabilité Nerveuse et Thérapeutique, Faculté de Médecine Créteil - Paris XII, 8 rue du Général Sarrail, 94010 Créteil cedex ;* [3] *Service de Physiologie - Explorations Fonctionnelles, Hôpital Henri Mondor, Assistance Publique - Hôpitaux de Paris, 51 avenue de Lattre de Tassigny, 94010 Créteil cedex ;* [4] *Service de Neurologie, Hôpital Henri Mondor, Assistance Publique - Hôpitaux de Paris, 51 avenue de Lattre de Tassigny, 94010 Créteil cedex, France*

** Corresponding author ; Tel : +33 (0)1 69 82 36 52 ; Fax : +33 (0)1 69 82 41 41 ;*
E-mail : boerio@nbcm.cnrs-gif.fr

Abstract

The conventional methods, usually performed in vivo*, provide limited information regarding neuromuscular excitability properties. In the present paper, we review the new non-invasive methods that have been improved to supplement the conventional electrophysiological methods. In particular, the automated sequence of multiple excitability tests developed by Professor Bostock (Qtrac©, Institute of Neurology, London, UK) to assess neuromuscular excitability in clinical neurophysiology, and its application to mouse models* in vivo*, are emphasized. Finally, we show that the efficiency of a substance injection (exemplified by means of the local anaesthetic lidocaine) renders the use of this method particularly appropriated for long-term follow-up of the effects of sub-lethal doses of a given toxin, in mice* in vivo*, which will help to a better characterization of toxin action on the neuromuscular excitability properties.*

Une méthode non invasive pour appréhender, in vivo*, les effets de toxines en fonction du temps sur l'excitabilité neuromusculaire chez la souris, et ses applications cliniques*

Les méthodes conventionnelles habituellement appliquées in vivo *ne donnent que peu d'informations relatives à l'excitabilité neuromusculaire. Dans cet article, nous présentons une synthèse des nouvelles méthodes non invasives qui ont été proposées pour accompagner les méthodes électrophysiologiques conventionnelles. Nous décrivons plus particulièrement la séquence automatique d'évaluation multiple de l'excitabilité développée par le Professeur Bostock (Qtrac©, Institute of Neurology, London, UK) pour caractériser l'excitabilité neuromusculaire en neurophysiologie clinique, puis adaptée à des modèles murins* in vivo*. Finalement, nous montrons que l'efficacité d'injection d'une substance (en prenant comme exemple la lidocaïne, un anesthésique local) rend l'utilisation de cette méthode particulièrement appropriée pour le suivi à long terme des effets de doses sub-létales d'une toxine donnée, chez la souris* in vivo*, ce qui permettra une meilleure caractérisation de l'action de toxines sur les propriétés d'excitabilité neuromusculaire.*

Keywords : *Long-term follow-up toxicity in mice, clinical applications,* in vivo *electrophysiology, neuromuscular system, membrane potential, ion channels, electrogenic pumps.*

Introduction

In the neuromuscular system, the impulse conduction relies on ion exchange processes through the membranes and, thus, is highly dependent on membrane potential and on the functional status of ion channels and/or electrogenic pumps. However, the conventional methods usually performed *in vivo* provide limited information regarding excitability properties in the neuromuscular system. Therefore, new non-invasive methods, involving a multimodal evaluation of ion transporters and membrane properties of the neuromuscular system, have been improved to supplement the conventional electrophysiological methods. In particular, an automated sequence of multiple excitability tests has been developed by Professor Bostock (Qtrac©, Institute of Neurology, London, UK) to appraise neuromuscular excitability in clinical neurophysiology (Kiernan *et al.*, 2000 ; Kuwabara *et al.*, 2000 ; Krishnan *et al.*, 2004), and was successfully used for studying changes in peripheral nerve excitability properties under various disease conditions

(Bostock *et al.*, 1995 ; Kuwabara *et al.*, 2002 ; Nodera *et al.*, 2004). It has been applied to animal studies first in rat (Yang *et al.*, 2000 ; George and Bostock, 2007 ; Maurer *et al.*, 2007), and recently a method has been developed for long-term follow-up in mouse (Boërio *et al.*, 2009a).

In the present paper, we review these new non-invasive methods and their applications in clinical neurophysiology and animal models. Finally, we demonstrate their efficiency to appraise the effects of a substance injection (exemplified by means of the local anaesthetic lidocaine).

Conventional electrophysiological methods

Standard electrophysiological methods rely, on the one hand, on detection studies by means of indwelling electromyography (EMG) to characterize motor units activity. On the other hand, conduction studies imply the stimulation of a nerve trunk and the recording of the innervated muscle by means of surface electrodes. The examinations of conduction velocity, distal latencies and compound muscle action potential (CMAP) amplitude allow the identification of a process of demyelination, axonal loss or conduction block. Nevertheless, these evaluations provide limited information regarding axonal excitability. Furthermore, a reduction of conduction velocity may not only underlie a demyelination process but could also imply morphological abnormalities (such as reduction of the internodal distances or smaller axonal size) and functional impairments (such as alteration of the membrane potential or blockade of sodium channels). Therefore, new methods have been developed to explore the underlying mechanisms such as membrane potential and ion exchange processes (ion channels and electrogenic pumps), involved in neuromuscular excitability.

New non-invasive electrophysiological methods

Several methods have been developed to explore neuromuscular excitability. Each one provides complementary information regarding excitability properties, and a multimodal evaluation is thus of great interest (Kiernan and Bostock, 2000 ; Lefaucheur *et al.*, 2006). This multimodal evaluation has been facilitated by the development of the computer assisted process : Qtrac© protocol, written and continually improved by Professor Hugh Bostock (see for review, Bostock *et al.*, 1998). The principle relies on the threshold tracking techniques which consists in tracking the threshold changes to evoke a target potential equal to 40% of maximal amplitude, depending on the various conditions applied (different intensities, pulse durations and subthreshold polarizing currents).

The different tests, the physiological mechanisms underlined and the parameters specially issued from the Qtrac© program are detailed below. The configuration implies the stimulation of a motor nerve and the recording of a CMAP from the muscle and, thereby, involves the peripheral nerve, the neuromuscular junction and the muscle itself. It is therefore legitimate to characterize this method as a neuromuscular evaluation. Nevertheless, it is worth noting that most excitability tests, in particular the electrotonus, the current-threshold relationship, the strength-duration properties and the superexcitability explained below, allow more specifically to infer about axonal membrane properties (see for review, Krishnan *et al.*, 2008). Although the present manuscript focuses on motor nerve exploration, similar procedure can be transferred to explore cutaneous afferents.

Stimulus-response curve

First introduced by Tom Brismar (1985), the stimulus-response curve is established with respect to threshold intensities required to evoke a CMAP of target amplitude from 10% (i_{10}) to 90% (i_{90}) of maximal CMAP amplitude (CMAPmax), by 10% increasing steps. Two pulse durations are currently applied : 0.2 and 1 ms. Most often, threshold intensity to evoke a CMAP equal to 50% CMAPmax : i_{50} (Kiernan *et al.*, 2000) and intensity ratios (Brismar, 1985 ; Boërio *et al.*, 2008) are retained for analysis. As Qtrac© is concerned, threshold intensity (i_{50}) is mostly observed. This later parameter is a hallmark of mean threshold intensity and provides information regarding nodal properties, while intensity ratios allow inferring about internodal properties.

Strength-duration curve

The purpose of this second test is to determine the threshold intensity required to evoke a target CMAP, depending on the pulse duration of the applied current. Longer current durations involve smaller intensities. Two parameters are basically derived from the strength-duration relationship : the strength-duration time constant (τ) and the rheobase. Both are highly dependent on membrane potential and also regulated by persistent sodium currents (Bostock and Rothwell, 1997). Under a threshold tracking recording, strength-duration time constant and rheobase are determined from the charge-duration relationship. Strength-duration time constant is given by the negative intercept on the x-axis and the rheobase by the slope.

Recovery cycle

The recovery cycle is defined by consecutive excitability changes induced by impulse conduction. Immediately after an action potential, peripheral nerve axons become unexcitable, owing to inactivation of transient sodium channels. This refractory period is first total, so the axons cannot generate another action potential, whatever the membrane solicitation. Next, the axons pass into the relative refractory period, due to gradual recovery of sodium channel inactivation. Thus, a stronger than normal depolarizing stimulus is required to generate an action potential. Afterwards, a period of increased excitability occurs. This supernormal period corresponds to a post-potential depolarization and is limited by fast paranodal potassium channels (Kiernan *et al.*, 1996). Finally, a prolonged period of reduced excitability, the so-called late subnormal period, takes place. This later period is more specifically regulated by nodal and internodal slow potassium channels

(Lefaucheur *et al.*, 2006). Resting excitability level is recovered between 100 and 200 ms after the initial impulse (Kuwabara *et al.*, 2000).

Various protocols have been developed to explore the recovery cycle (see for review, Boërio *et al.*, 2004). Under threshold tracking procedure, sub-maximal paired pulses are applied with progressively reduced interpulse intervals. Refractoriness and late subnormal period are expressed by an increase in the threshold to evoke the target CMAP. The refractoriness is generally estimated for 2 and 2.5 ms interpulse intervals (Bostock *et al.*, 1998 ; Krishnan and Kiernan, 2005). The superexcitability is expressed by a reduction of threshold and usually estimated at 7 ms interpulse interval, when it is known to be maximal (Kiernan *et al.*, 1996).

The next two evaluations are exclusively performed under the threshold tracking techniques.

Threshold electrotonus

The electrotonus is a combination of long-lasting, subthreshold, depolarizing or hyperpolarizing current and a single test pulse, applied at different time points along the 100 ms polarizing current. Indeed, the polarizing current induces changes in the membrane potential and the accommodation properties of the axonal membrane are highlighted by threshold changes to evoke the target single CMAP. The electrotonus is an indicator of membrane potential and allows more particularly inferring about internodal properties of the axonal membrane (Bostock *et al.*, 1998). The polarizing current induces initial, immediate threshold changes due to excitability changes at the node of Ranvier. Then, the current spreads towards the internode and consecutive phases (the so-called early and late electrotonus) are characterized. As a depolarizing current is applied, threshold changes more particularly emphasize the activity of slow potassium channels whereas slow persistent sodium channels and inward rectifier potassium channels are involved in response to hyperpolarizing currents. In particular, the inward rectifier channels are only activated when strong negative currents are applied, to prevent hyperpolarization.

Current-threshold relationship

The current-threshold relationship is complementary to the electrotonus. In this case, the polarizing current lasts for 200 ms and the single pulse is always delivered after the long-lasting current. The polarizing current is gradually increased from 50% depolarizing to 100% hyperpolarizing of the unconditioned threshold by 10% increasing steps. It reflects the rectifying properties of the axon. The outward rectification, more specifically involved when a depolarizing current is applied, results from the activity of fast and slow potassium channels while the inward rectification, involved when a hyperpolarizing current is applied, represents the accommodation due to inward rectifier potassium channels that are activated for strong negative currents, as aforementioned (Krishnan *et al.*, 2008).

Threshold intensities and the various parameters involved in axonal excitability are prone to be influenced by various pathophysiological phenomena, either functional or morphological.

Clinical neurophysiology

Applications to clinical neurophysiology were mostly explored in dysimmune peripheral neuropathies (see for review, Lefaucheur *et al.*, 2006) and in toxic neuropathies (Krishnan *et al.*, 2005 ; Ng *et al.*, 2007). Furthermore, few applications were reported in patients with motor neuron diseases (Bostock *et al.*, 1995 ; Kanai *et al.*, 2006 ; Vucic and Kiernan, 2006 ; Vucic and Kiernan, 2007), with demyelinating diseases of the central nervous system (Boërio *et al.*, 2007a ; Misawa *et al.*, 2008) and, finally, with muscular disorders (Krishnan and Kiernan, 2006 ; Boërio *et al.*, 2007b). Most results are summarized in *Table 1*.

Animal studies

Threshold tracking techniques have also been adapted to animal models, initially in rats *in vivo* (Yang *et al.*, 2000 ; George and Bostock, 2007) and *in vitro* (Maurer *et al.*, 2007) and, more recently, in mice using indwelling (Moldovovan and Krarup, 2006) or surface electrodes (Susuki *et al.*, 2007 ; Sawai *et al.*, 2008) for the stimulation. Considering the potential interest of mouse models in various disease conditions, a minimally invasive method has been recently adapted to assess peripheral nerve excitability in mouse models and was found suitable for repeated recordings from the same animal, which makes it a promising tool to appraise the progression along disease course and also the effects of a given treatment in animal models *in vivo* (Boërio *et al.*, 2009a).

Methodology

Excitability properties are usually recorded under inhalated anesthesia, using isoflurane. The stimulation are delivered on a motor nerve by means of surface electrodes, and the CMAP are recorded using needle electrodes inserted into the innervated muscle. Two paradigms were presented by Boërio and colleagues : (i) the caudal motor nerve was stimulated at the base of the mouse tail, and CMAP recorded from the tail muscle (*Figure 1*), and (ii) the evaluation was performed by stimulating the tibial branch of the sciatic nerve above the ankle and recording the CMAP from the plantar muscles (Boërio *et al.*, 2009a).

As in human studies, the multiple excitability program includes the recording of stimulus-response, strength-duration and current-threshold relationships, as well as threshold electrotonus and recovery cycle.

The effects of maturation (from juvenile to young adults) highlight the importance of careful age-matching between wild-type (WT) and diseased mice, especially in younger animals. A previous study

reveals that most excitability properties have stabilized in 13 and 14 week-old animals. In addition, this evaluation, repeated up to eight times from the same animal, showed satisfactory reproducibility and no side effects either from the repetitive anesthesia or needle insertions (Boërio *et al.*, 2009a).

Table 1. Excitability properties in various diseases.

Tableau 1. *Propriétés d'excitabilité dans diverses pathologies.*

Pathology	Stimulus-Response	Strength-Duration	Electrotonus	Current-Threshold	Recovery Cycle	Underlying mechanisms	Reference
MS					PR ↑ SN ↓	Alteration of the myelin sheath	Boërio et al. (2007a)
ALS		SDTC ↑	Fanning out		SN ↑	↑ Na conductance ↓ K conductance	Kanai et al. (2006) Vucic and Kiernan (2006)
Kennedy		SDTC ↑	Fanning out	Hyperpol ↑		Membrane Hyperpolarization	Vucic and Kiernan (2007)
CMT1A		Normal	Fanning out		RP ↓ SN ↓	↑ Fast K conductance	Nodera et al. (2004)
MMN	Slope ↑ I_{50} ↑	Rheobase ↑	Fanning out		PR ↓ SN ↑	Axonal Hyperpolarization next to blocks	Kiernan et al. (2002)
CIDP		SDTC ↓	Normal		RP, SN, SbN ↓	Morphological abnormalities	Cappelen-Smith et al. (2001)
AIDP	Normal	Normal	Normal		Normal	Normal	Kuwabara et al. (2002)
AMAN	Slope ↓ I_{50} ↑	Normal	Normal		Refractoriness ↑	Sodium channels dysfunction	Kuwabara et al. (2002)
Diabetic Np		SDTC ↓	Fanning in		RP, SN, SbN ↓	Na/K electrogenic pump dysfunction	Kiernan and Krishnan (2005)
Uremic Np		SDTC ↑	Fanning in		RP ↑ SN, SbN ↓	Membrane Depolarization	Krishnan et al. (2005)
Hepatic Failure	Normal	Normal	Fanning in		SN ↓	Membrane Depolarization	Ng et al. (2007)
Myotonic Dystrophy					PR ↑ SN ↓	Membrane Depolarization	Boërio et al. (2007b)
Critical illness Neuropathy		Normal	Fanning in		RP ↑ SN, SbN ↓	Membrane Depolarization	Z'Graggen et al. (2006)

MS : multiple sclerosis ; ALS : amyotrophic lateral sclerosis ; CMT1A : Charcot-Marie Tooth type 1A ; MMN : multifocal motor neuropathy with conduction block ; CIDP : chronic inflammatory demyelinating polyneuropathy ; AIDP : acute inflammatory demyelinating polyneuropathy ; AMAN : acute motor axonal neuropathy ; Np : neuropathy ; RP : refractory period ; SN : supernormality ; SbN : late subnormal period ; Fanning in : smaller threshold changes in response to polarizing currents ; Fanning out : greater changes in response to polarizing currents.

MS : sclérose en plaques ; ALS : sclérose latérale amyotrophique; CMT1A : Charcot-Marie Tooth de type 1A ; MMN : neuropathie motrice avec blocs de conduction; CIDP : polyradiculonévrite chronique; AIDP : Guillain-Barré démyélinisant ; AMAN : Guillain-Barré axonal ; Np : neuropathie ; RP : période réfractaire ; SN : supernormalité ; SbN : sous-normalité tardive ; Fanning in : réduction des fluctuations de seuil en réponse aux courants polarisants ; Fanning out : majoration des fluctuations de seuil en réponse aux courants polarisants.

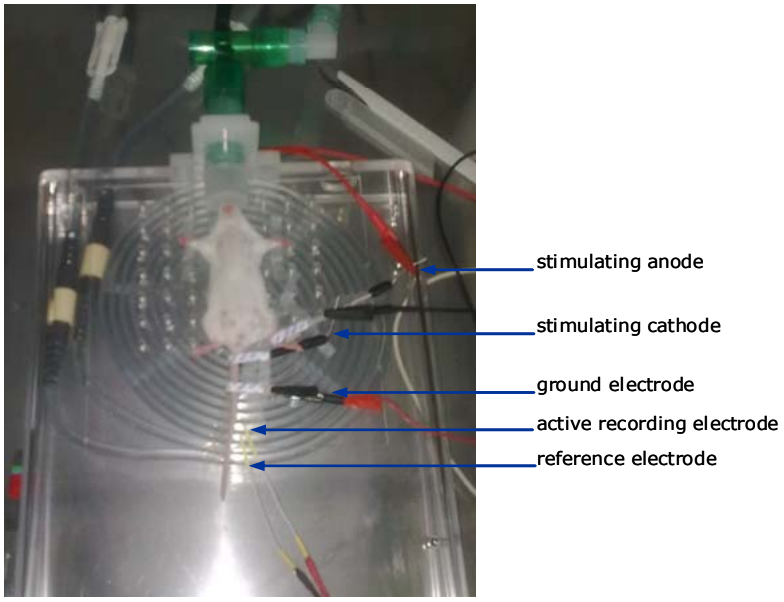

Fig. 1. Assessment of neuromuscular excitability in a mouse *in vivo* by stimulating the caudal motor nerve and recording CMAP from the tail muscle. Cathode stimulating electrode being located at the base of the tail and the anode on the rear leg. Recording electrodes are inserted in the tail muscle.

Fig. 1. *Enregistrement de l'excitabilité neuromusculaire à partir de la région caudale chez la souris* in vivo. *L'électrode de stimulation active est placée à la base de la queue de la souris et la référence au niveau de la cheville. Les électrodes de recueil sont insérées dans le muscle caudal.*

We recently performed recordings from 34 WT Swiss female mice, using the Qtrac© program, to investigate the reproducibility of excitability waveforms between different animals (*Figure 2*).

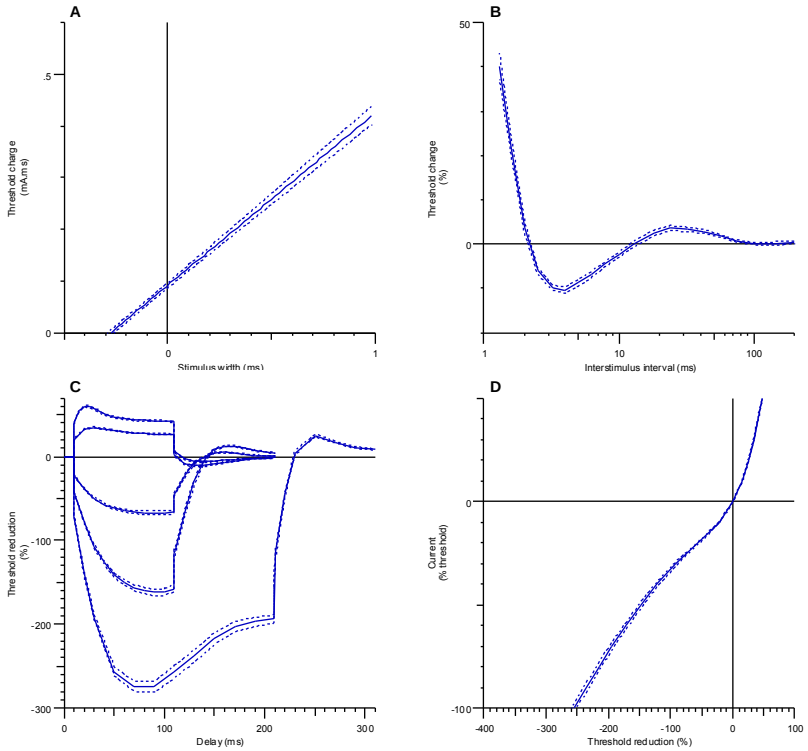

Fig. 2. Excitability waveforms recorded from the mouse caudal area *in vivo*, by means of the Qtrac© program. Means ± SEM of 34 mice.

Fig. 2. *Courbes d'excitabilité enregistrées à partir de la région caudale de souris* in vivo, *au moyen du logiciel Qtrac©. Moyennes ± ESM de 34 souris.*

The charge-duration relationship (*Figure 2A*) brings strength-duration time constant and rheobase estimates. The recovery cycle (*Figure 2B*) provides the refractory, supernormal and late subnormal periods. Threshold electrotonus and current-threshold relationship are illustrated in *Figures 2C* and *2D*, respectively. It is worth noting that, on the electrotonus, the five waveforms display excitability changes with respect to polarizing currents : from depolarizing current at 40% (upper trace) and 20% to hyperpolarizing currents at 20%, 40% and at last 70% (bottom) of the unconditioned threshold. It is clear that a great homogeneity of recordings occurs from the different animals.

Effects of disease conditions in mouse models

Only few studies reported in the literature explored excitability properties in mouse models of neurological diseases (Susuki *et al.*, 2007 ; Boërio *et al.*, 2009b), and long-term follow-up from the same animal cohort was documented only once. Repeated recordings were performed to appraise the progression along disease course (*i.e.* from 4 to 19 weeks of age) in the $SOD1^{G93A}$ mouse model of amyotrophic lateral sclerosis. As early as 8 weeks (a pre-symptomatic stage of disease), the $SOD1^{G93A}$ mice provided evidence of nerve excitability impairments consistent with a modest depolarization of the axonal membrane (Boërio *et al.*, 2009b).

Effects of toxin injection

In order to apply the multiple excitability method to the studies of the effects of toxin injection on the mouse neuromuscular excitability properties, *in vivo*, we have investigated the efficiency of a substance injection using lidocaine, a local anaesthetic well-known to block voltage-gated sodium channels and, thus, to inhibit CMAP. It is worth nothing that, although the excitability changes induced by lidocaine were explored on human sural nerve *in vitro* by means of threshold tracking techniques (Lang *et al.*, 2007), no study has previously assessed the effects of lidocaine on the neuromuscular excitability *in vivo*, to the best of our knowledge.

The effects of a local injection of lidocaine, at the base of animal tail, were studied on three 15 week-old female Swiss mice under anesthesia (by means of isoflurane inhalation), using the Qtrac© software. Stimulations were delivered at the base of animal tail, and CMAP recorded from the tail muscle as aforementioned. For each animal, multiple excitability measurements were performed before and after the injection, at the stimulation site, of 100 µL of a physiological solution containing 4 mg lidocaine. Regarding the relatively important volume of injected solution, the injection was delivered through three different points in a close area. The results of a representative experiment are presented below.

Immediately after the injection, on-line recordings were initiated to observe the effects of lidocaine on the excitability threshold and CMAP amplitude registered continuously. As shown in *Figure 3*, the major effects of lidocaine were to increase the threshold (*Figure 3A*, middle raw) and to markedly reduce the CMAP

amplitude (*Figures 3A*, lower raw, and *3B*). A CMAPmax dropping, from 2.3 mV at 12 min post-injection to 1 mV at 18 min post-injection, was observed.

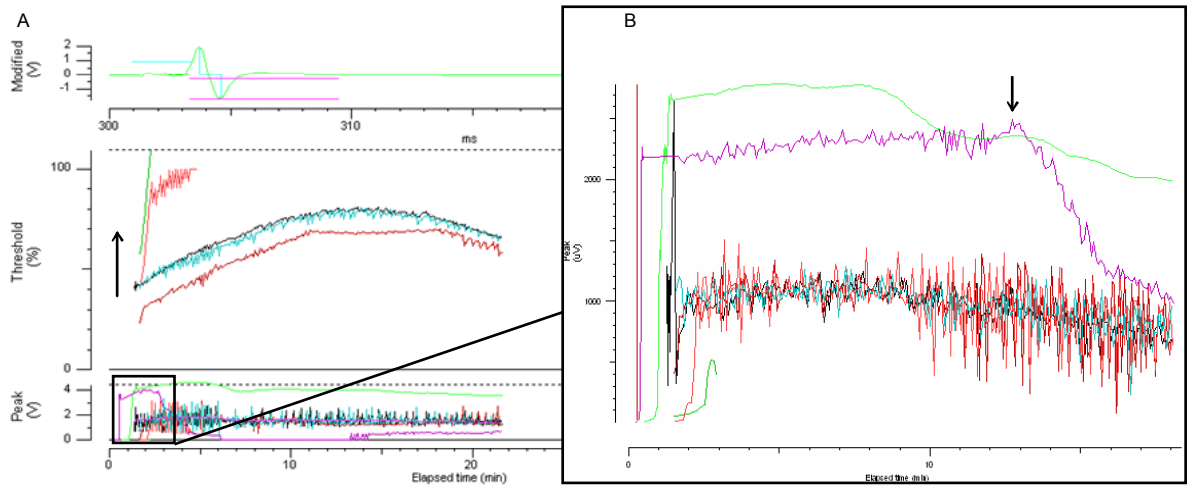

Fig. 3. On-line recordings of the effects of lidocaine on the excitability threshold and CMAP amplitude registered continuously. (**A**) Trace of a CMAP (upper raw), unconditioned threshold (black trace, middle raw) and evolution of CMAP amplitude (lower raw). The arrow indicates an increase in threshold (**B**) Magnification of the square part indicated in A provides a better appraisal of the drastic CMAP amplitude reduction (magenta trace) induced by lidocaine, as indicated by the arrow.

Fig. 3. *Enregistrements continus des effets de la lidocaïne sur le seuil d'excitabilité et l'amplitude du potentiel d'action global (CMAP). (**A**) Trace d'un CMAP (en haut), seuil d'excitabilité (tracé noir, au milieu) et amplitude du CMAP (en bas). La flèche témoigne de l'augmentation du seuil d'excitabilité (**B**) Amplification de la partie indiquée par un carré en A. Notez la réduction drastique de l'amplitude du CMAP (trace en magenta) produite par la lidocaïne, matérialisée par la flèche.*

Off-line treatment of the results, performed before and 20 min post-injection of lidocaine, reveals that the local anaesthetic induced marked neuromuscular excitability changes expressed by an increased threshold (*Figure 4A*), associated with a suppression of the supernormality, a prolongation of the refractory period, indicated by a shift of the curve to the right (*Figure 4B*) and a smaller threshold changes in response to depolarizing electrotonus (*Figure 4C*).

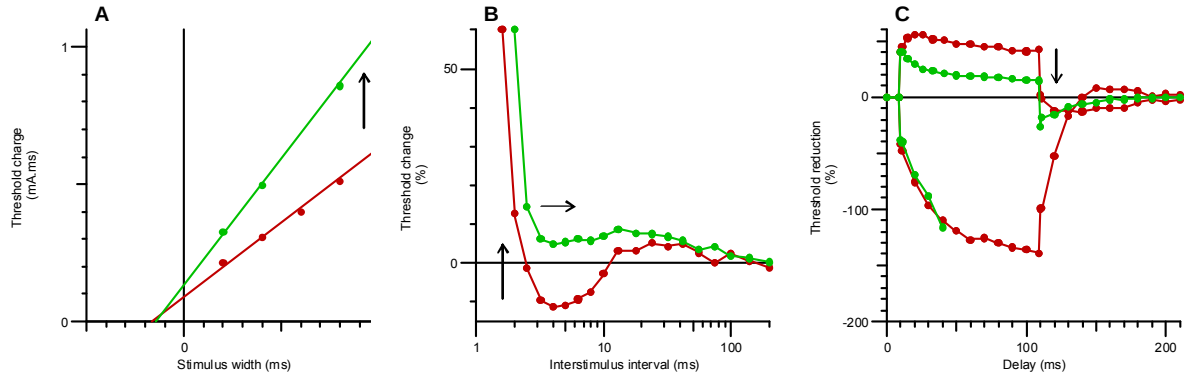

Fig. 4. Excitability waveforms recorded from a mouse tail muscle following caudal nerve stimulations *in vivo*, before (red) and 20 min post-injection (green) of lidocaine. (**A**) Charge-duration relationship. The arrow indicates an increase in threshold (**B**) Recovery cycle. The vertical arrow indicates a reduction in supernormality while the horizontal one indicates an enhanced refractoriness (**C**) Threshold electrotonus. The arrow indicates a greater accommodation.

Fig. 4. *Courbes d'excitabilité enregistrées à partir du muscle caudal d'une souris en réponse à des stimulations du nerf caudal* in vivo, *avant (en rouge) et 20 min après (en vert) l'injection de lidocaïne. (**A**) Relation charge-durée.* La flèche représente une augmentation du seuil *(**B**) Cycle de l'excitabilité. La flèche verticale témoigne d'une réduction de la supernormalité et la flèche horizontale indique une plus grande réfractorité (**C**) Courbes d'électrotonus. La flèche indique une meilleure accommodation. Ces paramètres renseignent plus spécifiquement sur les propriétés de l'axone moteur à la fois au niveau nodal et internodal.*

The present study provides evidence of the efficiency of a substance injection since lidocaine produced a drastic CMAP amplitude reduction. This reduction, as well as the prolongation of the refractory period induced by the local anaesthetic, are in accordance with the well-known effect of lidocaine consisting in a blockade of voltage-gated sodium channels, more specifically when they are inactivated. In addition, lidocaine produced specific changes in axonal excitability, as expressed by a greater accommodation to depolarizing electrotonus and a reduced superexcitability. Taken together, these changes are a primary hallmark of

membrane depolarization (Kiernan and Bostock, 2000 ; Boërio *et al.*, 2009b). It is worth noting that this membrane depolarization participates also in the increase in refractory period and percentage of refractoriness (Krishnan *et al.*, 2005).

Conclusion

Multiple excitability testing provides an accurate overview of neuromuscular excitability properties *in vivo*, and can be easily transferred from clinical neurophysiology to animal models. It is particularly appropriate for substance injections and repeated recordings from the same animal cohort and, thus, for a long-term follow-up of the effects of sub-lethal doses of toxins, in mice *in vivo*. It is indubitable that this method will bring specific information regarding changes in ion transfer and membrane properties induced by a given toxin which, thereby, will help to a better characterization of toxin action on the neuromuscular excitability properties, *in vivo*.

Acknowledgements. *This work was supported in part by grant STC-CP2008-1-555612-Atlantox.*

References

Boërio D, Hogrel JY, Créange A, Lefaucheur JP (2004) Methods and clinical value of peripheral nerve refractory period measurement in man. *Neurophysiol Clin* **34**: 279-291

Boërio D, Créange A, Hogrel JY, Lefaucheur JP (2007a) Alteration of motor nerve recovery cycle in multiple sclerosis. *Clin Neurophysiol* **118**: 1753-1758

Boërio D, Hogrel JY, Bassez G, Lefaucheur JP (2007b) Neuromuscular excitability properties in myotonic dystrophy type 1. *Clin Neurophysiol* **118**: 2375-2382

Boërio D, Hogrel JY, Lefaucheur JP, Wang FC, Verschueren A, Pouget J, Carrera E, Kuntzer T (2008) Stimulus-response curve of human motor nerves: multicenter assessment of various indexes. *Neurophysiol Clin* **38**: 31-38

Boërio D, Greensmith L, Bostock H (2009a) Excitability properties of motor axons in the maturing mouse. *J Peripher Nerv Syst* **14**: 45-53

Boerio D, Kalmar B, Greensmith L, Bostock H (2009b) Excitability properties of mouse motor axons in the mutant $SOD1^{G93A}$ model of ALS. *Muscle and Nerve* (in press)

Bostock H, Sharief MK, Reid G, Murray NM (1995) Axonal ion channel dysfunction in amyotrophic lateral sclerosis. *Brain* **118**: 217-225

Bostock H, Rothwell JC (1997) Latent addition in motor and sensory fibres of human peripheral nerve. *J Physiol Lond* **498**: 277-294

Bostock H, Cikurel K, Burke D (1998) Threshold tracking techniques in the study of human peripheral nerve. *Muscle and Nerve* **21**: 137-158

Brismar T (1985) Changes in electrical threshold in human peripheral neuropathy. *J Neurol Sci* **68**: 215-223

Cappelen-Smith C, Kuwabara S, Lin CS, Mogyoros I, Burke D (2001) Membrane properties in chronic inflammatory demyelinating polyneuropathy. *Brain* **124**: 2439-2447

George A, Bostock H (2007) Multiple measures of axonal excitability in peripheral sensory nerves: an in vivo rat model. *Muscle and Nerve* **36**: 628-636

Kanai K, Kuwabara S, Misawa S, Tamura N, Ogawara K, Nakata M, Sawai S, Hattori T, Bostock H (2006) Altered axonal excitability properties in amyotrophic lateral sclerosis: impaired potassium channel function related to disease stage. *Brain* **129**: 953-962

Kiernan MC, Mogyoros I, Burke D (1996) Differences in the recovery of excitability in sensory and motor axons of human median nerve. *Brain* **119**: 1099-1105

Kiernan MC, Bostock H (2000) Effects of membrane polarization and ischaemia on the excitability properties of human motor axons. *Brain* **123**: 2542-2551

Kiernan MC, Burke D, Andersen KV, Bostock H (2000) Multiple measures of axonal excitability: a new approach in clinical testing. *Muscle and Nerve* **23**: 399-409

Kiernan MC, Guglielmi JM, Kaji R, Murray NM, Bostock H (2002) Evidence for axonal membrane hyperpolarization in multifocal motor neuropathy with conduction block. *Brain* **125**: 664-675

Krishnan AV, Lin CS, Kiernan MC. Nerve excitability properties in lower-limb motor axons: evidence for a length-dependent gradient (2004) *Muscle and Nerve* ***29***: 645-655

Krishnan AV, Kiernan MC (2005) Altered nerve excitability properties in established diabetic neuropathy. *Brain* **128**: 1178-1187

Krishnan AV, Phoon RK, Pussell BA, Charlesworth JA, Bostock H, Kiernan MC (2005) Altered motor nerve excitability in end-stage kidney disease. *Brain* **128**: 2164-2174

Krishnan AV, Kiernan MC (2006) Axonal function and activity-dependent excitability changes in myotonic dystrophy. *Muscle and Nerve* **33**: 627-636

Kuwabara S, Cappelen-Smith C, Lin CS, Mogyoros I, Bostock H, Burke D (2000) Excitability properties of median and peroneal motor axons. *Muscle and Nerve* **23**:1365-1373

Kuwabara S, Ogawara K, Sung JY, Mori M, Kanai K, Hattori T, Yuki N, Lin CS, Burke D, Bostock H (2002) Differences in membrane properties of axonal and demyelinating Guillain-Barré syndromes. *Ann Neurol* **52**:180-187

Lang PM, Hilmer VB, Grafe P (2007) Differential contribution of sodium channel subtypes to action potential generation in unmyelinated human C-type nerve fibers. *Anesthesiology* **107**: 495-501

Lefaucheur JP, Boërio D, Hogrel JY, Créange A (2006) [Nerve excitability studies in the assessment of dysimmune neuropathies]. Rev Neurol (Paris) **162 S1**:3S17-3S26

Maurer K, Bostock H, Koltzenburg M (2007) A rat *in vitro* model for the measurement of multiple excitability properties of cutaneous axons. *Clin* Neurophysiol **118**: 2404-2412

Misawa S, Kuwabara S, Mori M, Hayakawa S, Sawai S, Hattori T (2008) Peripheral nerve demyelination in multiple sclerosis. *Clin Neurophysiol* **119**: 1829-1833

Moldovan M, Krarup C (2006) Evaluation of Na+/K+ pump function following repetitive activity in mouse peripheral nerve. *J Neurosci Methods* **155**: 161-171

Ng K, Lin CS, Murray NM, Burroughs AK, Bostock H (2007) Conduction and excitability properties of peripheral nerves in end-stage liver disease. *Muscle and Nerve* **35**: 730-738

Nodera H, Kaji R(2006) Nerve excitability testing and its clinical application to neuromuscular diseases. *Clin Neurophysiol* **117**: 1902-1916

Sawai S, Kanai K, Nakata M, Hiraga A, Misawa S, Isose S, Hattori T, Kuwabara S (2008) Changes in excitability properties associated with axonal regeneration in human neuropathy and mouse Wallerian degeneration. *Clin Neurophysiol* **119**:1097-1105

Susuki K, Baba H, Tohyama K, Kanai K, Kuwabara S, Hirata K, Furukawa K, Furukawa K, Rasband MN, Yuki N (2007) Gangliosides contribute to stability of paranodal junctions and ion channel clusters in myelinated nerve fibers. *Glia* **55**:746-757

Vucic S, Kiernan MC (2006) Axonal excitability properties in amyotrophic lateral sclerosis. *Clin Neurophysiol* **117**: 1458-1466

Vucic S, Kiernan MC (2007) Pathophysiologic insights into motor axonal function in Kennedy disease. *Neurology* **69**: 1828-1835

Yang Q, Kaji R, Hirota N, Kojima Y, Takagi T, Kohara N, Kimura J, Shibasaki H, Bostock H (2000) Effect of maturation on nerve excitability in an experimental model of threshold electrotonus. *Muscle and Nerve* **23**: 498-506

Z'Graggen WJ, Lin CS, Howard RS, Beale RJ, Bostock H (2006) Nerve excitability changes in critical illness polyneuropathy. *Brain* **129**: 2461-2470

Toxines et Signalisation – Toxins and Signalling
Rencontres en Toxinologie – Meeting on Toxinology, 2009
Editions de la SFET – SFET Editions
Accès libre en ligne sur le site – Free access on line on the site : http://www.sfet.asso.fr

Effects of ostreolysin, a protein from the oyster mushroom Pleurotus ostreatus*, on the mouse neuromuscular system* in vivo

Delphine BOERIO-GUEGUEN[1], Robert FRANGEŽ[2], Kristina SEPČIĆ[3], Evelyne BENOIT[1*]

[1] *CNRS, Institut de Neurobiologie Alfred Fessard - FRC2118, Laboratoire de Neurobiologie Cellulaire et Moléculaire - UPR9040, 91198 Gif sur Yvette cedex, France ;* [2] *Institute of Physiology, Pharmacology and Toxicology, Veterinary Faculty, University of Ljubljana, Slovenia ;* [3] *Department of Biology, Biotechnical Faculty, University of Ljubljana, Slovenia*

** Corresponding author ; Tel : +33 (0)1 69 82 36 52 ; Fax : +33 (0)1 69 82 41 41 ; E-mail : benoit@nbcm.cnrs-gif.fr*

Abstract

The effects of ostreolysin, a cytolytic protein from the edible oyster mushroom Pleurotus ostreatus*, were studied on the excitability properties of the mouse neuromuscular system,* in vivo*, by means of a minimally-invasive electrophysiological method. Experiments were performed by stimulating the caudal motor nerve and recording the compound muscle action potential (CMAP) from the tail muscle. The solutions containing ostreolysin (0.5 and 1 µg per g of body weight) were injected at the base of mice tail. The effects of the protein consisted mainly in a reduction of CMAP amplitude, associated with an increased excitability threshold and smaller threshold changes to depolarizing electrotonus. These effects provide additional insights for a better understanding and characterization of the mechanism of action of ostreolysin and are, therefore, particularly promising to further counteract its toxic action on the neuromuscular system* in vivo*.*

Effets de l'ostréolysine, une protéine du champignon Pleurotus ostreatus*, sur le système neuromusculaire de la souris* in vivo

Les effets de l'ostréolysine, une protéine cytolytique du champignon Pleurotus ostreatus*, ont été étudiés,* in vivo*, sur les propriétés d'excitabilité du système neuromusculaire chez la souris, en utilisant une méthode électrophysiologique très peu invasive. Les évaluations étaient effectuées par la stimulation du nerf caudal moteur et l'enregistrement du potentiel d'action musculaire composé (CMAP) du muscle caudal. Les solutions contenant l'ostréolysine (0,5 et 1 µg par g de poids corporel) ont été injectées à la base de la queue des souris. Les effets de la protéine ont principalement consisté en une réduction de l'amplitude du CMAP, associée à une augmentation du seuil d'excitabilité et une diminution des variations du seuil en réponse à l'électrotonus dépolarisant. Ces effets permettent d'approfondir et d'améliorer les compréhension et caractérisation du mécanisme d'action de l'ostréolysine et sont, de ce fait, particulièrement prometteurs pour contrebalancer, plus en avant, son action toxique sur le système neuromusculaire* in vivo*.*

Keywords : Pleurotus ostreatus*, ostreolysin, pore-forming protein,* in vivo *electrophysiology, mouse neuromuscular system.*

Introduction

Ostreolysin, a 15 kDa thermolabile protein, is specifically expressed during the formation of primordia and fruit bodies of the edible oyster mushroom *Pleurotus ostreatus* (Berne *et al*., 2002). This protein seems to be responsible for the adverse reactions observed after the ingestion of large quantities of oyster mushrooms (Al-Deen *et al.*, 1987). The cDNA nucleotide sequence of ostreolysin has a high homology with hemolysins from moulds and bacteria, such as *Aspergillus fumigatus* and *Clostridium bifermentans* (Berne *et al*., 2009). Previous studies showed that ostreolysin is toxic to rodents when intravenously injected (the dose producing 50 % lethality being 1.17 µg/g of body weight), leading to death by cardiorespiratory arrest. This arrest, which did not depend on the parasympathetic activity of the vagus nerve, was accompanied by blood hyperkaliemia (Žužek *et al.*, 2006). The protein also increased aortic ring tension (Rebolj *et al.*, 2007). In addition, nanomolar concentrations of ostreolysin have been shown to exert cytolytic effects on erythrocytes and tumor cells (Sepčić *et al.*, 2003). All these protein effects are assumed to result from ostreolysin-induced pores in the plasma membrane.

In the present study, we investigated the consequence of the membrane-damaging effect of ostreolysin on the excitability properties of the mouse neuromuscular system *in vivo*, using a minimally-invasive electrophysiological method.

Experimental procedures

The experiments, regarding the effects of ostreolysin on neuromuscular excitability properties *in vivo,* were performed in accordance with the guidelines established by the French Council on animal care "Guide for the Care and Use of Laboratory Animals" : EEC86/609 Council Directive - Decree 2001-131, on four Swiss female mice, at 19 weeks of age, under anesthesia (by means of isoflurane inhalation). Neuromuscular excitability properties were assessed using the Qtrac© software written by Prof. Bostock (Institute of Neurology, London), as previously described in mice *in vivo* (Boërio *et al.*, 2009). The electrical stimulations were delivered to the caudal motor nerve (at the base of the tail), by means of surface electrodes, and compound muscle action potentials (CMAPs) were recorded using needle electrodes inserted into the tail muscle.

To better identify the underlying mechanism(s) of action of ostreolysin, five different excitability tests (stimulus-response, strength-duration and current-threshold relationships, as well as threshold electrotonus and recovery cycle ; see Boërio-Guéguen *et al.*, 2009 for a review) were performed together before, 15-20 min after a first injection of 100 µL of physiological solution containing ostreolysin (0.5 µg per g of body weight), and 10-15 min after a second injection, identical to the first one (thus leading to a final dose of 1 µg protein per g of body weight). Injections were delivered at the stimulation site.

As a whole, more than 35 parameters were determined from the five different excitability tests, and analyzed. It is worth noting that each specific excitability test provides additional and complementary information regarding, on one hand, the functional status of ion channels and electrogenic pumps and, on the other hand, membrane properties (Kiernan *et al.*, 2000 ; Lefaucheur *et al.*, 2006 ; Krishnan *et al.*, 2008).

Results and Discussion

The most pronounced effect of ostreolysin was a decrease of CMAPs amplitude. In addition, off-line treatment of results revealed that the protein induced an increased excitability threshold associated with smaller threshold changes in response to depolarizing electrotonus, as illustrated in *Figure 1* by the effects of 1 µg ostreolysin per g of body weight during a representative experiment.

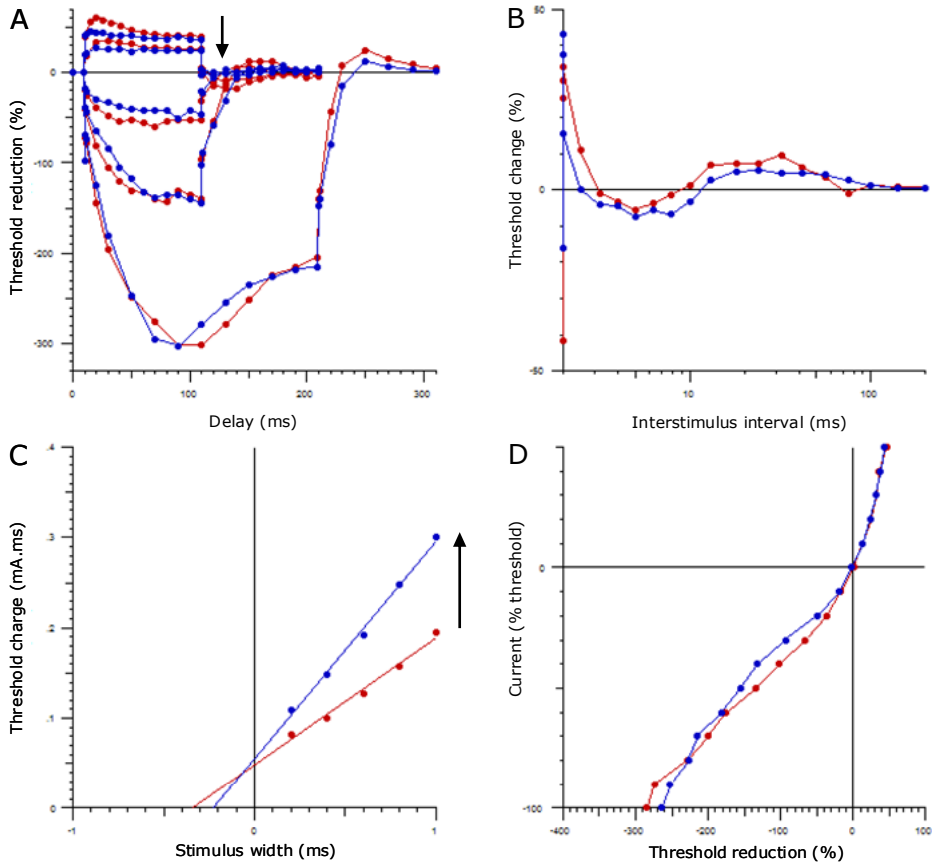

Fig. 1. Excitability waveforms obtained by stimulation of the caudal nerve and recordings from the tail muscle in a mouse *in vivo*, before (red) and 15 min post-injection (blue) of 1 µg ostreolysin per g of body weight. (**A**) Threshold electrotonus. (**B**) Recovery cycle. (**C**) Charge-duration relationship established from strength-duration curve. (**D**) Current-threshold relationship.

Fig. 1. *Courbes d'excitabilité établies par la stimulation du nerf caudal moteur et le recueil de l'activité électromyographique du muscle caudal d'une souris* in vivo, *avant (en rouge) et 15 min après (en bleu) l'injection d'1 µg d'ostréolysine par g de poids corporel. (**A**) Courbes d'électrotonus. (**B**) Cycle d'excitabilité. (**C**) Relation charge-durée établie à partir de la courbe intensité-durée. (**D**) Courbe courant-seuil.*

Among the 35 parameters determined and analyzed from the five different excitability tests, those related to CMAPs amplitude, excitability threshold and threshold changes to depolarizing electrotonus were altered by ostreolysin, as exemplified by three of them in *Figure 2*. It is worth noting that, although the effects of the protein could already be detected at a dose of 0.5 µg per g of body weight, the level of significance was enhanced at a dose of 1 µg per g of body weight.

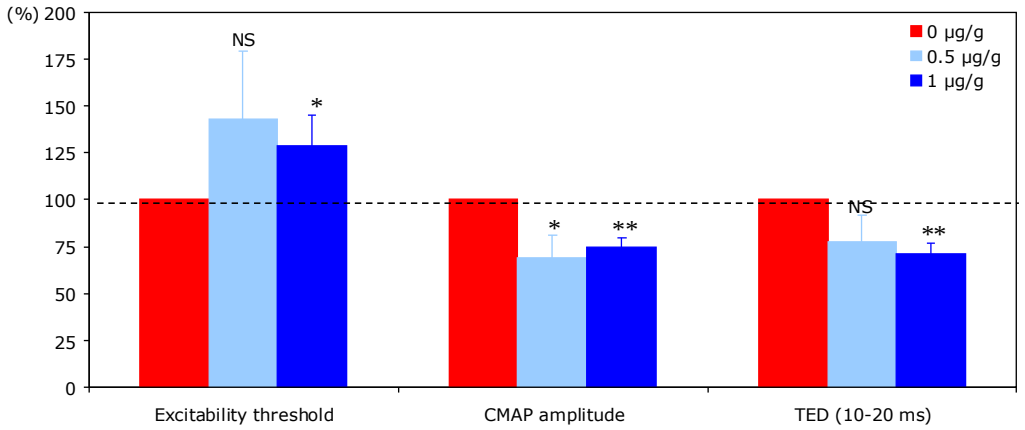

Fig. 2. Excitability threshold, CMAP amplitude and threshold changes to depolarizing electrotonus [TED (10-20 ms), *i.e.* single test-pulse applied 10-20 ms after the beginning of a long-lasting (100 ms), subthreshold, depolarizing current], determined before and after injections of the indicated doses of ostreolysin. Mean ± SEM of 4 mice.

Fig. 2. *Seuil d'excitabilité, amplitude du CMAP et changements du seuil en réponse à l'électrotonus dépolarisant [TED (10-20 ms),* i.e. *stimulation test unitaire appliquée 10-20 ms après le début d'un courant dépolarisant infraliminaire, maintenu pendant 100 ms], déterminés avant et après les injections des doses d'ostréolysine indiquées. Moyennes ± ESM de 4 souris.*

The fact that the amplitude of CMAPs is decreased and the threshold increased provides evidence of a reduced neuromuscular excitability induced by ostreolysin. Although the involvement of the muscle itself cannot be excluded, it is likely that ostreolysin also interferes directly with the motor nerve functioning, in particular by altering internodal properties of the axonal membrane if one considers the threshold changes in response to depolarizing electrotonus (Bostock *et al.*, 1998 ; Krishnan *et al.*, 2008). As a whole, these effects of ostreolysin are in accordance with the assumption that the protein induces ion-conducting pores both in the nerve and muscle plasma membranes.

Conclusion

As a conclusion, the fact that ostreolysin exhibits, *in vivo*, alterations of mouse neuromuscular excitability properties is encouraging in the way that it provides additional insights for a better understanding and characterization of the mechanism of action of this protein, which is therefore promising to counteract its toxic action on the neuromuscular system *in vivo*.

Acknowledgements. *This study was supported by the Slovenian Research Agency grant P4-0053, by the CNRS, and by the Proteus cooperation program funded by the French and Slovenian governments (PHC project BI-FR/08-09-Proteus-010/EGIDE-17933YD).*

References

Al-Deen IHS, Twaij HAA, Al-Badr AA, Istarabad TAW (1987) Toxicologic and histopathologic studies of *Pleurotus ostreatus* mushroom in mice. *J Ethnopharm* **21**: 297-305

Berne S, Križaj I, Pohleven F, Turk T, Maček P, Sepčić K (2002) *Pleurotus* and *Agrocybe* hemolysins, new proteins hypothetically involved in fungal fruiting. *Biochim Biophys Acta* **1570**: 153-159

Berne S, Lah L, Sepčić K (2009) Aegerolysins: structure, function and putative biological role. *Protein Sci* **18**: 694-706

Boërio D, Greensmith L, Bostock H (2009) Excitability properties of motor axons in the maturing mouse. *J Peripher Nerv Syst* **14**: 45-53

Boërio-Guéguen D, Lefaucheur JP, Créange A, Benoit E (2009) A non-invasive method to appraise time-dependent effects of toxins on the mouse neuromuscular excitability *in vivo*, and its clinical applications. In *Toxins and Signalling*, Benoit E, Goudey-Perrière F, Marchot P and Servent D (eds) pp 123-130. SFET Publications, Châtenay-Malabry, France, Epub on http://www.sfet.asso.fr (ISSN 1760-6004)

Bostock H, Cikurel K, Burke D (1998) Threshold tracking techniques in the study of human peripheral nerve. *Muscle and Nerve* **21**: 137-158

Kiernan MC, Burke D, Andersen KV, Bostock H (2000) Multiple measures of axonal excitability: a new approach in clinical testing. *Muscle and Nerve* **23**: 399-409

Krishnan A, Park S, Lin CS, Kiernan MC (2008) Assessment of nerve excitability in toxic and metabolic neuropathies. *J Peripher Nerv Syst* **13**: 7-26

Lefaucheur JP, Boërio D, Hogrel JY, Créange A (2006) Nerve excitability studies in the assessment of dysimmune neuropathies. *Rev Neurol (Paris)* **162-S1**: 3S17-3S26

Rebolj K, Batista U, Sepčić K, Cestnik V, Maček P, Frangež R (2007) Ostreolysin affects rat aorta ring tension and endothelial cells viability *in vitro*. *Toxicon* **49**: 1211-1213

Sepčić K, Berne S, Potrich C, Turk T, Maček P, Menestrina G (2003) Interaction of ostreolysin, a cytolytic protein from the edible mushroom *Pleurotus ostreatus*, with lipid membranes and modulation by lysophospholipids. *Eur J Biochem* **270**: 199-210

Žužek MC, Maček P, Sepčić K, Cestnik V, Frangež R (2006) Toxic and lethal effects of ostreolysin, a cytolytic protein from edible oyster mushroom (*Pleurotus ostreatus*), in rodents. *Toxicon* **48**: 264-271

Toxines et Signalisation – Toxins and Signalling
Rencontres en Toxinologie – Meeting on Toxinology, 2009
Editions de la SFET – SFET Editions
Accès libre en ligne sur le site – Free access on line on the site : http://www.sfet.asso.fr

Renewed taxonomy : phylogeny and species delimitation in an integrative framework

Nicolas PUILLANDRE
Department of Biology, University of Utah, 257 South 1400 East, Salt Lake City, UT 84112
Tel : +(001) 801 581 8370 ; Fax : +(001) 801 581 5010 ; E-mail : puillandre@biology.utah.edu

Abstract

The vast diversity of species included in the genus Conus *and in the superfamily Conoidea make them one of the most promising taxa for the discovery of new toxin-derived drugs. To rationalize the search for new peptides, integrative taxonomy can be used to quickly identify new lineages that potentially evolved new toxins. In this context, molecular characters are now a major tool, whether for specimen identification ("barcoding"), species delimitation (alpha-taxonomy) or phylogeny. At the species level, different criteria have been successfully applied to analyze DNA sequences and propose hypotheses of species delimitation in the genus* Benthomangelia *that are supported by other characters such as morphology. At the phylogenetic level, molecular characters were also used to define highly divergent lineages within Conoidea and to infer their relationships. The methodology used, based on clearly stated concepts and integrating different criteria and characters allow the definition of robust, reproducible and testable hypotheses. Furthermore, discriminating these lineages (families, subfamilies, genera or species) is of great value in toxin research, as illustrated with the family Terebridae where three different lineages have been identified each of them susceptible to have evolved their own set of toxins.*

Le renouveau de la taxonomie : phylogénie et délimitation d'espèces dans un contexte intégratif

La grande diversité spécifique inclue dans le genre Conus *et dans la superfamille des Conoidea font de ces groupes certains des plus prometteurs pour la découverte de nouvelles thérapies dérivées de toxines. Pour rationaliser la recherche de nouveaux peptides, une approche de taxonomie intégrative peut permettre d'identifier rapidement des lignées évolutives qui auraient potentiellement développé de nouvelles toxines. Dans ce contexte, les caractères moléculaires sont devenus un outil majeur, que ce soit pour l'identification de spécimens (« barcoding »), la délimitation d'espèces (alpha-taxonomie) et la phylogénie. Au niveau spécifique, différents critères ont été appliqués avec succès pour analyser des séquences ADN et proposer des hypothèses de délimitation d'espèces au sein du genre* Benthomangelia*, hypothèses soutenues par d'autres caractères (morphologiques). Au niveau phylogénétique, les caractères moléculaires ont été également utilisés pour définir différentes lignées au sein des Conoidea. La méthodologie utilisée, basée sur des concepts clairement établis et intégrant différents critères et caractères, permet de proposer des hypothèses robustes, reproductibles et testables. De plus, discriminer ces lignées (familles, sous-familles, genres et espèces) est important pour la recherche de toxines, comme le montre l'analyse de la famille des Terebridae, où trois différentes lignées ont été identifiées, chacune susceptible d'avoir développé des toxines uniques.*

Keywords : *Conoideans, conotoxin, DNA barcoding, integrative taxonomy, molecular phylogeny.*

Introduction

Cone snails are certainly one of the most diverse genus of marine invertebrates, with more than 600 described species (Kohn, 1990 ; Duda and Kohn, 2005). Their ornamentation, their accessibility and the "deadly" fascination for these venomous animals make this group one of the most famous in the naturalist collectors community. Furthermore, cone snails are also of great scientific value particularly because of the therapeutic applications of their toxins. Several different *Conus* peptides are now being clinically tested and one is currently commercialized under the name Prialt (Olivera, 2006). These toxins are also characterized by their huge diversity, as each species displays its own set of 100-200 specific toxins, which lead to the estimated number of 60,000-120,000 different toxins in this single genus.

Several species have already been investigated and several hundreds of toxins are now described. Known as conotoxins, they all share a common structure (Olivera, 2008) and are classified in ~ 20 superfamilies. Some of these toxins are functionally characterized, and a huge diversity of molecular targets has been found (Terlau and Olivera, 2004), echoing the vast potential therapeutic applications of these conotoxins.

However, despite the considerable amount of data accumulated, only a few C*onus* species have been analyzed proportionately. Furthermore, recent phylogenetic analyses have shown that most of the analyzed species are concentrated in a few clades within *Conus* and are thus not representative of the diversity of the genus (Olivera, 2008 ; unpublished results). To balance this bias, Olivera proposed a "concerted discovery" strategy, where modern taxonomic tools, such as molecular phylogeny and integrative taxonomy, could be use to identify independent lineages within *Conus*, where different toxins may have evolved, and thus accelerate the discovery of new toxins (Olivera, 2006).

To do so, a good knowledge of the taxonomy of the group is necessary, which is not currently the case. Traditionally, all cone snails are grouped in a single genus (*Conus*), though several authors have attempted to separate it into several genera (*e.g.* da Motta, 1991). Recent molecular phylogeny analyses (see Olivera, 2008, *Figure 1*) confirm that several highly divergent lineages are actually included in *Conus*. Investigating toxin diversity in these divergent lineages should lead to the discovery of new toxins. Recent results (*e.g.* Watkins *et al*., 2006 ; Imperial *et al*., 2007) also have shown that *Conus* is only the tip of the iceberg. Actually, *Conus* are included in the superfamily Conoidea, considered as the most diverse groups of marine molluscs (Bouchet *et al*., 2002). With an estimated species number over 10,000, revealed particularly by recent cruises set up by the Muséum National d'Histoire Naturelle de Paris (Bouchet *et al*., 2008), conoidean toxins could reach the unlikely number of one or two million...

The potential is evident, but how can we optimize the toxin discovery in such a diverse group? Which species should be investigated first? The "concerted discovery" strategy seems appropriate, but one should not ignore the difficulty encountered by malacologists in their attempt to classify the conoideans. Turrids, one of the three traditionally recognized groups within Conoidea, together with Conidae and Terebridae, is considered "a taxonomic nightmare" (*e.g.* Tryon, 1884). Whatever the taxonomic level considered (families, subfamilies, genera, species), taxonomists do not agree and contradictions are common : what will be considered as intraspecific variability for one of them will be considered as different species for another. With conoideans, and to some extent with molluscs, taxonomists face two major problems. First, most – if not all – species' descriptions are based on shell characters. Several studies have shown the plasticity of such characters : they may reflect environmental differences rather than differences between species (Hollander *et al*., 2006 ; Brookes and Rochette, 2007). Second, taxonomical practices do not allow a clear scientific evaluation of the groups delimited. Species are more opinions than testable hypotheses : specimens are grouped in species using non-formalized characters (a problem also linked to the use of shell characters), generally impossible to reproduce.

Thus, the challenge for taxonomy is to define a new methodology based on proposing hypotheses that are reproducible and testable (Wiens, 2007). Furthermore, as morphological characters are clearly not adapted, new characters will have to be analysed in an integrative framework. I propose here to review some taxonomical practices that are proposed to overcome these difficulties. First will be described the not-so-new character now commonly used in taxonomy : DNA, and its use as an identification tool (*i.e.* the barcoding). Then, methodological and conceptual issues at both the phylogenetic (families and subfamilies) and species levels will be presented, each illustrated by several case studies in conoideans.

Molecular characters and barcoding

Although DNA has been applied in taxonomy since the 1980's, its use still remains unconventional. Most species' descriptions are still primarily based on morphological characters, and DNA is generally restricted to an *a posteriori* confirmation of the species delimitation (*e.g.* Reid *et al*., 2006 ; Meyer *and Paulay*, 2005). However, DNA has several advantages over morphological characters. One of the most important advantages being, by definition, that it is genetically determined : DNA differences are supposed to reflect species boundaries and not environment variability. Furthermore, DNA sequences are now easily accessible and can provide a high number of formalized characters. These advantages have been highlighted recently by Hebert *et al*. (2003) when he proposed to use short DNA sequences has a "molecular barcode" to identify unknown specimens (*Figure 1D*). The principle is not new, but the novelty of the barcoding project resides in the standardization of the technique *i.e.* the same gene fragment, a ~650 bp fragment of the Cytochrome Oxidase I (COI), should be used for all animals.

The barcode system lies on one major principle : the COI sequence of a given specimen is more similar to the COI sequences of conspecific specimens than specimens of other species. The goal of most DNA barcode projects (see www.barcodinglife.org) is to test this assertion by sequencing several specimens of all the species for a given taxa. In most cases, the intraspecific variability is less than the interspecific variability. These sequences can then constitute the database used to identify an unknown specimen; the most similar sequence in the database will provide the species name.

In order to identify marine gastropods' egg capsules collected in the Philippines in 2007, we used a barcoding approach by comparing mitochondrial sequences (the COI gene, but also fragments of the 12S and 16S genes) to two online databases : BOLD (Barcode Of Life Database) and GenBank (Puillandre *et al*., 2009b). Two methods were used : the BLAST algorithm based on the similarity between sequences and a phylogenetic analysis where all sequences from GenBank were combined with the unknown ones to construct a phylogenetic tree (bayesian analysis, Huelsenbeck *et al*., 2001). This methodology has been tested with a known egg capsule (*Erosaria spurca*, Cypraeidae), first identified due to the proximity of the adults (*Figure 2A*) The first hit of the BLAST analysis and the sister-group of the "unknown" sequence were a sequence of *E. spurca*. Several egg capsules were identified this way, and some examples are shown in *Figure 2*. Some identifications were not surprising as the egg capsule morphology is somewhat characteristic of the corresponding group (*Figure 2B*), but others were more unexpected such as the *Granulifusus* (*Figure 2C*) that displays a morphology never found in Fasciolariidae (Knudsen, 1950). However, most egg capsules were not identified at the species level but only at the genus or even familial level. The database's incompleteness,

where some molluscan groups are not represented at all, may explain this result.

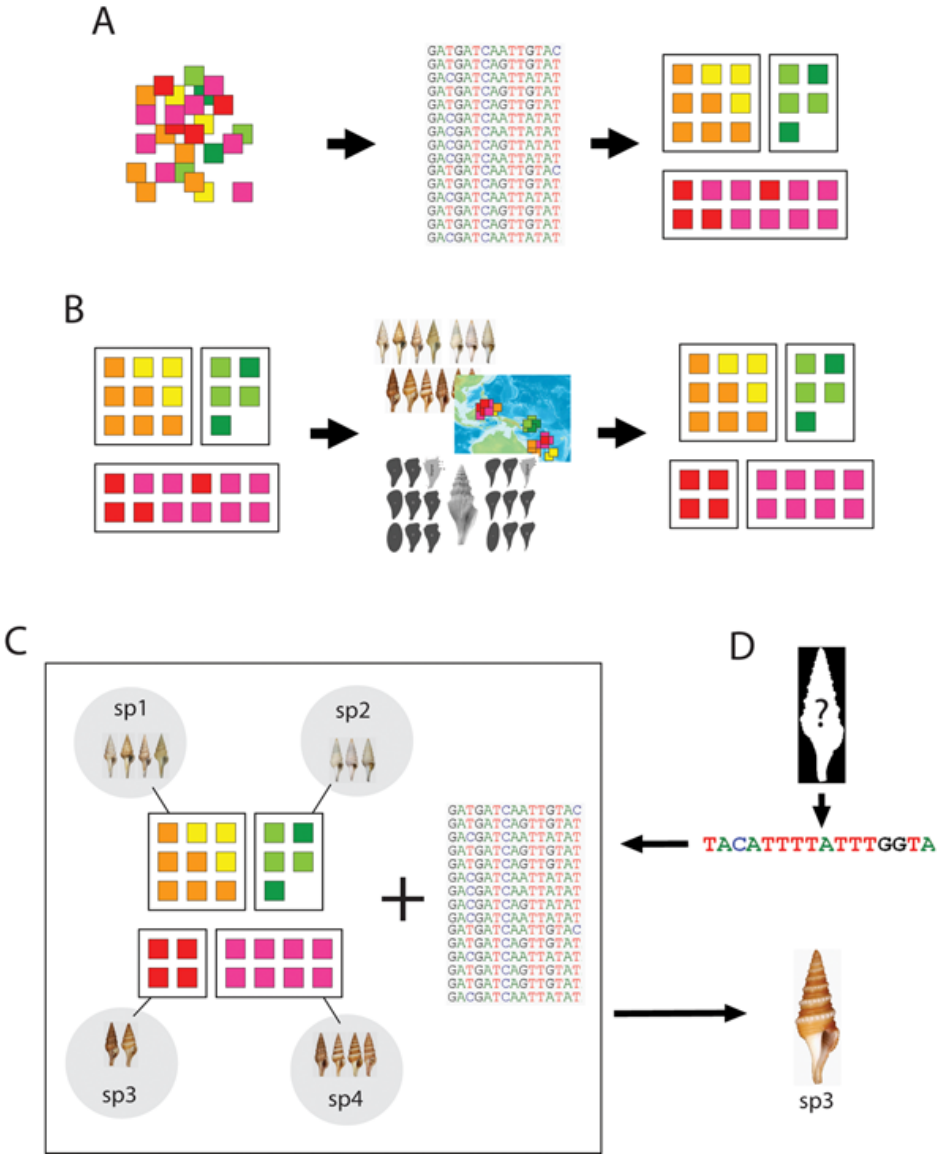

Fig. 1. Integrative taxonomy and Barcoding. (**A**) Several specimens are sequenced and placed in different primary hypotheses of species delimitation. (**B**) These hypotheses are then evaluated with other data (morphology, geography, ecology, etc) and may be modified. (**C**) Each delimited species is then associated to vouchers in a database and to their corresponding DNA sequences. (**D**) The DNA sequence from an unknown specimen can then be compared to the sequences included in the database. The most similar sequence will give the species identification.

Fig. 1. *Taxonomie intégrative et barcoding. (**A**) Plusieurs spécimens sont séquencés et placés dans différents groupes homogènes. (**B**) Ces groupes sont ensuite discutés en analysant d'autres données (morphologie, géographie, écologie…), et peuvent être modifiés. (**C**) Chaque espèce délimitée est ensuite associée dans une base de données à des spécimens de références ("vouchers") et à leurs séquences ADN correspondantes. (**D**) La comparaison d'une séquence ADN d'un spécimen inconnu permet d'identifier à quelle séquence elle ressemble le plus, et donc à quelle espèce le spécimen appartient.*

Thus, DNA Barcoding seems to be a powerful tool for species identification. Contrary to morphological characters, it does not need any knowledge about the taxa and can be used whatever the developmental stage (eggs, larvae, adults, etc) or the tissue available (Janzen *et al.*, 2005). However, several limits have been highlighted most of them being linked to the gene chosen : (i) a nuclear copy of the COI can be sequenced instead of the mitochondrial gene (Moritz and Cicero, 2004 ; Lorenz *et al.*, 2005), (ii) the COI gene does not always fulfill the requirement of a molecular barcode as in amphibians where the intraspecific variability is equivalent to the interspecific variability (Smith *et al.*, 2008), or in cnidarians where the intraspecific variability is null (Shearer and Coffroth, 2008), and (iii) the gene tree obtained with the COI (or with another mitochondrial gene) can be different from the species tree (Nichols, 2001 ; Rosenberg and Tao, 2008) because of problems of ancestral polymorphism for example (Fu and Zeng, 2008).

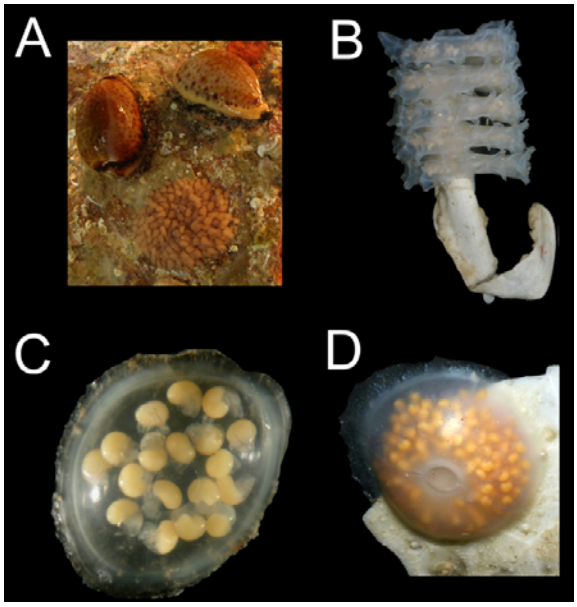

Fig. 2. Some egg capsules identified using DNA barcodes. (**A**) *Erosaria spurca*, Cypraeidae (egg capsule with adults). (**B**) *Conus sp*., Conidae. (**C**) *Granulifusus sp*., Fasciolariidae. (**D**) *Comitas sp*., Turridae.

Fig. 2. *Quelques capsules d'œufs identifiés par leur Barcode ADN.* (**A**) Erosaria spurca*, Cypraeidae (œufs et adultes).* (**B**) Conus sp.*, Conidae.* (**C**) Granulifusus sp.*, Fasciolariidae.* (**D**) Comitas sp.*, Turridae.*

For all these reasons, many authors claim that DNA barcoding is only an identification tool powerful when species are clearly differentiated with the COI gene (*e.g.* Ebach and Holdredge, 2005 ; Godfray, 2006). However, DNA barcoding can be used to discover cryptic species. This has been the case, for example, in already well-known groups, such as birds or lepidoptera (Hebert *et al.*, 2004 ; Hajibabaei *et al*., 2006 ; Vaglia *et al*., 2008). In these cases, the DNA barcode is used to point out problematic cases, but should not be used solely to describe new species. New standards for taxonomy are now being developed, and if they include the use of molecular data such as DNA barcodes, they also advocate their association with the analysis of other characters and criteria in an integrative framework.

Integrative alpha-taxonomy

Defining species is certainly one of the most controversial topics in biology. There are dozens of concepts of species available in literature (reviewed in Agapow *et al*., 2004 or in de Queiroz, 2007), but as de Queiroz (1998) first pointed out, they all correspond to properties shared by some but not all species, and not to a definition that can be applied to all organisms. He thus proposed a unified concept, formalized by Samadi and Barberousse (2006), where species are considered as definitely divergent lineages, known as the Lineage Species Concept (LSC). Because recovering these lineages would necessitate tracing back the network of all relationships between all individuals (who are the parents of who?), which is impossible, the taxonomist will have to indirectly infer this network using different species properties (the so-called "species concepts"). In this framework, species will thus be hypotheses constantly engaged in a process of modification/validation as new characters are analyzed and new criteria applied.

From the LSC, three criteria for defining species can be derived : (i) a species is a reproductive community that share a common gene pool. As a consequence, conspecific specimens will look similar; (ii) specimens from the same species are able to reproduce together, a criterion that can be tested directly (cross tests) or indirectly (no gene exchange between different species); (iii) all the specimens from the same species share a common history and should thus correspond to a monophyletic lineage in a phylogenetic tree. Taxonomists generally agree now that species delimitation should be based on several criteria, as some species may not be found if only one criterion is applied. For example, species that are too recent will share common haplotypes if they did not have enough time to accumulate differences (ancestral polymorphism). A phylogenetic analysis will not successfully recover the species boundaries in this case but another criterion might. Furthermore, the more characters that are analysed, the more supported the hypotheses will be. Even if some characters seem more approriate (DNA for example), none of them will be infallible, as we saw earlier, and the combination of molecular, morphological, ecological, behavioural, etc, characters is now advocated by most taxonomists (*Figures 1A and B*). Optimizing the number of criteria and characters to propose testable and reproducible hypotheses of species delimitation constitutes the standards of the integrative taxonomy (Sites and Marshall, 2003 ; Dayrat, 2005 ; Vogler and Monaghan, 2007 ; Wiens, 2007).

Following these rules, we analyzed the species diversity in the genus *Benthomangelia* (Puillandre *et al.,* 2009a). This genus is included in the subfamily Mangeliinae, closely related to the genus *Conus* (Taylor *et al.,* 1993 ; Puillandre *et al.,* 2008). Several species are already described in *Benthomangelia*, using only morphological characters. Our strategy was to sequence the COI barcode gene of 42 specimens available in the Muséum National d'Histoire Naturelle (MNHN) of Paris, collected recently in South-West Pacific, without any *a priori* hypotheses of species delimitation. As shown in *Figure 3A*, the analysis of genetic distances

between all specimens reveals a gap between low and high genetic distances. This gap has been used to define five entities, each including specimens separated by low genetic distances. A phylogenetic approach, using both likelihood (PhyML ; Guindon and Gascuel, 2003) and bayesian (Mr. Bayes ; Huelsenbeck *et al*., 2001) methods found the same five entities (*Figure 3B*). These entities were also recovered with an independent nuclear gene, a fragment of the 28S, confirming the lack of genetic exchange between them. The three criteria (similarity, common evolutionary history and genetic exchange) are successfully applied to all five entities.

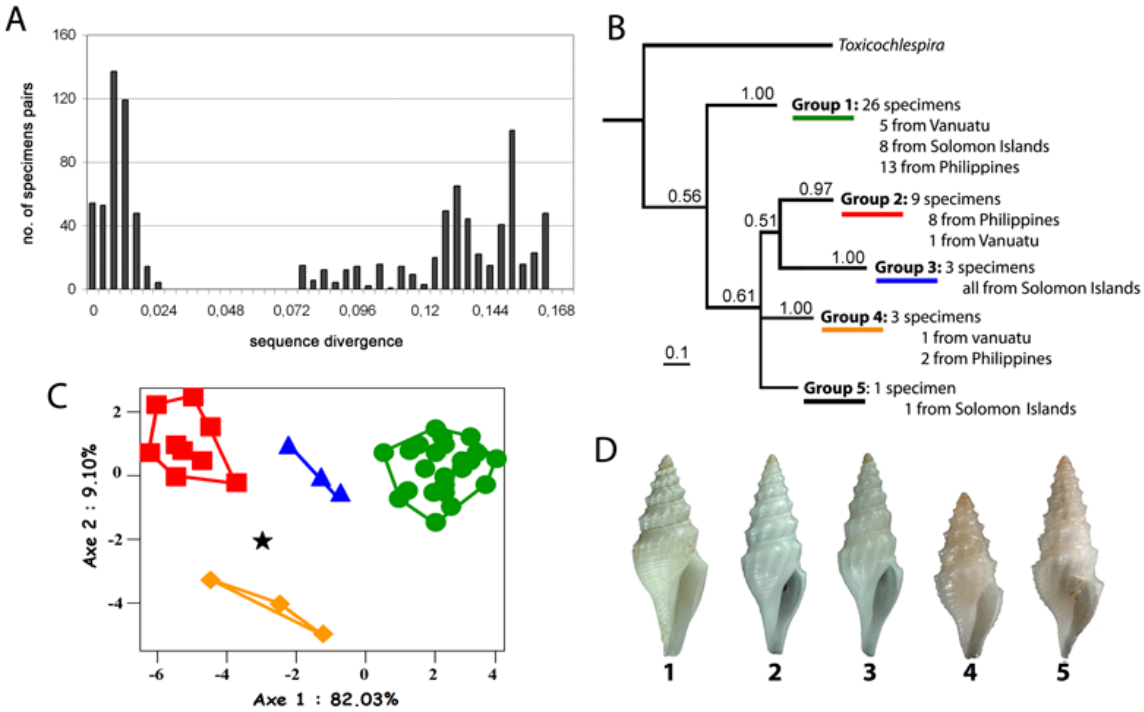

Fig. 3. Species delimitation in *Benthomangelia*. (**A**) Histogram of genetic distances calculated between all sequences. (**B**) Phylogenetic tree obtained with the COI gene. Five groups are delimited (intra-groups relationships are not shown). (**C**) Discriminate analysis between genetic groups. (**D**) One shell is illustrated for each delimited group.

Fig. 3. *Délimitation d'espèces au sein du genre* Benthomangelia*. (**A**) Histogrammes des distances génétiques calculées entre chaque paire de séquences. (**B**) Arbre phylogénétique obtenu avec le gène COI (les branchements au sein des groupes ne sont pas montrés). (**C**) Analyse discriminante entre les groupes génétiques. (**D**) Chaque groupe est illustré par une coquille.*

We also performed a morphological analysis on the same 42 specimens. The outline of the last whorl of each shell was reconstructed using an Elliptic Fourier Analysis (EFA) (Rohlf, 1996). This approach is supposed to detect slight differences in shape often not detectable by eye. A discriminate analysis, used to maximize the morphological variability between the five entities defined genetically, revealed strong differences in the shape of the last whorl (*Figure 3C*). However, morphological differences were also found between geographical region revealing a potential combined effect of genetics and environment on this morphological character. Nonetheless, finding morphological differences between the genetic groups strongly support our hypotheses of species delimitation. We also applied the same methodology to other conoidean groups (*Gemmuloborsonia*, *Bathytoma*, Turrinae, etc), each time delimiting cryptic species that were not detected with morphological characters. This is particularly striking in the genus *Bathytoma*, where the species *B. atractoides*, thought to include most of the South-West Pacific variability (Sysoev and Bouchet, 2001), was separated in at least 10 different species (Puillandre *et al*., submitted).

Phylogenetic reconstruction

What is true at the species level ("alpha-taxonomy") is also true at higher taxonomic levels ("beta-taxonomy"). The use of molecular characters has changed our understanding of classification by revealing unexpected relationships and by clarifying conoidean evolution. The classification of conoideans (*e.g.* Thiele, 1929 ; Powell, 1942, 1966 ; McLean, 1971) traditionally recognizes three main families : Conidae, with the genus *Conus*, Terebridae ("auger snails"), and Turridae, a heterogeneous group more or less defined as "all conoideans except cone and auger snails". Taylor *et al.* (1993) completely reorganized this classification by including several subfamilies in Conidae previously placed in Turridae. Although most of the previous authors based their conclusions on the analysis of shell and radula characters, Taylor *et al*. mainly relied on anatomical characters. A molecular phylogeny based on several mitochondrial (COI) and nuclear markers (28S, 18S, H3) globally confirmed their results, as the family Turridae (*sensu lato*) was paraphyletic, *i.e.* it included the two other families of the group (Conidae and Terebridae), some turrids being more closely related to *Conus* than to other turrids (*Figure 4*) (Puillandre *et al*., 2008).

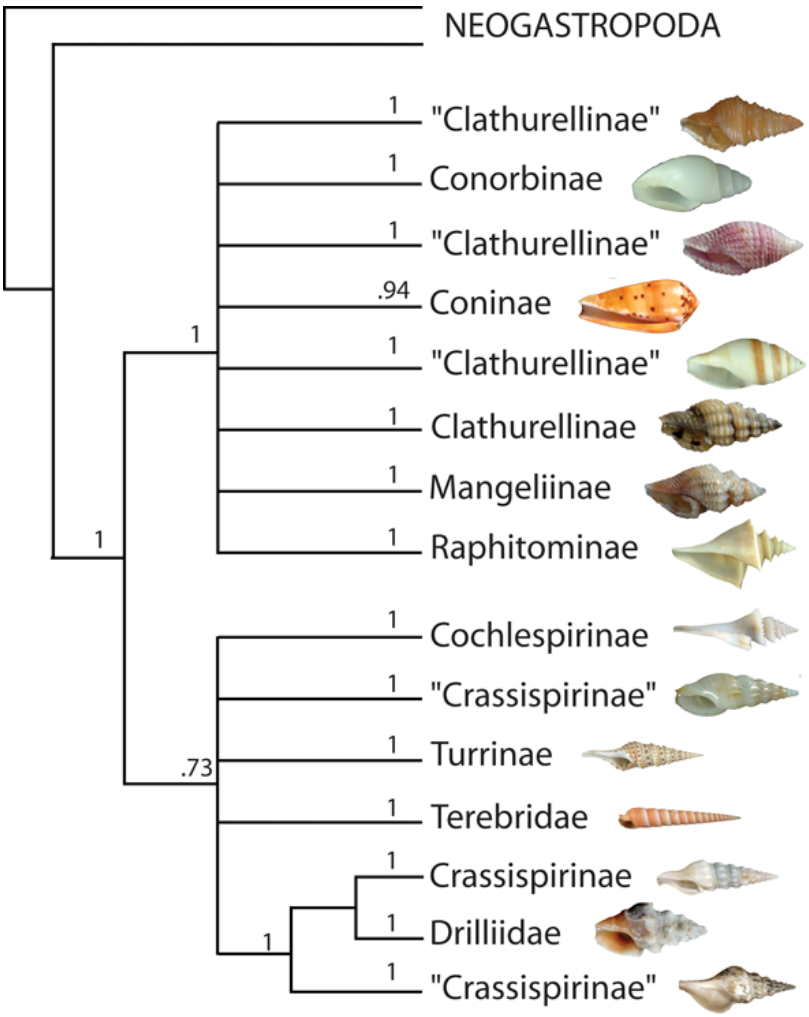

Fig. 4. Molecular phylogeny of Conoidea. Posterior probabilities are given for each node.

Fig. 4. *Phylogénie moléculaire des Conoidea. Les probabilités postérieures sont précisées pour chaque noeud.*

This molecular phylogeny, recently updated by the inclusion of several taxa missing in the tree shown in *Figure 4*, will be used to prepare a new classification for conoideans (Puillandre *et al*., in preparation). Actually, the genus *Conus* (*i.e*. the Conidae *sensu stricto*) and Terebridae are only two lineages among the fifteen currently recognized. A new classification will have to take into account this result and Turridae *sensu lato* will no longer be a valid family, as it includes lineages as divergent as Conidae and Terebridae could be. This result is not without consequence for the biochemist as each lineage may have evolved different toxins.

In another analysis, three mitochondrial genes (COI, 12S and 16S) were sequenced and used to infer the phylogenetic relationships between ~50 Terebridae species included in 10 different genera (*Figure 5*) (Holford *et al*., 2009). Five major lineages were defined : the first included the species "*Terebra*" *jungi*, the second the genus *Acus*, the third the genera *Cinguloterebra* and *Terebra* (both of them being polyphyletic), the fourth the genera *Hastula* and *Impages* (*Impages* being included in *Hastula*), and the last included the genera *Hastulopsis*, *Myurella*, *Strioterebrum*, *Clathroterebra* and *Terenolla*, all of them except *Terenolla* being polyphyletic. We also mapped on the tree the presence and absence of the venom apparatus in most of the species included in the analysis. Two independent lineages do not possess a venom apparatus, suggesting that it has been lost twice independently during the evolution of Terebridae.

This result is of great value to facilitate the discovery of new toxins. The tree constitutes a real "map" to guide the biochemist. Three lineages are susceptible to have evolved different toxins. In particular, the species "*Terebra*" *jungi* - morphologically not suspected to be so different from the other auger snails - is actually the first lineage to diverge in terebrid evolution, and thus constitutes a good target for toxin investigation.

Conclusion : taxonomy-based toxin discovery

This renewed taxonomy is thus both conceptual, as the taxonomic practices are replaced in a rigorous scientific framework, and methodological, through the use of a combination of several characters and criteria. For marine molluscs, and especially for conoideans, taxonomy and phylogeny integrating molecular characters are now causing a major shift in our perception of the classification and species diversity. At the

species level, morphological approaches generally led to an underestimation of the diversity, and the discovery of new species is promising for the search for new toxins. Analyses within *Conus* also indicate that some species actually include several cryptic species, each of them thought to produce its own sets of conotoxins (Duda *et al*., 2008 ; unpublished results).

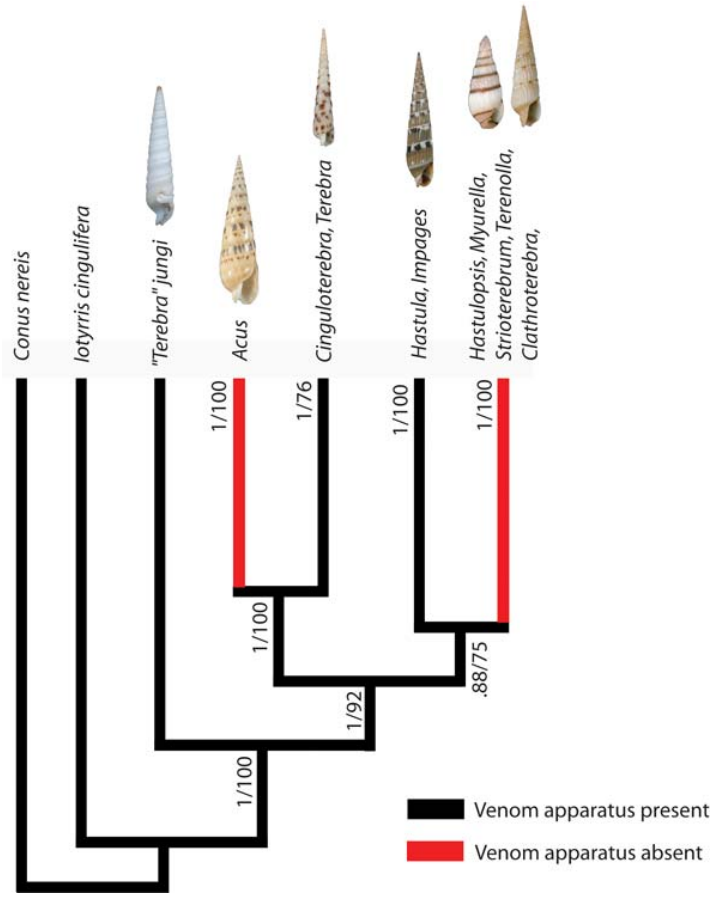

Fig. 5. Evolution of the venom apparatus in Terebridae. The molecular phylogeny defined five major lineages, each including several species not represented here. Posterior probabilities and boostraps are given for each node.

Fig. 5. *Evolution de l'appareil venimeux chez les Terebridae. La phylogénie moléculaire a permis de définir cinq lignées principales, chacune incluant plusieurs espèces non détaillées ici. Les probabilités postérieures et les « bosstraps » sont précisés pour chaque nœud.*

Phylogenetic analyses also proved their utility, as we saw for examples in the family Terebridae. We furthermore performed a phylogenetic analysis of the A-superfamily of conotoxins within the *Pionoconus* clade (Puillandre *et al*., submitted). Several lineages have been defined, each being the result of duplication events, followed by a rapid evolution by positive selection. Consequently, each defined clade has evolved its own function. This property could be used to accelerate the discovery of new toxins, by focusing the effort on lineages for which functions are still unknown and whose divergence with other lineages might have led to the apparition of unique functions. As illustrated by this direct correlation between the work of the taxonomist and the biochemist, we are entering in a new "gold age" for taxonomy that will not only benefit to a better knowledge, and thus a better conservation of the biodiversity, but also to most other researchers for whom taxa delimitation is a cornerstone.

Acknowledgements. *The research work presented in this article has been done in the MNHN of Paris and in the Olivera lab at the University of Utah, in collaboration with Michel Baylac, Marie-Catherine Boisselier, Philippe Bouchet, Mandë Holford, Yuri Kantor, Baldomero Olivera, Sarah Samadi, Ellen Strong, Alexander Sysoev, Yves Terryn and Maren Watkins. I am also pleased to thank Nicole Kraus for constructive comments on the manuscript and English improvements.*

References

Agapow PM, Bininda-Edmonds ORP, Crandall KA, Gittleman JL, Mace GM, Marshall JC, Purvis A (2004) The impact of species concept on biodiversity studies. *Q Rev Biol* **79**: 161-179

Bouchet P, Lozouet P, Maestrati P, Héros V (2002) Assessing the magnitude of species richness in tropical marine environments: exceptionally high numbers of molluscs at a new Caledonian site. *Biol J Linn Soc* **75**: 421-436

Bouchet P, Héros V, Lozouet P, Maestrati P (2008) A quater-century of deep-sea malacological exploration in the South and West Pacific: Where do we stand? How far to go? In *Tropical Deep-Sea Benthos,* Héros V, Corwie RH and Bouchet P (eds) pp 1-40. Mémoires du Muséum national d'Histoire naturelle, Paris

Brookes JI, Rochette R (2007) Mechanism of a plastic phenotypic response: predator-induced shell thickening in the intertidal gastropod *Littorina obtusata*. *J Evolution Biol* **20**: 1015-1027

da Motta AJ (1991) *A Systematic Classification of the Gastropod Family Conidae at the generic level*. La Conchiglia, Roma

Dayrat B (2005) Towards integrative taxonomy. *Biol J Linn Soc* **85**: 407-415

De Queiroz K (1998) The general lineage concept of species, species criteria, and the process of speciation: a conceptual unification and terminological recommendations. In *Endless Forms: Species and Speciation*, Howard DJ and Berlocher SH (eds) pp 57-75. Oxford University Press, Oxford

De Queiroz K (2007) Species concepts and species delimitation. *Syst Biol* **56**: 879-886

Duda TF, Bolina MB, Meyer C, Kohn AJ (2008) Hidden diversity in a hyperdiverse gastropod genus: Discovery of previously unidentified members of a *Conus* species complex *Mol Phylogenet Evol* **49**: 867-876

Duda TF, Kohn AJ (2005) Species-level phylogeography and evolutionary history of the hyperdiverse marine gastropod genus *Conus*. *Mol Phylogenet* **34**: 257-272

Ebach MC, Holdrege C (2005) DNA barcoding is no substitute for taxonomy. *Nature* **434**: 697

Fu J, Zeng X (2008) How many species are in the genus *Batrachuperus*? A phylogeographical analysis of the stream salamanders (family Hynobiidae) from southwestern China. *Mol Ecol* **17**: 1469-1488

Godfray HCJ (2006) To boldly sequence. *Trends Ecol Evol* **21**: 603-604

Guindon S, Gascuel O (2003) A simple, fast, and accurate algorithm to estimate large phylogenies by maximum likelihood. *Syst Biol* **52**: 696-704

Hajibabaei M, Janzen DH, Burns JM, Hallwachs W, Hebert PDN (2006) DNA barcodes distinguish species of tropical Lepidoptera. *Proc Nat Acad Sci* **103**: 968-971

Hebert PDN, Cywinska A, Ball SL, deWaard JR (2003) Biological identifications through DNA Barcodes. *Proc R Soc B* **270**: 313-321

Hebert PDN, Stoeckle MY, Zemlak TS, Francis CM (2004) Identification of birds through DNA barcodes. *PLoS Biol* **2**: 1657-1663

Holford M, Puillandre N, Terryn Y, Cruaud C, Olivera BM, Bouchet P (2009) Evolution of the Toxoglossa Venom Apparatus as Inferred by Molecular Phylogeny of the Terebridae. *Mol Biol Evol* **26**: 15-25

Hollander J, Collyer ML, Adams DC, Johannesson K (2006) Phenotypic plasticity in two marine snails: constraints superseding life history. *J Evol Biol* **19**: 1861–1872

Huelsenbeck JP, Ronquist F, Hall B (2001) MrBayes: bayesian inference of phylogeny. *Bioinformatics* **17**: 754-755

Imperial JS, Kantor Y, Watkins M, Heralde FM, Stevenson B, Chen P, Hansson K, Stenflo J, Ownby J-P, Bouchet P, Olivera BM (2007) Venomous Auger Snail *Hastula* (*Impages*) *hectica* (Linnaeus, 1758): Molecular Phylogeny, Foregut Anatomy and Comparative Toxinology. *J Exp Zool* **308B**: 744–756

Janzen DH, Hajibabaei M, Burns JM, Hallwachs W, Hebert PDN (2005) Wedding biodiversity inventory of a large and complex lepidopteria fauna with DNA Barcoding. *Philos T R Soc B* **360**: 1835-1845

Knudsen J (1950) Egg capsules and development of some marine prosobranchs from tropical West Africa. *Atlantide Report* **1**: 85-130

Kohn AJ (1990) Tempo and mode of evolution in Conidae. *Malacologia* **32**: 55-67

Lorenz JG, Jackson WE, Beck JC, Hanner R (2005) The problems and promise of DNA barcodes for species diagnosis of primate biomaterials. *Philos T R Soc B* **360**: 1869-1877

McLean JH (1971) A revised classification of the family Turridae, with the proposal of new subfamilies, genera and subgenera from the Eastern pacific. *The Veliger* **14**: 114-130

Meyer PC, Paulay G (2005) DNA Barcoding: error rates based on comprehensive sampling. *PLoS Biology* **3**: 1-10

Moritz C, Cicero C (2004) DNA Barcodes : promise and pitfalls. *PLoS Biology* **2**: 1529-1531

Nichols R (2001) Gene trees and species trees are not the same. *Trends Ecol Evol* **16**: 358-364

Olivera BM (2006) *Conus* Peptides: Biodiversity-based Discovery and Exogenomics. *J Biol Chem* **281**: 31173-31177

Olivera BM (2008) Venom peptides from *Conus* and other Conoideans : prospects and perspectives. In *Toxines et fonctions cholinergiques neuronales et non neuronales*, Benoit E, Goudey-Perrière F, Marchot P and Servent D (eds) pp 33-41. Publications de la SFET, Châtenay-Malabry, France, Epub on http://www.sfet.asso.fr (ISSN 1760-6004)

Powell AWB (1942) The New-Zealand recent and fossil Mollusca of the family Turridae. With general notes on turrid nomenclature and systematics. *Bulletin of the Auckland Institute and Museum* **2**: 1-192

Powell AWB (1966) The molluscan families Speightiidae and Turridae. An evaluation of the valid taxa, both recent and fossil, with lists of characteristics species. *Bulletin of the Auckland Institute and Museum* **5**: 5-184

Puillandre N, Baylac M, Boisselier MC, Cruaud C, Samadi S (2009a) An integrative approach of species delimitation in the genus Benthomangelia (Mollusca: Conoidea). *Biol J Linn Soc* **96**: 696-708

Puillandre N, Samadi S, Boisselier MC, Sysoev AV, Kantor YI, Cruaud C, Couloux A, Bouchet P (2008) Starting to unravel the toxoglossan knot: molecular phylogeny of the "turrids" (Neogastropoda: Conoidea). *Mol Phylogenet Evol* **47**: 1122-1134

Puillandre N, Strong E, Bouchet P, Boisselier MC, Couloux A, Samadi S (2009b) Identifying gastropod spawn from DNA barcodes: possible but not yet practicable. *Mol Ecol Resources* doi: 10.1111/j.1755-0998.2009.02576.x

Reid DG, Lal K, Mackenzie-Dodds J, Kaligis F, Littlewood DTJ, Williams ST (2006) Comparative phylogeography and species boundaries in *Echinolittorina* snails in the central Indo-West Pacific. *J Biogeogr* **33**: 990-1006

Rohlf FJ (1996) TpsDig. *Stata University of New-York at Stony Brook, http://life.bio.sunysb.edu/morph/.*

Rosenberg NA, Tao R (2008) Discordance of species trees with their most likely gene trees: the case of five taxa. *System Biol* **57**: 131-140

Samadi S, Barberousse A (2006) The tree, the network, and the species. *Biol J Linn Soc* **89**: 509-521

Shearer TL, Coffroth MA (2008) Barcoding corals: limited by interspecific divergence, not intraspecific variation. *Mol Ecol Resources* **8**: 247-255

Sites JW, Marshall JC (2003) Delimiting species: a renaissance issue in systematic biology. *Trends Ecol Evol* **19**: 462-470

Smith MA, Poyarkov Jr. NA, Hebert PDN (2008) CO1 DNA barcoding amphibians: take the chance, meet the challenge. *Mol Ecol Resources* **8**: 235-246

Sysoev A, Bouchet P (2001) New and uncommon turriform gastropods (Gastropoda: Conoidea) from the South-West Pacific. In P. Bouchet & B. A. Marshall (eds), Tropical Deep-Sea Benthos, Volume 22. *Mémoires du Muséum National d'Histoire Naturelle* **185**: 271-320

Taylor JD, Kantor YI, Sysoev AV (1993) Foregut anatomy, feedings mechanisms and classification of the Conoidea (= Toxoglossa)(Gastropoda). *Bull Nat Hist Mus Lond (Zoology)* **59**: 125-170

Terlau H, Olivera BM (2004) *Conus* Venoms: A rich source of novel ion channel-targeted peptides. *Physiol Rev* **84**: 41-68

Thiele J (1929) *Handbuch der systematischen weichtierkunde*. Fischer G (ed) Jena

Tryon GW (1884) *Manual of Conchology, Structural and systematic, with illustrations of the species,* Tryon GW (ed) vol. VI, *Conidae*, *Pleurotomidae*, 544 p. Academy of Natural Sciences, Conchological Section, Philadelphia

Vaglia T, Haxaire J, Kitching IJ, Meusnier I, Rougerie R (2008) Morphology and DNA barcoding reveal three cryptic species within the Xylophanes neoptolemus and loelia species-groups (Lepidoptera: Sphingidae). *Zootaxa* **1923**: 18-36

Vogler AP, Monaghan MT (2007) Recent advances in DNA taxonomy. *J Zool System Evolution Res* **45**: 1-10

Watkins M, Hillyard DR, Olivera BM (2006) Genes Expressed in a Turrid Venom Duct: Divergence and Similarity to Conotoxins. *J Mol Evol* **62**: 247-256

Wiens JJ (2007) Species delimitation: new approaches for discovering diversity. *Syst Biol* **56**: 875-878

Toxines et Signalisation – Toxins and Signalling
Rencontres en Toxinologie – Meeting on Toxinology, 2009
Editions de la SFET – SFET Editions
Accès libre en ligne sur le site – Free access on line on the site : http://www.sfet.asso.fr

Les Mollusques marins venimeux

Anne DESCOURS[1], Philippe FAVREAU[2*]

[1] *Toxinomics Foundation, Ch. des Aulx 18, 1228 Plan-les-Ouates, Suisse ;* [2] *Atheris Laboratoires, CP314, 1233 Bernex, Suisse*

** Auteur correspondant ; Tél : +41 (0)22 850 05 85 ; Fax : +41 (0)22 850 05 86 ;*
Courriel : philippe.favreau@atheris.ch

Résumé

Les Mollusques marins constituent un groupe d'animaux extrêmement vaste et qui présente une richesse exceptionnelle, que ce soit en nombre ou en diversité d'espèces en fonction des sites géographiques étudiés. La majorité de ces animaux restent probablement à être identifiés et classés dans l'embranchement des Mollusques. Dans le groupe actuel, les Mollusques marins venimeux forment un ensemble non négligeable d'espèces (~5-10%), que l'on trouve dans deux classes distinctes. Ainsi, les Mollusques marins venimeux sont présents d'une part chez les Céphalopodes, caractérisés par un véritable cerveau et un pied muni de ventouses, et d'autre part chez les Gastéropodes, et plus précisément dans la superfamille Conoidea. Malgré leur parenté, ces deux classes de Mollusques montrent une totale divergence de leur système venimeux, et plus particulièrement sur les composants des venins.

Venomous marine molluscs

Marine molluscs constitute an extremely wide animal group, showing an exceptional richness either in number or in diversity of species depending on collecting sites. The vast majority of these animals still remain to be identified and classified in the mollusc phylum. In the current group, venomous marine molluscs represent a non negligible part of the species (~5-10%), that can be found in two distinct classes. Thus, venomous marine molluscs are present on one hand in cephalopods, characterised by a developed brain and feet with suckers, and on the other hand in gastropods, more precisely in the superfamily Conoidea. Despite their close relationships, these two classes of molluscs display a complete divergence in the venomous system, and more particularly on the venom content.

Keywords : *Mollusc, Cephalopod, Conoidea, conopeptides, venom.*

Introduction

Les Mollusques marins sont des animaux invertébrés caractérisés par un corps mou, recouvert ou non d'une coquille, et par un pied leur permettant de se mouvoir. Cet ensemble d'animaux marins constitue le groupe le plus vaste et le plus varié parmi tous les embranchements marins avec plus de 100.000 espèces (Glaubrecht, 2009). La diversité des Mollusques marins est telle que la découverte de nouvelles espèces continue à un rythme soutenu. A titre d'exemple, dans la seule région de la Nouvelle-Calédonie, l'échantillonnage de la faune benthique (100-1500 m) depuis environ 30 années, a permis de dénombrer plus de 1.000 espèces dont plus de la moitié sont nouvelles. La présence de zones de micro-endémisme, la difficulté de collectes exhaustives et les études en cours révèlent une probable diversité de plus de 15.000 espèces de Mollusques dans cette seule région Indo-Pacifique (Bouchet *et al.*, 2008).

Parmi les nombreuses familles de Mollusques, certaines ont développé un système venimeux leur permettant de capturer des proies et de se défendre contre des prédateurs (*Figure 1*). Dans la classe des Céphalopodes, et plus particulièrement chez les Octopodes, ces animaux carnivores utilisent un système venimeux leur permettant de capturer mollusques, crustacés et poissons. Dans la classe des Gastéropodes, les Mollusques de la superfamille Conoidea utilisent leur venin pour se nourrir de vers, mollusques et poissons. Bien qu'inclus dans le même embranchement, ces deux groupes d'animaux ont développé indépendamment deux systèmes venimeux différents, laissant cependant apparaître des similitudes avec les venins d'Arthropodes (scorpions, araignées, hyménoptères) ou de Chordés (serpents).

Les Céphalopodes venimeux

La classe des Céphalopodes compte à ce jour environ 800 espèces connues réparties en deux sous-classes et quatre ordres. Les espèces venimeuses sont uniquement présentes dans la superfamille *Coleoidea*, et plus particulièrement parmi les seiches (famille Sepiidae) et les pieuvres (famille Octopodidae). Les

calmars appartiennent au même groupe que les seiches (Décapodiformes) et partagent les mêmes caractéristiques, mais ne sont pas systématiquement venimeux.

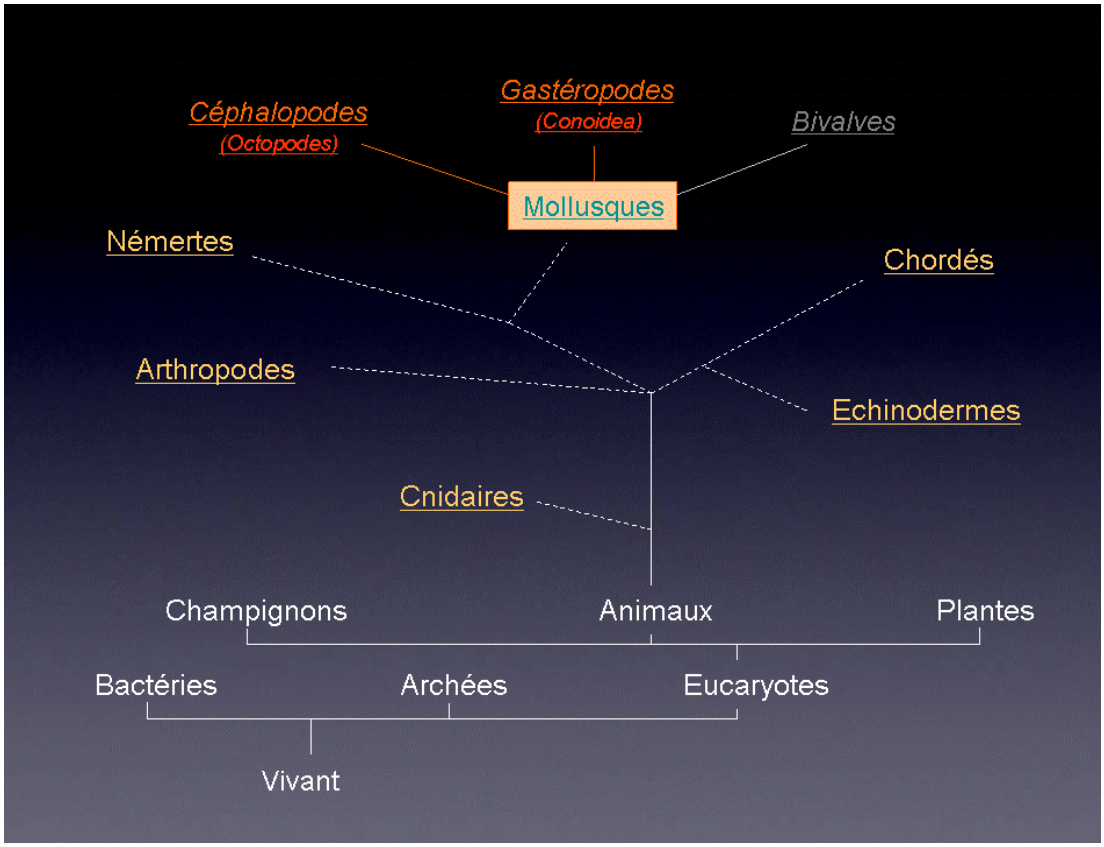

Fig. 1. Situation schématique des Mollusques marins venimeux (en rouge) dans l'arbre du vivant, adapté à partir du « Tree of Life Web Project » (Maddison *et al.*, 2007). A titre de comparaison, les embranchements incluant des animaux venimeux sont en jaune. Dans la classe Cephalopoda, seuls les Octopoda présentent des organismes venimeux dangereux pour l'homme. La classe Gasteropoda contient probablement plusieurs milliers d'espèces venimeuses, une partie importante étant rassemblée dans la superfamille Conoidea. Les nombreux autres embranchements, classes et familles n'ont pas été représentés pour une plus grande clarté. Il est à noter que les relations précises entre embranchements sont sujettes à continuelle révision (lignes pointillées).

Fig. 1. *Schematic situation of venomous marine molluscs (in red) in the Tree of Life, adapted from "Tree of Life Web Project" (Maddison et al., 2007). For comparison, phyla including venomous animals are underlined and in yellow. In the Cephalopoda class, only Octopoda include dangerous venomous animals. The Gastropoda class probably contains several thousands of venomous species, all of them gathered in the Conoidea superfamily. The numerous other phyla, classes and families have been omitted for clarity. One should note that precise phylogenetic relationships are subjected to constant changes (dashed lines).*

Les Céphalopodes sont présents dans tous les océans, sous toutes les latitudes et à toutes les profondeurs. Certaines espèces ont un mode de vie benthique, d'autres un mode de vie pélagique et d'autres encore peuvent en changer au cours de leur développement. Une grande variété de formes et de tailles existe parmi ces espèces qui vivent entre 1 et 7 ans pour les plus grandes. Tous les Céphalopodes, à l'exception des nautiles, ont la capacité de modifier rapidement l'apparence de leur tégument (couleur et texture) pour se camoufler, envoyer des signaux d'alarme ou pour communiquer avec leurs congénères.

Les Céphalopodes (du grec *képhalé* – tête et *podos* – pied) ont également pour caractéristiques communes : un cerveau contenu dans un crâne cartilagineux (beaucoup plus développé que celui de la plupart des invertébrés), de longs bras équipés de ventouses et un système de propulsion performant composé d'un manteau contractile et d'un siphon. Tous les membres de cette classe sont carnivores et possèdent, au centre de la base des tentacules, un bec corné qui leur permet de mordre leurs proies (mollusques, crustacés ou poissons) et, pour les espèces venimeuses, de créer une plaie où les toxines du venin pourront pénétrer et agir rapidement.

Chez les seiches ou les poulpes, qui sont tous venimeux, le venin est produit dans la glande salivaire postérieure ou glande à venin. Il suit ensuite un conduit parallèle à l'œsophage pour se mélanger à la salive produite par les glandes salivaires antérieures (Sutherland et Tibballs, 2001). Le mélange est ensuite appliqué par morsure, par simple pression de la masse buccale. L'action conjuguée du venin et des enzymes contenues dans la salive permet d'immobiliser la proie et de commencer rapidement la digestion de celle-ci. Tout comme les Gastéropodes, les Céphalopodes utilisent des radulas pour déchiqueter leur victime à l'intérieur de leur cavité buccale.

Les seiches (ordre des Sepioidea) et les calmars (ordre des Teuthoidea)

Les seiches (environ 120 espèces), tout comme les calmars (environ 350 espèces) sont des Décapodes munis de 8 bras et de 2 tentacules (*Figure 2*). Ces tentacules sont utilisés pour saisir une proie et l'amener jusqu'au bec de chitine où elle peut être envenimée. Ces Décapodes ont tous conservé au fil de l'évolution un squelette interne poreux, appelé os de seiche pour les Sepioidea ou plume pour les calmars, qui leur permet de contrôler leur flottabilité. Les seiches et les calmars sont généralement de petite taille, de 10 à 30 cm, et ont une durée de vie réduite (1 à 2 ans). Les seiches ont un cerveau très développé et sont capables d'apprentissage complexe, qualité généralement réservée aux Vertébrés (Hvorecny *et al.*, 2007).

En cas de danger, ces animaux sont également capables de sécréter un jet d'encre noire, appelée sépia, pour dissimuler leur fuite ou détourner l'attention d'un prédateur. Il semble que l'encre pourrait également agir sur les prédateurs comme moyen de défense chimique (Derby, 2007). L'encre, tout comme le venin de ces espèces, n'a été que très peu étudiée mais semble contenir un certain nombre de composés bioactifs à usage thérapeutique potentiel (Russo *et al*., 2003).

Si l'ensemble des Sepioidea et une partie des Teuthoidea sont venimeux, aucune espèce n'a été décrite comme dangereuse pour l'homme. Les venins des Céphalopodes, et des Décapodes en particulier, n'ont été que marginalement explorés. De façon générale, leurs venins montrent peu de ressemblances avec ceux de leurs lointains cousins, les Gastéropodes marins venimeux. Des similitudes étonnantes ont par contre été décrites entre le venin de *Sepia latimanus* et ceux d'animaux appartenant à d'autres embranchements. L'analyse de la glande postérieure de cette espèce a par exemple montré la présence de phospholipases A_2 (PLA_2) analogues aux toxines présentes dans les venins de lézards, de chenilles ou de scorpions (Fry *et al*., 2009). Par ailleurs, des céphalotoxines (toxines de céphalopodes), famille de glycoprotéines qui n'avait jusqu'à présent été décrite que pour les Octopodes, ont été récemment trouvées dans les glandes postérieures de plusieurs espèces de seiches et de calmars (Ueda *et al*., 2008). Ces toxines semblent provoquer une paralysie flasque chez les crustacés, et pour certaines chez les souris, rappelant l'activité de la tétrodotoxine. L'analyse des toxines issues de Décapodiformes reste un vaste terrain à explorer puisque la SE-céphalotoxine, extraite de l'espèce *Sepia esculenta* et décrite par Ueda en 2008, est la première céphalotoxine de décapodiforme dont la structure primaire a été identifiée. Il s'agit d'une glycoprotéine d'environ 100 kDa dont la séquence est originale. Une recherche par BLAST a cependant montré qu'elle comportait des domaines homologues à certains domaines du facteur de croissance épidermique (EGF), de la thrombospondine de type I et du récepteur LDL (low-density lipoprotein) de classe A.

F**ig. 2.** Les seiches et les calmars appartiennent au super-ordre des Décapodiformes alors que les pieuvres appartiennent à celui des Octopodiformes. Toutes les seiches et pieuvres, ainsi qu'une partie des calmars, sont venimeux. Ci-dessus, un calmar (espèce non identifiée) de Mer Rouge (Photo par Winfried Werzmirzowsky).

Fig. 2. *Cuttlefish and squids belong to the Decapodiforme superorder, while octopi belong to the Octopodiforme super-order. All cuttlefish and octopi, and some squids, are venomous. Above, a squid (unidentified species) from the Red Sea (Picture by Winfried Werzmirzowsky).*

Les pieuvres, poulpes et eledones (ordre des Octopoda)

Les Octopodes, comme leur nom l'indique, possèdent 8 bras et sont dépourvus de squelette. Ils ont par ailleurs beaucoup de traits communs avec leurs cousins Sepioidea. Ils utilisent les mêmes moyens de camouflage (jet

d'encre et capacité à changer de couleur et d'apparence) et sont dotés d'une intelligence et d'une mémoire bien supérieures à celles des autres invertébrés.

Parmi les 300 espèces d'Octopodes décrites, seules celles du genre *Hapalochlaena* sont potentiellement mortelles pour l'homme. Quelques cas d'envenimations sévères ou fatals ont été décrits, tous caractérisés par une morsure quasiment indolore puis par des symptômes paralytiques musculaires conduisant à une insuffisance respiratoire (Cavazzoni *et al.*, 2008). Ceci est dû à la présence de concentrations importantes de tétrodotoxine (TTX) dans la glande à venin et donc dans le venin des *Hapalochlaena* (Sutherland, 1969). La TTX agit comme inhibiteur des canaux sodiques musculaires et neuronaux, ce qui provoque une paralysie flasque chez les proies (crustacés ou vertébrés). Cette toxine a également été détectée dans de nombreux tissus de ces pieuvres (Yotsu-Yamashita *et al*., 2007) ainsi que dans leur encre (Williams & Caldwell, 2009). Comme chez d'autres animaux marins qui l'utilisent pour la défense ou la prédation, la TTX présente chez les *Hapalochalena* est d'origine bactérienne, produite par des bactéries endosymbiotiques du genre *Vibrio* (Simidu *et al*., 1987).

Outre la tétrodotoxine et autres molécules analogues comme la saxitoxine (Robertson *et al.*, 2004), très peu de composés issus de venin d'Octopodes ont été caractérisés. Quelques céphalotoxines, connues pour leur activité paralysante sur les crustacés, ont été isolées de la glande salivaire postérieure de plusieurs espèces de pieuvres (Cariello et Zanetti, 1977). L'élédoïsine, petit peptide extrait de la glande des *Eledone*, en est un autre exemple (Erspamer et Anastasi, 1962). Le genre *Eledone* semble montrer une diversité moléculaire intéressante pour la recherche de composés bioactifs (Key *et al*., 2002). C'est également le cas pour la plupart des autres Octopodes, puisque même la pieuvre commune a récemment donné lieu à la découverte de nouvelles toxines peptidiques, également de type tachykinine (Kanda *et al*., 2003). Dans les glandes salivaires des pieuvres sont aussi exprimées différentes protéines dont des enzymes et diverses toxines. Ces molécules ne semblent encore une fois pas directement apparentées à celles exprimées par les autres mollusques marins venimeux (Fry *et al*., 2009). Si certaines toxines, telles que les CAP (Protéines secrétées riches en cystéine) sont également présentes chez les cônes (présentés plus loin) comme chez plusieurs autres animaux venimeux, leurs séquences diffèrent assez largement et semblent être éloignées phylogénétiquement. D'autres familles de protéines décelées chez les pieuvres sont totalement absentes du protéome des *Conoidea* mais sont exprimées par d'autres taxons. C'est le cas des chitinases que l'on retrouve dans le venin des Octopodes et dans celui des guêpes.

Les venins de Céphalopodes n'ont jusqu'à présent pas retenu la même attention que ceux de leurs cousins Conoidea. Mais l'étude du transcriptome des glandes salivaires postérieure et antérieure de ces animaux et de leur protéome n'est pas dénuée d'intérêt pour autant. Leurs sécrétions recèlent certainement une diversité moléculaire tout aussi riche que celle connue pour les autres animaux venimeux. Et il est probable que l'étude de ces espèces, jusqu'à présent négligées par la recherche, révélerait l'existence de nouvelles familles de protéines et alimenterait le réservoir des molécules d'origine naturelle à usage thérapeutique.

Les Mollusques Gastéropodes

La majorité des Mollusques Gastéropodes vivent en milieu marin et forment le groupe le plus étendu des mollusques avec plus de 90.000 espèces répertoriées. Ces animaux se caractérisent par leur système digestif (du grec « gaster », estomac) et leur pied (du grec « podos ») permettant de se mouvoir. Une partie des Gastéropodes marins sont des prédateurs carnivores et utilisent des systèmes de capture plus ou moins complexes. La famille de Mollusques Gastéropodes la plus étudiée sur le plan des venins est celle des Conoidea (discutée au paragraphe suivant) mais certaines autres familles présentent des espèces produisant des substances similaires aux venins dans leurs glandes salivaires.

Comme chez les Céphalopodes, il semble que la frontière entre glande salivaire et glande venimeuse soit ténue, et il est vraisemblable que les sécrétions « salivaires » de nombreux Mollusques Gastéropodes soient proches de substances venimeuses. La présence de tétramine (ion tetramethylammonium) dans les glandes salivaires de nombreux Buccinidae est par exemple à l'origine de cas d'empoisonnements humains, notamment au Japon (Kawashima *et al*., 2004). D'autres composés toxiques ont également été détectés dans les glandes salivaires de Buccinidae (*Buccinum schantaricum*), de Muricidae (*Acanthina spirata*, *Thais haemastoma*) et de Ranellidae (*Charonia sauliae*, *Cymatium echo*) (Shiomi *et al*., 2002). Les sécrétions de *Cymatium echo* ont fait l'objet d'études approfondies et plusieurs protéines toxiques, les echotoxines, ont été isolées et caractérisées (Kawashima *et al*., 2003). D'un poids moléculaire de 25 kDa, ces protéines ressemblent aux actinoporines isolées d'anémones de mer. Ces protéines hémolytiques, toxiques pour les mammifères, forment des pores dans les membranes cellulaires induisant une destruction des tissus. Malheureusement, les études concernant ces familles de Mollusques Gastéropodes restent très confidentielles et une grande partie des substances présentes chez ces organismes ne sont toujours pas connues.

La superfamille Conoidea

Parmi les nombreuses familles de Mollusques Gastéropodes, la superfamille Conoidea, appelée également Toxoglossa, est un groupe incluant des espèces comportant un système venimeux très élaboré. Le nombre d'espèces connues est actuellement de quelques milliers, mais la véritable quantité d'espèces et leurs diversités géographiques sont encore sous-estimées puisqu'il est accepté que la majorité des animaux de cette superfamille restent à découvrir, notamment dans les faunes profondes (Bouchet *et al.*, 2008). Par ailleurs, la phylogénie des toxoglosses est actuellement sujette à extrême révision. Du fait de la très grande diversité et de la complexité d'identification des espèces, la classification traditionnelle basée sur les caractères de la coquille ne permet pas d'établir une classification suffisamment claire et précise. Historiquement divisée en trois familles, les Conidae, les Terebridae et les Turridae, il est maintenant établi que la famille Turridae englobe les

précédentes, montrant la nécessité d'ajouter les caractéristiques anatomiques et ADN des espèces afin de revoir profondément la phylogénie de cette superfamille (Puillandre *et al.*, 2008). La connaissance de la phylogénie des Conoidea s'intègre parfaitement dans la recherche de composés du venin, en offrant une carte précieuse pour l'investigation ciblée du venin de certaines espèces afin de découvrir des composés originaux (Holford *et al.*, 2009b).

Quasiment toutes les espèces de ce groupe ont développé un système venimeux sophistiqué leur permettant de capturer des proies (poissons, mollusques ou vers) en dépit de leur relative lenteur de déplacement. Par exemple, chez les cônes, ce système venimeux est constitué d'une glande à venin tubulaire débouchant sur le pharynx, lui-même prolongé par un organe extensible, le proboscis. Afin de capturer une proie, l'animal porte une dent radulaire ou radula (*Figure 3*) à l'extrémité distale du proboscis qui va alors s'étendre au dehors de l'animal jusqu'à harponner sa proie. Le venin est alors immédiatement injecté à la victime, provoquant une paralysie et permettant au mollusque de glisser sa proie dans sa cavité buccale.

Une des caractéristiques du système venimeux de ces mollusques réside dans le développement plus ou moins marqué de la radula (Kantor et Taylor, 1991; Kantor et Taylor, 2000). Cette évolution a notamment conduit à l'utilisation des caractéristiques des radulae à des fins taxonomiques, notamment au rang familial (Taylor *et al.*, 1993). Dans certains cas, la morphologie de la radula est un indicateur précis permettant de différencier des spécimens supposés conspécifiques de par un premier examen conchyologique (Kantor *et al.*, 2008). Les Gastéropodes ayant développé les dents radulaires les plus sophistiquées restent les espèces du genre *Conus*. C'est également ce genre qui focalise l'attention des recherches sur le venin de ces animaux depuis plus de 30 années.

Les cônes

Les cônes (environ 700 espèces) peuvent être rencontrés dans tous les océans, généralement entre les 45ème parallèles nord et sud, avec une préférence pour les régions inter-tropicales, que ce soit dans les zones côtières ou les pentes continentales jusqu'à 800 m de profondeur. De forme conique ou biconique et une ouverture aux côtés parallèles, les coquilles de cônes présentent une extrême diversité de motifs et de couleurs ayant très tôt attiré l'attention des collectionneurs (*Figure 3*). Les envenimations humaines par les cônes sont rares et la dangerosité de la plupart des espèces n'est pas élevée. Cependant, plusieurs espèces sont considérées comme dangereuses, voire mortelles, comme le cône piscivore *Conus geographus* (Fegan et Andresen, 1997).

Les études du venin des cônes constituent 99% des publications sur les venins des toxoglosses depuis 30 ans, alors que les cônes représentent moins de 5% des espèces de ce groupe. L'intérêt suscité par ces animaux provient à la fois de la complexité et de la diversité de leur venin, offrant un potentiel pharmacologique démontré, mais aussi par un accès aisé aux spécimens et à des quantités raisonnables de venin. Par ailleurs, les molécules du venin sont généralement des peptides courts (10-50 acides aminés) et repliés par des ponts disulfure (1 à 5 ponts), accessibles par la synthèse chimique, facilitant ainsi leur utilisation et caractérisation. Les constituants des venins de cônes sont appelés conotoxines ou conopeptides, chacun appartenant à une famille en fonction de sa structure primaire et de son activité. Plus globalement, le terme conopeptide est maintenant utilisé pour les composants des venins des Conoidea. Un grand nombre de revues récentes permettent d'évaluer la composition et la nature des venins de cônes (Olivera, 2006b, 2008 ; Becker et Terlau, 2008). Cependant, trois caractéristiques majeures doivent être soulignées : la complexité, la variété de fonction des toxines et la diversité de ces venins.

La complexité d'un venin de cône est en grande partie liée au nombre de molécules constituant ce venin, généralement autour de 100-600 composés pour le venin injecté et plus de 1.000 pour un venin directement prélevé de la glande productrice (Biass *et al*., 2009). A cet égard, les venins de cônes peuvent être rapprochés des venins d'araignées ou de scorpions, extrêmement riches en molécules bioactives (Pimenta *et al.*, 2001; Escoubas *et al.*, 2008). La complexité des conopeptides repose à la fois sur un grand nombre de familles structurales, établies par l'agencement des ponts disulfure, mais aussi sur la combinaison des acides aminés à l'intérieur de ces structures. En effet, des mécanismes moléculaires spécifiques encore mal compris (Woodward *et al.*, 1990; Conticello *et al.*, 2001) provoquent une hypermutation des résidus (hors cystéine) à une fréquence bien supérieure au taux naturel, dans chaque famille structurale, générant un grand nombre de fonctions biologiques.

Très tôt, le nombre élevé de composés du venin de cône a montré une grande variété d'activités biologiques, plus particulièrement neurobiologiques (Olivera *et al*., 1990). Aujourd'hui, plus de 30 cibles physiologiques différentes appartenant à 11 classes de récepteurs et canaux ont été mises à jour, à partir de quelques dizaines d'espèces uniquement (Favreau et Stocklin, 2009). L'activité biologique du venin est principalement paralysante, soit par tétanie (action excitatrice continue), soit par blocage (action inhibitrice permanente) (Terlau *et al.*, 1996). D'un point de vue physiologique, cette activité peut être modulée par un très grand nombre de récepteurs et canaux ioniques, impliqués dans la transmission nerveuse. A titre d'exemple, le venin du cône piscivore *Conus consors* contient des α-, μ- et ω-conotoxines qui bloquent respectivement les récepteurs nicotiniques de l'acétylcholine, les canaux sodium et calcium sensibles au potentiel, provoquant un blocage de la transmission de l'influx nerveux et produisant une paralysie flasque de la proie (Favreau *et al*., 1999, 2001). Ce même venin contient également une toxine excitatrice, la CcTx (Le Gall *et al.*, 1999), induisant des trains de potentiels d'actions au niveau des fibres nerveuses, générant une paralysie tétanique. Le cône produit ainsi un venin « cocktail » actif sur un grand nombre de cibles différentes, lui permettant probablement une capture efficace et sécurisée des proies.

Enfin, les venins de cônes montrent une diversité extrêmement riche, que ce soit inter-espèce ou intra-

espèce. La diversité de venins entre espèces différentes n'est pas originale puisqu'une telle variété se retrouve aussi chez les autres espèces venimeuses, tels que les serpents, scorpions ou araignées (Menez, 1998). Un venin typique, propre à une espèce, peut même servir d'empreinte moléculaire comme cela a été montré à plusieurs reprises (Escoubas *et al*., 1997; Vianna Braga *et al*., 2005). Cela doit cependant être relativisé par la présence de variations significatives de venins intra-espèces, qui peuvent être liées à des paramètres d'âge, de sexe (mâles/femelles), de populations et/ou de localités (Herzig *et al.*, 2008 ; Abdel-Rahman *et al*., 2009 ; Barlow *et al.*, 2009). Ces variations à l'intérieur d'une même espèce se révèlent particulièrement importantes chez certains cônes. Une étude récente sur trois groupes de *Conus ventricosus* provenant de régions différentes a fait apparaître de fortes disparités dans la composition des venins de cette espèce méditerranéenne (Romeo *et al*., 2008). Cette grande variabilité a aussi été montrée pour plusieurs autres espèces (Jakubowski *et al*., 2005; Davis *et al.*, 2009), reflétant une caractéristique générale.

Cette complexité des venins, associée à une grande variété d'actions biologiques et une forte biodiversité montre à quel point ces venins constituent une richesse exceptionnelle de molécules bioactives. Un des aspects fondamentaux est l'étude du système venimeux dans son ensemble (Menez *et al*., 2006), et plus particulièrement des mécanismes à l'origine de l'évolution des venins (Olivera, 2006a). Cela pourra sans aucun doute permettre de mieux cerner les mécanismes d'une telle diversité et son utilisation à des fins biomédicales.

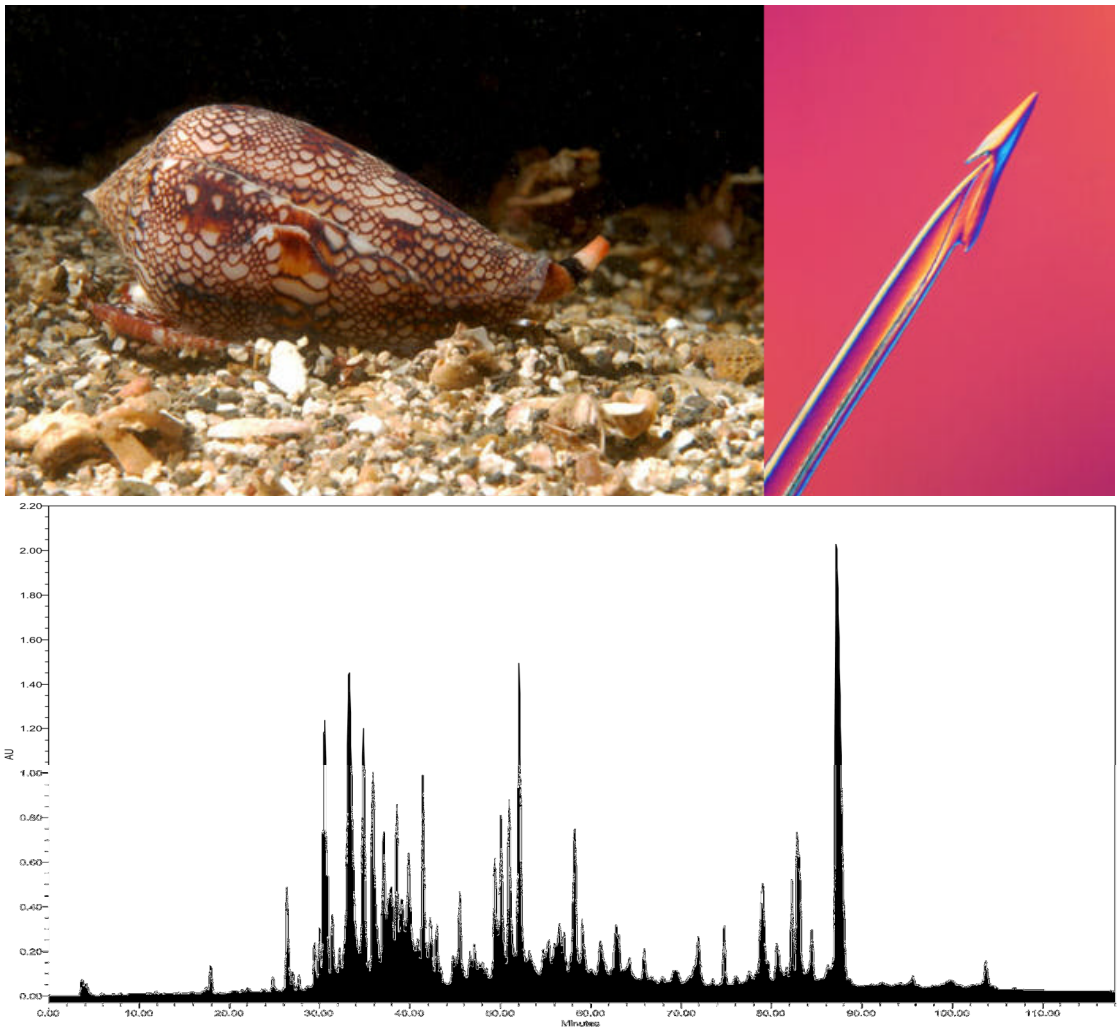

F**ig. 3.** La quasi totalité des études de venins de Conoidea sont focalisées sur la sous-famille Coninae, constituée du genre *Conus*. A gauche, *Conus textile textilinus*, cône malacophage, dans son environnement naturel (Iles Marquises, Photo par Joël Orempüller, IRD, ©Atheris Laboratories 2008). A droite, une photographie par contraste interférentiel montrant la morphologie d'une dent radulaire (radula ou harpon) de *Conus textile textile* (Photo par Jean-Jacques Soin, ©Atheris Laboratories 2008). En bas, un venin de *Conus textile* fractionné par chromatographie à phase inverse, montrant l'étendue des divers composés.

Fig. 3. *The near totality of conoidean venoms investigated to date are from the sub-family Coninae where the genus* Conus *is found. Left,* Conus textile textilinus*, a molluscivorous cone snail, in its natural environment (Marquesas Islands, Picture by Joël Orempüller, IRD, ©Atheris Laboratories 2008). Right, a picture by interferential contrast, showing the radula morphology of* Conus textile textile *(Picture by Jean-Jacques Soin, ©Atheris Laboratories 2008). Below, a venom from* Conus textile *fractionated by reverse phase chromatography, showing the extent of the component diversity.*

Les térèbres

Caractérisée par une coquille fortement acuminée et l'absence de canal siphonal, la famille des térèbres (environ 300 espèces) a fait l'objet de quelques études sur le contenu du venin. Ces coquilles montrent elles-aussi une grande variabilité de motifs et de couleur, les rendant attrayantes pour les amateurs de coquillages marins.

Un premier travail sur *Terebra subulata* a mis en exergue des différences significatives en comparaison des venins de cônes, ce qui a laissé suggérer une évolution tout à fait différente du système venimeux (Imperial *et al.*, 2003). L'analyse détaillée du système venimeux d'*Hastula hectica* a non seulement confirmé ces premiers résultats mais a aussi mis en lumière des différences importantes, notamment sur l'absence de modifications post-traductionnelles des composants du venin et la divergence génétique des familles de toxines (Imperial *et al.*, 2007). Cependant, les grandes caractéristiques biochimiques des venins de cônes sont conservées chez les térèbres, telles que la présence de précurseurs et l'expression de petits peptides repliés par des ponts disulfure, fournissant des venins de diversité comparable. Plus récemment, une analyse phylogénique de nombreuses espèces de térèbres, couplée à l'examen de leur appareil venimeux, a montré que certaines lignées ont perdu, de façon indépendante, le système typique producteur et inoculateur de venin (Holford *et al.*, 2009a). Même s'ils ont globalement conservé les caractéristiques majeures des venins des cônes, les Terebridae ont donc évolué de façon très divergente. A l'instar des turridés, on ne connaît à l'heure actuelle aucune cible moléculaire d'un conopeptide de térèbre.

Les turridés

Avec une coquille spiralée et la présence d'un canal siphonal, les turridés (*Figure 4*) rassemblent plus de 3.000 espèces répertoriées, mais le nombre d'espèces existantes pourrait se situer autour de 10.000. Alors qu'ils forment la majorité des espèces dans la superfamille Conoidea, peu de venins de turridés ont été étudiés jusqu'à présent. Trois raisons majeures peuvent être évoquées concernant la sous-représentation d'études de ces espèces. Tout d'abord, les Turridae ont largement été négligés car ils sont pour la plupart soit difficiles à identifier, soit non décrits. Ensuite, une grande partie de ces mollusques vivent dans les faunes profondes (>100 m) nécessitant donc une infrastructure importante pour la collecte d'échantillons (Richer de Forges, 1991). Enfin, une majorité de ces espèces sont de petite taille (<1 cm), ce qui offre peu de venin à analyser et réduit fortement les domaines d'investigations pour les tests de bioactivité.

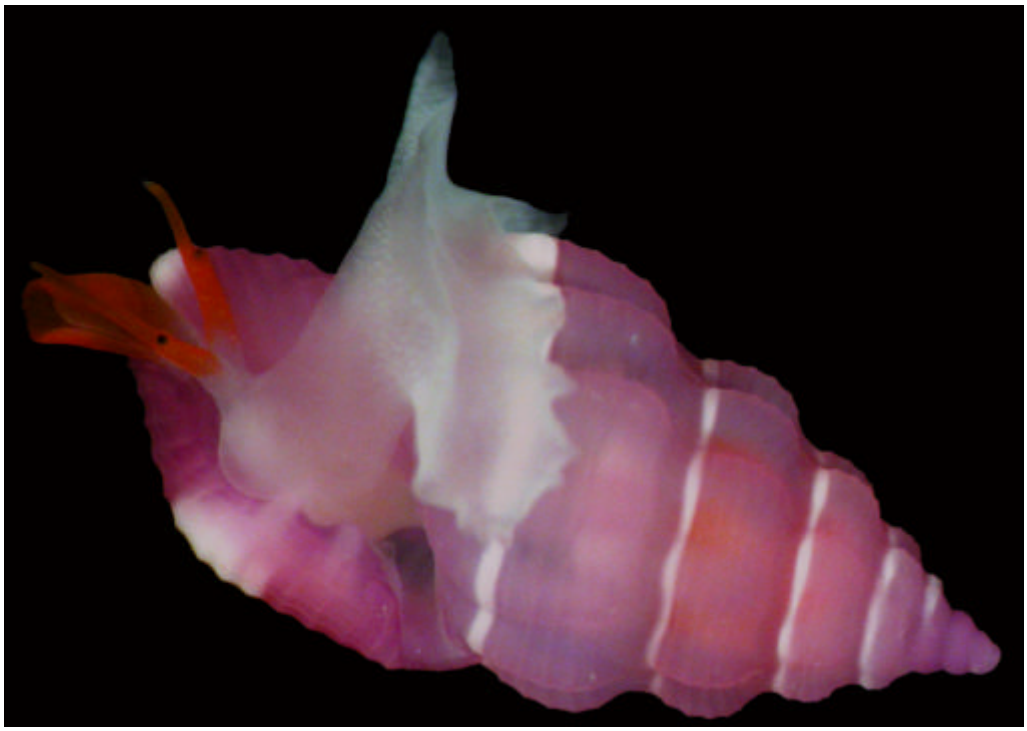

Fig. 4. Dans la famille des turridés (*sensu lato*), la plupart des espèces venimeuses existantes sont probablement encore inconnues. Ci-dessus, un turridé du genre *Lienardia*, pour lequel un grand nombre de noms d'espèces restent à définir (Philippines, Photo par Pierre Lozouet, MNHN, au cours du "Panglao Marine Biodiversity Project", Juin 2004).

Fig. 4. *In the family Turridae (*sensu lato*), most of venomous species are yet to be defined. Above, a turrid of the genus* Lienardia *from which numerous species remain to be characterized (Philippines, Picture by Pierre Lozouet, MNHN, during the "Panglao Marine Biodiversity Project", June 2004).*

Afin d'étudier les venins des turridés, des moyens d'analyse s'appuyant sur peu de matériel doivent donc être utilisés, par exemple par l'utilisation systématique des ARN messagers présents dans les conduits à venin.

Les techniques actuelles de séquençage d'ADN (Shendure et Ji, 2008) peuvent fournir un grand nombre d'information de séquences avec peu d'échantillon et dont le coût devient relativement accessible. Couplées à l'analyse protéique du venin, ces informations permettent d'avoir une vision globale de l'expression des constituants de ce mélange. Les quelques études disponibles sur les venins des turridés ont montré la présence de fluides complexes composés de conopeptides typiques mais présentant peu de similitudes avec les familles de peptides de cônes (Watkins *et al.*, 2006 ; Heralde, III *et al.*, 2008). Alors qu'aucune cible moléculaire n'a été caractérisée pour un conopeptide de venin de turridé, tout le potentiel pharmacologique présent chez ce groupe d'animaux reste à démontrer.

Conclusion

Les systèmes venimeux présents dans les Cephalopoda et Conoidea montrent une forte disparité, que ce soit dans leur organisation morphologique ou dans leur composition. Bien que constituant une partie très minoritaire des venins de Mollusques Gastéropodes, les cônes ont fourni l'essentiel des études de venin de cet embranchement. La mise sur le marché récente du Prialt®, médicament issu de *Conus magus*, pour traiter les douleurs chroniques sévères (Miljanich, 2004) et le développement de nombreux conopeptides en phase préclinique et clinique (Lewis, 2009), souligne le potentiel pharmacologique important de ces venins. Cela peut potentiellement être étendu à toute la superfamille Conoidea et aux Cephalopoda, dont l'activité biologique des composés reste à élucider. Ces venins constituent une source si vaste de composés bioactifs qu'il est très probable que certains apporteront de nouveaux outils de recherche en neurobiologie, et peut-être de futurs médicaments.

Remerciements. *Nous remercions Reto Stöcklin, Sébastien Dutertre et Daniel Biass pour une relecture critique de ce manuscrit. Nous souhaitons également remercier les rapporteurs de ce manuscrit pour leurs commentaires pertinents. Les études réalisées par les auteurs sur les venins de Conoidea sont financées par le projet européen CONCO (http://www.conco.eu/), LIFESCIHEALTH-6 Projet Intégré LSHB-CT-2007-037592.*

Références bibliographiques

Abdel-Rahman MA, Omran MA, Abdel-Nabi IM, Ueda H, McVean A (2009) Intraspecific variation in the Egyptian scorpion *Scorpio maurus palmatus* venom collected from different biotopes. *Toxicon* **53**: 349-359

Barlow A, Pook CE, Harrison RA, Wuster W (2009) Coevolution of diet and prey-specific venom activity supports the role of selection in snake venom evolution. *Proc Biol Sci* **276**: 2443-2449

Becker S, Terlau H (2008) Toxins from cone snails: Properties, applications and biotechnological production. *Appl Microbiol Biotechnol* **79**: 1-9

Biass D, Dutertre S, Gerbault A, Menou JL, Offord R, Favreau P, Stocklin R (2009) Comparative proteomic study of the venom of the piscivorous cone snail *Conus consors*. *J Proteomics* **72**: 210-218

Bouchet P, Héros V, Lozouet P, Maestrati P (2008) A quater-century of deep-sea malacological exploration in the South and West Pacific: Where do we stand? How far to go?, In *Tropical Deep-Sea Benthos*, Héros V, Cowie RH and Bouchet P (eds) volume 25, pp 9-40

Cariello L, Zanetti L (1977) Alpha- and beta-cephalotoxin: two paralysing proteins from posterior salivary glands of *Octopus vulgaris*. *Comp Biochem Physiol C* **57**: 169-173

Cavazzoni E, Lister B, Sargent P, Schibler A (2008) Blue-ringed octopus (*Hapalochlaena sp.*) envenomation of a 4-year-old boy: a case report. *Clin Toxicol (Phila)* **46**: 760-761

Conticello SG, Gilad Y, Avidan N, Ben-Asher E, Levy Z, Fainzilber M (2001) Mechanisms for evolving hypervariability: the case of conopeptides. *Mol Biol Evol* **18**: 120-131

Davis J, Jones A, Lewis RJ (2009) Remarkable inter- and intra-species complexity of conotoxins revealed by LC/MS. *Peptides* **30**: 1222-1227

Derby CD (2007) Escape by inking and secreting: Marine molluscs avoid predators through a rich array of chemicals and mechanisms. *Biol Bull* **213**: 274-289

Erspamer V, Anastasi A (1962) Structure and pharmacological actions of eledoisin, the active endecapeptide of the posterior salivary glands of *Eledone*. *Experientia* **18**: 58-59

Escoubas P, Celerier ML, Nakajima T (1997) High-performance liquid chromatography matrix-assisted laser desorption/ionization time-of-flight mass spectrometry peptide fingerprinting of tarantula venoms in the genus *Brachypelma*: Chemotaxonomic and biochemical applications. *Rapid Commun Mass Spectrom* **11**: 1891-1899

Escoubas P, Quinton L, Nicholson GM (2008) Venomics: Unravelling the complexity of animal venoms with mass spectrometry. *J Mass Spectrom* **43**: 279-295

Favreau P, Krimm I, Le Gall F, Bobenrieth MJ, Lamthanh H, Bouet F, Servent D, Molgo J, Menez A, Letourneux Y, Lancelin JM (1999) Biochemical characterization and nuclear magnetic resonance structure of novel alpha-conotoxins isolated from the venom of *Conus consors*. *Biochemistry* **38**: 6317-6326

Favreau P, Gilles N, Lamthanh H, Bournaud R, Shimahara T, Bouet F, Laboute P, Letourneux Y, Menez A, Molgo J, Le Gall F (2001) A new omega-conotoxin that targets N-type voltage-sensitive calcium channels with unusual specificity. *Biochemistry* **40**: 14567-14575

Favreau P, Stocklin R (2009) Marine snail venoms: Use and trends in receptor and channel neuropharmacology. *Curr Opin Pharmacol* **9**: 1-8

Fegan D, Andresen D (1997) *Conus geographus* envenomation. *The Lancet* **349**: 1672

Fry BG, Roelants K, Norman JA (2009) Tentacles of venom: Toxic convergence in the kingdom animalia. *J Mol Evol* **68**: 311-321

Glaubrecht M (2009) On "Darwinian mysteries" or molluscs as models in evolutionary biology: From local speciation to global radiation. *Am Malacol Bull* **27**: 3-23

Heralde FM III, Imperial J, Bandyopadhyay PK, Olivera BM, Concepcion GP, Santos AD (2008) A rapidly diverging superfamily

of peptide toxins in venomous *Gemmula* species. *Toxicon* **51**: 890-897

Herzig V, Khalife AA, Chong Y, Isbister GK, Currie BJ, Churchill TB, Horner S, Escoubas P, Nicholson GM, Hodgson WC (2008) Intersexual variations in Northern (*Missulena pruinosa*) and Eastern (*M. bradleyi*) mouse spider venom. *Toxicon* **51**: 1167-1177

Holford M, Puillandre N, Terryn Y, Cruaud C, Olivera B, Bouchet P (2009a) Evolution of the Toxoglossa venom apparatus as inferred by molecular phylogeny of the Terebridae. *Mol Biol Evol* **26**: 15-25

Holford M, Zhang MM, Gowd KH, Azam L, Green BR, Watkins M, Ownby JP, Yoshikami D, Bulaj G, Olivera B M (2009b) Pruning nature: Biodiversity-derived discovery of novel sodium channel blocking conotoxins from *Conus bullatus*. *Toxicon* **53**: 90-98

Hvorecny LM, Grudowski JL, Blakeslee CJ, Simmons TL, Roy PR, Brooks JA, Hanner RM, Beigel ME, Karson MA, Nichols RH, Holm JB, Boal JG (2007) Octopuses (*Octopus bimaculoides*) and cuttlefishes (*Sepia pharaonis, S. officinalis*) can conditionally discriminate. *Anim Cogn* **10**: 449-459

Imperial JS, Kantor Y, Watkins M, Heralde FM III, Stevenson B, Chen P, Hansson K, Stenflo J, Ownby JP, Bouchet P, Olivera BM (2007) Venomous auger snail *Hastula* (*Impages*) *hectica* (Linnaeus, 1758): Molecular phylogeny, foregut anatomy and comparative toxinology. *J Exp Zoolog B Mol Dev Evol* **308**: 744-756

Imperial JS, Watkins M, Chen P, Hillyard DR, Cruz LJ, Olivera BM (2003) The augertoxins: Biochemical characterization of venom components from the Toxoglossate gastropod *Terebra subulata*. *Toxicon* **42**: 391-398

Jakubowski JA, Kelley WP, Sweedler JV, Gilly WF, Schulz JR (2005) Intraspecific variation of venom injected by fish-hunting *Conus* snails. *J Exp Biol* **208**: 2873-2883

Kanda A, Iwakoshi-Ukena E, Takuwa-Kuroda K, Minakata H (2003) Isolation and characterization of novel tachykinins from the posterior salivary gland of the common octopus *Octopus vulgaris*. *Peptides* **24**: 35-43

Kantor YI, Taylor JD (1991) Evolution of the toxoglossan feeding mechanism - New information on the use of the radula. *J Mollus Stud* **57**: 129-134

Kantor YI, Taylor JD (2000) Formation of marginal radular teeth in Conoidea (Neogastropoda) and the evolution of the hypodermic envenomation mechanism. *J Zool* **252**: 251-262

Kantor YI, Puillandre N, Olivera BM, Bouchet P (2008) Morphological proxies for taxonomic decision in Turrids (Mollusca, Neogastropoda): A test of the value of shell and radula characters using molecular data. *Zool Sci* **25**: 1156-1170

Key LN, Boyle PR, Jaspars M (2002) Novel activities of saliva from the octopus *Eledone cirrhosa* (Mollusca; Cephalopoda). *Toxicon* **40**: 677-683

Kawashima Y, Nagai H, Ishida M, Nagashima Y, Shiomi K (2003) Primary structure of echotoxin 2, an actinoporin-like hemolytic toxin from the salivary gland of the marine Gastropod *Monoplex echo*. *Toxicon* **42**: 491-497

Kawashima Y, Nagashima Y, Shiomi K (2004) Determination of tetramine in marine gastropods by liquid chromatography/electrospray ionization-mass spectrometry. *Toxicon* **44**: 185-191

Le Gall F., Favreau P, Benoit E, Mattei C, Bouet F, Menou JL, Menez A, Letourneux Y, Molgo J (1999) A new conotoxin isolated from *Conus consors* venom acting selectively on axons and motor nerve terminals through a Na^+-dependent mechanism. *Eur J Neurosci* **11**: 3134-3142

Lewis RJ (2009) Conotoxins: Molecular and therapeutic targets. *Prog Mol Subcell Biol* **46**: 45-65

Maddison DR, Schulz KS, Maddison WP (2007) The tree of life Web project. *Zootaxa* **1668**: 19-40

Menez A (1998) Functional architectures of animal toxins: A clue to drug design? *Toxicon* **36**: 1557-1572

Menez A, Stocklin R, Mebs D (2006) 'Venomics' or : The venomous systems genome project. *Toxicon* **47**: 255-259

Miljanich GP (2004) Ziconotide: Neuronal calcium channel blocker for treating severe chronic pain. *Curr Med Chem* **11**: 3029-3040

Olivera BM, Rivier J, Clark C, Ramilo CA, Corpuz GP, Abogadie FC, Mena EE, Woodward SR, Hillyard DR, Cruz LJ (1990) Diversity of *Conus* neuropeptides. *Science* **249**: 257-263

Olivera BM (2006a) *Conus* peptides: Biodiversity-based discovery and exogenomics. *J Biol Chem* **281**: 31173-31177

Olivera BM (2006b) *Conus* snail venom peptides. In *Handbook of Biologically Active Peptides*, Kastin AJ (ed) pp 381-388. Academic Press

Olivera BM (2008) Venom peptides from *Conus* and other Conoideans : Prospects and perspectives. In *Toxines et fonctions cholinergiques neuronales et non neuronales*, Benoit E, Goudey-Perrière F, Marchot P et Servent D (eds) pp 33-41. Publications de la SFET, Châtenay-Malabry, France, Epub on http://www.sfet.asso.fr (ISSN 1760-6004)

Pimenta AM, Stocklin R, Favreau P, Bougis PE, Martin-Eauclaire MF (2001) Moving pieces in a proteomic puzzle: Mass fingerprinting of toxic fractions from the venom of *Tityus serrulatus* (Scorpiones, Buthidae). *Rapid Commun Mass Spectrom* **15**: 1562-1572

Puillandre N, Samadi S, Boisselier MC, Sysoev AV, Kantor YI, Cruaud C, Couloux A, Bouchet P (2008) Starting to unravel the toxoglossan knot: Molecular phylogeny of the "Turrids" (Neogastropoda: Conoidea). *Mol Phylogenet Evol* **47**: 1122-1134

Richer de Forges B (1991) Les fonds meubles des lagons de Nouvelle-Calédonie: Généralités et échantillonnages par dragages. In *Le Benthos des Fonds Meubles des Lagons de Nouvelle-Calédonie*, Richer de Forges B (ed) pp 7-148. Paris

Robertson A, Stirling D, Robillot C, Llewellyn L, Negri A (2004) First report of saxitoxin in octopi. *Toxicon* **44**: 765-771

Romeo C, Di F L, Oliverio M, Palazzo P, Massilia GR, Ascenzi P, Polticelli F, Schinina ME (2008) *Conus ventricosus* venom peptides profiling by HPLC-MS: A new insight in the intraspecific variation. *J Sep Sci* **31**: 488-498

Russo GL, De Nisco E, Fiore G, Di Donato P, d'Ischia M, Palumbo A (2003) Toxicity of melanin-free ink of *Sepia officinalis* to transformed cell lines: Identification of the active factor as tyrosinase. *Biochem Biophys Res Commun* **308**: 294-299

Shendure J, Ji H (2008) Next-generation DNA sequencing. *Nat Biotechnol* **26**: 1135-1145

Shiomi K, Kawashima Y, Mizukami M, Nagashima Y (2002) Properties of proteinaceous toxins in the salivary gland of the marine gastropod (*Monoplex Echo*). *Toxicon* **40**: 563-571

Simidu U, Noguchi T, Hwang DF, Shida Y, Hashimoto K (1987) Marine bacteria which produce tetrodotoxin. *Appl Environ Microbiol* **53**: 1714-1715

Sutherland SK, Lane WR (1969) Toxins and mode of envenomation of the common ringed or blue-banded octopus. *Med J Aust* **1**: 893-898

Sutherland SK, Tibballs J (2001) Australian animal toxins. Oxford University Press, Melbourne

Taylor JD, Kantor Y, Sysoev A (1993) Foregut anatomy, feeding mechanisms, relationships and classification of the Conoidea (=Toxoglossa) (Gastropoda). *Bull Br Mus nat Hist (Zool) London* **59**: 125-170

Terlau H, Shon KJ, Grilley M, Stocker M, Stuhmer W, Olivera BM (1996) Strategy for rapid immobilization of prey by a fish-hunting marine snail. *Nature* **381**: 148-151

Ueda A, Nagai H, Ishida M, Nagashima Y, Shiomi K (2008) Purification and molecular cloning of SE-cephalotoxin, a novel proteinaceous toxin from the posterior salivary gland of cuttlefish *Sepia esculenta*. *Toxicon* **52**: 574-581

Vianna Braga MC, Konno K, Portaro FC, de Freitas JC, Yamane T, Olivera BM, Pimenta DC (2005) Mass spectrometric and high performance liquid chromatography profiling of the venom of the Brazilian vermivorous mollusk *Conus regius*: Feeding behavior and identification of one novel conotoxin. *Toxicon* **45**: 113-122

Watkins M, Hillyard DR, Olivera BM (2006) Genes expressed in a turrid venom duct: Divergence and similarity to conotoxins. *J Mol Evol* **62**: 247-256

Williams BL, Caldwell RL (2009) Intra-organismal distribution of tetrodotoxin in two species of blue-ringed octopuses (*Hapalochlaena fasciata* and *H. lunulata*). *Toxicon* **54**: 345-353

Woodward SR, Cruz LJ, Olivera BM, Hillyard DR (1990) Constant and hypervariable regions in conotoxin propeptides. *EMBO J* **9**: 1015-1020

Yotsu-Yamashita M, Mebs D, Flachsenberger W (2007) Distribution of tetrodotoxin in the body of the blue-ringed octopus (*Hapalochlaena maculosa*). *Toxicon* **49**: 410-412

Toxines et Signalisation – Toxins and Signalling
Rencontres en Toxinologie – Meeting on Toxinology, 2009
Editions de la SFET – SFET Editions
Accès libre en ligne sur le site – Free access on line on the site : http://www.sfet.asso.fr

Le point sur les chlorotoxines des venins de scorpion

Jean-Pierre ROSSO*, Pierre-Edouard BOUGIS, Marie-France MARTIN-EAUCLAIRE

Equipe ToxCiM, Département de Signalisation Neuronale, Centre de Recherche en Neurobiologie-Neurophysiologie (CRN2M, CNRS UMR-6231), Universités de la Méditerranée et Paul Cézanne, Marseille, France

** Auteur correspondant ; Tél : +33 (0)4 91 69.89 08 ; Courriel : jean-pierre.rosso@univmed.fr*

Résumé

Chez les Buthidés, des toxines isolées à partir de venins obtenus par stimulation électrique ont été regroupées par homologie de structure primaire. Elles sont caractérisées par leur toxicité spécifique envers les Arthropodes. Jusqu'à ce jour, la cible naturelle de ces protéines (composées de 34 à 38 résidus d'acides aminés réticulés par quatre ponts disulfure), est controversée. Pour l'une d'entre-elles, appelée Chlorotoxine (Cltx) une interaction directe avec une métalloprotéase de la matrice extracellulaire de gliomes humains est démontrée.

Update on chlorotoxins of scorpion venoms

Toxins isolated from venoms of Buthids obtained by electric stimulation, are gathered by primary structure homology. They are characterized by their specific toxicity towards arthropods. So far, the natural target of these proteins made of 34 to 38 amino acid residues reticulated by four bridges disulphides, is still controversial. For one of them, called Chlorotoxin (Cltx), a direct interaction with a metalloprotease of the extracellular matrix of human gliomas is proved.

Keywords : *Scorpion chlorotoxins, chloride channel, metalloproteases.*

Introduction

Le terme de chlorotoxine a été employé pour la première fois lors de la caractérisation d'un peptide basique de 36 résidus d'aminoacides isolé à partir d'une stimulation électrique du venin du scorpion *Leiurus quinquestriatus quinquestriatus* (De Bin *et al.*, 1993) ; il possède une activité toxique sur les Arthropodes avec le modèle de l'écrevisse pour les Crustacés et le modèle de la blatte pour les Insectes. Les doses efficaces pour induire la paralysie chez ces animaux est de l'ordre de 2 à 5 μg /g. Ce peptide montre aussi une sélectivité pour un canal chlorure reconstitué à partir de cellules épithéliales d'intestin de rat qui se traduit par l'inhibition de ce courant ionique.

La chlorotoxine chimiquement modifiée s'est révélée utile pour le marquage spécifique des gliomes humains (Soroceanu *et al.*, 1998) où elle se lie de manière spécifique à une protéine de 72 kDa pouvant être un canal chlorure spécifique des gliomes ou bien un récepteur qui module l'activité de ce canal. L'hypothèse selon laquelle la métalloprotéase MMP-2, surexprimée dans la matrice extracellulaire des gliomes humains serait une cible moléculaire spécifique de la chlorotoxine, a été confirmée plus récemment (Deshane *et al.*, 2003).

Des peptides présentant des séquences en aminoacides homologues ont été purifiés et caractérisés à partir du venin d'un grand nombre de scorpions buthidés. Ils sont regroupés à l'intérieur d'une même famille (*Tableau 1*). Il n'existe pas à ce jour une nomenclature précise pour ces peptides souvent dénommés «insectotoxines» ou chlorotoxines «like».

Tableau 1*. Chlorotoxine (Cltx) et toxines homologues caractérisées à ce jour à partir des venins de scorpion.*

Table 1. *Chlorotoxin (Cltx) and homologs from scorpion venoms.*

Toxines	**Scorpion**
Chlorotoxin (Cltx)	*Leiurus quinquestriatus quinquestriatus*
Toxin 8/6 , Gatx1 , Chlorotoxins : –a, -b, -c, -d	*Leiurus quinquestriatus hebraeus*
Insectotoxins I1, I3, I4, I5, I5A	*Buthus eupeus*
Bs 8 chlorotoxin like, Bs 14 chlorotoxin like	*Buthus sindicus*
BmK CT, BmK 12, BmK 12-b,	*Buthus martensii Karsh*
Buta IT lepidopteran selective toxin, Bt V-6, Bt ITx3	*Buthus tamulus*
AmmP2	*Androctonus mauretanicus mauretanicus*

Homologues structuraux de la chlorotoxine

Bien que regroupés dans une même famille de toxines en raison de leur large degré d'homologie, on remarque cependant des différences en terme de pHi et de séquences N et C terminales *(Figure 1)*. Jusqu'a présent aucune information n'étant publiée dans le cadre relation structure fonction, il est impossible d'affirmer si les résidus les mieux conservés ont un rôle majeur dans l'interaction avec leurs cibles potentielles. Les structures tridimensionnelles et l'emplacement des ponts disulfure ont été établis pour l'insectotoxine I15a (Arseniev *et al.*, 1984) et la chlorotoxine (Cltx ; Lippens *et al.*, 1995).

Toxines	pHi	Séquences d'amino-acides	% homologie
AmmP2	8.21	-CGPCFTTDPYTESKCATCCGGRGK--CVGPQCLCNRI	100
Bs 14	8.20	-CGPCFTKDPETEKKCATCCGGIGR--CFGPQCLCNRGY	81
Cltx-d	6.69	-CGPCFTTDHQTEQKCAECCGGIGK--C-GPQCLCNRG	80
Cltx-b	6.69	-CGPCFTTDHQTEQKCAECCGGIGK--CYGPQCLC-RG	77
GaTx1	6.69	-CGPCFTTDHQMEQKCAECCGGIGK--CYGPQCLCNR-NH_2	77
Cltx-c	7.69	-CGPCFTTDRQMEQKCAECCGGIGK--CYGPQCLC-RG	74
BmK CT	8.53	-CGPCFTTDANMARKCRECCGGIGK--CFGPQCLCNRI	74
BmK 12	8.75	-CGPCFTTDANMARKCRECCGGIGK--CFKPQCLCNRI	71
Bmk 12-b	8.22	-CGPCFTTDANMARKCRECCGGNGK--CFGPQCLCNRE	71
Bs 8	8.90	RCKPCFTTDPQMSKKCADCCGGKGKGKCYGPQCLC	69
Be I5A	8.50	MCMPCFTTDPNMAKKCRDCCGGNGK--CFGPQCLCNR-NH_2	69
Be I4	8.51	MCMPCFTTDHNMAKKCRDCCGGNGK--CFGPQCLCNR	67
Be I5	8.50	MCMPCFTTDPNMANKCRDCCGG-GK-KCFGPQCLCNR	67
Buta It	8.52	RCGPCFTTDPQTQAKCSECCGRKG-GVCKGPQCICGIQ	65
Cltx	8.50	MCMPCFTTDHQMARKCDDCCGGKGRGKCYGPQCLC-R	63
Cltx-a	8.50	MCMPCFTTDHQMARKCDDCCGGKGRGKCYGPQCLC-RG	63
Tox 8/6	8.70	RCSPCFTTDQQMTKKCYDCCGGKGKGKCYGPQCICAPY	62
Be I3	8.51	MCMPCFTTDHQTARRCRDCCGGRGR-KCFG-QCLCGYD	59
Be I1	8.50	MCMPCFTTRPDMAQQCRACCKGRGK--CFGPQCLCGYD	58
Bt ITx3	8.21	RCPPCFTTNPNMEADCRKCCGGRGY--CASYQCICPGG	56
Bt V-6	8.52	RCPPCFTTNPNMEANCRKCCGGRGY--CASYQCICPG 1 10 20 30	54

Fig. 1. pHi , séquence primaire et pourcentage d'homologie de la chlorotoxine (Cltx) et ses homologues.

Fig. 1. *pHi, primary sequence and percentage of homology of chlorotoxin (Cltx) and its homologs.*

Activité biologique des homologues structuraux de la chlorotoxine

Dans le tableau 2 sont présentées les toxines pour lesquelles une activité biologique a pu être démontrée. La plupart d'entre elles sont toxiques pour les insectes. Les doses toxiques de l'ordre de quelques µg/g restent très élevées (jusqu'à 1000 fois plus), par comparaison avec les toxines «anti insectes» dites longues caractérisées dans ces mêmes venins et modulant les canaux sodiques de ces animaux (Zlotkin *et al.*, 1985).

Récemment, la toxine BmK CT obtenue de manière recombinante et initialement caractérisée à partir du venin de scorpion *Buthus martensii* Karsch a été présentée comme ayant le même potentiel thérapeutique sur les gliomes que la chlorotoxine (Fu *el al.*, 2007).

De plus, une toxine GaTx1 isolée du scorpion *Leurius quinquestriatus hebraeus* a été décrite comme ayant une très forte spécificité pour le canal chlorure porté par la protéine CFTR (K_D proche de 42nM), l'inhibant de manière réversible lorsqu'elle est liée à l'état fermé du canal ; cette toxine aurait donc un effet direct sur ce canal chlorure et serait la première toxine de scorpion active sur un canal de type anionique (Fuller *et al.*, 2007).

Le peptide AmmP2 a été purifié dans notre laboratoire à partir d'un venin obtenu par stimulation électrique du scorpion *Androctonus mauretanicus mauretanicus* (Rosso et Rochat, 1985). Une activité paralysante (3 à 8 □g/animal) a pu être enregistrée sur les larves de mouches (*Sarcophaga facultata*) et les crustacés terrestres (*Armadillidium vulgare*). Il est cependant très important de remarquer que plusieurs purifications à partir de venins dit «manuels», obtenus par stimulation manuelle et non électrique du post-abdomen et susceptible de simuler une sécrétion naturelle, n'a jamais permis de retrouver le peptide AmmP2 alors qu'il représente plus de 8% des protéines dans le venin obtenu par stimulation électrique (Zerrouk *et al.*, 1991).

Tableau 2. *Activité biologique de la chlorotoxine et des toxines homologues.*

Table 2. *Biological activity of the chlorotoxin and its homologs.*

Toxines	**Activité biologique**
Chlorotoxine	Toxicité envers les Arthropodes Blocage d'un canal chlorure de faible conductance reconstitué à partir de cellules épithéliales de colon de rat Inhibition de l'activité de la métalloprotéase MMP-2 Inhibition du développement des gliomes
GaTx-1	Inhibition réversible du canal chlorure du CFTR (Fuller *et al*., 2007)
Insectotoxines I1, I3, I4, I5 I5A	Toxicité envers les insectes (blattes) (Grischin *et al*., 1982)
BmK 12	Toxicité envers les insectes (blattes) (Escoubas *et al*., 1997)
Bt v-6	Toxicité envers les insectes (blattes, grillons, mouches, chenilles) (Escoubas *et al*., 1997)
BmK CT	Inhibition du développement des gliomes (Fu *et al*., 2007)
Bt ITx3	Toxicité envers les insectes (chenilles), paralysie de type flaccide (Dhawan *et al*., 2002)
Buta IT	Toxicité sélective envers les lépidoptères (*Heliothis virescens*) (Wudayagiri *et al*., 2001)
AmmP2	Toxicité envers les insectes (larves de mouches) et crustacés (Isopodes terrestres) (Rosso et Rochat, 1985)

Conclusion

L'hypothèse formulée (De Bin *et al*., 1993) selon laquelle la cible naturelle des chlorotoxines chez les Arthropodes serait un type de canal anionique musculaire extrajonctionnel n'est pas confirmée aujourd'hui. Le site d'interaction intracellulaire directe de la chlorotoxine et de la toxine GaTx1 sur certains types de canaux chlorure (De Bin *et al*., 1993 ; Fuller *et al*., 2007) est fondamentalement différent de celui décrit pour les autres neurotoxines des venins de scorpion, toxines alpha et beta, interagissant avec le domaine extracellulaire des canaux cationiques (Martin-Eauclaire et Couraud, 1995).

La seule cible moléculaire identifiée est une protéase à zinc présente dans la matrice extracellulaire de gliomes humains et sur laquelle la chlorotoxine exerce un effet inhibiteur. L'inhibition du courant chlorure mesuré à la surface de ces cellules tumorales n'est qu'un effet indirect de la présence de la toxine (Deshane *et al*., 2003). Les inhibiteurs naturels endogènes de ces métalloprotéases matricielles interagissent directement avec le site actif de l'enzyme (atome de zinc) par l'intermédiaire de leur séquence N-terminale, comparable à celle des chlorotoxines, contenant un pont disulfure jouant un rôle important dans chélation de l'ion métallique (Visse et Nagase, 2003). On peut dès lors émettre l'hypothèse que cette famille de peptides représenterait des inhibiteurs naturels de métalloprotéases de scorpion. Bien que présents dans la glande à venin, ils ne feraient pas partie de la sécrétion naturelle comme semble le démontrer l'absence de AmmP2 dans le venin du scorpion *Androctonus mauretanicus mauretanicus* obtenu par stimulation manuelle. Cette étude comparative du venin d'un même scorpion obtenu selon deux techniques différentes reste la seule à notre connaissance aujourd'hui. Dans la quasi-totalité des études scientifiques, les venins des scorpions buthidés sont extraits par stimulation électrique dans le but d'en obtenir des quantités importantes (Gopalakrishnakone *et al*., 1995). Cette méthode rentable entraine cependant la lésion des tissus glandulaires favorisant l'apparition de protéines intracellulaires dans le liquide sécrété (Chhatwal et Habermann, 1981 ; Goyffon, 2002).

Si la composition d'un venin physiologiquement naturel reste difficile à établir (Pimenta *et al*., 2003), il n'en demeure pas moins qu'en plus des neurotoxines, d'autres protéines issues de la glande à venin peuvent présenter un intérêt thérapeutique certain.

Références bibliographiques

Arseniev AS, Kondakov VI, Maiorov VN, Bystrov VF (1984) NMR solution spatial structure of *Buthus eupeus* insectotoxin I5A. *FEBS Lett* **165**: 57-61

Chhatwal GS, Habermann E (1981) Neurotoxins, protease inhibitors and histamine releasers in the venom of the Indian red scorpion (*Buthus tamulus*): Isolation and partial characterization. *Toxicon* **19**: 807-823

De Bin JA, Maggio JE, Strichartz GR (1993) Purification and characterization of chlorotoxin, a chloride channel ligand from the venom of the scorpion. *Am J Physiol* **264**: C361-C369

Deshane J, Garner CC, Sontheimer H (2003) Chlotoxin inhibits glioma cell invasion vai matrix metalloproteinase -2. *J Biol Chem* **278**: 4135-4144

Dhawan R, Joseph S, Sethi A, Lala AK (2002) Purification and characterization of a short insect from the venom of the scorpion *Buthus tumulus*. *FEBS Lett* **528**: 261-266

Escoubas P, Romi-Lebrun R, Wu FQ, Herrmann R, Moskovitz H, Rajendra W, Hammock B, Nakajima T (1997) Two novel short insectotoxins from the asian scorpion *Buthus martensi* and *Buthus tamulus. Toxicon* **35**: 490

Fu YJ, Yin LT, Liang AH, Zhang CF, Wang W, Chai BF, Yang JY, Fan XJ (2007) Therapeutic potential of chlorotoxin-like neurotoxin from the Chinese scorpion for human gliomas. *Neurosci Lett* **412**: 62-67

Fuller MD, Thompson CH, Zhang ZR, Freeman CS, Schay E, Szakacs G, Bakos E, Sarkadi B, McMaster D, French RJ, Pohl J,

Kubanek J, McCarty NA (2007) State dependent inhibition of cystic fibrosis transmembrane conductance regulator chloride channels by a novel peptide toxin. *J Biol Chem* **282**: 37545-37555

Gopalakrishnakone P, Cheah J, Gwee MCE (1995) Black scorpion (*Heterometrus longimanus*) as a laboratory animal: maintenance of a colony of scorpion for milking of venom for research, using a restraining device. *Laboratory Animals* **29**: 456-458

Goyffon M (2002) Le scorpionisme. *Revue Française des Laboratoires* **342**: 41-48

Grishin EV, Volkova TM, Soldatova LN (1982) Study of toxic components from the venom of Caucasus subspecies of scorpion *Buthus eupeus*. *Bioorg Khim* **8**: 155-164

Lippens G, Najib J, Wodak SJ, Tartar A (1995) NMR sequential assignments and solution structure of chlorotoxin, a small scorpion toxin that blocks chloride channels. *Biochemistry* **34**: 13-21

Martin-Eauclaire MF, Couraud F (1995) Scorpions neurotoxins : Effects and mechanisms. In *Handbook of Neurotoxicology*, Chang LW and Dyer RS (eds) pp 683-716. Marcel Dekker: New-York

Pimenta AMC, De marco Almeida F, De Lima ME, Martin Eauclaire MF, Bougis PE (2003) Individual variability in *Tityus serrulatus* (Scorpiones, Buthidae) venom elicited by matrix-assisted laser desorption/ionization time-of-flight mass spectrometry. *Rapid Commun Mass spectrum* **17**: 413-418

Rosso JP, Rochat H (1985) Characterization of ten proteins from the venom of the Moroccan scorpion *Androctonusmauretanicus mauretanicus* six of which are toxic to mouse. *Toxicon* **23**: 113-125

Soroceanu L, Gillespie Y, Khazaeli MB, Sontheimer H (1998) Use of chlorotoxin for targeting of primary brain tumors. *Cancer Res* **58**: 4871-4879

Visse R, Nagase H. (2003) Matrix metalloproteases and tissue inhibitors of metalloproteases. Structure, Function andBiochemistry. *Circulation Res* **92**: 827-839

Wudayagiri R, Inceoglu B, Herrmann R, Derbel M, Choudary PV, Hammock BD (2001) Isolation and characterization of a novel lepideptoran-selective toxin from the venom of south Indian red scorpion, *Mesobuthus tumulus*. *Biochemistry* **2**: 16-23

Zerrouk H, Bougis PE, Céard B, Benslimane A, Martin-Eauclaire MF (1991) Analysys by high-performance liquid chromatography of *Androctonus mauretanicus mauretanicus* (black scorpion) venom. *Toxicon* **29**: 951-960

Zlotkin E, Kadouri D, Gordon D, Pelhate M, Martin MF, Rochat H (1985) An excitatory and a depressant insect toxin from scorpion venom both effect sodium conductance and possess a common binding site. *Arch Biochem Biophys* **240**: 877-887

Toxines et Signalisation – Toxins and Signalling
Rencontres en Toxinologie – Meeting on Toxinology, 2009
Editions de la SFET – SFET Editions
Accès libre en ligne sur le site – Free access on line on the site : http://www.sfet.asso.fr

L'immunothérapie peut-elle réduire le dysfonctionnement rénal induit par le venin du scorpion Androctonus australis hector *?*

Djelila HAMMOUDI-TRIKI, Sonia ADI-BESSALEM, Amina MENDIL, Sassia SAMI-MERAH, Fatima LARABA-DJEBARI*

Laboratoire de Biologie Cellulaire et Moléculaire, Faculté des Sciences Biologiques, Université des Sciences et de la Technologie « Houari Boumédienne » USTHB, Bab Ezzouar, Alger, Algérie et Laboratoire de Recherche et de Développement sur les Venins, Institut Pasteur d'Algérie, Alger, Algérie

** Auteur correspondant ; Tél : +00 213 21336076 ; Fax : +00 213 21336077 ; Courriel : flaraba@hotmail.com*

Résumé

Après envenimation des rats par le venin du scorpion Androctonus australis hector*, l'analyse des variations fonctionnelles des reins révèle des lésions tissulaires avec une modfication des taux des marqueurs métaboliques dans le sang périphérique et dans les urines. L'utilisation de l'immunothérapie réduit partiellement ces modifications et la perte de l'équilibre électrolytique.*

Can immunotherapy reduce kidney dysfunction induced by Androctonus australis hector *venom ?*

Following envenomation of the rat with Androctonus australis hector *venom, analysis of the functional variations of kidney showed tissular damages associated with variation of metabolic markers in peripheral blood and urine. Immunotherapy reduced partially metabolic modifications and the lost in the electrolytic balance.*

Keywords : *Electrolytes, immunotherapy, metabolic parameters, venom.*

Introduction

Les voies d'élimination des toxines des venins sont mal connues. Il semblerait que la voie principale d'excrétion soit rénale car le venin se retrouve en quantité importante dans les reins des animaux envenimés (Revelo et *al*., 1996 ; Bessalem et *al*., 2003). L'immunothérapie associée à des traitements symptomatiques demeure le seul remède préconisé dans les cas d'envenimations accidentelles.

Exploration de la fonction rénale

Après envenimation de rats par le venin du scorpion *Androctonus australis hector* (*Aah)* suivie ou non par une immunothérapie, la fonction rénale a été explorée par le dosage de marqueurs physiologiques et par une analyse histologique. Les rats reçoivent une injection sub-létale (0,5 mg/kg) de venin d'*Aah* par voie sous-cutanée. L'administration des fragments $F(ab')_2$ par voie intra-péritonéale (40 mg/mL) est effectuée 30 min après l'envenimation (n = 3). Les témoins (n = 3) reçoivent le même volume de sérum physiologique. Après 24 h, des prélèvements de sang et d'urine sont effectués sur les trois séries d'animaux et les reins sont immergés dans du formol à 4% afin de réaliser l'étude histologique.

Les résultats des analyses urinaires ont montré une hyperprotéinémie, 24 heures après envenimation. La présence des protéines dans les urines pourrait être due à leur passage du sang vers les urines, conséquence du dysfonctionnement des glomérules. La créatinine est un marqueur de la fonction glomérulaire dans les conditions normales. Son dosage dans le sang et les urines permet d'évaluer la fonction rénale et en particulier la capacité de filtration. Sa teneur dans le sang augmente en raison de faible excrétion par les reins altérés, ce qui explique sa diminution dans les urines. En effet, dans les conditions expérimentales de cette étude, une augmentation de la créatinine sérique et sa diminution significative ($p<0,05$) dans l'urine est induite par le venin d'*Aah*. Parallèlement, les résultats obtenus ont montré que le venin d'*Aah* induit une augmentation de la concentration d'urée dans le sang et sa diminution dans les urines (*Figure 1*). L'urée naturelle est en effet, formée dans le foie lors du cycle de l'urée à partir de l'ammoniaque provenant de la dégradation des acides aminés. Avant d'être éliminée par l'urine, elle est filtrée par le glomérule rénal et réabsorbée partiellement par le tubule rénal. Une insuffisance rénale augmente donc sensiblement sa concentration dans le sang.

Une élimination significative des ions (Na^+ et K^+) est observée dans les urines (*Figure 1*). Le trouble électrolytique pourrait être expliqué par l'altération des cibles tissulaires (Corréa et *al*., 1997). Les

perturbations de l'excitabilité cellulaire causée par la liaison des neurotoxines sur leurs cibles cellulaires pourraient exercer un ralentissement de l'inactivation du canal et par conséquent un déséquilibre électrolytique.

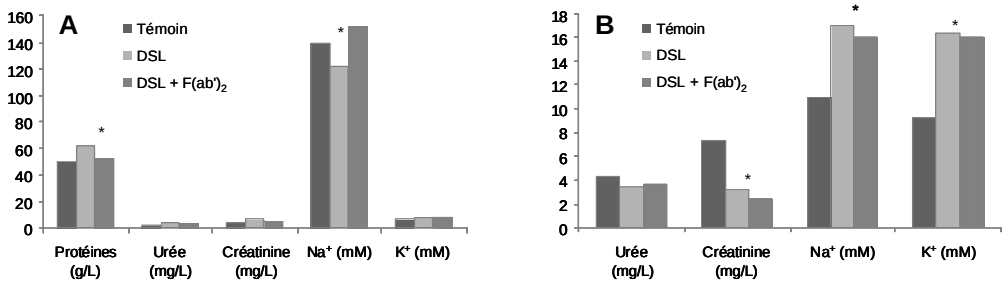

Fig. 1. Dosage des paramètres métaboliques et des électrolytes sériques (**A**) et urinaires (**B**) avant et après le traitement par immunothérapie. * Différence significative au seuil de 5% avec les témoins correspondants.

Fig. 1. *Dosage of metabolic parameters and electrolytes from serum (**A**) and urine (**B**) before and after immunotherapy.*

Afin de confirmer ce dysfonctionnement rénal, une analyse histologique du cortex rénal a été réalisée 24 heures après l'envenimation des animaux. L'observation des coupes histologiques a montré des altérations tissulaires importantes se manifestant par la présence d'hémorragies et d'oedèmes glomérulaires et tubulaires (*Figure 2*).

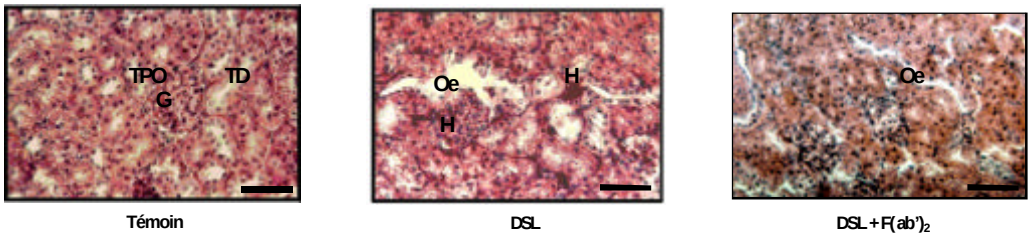

Fig 2. Analyse histologique du cortex rénal avant et après immunothérapie (Coloration Hématoxyline-Eosine). La barre d'échelle représente 33 µm. DSL : dose sublétale, G : glomérule, H : Hémorragie, Oe : Œdème, TD : Tubules distaux TP : Tubules proximaux. La barre représente 33 µm.

Fig 2. *Histological analysis of renal cortex before and after immunotherapy. Bar represents 33 µm.*

Le pouvoir neutralisant des fragments F(ab')$_2$ administrés par voie intra-péritonéale, 30 min après envenimation, n'est pas toujours suffisant pour réduire les perturbations tissulaires (*Figure 2*). Les concentrations urinaires de l'urée et la créatinine persistent partiellement 24 heures après envenimation (*Figure 1*). L'inefficacité de l'immunothérapie au niveau du cortex rénal pourrait s'expliquer par le fait que le rein, étant irrigué par un important flux sanguin lui ramenant de nombreux constituants toxiques, semble être une cible majeure des toxines du venin, lesquelles se fixent sur leurs récepteurs (Ismail et Abd-Elsalem, 1988 ; Revelo *et al*., 1996). L'étude pharmacocinétique entreprise par Devaux *et al*. (2004) a en effet montré que 78% de la toxine *Aah* I est détectée dans les reins.

Conclusion

Le rein constitue une cible majeure des toxines du venin du scorpion *Aah*. Les Fragments F(ab')2 administrés aux animaux réduisent partiellement les troubles physiologiques. La modification de la posologie d'administration de l'immunothérapie et son association à des traitements symptomatiques pourrait améliorer les fonctions physiologiques.

Références bibliographiques

Bessalem S, Hammoudi-Triki D, Laraba-Djebari F (2003) Effet de l'immunothérapie sur les modifications métaboliques et histopathologiques après envenimation scorpionique. *Bull Soc Pathol Exot*, **96**: 110-114

Corrêa MM, Sampaio SV, Lopez RA, Mancuso LC, Cunha OAB, Franco JJ, Giglio JR (1997) Biochemical and histopathological alterations induced in rats by *Tityus serrulatus* scorpion venom and its major neurotoxin Tityustoxin-I. *Toxicon* **35**: 1035-1067

Devaux C, Jouirou B, Krifi M, Clot-Faybesse O, El Ayeb M, Rochat H (2004). Quantitative variability in the biodistribution and in toxinokinetic studies of the three main alpha toxins from the *Androctonus australis hector* scorpion venom. *Toxicon* **43**: 661-669

Ismail M, Abd-Elsalam MA (1988) Are the toxicological effects of scorpion envenoming related to tissue venom concentration? *Toxicon* **26**: 233-256

Revelo MP, Bambirra EA, Ferriera AP, Diniz CR, Chavez-Olortegui C (1996) Body distribution of *Tityus serrulatus* scorpion venom in mice and effects of scorpion antivenom. *Toxicon* **34**: 1119-1125

Toxines et Signalisation – Toxins and Signalling
Rencontres en Toxinologie – Meeting on Toxinology, 2009
Editions de la SFET – SFET Editions
Accès libre en ligne sur le site – Free access on line on the site : http://www.sfet.asso.fr

L'augmentation de la perméabilité vasculaire serait-elle un facteur déclenchant de l'œdème pulmonaire induit par le venin du scorpion Androctonus australis hector *?*

Sassia SAMI-MERAH, Djelila HAMMOUDI-TRIKI, Sonia ADI-BESSALEM, Amina MENDIL, Fatima LARABA-DJEBARI*

Laboratoire de Biologie Cellulaire et Moléculaire, Faculté des Sciences Biologiques, Université des Sciences et de la Technologie « Houari Boumédienne » USTHB, Bab Ezzouar, et Laboratoire de Recherche et de Développement sur les Venins, Institut Pasteur d'Algérie, Alger, Algérie

** Auteur correspondant ; Tél : +00 213 21336076 ; Fax : +00 213 21336077 ; Courriel : flaraba@hotmail.com*

Résumé

Le venin du scorpion Androctonus australis hector *(*Aah*) induit chez la souris un œdème pulmonaire caractérisé par une augmentation de la perméabilité vasculaire. L'utilisation d'inhibiteurs de la réaction inflammatoire (dexaméthasone et indométhacine), une heure avant l'envenimation des souris, induit une diminution de l'extravasation du bleu d'Evans ainsi qu'une réduction du liquide accumulé dans les poumons. Le mécanisme d'induction de l'œdème pulmonaire par le venin d'*Aah *pourrait être dû à la libération de nombreux médiateurs inflammatoires dont les eicosanoïdes.*

May an increase in vascular permeability be responsible for the pulmonary edema induced by the venom of Androctonus australis hector *?*

Injection of the Androctonus australis hector *(*Aah*) venom to mice induces pulmonary edema, as assessed by an increase in the lung wet-to-dry weight ratio, and characterized by an increase in the lung vascular permeability, as revealed by accumulation of Evans blue in tissue. The vascular permeability increase and water accumulation in lung are inhibited by administration of inflammatory inhibitors (dexamethasone and indomethacin) prior to envenomation. The edema induced by* Aah *venom may be generated by multiple mediators including eicosanoids.*

Keywords **:** Androctonus australis hector *venom, anti-inflammatory, pulmonary oedema, vascular permeability.*

Introduction

L'œdème aigu du poumon est une complication commune à tous les sujets gravement envenimés par le scorpion *Androctonus australis hector* (*Aah*). Il représente la cause principale de décès, mais les mécanismes mis en jeu restent encore non élucidés. Les études cliniques et expérimentales suggèrent l'implication de l'augmentation de la perméabilité vasculaire pulmonaire dans la genèse de cette perturbation. Cette augmentation serait due à l'action des médiateurs moléculaires de l'inflammation (eicosanoïdes, kinines, histamine, sérotonine et facteur activateur des plaquettes [PAF]) secrétés après activation des leucocytes (Amaral et *al.*, 1994 ; De-Matos *et al.*, 2001 ; D'Suze et *al.*, 2004). Une réaction inflammatoire caractérisée par une infiltration des leucocytes au niveau des cavités péritonéale et pleurale ainsi que des organes cœur et poumons a été observée après injection du venin d'*Aah* ou de ses toxines (Sami-Merah *et al.*, 2007, 2008a, 2008b).

Cette étude a eu pour objectif, d'une part, de montrer l'implication de l'augmentation de la perméabilité vasculaire dans la formation de l'œdème pulmonaire, d'autre part, d'explorer le rôle de certains médiateurs de l'inflammation dans la genèse de l'œdème pulmonaire lors d'envenimation par le venin d'*Aah*.

Effets du venin du scorpion *Androctonus australis hector* sur la perméabilité vasculaire pulmonaire

L'augmentation de la perméabilité vasculaire pulmonaire a été évaluée 24 heures après envenimation de deux façons : d'une part, par l'estimation de l'ampleur de l'œdème formé dans les poumons par la mesure du rapport des poids humide et poids sec pulmonaires, le poids humide étant déterminé après prélèvement des poumons et le poids sec après incubation des poumons à 60°C pendant 48 h (Ipaktchi *et al.*, 2006) et, d'autre part, par la quantification du bleu d'Evans infiltré au niveau des poumons des souris envenimées. Dans ce second cas, le

bleu d'Evans (20 mg/kg) a été injecté à la souris par voie intraveineuse suivie par l'injection intrapéritonéale du venin d'*Aah* (0,5 mg/kg de poids corporel de souris). Après 24 h d'envenimation, les souris sont sacrifiées et les poumons sont prélevés et incubés dans le formamide à température ambiante pendant 72 h, la lecture de l'absorbance du bleu d'Evans est réalisée à 620 nm. La quantité de bleu d'Evans exprimée en µg/g de tissu est déduite à partir d'une courbe standard.

Les résultats obtenus montrent que l'injection de venin d'*Aah* à la souris induit une augmentation de la perméabilité vasculaire ainsi qu'une accumulation de liquide dans les poumons (*Tableau 1*). L'accumulation de liquide serait due à une élévation de la perméabilité vasculaire et au développement d'un œdème pulmonaire. Des travaux antérieurs ont suggéré que la libération des médiateurs de l'inflammation (histamine et eicosanoïdes) serait responsable de l'augmentation de la perméabilité vasculaire et de l'altération majeure de la membrane alvéolo-capillaire provoquant l'œdème pulmonaire observé lors d'envenimation scorpionique (Amaral *et al*., 1994; De Matos *et al*., 2001).

Tableau I. Evaluation de la perméabilité vasculaire pulmonaire en présence et en absence d'inhibiteurs de la réaction inflammatoire.

Table I. *Assessment of pulmonary vascular permeability with and without inhibitors of inflammatory response.*

Traitement	Indice de perméabilité vasculaire	
	Poids humide / poids sec *Wet weight / dry weight*	Concentration de bleu d'Evans *Evans Blue concentration* (µg/g de tissu)
Témoin	1,50 ± 0,03	4,8 ± 0,5
Venin (V)	7,66 ± 0,10	34,8 ± 2,5
Dexaméthasone + V	1,85 ± 0,06	4,2 ± 0,2
Indométhacine + V	2,66 ± 0,01	6,0 ± 0,3

Inhibition de l'augmentation de la perméabilité vasculaire induite par le venin d'*Aah* par différents inhibiteurs de la réponse inflammatoire

Les animaux ont été prétraités 1 h avant leur envenimation par la dexaméthasone, un inhibiteur de l'activité de la phospholipase A2 endogène responsable de la synthèse des métabolites de l'acide arachidonique (4 mg/kg) ou par l'indométhacine, un inhibiteur de l'activité de la cyclo-oxygénase responsable de la libération des prostaglandines (5 mg/kg). Après 24 h d'envenimation, ce traitement a entrainé une réduction de l'œdème pulmonaire et une diminution de la perméabilité vasculaire par rapport aux animaux envenimés, ainsi qu'en témoigne une diminution de l'extravasation du bleu d'Evans dans les poumons des animaux prétraités avant envenimation. En parallèle, la valeur du rapport poids humide/poids sec des poumons a révélé une réduction de la quantité de liquide accumulé dans les poumons des animaux envenimés. L'inhibition de l'augmentation de la perméabilité vasculaire semble être plus marquée avec le dexaméthasone (*Tableau 1*), inhibiteur de la synthèse des prostaglandines, des leucotriènes et du PAF impliqués dans l'augmentation de la perméabilité vasculaire.

Ces résultats suggèrent que les mécanismes de formation de l'œdème pulmonaire induit par le venin d'*Aah* seraient dus à la libération des médiateurs lipidiques de l'inflammation (PAF, leucotriènes et prostaglandines). Il a été démontré que l'injection intraveineuse des antagonistes du PAF (BN-52021 et WEB-2170), celle d'inhibiteurs de la lipo-oxygénase (MK-886) et de la cyclo-oxygénase (Aspirine et Indométhacine) induit une réduction significative de l'œdème pulmonaire provoqué par le venin de *Tityus serrulatus* chez le rat (De Matos et *al*., 1997). Ces médiateurs inflammatoires sont secrétés après activation des mastocytes par la substance P libérée à partir des terminaisons nerveuses après fixation de certaines toxines du venin du scorpion *Tityus serrulatus* sur les canaux sodium. Le traitement des rats envenimés avec un antagoniste du récepteur de la substance P provoque l'inhibition de l'œdème pulmonaire (De-Matos *et al*., 1999, 2001).

L'implication des médiateurs lipidiques de l'inflammation dans l'augmentation de la perméabilité vasculaire pulmonaire pourrait expliquer l'induction d'un œdème pulmonaire par le venin du scorpion *Aah* (Adi-Bessalem et *al*., 2008 ; Sami-Merah et *al*., 2008b).

Références bibliographiques

Adi-Bessalem S, Hammoudi-Triki D, Laraba-Djebari F (2008) Pathophysiological effects of *Androctonus australis hector* scorpion venom : Tissue damages and inflammatory response. *Exp Toxicol Pathol* **60**: 373-380

Amaral CSF, Barbosa AJA, Leite VHR, Tafuri WL, Rezende AA (1994) Scorpion sting-induced pulmonary oedema, evidence of alveolo capillary membrane permeability. *Toxicon* **32**: 999-1003

De-Matos IM, Rocha OA, Leite R, Freire-Maia L (1997) Lung oedema induced by *Tityus serrulatus* scorpion venom in the rat. *Comp Biochem Physiol C, Pharmacol Toxicol Endocrinol* **118**: 143-148

De-Matos IM, Souza DG, Seabra DG, Freire-Maia L, Teixeira MM (1999) Effects of tachykinin NK1 or PAF receptor blockade on the lung injury induced by scorpion venom in rats. *Eur J Pharmacol* **376**: 293-300

De-Matos IM, Talvani A, Rocha OO, Freire-Maia L, Teixeira MM (2001) Evidence for a role of mast cells in the lung edema induced by *Tityus serrulatus* venom in rats. *Toxicon* **39**: 863-867

D'Suze G, Salazar V, Díaz P, Sevcik C, Azpurua H, Bracho N (2004) Histopathological changes and inflammatory response induced by *Tityus discrepans* scorpion venom in rams. *Toxicon* **44**: 851-860

Ipaktchi K, Mattar A, Niederbichler AD, Hoesel LM, Vollmannshauser S, Hemmila MR, Su GL, Remick DG, Wang SC (2006) Attenuating burn wound inflammatory signaling reduces systemic inflammation and acute lung injury. *J Immunol* **177**: 8065-8071

Sami-Merah S, Hammoudi-Triki D, Martin-Eauclaire MF, Laraba-Djebari F (2007) La toxine Aah II d'*Androctonus australis hector*: effets inflammatoire et histopathologique. In *Toxines émergentes: nouveaux risques*, Goudey-Perrière F, Benoit E, Marchot P and Popoff MR (eds) pp 203-204. Coll. Rencontres en Toxinologie, Librairie Lavoisier, Paris

Sami-Merah S, Hammoudi-Triki D, Martin-Eauclaire MF, Laraba-Djebari F (2008a) Incidence de la fraction toxique du venin d'*Androctonus australis hector* dans la leucocytose pulmonaire. In *Toxines et fonctions cholinergiques neuronales et non neuronales*, Benoit E, Goudey-Perrière F, Marchot P and Servent D (eds) pp 129-130. Publications de la SFET, Châtenay-Malabry, France, Epub on http://www.sfet.asso.fr (ISSN 1760-6004)

Sami-Merah S, Hammoudi-Triki D, Martin-Eauclaire MF, Laraba-Djebari F (2008b) Combination of two antibody fragments F(ab')2/Fab : An alternative for scorpion envenoming treatment. *Intern Immuno Pharmacol* **8**: 1386-1394

Toxines et Signalisation – Toxins and Signalling
Rencontres en Toxinologie – Meeting on Toxinology, 2009
Editions de la SFET – SFET Editions
Accès libre en ligne sur le site – Free access on line on the site : http://www.sfet.asso.fr

Réponse inflammatoire induite par la fraction coagulante C1 isolée du venin de la vipère Cerastes cerastes

Fatah CHERIFI, Fatima LARABA-DJEBARI*

Laboratoire de biologie cellulaire et moléculaire, Faculté des sciences biologiques, Université des Sciences et de la Technologie « Houari Boumédienne » USTHB Bab Ezzouar, Alger, Algérie et Laboratoire de Recherche et Développement sur les Venins, Institut Pasteur d'Algérie, Alger, Algérie

** Auteur correspondant ; Tél : +00 213 21 33 60 76 ; Fax : +00 213 21 33 60 77 ;*
Courriel : flaraba@hotmail.com

Résumé

La fraction coagulante C1 isolée du venin de la vipère Cerastes cerastes *induit une réponse inflammatoire chez le rat après administration, par voie intrapéritonéale, d'une dose de 1 mg/kg de poids corporel. La réaction inflammatoire se traduit par une augmentation des taux de leucocytes totaux et plus particulièrement de polynucléaires neutrophiles et d'IL-6 dans le sang périphérique de l'animal. Cette fraction provoque également une hémolyse indirecte par activation du système du complément, accompagnée d'une importante libération de la peroxydase éosinophile pulmonaire. Cette réponse inflammatoire est comparable à celle induite par le venin total.*

Inflammatory response induced by coagulant fraction C1 isolated from Cerastes cerastes *venom*

The coagulant fraction C1 isolated from the venom of Cerastes cerastes, *induces an inflammatory response upon i.p. injection of 1 mg/kg into rats. The inflammatory reaction is reflected by high levels of total leukocytes and by neutrophils and IL-6 in the peripheral blood of the animal. This fraction caused indirect hemolysis through the activation of the complement system, along with a significant release of pulmonary eosinophilic peroxydase. This inflammatory response is similar to that induced by the whole venom.*

Keywords **:** Cerastes cerastes *venom, coagulant fraction, inflammation, leukocytosis, neutrophil.*

Introduction

Les venins composés de diverses substances à activités biologiques spécifiques sont de plus en plus utilisés en recherche biomédicale et à des fins diagnostiques ou thérapeutiques. La spécificité des propriétés coagulantes ou anticoagulantes des venins les rend utiles pour l'étude des mécanismes hémostatiques. Les protéinases qui représentent un groupe d'enzymes protéolytiques particulièrement impliquées dans la pathogenèse de la nécrose des tissus, d'hémorragies et des troubles de la coagulation sanguines, figurent parmi les constituants majeurs des venins de Viperidae. Certaines protéinases agissent sur les facteurs de coagulation sanguine et peuvent être pro-coagulantes ou anti-coagulantes selon qu'elles exercent des effets activateurs ou inhibiteurs de ces facteurs hémostatiques. Elles sont également douées d'activités fibrino(géno)lytiques de type thrombine (Laraba-Djebari *et al.,* 1992, 1995 ; Chérifi et Laraba-Djebari, 2008).

A partir du venin de la vipère *Cerastes cerastes,* trois sérine-protéinases différentes ont été purifiées et caractérisées (RP-34, Afaâcytine et la fraction coagulante C1) (Laraba-Djebari *et al.,* 1992, 1995 ; Chérifi et Laraba-Djebari, 2008). Plusieurs travaux antérieurs ont rapporté que les venins de Viperidae sont responsables d'importantes réponses inflammatoires et ont attribué cette inflammation aux protéinases qu'ils contiennent. Cependant, très peu d'études se sont focalisées sur l'action directe d'une molécule dans la réponse inflammatoire. Dans ce travail, nous montrons l'induction d'une réponse inflammatoire par la fraction coagulante C1 de type thrombine isolée du venin de *C. cerastes.* La réponse inflammatoire de cette fraction sera comparée avec celle du venin total.

Action du venin et de la fraction C1 sur le nombre de cellules inflammatoires

A partir de 1 g du venin de *Cerastes cerastes*, la fraction fortement coagulante (C1) a été purifiée après deux étapes de purification (gel-filtration sur Sephadex G-75 et chromatographie échangeuse d'anions sur DEAE-Sephadex A-50 ; Chérifi et Laraba-Djebari, 2008). Les rats ont reçu par voie intra-péritonéale (i.p.) une dose de 1 mg/500 µL de venin de *C. cerastes* ou de la fraction C1 par kg du poids corporel ; les témoins

sont traités dans les mêmes conditions par 500 µL de soluté physiologique. Le dénombrement des différentes populations cellulaires dans le sang périphérique est effectué après 3 h, 24 h ou 48 h. Il révèle une hyperleucocytose dont l'évolution varie en fonction du temps. En effet, 3 h après l'envenimation (résultat non illustré), le taux des leucocytes totaux passe de 3,7 x 10^3 à 5,6 x 10^3 cellules/µL pour atteindre 6,6 x 10^3 cellules/µL après 24 h (*Tableau 1*). La fraction C1 induit également une réponse inflammatoire et en particulier un recrutement massif des polynucléaires neutrophiles dans le sang périphérique (*Tableau 1*).

Tableau 1. Dénombrement cellulaire dans le sang des rats après 24 h d'administration du venin ou de la fraction coagulante C1 (moyennes ± écart-types de 2 expériences individuelles).

Table 1. *Leukocyte number in peripheral blood after administration (i.p. route) of the venom or coagulant fraction into rat (means ± S.D. ; n = 2).*

Population cellulaire	Témoin	Venin	Fraction C1
Leucocytes totaux (x 10^3/µL)	3,70 ± 0,51	6,60± 0,13	7,00 ± 1,02
Polynucléaires neutrophiles (cellules /µL)	382 ± 35	681 ± 93	1109 ± 52
Monocytes (cellules/µL)	207 ± 25	589 ± 38	649 ± 47

Effet du venin sur certains marqueurs de l'inflammation

De nombreux travaux ont déjà rapporté la libération de cytokines pro- et/ou anti-inflammatoires consécutive à des envenimations expérimentales ou accidentelles. Ainsi, l'injection d'une DL50 du venin de *Bothrops asper* provoque la libération de cytokines suivant une cinétique biphasique à 4 h et à 18 h d'envenimation (Vera *et al*., 2000). La réponse inflammatoire induite par une dose subléthale de venin total de *C. cerastes* a été évaluée par quantification de certains marqueurs de l'inflammation. Elle est corrélée à la synthèse d'une cytokine pro-inflammatoire (IL-6) et d'une cytokine anti-inflammatoire (IL-10) (résultat non illustré). La peroxydase des éosinophiles (EPO), autre marqueur de l'inflammation, a été dosée dans le tissu pulmonaire afin de déterminer l'effet du venin sur la cascade de l'inflammation. Les données montrent une activité enzymatique biphasique à 3 h et 24 h d'envenimation. L'activité hémolytique du système du complément a été également mise en évidence : le venin provoque une activité lytique triphasique observée 30 min, 24 h et 72 h après l'envenimation. Cependant, une quantification du taux du fibrinogène (qui peut être un marqueur inflammatoire pour certaines maladies) montre que le venin a provoqué une diminution de la concentration du fibrinogène plasmatique. Ce, probablement en raison de son contenu en protéases fibrinogénolytiques. Les valeurs mesurées 24 h après l'envenimation sont données dans le *Tableau 2*.

Action de la fraction C1 sur certains marqueurs de l'inflammation

L'inflammation provoquée par la fraction C1 se caractérise par une production importante de certains marqueurs (IL-6 et complément). L'EPO augmente aussi de façon significative dans le tissu pulmonaire (*Tableau 2*). Nos travaux antérieurs ont déjà montré que la fraction C1 contient une ß fibrinogenase et qu'elle dégrade significativement le fibrinogène plasmatique *in vivo* (2,01 *vs* 4 g/L chez les rats témoins) (Chérifi et Laraba-Djebari, 2008).

Tableau 2. Quantification de certains marqueurs inflammatoires 24 h après ladministration du venin ou de la fraction coagulante C1 (moyennes ± écart-types de 3 expériences individuelles).

Table 2. *Quantification of inflammatory markers after 24 h of venom or coagulant fraction administration into rats (means ± S.D. ; n = 3).*

Marqueurs inflammatoires	Témoin	Venin	Fraction C1
Activité hémolytique par le complément (%)	0	47,48 ± 1,87	44,43 ± 1,28
Taux d'IL-6 (pg/mL)	22,0 ± 1,7	243 ± 24	123 ± 17
Taux d'EPO (UA/mL à 490 nm)	0,09 ± 0,02	0,862 ± 0,188	0,649 ± 0,061
Taux du fibrinogène plasmatique (g/L)	4,0 ± 0,27	0,57 ± 0,06	2,01 ± 0,034

Discussion

Ces résultats montrent que la fraction coagulante C1 induit une réponse inflammatoire systémique qui semble être comparable à celle induite par le venin total. Cette inflammation se traduit par une infiltration des leucocytes dans le sang périphérique notamment les neutrophiles, une activation du système du complément et une augmentation de l'activité de l'EPO pulmonaire. Plusieurs cytokines sont impliquées dans le processus inflammatoire déclenché lors des envenimations vipérines. La mesure de la concentration sérique des cytokines permet de comprendre le processus inflammatoire. Parmi toutes les cytokines pro-

inflammatoires libérées lors des envenimations vipérines, l'IL-6 à un taux relativement élevé a toujours été considérée comme un marqueur de sévérité des envenimations. Dans cette étude, la mesure de l'activité de l'EPO a permis d'évaluer la séquestration des polynucléaires éosinophiles dans le tissu pulmonaire, en raison de la présence spécifique de cette enzyme dans les granules azurophiles des éosinophiles. L'EPO génère des radicaux libres qui exercent des effets cytotoxiques et des altérations protéiques notamment enzymatiques.

Références bibliographiques

Chérifi F, Laraba-Djebari F (2008) Mise en évidence et caractérisation d'une fraction coagulante et agrégante du venin de *Cerastes cerastes*. In *Toxines et fonctions cholinergiques neuronales et non neuronales*, Benoit E, Goudey-Perrière F, Marchot P et Servent D (eds) pp 324-325. Publications de la SFET, Châtenay-Malabry, France, Epub on http://www.sfet.asso.fr (ISSN 1760-6004)

Laraba-Djebari F, Martin-Eauclaire MF, Marchot PA (1992) A fibrinogen-clotting serine proteinase from *Cerastes cerastes* (Horned viper) with arginine–esterase and amidase activities, purification, characterization and kinetic parameter determination. *Toxicon* **30**: 1399-1410

Laraba-Djebari F, Martin-Eauclaire MF, Mauco G, Marchot P (1995) Afaacytin, an alpha beta-fibrinogenase from *Cerastes cerastes* (Horned viper) venom, activates purified Factor X and induces serotonin release from human blood platelets. *Eur J Biochem* **233***:* 756-765

Vera L, Gutièrrez JM, Denise V, Teixeira CFP (2000) Increments in serum cytokine and nitric oxide levels in mice injected with *Bothrops asper* and *Bothrops jararaca* snake venom. *Toxicon* **38**: 1253-1266

Toxines et Signalisation – Toxins and Signalling
Rencontres en Toxinologie – Meeting on Toxinology, 2009
Editions de la SFET – SFET Editions
Accès libre en ligne sur le site – Free access on line on the site : http://www.sfet.asso.fr

Implication des métalloprotéinases dans l'activité dermonécrotique du venin de la vipère Cerastes cerastes

Habiba OUSSEDIK-OUMEHDI, Fatima LARABA-DJEBARI*

Laboratoire de Biologie Cellulaire et Moléculaire, Faculté des Sciences Biologiques, Université des Sciences et de la Technologie « Houari Boumédienne » Bab Ezzouar, et Laboratoire de Recherche et de Développement sur les Venins, Institut Pasteur d'Algérie, Alger, Algérie

** Auteur correspondant ; Tél : +00 213 21336076 ; Fax : +00 213 21336077 ; Courriel : flaraba@hotmail.com*

Résumé

En plus des atteintes systémiques, l'envenimation vipérine se caractérise par des lésions locales au site de la morsure. Ces lésions peuvent évoluer vers la nécrose engendrant souvent des séquelles permanentes. Le venin de la vipère Cerastes cerastes *présente une forte activité dermonécrotique caractérisée par une dose minimale hémorragique de 19 µg pour une souris de 20 g. L'inhibition de cette activité par préincubation du venin avec un chélateur d'ions métalliques, le versenate disodique de calcium ($CaNa_2EDTA$), suggère une implication des métalloprotéinases du venin dans les lésions tissulaires induites.*

Involvement of metalloproteinases in the dermonecrotic activity of Cerastes cerastes *venom*

Snake envenomation is characterized by systemic alterations and by local tissue damage at the bite site. The venom of the viper, Cerastes cerastes, *displays a strong dermonecrotic activity with a minimal necrotic dose of 19 µg per 20 g mouse. Inhibition of this activity upon preincubation of the venom with a metal ion chelator, calcium disodium versenate ($CaNa_2EDTA$), suggests the involvement of venom metalloproteinases in the observed dermonecrosis.*

Keywords : *Dermonecrosis, metalloproteinase, venom, versenate.*

Introduction

L'activité demonécrotique des venins de Viperidae est le résultat de l'action de leurs différents composants touchant principalement l'intégrité des tissus et des cellules. Les molécules impliquées sont essentiellement des enzymes hydrolytiques de type protéinases et phospholipases (Gutièrrez et Rucavado, 2000). Le but de cette étude est de déterminer la classe de protéines impliquées dans l'activité dermonécrotique du venin de la vipère *Cerastes cerastes*.

Activité dermonécrotique du venin de *C. cerastes*

L'activité dermonécrotique est déterminée selon la méthode de Theakston et Reid (1983). Des doses de venin allant de 10 à 40 µg sont injectées par voie intradermique (i.d.) sur la peau dorsale à des lots de 4 souris. Les animaux sont sacrifiés après 72 heures, la peau dorsale est prélevée et les diamètres des lésions nécrotiques sont mesurés. Le logarithme du diamètre moyen de la lésion nécrotique est porté en fonction de la dose de venin injectée. La dose minimale nécrotique (DMN) est estimée par extrapolation à partir de la courbe obtenue.

Le venin de *C. cerastes* induit une activité dermonécrotique au niveau de la face interne de la peau dorsale des animaux. Cette activité est dépendante de la dose de venin injecté (*Figure 1*). La DMN est estimée à 19 µg/20 g de masse corporelle de souris.

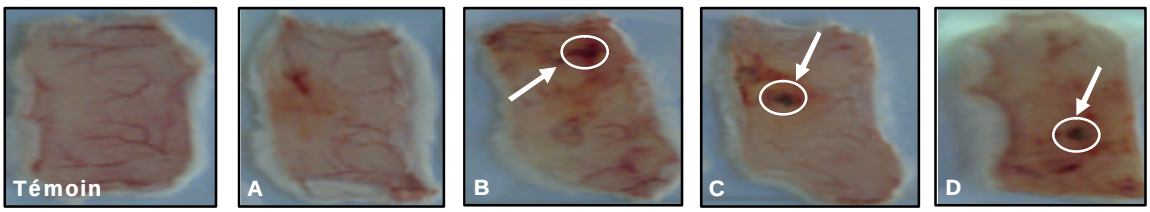

Fig. 1. Activité dermonécrotique du venin de *C. cerastes* (voie i.d.). Le panneau « Témoin » correspond à une injection de NaCl 0,15 M. Les panneaux A, B, C et D correspondent respectivement à des doses de 10, 20, 30 et 40 µg de venin.

Fig. 1. *Dermonecrotic activity after i.d. injection of* C. cerastes *venom. Panel "Témoin" corresponds to an injection of NaCl 0,15 M. Panels A, B, C and D correspond to doses of 10, 20, 30, and 40 µg of venom, respectively.*

Effet du $CaNa_2EDTA$ sur l'activité dermonécrotique du venin de *C. cerastes*

L'effet d'un chélateur d'ions métalliques, le versenate disodique de calcium ($CaNa_2EDTA$), sur l'activité dermonécrotique du venin, est analysé en incubant le venin (30 µg/20 g de masse corporelle de souris) pendant 1 heure à 37°C en présence de concentrations croissantes de $CaNa_2EDTA$ (5, 20, 40 mM). Des volumes de 100 µL de ces mélanges sont alors injectés par voie i.d. à des lots de quatre animaux. Après 72 h, les animaux sont sacrifiés, la peau dorsale est prélevée et les diamètres des lésions nécrotiques sont mesurés. Pour l'étude histologique, la tache nécrotique est découpée et les pièces de peau sont fixées dans du formaldéhyde à 4% pendant 48 h. Après inclusion dans de la paraffine, des coupes de 5 µm d'épaisseur sont colorées par l'hématoxyline-éosine.

Une régression significative de l'activité dermonécrotique du venin est observée avec une réduction de plus de 80% à 5 mM de $CaNa_2EDTA$ et une perte totale à partir de 10 mM (*Figure 2*). Ce résultat suggère une implication des métalloprotéinases du venin de *C. cerastes* dans son activité dermonécrotique. Les coupes histologiques montrent un épaississement et un brunissement de l'épiderme pouvant être dû à une infiltration par les mélanocytes. L'épiderme présente également des zones de rupture avec une structure nécrotique. L'œdème apparaît au niveau du derme et de la jonction épidermo-dermique. Le derme présente également des aires hémorragiques, une congestion des vaisseaux et une rupture des follicules pileux. La présence de polynucléaires et de macrophages au niveau des régions altérées indique une infiltration inflammatoire (*Figure 3*). En présence du $CaNa_2EDTA$, l'aspect tissulaire de la peau est comparable à celui du témoin. Il persiste cependant un petit œdème suggérant une faible activité œdématogène du chélateur.

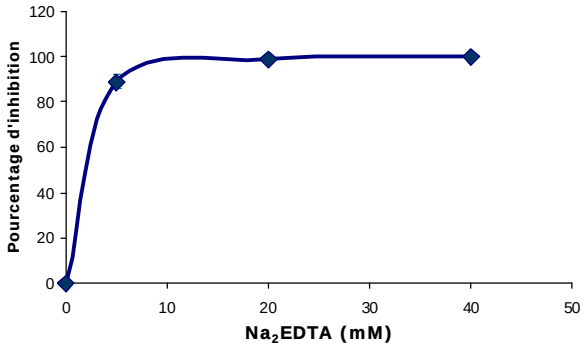

Fig. 2. Effet du $CaNa_2EDTA$ sur l'activité dermonécrotique du venin de *C. cerastes* (30 µg/20 g souris).

Fig. 2. *Effect of $CaNa_2EDTA$ on the dermonecrotic activity of* C. cerastes *venom (30 µg/20 g mouse).*

Ces résultats sont en accord avec ceux de Rucavado et *al*. (2000) montrant une inhibition totale de l'activité dermonécrotique du venin de *Bothrops asper* après incubation avec 40 mM de ce chélateur. Par ailleurs, l'inhibition totale de l'activité dermonécrotique provoquée par les sécrétions de la glande de Duvernoy du cobra *Philodryas patagoniensis* après incubation avec 1 mM de $CaNa_2EDTA$ suggère que cette activité serait associée aux métalloprotéinases (Peichoto et *al.* 2004).

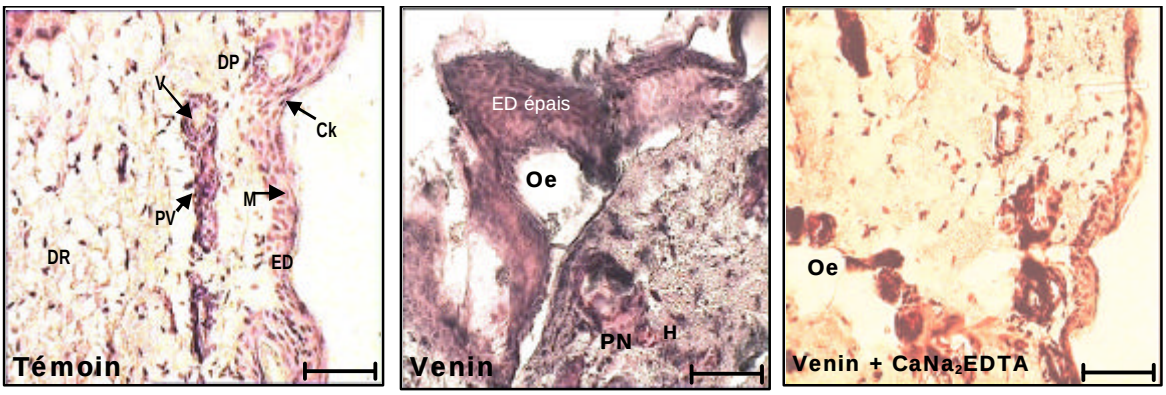

Fig. 3. Aspect histologique de la dermonécrose après trois jours d'envenimation. Le panneau « Témoin » correspond à une injection de NaCl 0,15 M. Les panneaux « Venin » et « Venin + $CaNa_2EDTA$ » correspondent à des injections de venin (30 µg/20 g de souris) sans et après préincubation avec $CaNa_2EDTA$ (40 mM). La coloration est effectuée avec de l'hématoxyline-éosine (**Ck** : Couche kératinisée. **D** : Derme, **DP** : Derme papillaire, **DR** : Derme réticulaire, **ED** : Epiderme, **F** : Follicule pileux, **H** : Hémorragie, **N** : Nécrose, **Oe** : Œdème, **PN** : Polynucléaires, **PV** : Plexus vasculaire). Echelle : 33 µm.

Fig. 3*. Histological aspect of dermonecrosis three days post envenomation. Panel "Témoin" corresponds to an injection of NaCl 0,15 M. Panels « Venin » and « Venin + $CaNa_2EDTA$ » correspond to injections of venom (30 µg/20 g de souris) directly and preincubated with $CaNa_2EDTA$ (40 mM), respectively. Staining used hematoxyline-eosine*. Scale bar : 33 µm.

Conclusion

La pré-incubation d'un chélateur d'ions métalliques, le $CaNa_2EDTA$, avec le venin de la vipère *C. cerastes* avant injection à la souris inhibe l'activité dermonécrotique du venin. Cette observation implique des métalloprotéinases dans les altérations tissulaires de la peau induites par le venin. Ces résultats suggèrent qu'un traitement avec ce chélateur à une concentration de 5 mM, dès les premiers instants qui suivent une envenimation, permettrait de neutraliser les enzymes à activité métallo-dépendante du venin avant leur diffusion et leur répartition dans les compartiments tissulaires. L'administration d'inhibiteurs de forte diffusibilité (tel le $CaNa_2EDTA$) pourrait neutraliser les composants dermonécrotiques du venin et les empêcher de générer des lésions tardives.

Références bibliographiques

Gutiérrez JM, Rucavado A (2000) Snake venom metalloproteinases: their role in the pathogenesis of local tissue damage. *Biochimie* **82**: 841-850

Peichoto ME, Acosta O, Leiva L, Teibler P, Marunak S, Ruiz R (2004) Muscle and skin necrotizing and edema-forming activities of Duvernoy gland secretion of the xenodentine colubrid snake *Philodryas patagoniensis* from the north-east of Argentina.*Toxicon* **44**: 589-596

Rucavado A, Escalante T, Franceschi A, Chaves F, León G, Cury Y, Ovadia M, Gutiérrez JM (2000) Inhibition of local hemorrhage and dermonecrosis induced by *Bothrops asper* snake venom: Effectiveness of early *in situ* administration of the peptidomimetic metalloproteinase inhibitor Batimastat and the chelating agent $CaNa_2EDTA$. *Am J Trop Med Hyg* **63**: 313-319

Theakston RDG, Reid HA (1983) Development of simple standard assay procedures for the characterization of snake venoms. *Bull WHO* **61**: 949-956

Toxines et Signalisation – Toxins and Signalling
Rencontres en Toxinologie – Meeting on Toxinology, 2009
Editions de la SFET – SFET Editions
Accès libre en ligne sur le site – Free access on line on the site : http://www.sfet.asso.fr

Cardiovascular and renal effects of Bothrops marajoensis *venom*

Rodrigo DANTAS[1*], Inez EVANGELISTA[1], Alba TORRES[2], Ramon MENEZES[2], Thiala da SILVA[2], Nilberto do NASCIMENTO[3], Marcos TOYAMA[4], Maria OLIVEIRA[1], Helena MONTEIRO[2], Alice MARTINS[2]

[1] *Department of Physiology and Pharmacology, Federal University of Ceará, Fortaleza, Ceará, Brazil* ; [2] *Department of Clinical and Toxicological Analysis, Pharmacy Faculty, Federal University of Ceará, Fortaleza, Ceará, Brazil* ; [3] *Veterinary Medicine Faculty, State University of Ceara, Fortaleza, Ceará, Brazil* ; [4] *São Vicente Unity, Campus of Litoral Paulista, Paulista State University (UNESP), São Paulo, Brazil*

** Corresponding author ; Tel : +55 (0) 85 3366-8269 ; Fax : +55 (0) 85 3366-8292 ;*
E-mail : tavaresdantas@gmail.com

Abstract

In Brazil, there is a large number of species of snakes, and some substances with pharmacological activity have already been gotten by means of studies of their venom. Among the Brazilian snakes, the genus Bothrops *is distinguished due to a high number of accidents. Botropic envenomations are characterized by prominent local tissue damage, haemorrhage, necrosis, oedema, as well as alterations in blood coagulation and acute renal failure. Therefore, we investigated the cardiovascular and renal effects of the* Bothrops marajoensis *(*Bmj*) venom, as well as its cytotoxic action on murine macrophages and Madin-Darby canine kidney (MDCK) cells.* Bmj *venom reduced the myocardial force of contraction and increased the perfusion pressure, without change in the coronary flow. The venom caused also hypotension accompanied by bradycardia and a block of electric conduction in the heart. In the kidney, the venom decreased the perfusion pressure, renal vascular resistance, urinary flow and glomerular filtration rate. Finally,* Bmj *venom reduced the viability of murine macrophages, but this reduction was not significant when compared to controls. In contrast, it promoted a dose-dependent cytotoxic effect on MDCK cells, with an* IC_{50} *(dose producing 50% cytotoxicity) value of 18 µg/mL.*

Effets cardio-vasculaires et rénaux du venin de Bothrops marajoensis

Au Brésil, il y a un grand nombre d'espèces de serpents et quelques substances présentant une activité pharmacologique ont déjà été obtenues par l'étude de leur venin. Parmi les serpents brésiliens, le genre Bothrops *se distingue du fait d'un nombre élevé d'accidents. Les envenimations par* Bothrops *sont caractérisées par des lésions intenses du tissu local, une hémorragie, une nécrose, un œdème ainsi que par des troubles de la coagulation du sang et une insuffisance rénale aiguë. Nous avons étudié les effets cardio-vasculaires et rénaux du venin de* Bothrops marajoensis *(*Bmj*) ainsi que son action cytotoxique sur les macrophages murins et les cellules rénales de chien Madin-Darby (MDCK). L'administration du venin de* Bmj *dans un modèle de cœur isolé-perfusé réduit la force de la contraction myocardique et augmente la pression de perfusion, sans changement de la circulation coronaire. Le venin provoque également une baisse de la pression artérielle moyenne et produit une hypotension et une bradycardie avec un bloc de la conduction électrique du cœur. Dans le rein, il diminue la pression de perfusion, la résistance vasculaire rénale, l'écoulement urinaire et le taux de filtrage glomérulaire. Finalement, au niveau des macrophages murins, le venin de* Bmj *induit une réduction non significative de la viabilité des cellules. Cependant, il exerce un effet cytotoxique sur les cellules MDCK, dépendant de la dose, avec une valeur d'*IC_{50} *(dose produisant 50% de cytotoxicité) de 18 µg/mL.*

Keywords : Bothrops marajoensis*, cardiotoxicity, nephrotoxicity, MDCK cells.*

Introduction

In Brazil, there is a large number of species of snakes, and some substances with pharmacological activity have already been obtained by means of studies of their venom. Among the Brazilian snakes, the genus *Bothrops* is distinguished due to the high number of accidents with these snakes (Brasil, 1998).

Botropic envenomations are characterized by prominent local tissue damage, haemorrhage, necrosis, oedema, as well as alterations in blood coagulation and acute renal failure (Ownby, 1990 ; Stocker, 1990 ; Bjarnason and Fox, 1994). Renal and cardiovascular effects have been described for venom of several species of the botropic genus (Barbosa *et al.*, 2005 ; Havt *et al.*, 2005 ; Sifuentes, 2008). Braga *et al.* (2008) demonstrated the effects of *Bothrops insularis* venom on isolated kidneys.

Bothrops marajoensis is an endemic species in the savannah of Marajó Island in the State of Pará and in some regions of Amapá State, in the north of Brazil. Despite its abundance in these regions, little is known about the venom of this species. In this work, we examined the renal and cardiovascular effects of the *Bothrops marajoensis* venom, as well as its cytotoxic action on murine macrophages and Madin-Darby canine kidney (MDCK) cells.

The kidney is a complex organ, consisting of cells whose growth and physiological functions are affected by poisons (Marotta *et al*., 2006). Differentiated epithelial kidney cell lines provide a convenient system to study the effects of poisons on these organ functions. The MDCK cell line, for example, bears close resemblance to transporting epithelia present in the kidney (Taub *et al*., 1979) and is the best established mammalian model for studying epithelial cell biology (Füllekrug *et al*., 2006).

Materials and methods

Venom, chemicals and drugs

The *Bothrops marajoensis (Bmj)* venom was kindly donated by Dr. Marcos H. Toyama (Paulista State University, UNESP, São Paulo, Brazil). Atropine and acetylcholine were purchased from Sigma (St Louis, MO) and were dissolved at the day of experiments.

Isolated perfused heart

Wistar rats (250-350 g body weight) were anesthetised by intraperitoneal (i.p.) injection of pentobarbital sodium (50 mg/kg), followed by i.p. administration of heparin (500 IU/kg). The thorax was opened, and the heart was frozen with a perfused solution according to the method of Ruskoaho and Leppäluoto (1988). The aorta was cannulated above the aortic valve, and Langendorff retrograde perfusion was performed with a Krebs-Henseleit solution containing : NaCl, 114.0 mM ; KCl, 4.96 mM ; KH_2PO_4, 1.24 mM ; $MgSO_4/7H_2O$, 0.5 mM ; $NaHCO_3$, 24.99 mM ; $CaCl_2/2H_2O$, 2.10 mM ; glucose, 3.60 mM. The solution was at pH 7.4, adjusted with NaOH, and gassed with 95% O_2 -5% CO_2 at 37°C.

Variations in the perfusion pressure were measured with a mercury manometer attached to the recording system. The isometric force of contraction was recorded by a strain gauge transducer (model FT03, Gould Instruments) connected to a Gould polygraph. The hearts were exposed to a resting tension of 2 g, and heart rate was counted from the contraction recordings using a Gould tachograph. During the equilibration period (60 min), the hearts were perfused with a peristaltic pump (Ismantec AS801) at a flow rate of 12 mL/min. The *Bmj* venom was used at various doses (0.3, 1.0, 3.0, 10.0 and 30.0 μg/mL ; n = 6 for each group) and its effects were compared to those of isovolumetric administration of saline (n = 6).

Blood pressure measurements

Male Wistar rats, weighing 250-300 g, were anesthetised with 50 mg/kg pentobarbital followed by i.p. administration of heparin (500 IU/kg), and, thereafter, the right carotid artery was cannulated with a polyethylene tube (PE50). The systemic blood pressure was recorded directly through a pressure transducer (P23 Gould Statham, Oxnard, CA, USA) connected to a polygraph (Narco Biosystems, Houston, Texas, USA). The mean arterial blood pressure was recorded continuously, and, after a 30 min equilibration period, atropine (1 μg/kg) and/or acetylcholine (1 μg/kg) were injected through a cannula implanted in the jugular vein. The *Bmj* venom (1, 3, 10, 30, 100 and 300 μg/kg ; n = 6 for each group) was injected at 15 min intervals and its effects were compared to those of isovolumetric injection of saline (n = 6) and 1 μg/kg acetylcholine (n = 6 ; Chen, 1967).

Electrocardiogram analysis

Male Wistar rats (250-300 g) were fasted for 24 h with free access to water. The rats were anesthetised with sodium pentobarbital (50 mg/kg, i.p.), and bipolar electrodes were implanted subcutaneously (limb lead II) and connected to an electrographic recorder (EKA-8 Burbik). The *Bmj* venom (100 μg/kg, n = 6) administration was probed against isovolumetric injection of saline (n = 6). The effects of *Bjm* were analysed on the duration of the PP, TQ, RR and PR intervals, as well as on QRS complex and P wave.

Kidney perfusion

Adult male Wistar rats (260-320 g) were fasted for 24 h with free access to water. The rats were anesthetised with sodium pentobarbital (50 mg/kg, i.p.) and, after careful dissection of their right kidney, the right renal artery was cannulated *via* the mesenteric artery without interrupting the renal blood flow, as described by Bowman (1970) and modified by Fonteles *et al*. (1983). The perfusion fluid was a modified Krebs-Henseleit (MKH) solution composed of (in mM) : 118 NaCl, 1.2 KCl, 1.18 KH_2PO_4, 1.18 $MgSO_4.7H_2O$, 2.5 $CaCl_2 2H_2O$ and 25 $NaHCO_3$, and added with bovine serum albumin (BSA, 6 g ; fraction V), urea (0.075 g), inulin (0.075 g) and glucose (0.15 g) for a final perfusate volume of 100 mL. The pH was adjusted to 7.4 with NaOH. In each experiment, 100 mL of MKH solution were recirculated for 120 min. The perfusion pressure was measured at the tip of the stainless steel cannula in the renal artery. Samples of urine and perfusate were collected at 10 min intervals for analysis of sodium and potassium levels by flame photometry. Inulin was analysed as described by Walser *et al*. (1955) and modified by Fonteles *et al*. (1983), and osmolality was measured using a vapour pressure osmometer (Wescor 5100C, USA). *Bmj* venom (30 μg/mL, n = 6) was added to the system 30 min after the beginning of each perfusion. The perfusion pressure, renal vascular resistance, urinary flow, glomerular filtration rate, and percents of sodium and potassium tubular transports were determined. The values obtained in the presence of *Bmj* venom were compared to those determined before venom addition.

Cytotoxicity on MDCK cells and murine macrophages

The viability of MDCK cells was determined using MTT (3-(4,5-dimethylthiazol-2-yl)-2,5-diphenyltetrazolium bromide) assay (Mosman, 1983). Macrophages, obtained from peritoneal cavity of Swiss female mice, and MDCK cells were cultivated in RPMI-1640 medium, supplemented with fetal bovine serum (FBS, 10%), penicillin (100 IU/mL) and streptomycin (100 µg/mL), and seed $1x10^6$ and $1x10^5$ cells/mL, respectively, in 96-well microplates for 2 h for attachment, at 37ºC in an atmosphere with 5% of CO_2. Cells were washed twice with medium at 37ºC and further incubated with various doses of *Bmj* venom for 24 h at 37ºC. After incubation, 100 µL of the medium was aspirated, 10 µL of MTT was added to the wells, and the plate was incubated for 4 h. Then, 90 µL of solution containing 10% SDS (sodium dodecyl sulfate)/HCl were added to solubilize the MTT-formazan product. After 17 h, the plate was read with a microplate reader at 570 nm. All the measurements were performed in quadruplicate.

Statistical analysis

Results are presented as the mean ± S.E.M. from six experiments for each group. Differences between groups were compared using the Student's *t*-test (non-parametric test) or analysis of variance (ANOVA) followed by the Bonferroni test with significance set at 5%.

Committee of Ethics

The study protocol was approved by the Committee of Ethics from Federal University of Ceará, in Fortaleza, Brazil (number 68/08).

Results and Discussion

Effects of *Bmj* venom on rat isolated perfused hearts

In rat isolated hearts, the perfusion of *Bmj* venom (0.1, 0.3, 1, 3, 10 and 30 µg/mL), in a dose-dependent manner, decreased the force of myocardial contraction (to 31.7 ± 13.2% ; *Figure 1a*) and increased the perfusion pressure (27.5 ± 3.6% to 92.7 ± 24%) (*Figure 1b*) without changes in the perfusion flow (*Figure 1c*). Bradycardia was also observed in the presence of the venom (see also *Figure 4*). The result obtained indicates an inverse relationship between the force of contraction and perfusion pressure without altering the flow of perfusion.

The system used in the present study was based on Langendorff retrograde perfusion (*via* the aorta) of an isolated heart. The effect of pressure that accompanies bradycardia in isolated hearts perfused with crystalloid solutions likely reflects the inability of solutions to adequately supply the energy demand of the myocardium. Thus, a reduction in myocardial energy consumption may have occurred, allowing an improvement in contractile performance and, consequently, an increase in the systolic pressure.

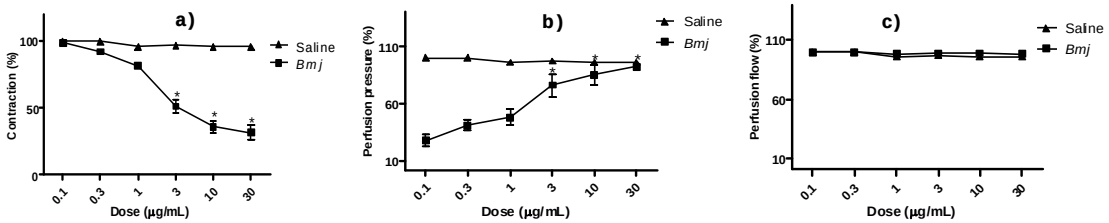

Fig. 1. Effects of *Bmj* venom on myocardial contraction (**a**), cardiac perfusion pressure (**b**) and perfusion flow (**c**). Results expressed as means ± SEM. *p<0.05 compared to the saline solution.

Fig. 1. *Effets du venin de* Bmj *sur la contraction du myocarde (**a**), la pression de la perfusion cardiaque (**b**) et le flux de perfusion (**c**). Les résultats sont indiqués par les moyennes ± ESM. *p<0,05 comparé à la solution saline.*

Effects of *Bmj* venom on arterial blood pressure

Whole venom from *Bmj* (1, 3, 10, 30, 100 and 300 µg/kg) produced a decrease of the mean arterial pressure (to 31.6 ± 5.3% with 300 µg/kg ; *Figure 2a*) and cardiac frequency (to 66.9 ± 5.4% with 300 µg/kg ; *Figure 2b*), without significant changes in the respiratory rate (*Figure 2c*).

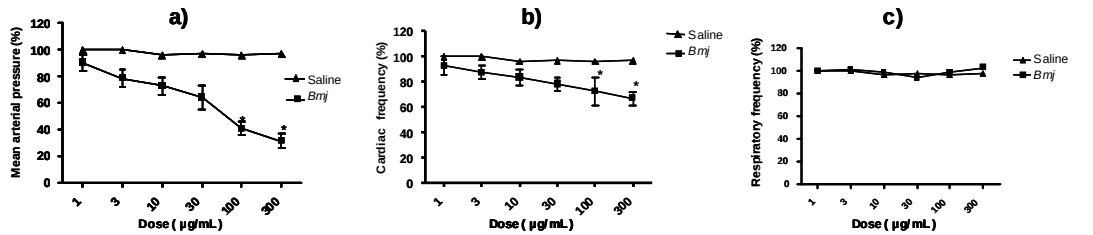

Fig. 2. Effects of the *Bmj* venom on isolated heart perfused. Mean arterial pressure (**a**), cardiac frequency (**b**) and respiratory frequency (**c**)**,** expressed as means ± SEM. *p<0.05 compared to the saline solution.

Fig. 2. *Effets du venin de* Bmj *sur le cœur isolé perfusé. Pression artérielle moyenne (**a**), fréquences cardiaque (**b**) et respiratoire (**c**) exprimées par les moyennes ± ESM. *p<0,05 comparé à la solution saline.*

The changes in the mean arterial pressure induced by venom perfusion (300 µg/kg) were 73.9 ± 15.6%, and, in rats treated with atropine, 72.9 ± 11.7% (data not shown). The heart rates, recorded in the presence of the highest dose of venom (300 µg/kg), were 66.9 ± 15% and, in animals treated with atropine, 67.7 ± 17% (*Figure 3*). It is worth noting that, in the absence of venom, atropine was observed to reverse the acetylcholine-induced decrease of the cardiac frequency. Finally, in the presence of *Bmj* venom, atropine induced no change in the respiratory rate : 97.9 ± 9.6% with whole venom alone, and 98.3 ± 7.4% with whole venom and atropine (data not shown).

Cardiovascular changes have been previously described for the venom of several species of the botropic genus (Rocha *et al*., 1949 ; Lomonte and Gutierrez, 1989 ; Selistre *et al*., 1990 ; Sifuentes, 2008).

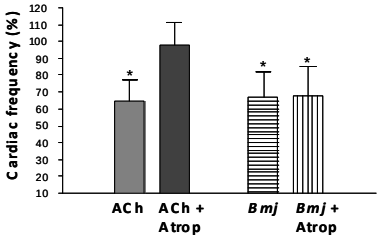

Fig. 3. Effects of *Bmj* venom (300 µg/kg) on the cardiac frequency. Results are expressed as the mean ± SEM. ACh : acetylcholine (1 µg/kg), Atrop : atropine (1 µg/kg). *p<0.05 compared to control.

Fig. 3. *Effets du venin de* Bmj *(300 µg/kg) sur la fréquence cardiaque, exprimée par la moyenne ± ESM. ACh : acetylcholine (1 µg/kg), Atrop : atropine (1 µg/kg). *p<0,05 en comparant au contrôle.*

The Bezold-Jarisch reflex describes cardiovascular reflexes involving sensory receptors located mainly in the left cardiac ventricle, when unmyelinated vagal afferent pathways are influenced by mechanical or chemical stimulation. The stimulation of these pathways increases parasympathetic activity and inhibits sympathetic activity, which results in bradycardia, hypotension and nausea. Atropine, a well-known muscarinic antagonist is effective in reducing the severity of these symptoms (Bezold, 1867 ; Jarisch and Henze, 1937 ; Mark, 1983).

To determine whether the hypotensive effects produced by *Bmj* venom resulted from the Bezold-Jarisch reflex involving ventricular receptors, the venom was administered in rats pre-treated with atropine. The cholinergic (muscarinic) block with atropine did not alter the drop in blood pressure induced by the venom (data not shown). This demonstrates that the hypotension and bradycardia induced by *Bmj* venom do not seem to result from parasympathetic system activation.

Electrocardiographic activity of *Bmj* venom

Intravenous injection of *Bmj* venom caused a gradual atrioventricular (AV) block that, in some experiments, resulted in a complete (third degree) AV block. During the gradual AV block, the ratio of atrial and ventricular frequencies was 2/1. In the presence of *Bmj* venom, an atrial flutter (67% per replicate) and a reversal in late hyperpolarisation were observed (*Figure 4*), indicating that QRS complex arrhythmia (P waves and QRS complexes appeared independently) and dysfunction of atrial conduction (complete AV dissociation) occurred.

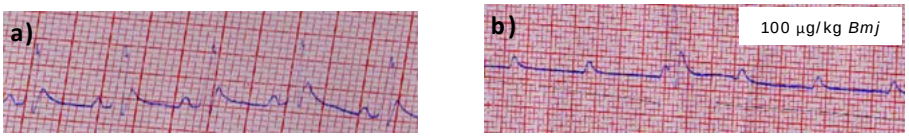

Fig. 4. Representative electrocardiograms (**a**, control ; **b**, *Bmj* venom).

Fig. 4. *Electrocardiogrammes représentatifs (**a**, témoin ; **b**, venin de* Bmj*).*

The changes produced by *Bmj* venom in the electrocardiogram segments are shown in *Table 1*. In particular, a significant increase in PP and RR intervals could be noted, indicating a decrease of heart rate.

Table 1. Effects of *Bmj venom* (100 µg/kg) on the different electrocardiogram segments.

Tableau 1. *Effets du venin de* Bmj *(100 µg/kg) sur les différents segments de l'électrocardiogramme.*

Parameters	Control	Saline	*Bmj venom*
PP interval (ms)	208 ± 6.2	208 ± 22.64	457 ± 0.75*
RR interval (ms)	182 ± 10.69	182 ± 6.12	414 ± 0.76*
QRS duration (ms)	98 ± 8.12	97.9 ± 1.1	101 ± 9.7
QRS amplitude (mV)	5.8 ± 0.8	5.5 ± 0.6	5.5 ± 1.2
TQ interval (ms)	14 ± 0.53	13.9 ± 0.2	12.6 ± 0.9
P wave amplitude (mV)	0.2 ± 0.032	0.18 ± 0.05	0.21 ± 0.02
PR interval (ms)	66 ± 0.8	66 ± 0.9	89 ± 1.6 *

Results are expressed as means ± SEM. *p<0.05 compared to control values.

*Les résultats sont exprimés par les moyennes ± ESM. *p<0,05 en comparant aux valeurs contrôles.*

Therefore, *Bmj* venom produced hypotension and bradycardia, with a block in electric conduction, in the heart.

Renal effects of *Bmj* venom

Bmj venom (30 μg/mL) caused a significant decrease of perfusion pressure (*Figure 5a*) and renal vascular resistance (*Figure 5b*) at 60, 90 and 120 min after perfusion of the venom.

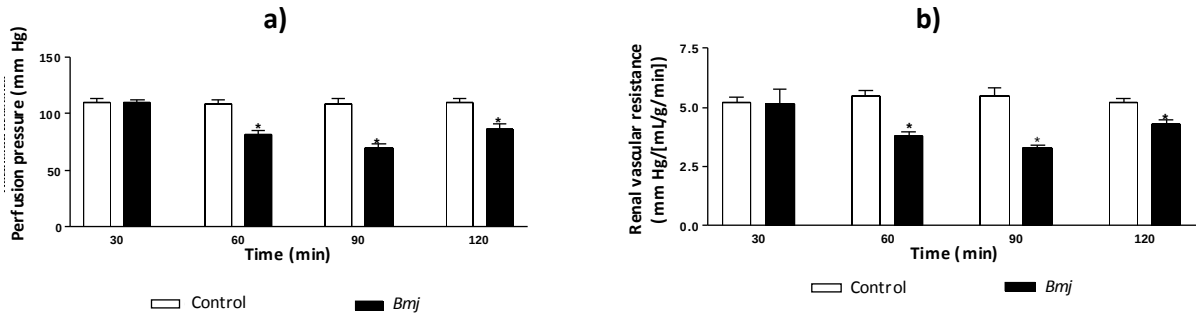

Fig. 5. Effects of *Bmj* venom (30 μg/mL) on perfusion pressure (**a**) and renal vascular resistance (**b**). Data are expressed as means ± SEM. *p<0.05 compared to the corresponding control groups.

Fig. 5. *Effets du venin de* Bmj *(30 μg/mL) sur la pression de perfusion (**a**) et la résistance vasculaire du rein (**b**). Les résultats sont exprimés par les moyennes ± ESM. * p<0,05 en comparant aux groupes témoins correspondants.*

The urinary flow and glomerular filtration rate were significantly decreased after perfusion of *Bmj* venom at 60 and 90 min (*Figures 6a*) and 60, 90 and 120 min (*Figure 6b*), respectively. The percent of sodium tubular transport was reduced at 90 and 120 min of perfusion from 85.14 ± 0.75% to 61.60 ± 2.30% and 60.60 ± 2.0%, respectively. Conversely, *Bmj* venom did not change the percent of potassium tubular transport ($control_{120min}$ = 56.98 ± 2.17% ; Bmj_{120min}=57.25 ± 3.19%).

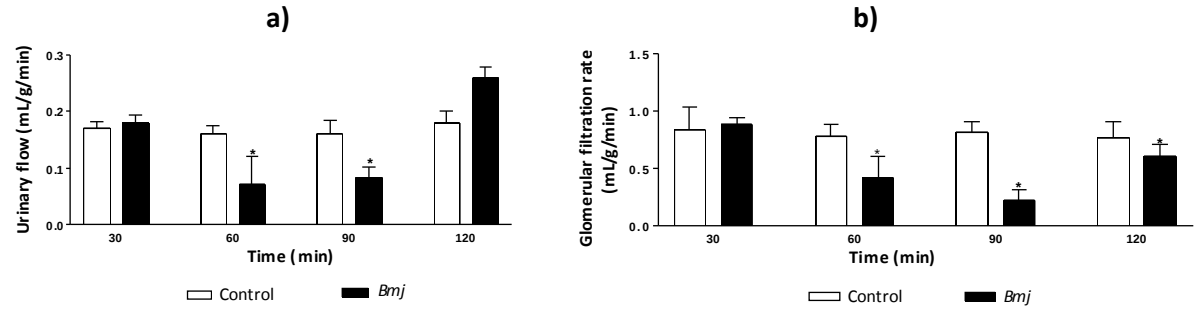

Fig. 6. Effects of *Bmj* venom (30 μg/mL) on urinary flow (**a**) and glomerular filtration rate (**b**). Data are expressed as means ± SEM. *p<0.05 compared to the corresponding control groups.

Fig. 6. *Effets du venin de* Bmj *(30 μg/mL) sur le flux urinaire (**a**) et le taux de filtration glomérulaire (**b**). Les résultats sont exprimés par les moyennes ± ESM. * p<0,05 en comparant aux groupes témoins correspondants.*

These observations are consistent with the results of previous studies concerning the venoms of other snakes from the same gender. Hence, Braga *et al.* (2006) assessed the renal and vascular effects of *Bothrops insularis* venom in the perfusion system and reported a decrease of vascular and functional parameters. In addition, *Bothrops jararaca* (Monteiro and Fonteles, 1999) and *Bothrops jararacussu* (Havt *et al*., 2001) venoms have been shown to decrease the perfusion pressure, renal vascular resistance, urinary flow and glomerular filtration rate in the rat isolated kidney.

Effects of *Bmj* venom on murine macrophages and MDCK cells

Analyses of *Bmj* venom cytotoxicity were performed on murine macrophages and MDCK cells using the MTT assay (see *Materials and methods*). At studied doses, the venom caused a reduction in the viability of murine macrophages. However, this reduction was not significant when compared to controls (p>0.05).

In MDCK cells, *Bmj* venom promoted a dose-dependent cytotoxic effect with an IC_{50} value (dose producing 50% cytotoxicity) of 18 μg/mL. The viability of cells, exposed to different doses of venom for 24 h, is shown in *Figure 7*. It is worth noting that treatment with venom caused cell death without membrane disruption when compared to controls (*Figure 8*).

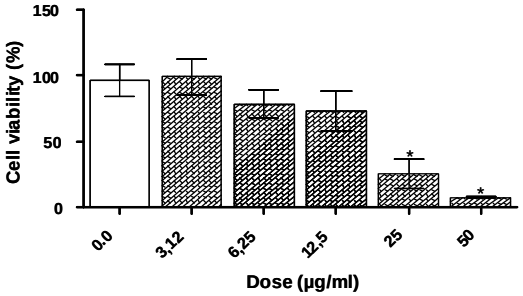

Fig. 7. Cytotoxic effect of different doses of *Bmj* venom on MDCK cells. The initial cell density was $1x10^5$ cells/mL. The graph presents mean ± SEM. *p<0.05 compared to control values.

Fig. 7. *Effet cytotoxique de différentes doses du venin de* Bmj *sur les cellules MDCK. La densité initiale de cellules est de $1x10^5$ cellules/mL. Le graphique représente la moyenne ± ESM. *p<0,05 en comparant aux valeurs contrôles.*

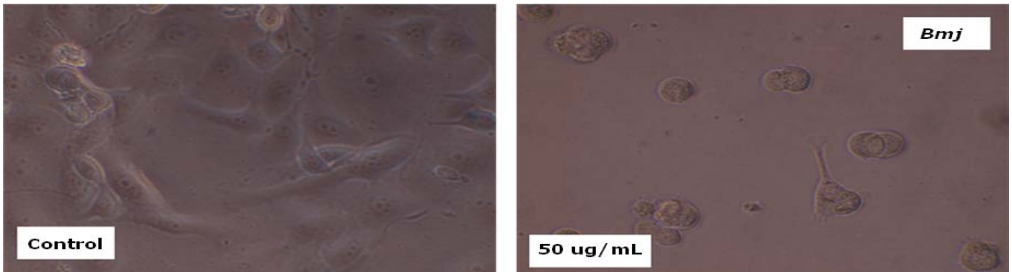

Fig. 8. Morphological changes of MDCK cells after exposure to 50 µg/mL *Bmj* venom. The MDCK cells treated with phosphate buffered saline (PBS) served as negative controls (Control).

Fig. 8. *Changements morphologiques des cellules MDCK après leur exposition au venin de* Bmj *(50 µg/mL). Les cellules MDCK incubées dans du PBS servent de témoins négatifs.*

Conclusion

The *Bmj* venom presents both cardiotoxic and nephrotoxic activities in the rat. It reduces the myocardial force of contraction, accompanied by an increase in the perfusion pressure, without change in the coronary flow. The venom produces also a drop in the mean arterial pressure and hypotension accompanied with bradycardia and block in electric conduction in the heart. The electrocardiographic analysis reveals that the venom causes a progressive, until a complete, atrioventricular block. In the kidney, *Bmj* venom decreases the perfusion pressure, renal vascular resistance, urinary flow and glomerular filtration rate, with a drop in the transport of sodium, potassium and chloride ions. Finally, the venom reduces the viability of murine macrophages. However, this reduction is not significant when compared to controls. In contrast, it promotes a dose-dependent cytotoxic effect on MDCK cells, with an IC_{50} value of 18 µg/mL.

Acknowledgements. *We are grateful to the CAPES, CNPQ and FUNCAP for financial support.*

References

Barbosa PS, Martins AM, Havt A, Toyama DO, Evangelista JS, Ferreira DP, Joazeiro PP, Beriam LO, Toyama MH, Fonteles MC, Monteiro HS (2005) Renal and antibacterial effects induced by myotoxin I and II isolated from *Bothrops jararacussu* venom. *Toxicon* **46**: 376-386

Bezold A von (1867) *Über die physiologischen Wirkungen des essigsäuren Veratrins.* With Ludwig Hirt (1844-1907). In: Untersuchungen aus dem physiologischen Laboratorium in Würzburg. Leipzig, **1**: 73-123

Bjarnason JB, Fox JW (1994) Hemorrhagic metalloproteinases from snake venoms. *Pharmacol Ther* **62**: 325-372

Braga MD, Martins AM, Amora DN, de Menezes DB, Toyama MH, Toyama DO, Marangoni S, Barbosa PS, de Sousa Alves R, Fonteles MC, Monteiro HS (2006) Purification and biological effects of C-type lectin isolated from *Bothrops insularis* venom. *Toxicon* **47**: 859-867

Braga MD, Martins AM, Amora DN, de Menezes DB, Toyama MH, Toyama DO, Marangoni S, Alves CD, Barbosa PS, de Sousa Alves R, Fonteles MC, Monteiro HS (2008) Purification and biological effects of L-amino acid oxidase isolated from *Bothrops insularis* venom. *Toxicon* **51**: 199-207

Brasil (1998) *Manual de diagnóstico e tratamento de acidentes por animais peçonhentos.* Brasília: FUNASA, Ministério da Saúde

Chen K K, Kovarakova¡ A (1967) Pharmacology and toxicology of toad venom. *J Pharm Sci* **56**: 1535-1541

Fonteles MC, Ganapathy V, Pashley, DH, Leibach FH (1983) Dipeptide metabolism in the isolated perfused rat kidney. *Life Sci* **33**: 431-436

Füllekrug J, Shevchenk A, Shevchenko A, Simons K (2006) Identification of glycosylated marker proteins of epithelial polarity in MDCK cells by homology driven proteomics. *BMC Biochemistry* **7**: 8

Gutiérrez JM, Nunez J, Escalante T, Rucavado A (2006) Blood flow is required for rapid endothelial cell damage induced by a snake venom hemorrhagic metalloproteinase. *Microvasc Res* **71**: 55-63

Havt A, Fonteles MC, Monteiro HS (2001) The renal effects of *Bothrops jararacussu* venom and the role of PLA_2 and PAF blockers. *Toxicon* **39**: 1841-1846

Havt A, Toyama MH, do Nascimento NR, Toyama DO, Nobre AC, Martins AM, Barbosa PS, Novello JC, Boschero AC, Carneiro EM, Fonteles MC, Monteiro HS (2005) A new C-type animal lectin isolated from *Bothrops pirajai* is responsible for the snake venom major effects in the isolated kidney. *Int J Biochem Cell Biol* **37**: 130-141

Jarisch A, Heinze C (1937) Über Blutdrucksenkung durch chemische Erregung depressorischer Nerven. *Archiv für experimentelle Phatologie und Pharmakologie* **187**: 706-730

Lomonte B, Gutiérrez JM (1989) A new muscle damaging toxin, myotoxin II, from the venom of the *Bothrops asper* (terciopelo). *Toxicon* **27**: 725-733

Mark AL (1983) The Bezold-Jarisch reflex revisited: clinical implications of inhibitory reflexes originating in the heart. *J Am Coll Cardiol* **1**: 90-102

Marotta AMM, Alencar MRP, Andrade TA, Xagoraris M, Ruivo GF (2006) Insuficiência renal aguda após acidente botrópico: um relato de caso. *Rev. biocên* **12**: 88-93

Monteiro HSA, Fonteles MC (1999) The effect of *Bothrops jararaca* venom on rat kidney after short-term exposure: preliminary results. *Pharmacol Toxicol* **85**: 198-200

Mosmann T (1983) Rapid colorimetric assay for cellular growth and survival: application to proliferation and cytotoxicity. *J Immunol Methods* **65**: 55-63

Ownby CL, Colberg TR (1990) Comparison of the immunogenicity and antigenic composition of several venoms of snakes in the family Crotalidae. *Toxicon* **28**: 189-199

Rocha SM, Beraldo WT, Rosenfeld G (1949) Bradykinin, a hipotensive smoth muscle stimulating factor released plasma globulin by snake venoms and by trypsin. *Am J Physiol* **156**: 261-273

Ruskoaho H, Leppaluoto J (1998) Immunoreactive atrial natriuretic peptide in ventricles, atria, hypothalamus, and plasma of genetically hypertensive rats. *Circ* **62**: 384-394

Selistre HS, Queiroz LS, Cunha OA, De Souza GE, Giglio JR (1990) Isolation and characterization of hemorrhagic, myonecrotic and edema-inducing toxins from *Bothrops insularis* (jararaca ilhoa) snake venom. *Toxicon* **28**: 261-273

Sifuentes DN, El-Kik CZ, Ricardo HD, Tomaz MA, Strauch MA, Calil-Elias S, Arruda EZ, Schwartz EF, Melo PA (2008) Ability of suramin to antagonize the cardiotoxic and some enzymatic activities of B*othrops jararacussu* venom. *Toxicon* **51**: 28-36

Stocker K, Meier J (1989) Snake venom proteins in hemostasis: new results. *Folia Haematol Int Mag Klin Morphol Blutforsch*. **116**: 935-953

Taub M, Chuman L, Saier Jr MH, Sato G (1979) Growth of Madin-Darby canine kidney epithelial cell (MDCK) line in hormone-supplemented, serum-free medium. *Proc Natl Acad Sci* **76**: 3338-3342

Walser M, Davidson DG, Orloff J (1955) The renal clearance of alkali-stable inulin. *J. Clin. Invest.* **34**: 1520-1523

Toxines et Signalisation – Toxins and Signalling
Rencontres en Toxinologie – Meeting on Toxinology, 2009
Editions de la SFET – SFET Editions
Accès libre en ligne sur le site – Free access on line on the site : http://www.sfet.asso.fr

Antimicrobial activities of phospholipase A_2 and L-amino acid oxidase from Bothrops *venom*

Alba TORRES[1*], Rodrigo DANTAS[2], Kamila LOPES[1], Gdaylon MENESES[1], Felipe DA COSTA[1], Nádia NOGUEIRA[1], Marcos TOYAMA[3], Eduardo FILHO[3], Helena MONTEIRO[2], Alice MARTINS[1]

[1] *Department of Clinical and Toxicological Analysis, Pharmacy Faculty, Federal University of Ceara, Fortaleza, Ceara, Brazil ;* [2] *Department of Physiology and Pharmacology- Federal University of Ceara, Fortaleza, Ceara, Brazil ;* [3] *São Vicente Unity, Campus of Litoral Paulista, Paulista State University (UNESP), São Paulo, Brazil*

** Corresponding author ; Tel : +55 (0) 85 3366-8269 ; Fax : +55 (0) 85 3366-8292 ;*
E-mail : alba.fabiola@gmail.com

Abstract

Snake venoms contain biologically active substances primarily consisting of proteins (90-95%). Some of these present enzymatic activities, such as phospholipases A_2 and L-amino acid oxidases. In this study we verify the effects of Bothrops leucurus *(BleuTV) and* Bothrops marajoensis *(BmarTV) venoms and their respective PLA_2 ($BleuPLA_2$ and BmarPLA2) and LAAO (BleuLAAO and BmarLAAO) fractions on bacteria and yeast strains. The susceptibility of the strains to antimicrobial potential of the venoms and fractions was analyzed using a disc-diffusion assay and the minimum inhibitory concentration (MIC) and minimum lethal concentration (MLC) values were determined using the microdilution method, with modifications. The results were statistically analyzed with the t or ANOVA test, followed by the Bonferroni's test when appropriate, with $p<0.05$. Fraction BmarLAAO inhibited the growth of the Gram-negative* Pseudomonas aeruginosa *and Gram-positive* Staphylococcus aureus *bacteria and of yeast* Candida albicans*. Venom BleuTV inhibited the growth of* S. aureus *a dose-dependent manner. The inhibitory effect was more significant on* S. aureus *with CIM= 50 µg/mL and CLM = 200 µg/mL for BmarLAAO and CIM = CLM = 25 µg/mL for BleuTV. In contrast, venom BmarTV and fractions $BmarPLA_2$, $BleuPLA_2$ and BleuL AAO inhibited none of the strains studied.*

Activités antimicrobiennes des enzymes phospholipase A_2 et L-acide aminé oxydase du venin du Bothrops

Les venins des serpents contiennent des substances biologiquement actives correspondant principalement à des protéines (90-95%). Certaines présentent des activités enzymatiques, telles les phospholipases A_2 (PLA_2) et les L-acide aminé oxydases (LAAO). Dans cette étude, nous avons vérifié l'action des venins des serpents Bothrops leucurus *(BleuTV) et* Bothrops marajoensis *(BmarTV) ainsi que de leurs fractions PLA_2 ($BleuPLA_2$ et $BmarPLA_2$) et LAAO (BleuLAAO et BmarLAAO) sur des cultures de bactéries et de levures. La sensibilité des souches de bactéries et levures au potentiel antimicrobien des venins et fractions a été analysée par la technique de diffusion en disques, et la concentration inhibitrice minimum (CMI) et la concentration létale minimum (CMB) ont été déterminées par la méthode de microdilution, avec des modifications. Les résultats ont été statistiquement analysés avec le test-t ou l'ANOVA puis avec le test du Bonferroni lorsque nécessaire, avec $p<0,05$. Nous avons observé que la fraction BmarLAAO empêche la croissance des bactéries Gram-négative* Pseudomonas aeruginosa et *Gram-positive* Staphylococcus aureus*, ainsi que de la levure* Candida albicans*. Le venin BleuTV empêche la croissance de* S. aureus *d'une manière dépendante de la dose L'effet inhibiteur est plus significatif sur* S. aureus *avec CMI = 50 µg/mL et CMB = 200 µg/mL pour BmarLAAO, et CMI = CMB = 25 µg/mL pour le BleuTV.En revanche, le venin BmarTV et les fractions BmarPLA2, BleuPLA2 et BleuLAAO n'inhibent aucune des souches étudiées.*

Keywords : *Antimicrobial activity,* Bothrops leucurus*,* B. marajoensis*, L-amino acid oxidase, phospholipase A_2.*

Introduction

Snake venoms contain many compounds with biological and/or biotechnological value. In accordance with Calvete *et al.* (2007), their proteomic characterization offers potential benefits for basic research and clinical diagnostic through the development of new tools for research and drugs of potential clinical use. These venoms are mixtures of active substances, which presenting a diversity of biological effects, *e.g.*

neurotoxicity, myotoxicity, cardiotoxicity, hemorrhagic, pro- and anticoagulants, antiparasitic and antibacterial effects (Kini, 2003 ; Torres *et al.,* 2003 ; Stábeli *et al.,* 2004 ; Santamaría *et al.,* 2005 ; Izidoro *et al.,* 2006).

About 90-95% of the dry weight of an ophidian venom relates to proteins (Bon, 1997). Among them are the phospholipase A_2 (PLA_2, EC 3.1.1.4) and L-amino acid: O_2 oxidoreductase (LAAO, EC 1.4.3.2) enzymes. The PLA_2s catalyze hydrolysis of glycerophospholipids at the *sn-2* position to release lysophospholipids and acid by-products (Verheij *et al.,* 1980 ; Kini, 2003). They are classified as secretory or cytosolic based on their cellular localization. They display various bioactivities as antibacterial (Nuñez *et al.,* 2004 ; Barbosa *et al.,* 2005 ; Xu *et al.,* 2007), anticoagulant (Oliveira *et al.,* 2002 ; Lu *et al.,* 2005), cell proliferation, antitumoral, inhibition of the platelet aggregation (Xu *et al.,* 2007), neurotoxic (Rodrigues *et al.,* 2004). Among the PLA_2s of snake venoms three types are recognized : those that contain an aspartic acid residue at position 49 (Asp49) and are catalytically active; and those that contain either a lysine or a serine residue at this position (Lys49 and Ser49) and are enzymatically inactive (Lomonte *et al.,* 2003).

The LAAOs are flavoenzymes which catalyze the stereospecific oxidative deamination of an L-amino acid substrate, to release the corresponding α-Keto acid with production of hydrogen peroxidase and ammonia (Du and Clemetson, 2002). The exact role of LAAO in snake venom is not yet understood. Studies indicate that it may induce apoptosis in endothelial vascular cells, what can contribute to the prolonged bleeding of the vessel damaged by the bite (Suhr and Kim, 1996 ; Torii *et al.,* 1997 ; Du and Clemetson, 2002). This protein represents approximately 30% of the whole venom of some snake species and generally presents a yellow color (Takasuka *et al*., 2001). LAAOs from different sources exhibit differences in their specificity, stability, and other biological activities. They seem to be involved in the allergic inflammatory response, induction of cytotoxicity against tumoral cells, bactericidal, leishmanicidal and trypanocidal actions, beyond induction of platelet aggregation and edema (Wei *et al.,* 2002 ; Stábeli *et al.,* 2004 ; Izidoro *et al.,* 2006 ; Toyama *et al.,* 2006 ; França *et al.,* 2007).

Materials and methods

Venoms and fractions

The *Bothrops leucurus* (BleuTV) and *Bothrops marajoensis (*BmarTV) venoms were obtained from the Butantan Institute (São Paulo, Brazil). The phospholipase A_2 (PLA_2) and L-amino acid oxidase fractions (LAAO) obtained by RP-HPLC and cation exchange chromatography (Toyama *et al*., 2001; Bonfim *et al*., 2001) were kindly provided by Prof. Dr. Marcos Hiraki Toyama (Paulista State University, UNESP, São Vicente Unity, Campus of Litoral Paulista, São Paulo, Brazil). Stock solutions of samples of BleuTV and BmarTV and of their respective $BleuPLA_2$ and BleuLAAO, and $BmarPLA_2$ and BmarLAAO fractions were 2 mg/mL in sterile phosphate saline buffer, pH 7.4.

Antimicrobial activity of venoms and fractions

The bacteria (*Salmonella choleraesuis* subsp. *choleraesuis sorotipo choleraesuis* ATCC 10708, *Staphylococcus aureus* ATCC 6538P, *Escherichia coli* ATCC 11229, *Pseudomonas aeruginosa* ATCC 15442) and yeast strains (*Candida albicans* ATCC 10231), free of microbial contamination and kept on agar at 4°C, were donated by the Laboratory for Reference Materials of the Oswaldo Cruz Foundation (FIOCRUZ). The antimicrobial potentials of the venoms and fractions were determined by the disk-diffusion (or Kirby Bauer) test (NCCLS, 2003a) with modifications. The strains were transferred to Brain Heart Infusion (BHI) broth and incubated at 35°C until they reached a turbidity equivalent (by eye) to the 0.5 scale of McFarland (approximately 10^8 CFU/mL). The bacterial inocula were spread onto the surface of sterile Mueller-Hinton agar (Merck) (for bacteria) or sterile Sabouraud-dextrose agar (Merck) (for yeast) using a sterile cotton swab. After 5 min, wells of 5 mm diameter were digged in the agar using a sterile punch and filled with 25 µL of decreasing concentrations (2, 1, 0.5, 0.25, 0.125 mg/mL) of each venom or fraction. Commercial antimicrobials (amikacin 2 mg/mL and ketoconazole 1.2 mg/mL) were used as positive controls and PBS, pH 7.4, as the negative control (absence of microbial growth). After incubation at 35ºC for 18h, the diameters (in mm) of the inhibition zones were measured.

Determination of minimum inhibitory concentration (MIC)

The MIC was determined by the microdilution method (NCCLS, 2003b) with modifications. Venom and fraction concentrations of 200, 100, 50, 25 and 12.5 µg/mL were used. The microbial strains were subcultured and their density was adjusted as described above. The cultures were diluted 100-fold to reach ~$1{,}5x10^6$ CFU/mL. An inoculum of 125 µL of microbial culture was mixed with 25 µL of each of the concentrations of venom or fractions and 100 µL of BHI broth (bacteria) or Sabouraud-dextrose broth (*C. albicans)* in 96 well plates. Wells containing BHI or Sabouraud-dextrose broth and PBS buffer sterile (pH 7.4) were used as negative controls. Wells containing a microorganism inoculum, culture medium and an antimicrobian agent (amikacin for bacteria and ketoconazole for yeast) were used as positive controls (growth inhibition). The plates were incubated at 35°C for 24h and inhibition of the microorganism growth was determined by recording absorbance at 490 nm. The MIC was defined as the lower concentration of sample able to inhibit microbial growth (lack of visible turbidity). Three independent experiments were performed in triplicate.

Determination of minimum lethal concentration (MLC)

For MLC determination, aliquots of 25 µL were removed from wells without visible turbidity according to above criteria and were transferred to the surface of agar Plate-count (bacteria) or agar Sabouraud-dextrose

(*C. albicans*). After incubation at 35ºC for 24h the colonies grown in agar were counted. The sample concentration that was observed a growth of less than 0.1% the initial inoculum ($1,5x10^6$ CFU/mL) was defined as the MLC for the tested strains (NCCLS, 2003b).

Results

The antibacterial activity was evaluated through the presence of inhibition zone after inoculation in Mueller-Hinton agar (for bacteria) or Sabouraud-dextrose agar (for yeast) by radial diffusion assay. Fraction BmarLAAO was found to inhibit the growth of Gram-negative *P. aeruginosa* and Gram-positive *S. aureus* bacteria and of the yeast *C. albicans* in a dose-dependent manner, with an order of susceptibility as *S. aureus* > *C. albicans* > *P. aeruginosa* (*Figure 1*). BleuTV was found to inhibit the growth of *S. aureus* (*Figure 2*). In contrast, BmarTV and fractions $BmarPLA_2$, $BleuPLA_2$ and BleuLAAO did not inhibit the growth of any of the strains.

The BmarLAAO and BleuTV samples were further assayed for their MIC and MLC values. Their inhibitory effect was more significant on *S. aureus*, with MIC = 50 µg/mL and MLC = 200 µg/mL for BmarLAAO (*Figure 3*) and MIC = MLC = 25 µg/mL for BleuTV (*Figure 4*). The positive control (amikacin) presented MIC = 25 µg/mL and MLC = 50 µg/mL (*Figures 2 and 4*). In contrast, no accurate MIC and MLC values could be determined for *P. aeruginosa* and *C. albicans* (>200 µg/mL).

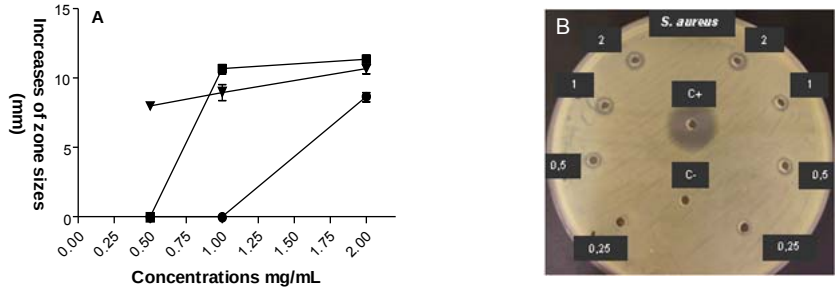

Fig. 1. Antibacterial activity of fraction BmarLAAO in disk-diffusion assay. (**A**) The activity was assayed on *P. aeruginosa* (●), *S. aureus* (▼) and *C. albicans* (■). The data points represent means ± SEM of three independent assays made in triplicate. (**B**) Typical disk-diffusion assay of BmarLAAO on *S. aureus* culture. The growth inhibition zone is measured in mm, including the 5 mm diameter of the well, after 18h of incubation at 35°C. The BmarLAAO concentrations (mg/mL) and the positive (C+) and negative controls (C-) are indicated.

Fig. 1. *Activité antibactérienne de la fraction BmarLAAO, selon le test de diffusion en disque. (**A**) L'activité a été mesurée sur* P. aeruginosa *(●),* S. aureus *(▼) et* C. albicans *(■). Chaque point représente la moyenne ± erreur standard de 3 essais indépendants faits en triplicats. (**B**) Exemple de disques de diffusion pour BmarLAAO sur une culture de* S. aureus*. La zone d'inhibition de croissance bactérienne est mesurée en mm, incluant le diamètre de 5 mm du puits, après 18 h d'incubation à 35°C. Les concentrations de BmarLAAO (en mg/mL) et les contrôles positif (C+) et négatif (C-) sont indiqués.*

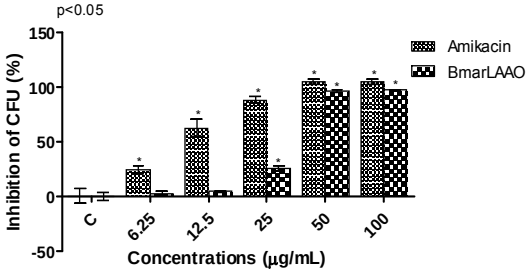

Fig. 2: Antibacterial activity of fraction BmarLAAO compared with amikacin on *S. aureus*, by the microdilution method. After incubation of BmarLAAO or amikacin (100, 50, 25, 12.5 and 6.25 µg/mL) the bacterial growth was measured by absorbance at 490 nm. The bars represent means ± SEM (n=3). *p<0.05 compared to the corresponding control group.

Fig. 2*. Activité antibactérienne de la fraction BmarLAAO et de l'amikacine sur* S. aureus*, par la méthode de microdilution. Après incubation de BmarLAAO ou de l'amikacine (100, 50, 25, 12.5 and 6.25 µg/mL), la croissance bactérienne a été quantifiée par absorbance à 490 nm. Les barres représentent les moyennes ± erreurs standard (n=3). *p<0,05 comparé au groupe contrôle correspondant.*

Discussion and conclusion

Samples BleuTV and BmarLAAO displayed significant antibacterial effect on *S. aureus,* while only BmarLAAO presented inhibited the growth of *P. aeruginosa* and *C. albicans*. For BleuTV, similar MIC and MLC values were found. According to Tavares (2007), the difference between MLC and MIC values should be in the order of magnitude of one or two times as observed in the present study, thus a large difference between these two values demonstrates tolerance of the microorganism to the drug.

In this context, other venoms were found to present antimicrobial activity, *e.g*. those of *Crotalus durissus terrificus* and *C. durissus cascavella* on *Xantomonas axonopodis* pv. *passiflorae* (Oliveira *et al.,* 2002 ; Toyama *et al.,* 2006) and the venom of *Bothrops jararaca* on *Saccharomyces cerevisae* and *Fusarium oxysparum* (Gomes *et al.,* 2005). Ciscotto *et al.* (2009) verified that venoms of the *Bothrops* genus (*B. jararaca* and *B. jararacussu*) are powerful inhibitors of *Staphylococcus aureus* growth. These venoms present an ample spectrum of action on Gram-positive and Gram-negative bacteria, although *Escherichia coli* and *Enterococcus fecalis* showed some resistance.

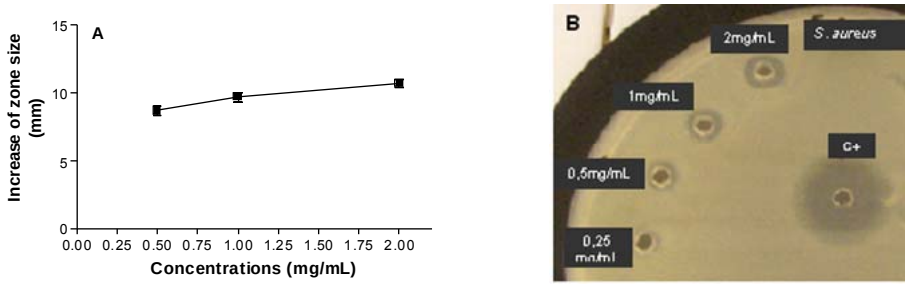

Fig. 3. Antibacterial activity of BleuTV on *S. aureus*, in disk-diffusion assay. (**A**) The data points represent mean ± SEM of three independent assays made in triplicate. (**B**) The inhibition zones are measured in mm, including the 5 mm diameter of the wells, after 18h of incubation at 35°C. The BleuTV concentrations and the positive (C+) control are indicated.

Fig. 3. *Activité antibactérienne de BleuTV sur* S. aureus*, selon le test de diffusion en disque. (**A**) Chaque point représente la moyenne ± erreur standard de 3 essais indépendants fait en triplicats. (**B**) La zone d'inhibition de croissance bactérienne est mesurée en mm, incluant le diamètre de 5 mm du puits, après 18 h d'incubation à 35°C. Les concentrations de BleuTV et le contrôle positif (C+) sont indiqués.*

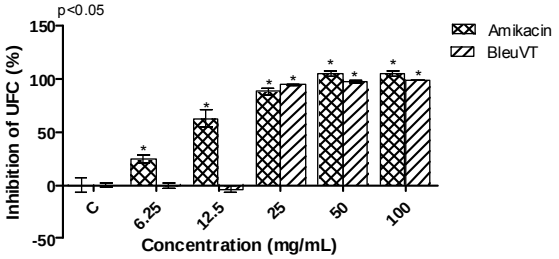

Fig. 4. Antibacterial activity of BleuVT compared with amikacin on *S. aureus*, by the microdilution method. After incubation of BleuVT or amikacin (100, 50, 25, 12.5 and 6.25 µg/mL) the bacterial growth was measured by absorbance at 490 nm. The bars represent means ± SEM of three independent assays realized in triplicate. *p<0.05 compared to the corresponding control group.

Fig. 4. *Activité antibactérienne de BleuTV et de l'amikacine sur* S. aureus*, par la méthode de microdilution. Après incubation de BleuTV ou de l'amikacine (100, 50, 25, 12.5 and 6.25 µg/mL), la croissance bactérienne a été quantifiée par absorbance à 490 nm. Les barres représentent les moyennes ± erreurs standard de trois essais indépendants faits en triplicats. *p<0,05 comparé au groupe contrôle correspondant.*

L-amino acid oxidases (LAAO) from snake venoms display antimicrobial activity on various microorganisms. Samy *et al.* (2007) demonstrated the antibacterial effect of LAAO from *Crotalus adamanteus* and *Bothrops asper* venoms on *Staphylococcus aureus* and *Proteus mirabilis*. In the same way, LAAO from *Bothrops pirajai* was found to inhibit the growth of *Pseudomonas aeruginosa* and *Escherichia coli* (Izidoro *et al.,* 2006). Some authors reported that the antimicrobial action of LAAO from snake venom is significantly diminished by the action of catalase (Toyama *et al.,* 2006 ; Wei *et al.,* 2002), a feature that suggests the importance of the subproduct of enzymatic action, *i.e*., hydrogen peroxide, for the observed biological activity.

Although the phospholipase A_2 (PLA_2) fractions did not significantly inhibit bacteria and yeast growth, many authors have reported antibacterial property of snake venom PLA_2. Some secretory PLA_2 are known to display powerful bactericidal activity on Gram-positive bacteria. A PLA_2, named BFPA, from the venom of *Bungarus fasciatus*, was reported to be active against *S. aureus* and *E. coli* (Xu *et al.,* 2007). Páramo *et al.* (1998) had described and characterized the bactericidal effect of a Lys49 PLA_2 from *B. asper* venom on Gram-positive and Gram-negative bacteria, and showed that a synthetic (115-129) peptide corresponded reproduces the effect of the complete protein, thus providing evidence that the bactericidal mechanism of this PLA_2 is not related to its enzymatic activity. In fact, other authors reported that snake venom PLA_2s present pharmacological effects through mechanisms that are either dependents to (Oliveira *et al.,* 2002 ; Barbosa *et al.,* 2005) or independent from their enzymatic activity (Lomonte *et al.,* 2003 ; Páramo *et al.,* 1998 ; Santamaría *et al.,* 2005).

In conclusion, the BleuTV and BmarLAAO interfere with the growth of several microorganisms as *Staphyloccocus aureus, Candida albicans* and *Pseudomonas aeruginosa*.

Acknowledgements. *We are grateful to the CNPq, CAPES and FUNCAP for financial support.*

References

Barbosa PSF, Martins AMC, Havt A, Toyama DO, Evangelhista JSAM, Ferreira DPP, Joazeiro PP, Beriam OS, Toyama MH, Fonteles MC, Monteiro HSA (2005) Renal and antibacterial effects induced by miotoxin I and II isolated from *Bothrops jararacussu* venom. *Toxicon* **46**: 376-386

Bon C (1997) Snake venom & pharmacopoeia. In *Snakes a natural history,* BAUCHOT R (ed) pp 194-209. Sterling Publishing Co, New York

Bonfim VL, Toyama MH, Novello JC, Hyslop S, Oliveira CRB, Rodrigues-Simioni L, Marangoni S (2001) Isolation and enzymatic characterization of a basic phospholipase A2 from *Bothrops jararacussu* snake venom. *J Protein Chem* **20**: 239-245

Calvete JJ, Juarèz P, Sanz L (2007) Snake venomics. Strategy and applications. *J Mass Spectrom* **42**: 1405-1414

Ciscotto CJ, Machado De Avila RA, Coelho EA, Oliveira J, Diniz CG, Farías LM, De Carvalho MA, Maria WS, Sanchez EF, Borges A, Chávez-Olórtegui C (2009) Antigenic, microbicidal and antiparasitic properties of na L-amino acid oxidase isolated from *Bothrops jararaca* snake venom. *Toxicon* **53**: 330-341

Du XY, Clemetson KJ (2002) Snake venom L-amino acid oxidases. *Toxicon* **40**: 659-665

França SC, Kashima S, Roberto PG, Marins M, Ticli FK, Pereira JO, Astolfi-Filho S, Stábeli RG, Magro AJ, Fontes MRM, Sampaio SV, Soares AM (2007) Molecular approaches for structural characterization of *Bohtrops* L-amino acid oxidases with antiprotozoal activity: cDNA cloning, comparative sequence analysis, and molecular modeling**.** *Biochem Biophys Res Commun* **355**: 302-306

Gomes VM, Carvalho AO, Da Cunha M, Keller MN, Bloch JR. C, Deolindo P, Alves EW (2005) Purification and characterization of a novel peptide with antifungal activity from *Bothrops jararaca* venom. *Toxicon* **45**: 817-827

Izidoro LFM, Ribeiro MC, Souza GRL, Sant'ana CD, Hamaguchi A, Homsi-Brandeburgo MI, Goulart LR, Beleboni RO, Nomizo A, Sampaio SV, Soares AM, Rodrigues VM (2006) Biochemical and functional characterization of na L-amino acid oxidase isolated from *Bothrops pirajai* snake venom. *Bioorg Med Chem* **14**: 7034-7043

Kini RM (2003) Excitement ahead: structure, function and mechanism of snake venom phospholipase A_2 enzymes. *Toxicon* **42**: 827-840

Lomonte B, Ângulo Y, Calderón L (2003) An overview of lysine-49 phospholipase A_2 myotoxins from crotalid snake venoms and their structural determinants of myotoxic action. *Toxicon* **42**: 885-901

Lu Q, Clemetson JM, Clemetson KJ (2005) Snake venoms and hemostais. *J Thromb Haemost* **3**:1791-1799

National Committee for Clinical Laboratory Standards (NCCLS). **NCCLS M2-A8**: Performance Standards for Antimicrobial Disk Susceptibility Tests: Approved Standard. 8th ed. Wayne, PA, 2003a.

National Committee for Clinical Laboratory Standards (NCCLS). **NCCLS M7-A6:** methods for dilution antimicrobial susceptibility tests for bacteria that grow aerobically: approved. 6th ed. Wayne, PA, 2003b.

Nuñez V, Arce V, Gutiérrez JM, Lomonte B (2004) Structural and functional characterization of myotoxin I, a Lys49 phospholipase A_2 homologue from the venom of the snake *Bothrops atrox. Toxicon* **44**: 91-101

Oliveira DG, Toyama MH, Novello JC, Beriam LOS, Marangoni S (2002) Structural and functional characterization off basic PLA_2 isolated from *Crotalus durissus terrificus* venom. *J Prot Chem* **21**: 161-168

Páramo L, Lomonte B, Pizarro-Cerdá J, Bengoechea J, Gorvel J, Moreno E (1998) Bactericidal activity of Lys49 and Asp49 myotoxic phospholipase A_2 from *Bothrops asper* snake venom: synthetic Lys49 myotoxin II-(115-129)-peptide identifies its bactericidal region. *Eur J Biochem* **253**: 452-461

Rodrigues VM, Marcussi S, Cambraia RS, Araújo Alde, Malta-Neto NR, Hamaguchi A, Ferro EAV, Homsi-Brandeburgo MI, Giglio JR, Soares AM (2004) Bactericidal and neurotoxic activities of two myotoxic phospholipases A_2 from *Bothrops neuwiedi pauloensis* snake venom. *Toxicon* **44**: 305-314

Samy RP, Gopalakrishnakone P, Thwin MM, Chow TKV, Bow H, YAP EH, Thong TWJ (2007) Antibacterial activity of snake, scorpion and bee venoms: a comparison with purified venom phospholipase A_2 enzymes. *J Appl Microbiol* **102**: 150-159

Santamaría C, Larios S, Ângulo Y, Pizarro-Cerdá J, Gorvel JP, Moreno E, Lomonte B (2005) Antimicrobial activity of myotoxic phospholipase A_2 from crotalid snake venoms and synthetic peptide variants derived from their C-terminal region. *Toxicon* **45**: 807-815

Stábeli RG, Marcussi S, Carlos GB, Pietro RCLR, Selistre-De-Araújo HS, Giglio JR, Oliveira EB, Soares AM (2004) Platelet aggregation and antibacterial effects of an L-amino acid oxidase purified from *Bothrops alternatus* snake venom. *Bioorg Med Chem* **12**: 2881-2886

Suhr SM, Kim DS (1996) Identification of the snake venom substance that induces apoptosis. *Biochem Biophys Res Commun* **224**: 134-139

Takatsuka H, Sakurai Y, Yoshioka A, Kokudo T, Usami Y, Suzuki M, Matsui T, Titani K, Yagi H, Matsumoto M, Fujimura Y (2001) Molecular characterization of L-amino acid oxidase from *Agkistrodon halys blomhoffii* with special reference to platelet aggregation. *Biochim Biophys Acta* **1544**: 267-277

Tavares W (2007) Resistência Bacteriana. In *Antibióticos e quimioterápicos para o clínico*, TAVARES W (ed) pp 37-51. : Atheneu, São Paulo

Torii S, Naito M, Tsuruo T (1997) Apoxin I, a novel apoptosis-inducing factor with L-amino acid oxidase activity purified from Western diamondback rattlesnake venom. *J Biol Chem* **272**: 9539-9542

Torres AM, Wong HY, Desai M, Moochhla S, Kuchel PW, Kini RM (2003) Identification of a novel family of proteins in snake venoms : purification and structural characterization of nawaprin from *Naja nigricollis* snake venom. *J Biol Chem* **278**: 40097-40104

Toyama MH, Toyama Ddeo, Passero LFD, Laurenti MD, Corbett CE, Tomokane TY, Fonseca FV, Antunes E, Joazeiro PP, Beriam LOS, Martins AMC, Monteiro HSA, Fonteles MS (2006) Isolation os new L-amino acid oxidase from *Crotalus durissus cascavella* venom. *Toxicon* **47**: 47-57

Verheij HM, Boffa MC, Rothen C, Bryekert MC, Verger R, Hass GH (1980) Correlation of enzimatic activity and anticoagulant properties of phospholipase A_2. *Eur J Biochem* **112**: 25-32

Wei JF, Wei Q, Lu QM, Tai H, Jin Y, Wang WY, Xiong YL (2002) Purification, characterization and biological activity of an L-amino acid oxidase from *Trimeresurus mucrosquamatus* venom. *Acta Biochim Biophys Sin* **35**: 219-339

Xu C, Ma D, Yu H, Li Z, Liang J, Lin G, Zhang Y, Lai R (2007) A bactericidal homodimeric phospholipases A_2 from *Bungarus fasciatus* venom. *Peptides* **28**: 969-973

Toxines et Signalisation – Toxins and Signalling
Rencontres en Toxinologie – Meeting on Toxinology, 2009
Editions de la SFET – SFET Editions
Accès libre en ligne sur le site – Free access on line on the site : http://www.sfet.asso.fr

Structure and function of sarafotoxins from Atractaspididae snake venoms

Yves TERRAT, Frédéric DUCANCEL*

Laboratoire d'Ingénierie des Anticorps pour la Santé (LIAS/SPI/iBiTec de Saclay/DSV/CEA), Bâtiment 152, CE de Saclay, 91191 Gif sur Yvette Cedex, France

** Corresponding author ; Tel : +33 (0)1 69 08 81 54 ; Fax : +33 (0)1 69 08 90 71 ; E-mail : frederic.ducancel@cea.fr*

Abstract

Snake venom sarafotoxins (SRTXs) and mammalian endothelins (ETs) comprise structurally and functionally related isopeptides that act as potent vasoconstrictors via identical receptors. This similarity is remarkable, since SRTXs are highly toxic components isolated from the venoms of snakes of the Atractaspis *genus within the Atractaspididae family (mole vipers), while ETs are endogenous hormones of the mammalian vascular system. Since the functional and structural characterization of SRTXs in 1988, the full extent of their natural diversity has become increasingly apparent, and this has led to the characterization of new families of ET-like peptides. Based on a combination of conventional biochemical approaches and more recent molecular biology and mass spectrometry techniques, this article describes the actual panel of SRTX isopeptides characterized in various snake species within the Atractaspididae family, but also the similarities and differences that exist between SRTXs and ETs in terms of their metabolism, genetic origin, structure and functional activities. Finally, very recent data concerning engineered SRTXs both to design protecting antisera and to generate matrix metalloproteinase inhibitors, are presented.*

Structure et fonction des sarafotoxines des venins des serpents de la famille des Atractaspididae

Les sarafotoxines (SRTXs) des venins de serpents et les endothelines (ETs) des mammifères forment une famille de puissants isopeptides structuralement et fonctionnellement homologues, qui agissent sur le système vasculaire via des récepteurs identiques. Cela est d'autant plus remarquable, que les SRTXs sont des composés hautement toxiques isolés uniquement à partir des venins des serpents du genre Atractaspis *au sein de la famille des Atractaspididae* (serpents taupe) *, alors que les ETs sont des hormones endogènes du système vasculaire des mammifères. Depuis leur découverte en 1988, la diversité naturelle des isoformes des SRTXs n'a cessé de croître, aboutissant à l'identification de nouvelles familles d'analogues des ETs. En s'appuyant sur des approches de biochimie classique ainsi que sur les techniques de biologie moléculaire et de spectrométrie de masse, cet article fait le point sur les dernières données concernant : a) la biodiversité des SRTXs, b) les différences et similitudes qui existent entre les SRTXs et les ETs quant à leur métabolisme, organisation génétique, ou encore de leurs structures et fonctions biologiques. Finalement, des résultats récents décrivant les premiers travaux d'ingénierie des SRTXs, réalisés afin de développer un antisérum protecteur ainsi que pour générer de nouveaux inhibiteurs des métalloprotéases matricielles, sont présentés.*

Keywords : Atractaspis*, endothelins, precursors, sarafotoxins, vasoactive peptides.*

Introduction

Snake venom sarafotoxins (SRTXs) and mammalian endothelins (ETs) form a structurally and functionally related family of potent vasoconstrictor peptides. SRTXs are isopeptides solely found in the venoms of snakes of the genus *Atractaspis* within the family Atractaspididae. The name of SRTXs derives from the Hebrew spelling of the species *A. engaddensis – Saraf Ein Gedi –* from which these peptides were first isolated and characterized (Kochva *et al.*, 1982 ; Kloog *et al.*, 1988). These oviparous burrowing snakes (*Figure 1A*) live underground and are distributed throughout subSaharan Africa with a limited penetration into the Israel territory and the south-western part of the Arabian peninsula. Eighteen species of very similar appearance of these burrowing asps are known (David and Ineich, 1999). They are relatively small, averaging 30 to 70 cm in length, and mainly feed on small reptiles, amphibians and small rodents, which they catch with their mouth closed, a feature which is unique among reptiles (*Figure 1B*) (Golani and Kochva, 1988).

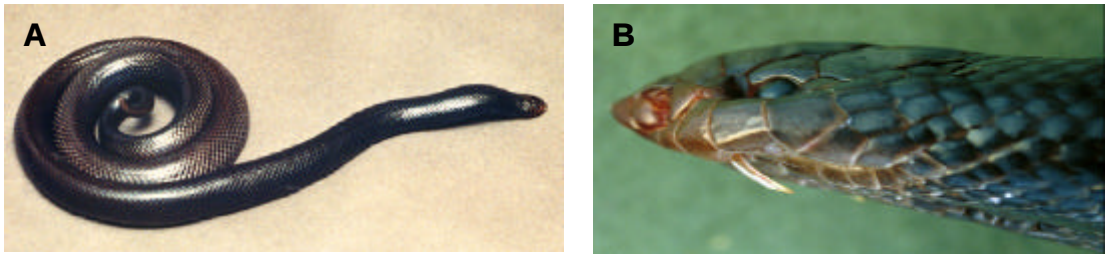

Fig. 1. Views of an *Atractaspis engaddensis* specimen. (**A**) *A. engaddensis* in a combined defensive/offensive position. Note the arched neck and the beginning of the coiled body with exposed tip of the tail. (**B**) Illustration of the capacity of Atractaspididae snakes to strike with one fang which protrudes from the closed mouth during the bite.

Fig. 1. *Photos d'un spécimen d'*Atractaspis engaddensis. *(**A**)* A. engaddensis *en position attaque/défense. Notez la forme arcboutée du cou, ainsi que la position sortante de l'extrémité de la queue. (**B**) Illustration de la capacité des serpents de la famille des Atractaspididae à frapper leur proie la gueule fermée avec un seul crochet.*

Within the genus *Atractaspis*, venom toxicity varies greatly from one species to another. The major clinical manifestations of *Atractaspis* bites are nausea, vomiting, abdominal pain, diarrhea, sweating, profuse salivation, loss of oculomotor accommodation, loss of consciousness, and respiratory difficulties (Bdolah *et al.*, 1991). Among the different venoms tested, that one of *A. engaddensis* is the most potent (Kochva, 2002). The latter mainly targets the cardiovascular system, and especially the heart, and this without pre- or post-synaptic neurotoxic effects (Weiser *et al.*, 1984). SRTXs from *A. engaddensis* are among the most lethal snake toxins ever described, causing death within minutes in mice and in under one hour in humans: the mean lethal dose 50 (LD_{50}) is approximately 15 µg per kg (Kochva *et al.*, 1993).

On the contrary of SRTXs that are over-expressed by the venom gland cells (they may account for 30% of the venom content), ETs (which are present in all vertebrates) in mammals are produced in very small amounts with sub-picomolar concentrations in plasma. ETs are mainly synthezised by endothelial cells but also by other cells in vertebrates, and they function as autocrine or paracrine hormonal factors (Yanagisawa *et al.*, 1988a, 1988b ; Kedzierski and Yanagisawa, 2001 ; Barton and Yanagisawa, 2008). The ET-system in mammals consists of four isoforms of 21 residues each (*Figure 2B*): ET-1, ET-2 and ET-3 in human, and the so-called vasoactive intestinal contractor (VIC) in rodents (Bloch *et al.*, 1991 ; Saida and Misui, 1991).

Other bioactive ETs of 31 amino-acids have also been described (Nakano *et al.*, 1997 ; Kishi *et al.*, 1998) (*Figure 2B*), when in fish only one ET-like sequence has been identified (Wang *et al.*, 1999 ; Hyndman and Evans, 2007). Based on their diverse pattern of expression in mammals, the ET-system components are associated with a large variety of physiological and pathological roles (Sakurai *et al.*, 1992 ; Miyauchi and Masaki, 1999 ; Kedzierski and Yanagisawa, 2001). Owing to their basal vasoconstrictor activity, ET-peptides are mainly involved in regulation of the vascular system (at the level of the vessels) but also in the development of various cardiovascular diseases such as hypertension and atherosclerosis. In the heart, the ET-system has cardiotropic actions and it contributes to cardiac hypertrophy and remodeling in the case of heart failure. In the lung it is involved in the development of pulmonary hypertension. In the kidney, it controls homeostatic functions and is associated with acute and chronic renal failure. In the brain it modulates the activity of the cardiorespiratory centers and the release of hormones (Stojilkovic and Catt, 1992). Finally, ETs are involved in fibrosis, cellular proliferation, hepatic glycogenolysis (Shaw and Boden, 2005), and along with their receptors they are clearly involved in the development of many cancers (Bagnato and Natali, 2004 ; Cazaubon *et al.*, 2006).

The structural and pharmacological similarities between SRTXs and ETs strongly suggest that ETs are "endogenous toxins" in vertebrates and that SRTXs are “ET-like” peptides in snake venoms. However, in view of the pharmacological complexity of the ET-system, the study of SRTXs appears particularly attractive to gain further progress in the functional and pharmacological knowledge that physiological system (Remuzzi *et al.*, 2002). Thus, characterization of novel SRTX isopeptides from *de novo* studied *Atractaspis* snakes could be of particular value in identifying new ET receptor subtypes and/or designing clinically useful agonists or antagonists for existing ET receptors. Here we will review all the data gathered since the discovery of SRTXs in 1982, up to the most recent findings on their structural and functional diversity, original organization, precursor maturation, and the structure of their genes. These data will be analyzed and compared with those on ETs as to establish the molecular and genetic bases of the similarities and differences between SRTXs and ETs.

Discovery and structural characteristics of sarafotoxins

Six years after the first reference to the existence of low-molecular-weight components in the venom of *A. engaddensis* (Kochva *et al.*, 1982), the primary sequences of three vasoconstrictor peptides named SRTX-a, SRTX-b and SRTX-c (*Figure 2A*) were published (Kloog *et al.*, 1988). Later on, bibrotoxin, a new SRTX that differs from SRTX-b solely by the presence of an Ala instead of a Lys at position +4, was characterized from the venom of *A. bibroni* (Becker *et al.*, 1993) (*Figure 2A*). SRTX-a, SRTX-b and SRTX-c, which display at least 85% strict identity and an identical C-terminus, have isoelectric points, of 5.8, 4.8 and about 3.5, respectively. SRTX-a and SRTX-b, which differ by a single substitution at position +13 (*Figure 2A*), have the same toxicity with an LD_{50} of about 0.01 $\mu g.g^{-1}$ in mice. SRTX-c, which is the most abundant isoform in this venom, is 30 times less toxic (LD_{50} = 0.3 $\mu g.g^{-1}$). Comparison with mammalian 21 amino-acid ET isopeptides (*Figure 2B*) reveals about 60% homology with SRTXs, the most significant differences being at the N-terminus (region

formed by residues +4 to +7) with several non-conservative amino-acid substitutions, contrasting with the high homology of the C-terminal hexapeptides (Ducancel, 2002).

A)	**C**	S	**C**	K	D	M	T	**D**	K	**E**	**C**	L	N	F	**C**	H	Q	D	V	I	**W**								**SRTX-a**
	C	S	**C**	K	D	M	T	**D**	K	**E**	**C**	L	Y	F	**C**	H	Q	D	V	I	**W**								**SRTX-b**
	C	T	**C**	N	D	M	T	**D**	E	**E**	**C**	L	N	F	**C**	H	Q	D	V	I	**W**								**SRTX-c**
	C	S	**C**	A	D	M	T	**D**	K	**E**	**C**	L	Y	F	**C**	H	Q	D	V	I	**W**								**Btx**
B)	**C**	T	**C**	F	T	Y	K	**D**	K	**E**	**C**	V	Y	Y	**C**	H	L	D	I	I	**W**								**ET-3**
	C	T	**C**	F	T	Y	K	**D**	K	**E**	**C**	V	Y	Y	**C**	H	L	D	I	I	**W**	I	N	T	P	E	Q	T	V	P	Y	**ET-3$_{31}$**
	C	S	**C**	S	S	L	M	**D**	K	**E**	**C**	V	Y	F	**C**	H	L	D	I	I	**W**								**ET-1**
	C	S	**C**	S	S	L	M	**D**	K	**E**	**C**	V	Y	F	**C**	H	L	D	I	I	**W**	V	N	T	P	E	H	V	V	P	Y	**ET-1$_{31}$**
	C	S	**C**	S	S	W	L	**D**	K	**E**	**C**	V	Y	F	**C**	H	L	D	I	I	**W**								**ET-2**
	C	S	**C**	S	S	W	L	**D**	K	**E**	**C**	V	Y	F	**C**	H	L	D	I	I	**W**	V	N	T	P	E	Q	T	A	P	Y	**ET-2$_{31}$**
	C	S	**C**	N	S	W	L	**D**	K	**E**	**C**	V	Y	F	**C**	H	L	D	I	I	**W**								**VIC**
	C	S	**C**	A	T	F	L	**D**	K	**E**	**C**	V	Y	F	**C**	H	L	D	I	I	**W**								**ET-fish**
C)	**C**	S	**C**	K	D	M	S	**D**	K	**E**	**C**	L	N	F	**C**	H	Q	D	V	I	**W**								**SRTX-a1**
	C	S	**C**	K	D	M	S	**D**	K	**E**	**C**	L	Y	F	**C**	H	Q	D	V	I	**W**								**SRTX-b1**
	C	T	**C**	K	D	M	T	**D**	K	**E**	**C**	L	Y	F	**C**	H	Q	G	I	I	**W**								**SRTX-e**
D)	**C**	S	**C**	N	D	I	N	**D**	K	**E**	**C**	M	Y	F	**C**	H	Q	D	V	I	**W**	D	E	P								**SRTX-m$_{24}$**
	C	S	**C**	N	D	M	N	**D**	K	**E**	**C**	M	Y	F	**C**	H	Q	D	V	I	**W**	D	E	P								**SRTX-m1$_{24}$**
	C	S	**C**	N	D	I	N	**D**	K	**E**	**C**	M	Y	F	**C**	H	Q	D	I	I	**W**	D	E	P								**SRTX-m2$_{24}$**
	C	S	**C**	N	D	M	N	**D**	K	**E**	**C**	V	Y	F	**C**	H	L	D	I	I	**W**	D	E	P								**SRTX-m3$_{24}$**
	C	S	**C**	N	N	M	S	**D**	K	**E**	**C**	L	N	F	**C**	N	L	D	I	I	**W**	E	N	V								**SRTX-m4$_{24}$**
	C	S	**C**	N	D	M	N	**D**	K	**E**	**C**	V	Y	F	**C**	H	Q	D	I	I	**W**	D	E	P								**SRTX-m5$_{24}$**
E)	**C**	S	**C**	N	N	M	S	**D**	K	**E**	**C**	L	N	F	**C**	N	L	D	I	I	**W**	E	N	A								**SRTX-f4$_{24}$**
								D	Q	**E**	**C**	M	Y	F	**C**	H	Q	D	V	I	**W**	D	E	P								**SRTX-f**
								D	Q	**E**	**C**	L	N	F	**C**	H	L	D	I	I	**W**	D	E	P								**SRTX-f3**
								D	K	**E**	**C**	V	N	F	**C**	H	L	D	I	I	**W**	D	E	P								**SRTX-f2**
F)	**C**	S	**C**	T	D	M	S	**D**	L	**E**	**C**	M	N	F	**C**	H	K	D	V	I	**W**	I	N	R	N							**SRTX-i1$_{25}$**
	C	S	**C**	A	D	M	S	**D**	L	**E**	**C**	M	N	F	**C**	R	L	D	V	M	**W**	V	N	R	N							**SRTX-i2$_{25}$**
	C	S	**C**	T	D	M	S	**D**	L	**E**	**C**	M	N	F	**C**	H	K	D	V	I	**W**	V	N	R	N							**SRTX-i3$_{25}$**
G)	**C**	S^{21} T^{4}	**C**	N^{9} K^{6} S^{4} A^{3} T^{2} F^{2}	D^{15} S^{5} T^{3} N^{2}	M^{15} W^{3} L^{2} I^{2} Y^{2} F^{1}	S^{7} T^{5} N^{5} L^{4} M^{2} K^{2}	**D**	K^{22} L^{3} Q^{2} E^{1}	**E**	**C**	V^{11} L^{10} M^{7}	Y^{18} N^{10}	F^{26} Y^{2}	**C**	H^{25} N^{2} R^{1}	L^{14} Q^{12} K^{2}	D^{27} G^{1}	I^{16} V^{12}	I^{27} M^{1}	**W**	D^{8} V^{4} I^{2} E^{2}	N^{8} E^{8}	P^{8} R^{3} T^{3} V^{1} A^{1}	P^{3} N^{3}	E^{3}	Q^{2} H^{1}	T^{2} V^{1}	V^{2} A^{1}	P^{3}	Y^{3}	

Fig. 2. Sequence alignments of various SRTXs and ETs. (**A**) SRTX isoforms previously isolated from the venom of *A. engaddensis* (SRTX-a, -b, and –c), and from *A. bibroni* (Btx). (**B**) Short (21 residues) and "long-ETs" (31 residues) from mammals, VIC peptide, and ET from fish. (**C**) Deduced SRTX sequences from *A. engaddensis* precursors. (**D**) Newly characterized 24 amino-acid SRTX sequences from *A. m. microlepidota*. (**E**) *De novo* characterized SRTX sequences from *A. fallax*. (**F**) Newly characterized SRTX sequences from *A. irregularis*. (**G**) Amino-acid variability. Invariant residues are in bold. The frequencies for occurrence of the amino-acid residues at the indicated positions are indicated as superscripts.

Fig. 2. *Alignement des séquences en acides amines des SRTXs et des ETs. (**A**) Isoformes de SRTXs préalablement isolées du venin d'*A. engaddensis *(SRTX-a, -b, et –c), et d'*A. bibroni *(Btx). (**B**) ETs courtes (21 acides aminés) et longues (31 acides aminés) de mammifères, peptide VIC et ET de poisson. (**C**) Séquences de SRTXs d'*A. engaddensis *déduites de leurs précurseurs nucléiques. (**D**) Nouvelles séquences de SRTXs de 24 acides aminés chez* A. m. microlepidota*. (**E**) Premières séquences de SRTXs chez* A. fallax*. (**F**) Nouvelles séquences de SRTXs de 25 acides amines chez* A. irregularis*. (**G**) Variabilité en acides amines. Les acides aminés invariants sont indiqués en caractères gras. Le nombre de fois où un acide aminé donné est retrouvé à une position particulière est indiqué en exposant.*

All these isopeptides contain a common core of 21 amino-acids and two conserved disulfide bridges between cysteines +1/+15 and +3/+11, which constitute a typical and unique Cys_1-X-Cys_3...Cys_{11}-X-X-X-Cys_{15} "signature" among mammalian bioactive peptides. NMR resolution and molecular modeling of the three-dimensional structures of ET-1 (Tamoaki *et al.*, 1991 ; Andersen *et al.*, 1992) and SRTX-b (Atkins *et al.*, 1995) have identified several structural features common to the whole family of these peptides. SRTXs and ETs adopt a cysteine-stabilized α-helical motif characterized by: a) an extended structure of the first three or four residues ; b) a β-turn structure between positions +5 and +8 ; c) an α-helical or helix-like conformation of the Lys_9-Cys_{15} segment ; d) the absence of a specific conformation for the C-terminal domain (*Figure 3*). It is noteworthy that formation of the α-helical conformation in segment Lys_9-Cys_{15} is unrelated to the formation of the two disulfide bridges (Chandralal *et al.*, 1999).

Biosynthesis of sarafotoxins: precursor organization and identification of new isoforms

To study the metabolism of SRTXs by venom gland cells, their precursors have been cloned from four different species of the genus *Atractaspis*: *A. engaddenis* (Ducancel *et al.*, 1993), *A. microlepidota microlepidota* (Hayashi *et al.*, 2004), *A. irregularis* (Quinton *et al.*, 2005), and very recently *A. fallax* (unpublished results). The structure and organization of these SRTX precursors were investigated and compared with those of ET precursors (Ducancel *et al.*, 1995, 1999).

The precursor of SRTXs from *A. engaddensis*: an original organization

The complete nucleotide sequence of one of the cDNAs encoding SRTXs in *A. engaddensis* is presented in *Figure 4*. It includes one open reading frame (ORF) of 1629 bp coding for a long pre-pro-polypeptide of 543 residues

and which starts with a Met followed by a hydrophobic peptide characteristic of a signal sequence (Ducancel *et al.*, 1993). This sequence presents no significant homology with the signal sequences of other precursors of snake toxins (Ducancel *et al.*, 1991).

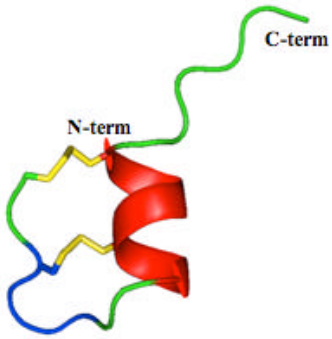

Fig. 3. NMR structure of sarafotoxin-b**.** Schematic representation of the structure adopted by one SRTX-b conformer. The two disulfide bridges are displayed in yellow, the extended structures in green, the β-turn in blue and the α-helical segment in red. (PDB accession code, 1SRB).

Fig. 3. *Structure RMN de la SRTX-b. Représentation schématique de la structure tridimensionnelle adoptée par la SRTX-b. Les deux ponts disulfure sont indiqués en jaune, le coude b en bleu et l'hélice alpha en rouge. (Code d'accession PDB : 1SRB).*

The amino-acid sequence deduced for this precursor has an original repetitive structure, comprising one sequence of 39 residues followed by 11 sequences of 40 residues (*Figure 4*). Each of these contains a SRTX sequence preceded by an invariant spacer peptide of 19 amino-acids (18 upstream of the first sequence of SRTXs). The last copy of SRTX is followed by an unrelated peptide. Five different isoforms of SRTXs: SRTX-a, SRTX-a1, SRTX-b, SRTX-c and SRTX-e, are encoded by this precursor. A sixth isoform, SRTX-b1, that differs from SRTX-b in the same way as does SRTX-a1 relative to SRTX-a, was identified during sequencing of an incomplete cDNA. Hence, in the *A. engaddensis* venom, six different SRTX isoforms are produced from two precursors. This so-called "rosary-type" organization is unique within precursors of disulfide-bridged snake toxins. Indeed, "three-fingered" toxins, such as neuromuscular toxins, muscarinic toxins, fasciculins and type A_2 phospholipases for which numerous isoforms have been identified, are all produced from mono-cistronic precursors (Ducancel *et al.*, 1991). Thus, this peculiar organization seems to constitute a simple and effective way of amplifying the production of SRTXs in the venom gland of *A. engaddensis*. It is note worthy that the SRTX-c, which is the most abundant isoform in the venom, is also the sequence with the greatest number of copies: five, in the precursor. However, such a peculiar organization poses the problem of the complete maturation of these precursors, which must end with the release of SRTX isoforms into the lumen of the venom gland (see below).

Identification of long-SRTX isoforms in the venom of *A. m. microlepidota*

A second poly-cistronic precursor encoding SRTXs was recently described in an exhaustive study of the venom of a specimen of *A. m. microlepidota* (Hayashi *et al.*, 2004). Combination of mass spectrometry analysis of the venom composition (Mennin *et al.*, 2004), with molecular cloning of the precursors encoding SRTXs, allowed identification of a new family of longer SRTXs which, compared to the other SRTXs, contain three additional residues at their C-terminus. *Figure 5* shows the nucleotide sequence and the deduced amino-acid sequence for a 1 100 bp fragment of DNA, corresponding to the C-terminal end of a precursor encoding *A. m. microlepidota* SRTXs.

This DNA fragment contains seven 144-nucleotide repeats, each encoding for a peptide link followed by a SRTX sequence. Although incomplete, this fragment displays a poly-cistronic organization as found for the precursor encoding SRTXs from *A. engaddensis*. However, there are several differences between these two "rosary-type" precursors (see below). Five different isoforms: SRTX-m and SRTX-m1 to -m4, are encoded by this incomplete precursor, and all but SRTX-m4 present an Asp-Glu-Pro tripeptide downstream of the invariant Trp at position +21. At the C-terminal extremity of the SRTX-m4 isoform the extension comprises a different tripeptide Glu-Asp-Val. Comparison of the primary structures of the five isoforms reveals 54% to 96% homology (*Figure 2D*). A sixth long isoform, SRTX-m5 (*Figure 2D*) was identified in another incomplete precursor that differs from SRTX-m2 by a single substitution at position +6 (unpublished data). SRTX-m was chemically synthesized and analysis of its biological properties showed that despite its longer C-terminus, SRTX-m a) adopts a typical SRTX-like three-dimensional structure ; b) is toxic to mice, mostly due to vasoconstriction ; and c) has only two-fold lower toxicity than the most toxic SRTX described to date, i.e., SRTX-b from *A. engaddensis* (Hayashi *et al.*, 2004).

All together, these findings establish that *A. m. microlepidota* venom contains a new family of SRTX isopeptides. It is note worthy, that we have just initiated the cloning of the precursors encoding SRTXs from *A. fallax*. The first data that we obtained, clearly demonstrate that SRTXs from *A. fallax* are encoded by poly-cistronic precursors sharing a highly homologous organization with the precursors of SRTXs from *A. m. microlepidota*. Figure 2E shows the first complete (SRTX-f4) or partial sequences (isoforms named SRTX-f, -f2 and –f3) of these new 24 amino-acid long-SRTXs.

A. irregularis : a different SRTX-precursor organization encoding an even larger family of new SRTX isoforms

A first molecular study on the venom of a fourth Atractaspididae species, *A. irregularis*, was reported (Quinton *et al.*, 2005). Direct analysis of the crude venom by nanospray-FT-ICR revealed about 60 distinct molecular masses in the 0.6-15.0 kDa range, of which one half with masses of 2.0-3.5 kDa correspond to peptides of 20-30 amino-acids, a length characteristic for SRTXs. To gain more insight into the sequences of these peptides, the putative precursors of *A. irregularis* SRTXs were cloned and *de novo* sequencing of the peptides was carried out by mass spectrometry on the reduced crude venom. *Figure 6A* shows the structure of one of the two mRNAs cloned.

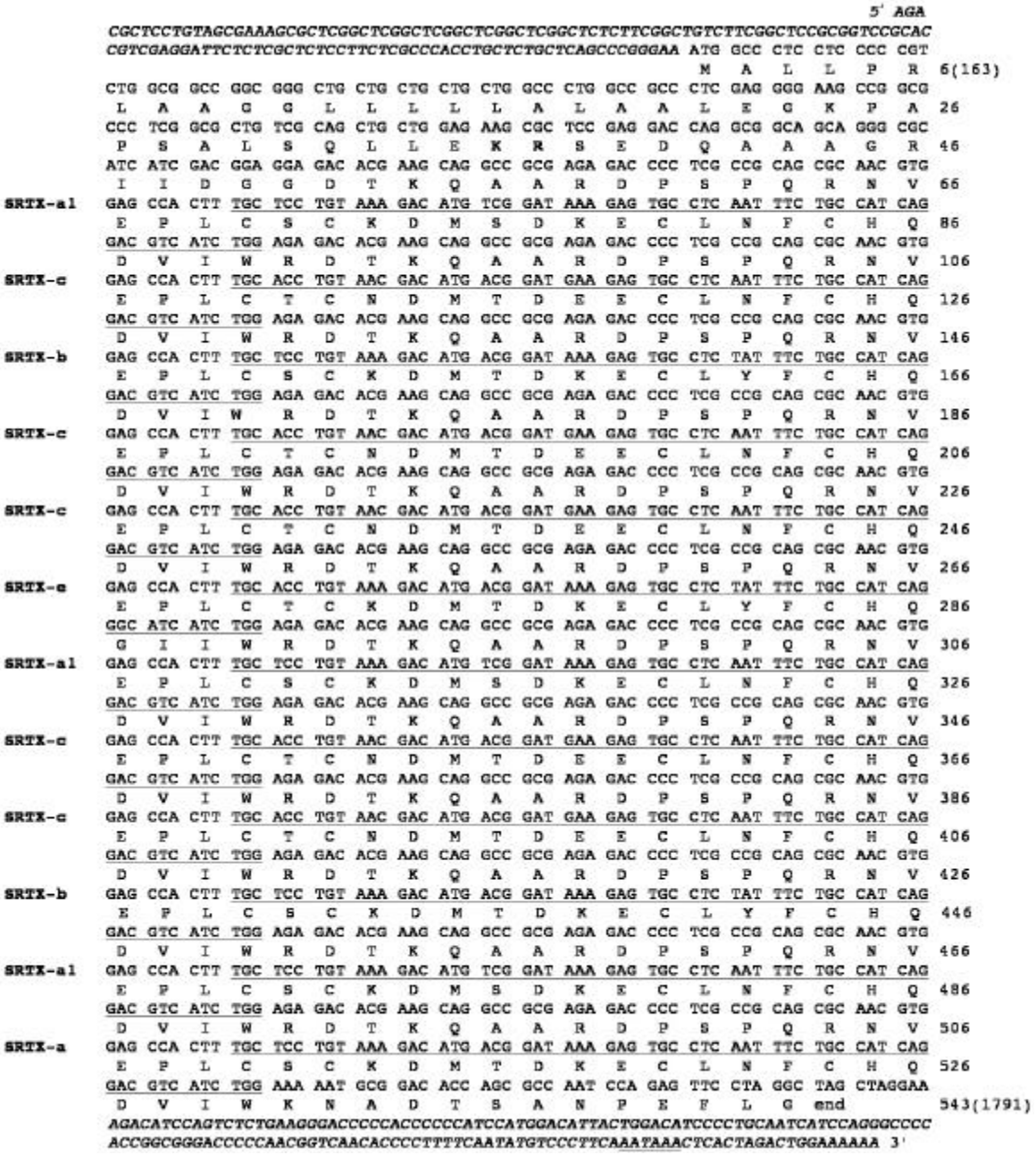

Fig. 4. Nucleotide and deduced amino-acid sequences of a full-length cDNA encoding SRTXs of *A. engaddensis* sarafotoxin. The 5' and 3' non-coding ends are shown in italics. The polyadenylation site "AATAAA" is underlined. The amino-acid sequence deduced from the nucleotide sequence that constitutes the open reading frame is numbered on the right of the figure. Numbers in parentheses indicate nucleotide numbering. Each SRTX sequence is underlined in the precursor, and its name indicated on the left of the figure. The dipeptide of basic amino-acids K-R is in bold.

Fig. 4*. Structure complète du précurseur codant les SRTXs d'*A. engaddensis*. Les extrémités 5' et 3' non codantes sont représentées en italique. Le site de polyadénylation « AATAAA » est souligné. Les séquences nucléotidiques et déduites en acides aminés qui constituent la phase ouverte de lecture sont numérotées sur la droite de la figure. Chaque séquence de SRTX est soulignée dans le précurseur, et son nom indiqué en caractères gras sur la gauche de la figure. Le doublet d'acides aminés basiques K-R est indiqué en caractères gras.*

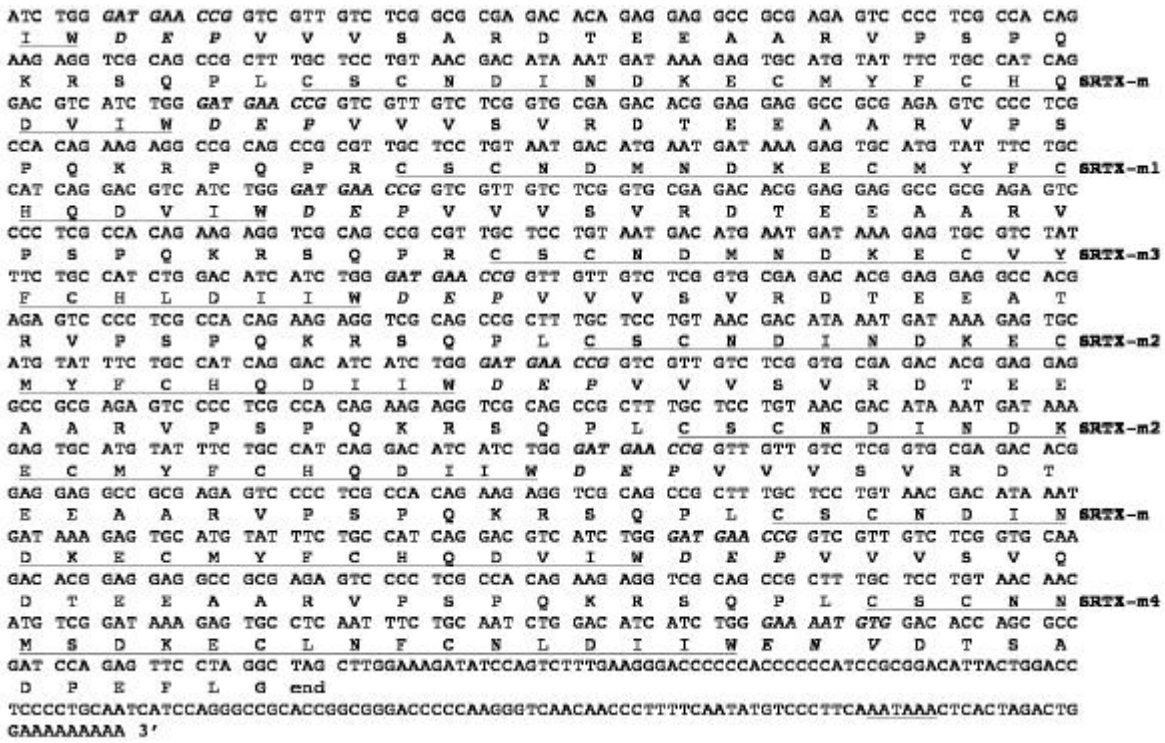

Fig. 5. Nucleotide and deduced amino-acid sequences of a large C-terminal cDNA fragment of an incomplete precursor encoding *A. m. microlepidota* SRTXs. The sequence of each SRTX isoform is underlined, and their names are indicated on the right. The poly (A+) addition signal is underlined within the 3' untranslated region. The three additional C-terminal amino-acid residues are in italics. GenBank accession number: AY485934.

Fig. 5. *Séquences nucléotidique et déduite en acides aminés de l'extrémité C-terminale de la phase ouverte de lecture d'un précurseur des SRTXs chez* A. m. microlepidota*. Les différentes séquences de SRTXs sont soulignées. Le site de polyadénylation « AATAAA » est souligné. Les trois résidus additionnels présent en C-terminal des SRTXs, sont en italique. Le numéro d'accession GenBank est : AY485934.*

In conclusion, during the latest 12 years a combination of cloning and mass spectrometry approaches has led to the identification of an increased number of ET-like peptides forming three families of SRTX isopeptides characterized by 21, 24 or 25 amino-acids (*Figure 2*). At the pharmacological level, it was only shown that SRTX-m (one of the isopeptides of the 24 amino-acid SRTX family) and SRTX-b have similar effects upon injection in mice. However, the potency of SRTX-m is two-fold lower than that of SRTX-b and binding studies, performed using brain or atrial membrane preparations, failed to reveal competition between these two isopeptides (Hayashi *et al.*, 2004). Hence it is tempting to hypothesize that an ET/SRTX receptor subtype that does not bind SRTX-b (Zeng *et al.*, 1997, Valdenaire *et al.*, 1998) could mediate the effects of some of these new SRTX members, as is probably the case for long-ETs (Kitamura *et al.*, 2003).

Precursors and gene organization of sarafotoxins *versus* endothelins

Comparison of SRTX precursors reveals two structurally distinct organizations: mono *versus* poly-cistronic, which is unique for isopeptides that belong to a same superfamily of compounds within a same *genus* of venomous animals. However, and despite their distinct overall organization, these two types of SRTX precursors share several common features, such as the predicted signal peptides that display about 95% sequence identity. Also, the pro-sequence located between the predicted signal peptides and the first SRTX sequence are similar both in their length, with 61 *versus* 69 amino-acids, and sequence, with 72% identity and/or homology. However, and although SRTXs from *A. engaddensis*, *A. m. microlepidota* and *A. fallax* come from repeated precursors, the length and composition of the repeats are significantly different (Ducancel, 2005). Finally, the C-terminal peptides that follow the last (in "rosary-type" precursors) or the unique (in *A. irregularis* precursors) SRTX sequence are identical in length, with 13 amino-acids. However, whereas the C-terminal peptides of the three poly-cistronic precursors are conserved (85% sequence identity), those of *A. irregularis* precursors have only two identical amino-acid residues. These observations strongly suggest that the genes encoding these two types of precursors followed different evolutionary pathways: a plausible complete duplication of a common ancestral gene in the case of *A. irregularis*, whereas the "rosary-type" precursor organization most probably reflects a combined duplication/mutation event of the SRTX-encoding exon only. This hypothesis is further supported by the structural characterization of an *A. engaddensis* exon encoding SRTX-c (Takasaki *et al.*, 1992). The latter contains the sequence of a mature 21 amino-acid SRTX preceded by a 16 amino-acid pro-peptide that appears to be conserved in both mono- and poly-cistronic types of SRTX precursors, suggesting that such an SRTX-encoding exon might be present in the corresponding genes. However, the differences observed between the two types of precursors also suggest that the genes encoding SRTXs and long-SRTXs could have evolved independently.

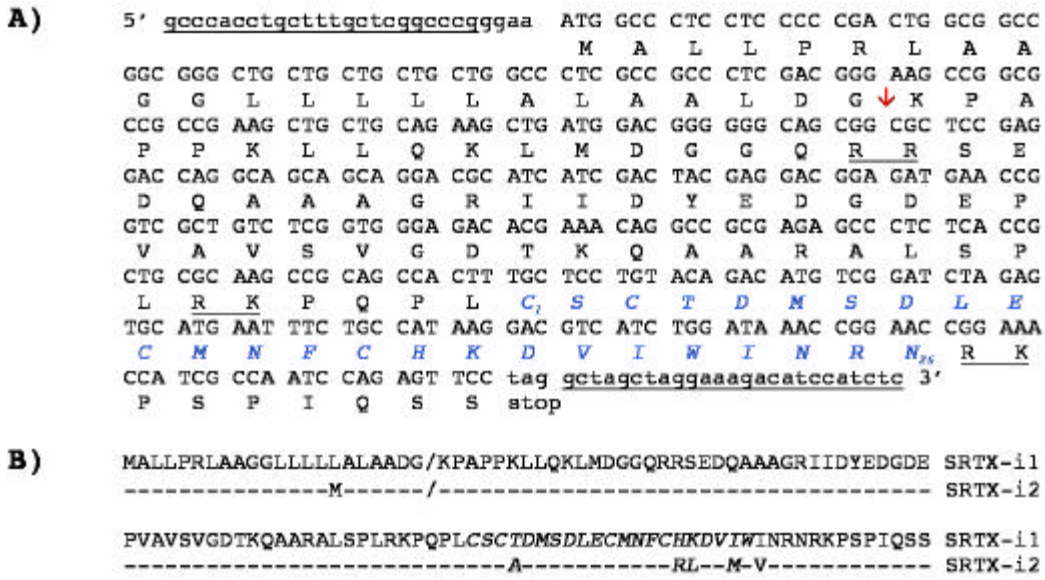

Fig. 6. Organization and deduced amino-acid sequences of the precursors encoding SRTXs from *A. irregularis*. (**A**) Nucleotide and deduced amino-acid sequences of the cDNA encoding SRTX-i1 isoform from *A. irregularis*. The amino-acid sequence is displayed with the single letter code. Positions of the PCR-primers are underlined. The red arrow indicates the probable cleavage site of the signal peptide. The mature 25 amino-acid SRTX-i1 sequence is displayed in blue and italics. Predicted dibasic processing sites are underlined. (**B**) Deduced amino-acid sequences of the two cloned precursors. The names of the isoforms are indicated on the right. « / » indicates the putative cleavage site of the signal peptide. The classical signature sequence of SRTXs is indicated in italics. Identical amino-acid residues are represented by «-».

Fig. 6. *Structure et séquences en acides aminés déduites de deux précurseurs codant des SRTXs chez* A. irregularis. *(**A**) Séquences nucléotidique et déduite en acides aminés du précurseur codant l'isoforme SRTX-i1 chez* A. irregularis. *La séquence en acides aminés est indiquée en code international à une lettre. La position des deux amorces de PCR est soulignée. La flèche rouge indique le site probable de coupure de la séquence signal. La séquence mature de 25 acides aminés de la SRTX-i1 est indiquée en bleu. Les doublets d'acides aminés basiques susceptibles d'être impliqués dans la maturation du précurseur sont soulignés. (**B**) Séquences déduites en acides aminés des précurseurs clonés. Le nom de chaque isoforme est indiqué sur la droite. « / » indique le site de coupure probable de la séquence signal. La séquence typique des SRTXs est indiquée en italique. Les acides aminés identiques sont représentés par « -».*

The structure and organization of the precursors encoding ETs and VIC appear to be intermediate between those of the poly- and mono-cistronic pre-pro-polypeptides encoding SRTXs. The precursors of ET and VIC contain a single and complete ET or VIC sequence, followed by one ET- or VIC-like peptide of 16 amino-acid residues that displays a highly divergent amino-acid composition, except for the conserved cysteine residues. However, comparison with the precursors encoding SRTXs reveals a higher variability in the length and sequence of the ET or VIC signal peptides, and no similarity between the pro-peptides and the linker sequences. Finally, cloning and characterization of the ET genes show that the latter are split into five different exons and that the ET and ET-like sequences, which coexist in the same precursor, are encoded by two different exons (Bloch *et al.*, 1989, 1991 ; Inoue *et al.*, 1989 ; Onda *et al.*, 1990). However, apart from this parallel between the existence of distinct exons encoding for the different isoforms of SRTXs and the presence of both ET and ET-like sequences within the precursor encoding ETs, no other similarity in sequence and structure is observed. In spite of occurence of strong homologies in the structures and biological activities of SRTXs and ETs, and despite cloning of a complete SRTX gene, it is likely that their genes have different organizations, suggesting distinct evolutionary paths.

Maturation of sarafotoxin *versus* endothelin precursors

Maturation of endothelin precursors

The precursors of mammalian ETs (Yanagisawa *et al.*, 1998a, 1998b ; Itoh *et al.*, 1988 ; Bloch *et al.*, 1991 ; Saida and Misui, 1991 ; Marsden *et al.*, 1992) and those of SRTXs have different structures, suggesting distinct maturation processes. ETs are produced as big-ETs, an inactive pro-form of 39 amino-acids produced by the maturation of long precursors of 178 to 224 amino-acids, owing to the presence of two basic doublets on either side of the big-ET. Such basic doublets are known to be cleavage sites for trypsin-like processing enzymes such as Kex2-like serine protease, and they are often involved in the post-translational maturation processes of numerous peptide precursors (Gubler *et al.*, 1982 ; Steiner, 1998). One biologically active molecule of ET is generated per precursor molecule, after the action of the ET-converting enzyme (ECE) that is specific for the peptide bond -Trp_{21}-Val_{22}- (Opgenrth *et al.*, 1992 ; Xu *et al.*, 1994).

Maturation of SRTXs precursors

Conversely, the difference in organization of SRTX precursors implies different maturation processes necessary

for the release of SRTXs into the lumen of the venom glands. It is likely that maturation of the SRTX precursors starts by the recognition *via* a trypsin-like endoprotease of the pairs of basic residues that are present within the pro-sequences of the precursors of SRTXs from *A. engaddensis* and *A. irregularis*, respectively. At this stage, several scenarii for the maturation of the intermediate pro-polypeptides can be envisaged, that likely require the action of uncharacterized and unlocalized endoproteases with particular specificity of cleavage, combined or not with amino and/or carboxy peptidases. It also remains to be established whether the invariant peptide link plays a role in the maturation process and, if so, whether this role is structural or functional, or both. The only information available at present is the mass spectrometry data on venom of a *A. engaddensis* specimen which shows that this venom lacks protein fractions of masses compatible with those of the peptide link, either alone or combined with an SRTX sequence (Mennin *et al.*, 2004). Finally, it has been shown that yeast cell is able to mature the poly-cistronic precursor of SRTXs from *A. engaddensis* (Borgheresi *et al.*, 2001), which means that yeast contains an appropriate maturation enzymatic machinery.

Cellular targets and biological activities of sarafotoxins

Binding characteristics of SRTXs

Iodinated (^{125}I-) SRTX-b binds specifically, and with high affinity to preparations of atrial membranes in a saturable, rapid and reversible manner (Kloog *et al.*, 1988). Scatchard analyses show that ^{125}I-SRTX-b recognizes a homogeneous population of sites, with a maximum binding capacity of 110 fmol per mg of protein and a dissociation constant (K_D) of 3 to 5 nM. This binding is efficiently inhibited by unlabelled SRTX-a, SRTX-b and SRTX-c, at mean inhibitory concentrations (IC_{50}) of 30, 25 and 100 nM, respectively. In contrast, various ligands of ion channels and of receptors and various bioactive peptides are unable compete with the binding of ^{125}I-SRTX-b. Other binding experiments also showed that ^{125}I-SRTX-b recognizes sites in rat brain, particularly in the cerebellum (K_D = 3.5 nM) and cerebral cortex (K_D = 0.3 nM) (Ambar *et al.*, 1988).

Biological properties and molecular targets of SRTXs

It has been shown that: a) the biological activity of SRTXs is associated with a mobilization of intracellular Ca^{2+} ions ; b) the binding of ^{125}I-SRTX-b is unaffected by the action of blockers specific to Ca^{2+} channels, such as verapamil or ninodipine, and c) the binding of SRTXs induces the hydrolysis of phosphoinositides, as shown by the accumulation of inositol mono-, di- and triphosphate. The concentrations of the three isotoxins that induced 50% of maximal phosphoinositide hydrolysis are 100, 60, and 300 nM for SRTX-a, SRTX-b, and SRTX-c, respectively. Thus, SRTX-c is both the less toxic and potent isotoxin of *A. engaddensis*, whereas SRTX-b induces phosphoinositide hydrolysis in other regions of the brain. Taken together, these results strongly suggest that SRTXs and ETs use the phosphoinositide signal transduction pathway *via* specific rhodopsin-like G-protein-coupled receptors (Kloog and Sokolovsky, 1989 ; Sakurai *et al.*, 1992 ; Sokolovsky, 1994). These glycosylated receptors (Bousso-Mittler *et al.*, 1991 ; Davenport and Maguire, 1995) range in size from 30 to 70 kDa and contain seven potential transmembrane domains, and share numerous structural features with other receptors coupled to G proteins. The recombinant forms of these receptors for the different isoforms of ETs and SRTXs are classified into two main subtypes, ET_A-R and ET_B-R, depending on their relative affinities. The isoforms ET-1 and ET-2 have similar and high affinities for ET_A-R, whereas ET-3 recognizes ET_A-R 1,000 times less well. The second family of receptors, ET_B-R, appears less selective since the three isoforms of ETs and SRTXs interact with the same affinity. A third subtype of ET receptor, called ET_{B1}-R, has been identified (Sokolovsky *et al.*, 1992). ET_{B1}-R is characterized by high-affinity (picomolar) sites that do not hydrolyze phosphoinositides and whose properties are affected differently depending on the degree of glycosylation. On the other hand, it has been suggested that the capacity of the Egyptian mongoose to resist to very high concentrations of SRTX-b or ET-1 is due to a new family of binding sites specific to SRTXs and ETs in the brain and cardiovascular tissue (Bdolah *et al.*, 1997). All these findings and observations underscore the incompleteness of our knowledge of the pharmacology of ETs and toxicology of SRTXs, in terms of the variable, tissue-dependent concentrations of ETs and/or SRTXs, and with regard to the equally broad heterogeneity among the receptors.

Structure-function relationships of sarafotoxins

Structure-function analysis of SRTXs

Numerous structure-function studies have been devoted to identifying the functional sites by which SRTXs and ETs recognize their receptors and act as vasoconstrictors. It has been established that the vasoconstrictor potencies of the three SRTX isoforms on rabbit aorta preparations range as SRTX-b > SRTX-a > SRTX-c (Wollberg *et al.*, 1989). STRX-b differs from SRTX-a by a Tyr substitution to Asn at position +13. The three ETs and the VIC peptide also have a Tyr at this position (*Figure 2B*). SRTX-c, the less toxic isoform of *A. engaddensis* SRTXs, has respectively three and four substitutions compared with the -a and -b isoforms, including a replacement of a Ser by a Thr at position +2, which is also observed in the ET-3 isoform, the less active of the ETs (*Figure 2A-C*). A study has sought to establish the biological characteristics of [Thr2]SRTX-b, a synthetic analogue of SRTX-b which, together with ET-1, is one of the two most toxic isopeptides and whose contractile activity is greater on the smooth muscles of organs such as the uterus, intestine, aorta and blood vessels (Lamthanh *et al.*, 1994). The results of this study confirm that presence of a Ser at position +2 is required for a high vasoconstrictor activity, as confirmed by sequence alignments (*Figure 2*), although replacement of this Ser by a Thr does not alter the overall toxicity of this analogue. This suggests that other substitutions contribute also to the weak pharmacological activity of SRTX-c and ET-3.

Structure-function analysis of ETs

Other structure-function relationships studies have completed the identification of the amino-acids responsible for the vasoconstrictor potency of ETs and SRTXs. Kimura *et al.* (1988) have shown that the C-terminus of ET-1, and particularly Trp21 and the two disulfide bridges, are crucial for its vasoconstrictor activity. The functional importance of the N- and C-terminus ends, and that of the carboxylic groups of Asp8 and Glu10 were established by chemical modification or mutagenesis of ET-1 (Nakajima *et al.*, 1989). Thus, the differences in biological activity and in toxicity which characterize these isoforms depend both on the nature of the amino-acids constituting the loop formed between the cysteines +3 and +11 where the principal sequence variations are located, and on the recognized receptor subtypes. Hence, various observations suggest that ETA-R recognizes the N- and C-termini of the ETs, whereas ETB-R is more specific to the C-terminal segment between amino-acids Glu10 and Trp21 (Sakurai *et al.*, 1992). The importance of the unstructured C-termini of ET-1 to trigger binding with ETB-R is confirmed by the fact that an ET-1 mutant devoid of disulfide bridges is still active (Bigaud and Pelton, 1992). Thus we can define a "common" and "minimum" vasoconstrictor site at the surface of ETs and SRTXs that seems partially conformational, constituted by the N- and C-terminal ends, and by the COOH groups of the side-chains at positions +8 and +10 (*Figure 7*). This is confirmed by the fact that all amino-acids: Cyst1, Cyst3, Asp8, Glu10, Cyst11, Cyst15 and Trp21, are invariant (*Figure 2G*) in ETs and SRTXs.

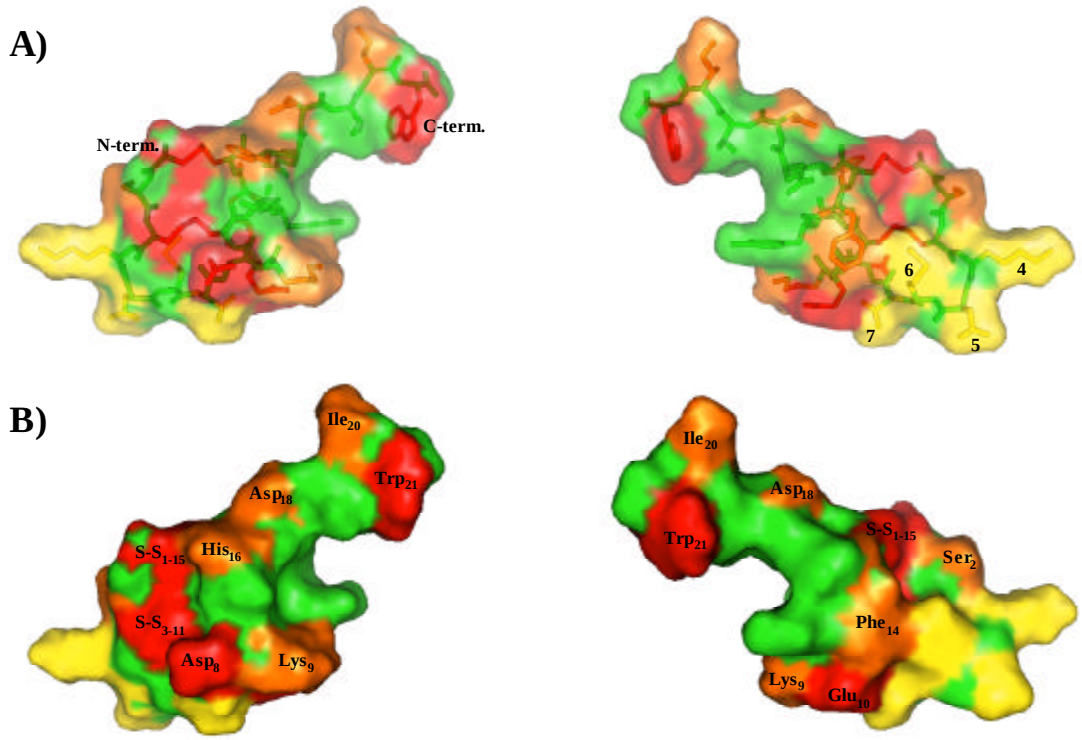

Fig. 7. Surface representations of the sarafotoxin-b molecule. (**A**) Faces A and B of SRTX-b are displayed. The backbone is shown by transparency. The N- and C-termini are indicated. Invariant and highly conserved amino-acid residues within SRTXs are indicated in red and orange, respectively. The four positions within the turn that are the most variable in ETs and SRTXs in terms of amino-acid composition are indicated in yellow and labeled from 4 to 7. The remainder of the molecule is shown in green. (**B**) Surface representations of faces A and B of SRTX-b. The residues that are labeled and numbered correspond to those found in SRTX-b. The pairing of the two disulfide bridges is indicated as S-S_{x-y}.

Fig. 7. *Représentations de la surface de la SRTX-b. (**A**) Les deux faces sont montrées. Le squelette est représenté par transparence. Les extrémités N- et C-terminales sont indiquées. Les résidus invariants et très conservés au sein des SRTXs et des ETs sont respectivement représentés en rouge et orange. Les quatre acides aminés les plus variables du coude des SRTXs et ETs sont numérotés de 4 à 7 et indiqués en jaune. Le reste de la molécule est en vert. (**B**) Représentations de la surface des deux faces de la SRTX-b. Les résidus qui sont mentionnés et numérotés correspondent à ceux de la SRTX-b. Le couplage des deux ponts disulfure est indiqué par « S-S_{x-y} ».*

Although little is known about the vasoconstrictor potencies of the newly identified SRTX isoforms, especially from the venoms of the snakes *A. m. microlepidota*, *A. fallax* and *A. irregularis*, and despite their differences in primary structure, these new isoforms display the overall structural and functional characteristics of the SRTXs of *A. engaddensis* and of ETs of mammals. However, although these long-SRTX isoforms share a common structural pattern with other SRTXs, we notice a diversification in the amino-acid composition since six new amino-acids are found in positions where they were absent until now: a) a Thr at position +4, b) an Iso at position +6, c) an Asn at position +7, d) a Leu or a Glu at position +9, e) a Met at position +12, and f) a Lys at position +17 (*Figure 2*). It is noteworthy that the higher sequence variability is located in the β-turn structure between positions +5 and +8 (*Figure 7*). Finally, the differences in length and amino-acid composition of the C-

termini downstream of the invariant Trp at position +21 could confer on these long-SRTXs or ETs a different receptor affinity and/or tissue specificity (Nakano *et al.*, 1997 ; Kishi *et al.*, 1998 ; Kitamura *et al.*, 2003 ; Hayashi *et al.*, 2004).

Engineering of sarafotoxins

Recently, two articles describing the chemical engineering of SRTXs, were published. A summary of each of them follows.

SRTXs: a scaffold to design matrix metalloproteinase inhibitors ?

The first article, by Lauer-Fields *et al.* (2007), describes the use of SRTXs as templates to design inhibitors of matrix metalloproteinases. The starting point of this work was that the ternary structure of SRTX-b shows topological similarity to the metalloproteinase interaction sites of the tissue inhibitors of metalloproteinases. While native SRTX-b induces very modest metalloproteinase inhibition, chemically engineered variants of SRTX-b showed enhanced inhibitory potencies. This was obtained by screening libraries of SRTX variants modified in their C-terminus, in combination or not with substitutions suggested by analogy with tissue inhibitors of metalloproteinases. The resulting SRTX variants with multiple substitutions folded correctly and formed native disulfide bounds, confirming the robustness and structural adaptability of the CSH-fold that characterizes the SRTXs. The best variant displayed improved affinity with micromolar K_i values for matrix metalloproteinase-1 and -9. NMR characterization of their structure in solution, indicate close similarity to SRTXs despite a more extended C-terminus helix. This result is interesting for several reasons. First, it confirms that the CSH scaffold that characterizes SRTXs and ETs is robust enough to tolerate major primary structure changes without major ternary structure modification. Second, it indicates that the primary structure of the C-terminus of SRTX is susceptible to vary in its amino-acid content (this work) or in length (see long-SRTXs). Finally, it appears that the C-terminus of SRTXs might be associated with a modulation of SRTX biological properties towards receptors or enzymes, an assumption that further emphasizes the interest of studying further the affinity and specificity of targets of the newly discovered long-SRTXs.

A first neutralizing antivenom against *A. m. microlepidota* envenomation

The second article, by Ismail *et al.* (2007), describes an original strategy to design a bivalent immunogenic conjugate aimed at inducing the production of neutralizing polyclonal antibodies in horse. To this end, the purified SRTX fraction *from A. m. microlepidota* was chemically coupled to T_{III}, the main neurotoxic compound found in the venom of the black desert cobra (*Walterinnesia aegytia*), a deadly snake found in Saudi Arabia. After immunization, the antibodies were extracted and purified from the serum and the $F(ab')_2$ fraction prepared. This $F(ab')_2$ fraction was shown to protect mice and rats against the lethal effects of either venom and to rescue rats challenged with lethal doses of the venom. The fraction was also found to neutralize the haemorrhagic, necrotizing and cardiotoxic effects of *A. m. microlepidota*. This is the first antivenom to be efficient against an *Atractaspis* envenomation.

Conclusions

Since the discovery of SRTXs in 1982, all the research results and particularly the recent molecular biology and mass spectrometry data show that the venoms of Atractaspididae snakes, like other venomous animals, contain a great variety of isoforms of a given toxin. This diversity, which is thought to reflect a predator's need to adapt evolutionarily to the ecological diversity of its prey, goes well beyond the scope of toxicology. Animal toxins are specific for precise molecular targets (receptors, ion channels, enzymes) and are involved in vital physiological machinery (central and/or peripheral nervous system, muscles, blood circulation). For this reason, animal toxins in general and ET-like peptides from Atractaspididae snakes in particular, constitute unique molecular probes for identifying and studying their targets. The data available on ET-like peptides also raise many questions. E.g., what are the enzymes responsible for the maturation of the SRTX precursors of and how do they function? Do these enzymes participate in the maturation of other poly-cistronic precursors, and do they have endogenous equivalents? Other questions concern the origin of and biological justification for the diversity of SRTXs. E.g., why do so many different isoforms exist? Does this feature reflect an equally great diversity among receptors and, if so, what are their molecular characteristics and where are they localized? What are the biological activity and recognition specificity of these various peptides? From a molecular evolutionary point of view, how is this diversity generated? What are the genomic structures that raise these differently organized precursors? For all these reasons, toxins in general and ET-like peptides in particular continue to fascinate researchers, clinicians and industrials alike.

Acknowledgements. *For their contributions to various aspects of current knowledge of* SRTXs*, we thank Avner Bdolah, Jean-Claude Boulain, Julie Bourdais-Jomaron, Julia Chamot-Rooke, Tolga Coskun, Yvon Doljansky, Philippe Favreau, Andrzej Galat, Mariana Hajj, Mirian Hayashi, Elazar Kochva, Hung Lamthanh, Jean-Pierre Le Caer, Caroline Ligny-Lemaire, Vilborg Matre, André Ménez, Laure Mennin, Gilles Mourrier, Bruno Muller, Tomohisha Ogawa, Gilles Phan, Loïc Quinton, Alexandra Savatier, Denis Servent, Reto Stöcklin, Michaël Wéry, Zvi Wollberg, and Sophie Zinn-Justin.*

References

Ambar I, Kloog Y, Kochva E, Wollberg Z, Oron U, Sokolovski M (1988) Characterization and localization of a novel neuroreceptor for the peptide sarafotoxin. *Biochem Biophys Res Comm* **157**: 1104-1110

Andersen NH, Chen C, Marschner TM, Krystek SR, Bassolino DA (1992) Conformational isomerism of endothelin in acidic aqueous media: a quantitative NOESY analysis. *Biochemistry* **31**: 1280-1295

Atkins AR, Martin RC, Smith R (1995) ^{1}H-NMR studies of sarafotoxin SRTb, a nonselective endothelin receptor agonist, and IRL 1620, and ET_B receptor-specific agonist. *Biochemistry* **34**: 2026-2033

Bagnato A, Natali PG (2004) Targeting endothelin axis in cancer. *Cancer treat Res* **119**: 293-314

Barton M, Yanagisawa M (2008) Endothelin: 20 years from discovery to therapy. *Can J Physiol Pharmacol* **86**: 485-498

Bigaud M, Pelton JT (1992) Discrimination between ET_A- and ET_B-receptor-mediated effects of endothelin-1 and [Ala^{1,3,11,15}]endothelin-1 by BQ-123 in the anaesthetized rat. *Br J Pharmacol* **1007**: 912-918

Bdolah A, Wollberg Z, Kochva E (1991) Sarafotoxins: a new group of cardiotoxic peptides from the venom of *Atractaspis*. In: Snake Toxins, Harvey AL (ed), pp. 415-423. New York: Pergamon Press.

Bdolah A, Kochva E, Ovadia M, Kinamon S, Wollberg Z (1997) Resistance of the Egyptian mongoose to sarafotoxins. *Toxicon* **35**: 1251-1261

Becker A, Dowdle EB, Hechler U, kauser K, Donner P, Schleuning WD (1993) Bibrotoxin, a novel member of the endothelin/sarafotoxin peptide family from the venom of the burrowing asp *Atractaspis bibroni*. *FEBS Letts* **315**: 100-103

Bloch KD, Friedrich SP, Lee ME, Eddy RL, Shows TB, Quertermous T (1989) Structural organization and chromosomal assignment of the gene encoding endothelin. *J Biol Chem* **264**: 10851-10857

Bloch KD, Hong CC, Eddy TB, Shows TB, Querternous T (1991) cDNA cloning and chromosomal assignment of the endothelin 2 gene: vasoactive intestinal contractor is rat endothelin 2. *Genomics* **10**: 236-242

Borgheresi RA, Palma MS, Ducancel F, Camargo AC, Carmona E (2001) Expression and processing of recombinant sarafotoxins precursor in *Pichia pastoris*. *Toxicon* **39**: 1211-1218

Bousso-Mittler D, Galron R, Sokolovsky M (1991) Endothelin/ sarafotoxin receptor heterogeneity: evidence for different glycosylation in receptors from different tissues. *Biochem Biophys Res Comm* **178**: 921-926

Cazaubon S, Deshayes F, Couraud PO, Nahmias C (2006) Endothelin-1, angiotensine II et cancer. *Med Sci* **22(4)**: 21-24

Chandralal MH, Lu J, Parkinson JA, Ramage R, Sadler IH (1999) A linear endothelin-1 analogue: solution structure of ET-1[Aib^{1,3,11,15}, Nle^{7}] by nuclear magnetic resonance spectroscopy and molecular modeling. *Neurochemistry International* **35**: 35-45

Davenport AP, Maguire JJ (1995) Endothelins in endocrinology: new advances. Endothelin receptor sub-types and their function. In: Frontiers in endocrinology. Baldi E, Maggi M, Cameron IT, Dunn MJ (ed) Vol. 15, pp. 35-45. Ares Serono Symposia

David P, Ineich I (1999) Venomous snakes in the world: systematic and repartition. *Dumerilia* **3**: 18-28

Ducancel F, Bouchier C, Tamiya T, Boulain JC, Ménez A (1991) Cloning and expression of toxin cDNAs. In Snake Toxins. Harvey AL (ed) pp. 385-414. New York: Pergamon Press

Ducancel F, Matre V, Dupont C, Lajeunesse E, Wollberg Z, Bdolah A *et al.* (1993) Cloning and sequence analysis of cDNAs encoding precursors of sarafotoxins. *J Biol Chem* **268**: 3052-3055

Ducancel F, Matre V, Dupont C, Wollberg Z, Bdolah A, Kochva A *et al.* (1995) Endothelins in endocrinology: new advances. Structure and function of mRNAs encoding sarafotoxin precursors. In: Frontiers in endocrinology. Baldi E, Maggi M, Cameron IT, Dunn MJ (ed) Vol. 15, pp. 35-45. Ares Serono Symposia

Ducancel F, Wery M, Hayashi MAF, Muller BH, Stöcklin R, Ménez A (1999) Les sarafotoxines de venins de serpent. *Ann Inst Pasteur* **10(2)**: 183-194

Ducancel F (2002) The sarafotoxins. *Toxicon* **40**: 1541-1545

Ducancel F (2005) Endothelin-like peptides. *Cell Mol Life Sci* **62(23)**: 2828-2839

Golani I, Kochva A (1988) Biting behaviour of *Atractaspis*. *Copeia* 792-797

Gubler U, Seeburg P, Hoffman BJ, Gage PL, Udenfrirnd S (1982) Molecular cloning establishes proenkephalin as precursor of enkephalin-containg peptides. *Nature* **295**: 206-208

Hayashi MAF, Ligny-Lemaire C, Wollberg Z, Wery M, Galat A, Ogawa T *et al.* (2004) Long-sarafotoxins: characterization of a new family of endothelin-like peptides. *Peptides* **25**: 1243-1251

Hyndman KA, Evans DH (2007) Endothelin and endothelin converting enzyme-1 in the fish gill: evolutionary and physiological perspectives. *J Exp Biol* **210**: 4286-4297

Inoue A, Yanagisawa M, Kimura S, Kasuya Y, Miyauchi T, Goto K *et al.* (1989) The human endothelin family: three structurally and pharmacologically distinct isopeptides predicted by three separate genes. *Proc Natl Acad Sci USA* **86**: 2863-2867

Ismail M, Al-Ahaidib MS, Abdoon N, Abd-Elsalam MA (2007) Preparation of a novel antivenom against *Atractaspis* and *Walterinnesia* venoms. *Toxicon* **49**: 8-18

Itoh Y, Yanagisawa M, Ohkubo S, Kimura C, Kosaka T, Inoue A, *et al.* (1988) Cloning and sequence analysis of cDNA encoding the precursor of a human endothelium-derived vasoconstrictor peptides, endothelin: identity of human and porcine endothelin. *FEBS Letts* **231**: 440-444

Kedzierski RM, Yanagisawa M (2001) Endothelin system: the double-edged sword in health and disease. *Annu Rev Pharmacol Toxicol* **41**: 851-876

Kimura S, Kasuya Y, Sawamura T, Shinmi O, Sugita Y, Yanagisawa T *et al.* (1988) Structure-activity relationships of endothelin: importance of the C-terminus moiety. *Biochem Biophys Res Comm* **156**: 1182-1186

Kitamura H, Cui P, Sharmin S, Yano M, Kido H (2003) Binding of new bioactive 31-amino-acid endothelin-1 to an endothelin ET_B or ET_B-like receptor in porcine lung. *Eur J of Biochem* **465**: 31-38

Kishi F, Minami K, Okishima N, Murakami M, Mori S, Yano M *et al.* (1998) Novel 31-amino-acid-length endothelins cause constriction of vascular smooth muscle. *Biochem Biophys Res Com.* **248**: 387-390

Kochva E, Viljoen CC, Botes DP (1982) A new type of toxin in the venom of snakes of the genus *Atractaspis* (*Atractaspidinae*). *Toxicon* **20**: 581-592

Kochva E, Bdolah A, Wollberg Z (1993) Sarafotoxins and endothelins: evolution, structure and function. *Toxicon* **31**: 541-568

Kochva E (2002) *Atractaspis* (Serpentes, Atractaspididae) the burrowing asp: a multidisciplinary minireview. *Bull Nat Hist Mus Lond* **68**: 91-99

Kloog Y, Ambar I, Sokolovsky M, Kochva E, Wolberg Z, Bdolah A (1988) Sarafotoxin, a novel vasoconstrictor peptide: phosphoinositide hydrolysis in rat and brain. *Science* **242**: 268-270

Kloog Y, Sokolovski M (1989) Similarities in mode and sites of action of sarafotoxins and endothelins. *Trends in Pharmacological Sci* **10**: 212-214

Lamthanh H, Bdolah A, Créminon C, Grassi J, Ménez A, Wollberg Z *et al.* (1994) Biological activities of [Thr^2]sarafotoxin-b, a synthetic analogues of sarafotoxin-b. *Toxicon* **32**: 1105-1114

Lauer-Fields JL, Cudic M, Wei S, Mari F, Fields GB, Brew K (2007) Engineered sarafotoxins as tissue inhibitor of metalloproteinases-like matrix metalloproteinase inhibitors. *J Biol Chem* **282(37)**: 26948-26955

Marsden PA, Sultan P, Cybulsky M, Gimbrone MA, Brenner BM, Collins T (1992) Nucleotide sequence of endothelin-1 cDNA from rabbit endothelial cells. *Biochem Biophys Acta* **1129**: 249-250

Mennin L, Favreau P, Doljansky Y, Ducancel F, Stöcklin R (2004) The proteome of *Atractaspis microlepidota microlepidota* snake venom reveals long-sarafotoxins, a family of endothelin-like peptides. Proceedings of the 15th European Symposium on Animal, Plant and Microbial Toxins (Slovenia), pp. 68

Miyauchi T, Masaki T (1999) Pathophysiology of endothelin in the cardiovascular system. *Annu Rev Physiol* **61**: 391-415

Nakajima K, Kubo S, Kumagaye SI, Nishio H, Tsunemi M, Inui T *et al.* (1989) Structure-activity relationship: importance of charged groups. *Biochem. Biophys Res Comm* **163**: 424-429

Nakano A, Kishi F, Minami K, Wakabayashi H, Nakaya Y, Kido H (1997) Selective conversion of big-endothelins to tracheal smooth muscle-contracting 31-amino acid-length endothelins by chymase from human mast cells. *J of Immunol* **159**: 1987-1992

Onda H, Ohkubo S, Ogi K, Kosaka T, Kimura C, Matsumoto H *et al.* (1990) One of the endothelin gene family, endothelin 3 gene, is expressed in the placenta. *FEBS Letts* **261**: 327-330

Opgenrth TJ, Wu-Wong JR, Shiosaki K (1992) Endothelin-converting enzymes. *FASEB J* **6**: 2653-2659

Quinton L, Le Caer JP, Phan G, Ligny-Lemaire C, Bourdais-Jomaron J, Ducancel F *et al.* (2005) Characterization of new toxins within crude venoms by combined use of Fourier Transform Mass Spectrometry and cloning. *Analytical Chem* **77(20)**: 6630-6639

Remuzzi G, Perico N, Benigni A (2002) New therapeutics that antagonize endothelin: promises and frustrations, *Nature reviews. Drug discovery* **1**: 986-1001

Saida K, Misui Y (1991) cDNA cloning, sequence analysis and tissue distribution of a precursor for vasoactive intestinal contractor (VIC). *Biochem Biophys Acta* **1089**: 404-406

Sakurai T, Yanagisawa M, Masaki T (1992) Molecular characterization of endothelin receptors. *TIPS Reviews* **13**: 103-108

Shaw SG, Boden PJ (2005) Insulin resistance, obesity and metabolic syndrome. Is there a therapeutic role for endothelin-1 anatgonists? *Curr Vasc Pharmacol* **3(4)**: 359-363

Sokolovsky M, Ambar I, Galron R (1992) A novel subtype of endothelin receptor. *J Biol Chem* **267**: 20551-20554

Sokolovsky M (1994) Endothelins and sarafotoxins: receptors heterogeneity. *Int J Biochem* **26**: 335-340

Steiner DF (1998) The proprotein convertase. *Curr Opinion Chem Biol* **2**: 31-39

Stoijilkovic SS, Catt KJ (1992) Neuroendocrine actions of endothelins. *Trends Pharmacol Sci* **13(10)**: 385-391

Takasaki C, Itoh Y, Onda H, Fujino M (1992 Cloning and sequence analysis of a snake *Atractaspis engaddensis* gene encoding sarafotoxin S6C. *Biochem Biophys Res Comm* **189**: 1527-1533

Tamoaki H, Kobayashi Y, Nishimura S, Ohkubo T, Kyogoku Y, Nakajima K *et al.* (1991) Solution conformation of endothelin determined by means of ^{1}H-NMR spectroscopy and distance geometry calculations. *Prot Eng* **4**: 509-518

Valdenaire O, Giller T, Breu V, Ardati A, Schweizer A, Richard JG (1998) A new family of orphan G protein-coupled receptors predominantly expressed in the brain. *FEBS Letts* **424**: 193-196

Wang Y, Olson KR, Smith MR, Russell MJ, Conlon JM (1999) Purification, structural characterization, and myotropic activity of endothelin from trout, Oncorhynchus mykiss. *Am J Physiol* **277**: 1605-1611

Weiser E, Wollberg Z, Kochva E, Lee SY (1984) Cardiotoxic effects of the venom of the burrowing asp, *Atractaspis engaddensis* (Atractaspididae, Ophidia). *Toxicon* **22**: 764-774

Wollberg Z, Bdolah A, Kochva E (1989) Vasoconstrictor effects of sarafotoxins in rabbit aorta: structure-function relationships. *Biochem Biophys Res Comm* **162**: 371-376

Xu D, Emoto N, Giaid A, Slaughter C, Kaw S, deWit D *et al.* (1994) ECE-1: a membrane-bound metalloprotease that catalyses the proteolytic activation of big endothelin-1. *Cell* **78**: 473-485

Yanagisawa M, Kurihara H, Kimura S, Tomobe Y, Kobayashi M, Yasaki Y *et al.* (1988a) A novel potent vasoconstrictor peptide produced by vascular endothelial cells. *Nature* **332**: 411-415

Yanagisawa M, Inoue A, Ishikawa T, Kasuya Y, Kimura S, Kumagaye SI *et al.* (1988b) Primary structure, synthesis and biological activity of rat endothelin, and endothelin-derived vasoconstrictor peptide. *Proc Natl Acad Sci USA* **85**: 6964-6967

Zeng Z, Su K, Kyaw H, Li Y (1997) A novel endothelin receptor type-B-like gene enriched in the brain. *Biochem Biophys Res Comm* **233**: 559-567

Toxines et Signalisation – Toxins and Signalling
Rencontres en Toxinologie – Meeting on Toxinology, 2009
Editions de la SFET – SFET Editions
Accès libre en ligne sur le site – Free access on line on the site : http://www.sfet.asso.fr

AdTx1, un antagoniste peptidique spécifique du récepteur adrénergique α1a

Arhamatoulaye MAIGA[1], Loïc QUINTON[2], Stefano PALEA[3], Moèz REKIK[3], Maud LARREGOLA[4], Geoffrey MASUYER[5], Gilles MOURIER[1], Carole FRUCHART[1], André MENEZ[6], Julia CHAMOT-ROOKE[2], Denis SERVENT[1], Nicolas GILLES[1]*

[1] *CEA, iBiTecS, Service d'Ingénierie Moléculaire des Protéines (SIMOPRO), Gif sur Yvette, 91191, France ;* [2] *Laboratoire des Mécanismes Réactionnels, UMR 7651 CNRS, Ecole Polytechnique, 91128 Palaiseau, France ;* [3] *Faculté des Sciences Pharmaceutiques, Université Paul Sabatier, Toulouse ;* [4] *Laboratoire de Synthèse, Structure et Fonction de Molécules Bioactives, UMR 7613, 4 place Jussieu 75252 Paris Cedex 05 ;* [5] *Structural Molecular Biology, Department of Biology & Biochemistry, University of Bath, UK ;* [6] *Muséum national d'Histoire naturelle, 57 rue Cuvier, Paris, France*

** Auteur correspondant ; Tél : +33 (0)169086547. ; Fax : +33 (0)169089071 ; Courriel: nicolas.gilles@cea.fr*

Cet article est dédié à la mémoire d'André Ménez

Résumé

Les venins d'animaux sont extrêmement riches en toxines peptidiques interagissant avec une grande affinité sur les canaux ioniques et les récepteurs canaux. A l'inverse, on ne connaît que très peu de toxines ciblant les récepteurs couplés aux protéines G (RCPG), dont pourtant le rôle physiologique est primordial. Afin d'identifier de nouveaux ligands ciblant ces RCPG, nous avons entrepris de cribler le venin du mamba vert vis-à-vis des différents sous-types de récepteurs adrénergiques et mis en évidence un nouveau peptide nommé AdTx1. Constitué de 65 résidus et réticulé par 4 ponts disulfure, AdTx1 appartiendrait à la famille des toxines à « trois-doigts ». In vitro*, AdTx1 présente une affinité nanomolaire et une forte spécificité pour le récepteur adrénergique α1a humain alors qu'*ex vivo*, elle bloque la contraction musculaire induite par la phényléphrine du muscle prostatique de lapin. AdTx1 est donc le premier antagoniste peptidique présentant une forte sélectivité pour le récepteur α1a, à être décrit.*

AdTx1, an antagonist toxin specific of α1a adrenergic receptor

Animal venoms are rich in peptidic toxins interacting with high affinity with ionic channels and ligand-gated ion channels. The G Protein Coupled Receptors (GPCR), another family of receptors with crucial physiological roles, are targeted by only few known toxins. To find original peptidic ligands targeting GPCR, we screened the green mamba venom on the different adrenergic receptor subtypes and identify a new peptide : AdTx1. With 65 residues and reticulated by 4 disulfide bridges, AdTx1 belongs to the three-fingers fold toxin family. AdTx1 displays in vitro *a nanomolar affinity and a high selectivity for the human α1a adrenoceptor whereas* ex vivo *it blocks the phenylephrine-induced muscular contraction of the rabbit prostatic muscle. Therefore it is the first peptidic antagonist with strong selectivity for the α1a receptor to be described.*

Keywords : *α1a-AR, allosteric, binding experiment, lower urinary tracks symptoms, non-competitive antagonist, peptidic ligand, snake venom.*

Introduction

Les venins de serpent sont constitués entre autres d'un mélange complexe d'enzymes et de toxines peptidiques. Ces molécules confèrent aux venins la capacité d'interagir avec des cibles moléculaires diverses et variées, à l'origine de leur redoutable toxicité. Les toxines contenues dans les venins sont des peptides fortement réticulés de moins de 100 acides aminés. Elles sont en général très sélectives et affines d'un récepteur membranaire donné. De ce fait, ces toxines sont très utiles dans la caractérisation biochimique et pharmacologique des récepteurs auxquels elles se lient. Elles peuvent conduire également à la conception de nouveaux médicaments. Le Captopril, le plus connu de ces médicaments, a été conçu à partir d'une toxine appelée BPP (*Bradykinin Potentiating Peptide*) provenant du venin de la vipère *Bothrops jaracusa*. Le Captopril est un inhibiteur très efficace de l'enzyme de conversion de l'angiotensine et possède donc des propriétés hypotensives (Lewis et Garcia, 2003). A ce jour, la grande majorité des toxines est active sur les canaux ioniques et seules quelques-unes possèdent une activité ciblant les Récepteurs Couplés aux Protéines G (RCPG). Celles-ci sont principalement des toxines muscariniques actives sur les récepteurs muscariniques et des sarafotoxines actives sur les récepteurs aux endothélines (Bradley, 2000).

Les RCPG ou récepteurs à 7 domaines transmembranaires jouent un rôle physiologique particulièrement important. Ils activent des voies de signalisation intracellulaire suite à la fixation de ligands très variés (hormone, acides aminés, peptides, lumière …). Ils sont également la cible de près de 50% des médicaments actuellement sur le marché (Neubig *et al.*, 2003).

Dans le but de trouver de nouvelles molécules actives vis-à-vis de ces récepteurs et possédant d'éventuelles activités pharmacologiques originales, le venin du mamba vert (*Dendroaspis angusticeps*) connu pour contenir quelques toxines actives sur les RCPG, a été étudié. Les RCPG cibles ont été restreints à la famille 1 a, celle de la Rhodopsine, seule décrite comme interagissant avec des toxines. Dans cet article, nous nous focaliserons sur les récepteurs adrénergiques (AR), et plus particulièrement sur les sous types α1AR. Composé des classes (α1, α2, β), la famille des AR assure la médiation de la réponse aux catécholamines endogènes. Le sous-type α1AR (α1aAR, α1bAR et α1dAR) est exprimé dans le système périphérique au niveau post-synaptique. α1bAR contrôle la tonicité de certains muscles lisses du système veineux, α1aAR et α1dAR ceux des muscles lisses de la zone urogénitale (Martin *et al.*, 2007).

La stratégie de criblage choisie pour obtenir de nouveaux ligands actifs sur les α1AR consiste à mesurer la liaison d'un ligand radioactif (^{3}H-prazosine) spécifique des α1AR en présence de fractions de venin obtenues après séparation par chromatographies liquides. Le peptide actif est purifié par plusieurs cycles de chromatographie et sa séquence déterminée. Cette séquence est ensuite synthétisée chimiquement afin de confirmer l'activité biologique du peptide identifié à partir du venin. Cette stratégie nous a permis de mettre en évidence le premier peptide spécifique du récepteur α1aAR, nommé AdTx1. AdTx1 a une affinité de 0,41 nM pour le récepteur α1a et une sélectivité très élevée pour ce sous-type. Des expériences *ex-vivo* révèlent qu'AdTx1 bloque la contraction du muscle prostatique de lapin induite par la phényléphrine. Ces résultats démontrent ainsi qu'AdTx1 peut être un excellent candidat médicament dans le traitement de l'hypertrophie bénigne de la prostate.

Matériels et méthodes

Le venin de *Dendroaspis angusticeps* utilisé provient de Latoxan (France). Les produits radioactifs : ^{3}H-prazosine, ^{3}H-rauwolscine, ^{3}H-CGP-12177 et ^{3}H-N-méthyl-scopolamine (NMS) proviennent de Perkin Elmer (Courtaboeuf, France). Les cDNA codant pour les récepteurs adrénergiques ont été introduits dans le plasmide pcDNA3.1 et ont été généreusement fournis par Michael Brownstein (Craig Venter Institute, USA), à l'exception de celui codant pour le α1bAR, qui provient du Dr. Cotecchia (Suisse).

Isolement d'AdTx1

Un gramme de venin brut de *Dendroaspis angusticeps* est fractionné sur une colonne échangeuse de cation (2*15 cm, Source 15S Pharmacia) par un gradient de NaCl 0-3 M en 16h à pH 2,5 (acide acétique 10 mM). La fraction E issue de la première chromatographie est fractionnée par une chromatographie en phase inverse (Water 600) sur une colonne Vydac préparative (C18, 15 µm, 10 mL/min). Elle se fait sous un gradient linéaire en acétonitrile : 0-100% d'un mélange acétonitrile-0,1% de TFA en 100 min. Les HPLC analytiques sont réalisés sur une colonne Vydac (4,6 mm, 5 µm, 1mL/min) avec un gradient de 0,5% d'acétonitrile/min.

Dégradation d'Edman

Cinq cents picomoles de la fraction O sont resuspendues dans 50% d'acétonitrile. La suspension est vortexée vigoureusement, séchée à l'argon sur un filtre Biobrene. Le séquençage d'Edman est effectué sur un séquenceur modèle automatique 492 de Biosystèmes, PerkinElmer.

Synthèse d'AdTx1

La synthèse d'AdTx1, la purification du produit synthétisé et son repliement sont réalisées suivant la méthode décrite pour la toxine MT1 (Mourier *et al.*, 2003). Brièvement, la synthèse se fait sur phase solide suivant la stratégie fmoc. Après purification de la toxine par HPLC, elle est repliée à 4°C sur 2 jours dans du tampon Tris-HCl (50 mM, pH 8) en présence de 1 mM de glutathion réduit et oxydé dans 20% de glycérol.

Spectrométrie de masse

L'appareil de spectrométrie de masse utilisé est le 7-T APEX III FT-ICR (Bruker Daltonik, Bremen, Germany) relié à un générateur de 7 tesla. Un voltage de -700 V est appliqué à 50°C entre les aiguilles nano-electrospray (Proxeon, Odense, Denmark) et l'entrée du capillaire utilisé pour le transfert d'ions. Les spectres obtenus entre 200 et 3000 m/z ainsi que les pics monoisotopiques sont marqués en utilisant le logiciel XMASS 6.1.4 (Bruker Daltonics).

Culture des cellules et préparation des membranes

Des cellules COS sont cultivées à 37°C en milieu DMEM contenant 10% de sérum de veau fœtal, 1% de pénicilline et 1% de glutamine. A 80% de confluence, elles sont transfectées en utilisant du phosphate de calcium de façon à exprimer transitoirement les RCPG voulus. Après une incubation à 37°C pendant 24 h puis à 30°C pendant 48 h, les cellules sont récupérées afin de préparer les membranes comme décrit (Fruchart-Gaillard *et al.*, 2006). La concentration protéique des membranes est déterminée par un dosage de Lowry utilisant la BSA comme étalon.

Le cerveau de rat est utilisé comme source naturelle des récepteurs α1AR, α2AR et muscariniques, le cœur et le poumon comme sources des récepteurs β1AR et β2AR. Les synaptosomes de cerveau de rat sont préparés suivant la méthode décrite (Favreau *et al.*, 2001). Les membranes de poumons et de cœurs sont préalablement broyées par un Virtis avant d'être traitées comme les synaptosomes de cerveau. Les dosages protéiques sont réalisés avec le test de Bradford en utilisant la BSA comme standard.

Tests de liaisons

Toutes ces expériences sont réalisées dans un volume final de 100 µL, à température ambiante, pendant 16 h dans du tampon : 50 mM Tris-HCl, pH 7,4, 10 mM $MgCl_2$, 1 g/L BSA $MgCl_2$. La filtration est réalisée sur des plaques 96 filtres GF/C pré-incubées avec du PEI 0,5%. 25 µL de microscint 0 sont déposés sur chaque filtre après séchage. La radioactivité est quantifiée sur un compteur beta (Topcount, PerkinElmer). La liaison non-spécifique est mesurée en présence de 1 µM de prazosine, 1 µM de rauwolscine, 10 µM de propanolol et de 1 µM d'atropine, pour les ligands ^{3}H-prazosine, ^{3}H-rauwolscine, ^{3}H-CGP-12177 et ^{3}H-NMS, respectivement. Les courbes d'inhibition sont réalisées avec des quantités constantes de récepteurs et de ligands radioactifs et des concentrations croissantes du composé à tester. Les données sont analysées par le logiciel Kaleidagraph. Le Ki des ligands est déterminé à l'aide de l'équation de Cheng et Prussof (Cheng et Prusoff, 1973).

Test *ex-vivo* sur le muscle prostatique de lapin

Des morceaux de prostate dorsale de lapins albinos mâles (3,5 – 5,2 kg, CEGAV, France) sont disséqués et placés dans une solution de Krebs-Henseleit (114 mM NaCl, 4,7 mM KCl, 2,5 mM $CaCl_2$, 1,2 mM $MgSO_4$, 1,2 mM KH_2PO_4, 25 mM $NaHCO_3$, 11,7 mM glucose, pH 7,4) oxygénée (95% O_2 et 5% CO_2) à 37°C en présence de 1 µM de propanolol, 0,1 µM de désipramine, 3 µM de deoxycorticostérone et 1 µM de normétanéphrine. Les contractions sont mesurées avec des transducteurs isométriques de tension (EMKA technologies, France) raccordés en utilisant PowerLab16/s (ADInstruments Pty Ltd, UK). Après 60 min d'équilibration, les morceaux sont exposés à 30 µM de phényléphrine pour contrôler leur viabilité. Après 30 min, une première courbe cumulative dose-réponse à l'adrénaline est tracée. Les muscles sont incubés avec 10, 30 ou 100 nM d'AdTx1 ou du solvant pendant 180 min, puis une seconde courbe dose-réponse à l'adrénaline est réalisée.

Résultats

Découverte d'AdTx1

Le fractionnement initial de 1g de venin brut de *Dendroaspis angusticeps* réalisé sur une colonne échangeuse de cations a permis une subdivision du venin en 13 fractions (*Figure 1.A*). La capacité de chacune des fractions à déplacer la liaison spécifique de la prasozine tritiée (ligand spécifique des récepteurs α1aAR), sur des synaptosomes de cerveau de rat est étudiée (*Figure 1B*).

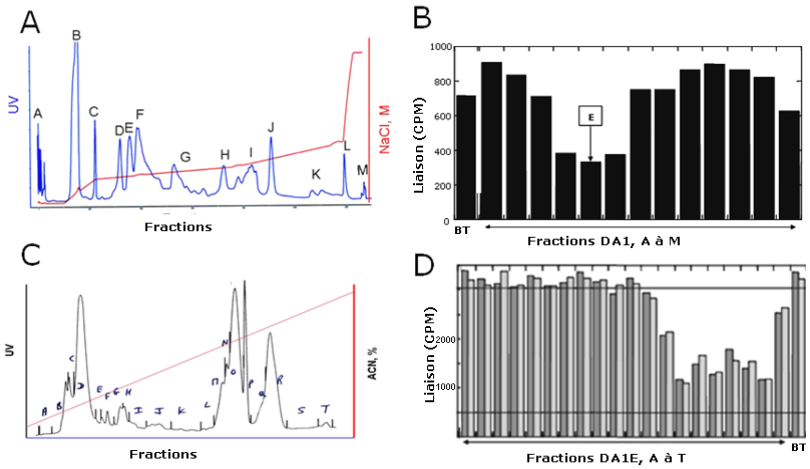

Fig. 1. Isolement d'AdTx1 dans le venin de *Dendroaspis angusticeps.* (**A**) Chromatographie échangeuse de cation du venin brut. (**C**) Chromatographie phase inverse de la fraction E. (**B** et **D**) Mesure de la liaison de la ^{3}H-prazosine sur synaptosomes de cerveaux de rats en présence de chacune des fractions isolées en A et C.

Fig. 1. *Discovery of AdTx1. (**A**) Ion-exchange chromatography of Dendroaspis angusticeps crude venom. We collected 13 fractions. (**C**) Reverse phase chromatography of fraction E on a Vydac C18 preparative column. We collected 20 fractions. (**B** and **D**) ^{3}H-prazosin binding to rat brain synaptosomes in the presence of each fraction isolated in A and C.*

Les fractions D, E et F diminuent considérablement la liaison spécifique de la ^{3}H-prazosine (*Figure 1.B*). La fraction E est séparée à son tour par une chromatographie en phase inverse (*Figure 1.C*). Elle conduit à 20 nouvelles fractions parmi lesquelles les fractions de M à R inhibent la liaison de ^{3}H-prazosine (*Figure 1.D*). Nous nous focaliserons sur la fraction O. Son analyse par HPLC analytique ne présente qu'un seul pic. L'analyse en masse indique que la fraction O est composée de 4 peptides dont un représente plus de 90% du signal. Sa masse mono isotopique, de 7278,3691 Da, devient, après réduction, 7286,3741 Da, indiquant la présence de 4 ponts disulfure. Le séquençage de la fraction O par dégradation d'Edman ainsi que par fragmentation massique des peptides issus de l'hydrolyse trypsique de la fraction O nous a permis de déterminer la séquence suivante :

LTCVTSKSIFGITTEDCPDGQNLCFKRRHYVVPKIYDSTRGCAATCPIPENYDSI-HCCKTDKCNE

Cette séquence est proche de celle des toxines muscariniques (*Tableau 1*), ce qui suggère que le peptide correspondant appartiendrait à la famille des toxines à trois doigts. Elle est ensuite synthétisée

chimiquement et oxydée afin de s'affranchir des contaminants présents dans la fraction O et d'en disposer en quantité importante (Mourier *et al.*, 2003). Le peptide synthétique possède les mêmes caractéristiques biochimiques (temps de rétention en phase inverse) et pharmacologiques (capacité de déplacement de la liaison de la ^{3}H-prazosine) que la fraction O. Il a été appelé AdTx1 et enregistré dans la base de données UniProt sous le numéro P8509.

Tableau 1. Séquence d'AdTx1 et comparaison avec les 9 séquences les plus proches.

Table 1. *AdTx1 sequence and comparison with the 9 most similar sequences.*

		--------mass sequencing--------	
		----------Edman dégradation----------	
		---boucle 1---- ------boucle 2----- ---boucle 3--	%id.
Edman Dégradation		LTXVTSKSIFGITTEDXPDGQNLXFKRRHYVVPKIYDSTRGXAATXPIPE	
Analyse de masse		IYDSTRGCAATCPIPENYDSI-HCCKTDKCNE ou LYDSTRGCATACPLPENYDLS-HCCKTDKCEN	
AdTx1	Da	LTCVTSKSIFGITTEDCPDGQNLCFKRRHYVVPKIYDSTRGCAATCPIPENYDSI-HCCKTDKCNE	100
MTβ	Dpp	LTCVTSKSIFGITTEDCPDGQNLCFKRRHYVVPKIYD**I**TRGC**V**ATCPIPENYDSI-HCCKTDKCNE	97
Cm3	Dpp	LTCVTSKSIFGITTEDCPDGQNLCFKRRHYVVPKIYD**I**TRGC**V**ATCPIPENYDSI-HCCKT**E**KCN**-**	95
MT3	Da	LTCVT**KNT**IFGITTE**N**CP**A**GQNLCFKR**W**HYV**I**P**RYTEI**TRGC**A**ATCPIPENYDSI-HCCKTDKCNE	80
MLT	Nak	LTCV**KE**KSIFG**V**TTEDCPDGQNLCFKR**WHMI**VP**GR**Y**KK**TRGCAATCPI**A**EN**RDVI**-**E**CC**S**TDKCN**-**	78
MT4	Da	LTCVTSKSIFGITTE**N**CPDGQNLCFKK**WY**Y**I**VP**RYS**D**I**T**W**GCAATCP**K**P**T**N**VRETI**HCC**E**TDKCN E	75
MT1	Da	LTCVTSKSIFGITTE**N**CPDGQNLCFKK**WY**Y**I**VP**RYS**D**I**T**W**GCAATCP**K**P**T**N**VRETIR**CC**E**TDKCN E	74
MT2	Da	LTCVT**T**KSI**GGV**TTEDCP**A**GQN**V**CFKR**W**HYV**T**PK**N**YD**IIK**GCAATCP**KVD**N**N**D**PI-R**CC**G**T**DKCN**D**	69
MTα	Dpp	LTCVTSKSIFGITTE**N**CPDGQNLCFK**KWY**Y**LNHRYS**D**I**T**W**GCAATCP**K**P**T**N**VRETI**HCC**E**TDKCN E	69
MT7	Da	LTCV**K**S**N**SI**WFP**T**S**EDCPDGQNLCFKR**WQ**Y**IS**P**R**M**YD**F**TRGCAATCP**KA**E**YR**D**VI**-**N**CC**G**TDKCN**K**	68

La lettre X correspond aux résidus non détectés par la dégradation de Edman. Les lettres en gras correspondent aux résidus différents de ceux d'AdTx1. Da: *Dendroaspis angusticeps*, Dpp: *Dendroaspis polylepis polylepis*, Nak: *Naja koauthia*.

The letter X corresponds to residues not detected by Edman degradation. Bold letters correspond to residues different from those of AdTx1. Da: Dendroaspis angusticeps*, Dpp:* Dendroaspis polylepis polylepis*, Nak:* Naja koauthia*.*

Sélectivité d'AdTx1 pour le sous-type α1aAR

L'inhibition par l'AdTx1 de la liaison de ^{3}H-prazosine, ^{3}H-rauwolscine, ^{3}H-CGP-12177 et ^{3}H-NMS sur des sources naturelles riches respectivement en récepteurs α1, α2, β adrénergiques et en récepteurs muscariniques, a été effectuée (*Figure 2*).

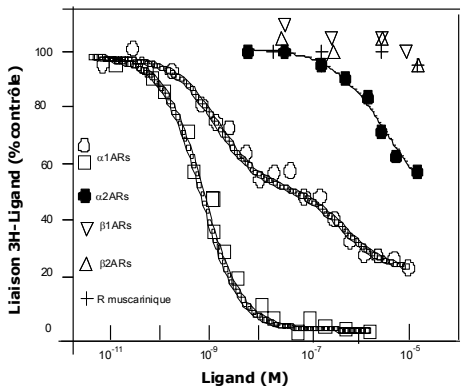

Fig.2. Sélectivité d'AdTx1 pour le récepteur adrénergique α1. Inhibition de la liaison de ^{3}H-prazosine par la prazosine (□) et par AdTx1(o) sur les récepteurs α1. Inhibition de la liaison de ^{3}H-rauwolscine sur α2 (●), ^{3}H-CGP-12177 sur β1 et β2 (triangle) et de ^{3}H- NMS sur les récepteurs muscariniques (+).

Fig.2. *AdTx1 selectivity. ^{3}H-prazosin binding inhibition by prazosin (□) and AdTx1 (o) on α1ARs. Binding inhibition of ^{3}H-rauwolscine on α2ARs (●), ^{3}H-CGP-12177 on β1 and β2 (triangles) and ^{3}H-NMS on muscarinic receptors (+) by AdTx1.*

L'inhibition de la liaison de ^{3}H-prazosine par AdTx1 montre une courbe biphasique avec un IC_{50} de haute affinité de 4 ± 0,5 nM et de basse affinité de 1500 ± 450 nM. L'inhibition de la rauwolscine n'est visible que pour des concentrations micromolaires d'AdTx1 alors que 10 µM d'AdTx1 n'inhibent pas la liaison de ^{3}H-CGP-12177 ni de ^{3}H-NMS sur leurs récepteurs respectifs. Ces résultats démontrent la forte sélectivité d'AdTx1 pour les récepteurs adrénergiques α1.

Afin de déterminer l'affinité de la toxine pour chacun des trois récepteurs α1AR, ces derniers sont exprimés transitoirement dans des cellules COS. AdTx1 inhibe la liaison de ^{3}H-prazosine sur α1aAR avec un IC_{50} de 1,3 nM et une pente proche de l'unité. Quelle que soit la concentration d'AdTx1 utilisée, l'inhibition de la prazosine est incomplète, laissant une liaison résiduelle de l'ordre de 20% (*Figure 3*). Sur les deux autres sous-types, α1bAR et α1dAR, AdTx1 inhibe la liaison de ^{3}H-prazosine avec des IC_{50} de 260 nM et de 6400 nM, respectivement. Comme sur le récepteur α1aAR, AdTx1 laisse une liaison résiduelle de ^{3}H-prazosine sur α1bAR. La liaison résiduelle observée sur ces récepteurs peut être due à une interaction non compétitive entre AdTx1 et la prazosine et peut suggérer un caractère allostérique de la toxine. Cependant les expériences réalisées jusqu'à présent ne permettent pas de conclure quant au mode d'interaction du peptide. Pour déterminer les constantes d'affinité de la toxine AdTx1 pour les trois récepteurs α1, nous supposerons qu'elle est un ligand compétiteur et utiliserons l'équation de Cheng et Prussof. Ainsi AdTx1 possède une affinité de 0,41 ± 0,02 nM pour le récepteur α1aAR, une affinité de 49 ± 17 nM pour le sous-type α1bAR et de 1200 ± 700 nM (n=4) pour α1dAR.

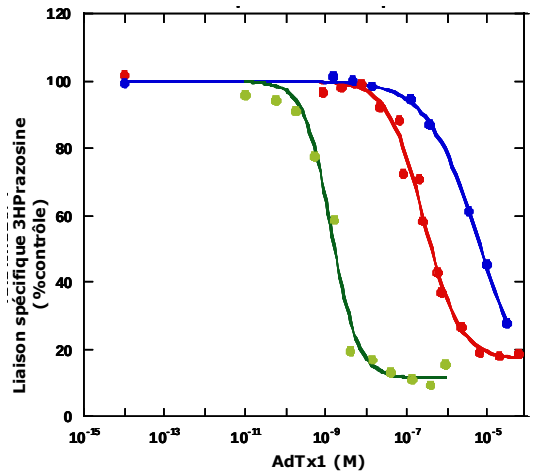

Fig. 3. Inhibition de la liaison spécifique de ^{3}H-prazosine par AdTx1 sur α1aAR (vert), α1bAR (rouge) et α1dAR (bleu) exprimés transitoirement dans les cellules COS.

***Fig. 3**. ^{3}H-prazosin binding inhibition by AdTx1 on α1aAR (green), α1bAR (red) et α1dAR (blue), expressed in COS eukaryotic cells.*

AdTx1 est un antagoniste du récepteur α1aAR

La contraction du muscle lisse prostatique de lapin est principalement contrôlée par les récepteurs α1AR (Delaflotte *et al*., 1996). Afin de comprendre le comportement fonctionnel d'AdTx1, nous avons étudié son influence sur cette contraction. L'addition cumulée de doses croissantes de phényléphrine entraîne des contractions de plus en plus importantes du muscle prostatique avec un pEC_{50} = 5,28 ± 0,05 et un effet maximal correspondant à 107 ± 2,2% de la réponse initiale à 30 µM phényléphrine. L'effet de la pré-incubation de concentrations croissantes d'AdTx1 (10, 30 et 100 nM) sur la courbe dose-réponse à la phényléphrine est représenté sur la *Figure 4*. 10 nM d'AdTx1 n'entraîne aucune modification significative de la courbe dose réponse. Par contre, 30 et 100 nM d'AdTx1 diminuent significativement la contraction maximale du muscle de 14,0 ± 2,2 % et 58,8 ± 4,3%, respectivement, tout en augmentant la pEC_{50} de la phényléphrine (pEC_{50} = 4,81 ± 0,14 et 4,27 ± 0,29). Ces résultats indiquent qu'AdTx1 est un antagoniste du récepteur α1aAR.

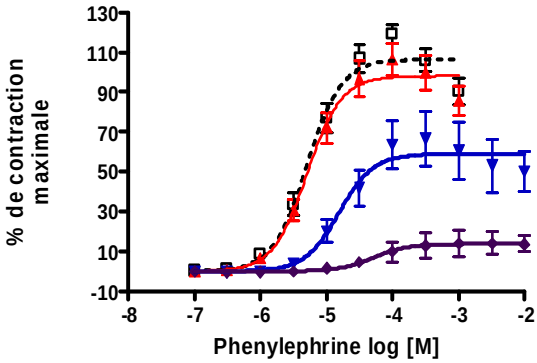

Fig. 4. Effet de différentes concentrations d'AdTx1 sur la contraction du muscle prostatique de lapin induite par la phényléphrine : (pointillés) en absence d'AdTx1, (rouge) en présence de 10 nM d'AdTx1, (bleu) 30 nM d'AdTx1 et (mauve) 100 nM d'AdTx1. Moyenne ± ESM (n = 6).

***Fig. 4**. In vitro activity test on prostate muscle. Cumulative concentration-response curves for PHE were obtained using isolated rabbit prostatic muscle after 30 min of incubation with solvent (dashes line), or 10 nM (red), 30 nM (blue) or 100 nM (purple) of AdTx1. Contractile responses to agonist were presented as a % of the maximal tension obtained with 30 µM of PHE. Mean ± SEM (n = 6).*

Discussion

Cette étude décrit une méthode originale d'isolement de peptide de venin de serpent spécifique de RCPG. Elle a permis d'obtenir, à partir du venin de mamba vert, AdTx1, un peptide spécifique du récepteur adrénergique α1a.

De par sa forte similarité de séquence avec les toxines muscariniques, AdTx1 appartiendrait à la famille des toxines de serpent à trois doigts. Elle possède respectivement 97% et 95% d'identité de séquence avec MTβ et Cm3. MTβ est décrite comme ayant une faible affinité sur des récepteurs muscariniques alors qu'aucune activité biologique n'a été identifiée pour Cm3 (Jolkkonen *et al.*, 1995 ; Joubert, 1985).

Par des tests de liaisons, nous avons montré qu'AdTx1 est le premier ligand peptidique ayant une affinité sub-nanomolaire et une sélective supérieure à un facteur 100 pour le sous-type α1aAR. Ces propriétés en font un outil pharmacologique particulièrement intéressant dans l'étude du récepteur α1aAR. D'autre part, les résultats des expériences *ex-vivo* réalisées sur le muscle prostatique de lapin montrent qu'AdTx1 provoque non seulement un décalage vers la droite de la pEC_{50} de la phényléphrine, ce qui traduit un effet antagoniste, mais aussi une baisse de la réponse contractile maximale, associée à une perte de l'efficacité de la phényléphrine.

L'hypertrophie bénigne de la prostate concerne 80% des hommes de 80 ans et provoque des symptômes indésirables tels que l'hyperactivité vésicale et la rétention d'urine. Les traitements actuellement sur le marché sont entre autres des bloqueurs de α1AR (tamsulosine, alfuzosine…) provoquant un relâchement des muscles prostatiques, mais aussi une hypotension du fait de leur action sur le sous-type α1bAR (Bullock et Andriole, 2006). AdTx1, de par sa sélectivité et son efficacité à relâcher le muscle prostatique, pourrait donc être un excellent candidat médicament dans le traitement de cette pathologie.

Références bibliographiques

Bradley KN (2000) Muscarinic toxins from the green mamba. *Pharmacol Ther* **85**: 87-109

Bullock TL, Andriole GL Jr (2006) Emerging drug therapies for benign prostatic hyperplasia. *Expert Opin Emerg Drugs* **11**: 111-123

Cheng Y, Prusoff WH (1973) Relationship between the inhibition constant (K1) and the concentration of inhibitor which causes 50 per cent inhibition (I50) of an enzymatic reaction. *Biochem Pharmacol* **22**: 3099-3108

Delaflotte S, Auguet M, Chabrier PE (1996) Pharmacological evidence that different alpha 1 adrenoceptor subtypes mediate contraction in rabbit prostate and hypogastric artery. *Acta Physiol Scand* **158**: 241-251

Favreau P, Gilles N, Lamthanh H, Bournaud R, Shimahara T, Bouet F, Laboute P, Letourneux Y, Menez A, Molgo J, Le Gall F (2001) A new omega-conotoxin that targets N-type voltage-sensitive calcium channels with unusual specificity. *Biochemistry* **40**: 14567-14575

Fruchart-Gaillard C, Mourier G, Marquer C, Menez A, Servent D (2006) Identification of various allosteric interaction sites on M1 muscarinic receptor using 125I-Met35-oxidized muscarinic toxin 7. *Mol Pharmacol* **69**: 1641-1651

Jolkkonen M, Adem A, Hellman U, Wernstedt C, Karlsson E (1995) A snake toxin against muscarinic acetylcholine receptors: amino acid sequence, subtype specificity and effect on guinea-pig ileum. *Toxicon* **33**: 399-410

Joubert FJ (1985) The amino acid sequence of protein CM-3 from Dendroaspis polylepis polylepis (black mamba) venom. *Int J Biochem* **17**: 695-699

Lewis RJ, Garcia ML (2003) Therapeutic potential of venom peptides. *Nat Rev Drug Discov* **2**: 790-802

Martin E, Capini C, Duggan E, Lutzky VP, Stumbles P, Pettit AR, O'Sullivan B, Thomas, R (2007) Antigen-specific suppression of established arthritis in mice by dendritic cells deficient in NF-kappaB. *Arthritis Rheum* **56**: 2255-2266

Mourier G, Dutertre S, Fruchart-Gaillard C, Menez A, Servent D (2003) Chemical synthesis of MT1 and MT7 muscarinic toxins: critical role of Arg-34 in their interaction with M1 muscarinic receptor. *Mol Pharmacol* **63**: 26-35

Neubig RR, Spedding M, Kenakin T, Christopoulos A (2003) International Union of Pharmacology Committee on Receptor Nomenclature and Drug Classification. XXXVIII. Update on terms and symbols in quantitative pharmacology. *Pharmacol Rev* **55**: 597-606

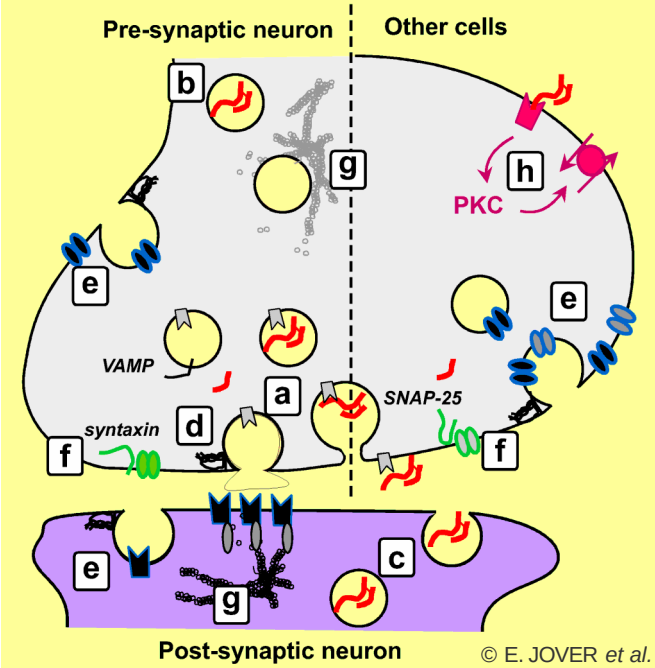

© E. JOVER *et al.*

Toxines et Signalisation

La plupart des protéines qui présentent une activité toxique démontrée, telles celles présentées dans cet ouvrage, interagissent avec divers types cellulaires. La majorité de ces protéines est dirigée vers des cibles exprimées à la surface de la cellule et altère les fonctions de la membrane plasmique ou perturbe leur intégrité. Par ailleurs, de nombreuses toxines produites par des micro-organismes, champignons, algues et plantes, interagissent tout d'abord avec la membrane plasmique mais c'est à l'intérieur de la cellule qu'elles exercent leur effet toxique. Cependant, le bénéfice que ces organismes retirent de la production d'une toxine à action intracellulaire n'est pas toujours évident. Des approches multidisciplinaires associant biologie moléculaire, microbiologie, biologie de la membrane, biochimie, physiologie, pharmacologie et protéomique ont permis un progrès considérable dans notre compréhension des mécanismes intracellulaires associés au mode d'action des toxines décrites dans cet ouvrage. Ces approches ont aussi conduit à définir les mécanismes qui dirigent ces molécules vers leurs cibles spécifiques au cœur des compartiments internes des cellules eucaryotes. Aujourd'hui, une image plus claire de leurs actions et partenaires intracellulaires se met en place. Des progrès récents démontrent que ces toxines constituent des outils performants pour élucider et caractériser des processus métaboliques cruciaux pour la cellule eucaryote, tels les voies de signalisation physiologiques et les mécanismes cellulaires constitutifs. Il est évident que les futurs développements pharmacologiques exploiteront les propriétés inhérentes à ces toxines d'agir au niveau intracellulaire pour délivrer des substances biologiquement actives à l'intérieur des cellules ou pour moduler des fonctions cellulaires altérées.

Toxins and Signalling

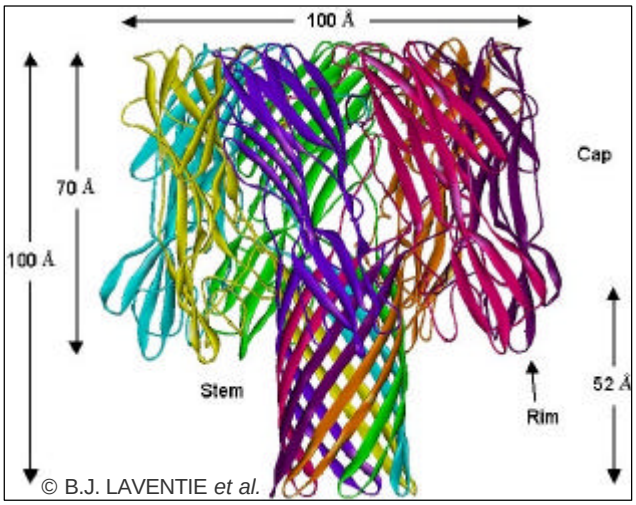

© B.J. LAVENTIE *et al.*

Most proteins with a demonstrated toxic activity, such as those presented in this e-book, interact with various cell types. Most animal toxins are directed against targets expressed at the cell surface and alter or disrupt plasma membrane functions. In turn, numerous toxins produced by micro-organisms, fungi, algae and plants, first interact with the plasma membrane but they express their effect inside the cell. However, it is often unclear what is the inherited benefit for these organisms to produce a toxin that acts intracellularly. Multi-disciplinary approaches combining molecular cell biology or microbiology, membrane biology, biochemistry, physiology, pharmacology and proteomics have made possible considerable progress in our understanding of the intracellular mechanisms of the toxins described in this e-book. These approaches have also led to define the mechanisms that address these molecules to their specific targets within the inner compartments of eukaryotic cells. Now a clearer picture of their intracellular actions and partners is emerging. Recent progress demonstrated them as useful tools to elucidate and characterize metabolic processes that are crucial for eukaryotic cells, such as physiological signalling pathways and constitutive cellular mechanisms. Most probably, future pharmacological developments will employ the inherent capability of these toxins to act intracellulary for delivering biologically-active substances into cells or for tuning altered cell functions.

Bernard Poulain,
Centre National de la Recherche Scientifique

ISSN : 1760-6004